The Dissertation Committee for Eric Chen Certifies that this is the approved version of the following dissertation:

Carbon Dioxide Absorption into Piperazine Promoted Potassium Carbonate using Structured Packing

Committee:

Gary T. Rochelle, Supervisor

A. Frank Seibert

David T. Allen

Benny D. Freeman

Richard L. Corsi

Carbon Dioxide Absorption into Piperazine Promoted Potassium Carbonate using Structured Packing

by

Eric Chen, B.S.; M.S.

Dissertation

Presented to the Faculty of the Graduate School of

The University of Texas at Austin

in Partial Fulfillment

of the Requirements

for the Degree of

Doctor of Philosophy

The University of Texas at Austin

December 2007

Dedication

To My Family

Acknowledgements

I would like to personally thank Dr. Gary Rochelle for his unwavering support throughout my graduate student tenure at the University of Texas at Austin. Since I have known Dr. Rochelle, he has held numerous titles that range from graduate school advisor and research supervisor, to trail guide and political activist, to choir singer and leading expert in his field, to colleague and friend. He has impressed upon me his exuberance and passion for chemical engineering, but yet has remained an approachable person.

I am deeply grateful for the financial support and material contributions that have made the completion of this work possible. I have had the privilege of receiving several fellowships, including the U.S. Environmental Protection Agency Science to Achieve Results (STAR) Fellowship, the John T. Files Endowed Graduate Fellowship in Engineering through the University of Texas at Austin College of Engineering Thrust Program, and the David Bruton Jr. Graduate Fellowship through the University of Texas at Austin Graduate School.

The majority of the pilot plant work was funded under U.S. Department of Energy Cooperative Agreement DE-FC26-02NT41440. A number of organizations have also provided invaluable contributions in the form of cost-sharing and in-kind donations. The Industrial Associates Program for CO_2 Capture, the UT Separation Research Program, and the UT College of

Engineering have provided equipment cost-sharing. Projects from CD Tech and Dyzacky/DOE also provided additional equipment through cost-sharing. Koch-Glitsch Inc. generously donated the Flexipac 1Y, Flexipac AQ, and IMTP #40 packing used in the absorber and stripper columns. Emerson Process and Rosemount Analytical donated the hardware and software for the DeltaV process control system and provided numerous pieces of process equipment at cost. Finally, Huntsman Corporation donated several heat-exchangers and numerous control valves for the pilot plant.

I would like to personally thank the personnel at the UT Separations Research Program (SRP). Frank Seibert has provided major support for the pilot plant work through the use of SRP personnel and cost-sharing with other projects. Christopher Lewis has provided his expertise with the DeltaV, Steve Briggs has provided mechanical and operational support, and Robert Montgomery has provided instrumentation and electrical support. Moreover, Alyson Sagle from Dr. Freeman's research group has graciously allowed me to perform the CO_2 loading analysis on the TOC analyzer and provided invaluable assistance with the setup and maintenance of the analyzer.

Finally, I would like to thank the members in my research group who directly contributed to the 24-hour operation of the pilot plant, which include Babatunde Oyenekan, John McLees, Andrew Sexton, Jennifer Lu, Marcus Hilliard, and Jason Davis. I would like to personally thank Ross Dugas for his time and effort from beginning to end of the pilot plant work. I would also like to thank Tim Rochelle and Daniel Ellenberger for the assistance that they have provided through sampling and sample analysis and Brian Daniels for his contribution to the development of an ion chromatograph method for piperazine and potassium analysis.

The absorber modeling work was completed using the Aspen Plus® and Aspen Properties® software donated by AspenTech. In addition, Dr. Chau-Chyun Chen of AspenTech has provided quick and responsive technical support, which made the absorber modeling effort worthwhile.

I would like to thank Jody Lester, Lane Salgado, and Maeve Cooney for their day-to-day non-technical help. I have also had the pleasure of interacting with the members of the Rochelle research group over the years, including: Dr. Sanjay Bishnoi, Dr. Norman Yeh, Dr. Sharmi Roy, Amy Nowlin, Stephano Freguia, Dyron Hamlin, Ian Wilson, Akin Alawode, Dr. Tim Cullinane, Dr. George Goff, Dr. Mohammed Al Juaeid, Bob Tsai, David Van Wagener, Jorge Plaza, Qing Xu, Sephideh Zialli, Stephanie Freeman, Thu Nguyen, and Fred Closmann.

In addition, I would to thank Lizhi Chen for his help and camaraderie as we slogged through the remedial undergraduate courses needed to become a chemical engineer. I thank Jacinto Lopez for his friendship and being a willing accomplice as we tested the various lunch spots around Austin. I would also like to thank Carmela Avila for her friendship and the inspiration she has provided on the last leg of this journey.

My neighbors from Cliffstone Cove have also been a constant source of distraction and entertainment. I would like to thank the Beamans for taking care of me like their own son. Sergio and Clare went out of their way to help me tend to the needs of my aging car. Ryan and Laura were the motivation and impetus behind the numerous and complicated remodeling projects around my house. I would like to thank Julian Sanchez for his benevolence, generosity and support for my home flooring and bathroom projects during my time here.

I would like to thank the members of my family who have been the bedrock and foundation since I began my earthly journey. During my time at UT,

my father has offered his time and financial support, and my mother has offered her practical sense. While growing up, my sister Emily always seemed to want to follow in the footsteps of her big brother. But now she has surpassed me in many ways and has become an inspiration to me. Finally, I would like to dedicate my dissertation to my grandfather, Yeh-Yeh, who passed away a few years ago. His infectious laughter, joyful exuberance, generosity, and sense of responsibility have left an indelible impression on me. My grandmother, Nie-Nie, continues his tradition of generosity and has helped start the next stage of my life.

Carbon Dioxide Absorption into Piperazine Promoted Potassium Carbonate using Structured Packing

Publication No._____

Eric Chen, Ph.D.

The University of Texas at Austin, 2007

Supervisor: Gary T. Rochelle

A large-scale pilot plant (0.43 m ID) was extensively modified and converted into an absorber/stripper system to demonstrate CO_2 capture technology using aqueous piperazine promoted potassium carbonate for coal-fired power plants. Four pilot plant campaigns were completed. Three campaigns were conducted using 5 m K^+/2.5 m PZ and 6.4 m K^+/1.6 m PZ. Flexipac 1Y and Flexipac AQ Style 20 structured packing were used in the absorber. The stripper was tested with 14 sieve trays, IMTP #40 random packing, and Flexipac AQ Style 20 packing. Monoethanolamine (7 m) was tested in the third campaign to establish a base case. An approximate rate analysis showed that 5 m K^+/2.5 m PZ is two times faster than 7 m MEA and three times faster than 6.4 m K^+/1.6 m PZ. The location of the temperature bulge moves from the top of the column to bottom as the liquid to gas flow rate ratio is increased. Foaming occurred in the absorber in the first two campaigns and occurred in the stripper in the fourth campaign.

Data from the pilot plant was used to develop a K^+/PZ absorber model in Aspen Plus® RateSep™. The Hilliard (2005) Aspen Plus® VLE model and the kinetics developed by Cullinane (2005) were incorporated in the model. Data-Fit was simultaneously used to reconcile pilot plant data and perform a regression of the interfacial area and heat loss parameters for the RateSep™ absorber model. The lean loading for the pilot plant data was shifted down by 10% to account for a discrepancy with the Cullinane vapor–liquid equilibrium data. The Data-Fit results showed that the average interfacial area for Flexipac 1Y was 80% of the value measure by the air-water column. The average interfacial area for Flexipac AQ Style 20 for 5 m K^+/2.5 m PZ was 56% of the air-water measurement. The CO_2 heat of absorption may not have been adequately predicted by the RateSep™ absorber model because the regressed values of heat loss were consistent with forced convection.

Table of Contents

List of Tables

List of Figures

Nomenclature

COMPONENT SPECIES

CO_3^{2-}	Carbonate
$H_2O(l)$	Liquid water
H_3O^+	Hydronium ion
HCO_3^-	Bicarbonate
K^+	Potassium
$KHCO_3$	Potassium bicarbonate
K_2CO_3	Potassium carbonate
OH^-	Hydroxide
PZ	Piperazine (liquid)
PZH^+	Protonated piperazine
$PZCOO^-$	Piperazine carbamate
$PZ(COO^-)_2$	Piperazine dicarbamate
H^+PZCOO^-	Protonated piperazine carbamate

ROMAN LETTERS

A	First term of equilibrium (K_{eq}) equation
A_b	Total active bubbling area on the tray [m^2]
A_h	Total area of the holes [m^2]
A_t	Cross-sectional area of the column [m^2]
a	Interfacial area per unit bubbling area for trays [−]
a_e	Effective surface area per unit volume of the column [m^2/m^3]
a_{eff}	Effective interfacial area of packing [m^2/m^3]
a^I	Interfacial area for mass transfer [m^2]
a_w	Wetted surface area per unit volume of the column [m^2/m^3]
a_p	Specific area of packing [m^2/m^3]
B	Second term of equilibrium (K_{eq}) equation
B	Base width of a corrugation [m] (Bravo et al. (1996)
C	Third term of equilibrium (K_{eq}) equation
C_E	Correction factor for surface renewal [−]

C_P	Specific molar heat capacity [J/kmol k]
$C_{p,\,prod}$	Heat capacity of products [cal/mol-K]
$C_{p,\,react}$	Heat capacity of reactants [cal/mol-K]
$\Delta C_{p,rxn}$	Heat capacity for the reaction [cal/mol-K]
D	Diffusion coefficient [m^2/s]
d	Characteristic length [m]
d_{eq}	Equivalent diameter [m]
d_h	Hydraulic diameter [m]
d_P	Nominal packing size [m]
F	Feed molar flow rate [kmol/s]
F_f	Fractional approach to flooding [−]
F_s	Superficial F-factor [$kg^{0.5}/m^{0.5}$-s]
$H_{f,prod}$	Heat of formation for products [kcal/mol]
$H_{f,react}$	Heat of formation for reactants [kcal/mol]
ΔH_a	Activation energy [KJ/kmol]
ΔH_{rxn}	Heat of reaction [kcal/mol]
$\Delta H\text{-}HD$	Heat duty calculated by Aspen Plus® [kcal/mol]
$\Delta H\text{-}VLE$	Heat duty calculated from Gibbs-Helmholtz [kcal/mol]
I	Ionic Strength [mol/L)
k	Kinetic rate constant [−]
$k_g^{'}$	Normalized Flux [mol/Pa-cm^2-s]
K	Equilibrium constant [−]
K_g	Overall mass transfer coefficient [mol/Pa-cm^2-s]
m	Molal [mol/kg H_2O]
M	Molar [mol/L]
MW	Molecular weight [g/mol]
N_{CO_2}	Molar flux [mol/hr]
$P^*_{CO_2}$	Equilibrium partial pressure of CO_2 [Pa]
$P_{CO_2,b}$	Partial pressure of CO_2 in the bulk gas [Pa]
$P_{CO_2,i}$	Partial pressure of CO_2 in at the gas-liquid interface [Pa]
R	Universal gas constant [8.3145 J/mol-K]
V	Liquid molar volume [m^3/mol]

T	Temperature [K]
x	Liquid mole fraction
y	Vapor mole fraction [−]
z	Charge [+/−]

GREEK LETTERS AND SYMBOLS

ε	Void fraction of packing [−]
ε_{solv}	Dielectric constant of solvent mixture [−]
γ	Activity [−]
η	Viscosity [N-sec/m^2]
λ	Thermal conductivity [W/m-K]
ρ	Density [kg/m^3]
σ	Surface Tension [N/m]

SUBSCRIPTS

b	Bulk solution or vapor property
eq	Equilibrium
for	Forward reaction
i	Component i
j	Stage or segment j
k	Component k
rev	Reverse reaction
t	Total

SUPERSCRIPTS

f	Film
I	Interface
L	Liquid
V	Vapor

ASPEN PLUS®

ANDKIJ/1,2	Binary Parameters for modified Andrade Equation, default is zero
ANDMIJ/1,2	Binary Parameters for modified Andrade Equation, default is zero
CHARGE	Ionic charge
CPAQ0	Aqueous phase heat capacity at infinite dilution. The Criss-Cobble equation is used to calculate heat capacity if no values is given.
CPIG	Ideal gas heat capacity coefficients
DHAQFM	Aqueous heat of formation at infinite dilution. Used in electrolyte solutions for ionic species and molecular solutes.
DHFORM	Standard heat of formation of ideal gas at 25°C
DHVLB	Heat of vaporization at the normal boiling point (TB)
DHVLWT	Watson heat of vaporization parameters
IONMOB	Parameter used in Jones-Dole model to calculate the liquid viscosity correction due to electrolytes.
SO25C	Criss-Cobble absolute entropy at 25°C. Used to estimate aqueous heat capacity at infinite dilution
TB	Normal boiling point

Chapter 1: Introduction

As the debate over global warming continues, it is indisputable that many countries have begun adopting policies aimed at reducing greenhouse gas (GHG) emissions such as carbon dioxide (CO_2). Within the last 10 years, research on CO_2 capture and sequestration has intensified dramatically. While the capture and sequestration of carbon dioxide is not a new technology, in its current state, it is very expensive. A combination of regulations and economics will drive the future of CO_2 capture and sequestration research and its ultimate implementation.

1.1 Sources and trends of U.S. Carbon Dioxide Emissions

One major source of anthropogenic emissions of carbon dioxide is the combustion of fossil fuel for energy. In 2004, 86 percent of the energy consumed in the United States was derived from the combustion of fossil fuels such as coal, natural gas, and petroleum. The combustion of fossil fuel accounted for 94 percent of U.S. CO_2 emissions in 2004 (U.S. EPA, 2006). According to Marland (2006), global CO_2 emissions from fossil fuel burning, cement manufacture, and gas flaring produced 26,760 Tg CO_2 eq. in 2003, of which the United States accounted for approximately 21 percent.

From 1990 to 2004, total CO_2 emissions from fossil fuel combustion have increased by about 20 percent, from 4,697 to 5657 Tg CO_2 eq. (U.S. EPA, 2006). Carbon dioxide emissions from electricity generation and transportation have increased by 26 and 28 percent, respectively, over the 14 year period. In 1990,

electricity generation accounted for 38 percent of all U.S. CO_2 emissions and the trend remained relatively constant, increasing to 40.5 percent in 2004, with coal combustion accounting for approximately 83 percent of the emissions from electricity generation. In 2004, coal-fired utility plants accounted for 34 percent of all carbon dioxide emissions in the United States (Figure 1-1).

The flue gases of coal-fired power plants typically contain between 10 to 15% CO_2, while gas-fired turbine plants contain about 2–3%. Therefore, the capture and sequestration of CO_2 from flue gases of coal-fired utility plants would represent a significant reduction in CO_2 emissions. It would represent the first and most cost effective method since utility plants are point sources. The target CO_2 removal rate from coal-fired power plants would be approximately 90%.

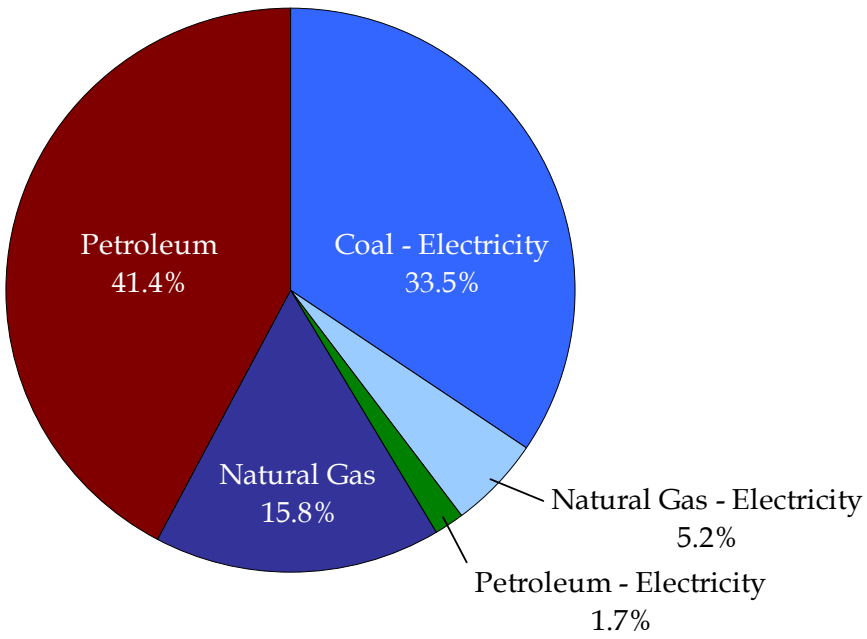

Figure 1-1. United States CO_2 Emissions by Fuel-Type and Sector in 2004, Total Emissions: 5657 Tg CO_2 Eq.

1.2 CO_2 Capture and Sequestration

There are a number of ways to remove CO_2 from the combustion process. Carbon dioxide capture processes can be divided into three categories: pre-combustion, post-combustion, and oxy-fuel combustion. Within each capture process, a number of separation technologies can employed as standalone technology or coupled with another separation processes to capture CO_2 for the purpose of sequestration. Once the CO_2 is removed, it is typically compressed and placed into storage. The carbon dioxide can be stored in abandoned gas and oil wells or used for enhanced oil recovery (EOR) when the market price of oil is favorable.

1.3 CO_2 Capture Processes

1.3.1 Oxy-fuel Combustion

In oxy-fuel combustion, pure oxygen is used in the combustion process instead of air. First, an air separation unit (ASU) separates oxygen from air. This is typically done with a cryogenic process. Membranes and adsorption processes can also be potentially used to separate out the oxygen. The fuel is combusted with pure oxygen to produce CO_2 and H_2O. A portion of the flue gas is recycled to control the flame temperature because of current material limitations. Pure CO_2 can be recovered once the water has been condensed. Oxy-fuel combustion power plants have been touted as zero emission technology. The production of thermal NO_x is also low because of the absence of nitrogen, but nitrogen in the fuel can still result in the production of NO_x. Pilot studies have shown that existing boilers can be retrofitted for oxy-fuel combustion. However, the development of new gas turbines (combustor and compressor) for oxy-combustion is needed. Existing technology for gas turbines cannot be used.

1.3.2 Pre-Combustion

There are a number of viable CO_2 capture technologies currently being researched for pre-combustion. One such technology that has been touted as "capture ready" is integrated gasification combined cycle (IGCC). In a typical IGCC system, synthesis gas is first produced from a gasification unit and possible feeds include coal, biomass, natural gas, and heavy petroleum residues. After the gasification process, the water gas shift reaction can be used to convert CO to CO_2 and H_2. The CO_2 can be separated at high partial pressure (15–40% at 15–40 bar) and the hydrogen is used as fuel for the gas turbine to generate electricity. A heat recovery steam generator (HRSG) produces superheated steam from the gas turbine exhaust heat at various pressures, which is used drive the steam turbines. Hence, the two power cycles are used to produce electricity. The efficiency of an IGCC plant is lower than a conventional pulverized coal-fired and has a much higher capital cost. In addition, several demonstration IGCC plants built in the U.S. have been plagued with numerous problems and resulted in unreliable operation. Physical absorption is the leading technology used for CO_2 removal. Chemical absorption can be used when the partial pressure is low, but the fuel gas must be cooled down to 40 °C.

1.3.3 Post-Combustion

While the pre-combustion technologies are typically more efficient, the large number of existing power plants, some of which may have 20 to 30 more years of life, will require the development of post-combustion technologies. In post combustion processes, the removal of CO_2 occurs at the tail end, where the flue gas is typically at low pressure (~1 bar) and the partial pressure of CO_2 varies between 3 to 20%. The CO_2 capture processes can be retrofitted to existing natural gas combined cycle (NGCC) and pulverized coal (PC) plants. Chemical

absorption is the leading technology for post combustion capture. This technology has been established for over 60 years. Other alternative technologies include adsorption, cryogenics, and membranes.

1.4 CO_2 Separation Technologies

A number of post-combustion technologies are available for CO_2 removal. These include chemical and physical absorption, membranes, adsorption, and cryogenic processes. A number of these processes are well established and commercially used. Other technologies require further development or a technological breakthrough in order to become competitive with existing technologies.

1.4.1.1 Adsorption

In this separation process, carbon dioxide is selectively removed from the flue gas via solid adsorbents that have a high surface area and desorbed through a regeneration process. Some solid adsorbents include natural or synthetic zeolites, activated carbon, alumina, molecular sieves, and polymers. The adsorption process is typically cycled between two beds of adsorbents. While one bed is adsorbing CO_2, the other bed is being regenerated. In the regeneration process, CO_2 can be desorbed by either pressure swing adsorption (PSA), temperature swing adsorption (TSA), or electrical swing adsorption (ESA), where a low voltage electric current is passed through the adsorbents. However, the technology suffers drawbacks from low capacity and selectivity for current adsorbents and is not ready for large scale CO_2 removal (CO2Net, 2006). In addition, the compression energy required for PSA is cost prohibitive.

1.4.1.2 Cryogenics

In cryogenic technology, the carbon dioxide is separated from other components by compression, cooling, condensation, and distillation to produce

liquid CO_2. However, as with any cooling process, there is a large energy penalty and the process would not be efficient for dilute streams of carbon dioxide. In addition, prior to the cooling process, water would need to be removed. Cryogenic technology would be most applicable for oxy-fuel and pre-combustion processes, where the partial pressure of carbon dioxide is high.

1.4.1.3 Membranes

Selective membrane gas separation is based on the diffusion rate of individual components through a thin membrane barrier. Membranes are commercially used to remove carbon dioxide from natural gas streams, which are at high pressure and have a high partial pressure of CO_2. Additional advantages include no moving parts, modularity, small footprint, and no regeneration energy. However, there is still a need to improve membrane selectivity, permeability and durability at high temperatures for CO_2 capture (CO2Net, 2006). Membrane technology is most suitable for bulk removal, but higher purities can be achieved when multiple stages and recycle streams are used. More recently, some researchers have focused on developing hybrid membrane technology, where membranes are combined with another separation process such as chemical absorption (Ducroux and Jean-Bapiste, 2004).

1.4.1.4 Physical Absorption

Physical absorption processes require relatively concentrated streams of CO_2 at high pressures, but have low energy requirements. They are commercially used to remove CO_2 and H_2S from natural gas (acid gas treating) and for removing CO_2 from synthesis gas in ammonia, hydrogen, and methanol production. Some commercially available solvents include dimethyl ether and polyethylene glycol (Selexol) and cold methanol (Rectisol). In physical absorption, the untreated gas is contacted with the solvent in an absorber column

and CO_2 is absorbed by the solvent. The CO_2 rich liquid stream exits the bottom of the absorber and then passes through a series of flash drums at varying pressures. The depressurization releases the carbon dioxide from the solvent. The lean solvent is then recycled back to the absorber column. Physical absorption processes typically operate near 40 °C and therefore the flue gas must be cooled accordingly. Physical absorption processes are the preferred method of CO_2 removal for pre-combustion processes.

1.4.1.5 Chemical Absorption

The technology for chemical absorption has existed for more than 60 years and was developed primarily for acid gas treating (Kohl and Neilsen, 1997). In this process, carbon dioxide chemically reacts with the solvent. The equipment for a typical chemical absorption process consists of an absorber column, a stripper column, and a cross-exchanger (Figure 1-2). Untreated gas enters the bottom of the absorber and lean solvent is fed to the top of the column. The lean solvent counter-currently contacts the flue gas and removes the CO_2. The CO_2 rich solvent leaves the bottom of the absorber and passes through the cross-exchanger where it preheated by the stream leaving the stripper. A temperature approach of 10 °C relative to the reboiler temperature is usually achieved in commercial practice. The pre-heated stream is fed into the top of the stripper column where the CO_2 is stripped out by the steam from the reboiler. The lean solvent exits the bottom of the stripper and is used to preheat the stripper feed stream. The lean stream is usually cooled before being returned to the absorber, where the process is repeated.

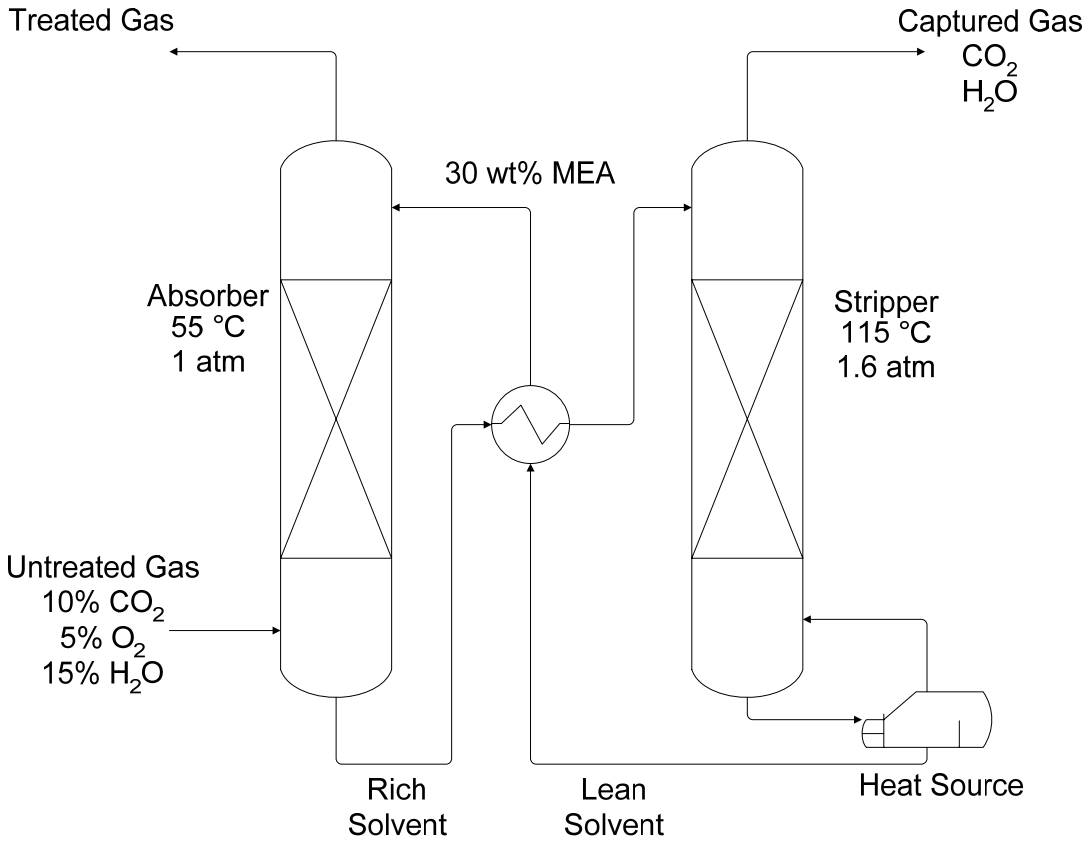

Figure 1-2. Schematic of Absorption and Stripping Process for CO_2 Removal

1.5 COST OF CO_2 CAPTURE

Economic studies on CO_2 capture for power plants have shown that while technically feasible, the high cost may make it impractical to implement in its current technological state. For a pulverized coal (PC) power plant based on current technology, the capture, transport and storage (CCS) of CO_2 would increase the cost of electricity (CoE) by 43–91% and for a natural gas combine cycle (NGCC) power plant the cost would increase by 37–85% (IPCC, 2005). For an IGCC power plant, the cost of electricity would increase by 21–78%. The bulk of the cost is from the CO_2 capture process and compression. For a PC plant, the cost of mitigation was \$30–71/tCO_2 avoided. Transportation and storage costs were estimated to be \$0–5/tCO_2 and \$0.6–8.3/tCO_2, respectively. Approximately

80% of the costs are attributed to capture and compression. Another study suggests that 70–80% of the operating cost is due to solvent regeneration and 50–80% of the capital cost is determined by the solvent circulation rate, which sets the absorber and stripper column size, pumps, and piping (Saxena and Flintoff, 2006). The IPCC study suggests that improvements to the current commercial technologies can reduce capture costs by 20–30% in the next decade.

1.6 RESEARCH AREAS

Improvements to the current chemical absorption technology will mostly likely occur with the development of better solvents and contactors. Some of the desirable solvent properties include: fast CO_2 absorption rate, high capacity for CO_2, low energy requirements for regeneration, low corrosivity, low degradation rates, low volatility, low solvent costs. Solvents with a fast reaction rate will result in a smaller absorber, less packing, and reduced pressure drop. As an alternative, the absorber could be operated closer to equilibrium, which would result in a more efficient stripper and lower regeneration costs. The working solvent capacity is defined as the amount of CO_2 that can be absorbed over a range of CO_2 partial pressures and is directly related to the vapor–liquid equilibrium characteristics of the solvent. Solvents with a high capacity typically result in a lower circulation rate and a lower energy requirement for regeneration. Solvents with low corrosivity can be used with equipment made of carbon steel, instead of stainless steel or other exotic alloys, which will dramatically reduce capital costs. In addition, low volatility and solvent stability will result in less solvent makeup and reduce the need for solvent reclaiming and reduce operating costs. Finally, there will a tradeoff between the cost of the solvent itself and the cost benefits derived from its use.

The selection of an efficient contactor has become more important as the difference in costs for random and structured packing has gradually been reduced. Random packing has been extensively used in the current gas treating industry. However, the newer generations of structured packing offer more surface area, lower pressure drop, lower liquid holdup and better mass transfer performance. More surface area will reduce the size of the absorber and stripper columns and lower pressure drop will eliminate the need for booster fans. In addition, one often overlooked piece of equipment is the distributor. For structured packing, proper liquid distribution is imperative.

1.7 PREVIOUS WORK

1.7.1 Solvents for Chemical Absorption

Over the years, there has been a lot of research that has focused on finding the ultimate solvent for chemical absorption. These solvents include the various classes of amines (primary, secondary, tertiary, and hindered). Some of these amines include monoethanolamine (MEA), diethanolamine (DEA), methyldiethanolamine (MDEA), and isobutanolamine (AMP). Promoted hot potassium carbonate (K_2CO_3) solvents have also been used in the acid gas treating industry (Littel *et al.*, 1990, Littel *et al.*, 1992a, b, Sartori and Savage, 1983, Say *et al.*, 1984).

Amines are generally considered to have fast reaction rates with CO_2, but have high heats of absorption. Potassium carbonate systems, on the other hand, have slower rates and a lower heat of absorption. The heat of absorption has been generally thought to be important in determining the steam requirement for the regeneration of the solvent, where high heats of absorption results in higher heat duties. However, this has been proven to be not necessarily the case in recent research published by Oyenekan (2007).

The current state of the art solvent is 15–30 wt% aqueous MEA with the addition of a corrosion inhibitor. Corrosion limits the use of MEA at higher concentrations until better corrosion inhibitors can be found. Acid gas treating technology was adapted for CO_2 capture from flue gas and MEA was one of the few solvents that could be used successfully at low partial pressures of CO_2. MEA has a fast absorption rate and a high capacity for CO_2. On the other hand, it has a high heat of absorption, is corrosive, and is prone to thermal and oxidative degradation. One approach to improving solvent performance is to blend the amine with potassium carbonate or with another amines (Bishnoi and Rochelle, 2002, Bosch *et al.*, 1989, Cullinane, 2002, Furukawa and Bartoo, 1997, Tseng *et al.*, 1988, 1998, Xiao *et al.*, 2000).

1.7.2 Aqueous Piperazine Promoted Potassium Carbonate

Cullinane (2005) developed a new solvent containing a blend of piperazine (PZ) and aqueous potassium carbonate. Piperazine is a diamine, which means it can absorb two moles of CO_2 per mole of amine and potentially results in a higher capacity for CO_2. It also has a fast CO_2 absorption rate that is comparable or even faster than MEA. When piperazine is blended with K_2CO_3, the amount of amine protonation is reduced by the buffering capacity of the potassium bicarbonate/carbonate, which leaves more amine free to react with CO_2.

In the Cullinane work, the vapor–liquid equilibrium of CO_2 over 0.0 to 6.2 molal (m) K^+ and 0.0 to 3.6 molal PZ was measured in a wetted wall column at 40 to 110 °C (Cullinane, 2005). In addition, equilibrium speciation of PZ in 2.5 to 6.2 m K^+ and 0.6 to 3.6 m PZ was measured using proton nuclear magnetic resonance (NMR). Using the same wetted wall column, Cullinane also measured the rate of CO_2 absorption in 0.0 to 6.2 m K^+ and 0.0 to 3.6 m PZ from 25 to 110 °C.

In addition, a thermodynamic model was developed using the electrolyte non-random two liquid (ENRTL) model and rate constants were regressed using a termolecular reaction mechanism.

Based on his bench-scale work, Cullinane found that a solution of 5 m K^+/2.5 m PZ has an absorption rate of CO_2 that is 1–1.5 times faster than 30 wt% MEA. Also, the heat of absorption is also approximately 10–25% less than MEA. The capacity of this solution is comparable or slightly less than that of 30 wt% MEA.

1.7.3 CO_2 Capture Pilot Plants

While there have been numerous bench-scale studies measuring the kinetics and VLE data of the various solvents, pilot plants are needed to complete the transition to a commercially operating system. Computer models can be used to simulate plant performance, but only a pilot plant study can truly demonstrate how a particular solvent or column internal will perform in an industrial operating environment and provide practical operating experience. Pilot plants also provide an opportunity to validate data obtained by bench-scale experiments. Pilot plants are expensive to build, maintain, and operate; as such, there only a handful of organizations that have pilot plants.

The International Test Centre (ITC) for CO_2 Capture has two pilot plant facilities (Wilson *et al.*, 2004a, Wilson *et al.*, 2004b). The Boundary Dam (BD) unit captures CO_2 from a coal-fired power plant and has a capture capacity of 4 tons of CO_2 per day. The diameters of the absorber and stripper columns are 45.7 and 40.6 cm, respectively. The other pilot unit is located at the University of Regina (UR) and removes CO_2 from the flue gas of natural gas fired boiler. The pilot unit has a removal capacity of 1 ton/day and the diameter of the absorption and desorption columns are both 30.5 cm. Experiments have been conducted on the

BD unit using 5 kmol/m^3 (30 wt%) MEA and a 4:1 MEA/MDEA blended solvent (Idem *et al.*, 2006). Experiments on the UR unit have been conducted with 5, 7, and 9 kmol/m^3 MEA and 4:1 MEA/MDEA solvent. Based on the pilot plant experiments, it was found that a reduction in heat duty could be achieved with the MEA/MDEA system.

The Korean Electric Power Research Institute (KEPRI) has a pilot plant unit that processes flue gas fired by natural gas (Hee-Moon *et al.*, 2004). The unit has a capacity of 2 ton/day and was operated with 10, 15, 25 wt% MEA using a license from ABB/Kerr McGee. The diameter of the absorber is 0.46 m and has a height of 18.8 m. The diameter of the stripper is 0.34 m and the height is 16.7 m. The plant was operated to attain 90% CO_2 removal and it was found that the CO_2 recovery rate is the same at 15 and 25 wt% MEA for high MEA liquid flow rates. It is possible that at the high MEA concentration (25 wt%), the absorber may have been pinched because the lean loading conditions were not optimized.

As part of the European Capture and Storage project (CASTOR), Europe's first CO_2 capture pilot plant was recently constructed at a coal-fired power plant in Esbjerg, Denmark (Knudsen *et al.*, 2006). The pilot plant has the capacity to process 24 tons of CO_2 per day. The absorber has an inner diameter of 1.1 m and was packed with IMTP #50 random packing, divided into 4 beds of 4.3 m. At the top of the absorber, the water wash section consisted of 3.0 m of 252Y Mellapak structured packing. The stripper has an inner diameter of 1.1 m and was packed with 10 meters of IMTP #50 random packing, divided into 2 beds. There was 3.0m water wash section containing IMTP #50 above the top bed. The first test was conducted from January to February 2006 using 25.4 wt% MEA. However, due to some of the problems encountered in the first test, Test 1 was to be repeated in August 2006, still using MEA. Additional tests will be conducted using two proprietary solvents, CASTOR-1 and CASTOR-2, for 5000 hrs.

The Kansai–Mitsubishi proprietary carbon dioxide recovery process (KM-CDR) was jointly developed by Kansai Electric Power Company and Mitsubishi Heavy Industries. The process used KS-1, a proprietary solvent that contains a hindered amine, which is resistant to O_2 degradation. KEPCO/MHI has also developed KP-1, a low pressure drop packing. KEPCO/MHI has several pilot/demo plants and a few commercial plants that utilize KM-CDR technology (Iijama *et al.*, 2004, Ohishi *et al.*, 2006, Yagi *et al.*, 2005). A summary of these plants are shown in Table 1-1.

Table 1-1. KEPCO/MHI CO_2 Capture Plants

Plant Name	Year in Operation	Capacity (ton/day)	Fuel
Nanko (Pilot)	1991	2	Nat Gas
MHI R&D (Pilot)	2004	1	Coal
Matsushima (Demo)	2006	10	Coal
Malaysia (Comm)	1999	210	Nat Gas
Malaysia (Comm)	2005	330	Nat Gas
India	2006	2 x 450	Nat Gas

A summary of the various CO_2 capture pilot plants is presented in Table 1-2. The steam requirements from the various pilot plant studies for MEA vary quite widely. Based on the literature review of the pilot plants, it appears that a number of pilot plant MEA baseline cases have been established. The studies also show that KS-1 and MEA with an inhibitor have similar heat requirements. In addition, structured packing is becoming a viable option because the cost of structured packing has dramatically decreased in the last 5 years. A pilot plant study is important because it confirms bench-scale experimental data and provides operational experience which cannot be simulated or obtained elsewhere.

Table 1-2. Pilot Plant Comparison

Pilot Plant	Capacity (ton/day)	Solvent	Steam (kcal/mol)
CASTOR	24	MEA	42
ITC – UR	1	MEA	39–75
ITC – BD	4	MEA	26–42
KEPCO/MHI	2	KS-1	27
KEPRI	2	MEA	–

1.8 RESEARCH OBJECTIVES AND SCOPE OF WORK

The motivation behind this work is to extrapolate the bench-scale work developed for aqueous piperazine promoted potassium carbonate into an industrial operating environment. This work aims to verify the results of the bench-scale work through a pilot plant study. The results from this study will focus on the absorber. An absorber model will be developed and validated with the pilot plant data and also be used to reconcile the pilot plant and bench scale results. Ultimately, the model can be used as a design and optimization tool for scale-up and also be used to dictate further bench-scale work to fill in gaps the needed for the model. A schematic of the process is illustrated in Figure 1-3.

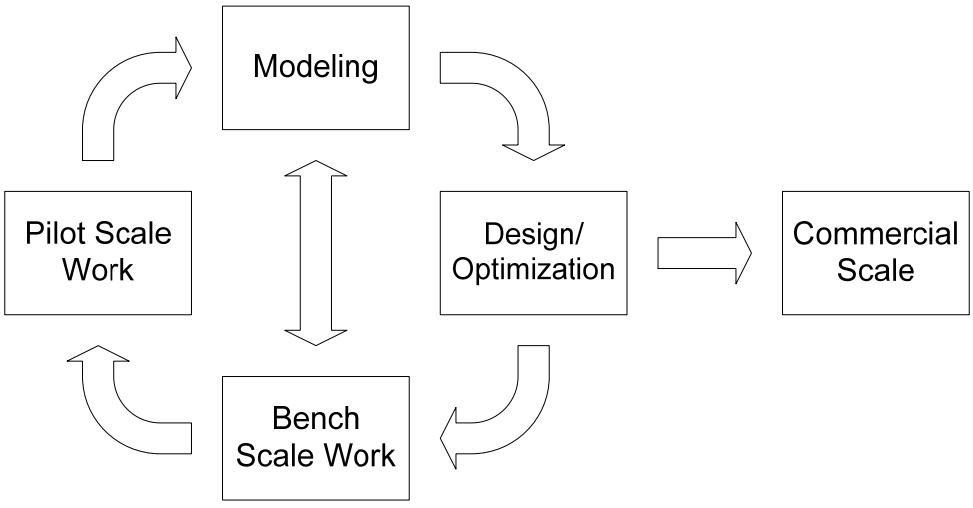

Figure 1-3. Schematic of Process Design Framework

The research objectives of this work are to:

1. Construct and demonstrate reliable operation of a pilot scale absorber/stripper system for CO_2 capture
2. Obtain good and consistent pilot plant data for the absorption of CO_2 into aqueous piperazine and potassium carbonate and verify bench-scale results with the pilot scale results through the extrapolation of raw data
3. Develop a rigorous rate-based absorber model in a commercially available simulation package
4. Validate the absorber model and reconcile the results from the pilot plant experiments

The first objective was accomplished through the extensive modification of the pilot plant facility operated by the Separation Research Program (SRP) at the University of Texas at Austin. The pilot distillation and extraction system was converted into an absorber/stripper system. The pilot plant has a removal capacity of 4 tons/day and unlike the other pilot facilities it is a closed loop system. A total of four campaigns were conducted with the pilot plant using both random and structured packing. Tests were performed with 30 wt% MEA to establish a baseline and with two piperazine and potassium carbonate solvent compositions, 5 m K^+/2.5 m PZ and 6.4 m K^+/1.6 m PZ.

The second objective was fulfilled through the material balances for the gas, liquid, and CO_2 recycle streams in the absorber and stripper. Engineering judgment and practical considerations were used to interpret and make corrections to the raw data. Mass transfer performance in the absorber was compared to the wetted wall column kg'. The temperature profile was quantified and used to help with the interpretation of the results. Effective

interfacial area measurements and performance evaluation of the Flexipac 1Y and Flexipac AQ Style 20 structured packing were also carried out.

The third objective was completed through the development of a rigorous rate-based model using Aspen Plus® RateSep™. The model uses the Aspen Plus® thermodynamic package developed by Hilliard (2005) and uses the rate constants obtained by Cullinane (2005) from the bench-scale wetted wall column. In addition, parameters for density and viscosity were regressed with Aspen Plus® Data Regression System (DRS) using bench-scale data and inputted into the absorber model.

Finally, the fourth objective was satisfied by simultaneously validating the absorber model and reconciling the pilot plant data using the Aspen Plus® Data-Fit regression package. The model parameters regressed by Data-Fit were the interfacial area factor and column heat loss. Reconciliation of the pilot plant data was made by Data-Fit through adjustments of the inlet and outlet CO_2 gas concentration, lean loading, inlet and outlet stream temperatures, and the temperature profile.

Chapter 2: Pilot Plant Experimental Setup, Methods, and Results

The experiments for this work were conducted at the pilot plant facility operated by the Separations Research Program (SRP) of The University of Texas at Austin (UT). The facility is located at the J.J. Pickle Research Center, 20 minutes north of the main UT campus. SRP typically uses the facility to conduct distillation and extraction experiments for industrial companies and also aids UT graduate students with pilot-scale work.

As part of this work, the existing pilot plant facility was extensively modified and converted into an absorber/stripper system prior to the startup of the first CO_2 capture campaign. The modification added new analytical equipment, process instrumentation, stainless steel process equipment and piping. A total of four pilot plant campaigns were conducted: three pilot plant campaigns that used aqueous piperazine promoted potassium carbonate and one campaign with monoethanolamine (MEA) to establish a base case for comparison. The four campaigns were completed over a period of four years. When the pilot plant was not being used for this work, it was reconfigured to the original setup and used to run distillation and extraction experiments.

This work focuses on the three potassium carbonate and piperazine campaigns. The results of the MEA campaign can be found in Dugas (2006). Incremental improvements and modifications to the pilot absorber/stripper system were made over the course of the four campaigns. This chapter details the pilot plant equipment and setup, the modifications that were made for each

campaign, sampling and analytical methods developed by this work, and the results from each of the K^+/PZ campaigns. An overview of the four campaigns is given in Table 2-1.

Table 2-1. Summary of the Four Pilot Plant Campaigns

Campaign	Solvent	Absorber Packing	Stripper Packing
1	5 m K^+/2.5 m PZ	Flexipac 1Y	Sieve Trays
2	5 m K^+/2.5 m PZ	Flexipac 1Y	IMTP #40
3	7 m MEA	Flexipac 1Y	IMTP #40
	7 m MEA	IMTP #40	Flexipac 1Y
4	5 m K^+/2.5 m PZ	Flexipac AQ Style 20	Flexipac AQ Style 20
	6.4 m K^+/1.6 m PZ	Flexipac AQ Style 20	Flexipac AQ Style 20

2.1 EXECUTIVE SUMMARY OF PILOT PLANT CAMPAIGNS

This section presents a summary of the major issues that were resolved, through trial and error over the course the four pilot plant campaigns. Preheating the stripper feed solvent was most efficiently done with a plate and frame heat exchanger in terms of performance and relative cost. The cross exchanger is a critical part of the absorption and stripping system. Preheating and saturating the absorber inlet gas was performed most effectively with a steam injector.

The in-situ CO_2 analyzers needed to be protected from non-condensing water and the extractive sampling system performed best when the sample lines were heated to prevent the condensation of water. Liquid sampling was best done using sample bombs to minimize the flashing of CO_2, especially at rich loadings and high temperatures. Allowing the hot sample bombs to be cooled prior to sample extraction is also recommended. The liquid analytical techniques need to be fully developed prior to the start of pilot plant experiments, and sample quality assurance and control are extremely important.

Due to the inherent variability of a pilot plant, all the possible unknowns must be eliminated for proper interpretation of critical data. The calibration of process equipment to validate the measured flow rates is critical and introduces additional unknowns if this is not done. Gas flow measurements are difficult and expensive, but are critical if any data is to be extracted. Measurement of water concentration in the gas may be critical in data interpretation because the transfer of enthalpy between the liquid and vapor is dependent on the water content of the inlet gas and the temperature of the inlet liquid.

In the pilot plant, the inlet liquid temperature may not have been adequately measured because the nearest temperature measurement was 15 meters away from the absorber inlet. Heat loss from the 5.1 cm pipe may have resulted in slightly lower temperatures than that measured. The titration and ion chromatography methods developed for measuring piperazine and potassium concentration needed to be reconciled. The difference in CO_2 loading between the on-campus inorganic carbon analyzer and that of the Shimadzu Total Organic Carbon analyzer should also be reconciled, possibly using a standard made up of both sodium bicarbonate and carbonate, as well as standards that contain only one of each. Also, the inlet CO_2 gas concentration appeared to cycle with the opening and closing of the stripper valve. A new process control technique should be developed to address this issue.

An efficient analysis of the CO_2 loading in the liquid is needed to allow a rapid material and heat balance during actual operation. The maintenance of water balance, temperature, and CO_2 loading is extremely important for the piperazine and potassium carbonate system in order to avoid solubility issues, which can result in instrument and equipment failure and possible plant shutdown.

It is recommended that antifoam be continuously added through a metering or peristaltic pump. Antifoam is typically designed for a once through process. In the pilot plant, the liquid solvent is continuously recycled and, over time, the antifoam loses its efficacy. Foaming was observed in all of the K^+/PZ campaigns. In the first two campaigns, foaming was observed in the absorber and in Campaign 4, foaming was observed in the stripper. It was found that the DOW Corning Q2-3183A antifoam worked well for the piperazine and potassium carbonate system.

2.2 TIMELINE OF PILOT PLANT CAMPAIGNS

Quarter	Action
2002 Q4	▪ Start of project
2003 Q1	▪ Order solvent cooler
2003 Q2	▪ Piping demolition ▪ Piping iso drawn ▪ Created welding bid ▪ Solvent cooler procured ▪ Ordered air cooler, 5 Micro Motion® flowmeters, Vaisala CO_2 analyzers, raw materials
2003 Q3	▪ Test plan ▪ Begin welding ▪ Air cooler procured ▪ Analytical method development, ▪ Purchased for RTD for absorber ▪ Installation of solvent heater, solvent cooler, control valves, Micro Motion® flowmeters, and filters on support racks
2003 Q4	▪ Pipe welding
2004 Q1	▪ Welding completed ▪ Installation of instrumentation 90% complete ▪ Excel absorber model completed ▪ Gas line
2004 Q2	▪ Campaign 1 commenced in May ▪ Measured effective interfacial area for Flexipac 1Y ▪ Load chemicals ▪ Begin operation mid-June for 7 days

2004 Q3	▪ Campaign 1 data analysis ▪ Campaign 2 modifications ▪ Test plan
2004 Q4	▪ Build sample bombs ▪ Construct bypass around blower to heat up gas ▪ Campaign 2 (mid-October to mid-November) ▪ Campaign 2 loading and data analysis
2005 Q1	▪ Loading analysis resolution ▪ MEA modifications ▪ Built new CO_2 makeup heater and 0–5%Horiba sampling unit ▪ Ordered new stainless steel reboiler ▪ Campaign 3 (MEA, mid-March to mid-April)
2005 Q2	▪ Replaced PVC airline with stainless steel ▪ Designed new air heater and cross-exchanger ▪ New reboiler procured ▪ Data analysis
2005 Q3	▪ Design carbon filter ▪ Procure parts for FTIR ▪ Installation of reboiler ▪ Test plan ▪ Solubility experiments
2005 Q4	▪ Bench-scale density and pH measurements ▪ IC method development ▪ Installation of cross-exchanger, carbon filter, heated lines, FTIR
2006 Q1	▪ Campaign 4 (January to February)

2.3 CAMPAIGN ONE – PILOT PLANT SETUP AND TROUBLESHOOTING

The main objectives of the first campaign were the design, modification, startup, and troubleshooting of the pilot absorber/stripper system. The existing distillation and extraction pilot plant was converted into an absorber and stripper system. The modifications were made such that the pilot plant easily could be converted between the two modes of operation. The second objective was to obtain characterization data for the absorber and stripper with Flexipac 1Y structured packing and sieve trays, respectively.

2.3.1 Existing Major Equipment

The pilot plant facility was constructed in 1986 and originally designed for distillation and extraction experiments. The pilot plant consists of two columns, each with an internal diameter of 0.43 m and constructed from 18-inch schedule 40 carbon steel pipe. Both columns have a number of penetration points, manways, and sight glass windows along the entire length of the vessel. The height of each column is approximately 13.3 meters. The distillation column is insulated with calcium silicate, but the extraction column is not insulated. In the CO_2 absorption campaigns, the distillation column was used as the stripper and the extraction column was used as the absorber. The absorption column is packed with 6.1 m of packing, which is divided into two beds (3.05 m). In between each packed bed, there is a spool piece that swings out to facilitate packing change-outs. Also, within each spool piece, there is a chimney tray and a redistributor just below. There is no water wash section above the top of the absorber packing, as in conventional plants. When trays are used, it is installed as one continuous section from the top of the column to the bottom. A picture of the pilot plant facility is shown in Figure 2-1 and a schematic of the absorber and stripper is given by Figure 2-2. A process and instrumentation diagram of the absorber and stripper are shown in Figure 2-3 and Figure 2-4, respectively.

The majority of the existing equipment was retained, which included a blower, six centrifugal pumps, several feed tanks, a reboiler, condenser, and vacuum pump (Table 2-2). The blower (C-103) is normally operated as a standalone unit and used to provide ambient air to the air-water column. During the operation of the CO_2 capture campaigns, the blower was used to recycle the gas from the top of the absorber back to the inlet. The silencer of the blower was removed and new piping was installed to connect the blower inlet to the outlet of the water knockout. The blower is also equipped with a variable speed drive.

In the first campaign, only four of the centrifugal pumps were used. The pumps have capacities that range from 3.4 to 22.7 m^3/hr (15 to 100 gpm). The impellers of the pumps are made of carbon steel. During the course of the campaigns, it was discovered that the pump seals needed to be made out of Ethylene–Propylene–Diene Monomer (EPDM) rubber. Other types of rubber seals eventually resulted in leaks. There are two pumps associated with the absorber, one that pumps lean solvent from the absorber feed tank to the top of the absorber (P-106) and one that pumps rich solvent from the bottom of the absorber to the stripper (P-104). There are two pumps associated with the stripper. One pump is used to pump liquid solvent from the bottom stripper reboiler to the solvent cooler (P-102). The other pump is used to pump the reflux from the overhead liquid condenser back to the stripper feed (P-103). Most of the pumps have variable speed drives, which eliminates the need for control valves and dramatically improves flow control.

In the existing facility, there are two identical liquid feed-tanks, one for each of the columns. For the CO_2 capture campaigns, only the absorber feed-tank was used (V-105). The feed tank is constructed out of carbon steel and has a volume of 3.6 m^3. The top of the feed-tank vented to the atmosphere to prevent a vapor lock. In addition, a portion of the solvent in the absorber feed-tank is continuously re-circulated. The overhead gas accumulator stores CO_2 gas from the condenser (V-103). It has a volume of 2.4 m^3 and is made of carbon steel. A control valve is installed downstream of the gas accumulator to regulate the pressure in the stripper column. There is also a vent on the gas accumulator which is regulated by a control valve. Water from the condenser is stored in the overhead liquid accumulator (V-106) before it is pumped back to the stripper feed as reflux. The overhead liquid accumulator has a volume of 0.2 m^3 and is made of carbon steel.

The carbon steel reboiler (H-102) on the stripper is a kettle-type boiler and has a surface area of 18.6 m^2. Liquid is circulated from the bottom of the stripper to the bottom of the reboiler. Liquid is pumped from the bottom of the reboiler, on the opposite end of the feed nozzle. Vapor generated by the reboiler is fed through a nozzle on the side of the stripper, just above the liquid level in the sump. The reboiler and associated piping are all insulated. Low pressure steam from the university gas-fired steam boiler at 930 kPa (135 psia) is used to heat the reboiler. The reboiler is located adjacent to the stripper and the reboiler level varies from 14 to 37 cm (5.4 – 15 in).

Figure 2-1. Pilot Plant Facility at UT SRP with the Stripper Column and Reboiler on the Left Side, Absorber Column on the Right Side, Absorber Feed Tank and Overhead Gas Accumulator on the First Platform (Picture Taken by C. Lewis)

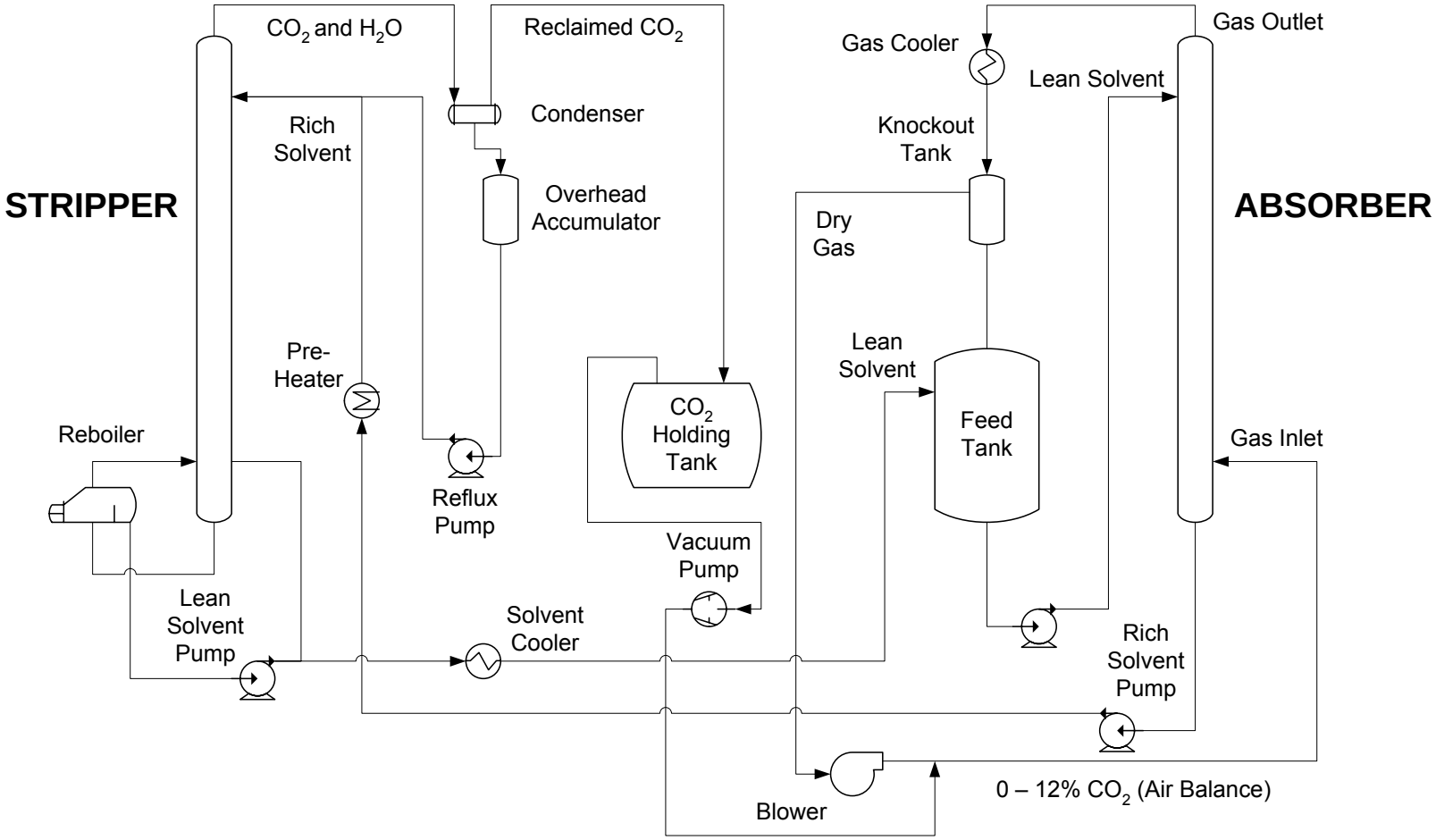

Figure 2-2. Process Flowsheet of Absorber/Stripper Pilot Plant for Campaign 1

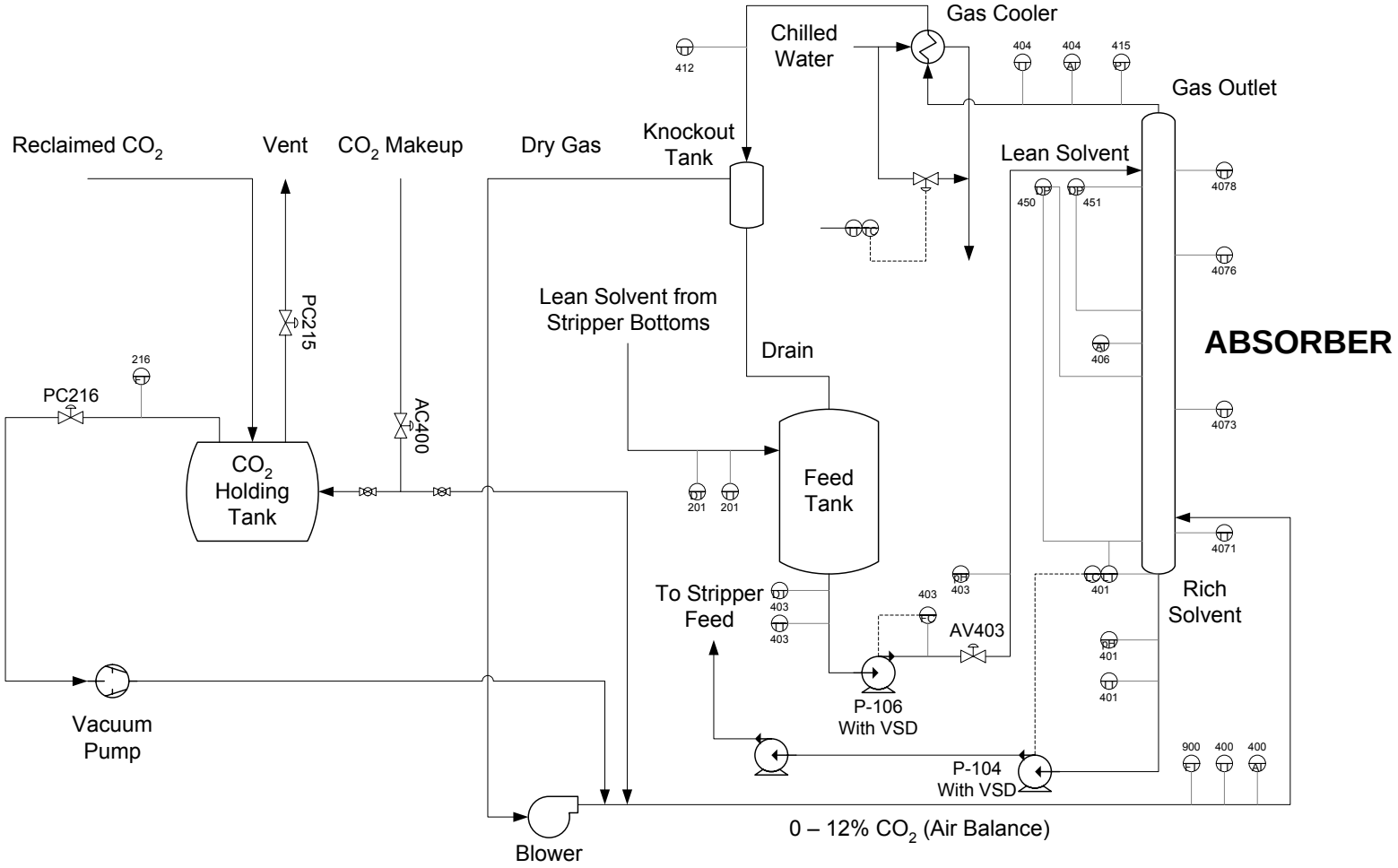

Figure 2-3. Process and Instrumentation Diagram of the Absorber for Campaign 1

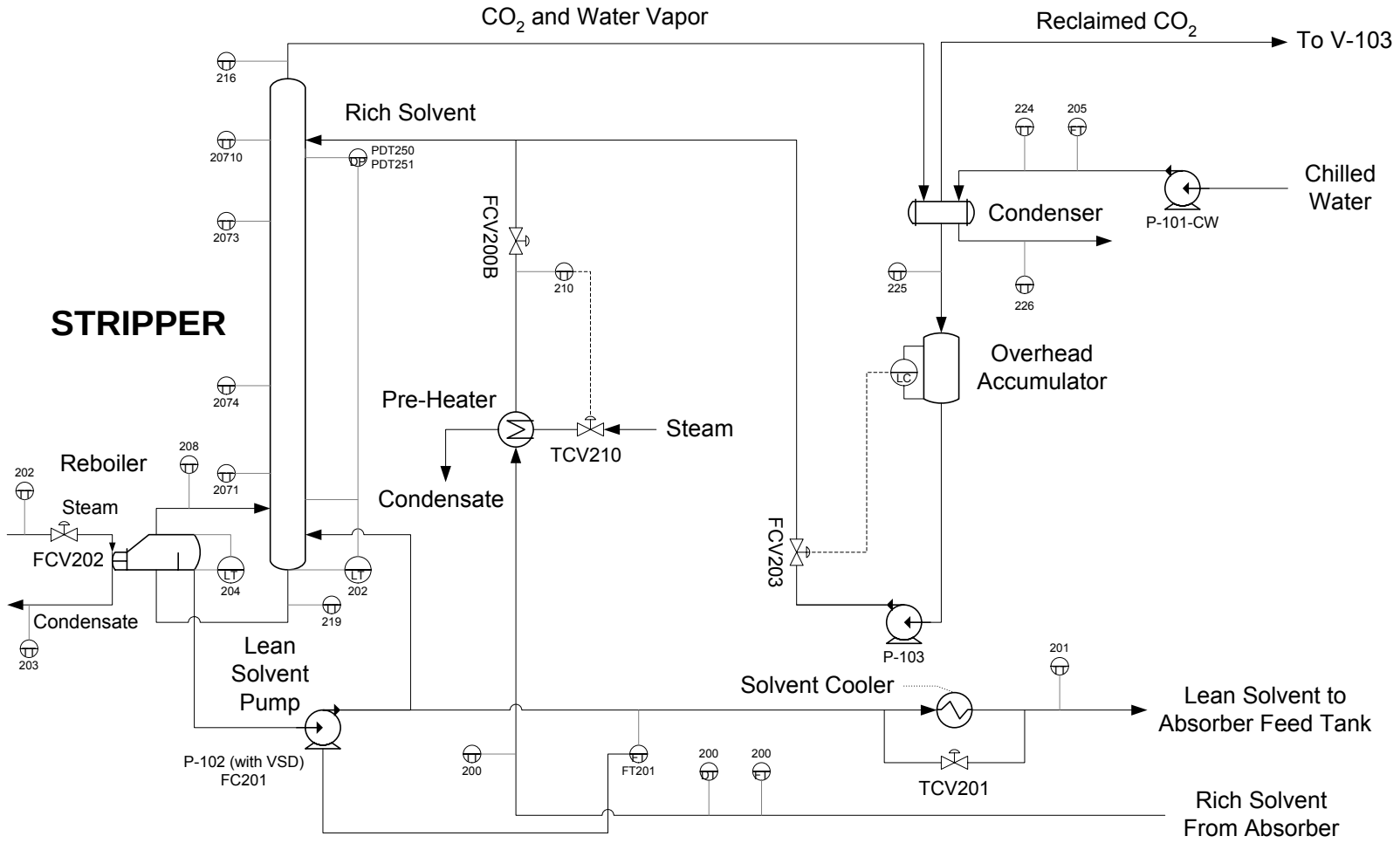

Figure 2-4. Process and Instrumentation Diagram of the Stripper for Campaign 1

Table 2-2. Pilot Plant Equipment Specifications

Equipment	Function	Status	Equipment Specification				MOC	T_{DSGN} (°C)	P_{DSGN} (kPag)	Phase
Vessels			Vol (m^3)	ID (cm)	No. Bed	Bed Ht (m)				
V-102	Stripper	Existing	-	42.7	2	3.05	CS	200	520	G/L
V-104	Absorber	Existing	-	42.7	2	3.05	CS	180	520	G/L
V-103	OVHD Horiz. Acc.	Existing	2.4	-	-	-	CS	200	520	G
V-105	Absorber Feed Tank	Existing	3.6	-	-	-	CS	230	520	L
V-106	OVHD Liq. Acc.	Existing	0.2	-	-	-	CS	150	520	L

Heat Exchangers			Type	Duty (MJ/hr)	Area (m^2)	Passes	Shell	Tube	Shell	Tube	Shell	Tube	Shell	Tube
H-101A	Feed Heater	New	Hairpin	840	9.9	1-1	CS	316	340	200	3450	3450	STM	L
H-101B	Feed Heater	New	Hairpin	840	9.9	1-1	CS	316	340	200	3450	3450	STM	L
H-107	Solvent Cooler	New	Fixed	1800	13.4	1-2	316	316	230	230	1550	1030	L	CW
H-111	Condenser Preheater	Existing	Fixed	230	1.5	1-4	316	316	230	230	1550	1030	STM	L
H-112	Air Cooler	New	Fixed	490	19.8	-	316	316	-	-	-	-	G	CW

Condensers/Reboilers			Type	Duty (MJ/hr)	Area (m^2)	Passes	Shell	Tube	Shell	Tube	Shell	Tube	Shell	Tube
H-102	Reboiler	Existing	Fixed	2500	18.6	1-2	CS	CS	200	200	690	1210	G/L	STM
H-104	Condenser	Existing	Fixed	2480	14.3	1-1	CS	CS	150	180	1030	1030	G/L	CW

Pumps			Cap (m^3/hr)	Diff Hd (m)	Eff. (%)	Type	Power (kW)				
P-102-DI	Stripper Bottoms Pump	Existing	6.8	59.4	27	Centrifugal	5.6	CS	180	1310	L
P-103-DI	OVHD Acc Pump	Existing	3.4	61.0	15	Centrifugal	5.6	CS	180	1310	L
P-104-DI	Absorber Pump	Existing	22.7	36.6	59	Centrifugal	5.6	CS	180	1660	L
P-105-DI	Absorber Pump	Existing	3.4	36.6	16	Centrifugal	3.7	CS	180	1660	L
P-106-DI	Absorber Feed Pump	Existing	11.4	41.1	42.5	Centrifugal	3.7	CS	180	1660	L

Blower/Vacuum Pump			Cap (m^3/hr)	DP (kPa)	Power (kW)				
C-102A	Vacuum Pump	Existing	730	100	11.2	CS	-	70	G
C-103	Blower	Existing	2550	20	29.8	CS	650	35	G

Notes:
DSGN = Design
ID = Inner Diameter
MOC = Material of Construction
OVHD = Overhead

The two phase condenser (H-104) for the stripper is located on the top level of the pilot plant structure. The 1–1 single pass condenser has a surface area of 14.3 m^2 and is constructed of carbon steel. In the condenser, water and CO_2 from the overhead vapor of the stripper are separated. Water is condensed as liquid and fed to the overhead liquid accumulator from the bottom of the condenser. The non-condensable CO_2 vapor is sent to the overhead gas accumulator, before being recycled back to the feed gas.

The vacuum pump (C-102A) is used when the stripper is configured for vacuum operation. The vacuum pump is connected to a 2.5 cm (1 in.) nozzle on the CO_2 vapor outlet of the condenser. Due to the size of the nozzle, there is a limitation in the amount of CO_2 that could be stripped, which reduces the range of gas flow rates used for vacuum operation. During the operation of the vacuum pump, the CO_2 vapor comes into intimate contact with the lubricating oil. An oil separator is installed downstream to minimize the amount of entrainment. The vacuum pump is made of carbon steel.

A reflux heater (H-111) is available, but was not used. The condensed water from the overhead liquid accumulator is pumped through the reflux before being mixed with the stripper feed stream.

The cooling water system consists of a feed-tank (T-101-CW), a heat exchanger (H-101-CW), and two pumps (P-101-CW and P-102-CW). The cooling water system is designed so that it is isolated from the university cooling water system. The pilot plant cooling water is cross-exchanged with the cooling water from the university and then stored in the cooling water feed-tank. Cooling water from the feed-tank is then pumped through the pilot plant system, in this case to the condenser of the stripper and/or the air cooler. If there is ever a leak in one of the process exchangers, only the pilot plant cooling water system becomes contaminated.

Figure 2-5. Vacuum Pump (C-102A) Draws Gas from the Right Side and Discharges from the Top of the Oil Reservoir (Picture Taken by C. Lewis)

2.3.2 New Major Equipment

In a typical industrial application, the rich solvent from the absorber is preheated by the lean stream leaving the stripper bottom through a plate and frame cross-exchanger. The exchanger is typically designed to achieve a temperature approach of 5–10 °C with the temperature of the reboiler. Preheating the rich solvent minimizes the reboiler heat duty. Due to the constraints of the pilot plant being a multi–use facility, the solvent preheater and cooler are kept as separate pieces of equipment. As part of this work, the existing solvent cooler and preheater were replaced and a new air cooler was purchased.

The existing solvent preheater was undersized and was replaced with two Brown Fintube heat exchangers (H-101A and H-101B) that were installed in

parallel (Figure 2-6). The hairpin exchangers were donated by Huntsman Chemical from an existing nearby facility. The U-tube heat exchangers each have a surface area of 9.9 m^2, 2.5 cm OD tubes, 7.6 cm shells, and 2.4 cm longitudinal fins. Exchanger drawings obtained from a local distributor showed that the tube side was constructed from stainless steel and the shell side was constructed of carbon steel. Therefore, in all of the CO_2 capture campaigns, the preheater exchangers were operated with the process stream on the tube side and 930 kPa (135 psi) low pressure steam was used on the shell side.

Figure 2-6. Solvent Preheater (H-101A & B), Micro Motion® Flowmeters, and Control Valves Installed on Support Rack (Picture Taken by C. Lewis)

An ITT standard model 08084 SSCFC heat exchanger was purchased and used as the new solvent cooler (H-107). The BEM type heat exchanger is

constructed from type-316 stainless steel and has an area of 144 ft^2 (Figure 2-7). The exchanger has a total of 210 tubes and is designed as a single pass on the shell side and 2 passes on the tube side. In the solvent cooler, the process stream flowed on the shell side and cooling water at 10 °C flowed on the tube side. The lean solvent from the stripper bottoms was cooled to approximately 40 °C before being pumped into the lean solvent feed tank. The solvent cooler and solvent heaters were mounted on custom–built support racks to centralize operational procedures and to minimize the footprint. The welding shop at the PRC campus fabricated the support racks.

Figure 2-7. Solvent Cooler (H-107) Installed on Support Rack. Cooling Water Piping (Green) Flows Tube Side (Picture Taken by C. Lewis)

Water in the gas leaving the top of the absorber column needed to be removed in order to protect the downstream blower and Vaisala CO_2 analyzer. A new air cooler (H-112) was purchased from Super Radiator Coils, model number 27x27-12R-58/156. The air cooler was sized to remove approximately 490 MJ/hr and has an area of 19.8 m^2. The cooler is constructed much like a radiator with a large number of coils consisting of 1.6 cm (5/8 in.) OD 316L stainless steel tubing. The rest of the structure is constructed from type 316 stainless steel. Cooling water at 10 °C was used to cool the process gas. Water condensed from the air cooler was drained back to the absorber feed tank.

Figure 2-8. Air Cooler (H-112) Installed on Top Platform of Structure. Radiator Coils are Located on the Opposite Side (Picture Taken by C. Lewis)

Downstream of the air cooler, a new water knockout was purchased and installed. The water knockout was used to remove entrained water that may have bypassed the air cooler and prevented water droplets from damaging the

impeller of the blower that was located downstream. The water knockout works as a centrifugal type separator. Gas enters the vessel tangentially near the bottom and exits out the top. The condensed liquid drains from the bottom of the knockout and to the lean feed tank.

Rosedale bagged filters were used to remove rust and debris in order to protect the Micro Motion® flowmeters downstream of the filters. The filter housing is made of type 316 stainless steel and the bag filters were made of cotton. Another bagged filter is used to filter the solvent from the reboiler. It was discovered through trial and error, that only the filter bag made of cotton could withstand the high temperature and corrosiveness of the piperazine and potassium carbonate solvent. The solvent eventually dissolved the bag filters made of polypropylene. If the manufacturer uses stitching made of synthetic material on the cotton bag filter, this also results in bag filter failure. Cotton filters with cotton stitching were requested for all of the bagged filters used in the campaigns.

2.3.3 Piping Modification

Due to the corrosive nature of the aqueous piperazine promoted potassium carbonate solvent, all of the carbon steel piping was replaced by type 304L stainless steel pipe. As part of this work, demolition of a portion of the carbon steel piping was performed as well as installation of the new stainless piping. The personnel at SRP performed the layout of the new piping iso and also purchased the new stainless steel pipe, flanges, and gaskets. Schedule 10 304L stainless steel pipe, 150# flanges, and Garlock gaskets were used for construction. The majority of the new stainless steel piping was welded by an outside contractor and took six months to complete.

2.3.4 CO_2 Delivery System

A carbon dioxide delivery system was required to initially charge the liquid solvent with CO_2 prior to startup and also for CO_2 makeup during the operation of the pilot plant. As part of this work, a steam heated CO_2 pressure regulator was purchased from Andon Specialties, model number H2-1A55Q5G114, and a storage rack was constructed of Unistrut to house up to three large CO_2 cylinders. The capacity of the cylinders varied in size from 150, 200, and 300 L. The CO_2 delivery system was housed indoors.

The steam–heated regulator was found to be inadequate. As the liquid carbon dioxide from the cylinder was being released, over time the lines would begin to freeze and eventually stop flowing. A simple shell and tube heat exchanger was built using 1.3 cm and 1.9 cm OD type 316 stainless steel tubing and stainless steel fitting from Swagelok. University steam was used to vaporize the liquid carbon dioxide from the shell side. A steam trap was also installed. The preheater worked adequately for makeup, but the initial charging of the liquid solvent required patience. Stainless steel tubing (1.3 cm OD) was run from the steam regulator to a control valve located outside. Initially, the makeup CO_2 was discharged downstream of blower. Later, the CO_2 makeup was discharged into the overhead gas accumulator because the CO_2 concentration could be better controlled.

2.3.5 Process Flowsheet

The pilot plant was operated as a closed-loop system, where both the gas and liquid were continuously recirculated. The aqueous piperazine and potassium carbonate solvent was stored in the absorber feed tank. The feed tank was used to maintain a constant lean loading and minimize any flow interruptions in the system. The residence time in the feed tank varied from 0.5

to 1.5 hr depending on the liquid flow rate. Lean solvent from the feed tank was pumped through a filter and then through a Micro Motion® flowmeter before being pumped to the top of the absorber column.

A distributor uniformly disperses the liquid onto the top of the packing. The solvent flows downward by gravity along the surface of the first section of packing, promoting gas liquid contact area. The liquid solvent at the gas–liquid interface of the wetted packing surface absorbs carbon dioxide from the upwardly flowing gas. At the middle of the column is a chimney tray to recollect the liquid and a redistributor for spreading the liquid over the second section of packing.

The solvent rich in CO_2 exits out the bottom of the absorber and is then pumped to another filter before passing through a second Micro Motion® flowmeter. After the flowmeter, the solvent flow is split and passes through the two solvent pre-heaters. Near the top of the column, the preheated stripper feed is mixed with the reflux and then fed at the top of the stripper column to a distributor. In the first campaign, sieve trays were used in the stripper. In later campaigns, random and structured packing were used. A chimney tray and distributor similar to the one in the absorber was used only when there was packing in the stripper. The rich solvent flows downward and the CO_2 is stripped by the steam generated from the solvent by the reboiler.

The lean liquid at the bottom of the stripper is circulated through the reboiler before being pumped to the solvent cooler. Instead of passing through the cooler, a portion of the lean solvent is diverted and pumped to the stripper sump. The solvent is cooled to approximately 40 °C and flows back into the absorber feed tank where the entire process is repeated.

The gas consists of ambient air with the addition of CO_2 from large compressed gas cylinders. The CO_2 concentration in the gas is varied from 3 to

17 mol%. The CO_2 rich gas enters the bottom of the absorber and counter-currently contacts the liquid solvent. The absorber column contains structured packing to maximize the amount of effective interfacial area and minimize pressure drop. Carbon dioxide is absorbed by the liquid solvent at the gas – liquid interface. The "clean" gas then exits out the top of the absorber and passes through the air cooler, where it chills to approximately 10 °C and most of the moisture is removed to protect the CO_2 analyzers and the blower located downstream.

The cooled gas then passes through the water knockout drum where any residual water that may have been entrained is finally removed. The gas is then mixed with the CO_2 from the overhead gas accumulator and recycled back to the blower, where the gas is, and the process is repeated. During the operation of the pilot plant, makeup CO_2 was added into the overhead gas accumulator. The overhead gas accumulator has a split vent valve. When the vent is 0–50%, the accumulator is vented where the vent is fully open at 0%. For 50–100%, nitrogen is added to the system, where at 100%, the vent is fully open for nitrogen addition. When the vent is 50%, both the vent and nitrogen valves are closed. In all of the campaigns, although the vent was at 100%, the gate valve for the nitrogen was closed shut, which resulted in zero nitrogen addition. There is a vent on the impeller housing of the blower; the casing around the hub has an opening that is approximately 2.5 cm in width. The absorber feed tank is vented to the absorber in order to equalize the pressure. During the steady state operation of the pilot plant, it is assumed that there is no leakage. Only when the process conditions are changed is there expected to be any leakage through the blower vent.

The vapor exiting the top of stripper contains carbon dioxide and water and flows to the two–phase condenser. The water is condensed out as liquid and

flows into the overhead liquid accumulator. The water is then pumped through the reflux heater and mixed with the stripper feed. In all of the campaigns, the reflux heater was not used and therefore the reflux was cooler than the stripper feed. The CO_2 gas exits the top of the condenser and then flows to the overhead gas accumulator. The CO_2 in the gas accumulator was mixed with the "clean" air that had passed through the absorber. A control valve downstream of the accumulator controlled the CO_2 concentration in the inlet gas to the absorber. Makeup CO_2 was added to the overhead gas accumulator. During vacuum operation, the vacuum pump was used to draw suction from the gas accumulator.

2.3.6 Online Process Instrumentation

As part of the pilot plant modification, a number of upgrades were made to the measurements of gas and liquid flow, pressure, and temperature. In addition, the capability of online pH measurement and gas phase CO_2 analysis were added. A list of process instrumentation used in the CO_2 capture pilot plant is given by Table 2-3.

Pressure measurements were performed using Ashcroft, Rosemount 1151 and Rosemount 3051 Series pressure transmitters. The Ashcroft pressure transmitters were used with the AN-75 Dietrich Standard annubar for gas flow measurements in Campaigns 1 and 2. The 3051 Series transmitters are smart transmitters and contain a microprocessor that allows communication through the HART protocol. The 3051 transmitters have an accuracy of ±0.1% of the reading and ranged from 0–3, 0–25, and 0–40 inches of water. The 1151 Series transmitters are analog and have a 4–20 mA output. The 1151 transmitters have an accuracy of ±0.5% of the calibrated span and ranged from 0–5, 0–30, and 0–150 inches of water. The pressure transmitters were used to measure absolute,

differential, and gauge pressure throughout the pilot plant. The pressure transmitters were also used to measure liquid level in the sump of the two columns, the absorber feed tank, overhead liquid accumulator and the reboiler.

Temperature measurements of the process streams and column profiles were made using K-type thermocouples and Rosemount Series 68 Platinum Resistance Temperature Detector (RTD) sensors. Rosemount 848T 8-Input temperature transmitters were used in conjunction with the RTD sensors. The RTD sensors have an accuracy of ±0.6 °C. In the first campaign, the temperature measurements on the stripper side were performed with thermocouples and on the absorber side, the thermocouples were replaced with RTD sensors. In later campaigns, all of the thermocouples in the pilot plant were gradually replaced with the Rosemount RTD sensors. As part of this work, some of the conduit and cabling associated with the RTD sensors were installed. Also, in Campaign 1, an infrared temperature gun was used to measure the surface temperature of the absorber column.

The liquid flow rate, temperature and density of the absorber lean and rich solvent streams were measured using Micro Motion® F-series Coriolis flowmeters and are manufactured by Emerson Process Management. The F-series flowmeters have an accuracy of ±0.20 vol% for the flow rate, ±2.0 kg/m^3 for the density, and ±1 °C for the temperature. The Micro Motion® flowmeters were used to measure the flow rates of the absorber inlet, stripper inlet, stripper reflux, and absorber feed tank inlet. The density measurement was used to monitor changes in the water balance.

Table 2-3. Pilot Plant Instrumentation Specification

Manufacturer	Model Number	Function	Range	Method	Accuracy
Dietrich Standard	AN-75	Gas Flow – Abs Inlet (C1/C2)	-	DP	±1% Actual Value
Dietrich Standard	Diamond II Annubar - GCR 15	Gas Flow – Abs Inlet (C3/C4)	-	DP	±1% Actual Value
Horiba	PIR-2000	CO_2 Conc - Abs Gas Mid	0-5/10/20%	NDIR	±1% Full-Scale
Horiba	PIR-2000	CO_2 Conc - Abs Gas Out	0-1/3/5%	NDIR	±1% Full-Scale
Micro Motion®	F-Series	Liquid Flow Rate	0 - 32650 L/hr	Coriolis	±0.20 Vol%
		Liquid Density	0 - 5000 kg/m3	-	±2.0 kg/m3
		Liquid Temperature	-100 to 180 °C	-	±1 °C
Rosemount	3095MFA Mass Probar Flowmeter	Gas Flow - CO_2 Recycle	-	DP	±0.9%
Rosemount	389VP pH/ORP Sensor	pH - Abs Inlet/Outlet	9 - 12	-	99% Linearity
Rosemount	5081-P pH/ORP Transmitter	pH - Abs Inlet/Outlet	-	-	±1 mV @ 25°C, ±0.01 pH
Rosemount	68 Series Platinum RTD	Temperature Sensor	-50 to 400C	Resistance	±0.6 °C
Rosemount	848T 8-Input Temp Transmitter	Temperature Transmitter	-	-	-
Rosemount	3051 Series - DP/GP/AP/LT	Pressure Transmitter	0-3/25/40 inch of H_2O	-	±0.1% Reading
Rosemount	1151 Series - DP/GP/AP/LT	Pressure Transmitter	0-5/30/150 inch of H_2O	-	±0.5% Calib Span (0.1% Smart)
Temet Instruments	Gasmet DX-4000 FTIR	CO_2 Conc - Abs Gas Inlet/Outlet	0-100%	FTIR	<2% Measuring Range
Vaisala	GMT221	CO_2 Conc - Abs Gas Outlet	0-5% CO_2	NDIR - CarboCap	<±[0.02% CO_2 + 2% Reading] @ 25°C
Vaisala	GMT221	CO_2 Conc - Abs Gas Inlet	0-20% CO_2	NDIR - CarboCap	<±[0.02% CO_2 + 2% Reading] @ 25°C
Vaisala	GMT222	CO_2 Conc - Abs Gas Outlet	0-10,000 ppm	NDIR - CarboCap	<±[20 ppm CO_2 + 2% Reading] @ 25°C

Notes:
AP = Absolute Pressure
DP = Differential Pressure
GP = Gauge Pressure
LT = Level Transmitter
FTIR = Fourier Transform Infrared Sensor
NDIR = Nondispersive Infrared Sensor
RTD = Resistance Temperature Detector

In Campaign 1, the inlet gas line to the absorber was 20.3 cm and made of PVC. The gas flow rate was measured using a Dietrich Standard AN-75 annubar, differential pressure transmitters with varying pressure ranges, and a temperature measurement. The flowmeter has an accuracy of ±1% of the actual value. The flow meter was calibrated for air and density corrections were made in the calculations of the actual gas rate to include CO_2 and water. The steam flow to the reboiler was measured using an orifice plate and Rosemount differential pressure transmitters.

The pHs of the absorber inlet and outlet solvent streams were continuously measured with Rosemount 389VP pH/ORP sensors and Rosemount 5081-P pH/ORP transmitters. The 389VP pH sensor has a measuring range of 9–12 pH units and a linearity of 99%. The 5081-P transmitters have an accuracy of ±0.01 pH units or ±1 mV at 25 °C. The connection cable is hardwired to the Rosemount transmitter and attached to the pH sensor on the other end via a quick-connect adapter. As discovered just before the startup of the first campaign, the quick-connect cables may not be waterproof and needed to be shielded by a shelter. Lean loading measurements were correlated to bench-scale pH measurements. The online pH measurements were used to monitor the lean loading and rich loading of the solution. The lean loading of the solution was changed by adjusting reboiler heat duty and CO_2 makeup flow rate.

The concentration of CO_2 in the gas was measured at the inlet, middle and outlet of the absorber column. The inlet and outlet concentrations were measured in situ using Vaisala GMT 221 and GMT 222 CO_2 analyzers. In the first campaign, the absorber inlet Vaisala probe was located downstream of the blower, while the absorber outlet probe was located just upstream of the air cooler. In later campaigns, the absorber outlet probe was moved downstream of the water knockout. The Vaisala CO_2 analyzers use a new silicon based non-

dispersive infrared (NDIR) sensor and use single-beam dual-wavelength NDIR. The probes are interchangeable with the transmitters. The inlet CO_2 concentration was measured with a 0–20 mol% probe and the outlet concentration was measured with either a 0–10,000 ppm or 0–5 mol% probe, depending on the range of the outlet gas. The analyzers have an accuracy <±(0.02% CO_2 + 2% of the reading) at 25 °C, an operating of limit of 60 °C and 0–100% relative humidity. The Vaisala analyzers have a temperature dependence of -0.1% of %full-scale/°C and a pressure dependence of +0.15% reading/hPa.

The concentration of CO_2 in the middle of the absorber column was measured with a Horiba PIR-2000 CO_2 analyzer with a range of 0–1, 0–3, and 0–5 mol%. The Horiba is also a NDIR analyzer and has an accuracy of ±1% full-scale. Unlike the in situ Vaisala analyzers, the middle gas samples use an extractive sampling system. The gas is extracted from the space between the chimney tray and redistributor in the spool piece, where there is no liquid. A diaphragm sample pump extracts the gas and it passes through a water knockout immediately after it exits the column (Figure 2-9). The gas then flows through approximately 30 meters of 0.6 cm polyethylene tubing and into a coalescing filter that removes water and excess gas, which is adjusted by a downstream needle valve. Next, the gas passes through a membrane filter before it flows to the PIR-2000 CO_2 analyzer. A rotameter on the outlet of the analyzer was adjusted to maintain a constant flow rate to the analyzer during online operation and the calibration process. The sampled gas was then discharged outside.

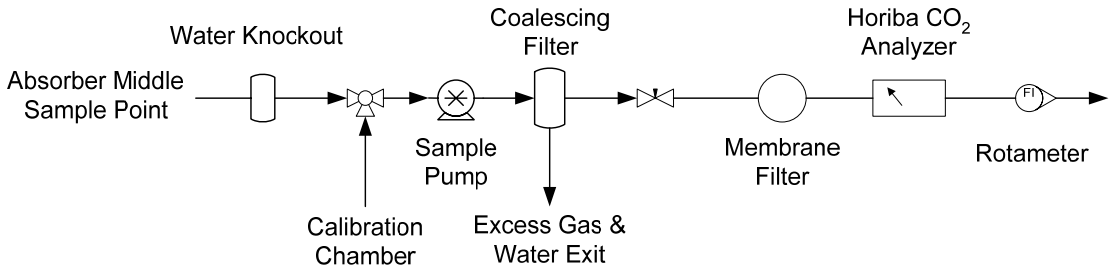

Figure 2-9. Schematic of Extractive Sampling System for Horiba CO_2 Analyzer

2.3.7 DeltaV Process Control System

The DeltaV digital automation system version 7.2 was used to log all the process data and control the operations of the pilot absorber/stripper system. DeltaV is a distributed control system (DCS) based on PlantWeb® digital plant architecture and is manufactured by Emerson Process Management. HART® and FOUNDATION™ field bus process instrumentation as well as 4–20 mA analog signals were fully integrated into the DeltaV system. The DeltaV consists of an operator interface, control hardware, and control software. DeltaV Operate, the operator interface, is run directly on standard PC hardware and operating system and allows the user to monitor and make changes to the process. The control hardware consists of I/O modules connected to a digital control computer, which are attached to a larger redundant DeltaV plant-wide network. The DeltaV control software can be configured to provide model predictive control, neural networks, fuzzy logic, and variability analysis. A schematic of the DeltaV architecture is shown in Figure 2-10.

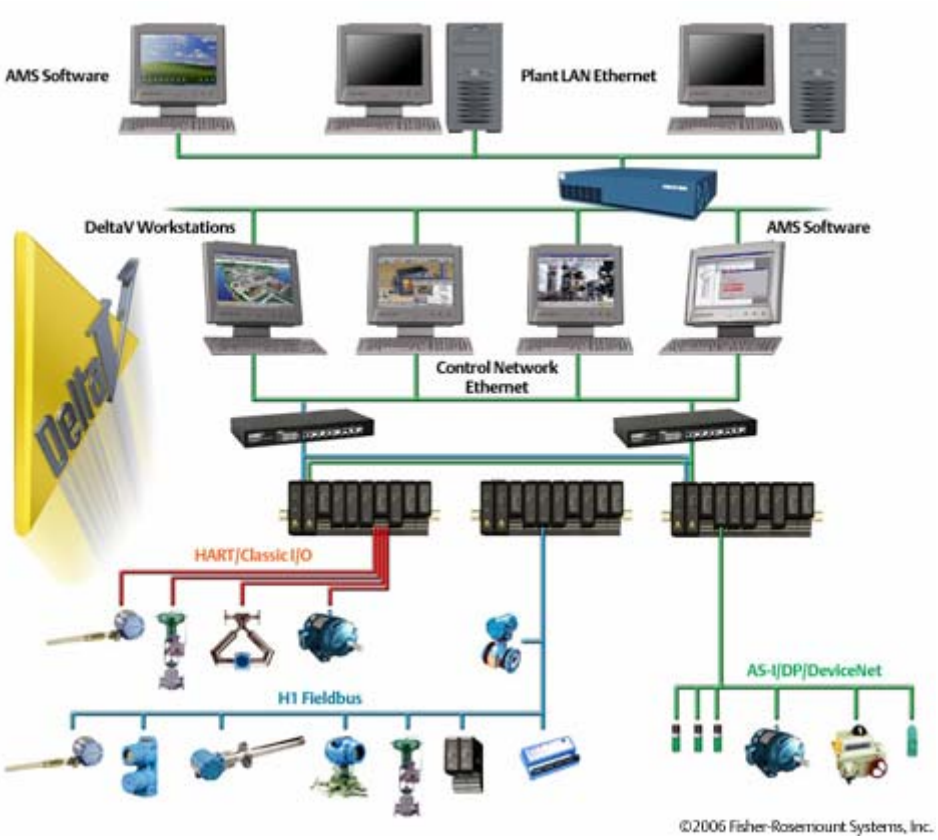

Figure 2-10. Schematic of DeltaV Architecture

2.3.8 Instrument Calibration

The Vaisala and Horiba CO_2 analyzers were calibrated approximately once every 24 to 48 hours with primary standards. In the first campaign, a total of four primary standards were used: 0, 1, 4, and 12 mol% CO_2. In later campaigns, calibration standards of 4.9 and 16.9 mol% CO_2 were added. An onsite nitrogen source was used as the zero calibration gas. The calibration gases consisted of air and carbon dioxide and were purchased from Praxair Inc. The cylinders were filled gravimetrically and have an analytical accuracy of ±0.02%. Certificates of analysis for the calibration gases provided by the vendor are listed in the appendix.

The calibration system consisted of a calibration panel and two calibration chambers, which are located at the inlet and outlet sample points. The calibration chamber is made of 5.1 cm PVC pipe and several tees. Calibration gas flows into the calibration apparatus at one end and exits the opposite end. The Vaisala probe and 0.64 cm tubing for the Horiba are inserted into the penetrations along the length of the calibration chamber. The calibration panel consists of several on-off ball valves, a rotameter, the CO_2 gas standards and the respective regulators, and needle valves for each of the CO_2 gas cylinders. The needle valves control the flow of the calibration gas from the individual cylinders and the rotameter is used to adjust the flow calibration chamber. The ball valves control to which calibration chambers the calibration gas is directed. The Horiba for absorber middle sample point is calibrated from the inlet calibration chamber. Sampling for the Horiba is switched from calibration chamber and absorber middle sample location at the calibration panel.

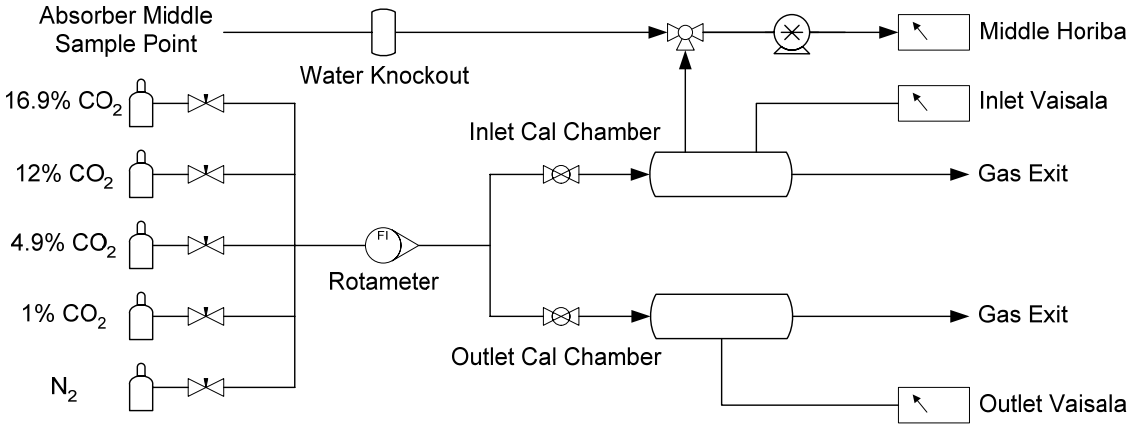

Figure 2-11. Schematic of Calibration Panel for CO_2 Analyzers

During the calibration process, the Vaisala probes were removed from the process line and inserted into a calibration chamber. The sample line of the Horiba was disconnected from the absorber and also connected to calibration

chamber. The CO_2 calibration gas was metered to the calibration chamber using a rotameter on the calibration panel. The raw output signals from the analyzers were recorded and a calibration curve was fitted to a linear equation. The results of the calibration curve were then inputted into DeltaV. The process to calibrate the Horiba analyzer took approximately 20–30 minutes, due to the extractive sampling system that was used. The in situ Vaisala had much quicker response time and could be calibrated in less than 10 minutes. The standard operating procedure for the calibration of CO_2 analyzers is listed in the appendix.

The Micro Motion® and orifice flowmeters are factory calibrated and are periodically checked by measuring the time it takes to fill a known volume. The Deitrich Standard annubar was calibrated using the Pitot tube traverse method. The Rosemount pressure transmitters are calibrated approximately once per month using manometers and pressure gauges. The Rosemount RTD sensors are calibrated before installation in the pilot plant with a dry block calibrator. The pH meters were calibrated with 7 and 10 pH standard solutions prior to the startup of each campaign.

2.3.9 Offline Analytical Methods

In this campaign, an acid-base titration method was used to determine the concentration of piperazine and potassium. The standard operating procedure for the titration procedure is listed in the appendix. An abbreviated summary of the method is enumerated as follows:

1. Add methyl orange to the undiluted sample
2. Titrate with 2N hydrochloric acid (HCl) until the endpoint is reached
3. Heat the solution to release residual CO_2 and allow the solution to cool
4. Titrate with 2N sodium hydroxide (NaOH) until the pH is approximately -265 mV.

The first endpoint represents the total alkalinity of solution and is given by the following equation:

$$Total\ Alkalinity = mol\ K^{+} + 2\ mol\ PZ \tag{2.1}$$

The back-titration endpoint represents the concentration of piperazine in the solution. The concentration of piperazine is calculated by dividing the amount of HCl that is added by two because piperazine contains two nitrogen atoms. The potassium concentration was calculated by taking the difference between the total alkalinity and piperazine concentration. The concentration measurements for K^+ and PZ are reported in units of mol/kg of solution, and not mol/kg of H_2O. For the CO_2 loading measurements, the piperazine and potassium concentrations were reported as total alkalinity.

The concentration of carbon dioxide (CO_2 loading) in the solution was measured using the Shimadzu TOC-5050A Total Organic Carbon Analyzer (TOC). The Shimadzu TOC can be used to measure both inorganic (IC) and total organic carbon (TC). For the measurements of inorganic carbon, 25 wt% phosphoric acid is used to evolve the CO_2 gas from the solvent. The stream of CO_2 is analyzed with a NDIR detector. For total organic carbon analysis, a precisely metered slipstream of the sample is combusted over platinum catalyst at 680 °C with ultra pure air. The resulting CO_2 is measured with the NDIR detector. The Shimadzu has a detection limit of four ppb and a range up to 4000 ppm for TOC and 5000 ppm for IC. The TOC analyzer has an autosampler, which allows it to perform up 89 analyses in one run. A 1000 ppm IC standard was prepared from a mixture of Na_2CO_3, $NaHCO_3$ and deionized (DI) water. The Na_2CO_3 was heated in an oven at 225 °C for several hours and allowed to cool in a desiccator jar. The sodium bicarbonate and carbonate were stored in sealed glass bottles in the desiccator jar when not being used. The 1000 ppm

standard was further diluted to make 50, 100, 150 and 200 ppm IC standards for the calibration curve. A new 1000 ppm standard was prepared each month.

In the first campaign, the total carbon standard was made from a solution of piperazine and potassium carbonate. The total carbon standard recommended by Shimadzu is made from hydrogen potassium phthalate (KHP). Total carbon calibration curves were generated with 50, 100, 200, and 300 ppm TC standards. The TOC has an auto sampler that allows the analyzer to be continuously operated without user intervention. However, the DI rinse water for the auto-sampler and the phosphoric acid for the IC analysis needed to be periodically monitored and was replenished when necessary.

The CO_2 loading was determined by the inorganic carbon analysis and the concentration of piperazine was determined by the taking the difference between the organic carbon and inorganic carbon analyses.

$$Total\ Carbon = Inorganic\ Carbon + Piperazine\ Carbon \tag{2.2}$$

Prior to analysis, approximately 0.9 grams of liquid sample was weighed and diluted to a volume of 1000 mL with DI water. The samples were pipetted into 8 mL vials and placed in the auto-sampler. The TOC measurements seemed drift over time. IC standards (100 ppm) were analyzed every 10th sample in the matrix. The standards appeared to trend upward in concentration at consistent rate over time. After the loading analysis for Campaign 1 had been completed, it was found that the 100 ppm IC standards absorbed CO_2 from the atmosphere, and up to 30% higher concentrations were observed. The 200 ppm IC standards seemed to absorb CO_2 at a much slower rate. It is also entirely possible that the diluted sample solutions may have absorbed CO_2 from the air. This problem was rectified in Campaign 2, when a new liquid sampling and new TOC analysis

method was developed. In later campaigns, all of vials were covered with parafilm to eliminate absorption of CO_2 from the atmosphere.

In Campaign 1, Inductively Coupled Plasma (ICP) emission spectroscopy was used to determine the concentration of potassium, vanadium and total iron in the solution. Due to the presence of carbon steel equipment in the system, 1000 ppm of vanadium (V^{5+}) was added to the solvent as a corrosion inhibitor. The iron concentration indicated the amount of rust that was being produced from carbon steel equipment in the pilot plant and was used to indirectly evaluate corrosion. The ICP analysis was performed by another member in our research group using the ICP analyzer that belonged to the UT Austin Civil Engineering Department.

2.3.10 Raw Materials Inventory

In Campaign 1, the effective interfacial area of the Flexipac 1Y structured packing was determined by absorbing CO_2 from ambient air into 0.1 N KOH. The solution was made using water (CAS No. 7732-18-5) from the City of Austin and KOH (CAS No. 1310-58-3) pellets in 22.7 kg bags purchased from UNIVAR USA. The starting 5 m K^+/2.5 m PZ solution was made by removing several drums of the KOH solution and adding 68 wt% aqueous piperazine (CAS No. 111-85-0) and 47 wt% aqueous potassium carbonate (CAS No. 584-08-7) from 300 kg drums. In addition, 4 bags of 22.7 kg bags of U.S.P. grade potassium bicarbonate (CAS No. 298-14-6) were purchased as makeup. The piperazine was donated by DOW Chemical and the potassium bicarbonate and carbonate were purchased from UNIVAR USA. The makeup CO_2 (CAS No. 124-38-9) was purchased from Texas Welding Supply and was dispensed from 150, 200, and 300L cylinders containing liquid carbon dioxide. Vanadium (V^{5+}) was added as a corrosion inhibitor in the form of potassium metavanadate (KVO_3). The

metavanadate (CAS No. 13769-43-2) is commercially sold under the trade name HotPot-922 by Pechiney World Trade USA and is typically used in hot potassium carbonate systems for inhibiting corrosion.

In the December of 2003, the purchased cost from UNIVAR USA for 6 drums of 47 wt% aqueous potassium carbonate, 45.5 kg of KOH pellets, and 90.9 kg of U.S.P. grade $KHCO_3$ was \$0.7/kg, \$3.04/kg, and \$3.85/kg. Per the Armand Products July 1, 2006 truckload price list, 47% K_2CO_3 solution costs \$0.45/kg for bulk and \$0.62/kg for 300 kg drums, FOB Muscle Shoals, Alabama. For U.S.P. grade potassium bicarbonate in 22.7 kg bags from Armand Products, the cost is \$6.53/kg for quantities less than 455 kg. The cost per pound decreases with increasing quantities. For quantities greater than 4546/kg, the cost of $KHCO_3$ is \$2.10/kg. Piperazine costs were estimated to be \$5.50/kg and MEA was estimated to cost about 5 times less than piperazine. The cost of the CO_2 gas from Texas Welding Supply was approximately \$0.37/kg.

2.3.11 Liquid Sample Collection

In Campaign 1, the liquid samples were taken at the inlet, middle, and outlet of the absorber. Erlenmeyer flasks with glass stoppers were used to take the samples. The sampling procedure involved opening a valve at the sample point and allowing the solution to flow out into the Erlenmeyer flasks. The pH and temperature was recorded for each liquid sample with a handheld pH meter. The sample was then poured into a 40 mL glass sample vial and capped. Samples were collected once the pilot operation had reached steady state for one hour. Two sets of liquid samples were taken for each run condition. It was later discovered that the sampling process made have resulted in the loss of CO_2 from the samples due to flashing. In the second campaign, the liquid sample

collection procedure incorporated the use of sample bombs, which minimized flashing.

2.3.12 Campaign 1 Plant Operation

Pilot plant operations commenced at the end of May 2004. The effective interfacial area of the Flexipac 1Y structured packing in the absorber was determined by absorbing CO_2 from ambient air into a solution of 0.1 N potassium hydroxide (KOH). The gas and liquid flow rates were varied from 300 to 770 m^3/hr and 8 to 40 m/hr, respectively. The starting solution inventory was 2.9 m^3 (14 drums). A Horiba VIA510 CO_2 gas analyzer was used to measure the outlet CO_2 concentration.

Upon completion of the effective area tests, 5 drums of the 0.1 N KOH solution were removed. The remaining solution was mixed with 3 drums of 68% piperazine AQ, 2 drums of water, 5 drums of 47% liquid K_2CO_3, and 0.03 m^3 (50 kg) of the HotPot-922 solution to give a vanadium concentration of 1000 ppm. Piperazine has a freezing point of 54 °C and is solid at room temperature. Drum heaters were used unsuccessfully to liquefy the solid piperazine. Numerous attempts to solubilize piperazine in the potassium carbonate solution were also unsuccessful. The piperazine was eventually added into the system by first adding CO_2 into the relatively lean starting potassium solution. Once the solution was loaded, it was heated in the reboiler. Via a batch process, hot bicarbonate solution was pumped into the piperazine drum. The resulting mixture was then pumped into the absorber feed tank. While the solvent was circulating, 40 mL of antifoam was added to the system. The process of charging the piperazine and potassium carbonate took approximately two weeks. Once the chemicals were loaded, troubleshooting on the absorber and stripper began. During startup, solids were discovered at the bottom of the absorber feed tank.

It was speculated that piperazine had precipitated. Hot solvent was circulated through the entire system to dissolve the piperazine and the absorber feed was withdrawn from the side of the absorber feed tank, instead of the bottom.

The pilot plant was operated for a total of seven days, beginning in mid June. A total of 35 runs and 19 operating conditions were conducted with three solvent compositions, while maintaining a K^+/PZ ratio of 2:1. The potassium and piperazine concentrations were 2.3, 2.9, and 3.1 mol K^+/kg soln and 1.15, 1.45, and 1.55 mol PZ/kg soln, respectively. The gas and liquid flow rates were varied from 0.5 to 3 kg/m^2-s and 1.3 to 5.1 kg/m^2-s, respectively. The liquid to gas (L/G) ratio was varied from 0.9 to 5.6 kg/kg. The synthetic flue gas contained 3–13% CO_2 in air at 25 to 50 °C. The temperature of the solvent to the absorber varied from 35 to 45 °C. The absorber was operated at atmospheric pressure. The stripper pressure varied from 1 to 1.7 bar. The absorber contained 6.1 m of Flexipac 1Y structured packing and the stripper contained 14 sieves trays with 45.7 cm tray spacing. Lean loading and CO_2 removal varied from 0.41 to 0.54 mol CO_2/(mol K^+ + 2 mol PZ) and from 84.5 to 99.8%, respectively. Vanadium concentrations were maintained at approximately 18 mmol/kg soln (1000 ppm). Dissolved iron concentration varied from 0.3 to 0.6 mmol/kg soln.

Foaming was observed in the absorber after several days of operation. Three hundred and seventy-five milliliters of silicone based GE antifoam were added throughout the duration of pilot plant operations. The online Rosemount pH meters failed after the first day of the operation. The rain may have short-circuited the probes because the quick-connect cables on pH meter were not designed for outdoor use.

Table 2-4. Campaign 1 Absorber Operation

Parameter	Value
Inlet CO_2 (mol%)	3 – 12
PZ Concentration (mol/kg of solvent)	1.2 – 1.6
K^+/PZ Ratio	2.0 – 2.05
Lean Loading (mol CO_2/(mol K^+ + 2 mol PZ))	0.39 – 0.50
G (kg/m^2-s)	0.5 – 3.0
L/G (kg/kg)	2.2 – 5.6
$T_{GAS,IN}$ (°C), Typical	32
T_{LEAN} (°C), Typical	40

There were also solubility issues with both the piperazine and the potassium carbonate. The absorber and stripper filters eventually became plugged and had to be bypassed. Based on a visual inspection, the stripper filter had plugged up with potassium carbonate and the absorber filter was filled with precipitated piperazine. When the solution is too lean, piperazine will precipitate and float. Potassium carbonate precipitates when the solution becomes too rich and sinks to the bottom. Also, both potassium carbonate and piperazine were near their respective solubility limits. After the loss of the filters, it was finally realized that additional water needed to be added to the system and that the liquid holdup in the overhead liquid accumulator should be minimized because there would always be water inventory in the accumulator. The loss of water from the solution resulted in the precipitation of both components and wreaked havoc on the plant operation. In addition, the some of the samples for the stripper lean, which tended to be slightly cooler, contained precipitate.

In the first campaign, the solvent was not adequately preheated by the heat exchanger. It was discovered that the steam traps were undersized and that the condensate eventually backed up into the exchanger and resulted in poor

performance. This issue was addressed in the next campaign. The inlet gas temperature was also too low. To much cooling occurred at the air cooler and the mechanical work from the blower could not get the temperature up to 40 °C. A control valve was not installed for the cooling water to the air cooler cooling and the flow rate could not be controlled. In addition, the inlet gas was not saturated with water, which was expected in an industrial process.

The orifice meter measuring the steam flow to the reboiler was too small. In some cases, the reboiler steam rate was operated beyond the measurement range. Finally, the middle absorber CO_2 gas sampling system was filled with water due to condensation from the saturated gas. The water knock-out filters for the Horiba sampling system were replaced and the entire sampling line was blown with compressed air.

2.3.13 Campaign 1 Results

The results from the KOH test in the carbon steel absorber column showed that the maximum effective area was approximately 49% of the total packing surface area. The specific area of the Flexipac 1Y structured packing is 410 m^2/m^3. The results are plotted in Figure 2-12. The figure shows that at high gas rates, the effective area approaches a maximum. These results are consistent with that obtained by UT-SRP (Separations Research Program) for a high surface area structured packing. The effective area for the 300 and 400 acfm gas rates were approximately the same, but the results for the 180 acfm gas rate was much lower. The data for the 180 acfm gas rate may not be reliable because the effective area is typically independent of gas flow rate.

The DeltaV control system was used to log the process data real-time. Measurements included the temperature, pressure, flow rate, density, CO_2 concentration, liquid level, steam flow, and cooling water flow. The logged data

was retrieved from DeltaV and imported into Excel spreadsheets on a daily basis. The data points were recorded once per minute. The reported process conditions were generated by averaging the points 10 minutes before and after the specified sample point. This reduces the effect from the disturbances caused by the liquid sample collection process.

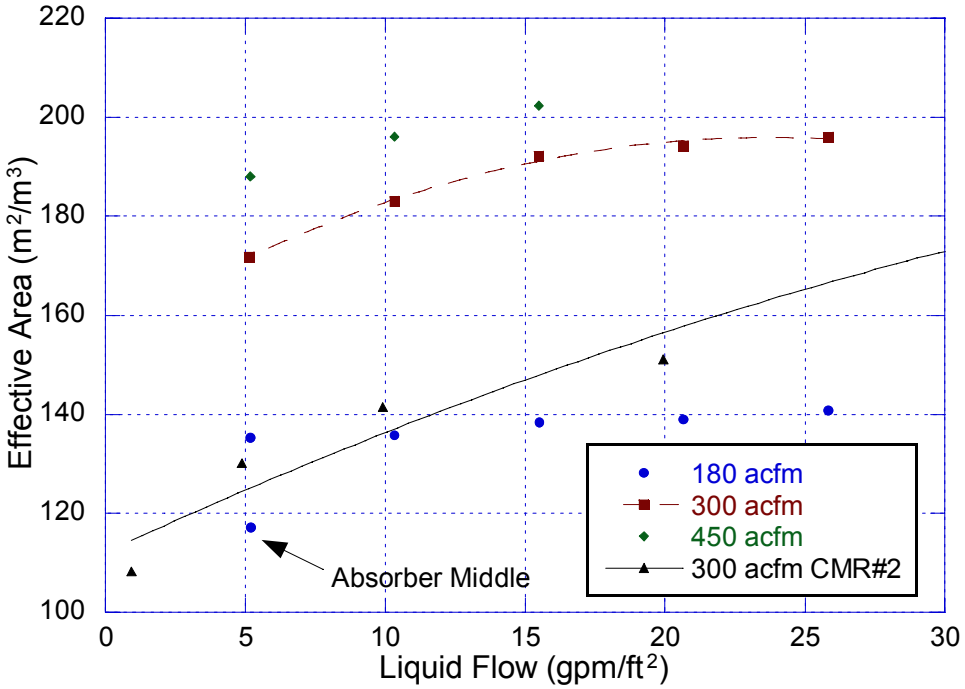

Figure 2-12. Effective Area of Flexipac 1Y Structure Packing from the Absorption of CO_2 into 0.1 N KOH

Titrations and ICP analyses were performed only at the beginning and end of each concentration change (Table 2-5). CO_2 loading and piperazine analysis was performed for absorber lean, middle, and rich solutions using the Shimadzu TOC. Some of the rich samples had precipitate and these samples were later diluted with water and re-analyzed. Parafilmed 100-ppm IC standards were placed in between every 10th sample, but the samples themselves were not parafilmed. Some of the samples may have absorbed CO_2 from the atmosphere before analysis and the inorganic carbon analysis may be

erroneously higher. The piperazine was calculated by subtracting the contribution of the inorganic carbon portion of the analysis. The loading and piperazine data reported in Campaign 1 should be used with caution. In addition, ion chromatography was used to analyze the concentration of piperazine and potassium prior to the start of Campaign 4. The results show that ion chromatography results are 15 to 20% higher than that obtained by the titration analysis.

In Run 1.1.1, the concentration of potassium carbonate was slightly low. Three-quarters of a drum of 47% potassium carbonate was added to the system. In Run 1.2.1 through 1.7.1, the potassium to piperazine concentration was maintained at approximately 2:1. For Runs 1.8.1 to 1.17.2, 5 drums of condensate were removed to further concentrate the solvent system. The potassium concentration appeared to have slightly changed and may have been due to operations with an increased level in the liquid accumulator. In the final set of runs, an additional drum of condensate was removed and the liquid accumulator was operated with a higher liquid level.

A summary of the absorber gas rate, liquid rate, CO_2 gas concentration, and stream temperatures is given in Table 2-6. Five absorber temperature profiles were acquired with the infrared temperature gun. The infrared gun measured the surface temperature of the absorber column, which also had a layer of white paint, whereas the RTD measurements consisted of probes inserted partially into the packing where it may contact gas, liquid or both. Both sets of results indicate that a large bulge occurred towards the top of the column. At the spool piece, a large temperature gradient also existed. The complete raw data set for Campaign 1 is listed in the appendix.

Table 2-5. Campaign 1 Absorber Analyses

Run ID	Date	Time	Titration			ICP			TOC		Ion Chromatograph		
			Ln Talk mol/kg	Lean PZ mol/kg	Lean K^+ mol/kg	Lean K^+ mol/kg	Lean V mmol/kg	Lean Fe mmol/kg	Lean PZ mol/kg	CO_2 Loading mol/kg	Ln Talk mol/kg	Lean PZ mol/kg	Lean K^+ mol/kg
1.1.1	6/16/04	15:30	4.51	1.22	2.06	2.00	18.7925	0.118	1.09	2.18	-	-	-
1.1.2	6/16/04	16:15	-	-	-	-	-	-	1.17	1.84	-	-	-
1.1.3	6/16/04	17:00	4.50	1.20	2.10	1.72	18.23	0.172	1.27	1.91	5.49	1.58	2.33
Added 3/4 Drum of K2CO3													
1.2.1	6/17/04	11:30	4.65	1.17	2.31	2.11	18.00	0.161	1.15	2.03	-	-	-
1.2.2	6/17/04	12:15	-	-	-	-	-	-	1.09	2.46	-	-	-
1.2.3	6/17/04	13:00	-	-	-	-	-	-	1.16	2.02	5.46	1.44	2.59
1.3.1	6/17/04	16:15	-	-	-	-	-	-	1.19	2.19	-	-	-
1.3.2	6/17/04	16:45	-	-	-	-	-	-	1.22	2.30	-	-	-
1.3.3	6/17/04	17:45	-	-	-	-	-	-	1.22	2.25	6.52	1.63	3.25
1.4.1	6/17/04	18:30	-	-	-	-	-	-	1.24	2.31	-	-	-
1.5.1	6/17/04	19:15	-	-	-	-	-	-	1.29	2.36	-	-	-
1.6.1	6/18/04	15:30	-	-	-	-	-	-	1.20	2.21	-	-	-
1.7.1	6/21/04	16:45	4.63	1.15	2.33	1.98	18.06	0.241	1.24	2.25	-	-	-
Removed Water													
1.8.1	6/22/04	17:45	5.66	1.40	2.87	1.87	18.55	0.172	1.41	2.63	-	-	-
1.8.2	6/22/04	18:30	-	-	-	-	-	-	1.48	2.66	-	-	-
1.9.1	6/22/04	19:30	-	-	-	-	-	-	1.46	2.63	6.49	1.63	3.23
1.9.2	6/22/04	20:15	-	-	-	-	-	-	1.44	2.67	-	-	-
1.10.1	6/22/04	21:15	-	-	-	-	-	-	1.49	2.76	-	-	-
1.10.2	6/22/04	22:00	-	-	-	-	-	-	1.44	2.70	-	-	-
1.11.1	6/23/04	8:15	-	-	-	-	-	-	1.47	2.75	6.53	1.64	3.25
1.11.2	6/23/04	9:00	-	-	-	-	-	-	1.46	2.84	-	-	-
1.12.1	6/23/04	14:30	-	-	-	-	-	-	1.44	2.93	-	-	-
1.12.2	6/23/04	15:15	-	-	-	-	-	-	1.28	3.37	-	-	-
1.13.1	6/23/04	17:30	-	-	-	-	-	-	1.36	2.94	-	-	-
1.14.1	6/23/04	18:15	-	-	-	-	-	-	1.41	3.07	6.64	1.66	3.31
1.15.1	6/24/04	9:00	-	-	-	-	-	-	1.42	3.05	-	-	-
1.15.2	6/24/04	9:30	-	-	-	-	-	-	1.49	3.08	-	-	-
1.16.1	6/24/04	10:30	-	-	-	-	-	-	1.48	3.09	-	-	-
1.16.2	6/24/04	11:00	-	-	-	-	-	-	1.48	3.09	-	-	-
1.17.1	6/24/04	12:15	-	-	-	-	-	-	1.42	3.12	-	-	-
1.17.2	6/24/04	12:30	5.84	1.44	2.96	2.42	21.97	0.593	1.48	3.15	-	-	-
Removed Water													
1.18.1	6/24/04	16:00	6.11	1.54	3.03	2.75	23.64	0.236	1.50	3.25	-	-	-
1.18.2	6/24/04	16:15	-	-	-	-	-	-	1.39	3.20	-	-	-
1.19.1	6/24/04	17:00	-	-	-	-	-	-	1.53	3.31	-	-	-
1.19.2	6/24/04	17:30	6.15	1.52	3.11	2.77	22.93	0.129	1.48	3.24	6.53	1.60	3.34

Table 2-6. Campaign 1 Absorber Results

Run#	Gas Rate Actual m^3/min	Liquid Rate L/min	L/G kg/kg	CO_2 In %	CO_2 Out %	CO_2 Removal %	Temp Gas In °C	Temp Gas Out °C	Temp Liq In °C	Temp Liq Out °C	Density Liq In kg/m^3	Density Liq Out kg/m^3	pH Liq In	DP Bot Bed kPa	DP Top Bed kPa
1.1.1	15.0	19.0	1.27	2.89	0.16	94.3	38.8	42.6	39.33	29.19	1145	1174	11.4	0.81	0.77
1.1.2	14.9	18.9	1.26	2.84	0.17	93.9	37.7	42.0	39.11	28.57	1146	1173	11.5	0.63	0.77
1.1.3	14.9	18.9	1.27	2.78	0.17	93.8	38.8	42.4	38.90	28.95	1147	1174	11.6	0.72	0.76
1.2.1	7.5	18.8	2.47	2.97	0.00	99.8	28.0	39.8	41.50	32.28	1163	1180	11.6	0.19	0.25
1.2.2	7.5	18.9	2.49	2.92	0.01	99.8	29.0	41.8	43.16	32.59	1163	1181	11.5	0.20	0.25
1.2.3	7.5	18.9	2.50	2.88	0.01	99.8	29.4	43.0	44.46	32.58	1162	1181	11.4	0.14	0.25
1.3.1	7.5	37.7	5.03	2.25	0.02	98.9	32.9	39.5	41.02	38.36	1165	1172	11.4	0.94	0.67
1.3.2	7.5	37.7	5.03	2.45	0.03	98.9	33.2	39.3	40.67	38.09	1165	1173	11.2	0.92	0.77
1.3.3	7.5	37.7	5.03	2.37	0.03	98.7	33.3	38.7	40.42	38.06	1166	1173	11.2	1.07	0.85
1.4.1	7.5	37.6	4.99	3.92	0.04	99.1	33.1	38.0	40.01	39.40	1166	1175	11.3	1.33	0.95
1.5.1	10.2	32.7	3.20	3.00	0.05	98.3	33.4	38.1	40.08	38.26	1166	1174	11.3	1.42	1.06
1.6.1	4.5	29.1	6.37	11.72	0.32	97.3	33.5	15.8	39.53	44.04	1165	1180	10.7	0.40	0.21
1.7.1	3.0	19.0	6.21	11.62	0.73	93.7	32.3	41.5	40.05	39.25	1163	1184	10.6	0.15	0.07
1.8.1	15.0	19.0	1.33	3.39	0.26	92.3	37.6	43.6	41.16	29.68	1207	1234	10.9	0.72	0.77
1.8.2	14.9	19.0	1.33	3.47	0.21	93.9	37.6	43.5	41.48	29.45	1207	1237	11.0	0.72	0.77
1.9.1	19.9	19.0	1.02	3.58	0.56	84.5	46.9	42.1	41.49	31.63	1206	1236	11.0	1.22	1.31
1.9.2	19.9	19.0	1.02	3.66	0.54	85.2	46.3	41.9	41.55	31.49	1207	1235	11.0	1.23	1.32
1.10.1	10.0	19.2	1.97	2.98	0.04	98.6	28.4	42.7	41.58	30.13	1208	1232	11.0	0.41	0.43
1.10.2	10.0	18.7	1.91	2.68	0.03	98.9	27.7	42.7	41.52	29.83	1208	1233	11.2	0.41	0.43
1.11.1	7.5	9.4	1.27	2.71	0.23	91.5	23.6	35.8	34.63	22.56	1212	1241	11.2	0.23	0.24
1.11.2	7.5	9.5	1.29	2.48	0.16	93.6	24.1	36.1	35.39	22.66	1211	1241	11.2	0.23	0.24
1.12.1	20.9	26.5	1.39	2.25	0.33	85.3	52.7	42.9	39.81	34.39	1211	1233	10.6	1.52	1.65
1.12.2	19.7	24.8	1.37	3.58	0.47	86.9	51.1	43.7	39.64	34.43	1211	1234	10.6	1.35	1.45
1.13.1	7.2	29.1	4.08	13.99	1.20	91.4	30.7	49.4	40.49	38.54	1211	1236	10.9	0.40	0.30
1.14.1	5.9	25.5	4.33	13.22	1.15	91.3	29.6	46.2	40.26	41.05	1212	1233	11.1	0.61	0.26
1.15.1	6.2	29.3	4.69	12.30	1.26	89.7	24.7	35.3	39.59	39.76	1216	1234	11.1	0.32	0.25
1.15.2	6.2	29.3	4.69	11.30	0.88	92.2	25.6	44.0	43.23	40.86	1214	1234	10.8	0.52	0.32
1.16.1	7.5	29.4	3.92	12.23	1.74	85.7	27.4	50.8	43.34	38.47	1212	1238	10.8	0.69	0.42
1.16.2	7.5	29.5	3.95	12.51	1.75	86.0	28.7	49.7	42.48	38.83	1213	1237	11.1	0.70	0.44
1.17.1	4.0	18.9	4.75	11.59	0.68	94.2	26.8	48.2	41.34	38.39	1214	1239	11.0	0.12	0.13
1.17.2	4.0	18.9	4.77	11.59	0.55	95.2	26.7	47.7	41.22	38.40	1214	1239	10.9	0.12	0.13
1.18.1	6.2	29.2	4.84	12.40	0.43	96.5	33.7	52.9	46.24	43.36	1229	1252	10.8	0.83	0.39
1.18.2	6.2	29.3	4.83	12.65	0.45	96.4	34.2	53.2	46.05	43.54	1228	1252	10.8	0.84	0.38
1.19.1	4.0	18.8	4.87	11.55	0.58	95.0	32.9	53.7	45.27	40.44	1229	1257	11.0	0.15	0.12
1.19.2	4.0	18.9	4.89	11.76	0.40	96.6	32.1	53.2	44.84	39.81	1228	1257	11.0	0.13	0.12

2.3.14 Campaign 1 Corrosion Evaluation

Corrosion coupons were purchased from Alabama Specialty Products Inc. Five different types of steel materials were tested: carbon steel (C1010), 304L stainless steel, 316L stainless steel, 317L stainless steel, and 2205 stainless steel (Duplex). All of the coupons are milled with a 120 grit finish and each coupon is stamped with a unique identification number. The corrosion coupons were mounted onto a 316L stainless steel 5 cm pipeline insertion rack with a 20 cm stem and three mounting holes. The coupons were mounted to the stem with 0.6 cm Teflon shoulder washers and 0.3 cm Teflon spacers were used in between each coupon. In all of the campaigns, the two sets of each material type were installed on two of the mounting holes. In addition, Z-core resin coupons manufactured by Smith Fibercast, which represented advance fiber reinforced plastic (FRP) material, was tested.

Corrosion coupons were inserted into a 5 cm pipe just downstream of the feed heater and left in the system over a one week period. Each coupon was weighed at the beginning and end of the week-long run and only visually inspected. Preliminary results show that all of the steel coupons remained relatively unchanged (Table 2-7). However, the FRP seemed to have absorbed some of the solvent, as the final weight was slightly higher.

Table 2-7. Campaign 1 Corrosion Coupon Results

Sample ID	Initial Mass g	Final Mass g	Difference
C1010-1	15.6816	15.6824	-0.0008
C1010-2	15.8699	15.8705	-0.0006
304L-1	14.6760	14.6762	-0.0002
304L-2	14.7226	14.7232	-0.0006
316L-1	14.3783	14.3791	-0.0008
316L-2	14.3493	14.3496	-0.0003
317L-1	14.7838	14.7839	-0.0001
317L-2	14.7172	14.7179	-0.0007
2205-1	15.1899	15.1903	-0.0004
2205-2	15.3256	15.3267	-0.0011
FRP	10.4145	10.4408	-0.0263

2.3.15 Campaign 1 Summary

In Campaign 1, an existing extraction/distillation pilot plant was modified into an absorber/stripper system for CO_2 capture. New process equipment and instrumentation was added to the existing system. The carbon steel piping was replaced with type 304 stainless steel. The pilot plant was operated for approximately one month, which included troubleshooting and one week of operation. The absorber contained Flexipac 1Y structured packing and the stripper contained 14 sieve trays at 45.7 cm spacing. The pilot plant was operated with 5 molal potassium carbonate and 2.5 molal piperazine.

In Campaign 1, several problems arose that needed to be resolved in latter campaigns. These issues include: (1) The loss of water from the solvent and low temperature points in the system resulted in the precipitation of piperazine and potassium compounds in the instrument lines and equipment. This created a number of problems during the operation plant and the pilot plant was shut down several times. (2) Foaming was observed in the absorber, which limited

the operating range of liquid and gas flow rates for pilot plant and required the addition of antifoam. (3) The steam traps for the stripper feed preheater were undersized. As a result, the stripper feed was not adequately preheated and the stripper had an excessively high heat duty. (4) The liquid sampling method used in Campaign 1 may have resulted in the loss of CO_2 from flashing. (5) The absorber inlet gas was not representative of expected flue gas conditions. The temperature was too low and was not saturated with water at 40 °C. (6) Due to the loss of both pH meters, at times the pilot plant was blindly operated because there was significant delay with the liquid loading analyses. (7) The CO_2 loading analysis may have been compromised by the absorption of CO_2 into the diluted samples. The samples were analyzed using an autosampler and may have been exposed to the atmosphere for an extended period prior to analysis. (8) The DeltaV log sheet recorded the raw signal for the inlet and outlet Vaisala CO_2 gas analyzers and not the calibrated values.

2.4 CAMPAIGN TWO – ABSORBER/STRIPPER CHARACTERIZATION

The first objective of Campaign 2 was to obtain a more complete data set on absorber performance as a function of gas rate, liquid rate, CO_2 gas concentration, and CO_2 lean loading with Flexipac 1Y structured packing. Due to the problems encountered during Campaign 1, a portion of Campaign 2 was devoted to obtaining additional absorber data with Flexipac 1Y. The second objective was to obtain performance data for the stripper over a range of solvent rates, rich loadings, and stripper pressures with IMTP #40 random packing.

2.4.1 Campaign 2 Modifications

Before the commencement of Campaign 2, several issues were resolved. The two online Rosemount pH meters that failed were replaced. The original probes and transmitters were sent to Rosemount Analytical for examination, but

it appeared that nothing was wrong. In the original setup, one end of the cable is hardwired to the transmitter and the pH probe is connected to the opposite end via a quick-connect. Apparently, the pH probes and transmitters are not designed for outdoor use. It was suspected that heavy rains had shorted the connection between the probe and transmitter, causing the pH meters to malfunction. Rosemount Analytical sent two new pH meters with one of the probes hardwired to the transmitter. Electrical tape was wrapped around the probe with the quick-connect cable to prevent water intrusion.

At 12% CO_2, the 0–5% Horiba analyzer was over-ranged when taking measurements at the middle of the absorber. An existing Horiba PIR-2000 CO analyzer was converted by the manufacturer to a 0–20% CO_2 analyzer. The new analyzer was initially used to measure the absorber middle CO_2 gas concentration. However, due to the new blower configuration, the saturated inlet gas caused the Vaisala analyzer to malfunction at the beginning of the campaign. The absorber middle Horiba sampling system was then used to measure absorber inlet CO_2 gas concentration and no absorber middle gas samples were analyzed during Campaign 2.

At the conclusion of the first campaign, it was discovered that the polyethylene bag filter for the reboiler had completely dissolved. The filters were replaced with bags made from cotton. The polyethylene bag filter had previously been used in a C6/C7 system with no adverse effects at approximately the same temperatures (~120 °C). Therefore, temperature should not have been an issue. However, it was discovered that although the new bags were made from cotton, the stitching was still made of a synthetic fiber, which eventually caused the bags to fail. In the third and fourth campaign, cotton filter bags with cotton stitching were used.

In the first campaign, the steam traps on the stripper feed heater were undersized. As a result, the solvent was not adequately heated. New steam traps were installed on the stripper feed heater to rectify the problem. A larger orifice was installed for steam flow measurement to the reboiler because the steam flow rates exceeded the measuring range of the orifice in the first campaign. The cooling water to the air cooler was blinded to permit operation at higher gas temperatures. A bypass around the blower was constructed with PVC pipe. The bypass allowed a portion of the gas to be recycled and increased the temperature of the inlet absorber gas to reach 40 °C. A manually adjusted butterfly valve was used to regulate the gas flow rate through the blower recycle. The process flowsheet and process and instrumentation diagram for Campaign 2 is shown below.

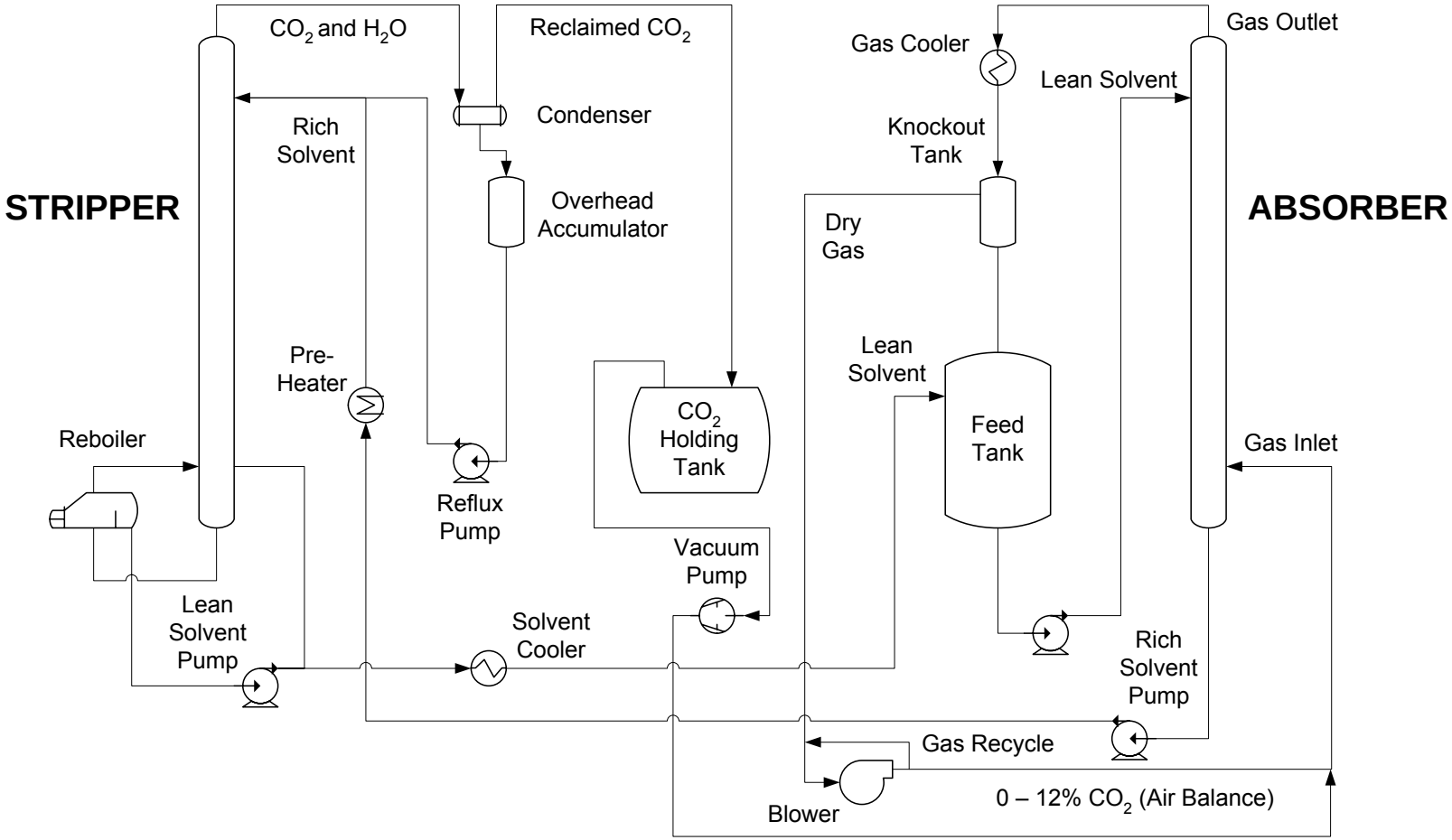

Figure 2-13. Process Flowsheet of Absorber/Stripper Pilot Plant for Campaign 2

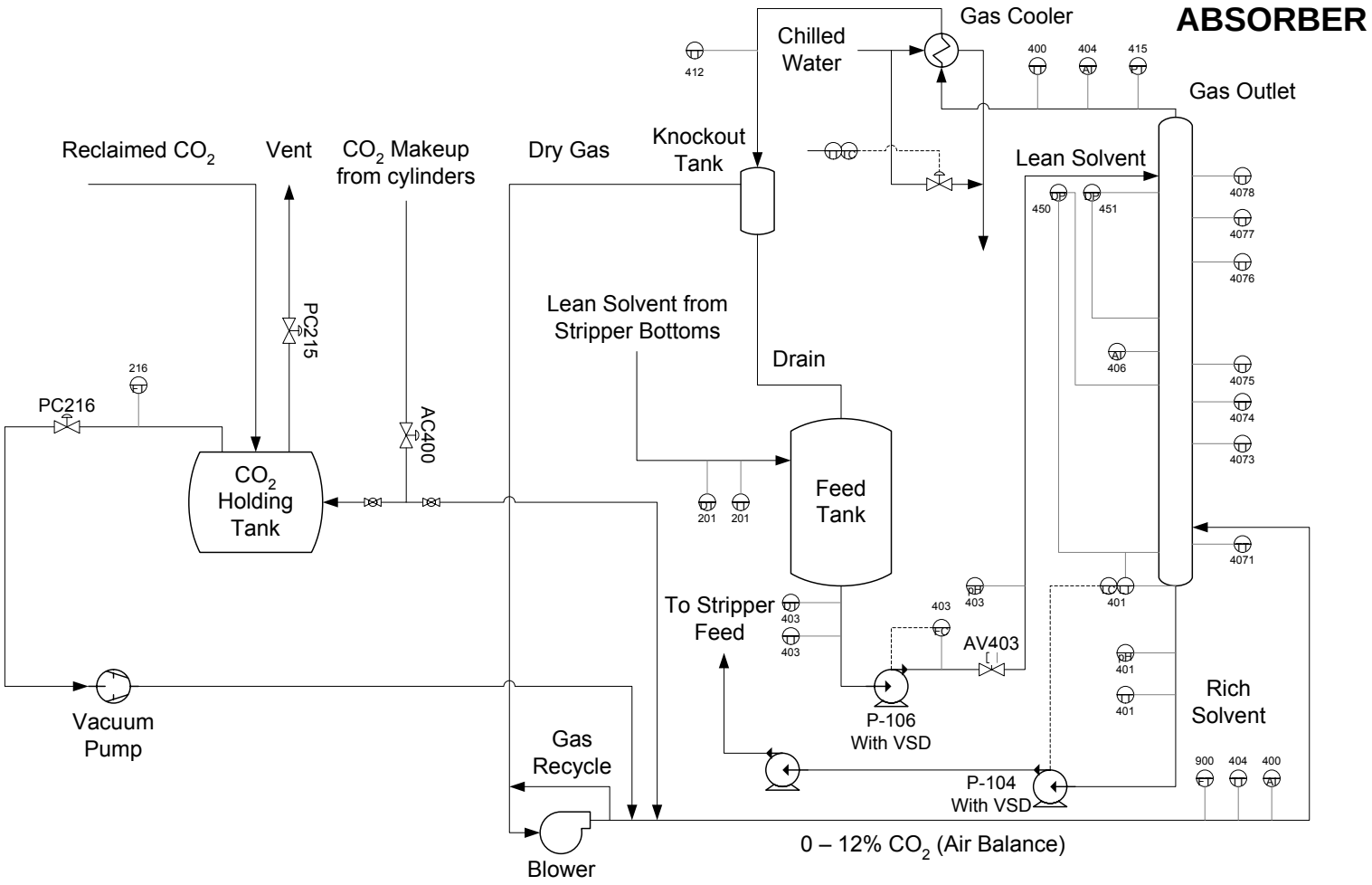

Figure 2-14. Process and Instrumentation Diagram of the Absorber for Campaign 2

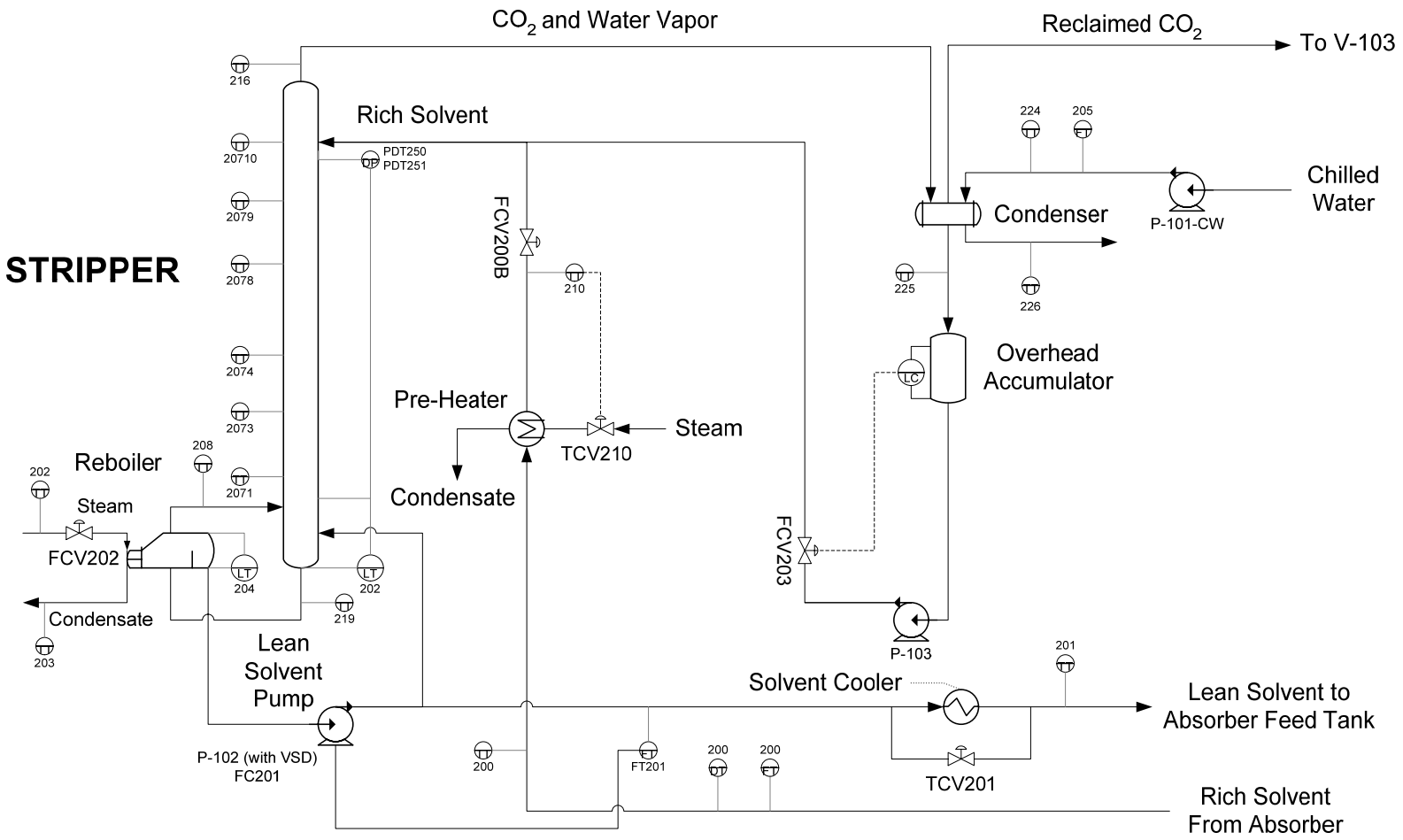

Figure 2-15. Process and Instrumentation Diagram of the Stripper for Campaign 2

2.4.2 Campaign 2 Liquid Sample Collection Method

In the first campaign, there were issues with material balance closure in the absorber column. It was believed that the CO_2 in the rich samples were flashing during the sample collection process. Sample bombs were constructed and used to take samples to eliminate this. The sample bombs were made from 1.3 cm OD stainless steel tubing and Swagelok® quick-connects and had a volume of about 10 mL. The stock o-rings in the quick-connects were replaced with EPDM o-rings.

A total of five liquid sample points were taken for Campaign 2: absorber lean, absorber middle, absorber rich, stripper middle, and stripper lean. Quick-connects and braided stainless steel hoses were attached to the pump discharge and suction of the pumps for the absorber lean, absorber rich, and stripper lean streams. The sample bomb was connected to the two ends of the sample hose and fluid was allowed to circulate for several minutes before the valves were shut and the sample bomb was disconnected. For the pump samples, the discharge valve was always shut first and then the suction side valve was closed. The sample bombs were colored coded to match the sample location.

For the absorber middle sample, fluid from the collector plate was allowed to flow through the sample bomb and discharge back into the absorber column for several minutes, before being disconnected. The stripper middle sample was taken from a bayonet collector, allowed to flow through the sample bomb and discharge into an eductor. Under vacuum operations, some of the stripper middle samples could not be withdrawn because the eductor did not provide enough suction.

The sample bombs were brought inside to the laboratory and attached to a sample extraction system. A syringe was used to extract the liquid sample from the sample bomb through a Teflon coated rubber septum. The sample was then

injected into a 40-mL vial containing 30 mL of chilled de-ionized (DI) water. The sample was injected underneath the surface of the DI water. The samples were diluted to minimize any flashing and to prevent precipitation. After, the mass of the injected sample was recorded and residual sample was allowed drain from the sample bomb. Nitrogen was used to blow out any residual liquid in the sample extraction system. Two set of samples were taken for each operating condition. The standard operating procedure for collecting the liquid samples is listed in the appendix.

2.4.3 Campaign 2 Analytical Methods

In Campaign 2, the concentration of piperazine and potassium was initially determined by titration with 2 N HCl and 2 N NaOH using the method developed for Campaign 1. In Campaign 2, the titration method was performed on samples that had been diluted by a ratio of 3:1. When the results from the titration method for the two campaigns are compared, for a given liquid density and temperature, the results from the second campaign were consistently lower than the first campaign. It was assumed that the concentration of potassium and piperazine were correlated with density. This may have been due to a change in the indicator endpoint resulting from sample dilution. It is possible that the endpoint may have been overshot during the titration of the dilute solution with a concentrated acid. A method for analyzing piperazine and potassium using ion chromatography (IC) was later developed in Campaign 4 and used to verify the correct the titration results. The IC results are given in the Campaign 4 Analytical Methods section of this chapter.

In Campaign 2, the Shimadzu 5050A TOC was used to determine the CO_2 loading in the solvent with the same method developed for Campaign 1. In addition, some of the diluted liquid samples from Campaign 2 were analyzed

with the inorganic carbon (IC) analyzer located on the main UT campus to validate the TOC results. The results from the campus IC and from the Shimadzu total organic carbon (TOC) analyzer located at the Pickle Research Center (PRC) were plotted against online pH measurements. The results are shown in Figure 2-16. It was found that the campus loading numbers were systematically lower than that analyzed by the Shimadzu TOC.

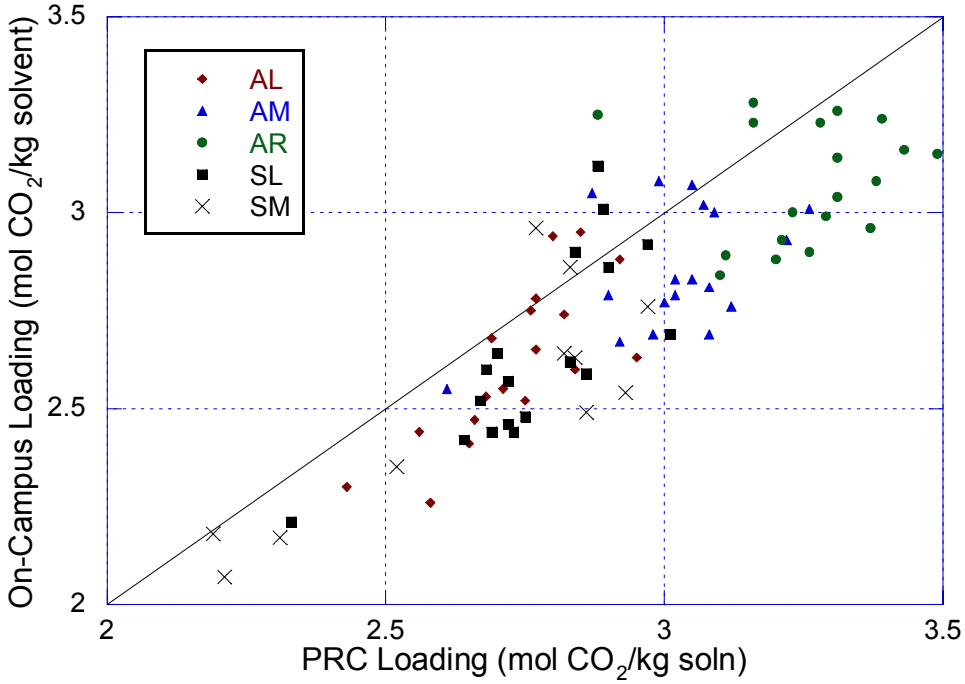

Figure 2-16. CO_2 Loading Results for PRC TOC analyzer and On-campus Inorganic Carbon Analyzer of Same Sample

In the process, it was discovered that the diluted sample solutions and the IC standard solutions absorbed CO_2 when left open to the atmosphere. The PRC IC standards are made up to a concentration of 1000 ppm of inorganic carbon using sodium carbonate and sodium bicarbonate. The on-campus IC standard is made up to a concentration of 7 molar (84 ppm) using sodium carbonate.

An experiment was conducted where the IC standard was parafilmed and the diluted samples were left open to the atmosphere and were analyzed over a

period of five days (Figure 2-17). The results show that the diluted samples absorbed between 20 to 30 ppm of CO_2 from the atmosphere within a 17 hour period. In earlier analyses, the TOC was operated over a period of 12 hours. Therefore, if the samples were not parafilmed, a large amount of CO_2 would have been absorbed.

The results also show that the 100 ppm IC standard did not absorb any CO_2 over a period of 4 days when covered with parafilm. The slight change in concentration for the 100 ppm IC standard may have been due to analyzer drift. It was noticed that sometimes the Shimadzu carrier gas fluctuated over time, which gave slightly different results for a particular IC standard concentration. To account for analyzer drift in latter TOC analyses, IC standards were analyzed every 5–6 samples in the sample matrix.

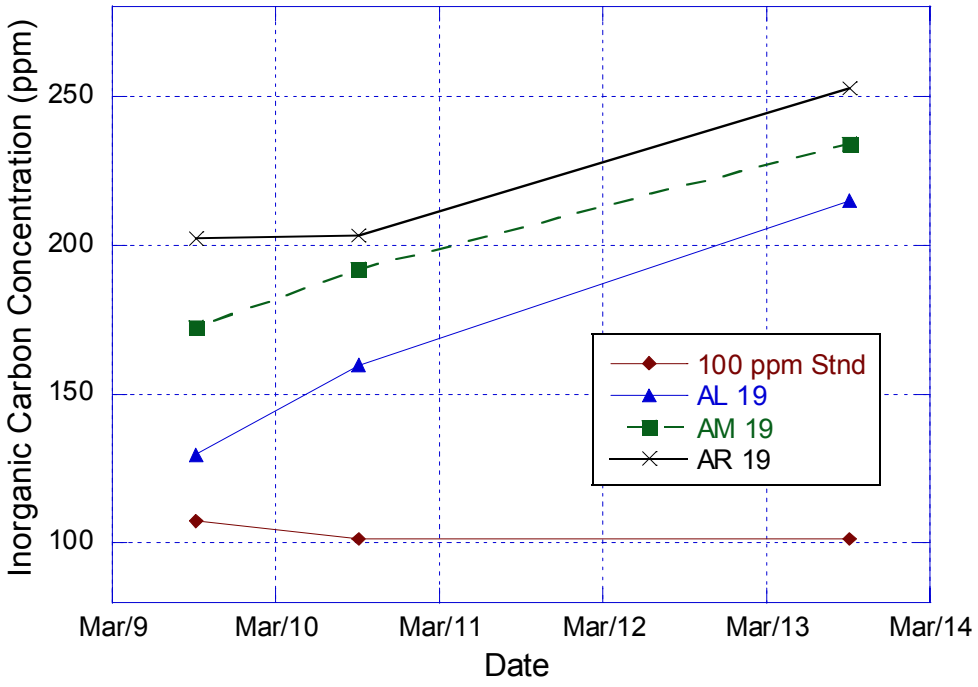

Figure 2-17. CO_2 Absorption in Diluted K^+/PZ Samples from Campaign 2

It was also observed that the 100 ppm IC standards consisting of sodium carbonate and bicarbonate will absorb up to 10 ppm of CO_2 when left open to the

atmosphere overnight. Three sets of IC standards consisting of 100, 150, 200 ppm were made at PRC and analyzed by the on-campus IC. The values were found to be about 10–15% lower by the on-campus IC (Figure 2-18). The PRC standards were freshly prepared, while the on-campus standard that was used to calibrate the analyzer was not. It is possible that the on-campus standard may have absorbed CO_2. In addition, the on-campus standard is made from Na_2CO_3, which readily absorbs water and CO_2 from the atmosphere. If the Na_2CO_3 was not properly heated or even heated before being used to make up the standard, this would also give erroneous results.

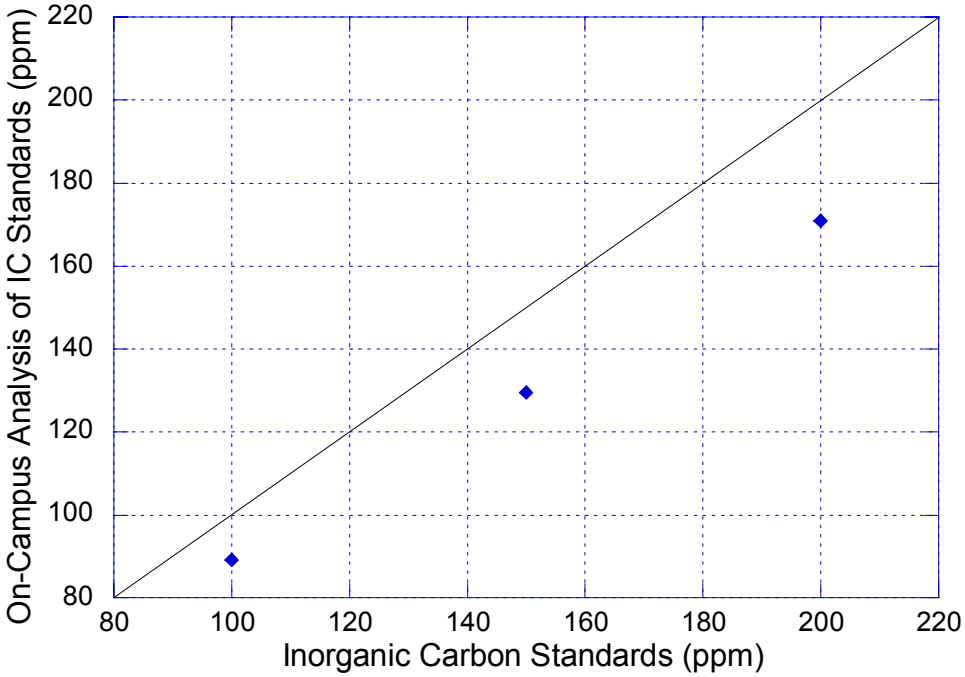

Figure 2-18. Analysis of 100, 150, 200 ppm Inorganic Carbon Standards by the On-campus Inorganic Carbon Analyzer

The sodium carbonate standard used for the main campus IC was measured by the Shimadzu and determined to be 96 ppm when the actual concentration should have been 84 ppm. This supports the observation that CO_2 is absorbed by the Na_2CO_3 standard. The on-campus standard is stored in a

stopped glass flask at ambient temperature and not in the refrigerator. Overtime, the standard may have absorbed CO_2 from the atmosphere.

Base on these results, the initial loading analysis was discarded and the absorber lean, middle, and rich samples were re-analyzed with the new and more rigorous method. In addition, the samples were diluted 40:1 with chilled DI water to minimize CO_2 losses. Inorganic carbon standards of 100 ppm were made up daily from the 1000 ppm standard and were analyzed after every 6 samples. The 1000 ppm IC standard was stored in a capped bottle and kept in the refrigerator when not in use. The diluted liquid samples were transferred to the sample tubes and immediately covered with parafilm to minimize the absorption of CO_2 from the atmosphere.

2.4.4 Campaign 2 Plant Operation

Pilot plant operation for Campaign 2 commenced at the end of October in 2004. The pilot plant was operated continuously for 10 days, 24 hours per day, except on weekends. A total of 40 runs and 23 operating condition were completed. Twenty-three runs were conducted at a single solvent composition. The solvent from the first campaign was used in the second campaign. The solvent has been stored in steel drums in between the two campaigns.

The piperazine and potassium concentrations were varied between 1.3 to 1.4 mol/kg soln and 2.8 to 2.9 mol/kg soln, respectively. The gas and liquid flow rates were varied from 1.2 to 2.2 kg/m^2-s and 2.7 to 11.9 kg/m^2-s, respectively. The L/G ratio was varied from 1.8 to 6.9 kg/kg. The inlet CO_2 concentrations were varied between 2.6 to 12.4 mole percent and the inlet gas temperatures were varied between 30 and 50 °C. The inlet temperature of the solvent to the absorber was maintained nominally at 40 °C. The stripper pressure was nominally varied between 0.3 to 1.8 bar, with one run at 3.4 bar.

The absorber contained 6.1 m of Flexipac 1Y structured packing and the stripper contained 6.1 m of IMTP #40 random packing, divided into two 3.05 m beds of packing. A chimney tray and liquid redistributor was located in between each bed of packing. In the stripper, two Koch 4C distributors were used as the distributor and redistributor for the top and bottom beds, respectively. The absorber contained a Koch 3C distributor at the top and a Montz II redistributor in the bottom bed. The CO_2 removal rate varied from 56.3 to 97.3 percent. No additional vanadium was added to the system. The lean loading varied from 0.43 to 0.53 mol/total alkalinity. The lean density varied between 1221 to 1230 kg/m^3.

In order to increase the inlet gas temperature, a bypass around the blower was constructed. A 15.2 cm PVC pipe run was added towards the beginning of the second campaign. As a result, water began to condense downstream of the knockout pot, accumulated in some of the lines, and leaked out through the blower casing. Water was periodically drained from the lines and pumped back into the system.

The supersaturated conditions in the inlet gas eventually resulted in the failure of the inlet Vaisala CO_2 gas analyzer. The Horiba PIR-2000 analyzer was switched from analyzing the absorber middle and used to measure the inlet CO_2 gas concentration. However, there was some time lag associated with the Horiba extractive gas sampling system. As a result, it was difficult to control the system and took longer to reach steady state. No absorber middle gas samples were analyzed in Campaign 2.

Table 2-8. Campaign 2 Absorber Operation

Parameter	Value
Inlet CO_2 (mol%)	2.6 – 12.6
PZ Concentration (mol/kg solvent)	1.3 – 1.4
K^+/PZ Ratio	2.0 – 2.3
Lean Loading (mol CO_2/(mol K^+ + 2 mol PZ))	0.43 – 0.54
G (kg/m^2-s)	1.2 – 2.2
L/G (kg/kg)	1.7 – 7.1
$T_{GAS,IN}$ (°C)	29 – 64
T_{LEAN} (°C)	39 – 48

Table 2-9. Campaign 2 Stripper Operation

Parameter	Value
ΔT Approach (°C)	31 – 81
Top Temperature (°C)	67 – 113
Bottom Temperature (°C)	74 – 143
Reboiler Heat Duty (kcal/mol CO_2)	107 – 223

Both of the online Rosemount pH meters were replaced prior to the commencement of the second campaign. The inlet pH meter was hardwired to the transmitter, but the outlet pH meter still had the quick-connect cabling. Electrical tape was wrapped around the quick-connect in lieu of constructing a shelter. The outlet online Rosemount pH meter failed again just before the commencement of the second campaign, possibly due to the rain. The inlet loading was monitored by the online Rosemount pH meter and controlled by the addition of makeup CO_2 or increasing the stream flow to the stripper reboiler.

Significant foaming was occasionally observed and limited the hydraulic rates. New antifoam from GE was used in the second campaign, which the manufacturer claimed to be better suited for the K^+/PZ solvent system. Antifoam was periodically added, which eliminated the problem for 10–20 hours

of operation. Foaming appeared to increase with high CO_2 gas concentration, large temperature bulges, and high gas rates.

2.4.5 Campaign 2 Results

A summary of the results for the liquid analyses of Campaign 2 is shown in Table 2-10. The acid-base titration method was used to determine the concentration of piperazine and potassium in the solvent. Before the start of Campaign 4, the ion chromatography method was used to measure piperazine and potassium concentration. The two analyses appear to agree with each other. In Campaign 2, the titration analysis was performed with a 4:1 pre-diluted sample. In Campaign 1, titrations were performed with undiluted pilot plant samples. It is possible that the dilution of the sample may have shifted the titration endpoint of methyl orange. CO_2 loading was measured using the Shimadzu TOC with the revised inorganic carbon analytical method. Piperazine analysis using organic carbon analysis was not performed in this campaign onward because of its unreliability. Table 2-11 is a summary of the absorber results from Campaign 2. The complete raw data set for Campaign 2 is given in the appendix. In Campaign 2, no corrosion coupons were installed.

Table 2-10. Campaign 2 Absorber Analyses for 5 m K^+/2.5 m PZ

Run ID	Date	Time	Ion Chromatograph		Titration		CO_2 Loading		
			PZ Lean mol/kg	K^+ Lean mol/kg	PZ Lean mol/kg	K^+ Lean mol/kg	Lean mol/kg	Mid mol/kg	Rich mol/kg
2.1.1	10/26/04	10:35	1.24	2.90	1.29	2.97	2.65	2.96	3.14
2.1.2	10/26/04	11:00	-	-	-	-	2.47	-	3.24
2.2.1	10/26/04	14:45	-	-	-	-	2.45	3.22	3.21
2.3.1	10/27/04	0:15	-	-	-	-	2.60	3.16	3.43
2.4.1	10/27/04	2:30	-	-	-	-	2.65	3.06	3.29
2.5.1	10/27/04	3:30	-	-	-	-	2.65	2.90	3.21
2.6.1	10/27/04	6:00	-	-	-	-	2.61	2.98	3.24
2.7.1	10/27/04	7:00	1.32	3.08	1.38	3.01	3.00	2.93	3.28
2.8.1	10/27/04	12:00	-	-	-	-	2.58	2.99	3.13
2.8.2	10/27/04	13:00	1.25	2.91	1.28	2.87	2.67	3.00	3.30
2.9.1	10/28/04	4:15	1.21	2.77	1.32	2.72	2.52	2.96	3.22
2.9.2	10/28/04	5:15			-	-	2.50	3.08	3.28
2.10.1	10/28/04	13:40	1.33	3.09	1.41	2.97	2.84	3.06	3.39
2.10.2	10/28/04	14:55	-	-	-	-	2.65	3.06	3.28
2.11.1	10/28/04	16:35	-	-	-	-	2.94	3.26	3.41
2.11.2	10/28/04	17:15	-	-	-	-	2.89	3.05	3.48
2.12.1	10/28/04	19:15	-	-	-	-	2.83	3.26	3.57
2.12.2	10/28/04	20:15	-	-	-	-	2.73	3.16	3.55
2.13.1	10/29/04	5:45	-	-	-	-	2.50	2.95	3.25
2.13.2	10/29/04	6:45	1.26	2.95	1.32	2.86	2.78	2.91	3.08
2.14.1	11/2/04	20:32	-	-	1.30	2.82	-	-	-
2.14.2	11/2/04	21:45	-	-	-	-	2.94	3.33	3.39
2.15.1	11/3/04	0:30	1.24	2.90	-	-	2.84	3.01	3.24
2.16.1	11/3/04	1:30	-	-	-	-	2.82	3.14	3.27
2.17.1	11/3/04	5:15	-	-	-	-	2.73	2.97	3.12
2.17.2	11/3/04	6:15	-	-	1.35	2.74	2.70	3.00	3.15
2.18.1	11/3/04	11:30	-	-	1.36	2.79	2.82	2.95	3.10
2.18.2	11/3/04	12:30	-	-	-	-	2.82	3.20	3.16
2.19.1	11/3/04	15:45	-	-	-	-	2.90	2.99	3.40
2.19.2	11/3/04	16:45	-	-	-	-	2.93	3.01	3.21
2.20.1	11/4/04	6:00	-	-	-	-	2.66	3.02	3.13
2.20.2	11/4/04	7:30	-	-	-	-	2.74	3.16	3.43
2.21.1	11/4/04	10:15	-	-	-	-	2.94	2.71	3.53
2.21.2	11/4/04	11:15	1.39	3.23	1.43	3.06	2.90	3.12	3.40
2.22.1	11/4/04	13:30	1.30	3.03	1.36	2.88	2.78	3.02	3.29
2.22.2	11/4/04	15:15	-	-	-	-	2.77	3.07	3.35
2.23.1	11/4/04	21:15	-	-	-	-	2.68	3.22	3.43
2.23.2	11/4/04	23:00	-	-	-	-	2.66	3.00	3.21
2.24.1	11/5/04	3:45	-	-	-	-	2.65	3.08	3.29
2.24.2	11/5/04	4:45	1.24	2.92	1.35	2.77	2.43	2.90	3.11

Table 2-11. Campaign 2 Absorber Results for 5 m K^+/2.5 m PZ

Run#	Gas Rate Actual m^3/min	Liquid Rate L/min	CO_2 In mol%	CO_2 Out mol%	CO_2 Removal %	Temp Gas In °C	Temp Gas Out °C	Temp Liq In °C	Temp Liq Out °C	Density Liq In kg/m^3	Density Liq Out kg/m^3	pH Liq In	DP Bot Bed kPa	DP Top Bed kPa
2.1.1	17.0	30.2	11.1	2.1	81.2	49.1	49.2	40.2	47.4	1224	1242	11.2	0.79	0.86
2.1.2	17.0	30.3	11.0	2.4	78.5	49.4	48.8	40.3	47.2	1225	1240	11.1	0.81	0.87
2.2.1	17.0	30.1	12.3	5.4	56.3	54.4	50.8	41.2	50.5	1226	1240	11.0	0.80	0.87
2.3.1	12.8	34.0	11.5	4.0	64.7	46.2	44.6	40.7	44.7	1227	1240	10.7	0.57	0.63
2.4.1	12.7	41.5	12.0	3.7	69.5	45.6	40.9	40.6	44.6	1227	1239	10.6	0.83	0.76
2.5.1	12.7	41.4	10.7	2.7	74.3	46.7	40.7	40.6	44.6	1227	1239	10.6	0.88	0.81
2.6.1	12.7	47.2	10.4	1.9	81.5	47.2	38.6	41.2	45.9	1228	1237	10.6	1.02	0.83
2.7.1	12.7	47.4	11.1	2.2	80.0	48.2	39.5	41.3	46.4	1228	1238	10.6	1.03	0.86
2.8.1	17.0	49.4	11.7	4.0	65.7	50.8	45.8	41.4	46.6	1227	1238	10.6	1.45	1.60
2.8.2	17.0	49.2	11.4	3.8	67.1	53.2	46.2	41.6	47.8	1227	1237	10.6	1.48	1.62
2.9.1	9.9	32.4	11.3	3.5	68.9	36.2	41.1	40.6	41.8	1226	1241	10.6	1.32	0.26
2.9.2	9.9	32.3	11.3	3.4	70.2	37.4	42.2	40.8	42.3	1226	1241	10.6	1.34	0.25
2.10.1	9.9	43.7	11.9	1.9	84.3	47.2	38.6	41.2	48.0	1228	1238	10.6	1.98	1.02
2.10.2	9.9	43.5	12.0	2.0	83.6	48.2	38.9	41.3	48.2	1228	1238	10.6	2.01	1.06
2.11.1	9.9	43.4	11.5	1.8	84.4	51.2	39.3	41.4	48.4	1229	1238	10.6	2.11	1.20
2.11.2	9.9	43.6	11.7	1.9	83.5	51.5	39.6	41.4	48.6	1229	1238	10.6	2.11	1.20
2.12.1	9.9	45.6	11.7	0.6	94.8	59.8	37.4	41.0	48.4	1229	1239	10.6	2.38	7.05
2.12.2	9.9	45.3	11.4	0.3	97.3	47.9	37.4	41.0	48.0	1229	1239	10.7	2.36	8.26
2.13.1	9.9	37.9	11.6	2.7	76.7	33.5	39.3	40.7	45.0	1230	1242	10.6	0.77	0.86
2.13.2	9.9	37.9	12.0	3.0	74.6	32.0	37.6	40.3	44.1	1230	1243	10.6	0.77	0.86
2.14.1	9.9	18.9	4.9	0.8	84.1	29.3	38.2	43.5	30.7	1227	1246	10.4	0.25	0.28
2.14.2	9.9	19.0	4.7	0.9	81.0	28.2	36.8	42.5	30.1	1227	1245	10.4	0.26	0.28
2.15.1	9.9	22.9	5.4	0.7	86.4	29.9	36.6	41.9	34.6	1229	1242	10.4	0.28	0.29
2.16.1	9.9	22.3	5.3	0.6	88.1	29.5	36.1	42.0	34.5	1230	1244	10.4	0.28	0.30
2.17.1	12.7	20.8	4.4	0.5	88.4	33.0	35.6	38.8	31.5	1231	1245	10.5	0.43	0.47
2.17.2	12.7	20.8	4.3	1.1	74.6	31.7	34.9	39.0	30.0	1232	1248	10.5	0.44	0.47
2.18.1	12.7	30.5	4.0	0.5	87.8	35.7	39.0	44.8	37.2	1222	1233	10.3	0.45	0.48
2.18.2	12.7	29.9	3.9	0.4	88.6	36.6	39.2	44.8	37.6	1222	1233	10.3	0.45	0.49
2.19.1	12.7	37.8	3.9	0.3	92.5	37.4	40.5	47.0	40.5	1222	1231	10.2	0.54	0.52
2.19.2	12.7	37.8	3.9	0.3	91.7	39.7	41.8	47.8	42.3	1222	1230	10.2	0.55	0.56
2.20.1	14.2	77.4	16.2	2.0	87.7	47.1	36.3	40.1	48.0	1226	1233	10.6	1.46	1.08
2.20.2	14.2	77.1	16.0	1.8	88.5	49.7	36.3	40.1	48.3	1226	1233	10.6	1.53	1.15
2.21.1	14.2	83.4	16.1	1.2	92.6	58.4	35.8	40.1	48.3	1226	1232	10.6	1.91	1.42
2.21.2	14.2	83.3	16.4	1.4	91.3	64.3	38.1	40.9	50.7	1225	1231	10.5	1.92	1.44
2.22.1	14.2	83.0	17.9	2.5	86.2	49.5	39.3	41.8	51.2	1220	1227	10.5	1.70	1.19
2.22.2	14.2	83.3	17.4	1.8	89.4	49.1	38.7	41.1	50.9	1223	1229	10.5	1.72	1.19
2.23.1	14.2	56.8	17.2	4.5	73.9	42.0	41.5	39.9	47.9	1227	1237	10.7	0.89	0.95
2.23.2	14.2	56.5	16.3	4.0	75.6	41.0	39.8	39.8	47.3	1227	1237	10.7	0.92	0.96
2.24.1	14.2	57.0	16.9	3.4	79.8	41.7	41.5	39.7	47.6	1229	1240	10.8	1.00	1.07
2.24.2	14.2	56.5	17.4	3.8	78.4	41.5	42.0	39.6	47.5	1229	1240	10.8	1.02	1.10

1. Run 2.13 High Stripper Pressure Case
2. Run 2.14-2.19 Vacuum Stripping Cases

2.4.6 Campaign 2 Summary

In Campaign 2, several issues from Campaign 1 were resolved, which include: (1) Sample bombs were used for the liquid sampling, which minimized CO_2 losses from flashing. (2) The liquid sampling method was improved through the use of syringes and injection of samples into vials containing chilled DI water to minimize CO_2 losses and eliminate precipitation from cooling. (3) The liquid samples and standards for the CO_2 loading analysis were covered with parafilm to minimized CO_2 absorption. (4) The absorber inlet gas was heated by the addition of a gas recycle. (5) The undersized steam traps for the stripper feed pre-heater were replaced.

In Campaign 2, there were several issues that needed to be resolved. These issues include: (1) The stripper feed still was not adequately pre-heated. (2) The absorber inlet gas was not saturated. (3) The absorber inlet gas temperature was not well controlled. (4) The Vaisala CO_2 gas analyzers were operated in a condensing environment which resulted in the failure of the absorber inlet analyzer and intermittent malfunction of the absorber outlet analyzer. (5) Foaming in the absorber was observed, which limited the matrix of run conditions. (6) The absorber outlet pH meter failed as a result of water intrusion. (7) The water balance was not well maintained because the air cooler was not operated. Water condensed in the gas lines and leaked out through the blower. (8) Steady state operation of the pilot plant was difficult due to the lag time associated with the extractive sampling method used with the Horiba CO_2 analyzer, which included the control of the steam flow to the reboiler, the CO_2 recycle flow rate, and the flow of CO_2 makeup. (9) The pilot plant was sometimes operated blindly because real-time analysis of the absorber lean loading was not available. (10) The CO_2 material balance for the gas and liquid

phase did not match after the commencement of vacuum operation. (11) The DeltaV log sheet recorded the raw signal for the absorber outlet Vaisala CO_2 analyzer and not the calibrated value.

2.5 CAMPAIGN THREE – MEA BASELINE

The main objective of the MEA campaign was to establish a benchmark for comparison to the aqueous piperazine and potassium carbonate system in terms of performance and plant operation. The same Flexipac 1Y structured packing was used in the absorber and IMTP #40 was used in the stripper. Another objective was to evaluate and compare mass transfer rate data obtained by the pilot plant to bench-scale data from a wetted wall column for the two solvent systems.

2.5.1 Campaign 3 Modifications

Prior to the start of the third campaign, the additional modifications were made to the pilot plant to correct the problems encountered in Campaign 2. At low gas rates, the annubar in the 20 cm PVC gas line gave erroneous results due to the low pressure drop and poor turndown characteristics. The 20.3 cm gas schedule 40 PVC line was replaced with 7.6 cm and 10.2 cm schedule 40 PVC gas lines. In the new setup, the gas could flow through either line or both and generate enough pressure drop to produce an accurate reading. Steam flow measurement for the solvent preheater was added. In addition, a Rosemount 3095MFA Mass Probar annubar was added to measure the gas flow rate of the CO_2 recycle stream leaving the overhead gas accumulator. The annubar has an accuracy of ±0.9% of the mass flow rate for gas and stream and a flow turndown of 8:1. The flowmeter was a way of verifying the gas and liquid material balance of the absorber and stripper when the system was at steady state. Unfortunately, the minimum Reynolds number for the flowmeter is 6000 and is equivalent to a

minimum flow rate of 63 ft^3/min at 293 K and 1 bar. In Campaign 4, this flow requirement was satisfied under only one run condition. However, in the MEA campaign, it appeared that the flowmeter gave reasonable results above 30 scfm. The results from the CO_2 recycle flowmeter were used only as a rough comparison.

Under vacuum conditions, the amount of CO_2 that could be stripped was limited by the diameter of the 2.5 cm gas line from the overhead condenser. This dictated the range of lean loadings and gas rates for the absorber and the range of stripper pressure for vacuum operation. To rectify this problem, a 5.1 cm gas line was added to the top of the overhead liquid accumulator and connected to the CO_2 gas accumulator. In the new configuration, excess CO_2 from the condenser could exit the bottom of the condenser along with the water and flow to the overhead liquid accumulator. The liquid accumulator functioned as a separator. The CO_2 gas could exit the top of the tank and flow into the overhead gas accumulator. A constant liquid level was maintained in the vessel, which prevented any gas from being returned with the liquid reflux. However, in Campaign 4, some of the condensed water became entrained with the CO_2 recycle stream and began to collect in the overhead gas accumulator. Water was periodically drained and pumped back into the system.

In Campaign 2, the solvent preheater still did not function properly. The solvent may have been flashing after the control valve, which was downstream of the heat exchangers, and created a vapor lock. In addition, the stripper did not have a two phase distributor, which would have helped with the two phase flow. To correct this problem, a spare pump was connected in series to the absorber outlet pump to increase the pressure of the solvent stream. The control valve was also relocated upstream of the stripper inlet nozzle.

A new extractive CO_2 sampling system was constructed for a second Horiba analyzer. The sampling system consists of a water knockout, sample pump, coalescing filter, membrane filter and rotameter. The gas flows from the sample point to a water knockout and then through the sample pump. Next the gas passes through a coalescing filter that removes any condensed water and then through a membrane filter that removes any residual moisture. The gas is then analyzed by the Horiba CO_2 analyzer. The gas flow rates are regulated by a rotameter located downstream of the Horiba analyzer. A large weather proof electrical cabinet was purchased and modified to fit two sampling pumps. A temperature controlled fan was added to help dissipate the heat inside the cabinet and to prevent the sample pump from overheating or melting the diaphragm.

A new CO_2 makeup heater was constructed and installed. The previous heater was not sized for high liquid CO_2 flow rates. As a result of being undersized, the heater began to leak due to the continuous stress resulting from differential thermal expansion. At high flow rates, the CO_2 was not adequately heated and the exchanger and makeup lines would freeze. The new double-pipe heat exchanger was constructed out of 2.5 cm steel black pipe and 1.3 cm OD stainless steel tubing. The heater consisted of two 10 foot sections and was operated in parallel. Steam flow was on the shell side and the liquid CO_2 was on the tube side. In the new design, steam flow was directed in parallel to the heat exchangers and to the CO_2 regulator, whereas before, the steam flowed in series with the heat exchanger and regulator.

In the third campaign, the Gasmet DX-4000 FTIR from Temet Instruments was used for the analysis the absorber outlet gas stream. The FTIR has an accuracy of less than 2% of the measuring. The FTIR measured the concentration of CO_2 and water, MEA volatility, and ammonia accumulation for the MEA

campaign. The FTIR was not connected to the DeltaV system because the Modbus hardware had not been purchased. Instead, the Calmet software that came with the FTIR was used to record the data. The results for the MEA campaign can be found in Dugas (2006).

2.5.2 Campaign 3 Summary

In Campaign 3, several issues from Campaign 1 were resolved, which include: (1) The control valve was moved upstream of the inlet nozzle. (2) Two pumps were used in series to pressurize the stripper feed. (3) The liquid sampling and handling procedure developed in Campaign 2 were successfully implemented. (4) The results for CO_2 loading were corrected with standards placed periodically in between samples during the analysis. (5) Diluted liquid samples and standards were covered with parafilm to minimize CO_2 absorption

After the completion of Campaign 3, it was found that there were several issues that needed to be resolved. These issues include: (1) The stripper feed pre-heater was undersized. (2) The stripper feed was flashing across the control valve at the top of the stripper, which resulted in poor mass transfer performance. (3) The absorber inlet and outlet conductivity meters were unreliable and the two meters eventually failed. (4) The reboiler developed pin-hole sized leaks. (5) The absorber gas flow measurement did not zero properly.

2.6 Campaign Four – Optimized K^+/PZ Process Configuration

The main objective of the last campaign was to obtain absorber and stripper data for the aqueous piperazine and potassium carbonate system with an optimized configuration. Based upon the learning experience from the three preceding campaigns, the optimized configuration included modifications such as a new plate and frame cross-exchanger, new high capacity Flexipac AQ Style 20 structured packing for the absorber and stripper, and a new heater for the

absorber inlet gas. Data for the 5 m K^+/2.5 m PZ solvent was generated with the new packing and was compared to the Flexipac 1Y packing used in the previous campaigns.

The second objective was to test another K^+/PZ solvent composition. The first half of Campaign 3 was conducted with the 5 m K^+/2.5 m PZ solvent and 6.4 m K^+/1.6 m PZ solvent was used in the latter half. The second solvent composition has a heat of absorption that is 50% lower than 5 m K^+/2.5 m PZ. The CO_2 capacity of 6.4 m K^+/1.6 m PZ is also expected to be 0–10% higher than 5 m K^+/2.5 m PZ. The CO_2 absorption rate is expected to be 40% less than the 5 m K^+/2.5 m PZ solvent. Experiments with the second solvent composition should help establish the tradeoffs between fast CO_2 absorption rates, low heat of absorption and higher capacity solvents.

2.6.1 Bench-scale Experiments and Results

2.6.1.1 Potassium Carbonate and Piperazine Solubility

In order to determine the absolute concentrations of the second solvent, solubility experiments were conducted with 4 different compositions: 6 m K^+/1.5 m PZ, 6.4 m K^+/1.6 m PZ, 6.8 m K^+/1.7 m PZ, and 7.2 m K^+/1.8 m PZ. The ratio of potassium to piperazine was maintained at four. Experiments were conducted at 40, 50, and 60 °C and four different CO_2 loadings for each solution. Higher piperazine and potassium concentrations result in faster absorption rates and larger solution capacities, respectively. However, as the total concentration increases, the risk of salting out the potassium bicarbonate or precipitating piperazine also increases. The results are shown in Table 2-12.

At low CO_2 loadings, piperazine tended to form a separate layer from the potassium carbonate/bicarbonate solution. At rich CO_2 loadings, the potassium bicarbonate tended to salt out, precipitating as fine white crystals. The table

shows that at 40 °C, only the 6.4 m K^+/1.6 m PZ solvent composition does not phase separate or form precipitates over the loading range that the pilot plant will be operated. This particular solvent composition was selected for the fourth campaign.

Table 2-12. Potassium Carbonate/Piperazine Solubility Experiments

Composition	Temp (°C)	Loading (mol CO_2/mol K^+ + 2mol PZ)	Observation
6 m K^+/1.5 m PZ	40	0.33	2 Liquid Layer
		0.44	Fully Dissolved
		0.56	Fully Dissolved
		0.67	$KHCO_3$ Precipitate
6.4 m K^+/1.6 m PZ	40	0.40	Fully Dissolved
		0.47	Fully Dissolved
		0.53	Fully Dissolved
		0.60	Fully Dissolved
6.8 m K^+/1.7 m PZ	40	0.40	Fully Dissolved
		0.47	White Precipitate
		0.53	White Precipitate
		0.60	White Precipitate
6.8 m K^+/1.7 m PZ	50	0.40	Fully Dissolved
		0.47	White Precipitate
		0.53	White Precipitate
		0.60	White Precipitate
6.8 m K^+/1.7 m PZ	60	0.40	Fully Dissolved
		0.47	White Precipitate
		0.53	White Precipitate
		0.60	Fully Dissolved
7.2 m K^+/1.8 m PZ	40	0.33	2 Layers, Solid Top Layer
		0.42	White Precipitate
		0.50	White Precipitate
		0.58	White Precipitate

2.6.1.2 Density and pH Measurements

Previous density measurements of the piperazine promoted potassium carbonate solvent were limited to a temperature of 40 °C. It was desired to measure the density of the solvent over a temperature ranging from 40 to 60 °C.

Hydrometers from Fisher Science were procured. A cylindrical water tank was constructed out of Plexiglas. A water bath was used to heat the water and circulate the warm water through the water tank. To make a density measurement, approximately 300 mL of solvent was poured into a graduated cylinder. The hydrometer was placed in the graduated cylinder, which was then immersed in the heated water tank. A K-type thermocouple measured the temperature of the solvent and a magnetic stir bar was used to mix the solvent and maintain a uniform temperature throughout the cylinder. The stir bar was turned off when density measurements were recorded.

Density measurements were taken for the 5 m K^+/2.5 m PZ solvent and for the 6.4 m K^+/1.6 m PZ solvent at two different loadings. In addition, a density measurement was taken for the pilot plant solution. The results from the density measurements show that density decreases linearly with an increase in temperature (Figure 2-19). The figure also shows that density is not very sensitive to CO_2 loading and piperazine concentration, which corroborates the density measurements made by Cullinane on a densitometer instrument.

Bench-scale measurements of pH were made for the 6.4 m K^+/1.6 m PZ solvent at four different CO_2 loadings and over a temperature range from 40 to 60 °C. The pH measurements will be used in the pilot plant operations for controlling lean loading to the absorber. Measurements were made with a Cole Parmer pH meter. Figure 2-20 shows bench-scale measurements of pH dependence on CO_2 loading at different temperatures. The trends indicate that there is inconsistent variation of pH with temperature. However, pH does vary with CO_2 loading. The general slope of the bench-scale measurements can be used to determine online CO_2 loading values of the pilot plant once a pH and corresponding CO_2 loading value is established.

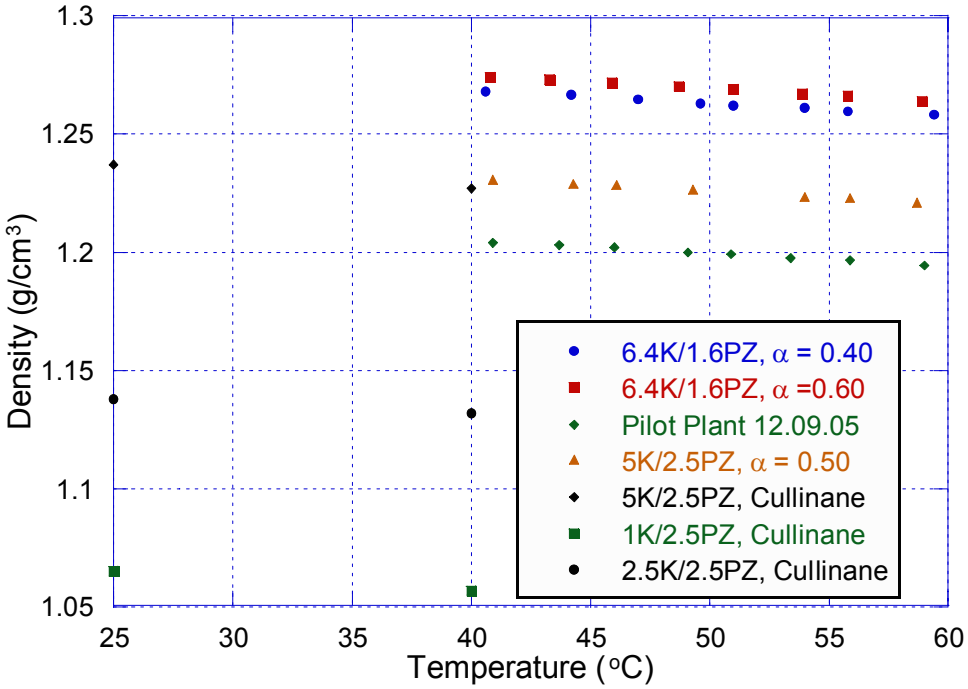

Figure 2-19. Bench-scale Measurements of Density for 5 m K^+/2.5 m PZ and 6.4 m K^+/1.6 m PZ as a Function of Temperature

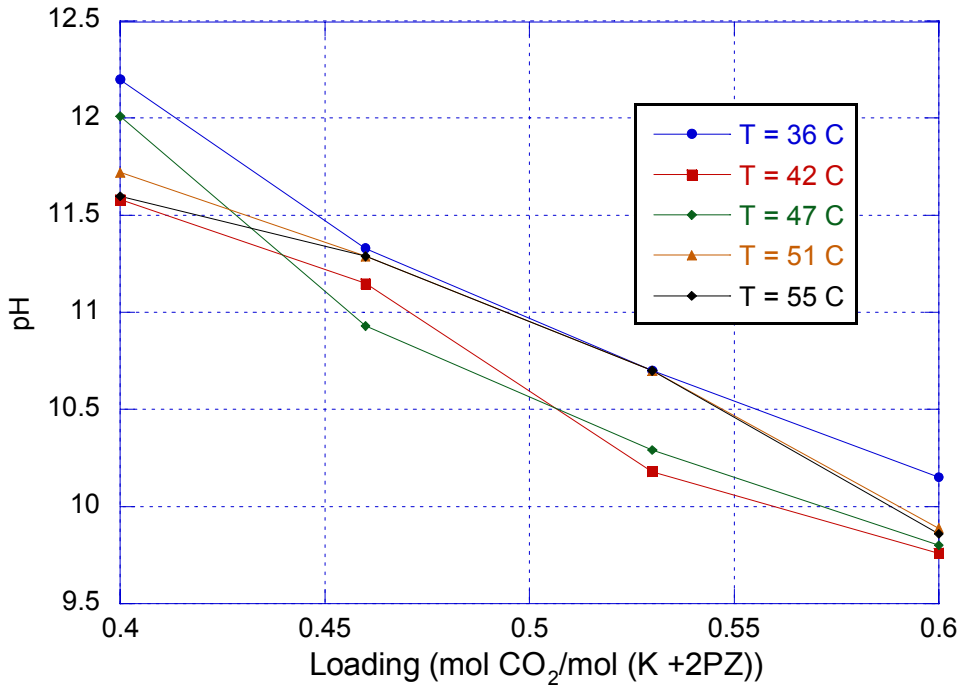

Figure 2-20. Measurements of pH for 6.4 m K^+/1.6 m PZ at 36 – 55 °C.

2.6.2 Campaign 4 Modifications

During the third campaign, even with the new modifications, the stripper feed stream was still pre-heated inadequately. In Campaign 4, a new plate and frame cross-exchanger was purchased from Alfa Laval. The Alfa Laval M6-FG exchanger was sized for a 10 °C temperature approach and a pressure drop of 1.0 bar. The exchanger has a heat transfer area of 14.8 m^2, consists of 99 plates and is arranged for 5 pass flow. It is constructed of type 316 stainless steel and contains EPDM gaskets. The cost of the plate exchanger was approximately $5000.

Figure 2-21 illustrates the new absorber/stripper configuration of Campaign 4. In the cross-exchanger, the hot lean stream from the reboiler is used to preheat the cold rich stream leaving the absorber outlet. The existing feed preheater was used as a trim heater and was installed downstream of the cross-exchanger to simplify the amount of flow instrumentation and reduce costs. The process and instrumentation diagram for the absorber and stripper are shown Figures 2-22 and 2-23, respectively.

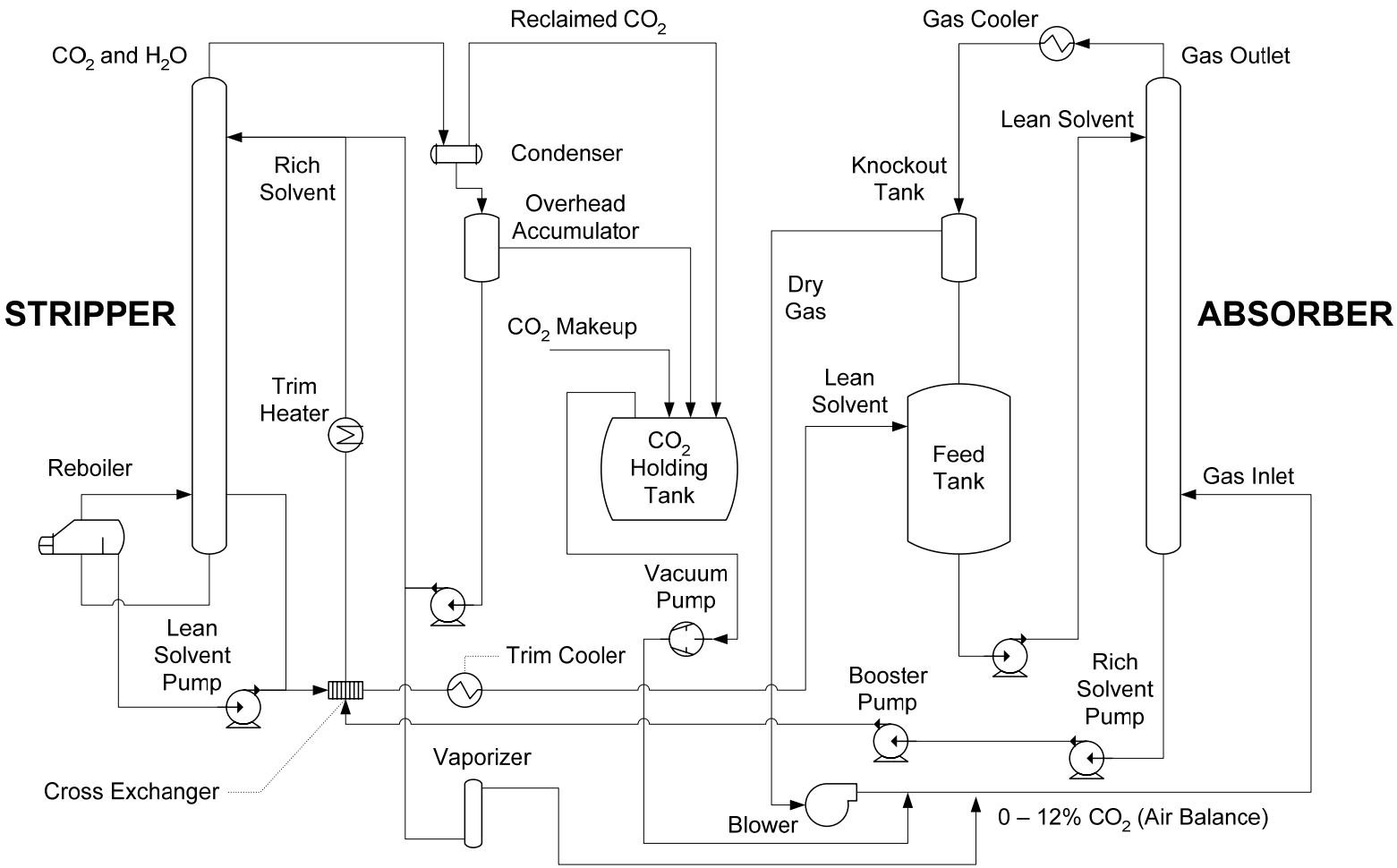

Figure 2-21. Absorber/Stripper Pilot Plant Configuration for Campaign 4

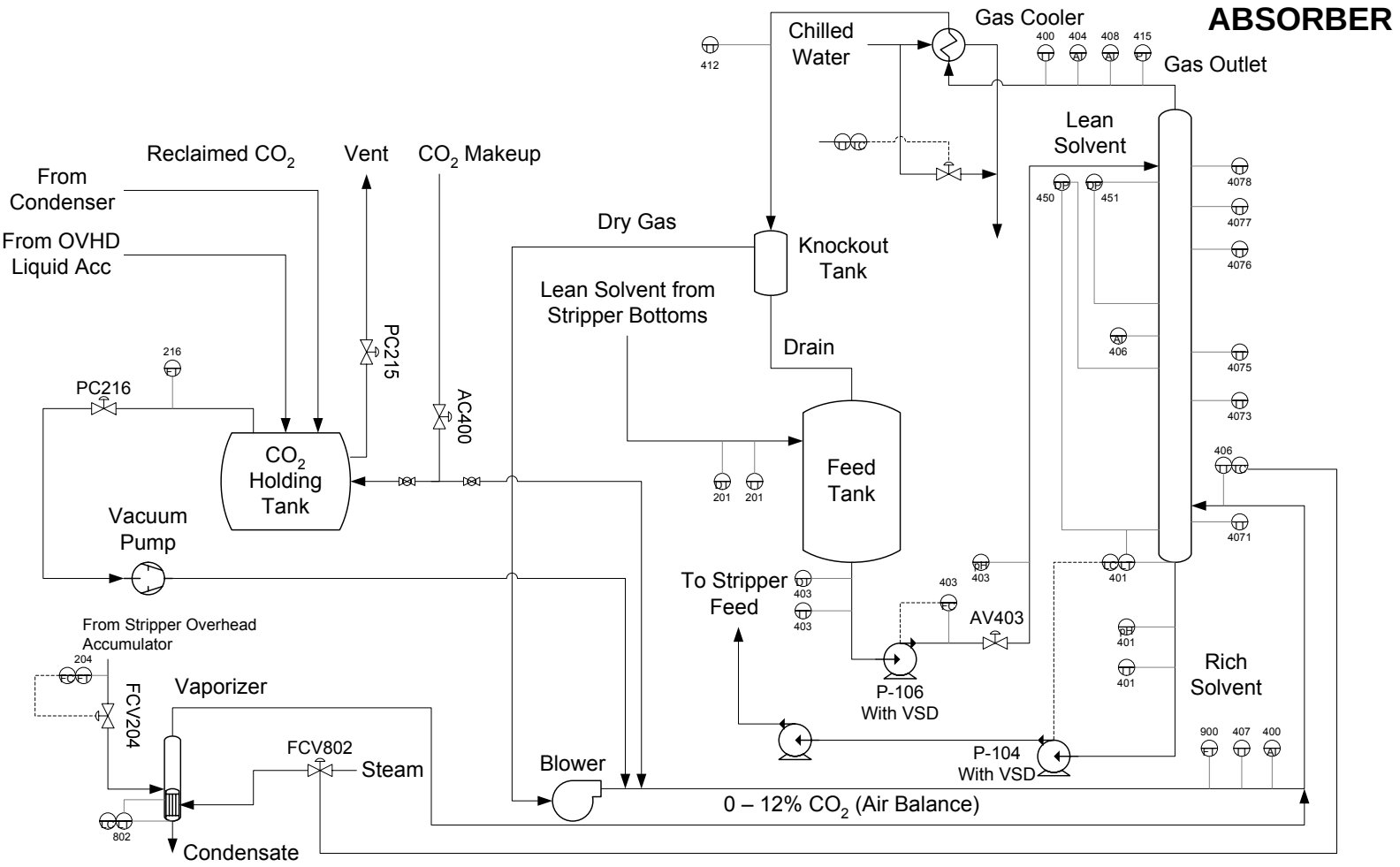

Figure 2-22. Process and Instrumentation Diagram of the Absorber for Campaign 4

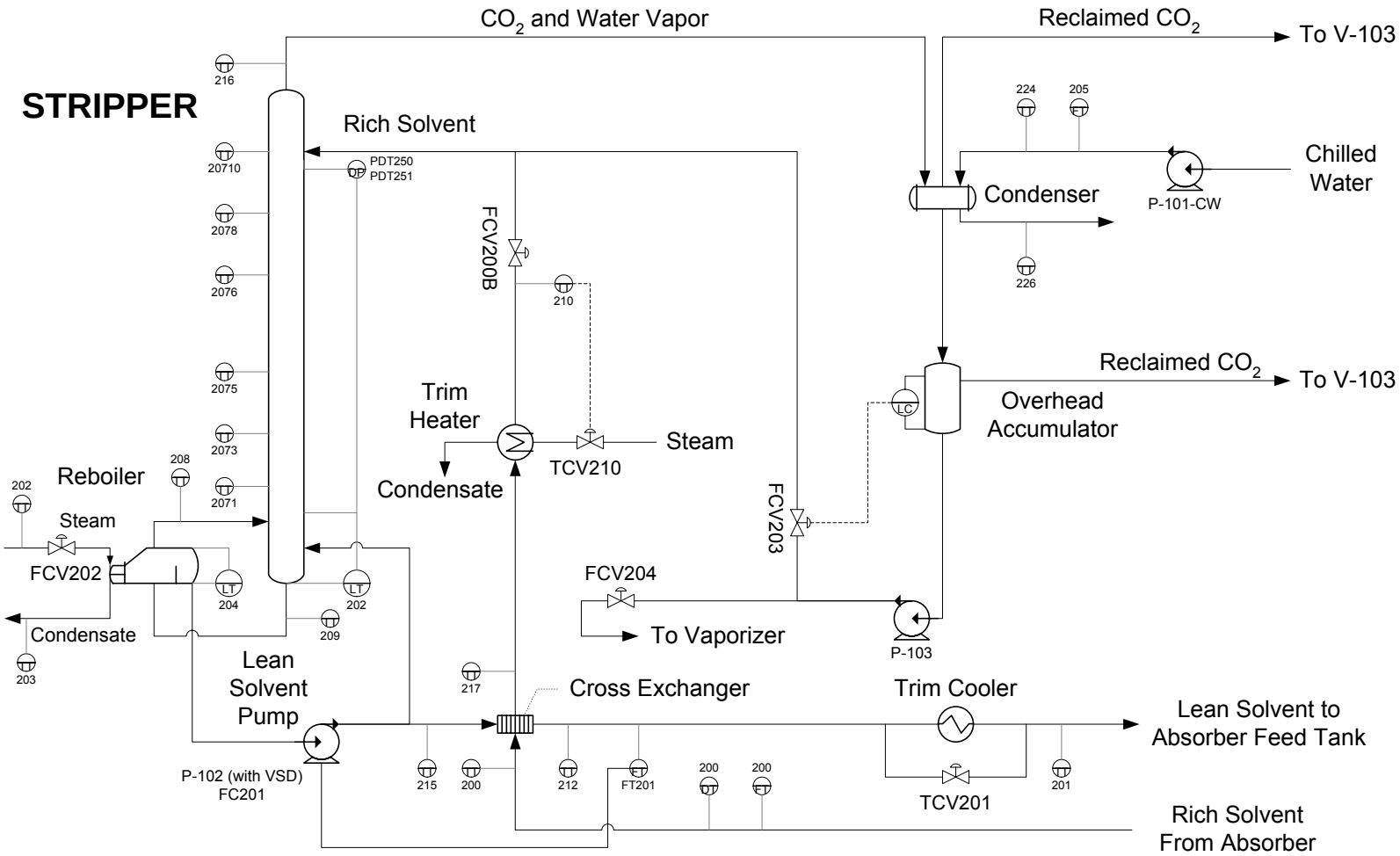

Figure 2-23. Process and Instrumentation Diagram of the Stripper for Campaign 4

In the MEA campaign, the air cooler was operated to protect the Vaisala CO_2 probe and the blower recycle was used to preheat the gas. However, the absorber inlet gas was not adequately preheated and was not saturated with water. To remedy this problem, an existing 10.2 cm reboiler was retrofitted and used to generate steam and heat the inlet gas. Distillate from the stripper condensate supplied the water for the reboiler. The level in the preheat reboiler was maintained by adjusting the steam flow to the 10.2 cm reboiler. Approximately 0.6 gpm of water is needed to saturate the inlet absorber gas to 20% water at a gas flow rate of 500 cfm. A 2.5 cm pipe was installed from the reboiler to the inlet gas line. The steam generated from the reboiler was injected into the inlet absorber gas downstream of the Vaisala CO_2 analyzers.

In the third campaign, the PVC pipe for the blower recycle was melted and partially destroyed due to the excessive heat that occurred during the loading of the MEA solution. The pipe for the blower recycle was replaced with stainless steel pipe. In the fourth campaign, the remaining 20.3 cm PVC gas lines were replaced with 20.3 cm 304 L stainless steel pipe. In addition, the 7.6 and 10.3 cm schedule 40 PVC pipe for the gas flow rate was replaced with a single 10.3 cm schedule 10 stainless steel pipes. The blower recycle was not operated during Campaign 4.

In the fourth campaign, the Dietrich Standard Diamond II GCR-15 Annubar used in the 10.3 cm line from Campaign 3 was used to measure gas flow rate. The annubar was originally sized for schedule 40, but was used in the new 10.3 cm schedule 10 pipe. Corrections to the inner diameter were made in DeltaV. In addition, three Rosemount differential pressure transmitters with different pressure ranges and a Rosemount RTD for temperature measurement were used. The flowmeter has an accuracy of ±1% of the actual value. Flow straighteners were installed upstream of the annubar to ensure the flow

measurement was accurate. The flow meter was calibrated for air. In the interpretation of the data, density corrections were made to account for CO_2 and water.

The existing carbon steel reboiler for the stripper developed pinhole-sized leaks during the MEA campaign. Prior to the start of the fourth campaign, a new stainless steel kettle reboiler was installed and insulated. The new reboiler has the same design and specification as the original carbon steel reboiler.

Figure 2-24. Stainless Reboiler and Stripper Column Sump with Calcium Silicate Insulation

An orifice plate was installed in the cooling water line to the air cooler instead of a control valve to simplify plant operation. The cooling water removed most of the moisture from the absorber outlet gas stream to protect the downstream Vaisala CO_2 probe. The condensate from the air cooler and the knockout filter drained to the absorber feed tank.

To provide the capability of measuring multiple gas components, the Gasmet DX-4000 FTIR from the MEA campaign was retrofitted into the pilot plant in the fourth campaign. Two 30.5 m heated lines were procured from Environmental Supply Company, one for the absorber inlet and one for the outlet. The heated lines consist of 0.6 and 1.0 cm OD PFA lines. An additional sample pump and heater module for the FTIR was purchased from Air Quality Analytical, Inc. Gas samples were simultaneously drawn from the absorber inlet and outlet. The temperature of the heated line was maintained at 180 °C. The gas analysis was alternated between the two sample-points via a three way valve located inside a heated box. A MODBUS card was used to connect the FTIR computer to the DeltaV process control system. The FTIR was used measure CO_2 and water concentration and piperazine volatility. In addition, two new Vaisala CO_2 probes with concentration ranges of 0–5% and 0–20% were purchased and used to replace the two existing Vaisala probes.

An activated carbon filter system was designed and installed to mitigate recurring foaming issues encountered during the first two campaigns. Two types of filters from Rosedale Products, Inc. were purchased: 4–12 filter housing with a single pass carbon holding basket (Part No. 4-12-SP-304) and 4–12 bag filter housing with EPR gaskets. Both filters were made of type 304 stainless steel. The filter system was based on literature recommendations and was designed to filter 10–15% of the total lean solvent stream. The design allowed for the removal of enough degradation products without removing antifoam. The filter that contained activated carbon was installed downstream of the absorber lean Micro Motion® flowmeter. The second bag filter was installed downstream of the carbon filter to capture fine charcoal particles.

Two types of activated carbon were available. Activated carbon from the filter manufacturer contained 10 x 50 mesh size activated carbon and was made

of virgin coconut hulls. In addition, a lignite-based 8 x 30-mesh PETRODARCO activated carbon from NORIT was purchased. Four different filter bag materials (Nomex®, cotton, viscous rayon, and nylon) were tested because of material compatibility issues arising from the use of polyethylene in the previous campaigns. The filter materials were tested in warm solvent solutions and it was found that cotton performed the best based on visual inspections.

2.6.3 Campaign 4 Analytical Methods

2.6.3.1 CO_2 Analysis

The fourth campaign used the same liquid sample collection and preservation method developed in Campaign 2. In the fourth campaign, the sample bombs were slightly modified through the use of clear PFA tubing instead of the stainless tubing originally used. This allowed the sample collector to visually verify whether the sample collection was successful. During the fourth campaign, the middle liquid samples for the absorber and stripper both seem to be problematic at times. It was possible that the sample lines may have become partially blocked, which resulted in very low flows.

The liquid sample extraction procedure followed the standard methods developed over the course the last 3 campaigns. Ten milliliters of sample are withdrawn from the sample bombs with a syringe and injected into a vial containing 30 mL of chilled deionized water. For CO_2 loading analysis, the samples were further diluted by a factor of 40 and then analyzed on the Shimadzu 5050 Total Organic Carbon analyzer by utilizing its inorganic carbon analysis feature. Inorganic carbon standards of 100 ppm were placed every 6–7 samples to maintain quality control.

2.6.3.2 *Piperazine and Potassium Analysis*

2.6.3.2.1 Ion Chromatography Method Development and Analysis

A new IC column was purchased and installed in the ion chromatography analyzer. The new column was better suited for piperazine and amine analysis. A new method was developed for measuring piperazine and potassium on the IC. The method takes approximately 5 minutes and uses 6 mM and 55 mM monosulphonic acid (MSA) as the eluent. The standards contained both piperazine and potassium and a calibration curve were generated over the following range of concentrations: 0, 10, 20, 30, 40, and 50 ppm K^+/PZ. The liquid samples analyzed on the ion chromatograph were further diluted by a factor of 2000 from the pre-diluted 4:1 samples. The ion chromatography analyzer was calibrated with standards that contained both piperazine and potassium. Additional details regarding the new IC method for measuring K^+ and PZ can be found in the appendix.

Prior to the start of Campaign 4, selected K^+/PZ samples from the first and second campaign were analyzed with new IC method. The concentrated pilot plant solutions from Campaign 1 were diluted by a factor of 4000 and the prediluted pilot plant samples from Campaign 2 were diluted by a factor of 1000. Tables 2-13 through 2-15 show the results of the sample analysis for the first two campaigns using the newly developed IC method. The results show that total alkalinity was not as well correlated to density measurements as previously assumed, which was based on Campaign 1 data. The total alkalinity results from the IC for Campaign 1 and Campaign 2 seem to show good agreement with the total alkalinity values obtained using the acid titration method used in those campaigns. The tables seem to show that there was some loss of potassium in between the transition from Campaign 2 to the current campaign. The pilot

plant samples were taken from the bottom of a large storage tank and therefore, may not have been a representative sample.

Table 2-13. Campaign 1 IC Results

Campaign 1 Data	K^+ gmol/kg	PZ gmol/kg	TAlk gmol/kg	K^+/PZ	Density kg/m^3
C1 6/16 AL 17:00	2.3293	1.5802	5.4896	1.4741	1146.6
C1 6/17 AL 13:00	2.5907	1.4356	5.4619	1.8046	1162.4
C1 6/22 AL 17:45	3.2496	1.634	6.5177	1.9887	1206.1
C1 6/22 AL 19:30	3.2348	1.6258	6.4864	1.9897	1206.4
C1 6/23 AL 08:15	3.2509	1.6377	6.5263	1.9851	1212.6
C1 6/23 AL 18:10	3.3146	1.6624	6.6393	1.9939	1211.9
C1 6/24 AL 17:30	3.3365	1.5987	6.5339	2.0870	1228.1

1. Results are in mol/kg of solvent
2. TAlk = Total Alkalinity (mol CO_2/(mol K^+ + 2 mol PZ))

Table 2-14. Campaign 2 IC Results

Campaign 2 Data	K^+ gmol/kg	PZ gmol/kg	TAlk gmol/kg	K^+/PZ	Density kg/m^3
C2 AL8	2.8981	1.2421	5.3823	2.3332	1224.3
C2 AL11	3.0807	1.3216	5.724	2.331	1228.2
C2 AL13	2.908	1.2493	5.4066	2.3278	1227.0
C2 AL14	2.7736	1.205	5.1836	2.3018	1226.2
C2 AL16	3.085	1.327	5.739	2.3248	1228.4
C2 AL22	2.9487	1.2591	5.4669	2.3418	1230.4
C2 AL37	3.2303	1.3927	6.0158	2.3194	1224.4
C2 AL38	3.027	1.3038	5.6346	2.3218	1219.5
C2 AL43	2.9179	1.2404	5.3987	2.3523	1229.1
C2 AL 26	2.8967	1.2393	5.3753	2.3373	1228.5

1. Results are in mol/kg of solvent
2. TAlk = Total Alkalinity (mol CO_2/(mol K^+ + 2 mol PZ))

Table 2-15. IC Results of Pilot Plant Composition Prior to Campaign 4 Start-up on 12/09/05

K^+	PZ	TAlk	K/PZ	Density
gmol/kg	gmol/kg	gmol/kg		kg/m3
3.0208	1.5888	6.1983	1.9013	1204

1. Results are in mol/kg of solvent
2. TAlk = Total Alkalinity (mol CO_2/(mol K^+ + 2 mol PZ))

The results from Campaign 2 of the titration and ion chromatograph are compared in Figure 2-25. The average difference between the ion chromatography and titration method for potassium, piperazine, and total alkalinity (mol K^+ + 2 mol PZ) was 2.8%, -5.2% and -0.89%, respectively. It can be concluded that the measurement of total alkalinity can be reliably determined by both methods. However, the piperazine concentration was consistently higher for the titration method and because the potassium concentration was calculated as a difference between total alkalinity, it was consequently lower. This discrepancy is most likely due to errors with the perceived endpoint (-265 mV) in the titration method (-265 mV). Instead the determination of piperazine concentration should have taken the difference between the two inflection points of NaOH titration. This technique is further detailed in the revised titration method section.

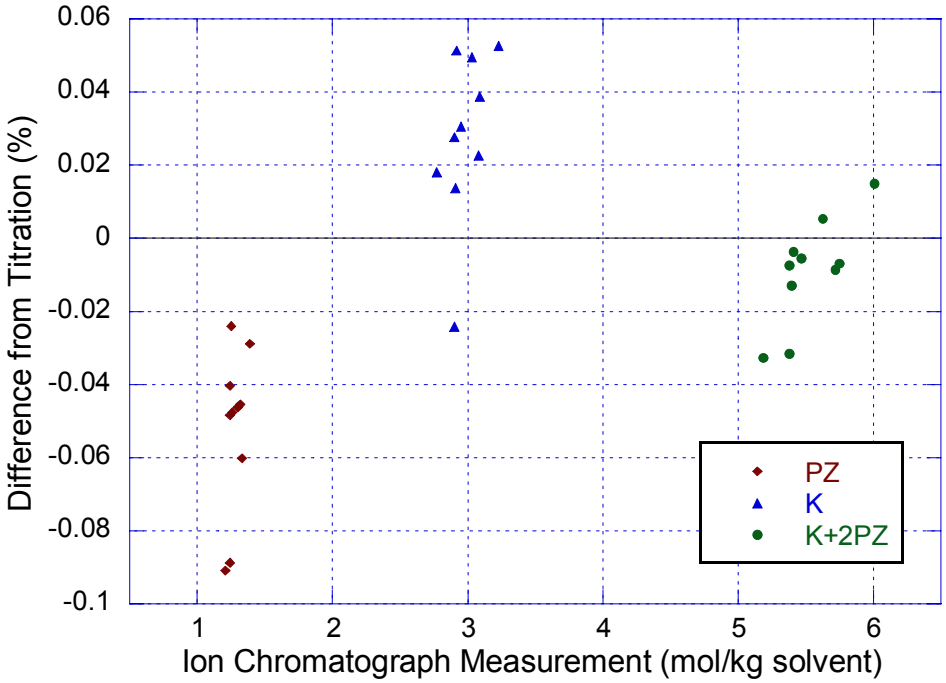

Figure 2-25. Comparison of Titration and Ion Chromatography Measurements of K^+ and PZ Concentration for Campaign 2

2.6.3.2.2 Revised Titration Method

In Campaign 4, the titration method that was used in Campaigns 1 and 2 was refined. However, it was only used during the campaign to perform a real-time check of the solution composition and was not used as the primary analysis of piperazine and potassium concentration. In the new titration method, due to the 3:1 dilution of liquid samples, the concentrations of both HCl and NaOH were changed to 0.2 N instead on 2 N. Also, the pH of the liquid sample was measured and recorded during the forward and back titrations instead of relying on methyl orange as the color indicator and titration to 265 mV to obtain piperazine concentration. The inflection point of the forward acid titration curve measures the total alkalinity of the solution (Figure 2-26).

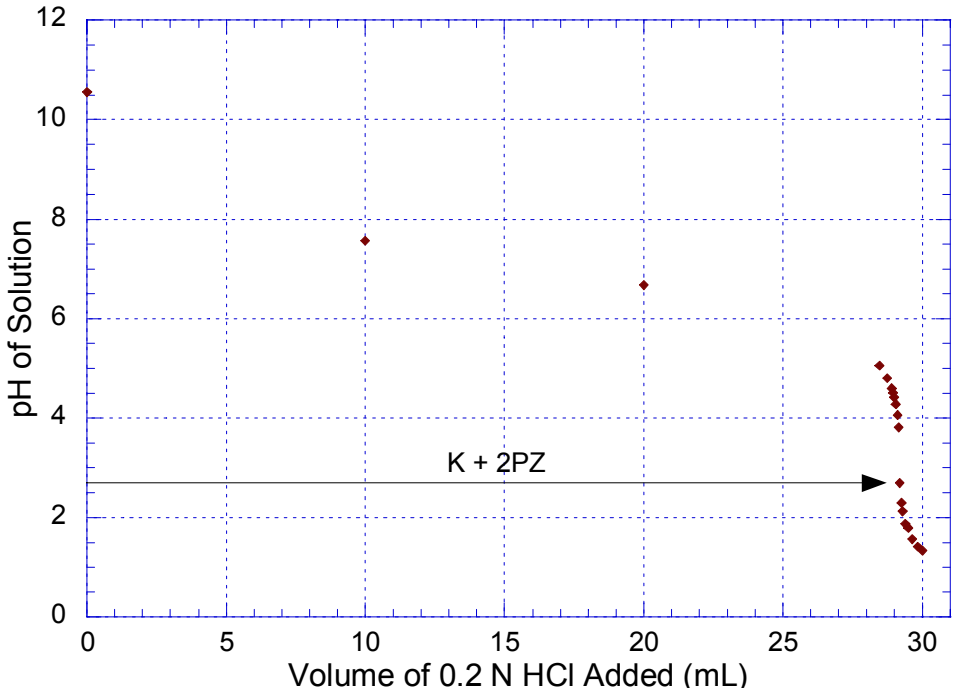

Figure 2-26. Forward Titration of 5 m K^+/2.5 m PZ solution with 0.2 N HCl to Determine the Total Alkalinity (mol K + 2 mol PZ)

The difference between the two inflection points for the back titration with 0.2 N NaOH gives the concentration of piperazine (Figure 2-27). The potassium concentration was determined by taking the difference between total alkalinity and two times the piperazine concentration. Two sets of titrations were performed on a known solution of 5 m K^+/2.5 m PZ solution to verify reproducibility (Table 2-16). Titrations were performed with 2 N HCl and 2 N NaOH with approximately of 10 grams of undiluted solution. The results indicate that using the two endpoints for the back titration method yielded results that were 1.5% higher than that calculated. However, the difference in measurement of total alkalinity was less than 1% in one case and approximately 9% in the other. In the 9% error case, the burette containing acid needed to be refilled during the titration process. It is possible that during the refilling process, CO_2 may have been absorbed by the sample and required excess HCl.

Table 2-16. Validation of Reproducibility of Modified Titration Method Using Acid-Base Endpoints Determined from Direct pH Measurements

Sample ID	K+2PZ Expected	K+2PZ Measured	Diff %	PZ Expected	PZ Measured	Diff %
1	5.83	6.35	8.9	1.46	1.44	1.3
2	5.83	5.83	0.05	1.46	1.44	1.2

The original method for determining piperazine by back titrating to a reading of ~265 mV was not accurate because significant errors were introduced if the forward acid titration was overshot. Additional NaOH would need to be added to neutralize the excess acid and would result in an erroneous higher piperazine concentration and lower potassium concentration.

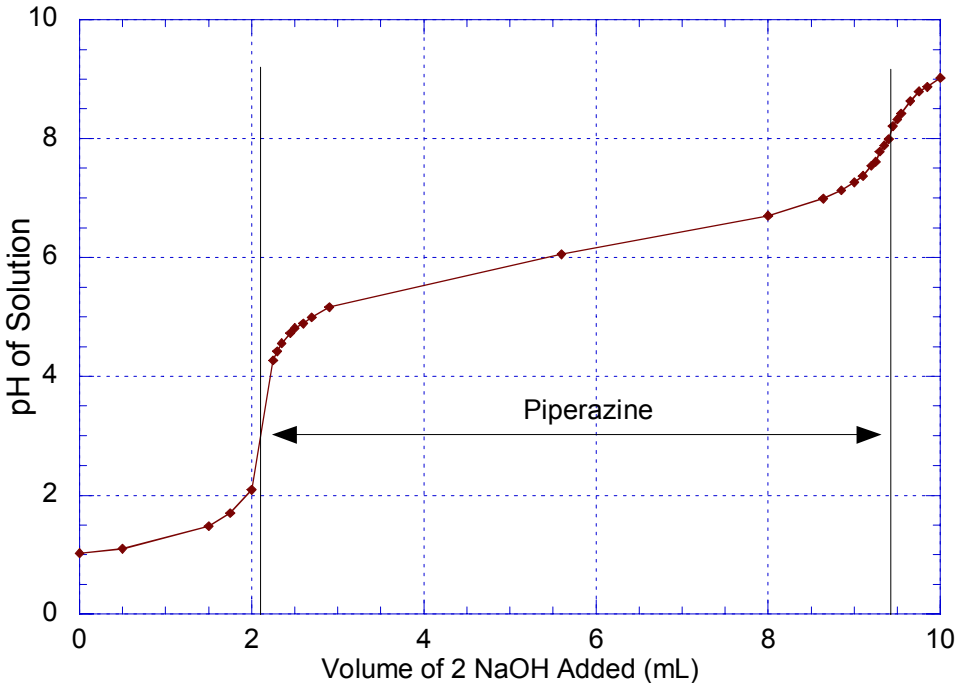

Figure 2-27. Back Titration of 5 m K^+/2.5 m PZ solution with 0.2 N NaOH to Determine the Piperazine Concentration

In addition, titration measurements were performed on absorber lean and absorber rich pilot plant solutions to verify that the endpoints from direct pH

measurements and methyl orange technique matched. The results show that if both methods are performed properly, a difference of approximately 1% could be achieved (Table 2-17). Approximately 49 grams of water was added to 0.55 grams of sample prior to the start of each titration. The pH of the solution was recorded while the 0.2N HCl acid was added continuously. The titration curve for the absorber lean sample is shown in Figure 2-28.

Table 2-17. Validation of Methyl Orange Indicator with pH Measurement Based Titration Method Using 0.2 N HCl and Pilot Plant Samples Diluted 90:1

Sample ID	Date/Time	Total Alkalinity Methyl Orange	Total Alkalinity pH	Difference %
AL	01/09/06 13:30	5.51	5.55	-0.6
AR	01/09/06 13:30	5.37	5.42	-1.0

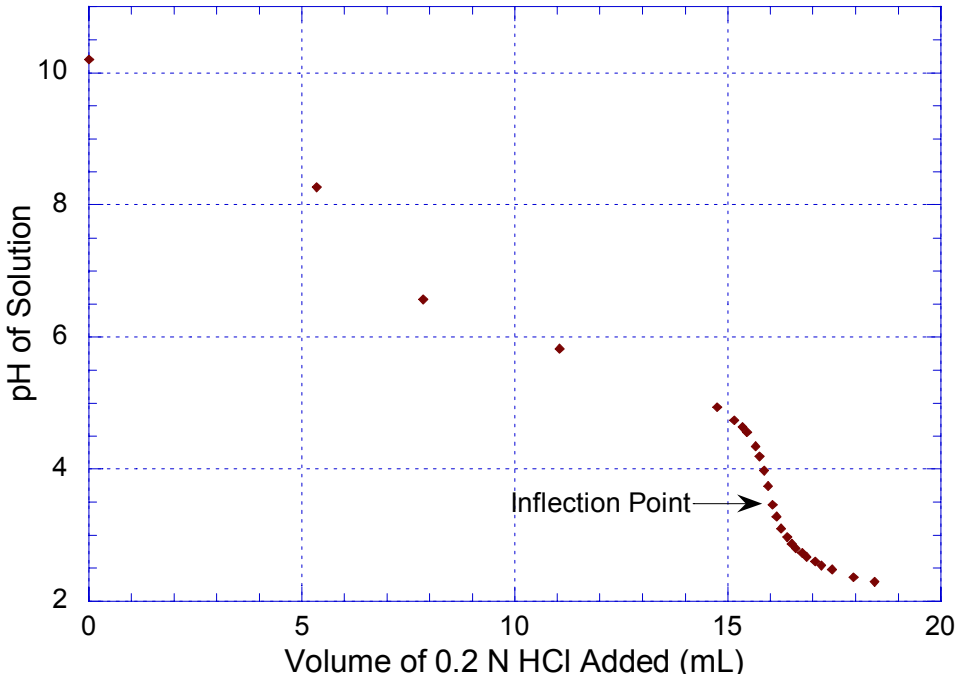

Figure 2-28. Titration of Absorber Lean Pilot Plant Sample (Taken 1/09/06 - 13:30) with 0.2 N HCl to Determine Total Alkalinity (mol K^+ + 2 mol PZ)

In Campaign 4, the ion chromatograph was used as the primary analysis of piperazine and potassium concentration. A few titrations were performed during the operation of the pilot plant for on-site verification of total alkalinity. The titration measurements were consistently lower than the results obtained by the post-campaign IC analysis (Table 2-18).

Table 2-18. Concentration of Piperazine and Potassium from Campaign 4 for the Titration and Ion Chromatograph Methods

Sample ID	Titration gmol/kg soln	Ion Chrom gmol/kg soln	Diff %
AL 97	5.55	6.12	10.4
AL 100	5.73	6.11	6.6
AL 103	5.66	6.00	6.2

Although the IC and titration total alkalinity results of Campaign 2 matched, the titration and IC methods were slightly changed. The new titration method used a more dilute acid, which should actually make the method more accurate. Also, the Campaign 4 titrations were conducted using the pH end-point method, whereas the Campaign 2 method was titrated to the methyl orange endpoint. Sometimes it was difficult to determine when a color change had occurred.

This section has shown that the results from the two endpoint methods have a difference of less than 2%. In Campaign 4, the IC method was slightly modified from that used in the Campaign 2 sample analysis. The original IC method had a retention time of approximately 30–40 minutes. Due to the high volume of samples that were collected and to achieve a higher throughput, the method was modified to have a retention time of approximately 5–10 minutes. This may have slightly degraded the precision of the ion chromatograph analyzer. The performance of the column may also have degraded due to the

build up of residual analytes. For certain sets of analyses, the absorber lean sample analysis seemed to have substantial deviation from the absorber middle and absorber rich samples. Other concerns include degradation products of piperazine that may further complicate interpretation of the IC results.

Overall, the IC method appeared to have a precision of approximately 10%. It was concluded while the IC method may be more efficient at analyzing a large number of samples, the titration method may be more accurate and precise for piperazine and potassium determination.

2.6.3.3 Revised CO_2 Gas Concentration Analysis

Initially, there was some confusion regarding whether the gas cylinders were in mole or weight percent. The certificate of analysis for the CO_2 standards states that the cylinders are gravimetrically filled with CO_2 and air. The concentration of CO_2 is then verified by the vendor through gas chromatography/thermal conductivity detection (TCD) analysis. In the earlier campaigns, it was assumed that the standards were in weight percent and a 16.9% gas cylinder was ordered, which was supposed to be in weight percent. Two of CO_2 cylinders were analyzed by another research group using gas chromatography (GC). The GC analyzer was calibrated to measure mixtures of CO_2, CH_4, and C4. Thus, slight discrepancies may be expected. Analysis of the 12% and 16.9% CO_2 cylinders by the GC method resulted in CO_2 concentrations of 13.2 mol% and 18.3 mol%, respectively. It was concluded that the CO_2 standards were in mole percent and not weight percent because the analysis was closer to the mole percent values.

2.6.4 Campaign 4 Plant Operation

The final pilot plant campaign using potassium carbonate and piperazine commenced at the beginning of January 2006 and was completed in early

February 2006. The pilot plant was operated for 12 days, 24 hours per day. A total of 59 runs and 33 operating condition were completed. Approximately 300 liquid samples were taken and analyzed for CO_2 loading, piperazine and potassium concentration. The newly installed cross-exchanger reduced the approach temperature to less than 10 °C.

The experiments were conducted with two different solvent compositions: 5 m K^+/2.5 m PZ and 6.4 m K^+/1.6 m PZ. The absorber and stripper were both packed with a new structured packing, Flexipac AQ Style 20, which was donated by Koch-Glitsch Inc. The new structured packing has a specific surface area of 213 m^2/m^3, which is approximately 50% less than the Flexipac 1Y packing used in the previous campaigns. Flexipac AQ Style 20 packing has a steeper corrugation angle (50 degrees), whereas the Flexipac 1Y packing has a corrugation angle of 45 degrees. As a result, the new packing has less surface area, a lower liquid holdup, and will be less efficient. The packing has a higher capacity and will permit operation at high gas rates with reduced pressure drop.

The absorber and stripper column each contained 6.1 m of Flexipac AQ structured packing, which was divided into two 3.05 m beds. In between the top and bottom bed of packing there was a chimney tray and an orifice riser redistributor. In the stripper, a Montz II distributor was used in the upper bed and a Koch collector plate with an inverted screen and a 4C redistributor was used for the bottom bed. The absorber contained a Koch 3C distributor at the top and a chimney tray and Montz II redistributor for the bottom bed.

In the fourth campaign, the air cooler was in full operation and was used to protect the Vaisala CO_2 analyzers that were downstream. The newly installed cross-exchanger performed as designed and the trim heater and cooler were not used during the campaign. A summary of the absorber and stripper operations is shown in Tables 2-19 and 2-20, respectively.

Table 2-19. Campaign 4 Absorber Operation

Parameter	5 m K^+/2.5 m PZ	6.4 m K^+/1.6 m PZ
Inlet CO_2 (mol%)	8.0 – 17.6	14.3 – 18.0
PZ Concentration[1] (mol/kg)	1.4 – 1.5	1.0 – 1.2
K^+/PZ Ratio	2.1 – 2.3	3.9 – 4.0
Lean Loading[2] (mol CO_2/TAlk)	0.39 – 0.45	0.45 – 0.51
G (kg/m^2-s)	1.2 – 2.0	1.2 – 2.0
L/G (kg/kg)	3.9 – 10.8	8.3 – 14.5
$T_{GAS,IN}$ (°C)	40	40 – 41
T_{LEAN} (°C)	40 – 46	39 – 46

1. Concentration in mol/kg of solvent
2. TAlk = Total alkalinity (mol K+2 mol PZ)

Table 2-20. Campaign 4 Stripper Operation

Parameter	5 m K^+/2.5 m PZ	6.4 m K^+/1.6 m PZ
ΔT Approach (°C)	6.9 – 8.9	3.7 – 6.4
Top Temperature (°C)	103 – 115	71.5 – 94
Bottom Temperature (°C)	117 – 118	77 – 97
Reboiler Heat Duty (kcal/mol CO_2)	85 – 290	90 – 180
NTU per pass (5 pass PFE)	1.5 – 2.1	1.5 – 1.9
$C_{P,COLD}/C_{P,HOT}$	1.04 – 1.08	1.05 – 1.11

In Campaign 4, foaming occurred in the stripper instead of the absorber, which occurred in the first 2 campaigns. The magnitude of the temperature bulge was not as significant in the absorber for the 6.4 m K^+/1.6 m PZ solvent due to the slower CO_2 absorption rate. The installation of the cross-exchanger resulted in a higher temperature profile across the stripper. It is possible that foaming may have had temperature dependence. Approximately 750 mL of DOW Corning DSP and DOW Corning Q2-3183A antifoam was added over the duration of the campaign. Both antifoams were silicon-based and were previously used in the MEA campaign. However, the Q2-3183A antifoam appeared to be more effective than the DSP antifoam for the piperazine and

potassium carbonate solvent. The antifoam was typically added into the absorber feed tank or into the suction side of the absorber rich pump (P-104).

Table 2-21. Campaign 4 Antifoam Addition Date, Location, and Type

Date	Time	Volume (mL)	Antifoam	Location
01/10/06	11:06	50	Q2-3183A	P-104
01/12/06	10:10	100	DSP	P-104
01/12/06	10:40	100	DSP	Feed tank
01/12/06	12:45	100	DSP	Feed tank
01/12/06	14:30	100	Q2-3183A	Feed tank
01/19/06	11:00	100	Q2-3183A	Feed tank
01/19/06	17:30	100	Q2-3183A	Feed tank
01/19/06	20:00	25	Q2-3183A	Feed tank
01/20/06	00:15	25	Q2-3183A	Feed tank
01/20/06	03:11	25	Q2-3183A	Feed tank
01/20/06	03:45	25	Q2-3183A	Feed tank

A carbon filter was installed in this campaign to remove the degradation products that may have been a source of the foaming issues encountered in the first 2 campaigns. However, it was uncertain whether the carbon filter performed its intended function. The orifice plate that was installed in series with the carbon filter was improperly sized and steps were not taken to address this issue. The flow rate through the carbon filter was not measurable on the rotameter and did not meet the design flow rate of 10–20% of the total liquid flow through the system.

Due to the lack of temperature control on the inlet absorber gas, a steam injector was installed. Steam was generated in the 10.2 cm reboiler using the distillate from the stripper and injected into the inlet gas to maintain a constant temperature of 40 °C. The steam generator worked well for most of the campaign. However, in the middle of the campaign, the steam generator became plugged due to the accumulation of solids from the distillate. The distillate

contained small amounts of potassium carbonate and piperazine. Since the reboiler was never bled, solids accumulated over time and eventually impeded steam production. The 10.2-cm reboiler was bled, washed, and restarted. The reboiler was operated without additional problems after the initial shutdown.

There were some solubility issues during the second half of the campaign after the composition was changed. The experiments with the 6.4 m K^+/1.6 m PZ solvent were designed to operate at the solubility limits of the solvent. As a result, any loss of water inventory in the system would cause solids to precipitate out. During the course of plant operation, water was continually lost and at first could not be found. It was later discovered that water had begun to accumulate in the overhead CO_2 gas accumulator. Therefore, water had to be periodically pumped from the gas accumulator and back into the solvent stream, which resulted in some density fluctuations.

Before the start of this campaign, the pH meters were repaired and the transmitters were shielded from possible water intrusion with a makeshift cover. Both pH meters did not fail as in the previous campaigns and performed well. Continuous online measurements were taken at the lean and rich end of the absorber. However, there were issues with maintaining a constant lean loading. It was concluded that having an additional pH meter upstream of the absorber feed tank would have facilitated this because it would give the operator direct feedback on the lean loading going into the feed tank. Adjustments to the heat duty could be made immediately instead of waiting for the contents of the feed tank to turn over and finding out that the loading was incorrect.

At the end of Campaign 4, an air-water test was conducted on the absorber to determine the effective wetted area of the Flexipac AQ Style 20 structured packing. Several water rinses was performed on the system to remove any residual solvent. The experiments were conducted by absorbing

atmospheric CO_2 into 0.1 N NaOH solution. However, the CO_2 absorption rate appeared to be too high. This may have been an indication that there was residual piperazine and potassium carbonate in the NaOH solution, which enhanced the absorption rate. The results were not used for the determination the effective interfacial area in the mass transfer calculations. Instead, effective area measurements from the PVC air-water column were used.

2.6.5 Campaign 4 Results

In the fourth campaign, a comprehensive analysis of the liquid samples was undertaken. CO_2 loading was measure for the five sample points using the Shimadzu TOC with the updated protocol. In addition, piperazine and potassium was analyzed using the ion chromatography method developed at the start of this campaign. The results of the absorber liquid analyses for the 5 m K^+/2.5 m PZ and 6.4 m K^+/1.6 m PZ solution are shown below. In addition, the results for the gas rate, liquid rate, CO_2 gas concentration, density, pH, temperature, and pressure drop are shown in the table below.

Table 2-22. Campaign 4 Absorber Analyses for 5 m K^+/2.5 m PZ

Run ID	Date	Time	Piperazine			Potassium			CO_2 Loading		
			Lean mol/kg	Mid mol/kg	Rich mol/kg	Lean mol/kg	Mid mol/kg	Rich mol/kg	Lean mol/kg	Mid mol/kg	Rich mol/kg
4.1	01/10/06	15:30	1.43	1.54	1.43	3.04	3.24	3.02	2.55	2.80	2.88
4.2.1	01/10/06	21:04	1.49	1.46	1.48	3.15	2.97	3.13	2.56	2.90	3.28
4.2.2	01/10/06	22:08	1.49	1.45	1.47	3.16	3.06	3.12	2.50	2.64	3.40
4.3.1	01/11/06	12:00	1.47	1.53	1.41	3.10	3.12	2.97	2.68	3.19	3.19
4.3.2	01/11/06	13:01	1.49	1.66	1.48	3.15	3.34	3.11	2.68	3.45	3.32
4.4.1	01/11/06	15:59	1.50	-	1.43	3.15	-	3.04	2.66	-	3.30
4.4.2	01/11/06	17:28	1.67	1.57	2.01	3.48	3.31	4.23	2.99	3.23	4.25
4.5.1	01/11/06	21:19	1.49	1.43	1.48	3.14	3.01	3.09	2.66	3.02	3.30
4.5.2	01/11/06	22:20	1.50	1.66	1.46	3.15	3.53	3.08	2.70	3.57	3.36
4.6.1	01/12/06	6:28	1.45	1.44	1.39	3.05	3.02	2.93	2.42	2.97	3.13
4.6.2	01/12/06	7:35	1.46	1.44	1.40	3.08	3.03	2.95	2.43	3.06	3.15
4.7.1	01/12/06	14:04	1.47	1.39	1.40	3.12	2.93	2.97	2.34	2.62	2.91
4.7.2	01/12/06	15:00	1.45	1.37	1.41	3.09	2.88	2.99	2.33	2.56	2.89
4.8	01/12/06	17:06	1.42	1.39	1.38	2.96	2.91	2.90	2.26	2.65	2.84
4.9.1	01/12/06	18:03	1.44	1.35	1.38	3.06	2.85	2.93	2.27	2.82	2.97
4.9.2	01/12/06	18:31	1.43	1.36	1.43	3.05	2.89	3.02	2.28	2.80	2.96
4.10.1	01/12/06	22:31	1.43	1.39	1.39	3.04	2.92	2.93	2.63	2.89	2.90
4.10.2	01/12/06	23:31	1.40	1.36	1.42	2.95	2.83	2.96	2.58	2.90	3.09
4.11.1	01/13/06	2:07	1.59	1.38	1.40	3.54	2.85	2.94	2.60	2.93	3.11
4.11.2	01/13/06	3:03	1.45	1.36	1.39	3.05	2.83	2.91	2.58	2.97	3.13
4.12.1	01/13/06	5:12	1.47	1.39	1.40	3.10	2.87	2.94	2.58	2.96	3.06
4.12.2	01/13/06	5:59	1.46	1.39	1.39	3.09	2.91	2.91	2.62	2.96	3.10
4.13.1	01/18/06	17:00	1.30	1.41	1.47	2.94	2.96	3.06	2.38	2.89	2.76
4.13.2	01/18/06	17:45	1.51	1.35	1.39	3.38	2.83	2.88	2.49	2.73	2.88
4.14.1	01/19/06	10:27	1.53	1.36	1.37	3.47	2.83	2.86	2.56	2.71	2.88
4.14.2	01/19/06	12:20	1.33	1.34	1.40	2.99	2.83	2.93	2.51	2.78	2.88
4.15.1	01/19/06	13:56	1.39	1.38	1.36	3.14	2.90	2.86	2.56	2.82	2.95
4.15.2	01/19/06	15:10	1.39	1.36	1.43	3.13	2.85	3.04	2.56	2.80	2.95
4.16.1	01/19/06	19:35	1.78	1.64	1.42	4.06	3.54	2.93	3.09	2.83	3.41
4.16.2	01/19/06	21:03	1.60	1.36	1.50	3.34	2.83	3.16	2.87	2.76	3.08
4.17.1	01/20/06	4:13	1.40	1.37	1.43	3.19	2.86	3.03	2.36	2.71	2.89
4.17.2	01/20/06	5:13	1.38	1.39	1.41	3.10	2.74	2.96	2.38	2.72	2.93
4.18	01/20/06	13:30	1.39	1.59	1.51	3.15	3.35	3.18	2.48	3.05	3.09
4.19	01/20/06	14:34	1.48	1.55	1.54	3.34	3.26	3.27	2.68	2.95	3.24

1. Piperazine and potassium measured using ion chromatography method developed by this work
2. CO_2 loading analysis done with Shimadzu TOC
3. Concentration in units of mol/kg of solvent

Table 2-23. Campaign 4 Absorber Results for 5 m K^+/2.5 m PZ

Run#	Gas Rate Actual m^3/min	Liq Rate L/min	CO_2 In mol%	CO_2 Out mol%	FTIR CO_2 mol%	CO_2 Removal %	Temp Gas In °C	Temp Gas Out °C	Temp Liq In °C	Temp Liq Out °C	Density Liq In kg/m^3	Density Liq Out kg/m^3	pH Liq In	pH Liq Out	DP Bot Bed kPa	DP Top Bed kPa
4.1	14.2	53.0	7.98	0.59	0.83	92.1	39.9	42.4	39.9	48.6	1226	1232	11.0	9.6	0.58	0.58
4.2.1	11.3	47.2	16.28	4.08	-	74.8	39.9	45.8	38.9	48.1	1230	1242	11.1	9.3	0.50	0.43
4.2.2	11.3	47.3	17.19	5.00	4.91	70.8	40.1	46.1	39.0	47.8	1231	1244	11.1	9.3	0.50	0.43
4.3.1	8.5	49.2	15.49	2.60	15.16	82.8	40.6	38.1	42.1	50.0	1232	1238	10.7	9.3	0.37	0.25
4.3.2	8.5	49.2	16.04	2.81	15.70	82.2	40.6	38.7	42.5	50.2	1232	1239	10.7	9.3	0.37	0.25
4.4.1	11.3	54.9	16.95	5.22	5.24	69.1	40.0	41.8	43.6	50.3	1232	1240	10.7	9.3	0.51	0.39
4.4.2	11.3	55.2	17.09	5.49	16.64	67.8	40.0	42.4	43.9	50.2	1232	1240	10.7	9.2	0.52	0.41
4.5.1	14.2	54.9	16.59	6.89	16.44	58.6	40.1	45.7	42.0	47.0	1233	1243	10.7	9.3	0.65	0.62
4.5.2	14.2	55.0	17.55	6.89	9.03	60.8	40.0	43.6	41.4	46.2	1234	1244	10.7	9.3	0.66	0.62
4.6.1	8.5	45.4	16.63	2.35	2.25	85.5	40.1	46.7	46.7	50.9	1217	1230	10.9	9.2	0.42	0.29
4.6.2	8.5	45.0	16.43	2.03	2.03	87.4	39.9	40.4	43.6	50.9	1219	1229	10.9	9.2	0.42	0.27
4.7.1	11.3	55.1	13.17	1.33	1.42	89.6	40.0	44.9	45.2	50.7	1218	1229	10.9	9.4	0.43	0.35
4.7.2	11.3	54.8	12.77	1.01	12.63	91.8	40.1	43.4	45.0	50.6	1218	1228	10.9	9.4	0.40	0.32
4.8	14.2	55.1	10.75	1.89	10.60	82.2	39.9	47.2	43.3	47.3	1215	1227	10.9	9.5	0.53	0.54
4.9.1	14.2	54.7	16.38	5.89	16.29	64.2	40.0	50.9	43.2	47.4	1216	1231	10.9	9.3	0.54	0.57
4.9.2	14.2	55.0	16.03	5.70	16.13	64.6	40.0	51.0	43.2	47.3	1216	1232	10.9	9.3	0.54	0.58
4.10.1	8.5	49.2	17.56	4.95	5.12	71.5	40.0	39.8	44.3	50.9	1219	1227	10.5	9.1	0.32	0.21
4.10.2	8.5	49.2	17.62	5.09	5.26	70.8	40.0	38.6	41.7	51.3	1221	1227	10.5	9.1	0.33	0.20
4.11.1	11.3	54.7	14.93	5.13	15.06	65.4	40.1	36.3	41.6	48.8	1221	1227	10.5	9.2	0.46	0.37
4.11.2	11.3	54.9	15.08	5.42	14.89	63.8	40.0	35.6	41.2	48.4	1222	1228	10.5	9.2	0.48	0.38
4.12.1	14.2	55.0	11.23	4.76	4.79	57.5	40.1	38.1	39.8	46.3	1223	1228	10.6	9.4	0.65	0.61
4.12.2	14.2	54.9	12.64	5.89	5.70	53.5	40.1	38.6	39.9	46.2	1223	1229	10.5	9.3	0.65	0.62
4.13.1	14.2	109.8	17.11	5.21	17.23	69.6	40.0	38.4	41.5	47.9	1218	1222	10.3	9.3	0.83	0.73
4.13.2	14.2	110.0	16.28	4.43	16.42	72.8	39.9	39.9	43.0	49.5	1217	1221	10.3	9.3	0.88	0.77
4.14.1	11.3	113.7	17.16	2.94	2.70	82.7	40.1	37.8	42.8	48.1	1219	1222	10.3	9.4	0.77	0.71
4.14.2	11.3	113.6	15.88	2.19	15.97	86.0	39.9	38.1	42.8	47.8	1219	1222	10.3	9.4	0.68	0.59
4.15.1	8.5	88.9	16.49	1.91	1.83	88.1	40.0	35.5	39.5	45.2	1221	1224	10.3	9.5	0.44	0.35
4.15.2	8.5	89.2	16.76	2.17	2.23	86.7	40.0	35.6	39.6	45.4	1221	1224	10.3	9.4	0.45	0.34
4.16.1	14.2	94.4	16.44	6.28	5.78	61.9	40.0	38.2	41.4	48.4	1219	1223	10.5	9.3	0.76	0.60
4.16.2	14.2	94.6	13.24	3.82	3.49	71.0	40.1	37.4	41.3	47.7	1218	1222	10.5	9.4	0.72	0.58
4.17.1	14.2	94.7	16.62	4.89	4.86	70.6	40.0	37.2	40.1	49.5	1217	1222	10.7	9.4	0.73	0.54
4.17.2	14.1	94.7	17.04	4.27	17.32	74.9	40.1	37.9	40.6	50.9	1217	1222	10.7	9.4	0.65	0.47
4.18	14.2	75.8	13.94	1.91	1.91	86.1	40.5	37.3	40.0	51.2	1223	1228	10.9	9.5	0.48	0.33
4.19	14.2	75.5	13.04	1.34	1.39	89.5	40.4	38.2	40.3	52.1	1224	1228	10.9	9.5	0.48	0.32

1. CO_2 OUT with no value means analyzer was over-ranged with 5.96 reading
2.FTIR CO_2 shown was includes water, while CO_2 In and Out has less than 2% water

Table 2-24. Campaign 4 Absorber Analyses for 6.4 m K^+/1.6 m PZ

Run ID	Date	Time	Piperazine			Potassium			CO_2 Loading		
			Lean mol/kg	Mid mol/kg	Rich mol/kg	Lean mol/kg	Mid mol/kg	Rich mol/kg	Lean mol/kg	Mid mol/kg	Rich mol/kg
4.20.1	01/23/06	18:40	0.96	0.99	1.00	3.79	3.64	3.72	2.97	3.10	3.18
4.20.2	01/23/06	21:40	0.99	0.98	0.95	4.04	3.71	3.88	2.94	3.09	3.15
4.21.1	01/24/06	7:38	0.99	0.98	0.99	3.64	3.57	3.59	2.83	2.95	3.02
4.21.2.	01/24/06	9:00	1.00	1.00	0.98	3.67	3.65	3.56	2.87	2.99	3.07
4.22.1	01/24/06	11:30	-	0.98	1.01	-	3.57	3.68	3.01	3.11	3.23
4.22.2	01/24/06	12:35	1.21	1.02	0.85	4.78	3.71	2.76	3.11	3.31	3.02
4.23	01/24/06	19:33	1.18	0.97	1.13	4.74	3.53	3.61	3.17	3.15	3.29
4.24	01/24/06	21:34	1.07	1.06	1.06	4.25	3.92	3.84	3.04	3.40	3.41
4.25	01/25/06	4:58	1.02	1.00	1.04	4.01	3.58	3.65	2.80	3.01	3.08
4.26.1	01/25/06	15:00	1.01	1.01	0.96	3.97	3.65	3.52	2.76	2.91	3.09
4.26.2	01/25/06	16:00	0.99	1.00	0.99	3.90	3.62	3.64	2.78	2.92	3.10
4.27.1	01/25/06	21:00	1.00	1.01	0.99	3.94	3.65	3.64	2.78	3.00	3.22
4.27.2	01/25/06	22:04	1.05	0.99	1.00	4.14	3.58	3.70	2.80	2.99	3.17
4.28.1	01/26/06	0:58	1.00	0.97	0.96	3.92	3.49	3.45	2.73	3.01	3.14
4.28.2	01/26/06	2:00	0.99	0.98	0.99	3.90	3.50	3.66	2.75	2.96	3.13
4.29.1	01/26/06	5:32	1.02	0.99	0.99	3.98	3.56	3.59	2.73	2.99	3.15
4.29.2	01/26/06	6:32	1.03	0.95	1.09	4.06	3.43	3.73	2.75	3.01	3.15
4.30.1	01/26/06	10:00	1.18	0.99	1.02	4.61	3.58	3.77	2.64	2.92	3.11
4.30.2	01/26/06	11:00	1.00	1.04	0.99	3.91	3.72	3.62	2.67	2.94	3.15
4.31.1	01/26/06	15:00	1.05	0.99	0.96	4.14	3.57	3.53	2.85	3.01	3.16
4.31.2	01/26/06	16:00	1.07	1.00	0.99	4.17	3.60	3.70	2.94	3.00	3.18
4.32.1	01/26/06	19:00	1.01	0.99	1.02	3.98	3.54	3.71	2.78	3.03	3.24
4.32.2	01/26/06	20:00	1.02	1.12	1.08	3.81	4.01	3.88	2.78	3.29	3.53
4.33.1	01/27/06	0:30	1.00	0.98	0.98	3.92	3.49	3.29	2.73	3.06	2.99
4.33.2	01/27/06	1:30	1.01	0.98	0.96	3.76	3.51	3.09	2.73	3.06	2.78

1. Piperazine and potassium measured using ion chromatography method developed by this work
2. **CO_2 loading analysis done with Shimadzu TOC**

Table 2-25. Campaign 4 Absorber Results for 6.4 m K^+/1.6m PZ

Run#	Gas Rate Actual m^3/min	Liquid Rate L/min	CO_2 In mol%	CO_2 Out mol%	FTIR CO_2 mol%	CO_2 Removal %	Temp Gas In °C	Temp Gas Out °C	Temp Liq In °C	Temp Liq Out °C	Density Liq In kg/m^3	Density Liq Out kg/m^3	pH Liq In	pH Liq Out	DP Bot Bed kPa	DP Top Bed kPa
4.20.1	8.5	87.0	15.72	4.98	-	68.0	41.1	34.1	38.8	43.7	1278	1275	10.3	9.7	0.33	0.36
4.20.2	8.5	87.1	15.73	5.26	-	66.5	41.1	34.4	38.6	43.5	1276	1275	10.3	9.7	0.37	1.51
4.21.1	8.5	98.2	14.32	3.23	-	77.1	41.1	33.3	39.0	43.1	1264	1262	10.4	9.8	0.38	0.27
4.21.2.	8.5	98.6	16.15	4.19	-	73.8	41.1	35.2	40.5	44.9	1267	1265	10.3	9.6	0.37	0.26
4.22.1	8.5	56.7	17.60	-	8.78	50.1	41.2	33.8	36.8	43.5	1273	1271	10.3	9.5	0.13	0.12
4.22.2	8.5	56.8	18.02	-	8.88	50.7	41.7	34.3	36.7	43.7	1274	1272	10.3	9.5	0.13	0.11
4.23	8.5	56.8	17.64	-	7.60	56.9	41.7	34.5	37.8	45.3	1276	1273	10.5	9.5	0.19	0.17
4.24	8.5	56.9	17.03	7.31	7.13	58.2	41.7	34.2	37.5	44.9	1276	1273	10.5	9.5	0.21	0.21
4.25	8.5	64.4	16.17	5.41	16.28	66.3	41.7	33.0	39.5	44.5	1267	1266	10.6	9.6	0.25	0.18
4.26.1	8.5	79.3	16.64	3.58	3.63	78.2	38.7	36.8	38.3	44.5	1265	1265	10.5	9.7	0.25	0.14
4.26.2	8.5	79.5	17.24	4.11	4.18	75.9	40.0	37.4	38.7	45.3	1266	1265	10.5	9.7	0.26	0.15
4.27.1	8.5	68.2	16.69	5.18	5.19	68.7	40.0	36.6	40.0	46.2	1266	1266	10.5	9.6	0.28	0.18
4.27.2	8.5	68.2	16.01	4.80	4.91	69.7	40.0	35.8	39.3	45.4	1268	1267	10.5	9.6	0.28	0.19
4.28.1	8.5	56.8	16.48	6.24	16.39	61.8	40.1	35.1	38.9	45.5	1264	1264	10.6	9.5	0.25	0.18
4.28.2	8.5	56.8	14.76	5.04	15.16	65.5	40.0	34.2	38.4	44.5	1265	1264	10.6	9.6	0.26	0.18
4.29.1	8.5	56.8	15.17	4.27	15.68	71.6	40.0	35.3	39.4	46.1	1268	1267	10.7	9.6	0.25	0.18
4.29.2	8.5	56.8	16.20	4.96	16.34	69.1	39.9	35.6	39.5	46.4	1270	1269	10.7	9.6	0.26	0.18
4.30.1	8.5	68.1	15.53	3.12	3.16	79.6	40.0	35.7	41.0	46.5	1265	1265	10.7	9.6	0.26	0.17
4.30.2	8.5	68.3	16.92	4.01	17.31	76.0	39.9	34.9	40.4	46.2	1267	1267	10.7	9.7	0.29	0.19
4.31.1	14.2	79.5	16.56	-	8.86	46.5	39.9	38.4	41.6	47.0	1263	1263	10.6	9.5	0.62	0.54
4.31.2	14.2	79.4	16.37	-	8.68	47.0	40.2	38.4	41.6	46.9	1265	1265	10.6	9.6	0.62	0.54
4.32.1	14.2	68.0	17.29	-	9.92	42.6	39.9	40.9	43.5	47.9	1266	1267	10.5	9.4	0.64	0.56
4.32.2	14.2	68.1	16.57	-	9.44	43.0	39.9	41.1	43.7	48.0	1266	1267	10.5	9.4	0.66	0.57
4.33.1	14.2	56.8	17.24	-	10.28	40.4	39.8	44.8	45.6	45.3	1260	1265	10.5	9.4	0.61	0.60
4.33.2	14.2	56.7	16.88	-	10.14	39.9	40.1	43.6	45.1	45.4	1261	1265	10.5	9.4	0.61	0.59

1. CO_2 OUT with no value means analyzer was over-ranged with 5.96 reading
2.FTIR CO_2 shown was includes water, while CO_2 In and Out has less than 2% water

In Campaign 4, corrosion coupons were inserted downstream of the trim heater. The coupons were weighed prior to installation at the beginning of the campaign and reweighed after removal approximately eight weeks later. The coupons were scrubbed and cleaned of accumulation prior to being reweighed. The results do not show a consistent trend (Table 2-26). For the same material some coupons exhibit somewhat significant losses (316L-5 and 2205-6), while other coupons showed an increase in weight. It was possible that the weighing scale was not performing properly. Based on the mixed results, it was concluded that there was no appreciable corrosion during Campaign 4.

Table 2-26. Campaign 4 Corrosion Coupon Results

Sample ID	Initial Mass g	Final Mass g	Difference Initial-Final
C1010-5	15.8236	15.8235	0.0001
C1010-6	16.0942	16.0966	-0.0024
304L-5	14.6822	14.6820	0.0002
304L-6	14.6066	14.6087	-0.0021
316L-5	14.3729	14.3693	0.0036
316L-6	14.3915	14.3986	-0.0071
317L-5	14.8248	14.8253	-0.0005
317L-6	14.8699	14.8716	-0.0017
2205-5	15.3240	15.3243	-0.0003
2205-6	15.3818	15.3773	0.0045
FRP	11.3150	11.4238	-0.1088

2.6.6 Campaign 4 Summary

Several issues from the previous campaigns that were resolved include: (1) An approach temperature of 10 °C for the stripper feed was finally achieved through a plate and frame exchanger. (2) The absorber inlet gas was saturated and consistently maintained at 40 °C by steam injection. (3) The Vaisala CO_2 analyzers were operated in a non-condensing gas stream. (4) The tubing of the sample bombs were replaced with PFA fluoroplastic tubing for sample verification. (5) A higher capacity pump for the stripper lean stream was

installed. (6) A slipstream carbon filter was installed to remove degradation products and reduce foaming.

In Campaign 4, some unresolved problems include: (1) The DeltaV log sheet recorded the raw signal for the absorber outlet Vaisala CO_2 analyzer and not the calibrated value. (2) The probe of the Vaisala CO_2 analyzer had an odd-size diameter. The pressure of the absorber outlet was under vacuum at times and there may have been a possible leak through fitting. (3) The CO_2 recycle flowmeter was over-sized for pressurized stripper operation. (4) The temperature and pressure from the recycle flowmeter were not recorded. (5) There was not enough flow through the carbon filter because the orifice plate on the main liquid line was too large. (6) Foaming was observed in the stripper and not in the absorber.

2.7 RECOMMENDATIONS FOR FUTURE PILOT PLANT STUDIES

2.7.1 Pilot Plant Operation

The proper operation of the pilot plant requires real-time analysis for the process control and steady state operation. The in-situ measurement by the Vaisala CO_2 gas analyzers allowed the operator to make adjustments and quickly reach steady state and accurately control the CO_2 concentration in the gas stream. Real-time liquid analysis is critical for the determining the steam rate to the reboiler and is also useful to the operator for determining the whether the lean loading conditions has been attained. It would be useful to develop a robust method of measuring CO_2 loading in real-time. In addition, measurements of loading should be taken both upstream and downstream of the absorber feed tank. The upstream measurement will provide the operator with real-time feedback and maintain a constant lean loading, which should dampen

composition variation in the feed tank. The system should also reach steady state more quickly.

2.7.2 Water Balance

Maintaining the water balance in the solvent system is critical for the operation of the pilot plant. Throughout the three piperazine and potassium carbonate campaigns, the loss of water from the system resulted in solubility issues. This caused process instrument error, plugged filters and instrument lines, and several major plant shutdowns. The water hold-up from the overhead liquid accumulator should be minimized or water should be added to the system to account for this loss in water.

To accommodate high gas flows at vacuum operation in the stripper, a portion of the gas was routed through the liquid accumulator because the diameter of overhead gas line from the condenser was too small. This caused significant carryover of water into the overhead gas accumulator where the CO_2 recycle stream was stored. It is recommended that the diameter of the gas line from the condenser be enlarged and to not use the dual flow path for the gas.

The loss of water also affects the measurement of pH in the solution. In the K^+/PZ an attempt was made to correlate pH with lean loading in order to control and maintain process conditions. Variations in water balance affect the precision of the pH measurements and could not be reliably used to control the steam flow to the reboiler of the stripper. Maintaining a constant water balance will enable the use of real time loading measurements and help with process control.

2.7.3 Process Instrumentation

Temperature measurements are an important indicator of mass transfer performance and are important in modeling and computer simulations. It would

be useful to add a gas temperature measurement at or near the outlet nozzle of the absorber. It would also be useful to have a temperature measurement at the absorber liquid inlet nozzle. A temperature measurement at the liquid inlet nozzle downstream of where the stripper feed and reflux is mixed would be useful.

A flowmeter on the cooling water of the solvent cooler would provide valuable heat capacity information for the process solvent. In the current configuration, the temperatures of the cooling water and process stream are measured and only the flow rate of the process fluid is measured. The heat capacity of the process fluid can be calculated if the flow rate of the cooling water is known.

2.7.4 Foaming

Foaming was observed in all of the K^+/PZ campaigns. In the first two campaigns, foaming was observed in the absorber. In Campaign 4, foaming was observed in the stripper. The higher temperatures approaches of the new cross-exchanger resulted in flashing across the control valve at the top of the stripper. The flashing feed may have caused foaming, which resulted in poor mass transfer performance in the stripper. It is recommended that a two-phase distributor be installed in the stripper for future service.

Experiments with organic liquids are routinely conducted in the pilot plant and there is typically some residue left in the system. During vacuum operation, the gas stream comes into intimate contact with the oil reservoir of the vacuum pump. Oil impurities may be present in the gas stream and get transferred into the liquid solvent over time. A slip-stream carbon filter was installed in the fourth to filter out residual organic compounds and piperazine degradation products to reduce foaming. However, during the operation of the

pilot plant there was essentially no flow through the carbon filter unit. It is recommended that a new orifice plate be installed to force some flow through the carbon filter.

During the operation of the pilot plant, antifoam was periodically added to the system to eliminate foaming. It was found that the DOW Corning Q2-3183A antifoam worked well for the piperazine and potassium carbonate system. According to the vendor, antifoam is typically designed for once-through processes. In the pilot plant, the liquid is continuously recycled and over-time the antifoam loses its efficacy. It is recommended that antifoam be continuously added through a metering or peristaltic pump.

2.7.5 Material Balance

In all of four of the pilot plant campaigns, the CO_2 material balance for the absorber consistently did not close. Some of the related issues such as better liquid sampling and analytical techniques were resolved over the course of the four campaigns. The closure of the material balance depends on precise measurements of the (1) gas and liquid mass flow rates, (2) CO_2 concentration in the gas, and (3) the loading of CO_2 in the liquid. In future experiments it is recommended that the critical measurements for the material balance be established prior to the start of the campaign. In the analysis of the data, it was found that the precision of the liquid phase measurements were more critical to the material balance. A 10% shift in the gas material balance was equivalent to a 2% shift in the liquid phase.

Several procedures are recommended to validate the accuracy and consistency of the critical measurements, which include: (1) Re-zero and run the three Micro Motion® flowmeters for the absorber lean, absorber rich, and stripper lean in series to make sure the density, flowrates, and temperature readings are

consistent. The flow check should be performed with both water and the process solvent (2) Run a flow check of the Micro Motion® flowmeters with the bucket and stopwatch method to validate flow and to compare density measurements with another method such as using a hydrometer. The actual process solvent should be used. (3) A second measurement of gas flow should be added at the absorber outlet to validate inlet gas flow measurements. (4) The liquid sampling and analytical method for CO_2 loading and solvent composition should be thoroughly developed and validated in the laboratory prior to the start of the campaign. (5) The calibration of the CO_2 gas analyzers should be validated both in the laboratory and in the field. (6) Gas phase water measurements are also critical in determining the gas flow measurements and CO_2 gas concentration. It is recommended that the FTIR be used for the gas phase measurement of CO_2 and H_2O.

2.7.6 Gas Analysis

During the pilot plant campaigns, the CO_2 gas analyzers were re-calibrated approximately once a week. Significant drift was observed in the Horiba over the course of the four campaigns and the outlet Vaisala analyzer exhibited some drift. It is recommended that two point calibration checks be conducted once every 24 hours and that the analyzers be recalibrated once every three days.

In Campaign 4, the CO_2 concentration measured by the FTIR and the Vaisala analyzers unexpectedly matched. The inlet and outlet FTIR measurements were performed at 40 °C and were assumed to be saturated with water. The inlet and outlet Vaisala measurements were conducted between 20 to 27 °C and between 10 to 15 °C, respectively. It was assumed that the Vaisala analyzers measured wet CO_2 concentration. Under different water

concentrations, the wet CO_2 concentrations were not expected to be the same. It is recommended that further testing be done to compare the CO_2 gas measurements of the Vaisala and FTIR at dry and wet conditions, different temperature ranges, and various degrees of water saturation. The pressure effects, in particular vacuum, should also be investigated for the Vaisala CO_2 analyzers.

2.7.7 Material Compatibility

Material compatibility is important for safety and long-term operation of pilot and industrial scale plants. During the operation of the pilot plant, it was found that Viton® seals were not compatible with the piperazine and potassium carbonate solvent. The pump seals eventually failed and were replaced with EPDM seals, which were compatible with the solvent. The o-rings in the sample bombs were also replaced with EPDM. The filters contained Viton® o-rings, which swelled in the presence of the K^+/PZ solvent. Cotton filters were compatible with the K^+/PZ solvent, but other materials such as polyethylene and polypropylene were dissolved by the solvent over time. The polyethylene bag filter for the stripper completely dissolved in the high temperature solvent. Although the vendors used cotton material for the bags, stitching made of polyethylene or polypropylene was still used, which also resulted in filter failure. Cotton bag filters with cotton stitching should be specified.

2.7.8 Data Acquisition

In all of the campaigns, the raw signal for the CO_2 gas concentration was recorded instead of the calibrated value. In DeltaV, after the coefficients for the calibration curve are entered, the new coefficients need to be manually uploaded into the system. In the course of the calibration procedure, this step may have been inadvertently left out. If the updated values are not uploaded, the values

from the previous calibration are used. Depending on the amount of analyzer drift, there may be significant error. Whenever new instrumentation is added, it should be verified that the calibrated signal and not the raw signal is being logged. It may be useful to record both the raw and calibrated signals of critical measurements such as CO_2 gas concentration.

Chapter 3: Analysis of Pilot Plant Data

The results of the data analysis for the K^+/PZ pilot plant campaigns are presented in this chapter. Real time process measurements of the gas and liquid flow rates, temperatures, densities, CO_2 gas concentration, and CO_2 gas recycle are examined. The liquid analyses for potassium and piperazine concentration and CO_2 loading are also evaluated. A material balance for the rate of CO_2 removal in the absorber and stripper was performed. Mass transfer performance between the Flexipac 1Y and Flexipac AQ Style 20 structured packing and the 5 m K^+/2.5 m PZ and 6.4 m K^+/1.6 m PZ solvents is evaluated and compared to bench-scale measurements made in the wetted wall column.. The location and magnitude of the temperature bulge in the absorber are identified for each run and are quantified by integrating the area under the temperature profile. In addition, the general trends for pressure drop, pH, loading, capacity, stripper heat duty, and cross-exchanger performance are presented.

3.1 Real Time Process Measurements

The process measurements are continuously logged in real-time by the DeltaV process control system. The data recorded by DeltaV is downloaded into an Excel spreadsheet at one minute intervals at the end of each 24 hour shift. The real time measurements of gas and liquid flow rates, liquid density, temperature and CO_2 concentration are analyzed in this section.

The volumetric flow rate of the absorber inlet gas is shown in Figure 3-1. The plot shows the actual measured gas flow rate from 11:00 to 13:00 on 1/24/06

for Campaign 4. During this period, the pilot plant was assumed to be at steady state and liquid samples were taken at 11:30 and 12:30. The plot shows slight variations in the measured gas rate, but remains relatively constant. The standard deviation for the gas flow rate was 0.03 m^3/min over the 2 hour period.

A plot of the molar gas flow rate, which accounts for pressure and temperature, for the same data is shown in Figure 3-2. The plot shows that the molar gas flow rate gradually decreases over time. The decrease in flow is a result of the rise in gas temperature. The gas pressure remained constant during the time interval. This figure suggests that maintaining a constant mole flow of gas rather than volumetric flow may be better. The standard deviation of the molar gas flow rate was ±0.6%. It was concluded that the real-time gas flow measurement was within reasonable error. Table 3-1 is a summary of the averages and standard deviations for the real-time measurement analysis.

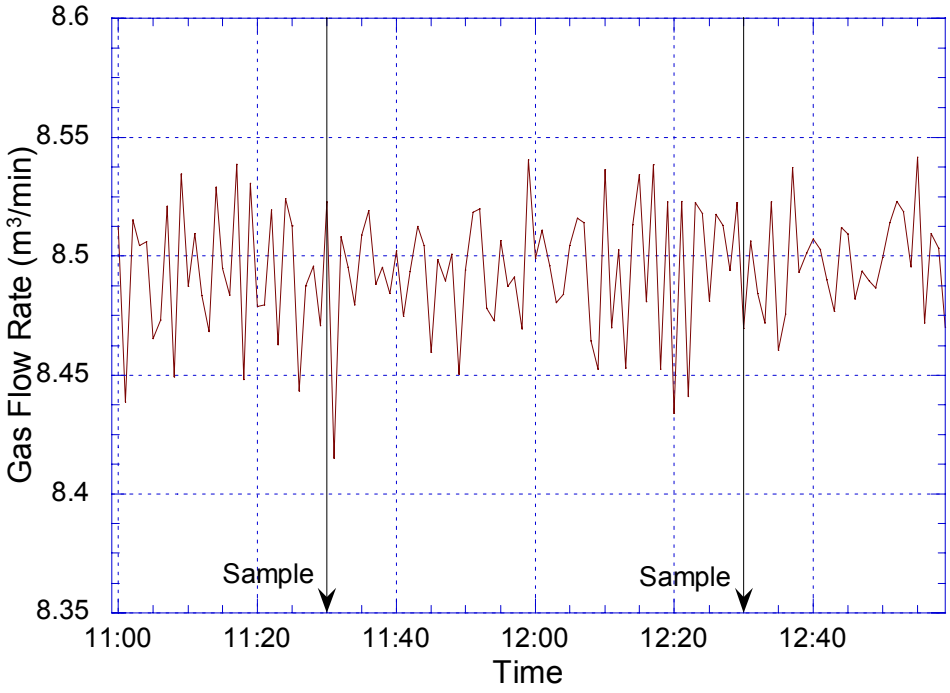

Figure 3-1. Real-time Volumetric Flow Rate of Absorber Inlet Gas for Campaign 4 (6.4 m K^+/1.6 m PZ, 1/24/06, 11:00 - 13:00)

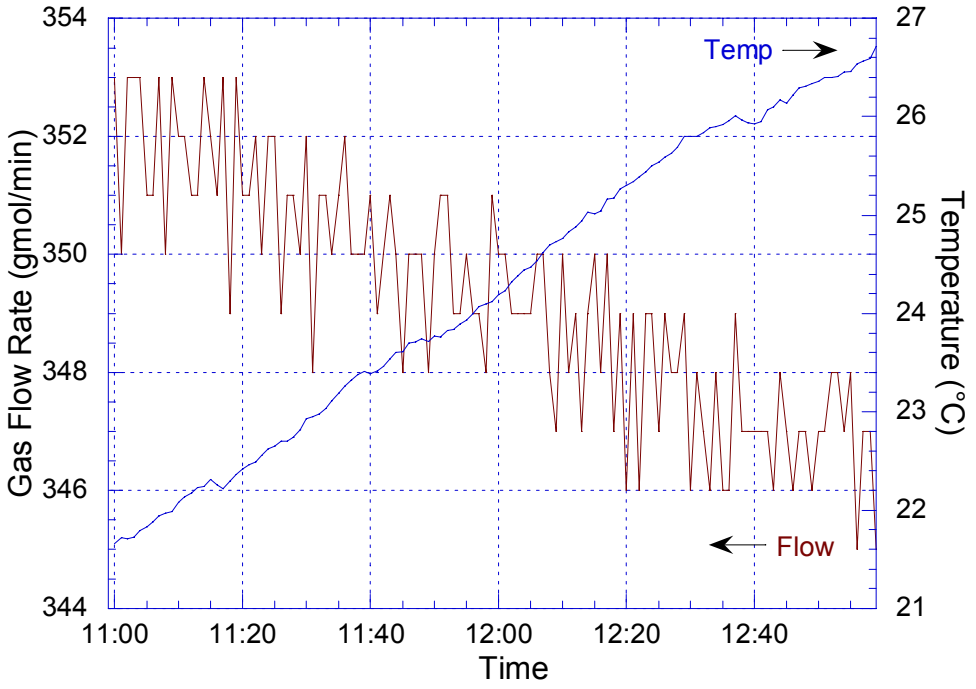

Figure 3-2. Real-time Molar Flow Rate of Absorber Inlet Gas for Campaign 4 (6.4 m K^+/1.6 m PZ, 1/24/06, 11:00 - 13:00)

Table 3-1. Average and Standard Deviation of Real time Process Measurements of Gas Flow Rate, Liquid Flow Rate, and Liquid Density for Campaign 4, 1/24/06, 11:00-13:00

Parameter	Unit	Location	AVE	STD DEV	SD/AVE %
Gas Vol Flow	m^3/min	Absorber Inlet	8.49	0.03	0.30
Gas Mole Flow	gmol/min	Absorber Inlet	349.23	2.06	0.59
Liq Vol Flow	L/min	Absorber Lean	56.78	0.58	1.02
Liq Vol Flow	L/min	Absorber Rich	58.67	0.48	0.82
Liq Vol Flow	L/min	Stripper Lean	56.72	2.24	3.95
Liq Density	kg/m^3	Absorber Lean	1273.38	0.36	0.03
Liq Density	kg/m^3	Absorber Rich	1271.41	0.43	0.03
Liq Density	kg/m^3	Stripper Lean	1271.27	0.61	0.05
Liq Mass Flow	kg/min	Absorber Lean	72.31	0.74	1.02
Liq Mass Flow	kg/min	Absorber Rich	74.60	0.61	0.82
Liq Mass Flow	kg/min	Stripper Lean	72.11	2.83	3.93

The volumetric flow rate and density for the absorber lean, absorber rich and stripper lean streams are measured by the Micro Motion® flowmeters

(Figure 3-3). The figure shows that the liquid flow rates oscillate over time. The flow rate for the stripper lean exhibits the highest degree of oscillation and the highest standard deviation among the three flows rates. The standard deviation for absorber lean, absorber rich, and stripper lean flow rates were 1.0, 0.8, and 4.0%, respectively. The density measurements also demonstrate a similar trend. The absorber lean and rich densities follow a smooth line and trend well with each other, whereas the density of the stripper lean tends to oscillate. The figure seems to indicate that a filter was used to smooth out the density measurements for the absorber lean and absorber rich, whereas the stripper lean density measurement did not have a filter. When a measurement is filtered, a running average over a period of 20 seconds is recorded instead of the instantaneous signal. The standard deviations of the absorber lean, absorber rich, and stripper lean densities were 0.03, 0.03, and 0.05%, respectively. The figure also seems to indicate that the density of the stripper lean matched the absorber rich instead of the absorber lean, which is unexpected. The stripper lean density was adjusted to match the absorber lean measurements in the Data Reconciliation section of this chapter.

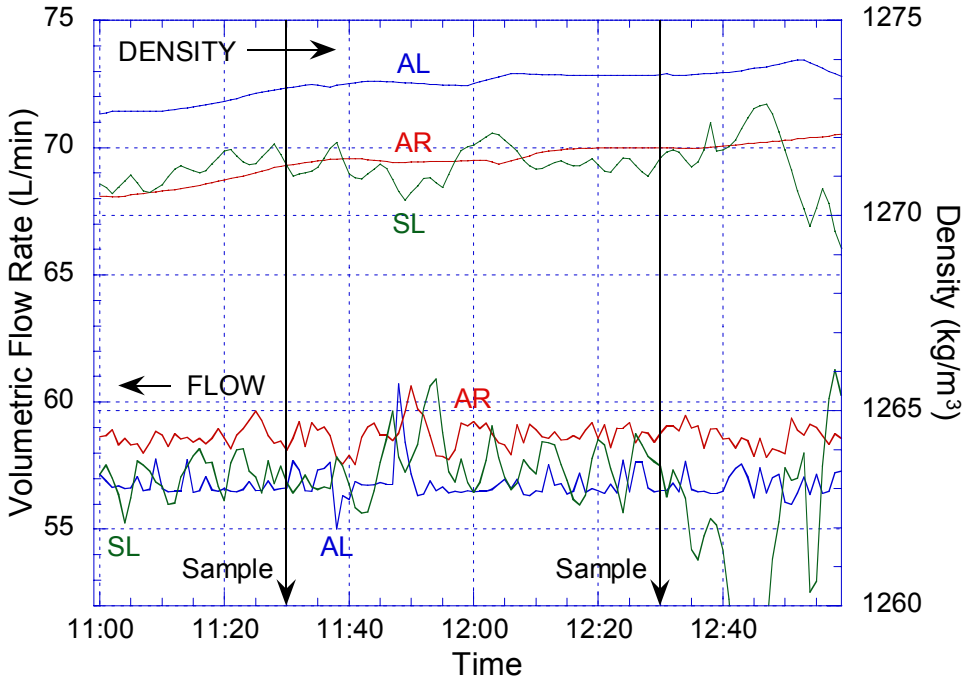

Figure 3-3. Real-time Liquid Flow Rate and Density Measurements of Absorber Lean (AL), Absorber Rich (AR), and Stripper Lean (SL) for Campaign 4 (6.4 m K^+/1.6 m PZ, 1/24/06 11:00 - 13:00)

The mass flow rates of the three liquid streams were calculated by multiplying the volumetric flow rate with the density (Figure 3-4). The mass flow rates exhibit the cycling trend observed for the volumetric flow rates. The absorber rich solution also has a consistently higher mass flow because of the absorption of CO_2. The figure also shows that after each liquid sample is taken, the stripper lean experiences a major upset and may take 20-30 minutes for it to recover from the disturbance.

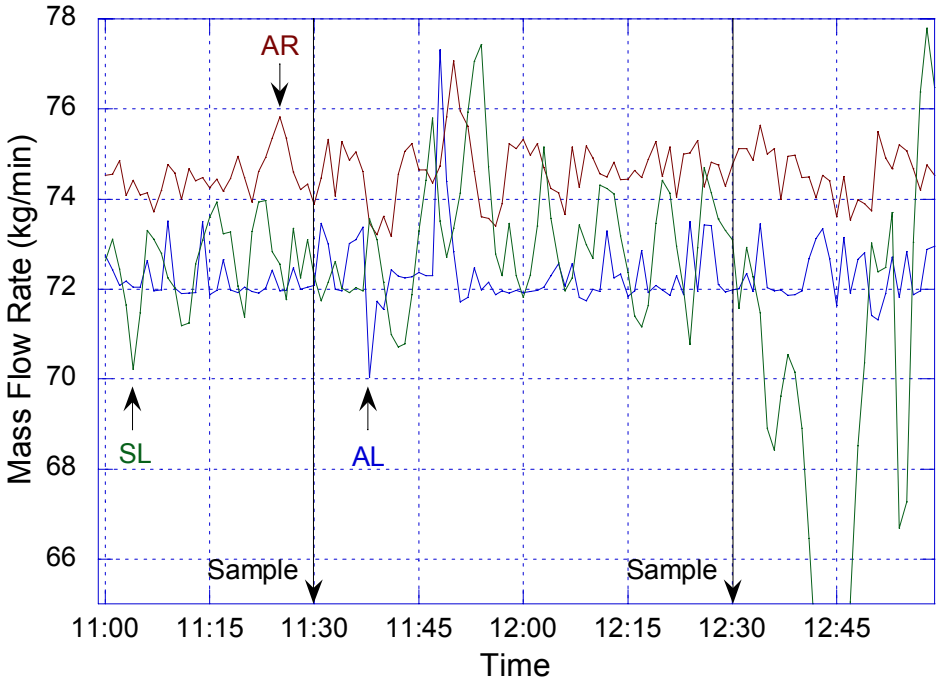

Figure 3-4. Real-time Mass Flow Rate Measurements of Absorber Lean (AL), Absorber Rich (AR), and Stripper Lean (SL) for Campaign 4 (6.4 m K^+/1.6 m PZ, 1/24/06, 11:00 - 13:00)

The temperature of the absorber lean, absorber rich, and stripper lean streams are measured by the Micro Motion® flowmeters (Figure 3-5). The measurements show that the absorber rich temperature is consistently higher than the absorber lean temperature by approximately 7.5 °C and that the absorber lean and absorber rich temperatures trend well each other. The figure also shows that the stripper lean temperature oscillates excessively, similar to the density and flow measurements. Finally, the stripper lean temperature did not match the absorber lean temperature in the first 30 minutes of the time interval.

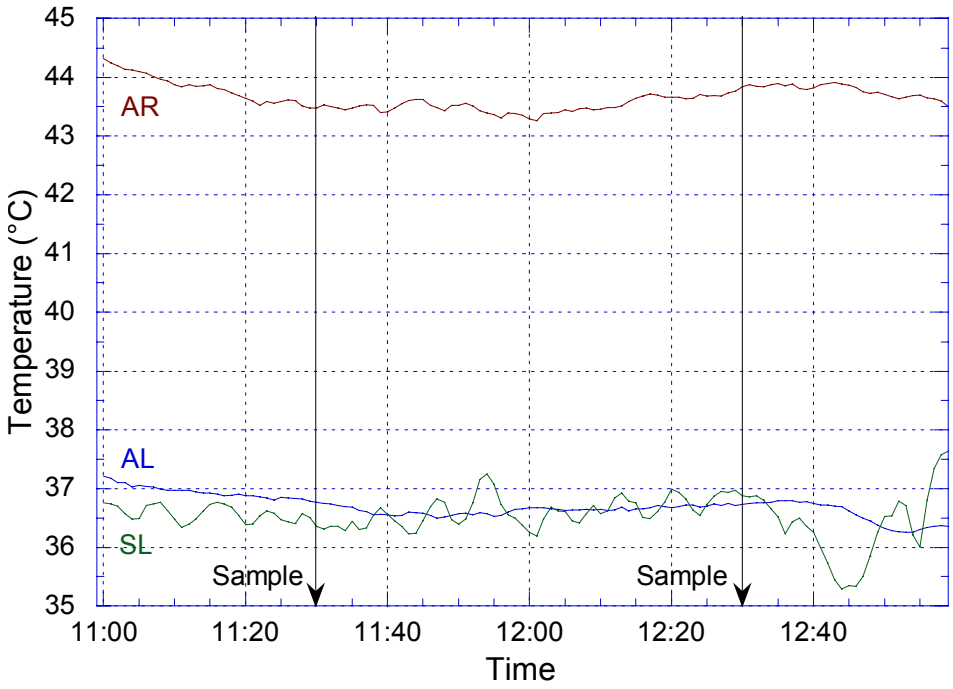

Figure 3-5. Real-time Temperature Measurements of Absorber Lean (AL), Absorber Rich (AR), and Stripper Lean (SL) for Campaign 4 (6.4 m K^+/1.6 m PZ, 1/24/06, 11:00 - 13:00)

The stripper lean Micro Motion® measures the liquid flow from the stripper reboiler. The level in the reboiler is maintained by the stripper bottoms pump (P-102) through a variable speed drive (VSD). Due to the inherent design of the kettle reboiler, the volume of liquid is spread out over a large area. Slight changes to the reboiler level results in a large displacement of liquid volume. As a result, maintaining a constant level in the reboiler was difficult. Also, the stripper bottoms pump is controlled in CASCADE mode base on the level of the reboiler. In CASCADE mode, the level of the reboiler is manually set by the operator and the VSD of the pump is varied to maintain the specified reboiler level. Therefore, the liquid flow to the stripper lean flowmeter constantly oscillated due to changes of the pump VSD. In addition, upstream of the Micro Motion® flowmeter, there is a control valve which regulates the amount of

stripper lean liquid that is bypassed around the solvent cooler. The two liquid streams are recombined just upstream of the flowmeter. This may have also contributed to the fluctuations in temperature and flow measurements. The oscillating temperatures resulted in fluctuating density readings. Based on the above analysis, it was found that both the absorber lean and absorber rich flow rates had a standard error of ±1%, while the stripper lean had a standard error of ±4%.

The real time measurements of CO_2 concentration for the inlet, middle, and outlet of the absorber for Campaign 4 on 1/20/06 from 3:00 to 5:30 AM are shown in Figure 3-6. The inlet and outlet CO_2 concentrations were measured with the in-situ Vaisala analyzers; the middle concentration was measured with the Horiba analyzer. The figure also shows the concentration of carbon dioxide and water measured by the FTIR analyzer at the inlet and outlet of the absorber. The FTIR and Horiba analyzers use an extractive sampling system and the measurements for the two instruments were shifted by several minutes to account for the residence time in the sampling system.

The Horiba measures dry CO_2 gas concentration and the FTIR measures wet CO_2 gas concentration. Experiments indicated that the Vaisala analyzer measured wet CO_2 gas concentration and this was assumed. The figure shows that all of the measured CO_2 gas concentrations trend relatively well with each other. The slight oscillation in CO_2 concentration over time was concluded to be reflective of real-time changes in the concentration and not associated with instrument noise or sampling error because all four measurements demonstrated the same peaks and valleys at the same time.

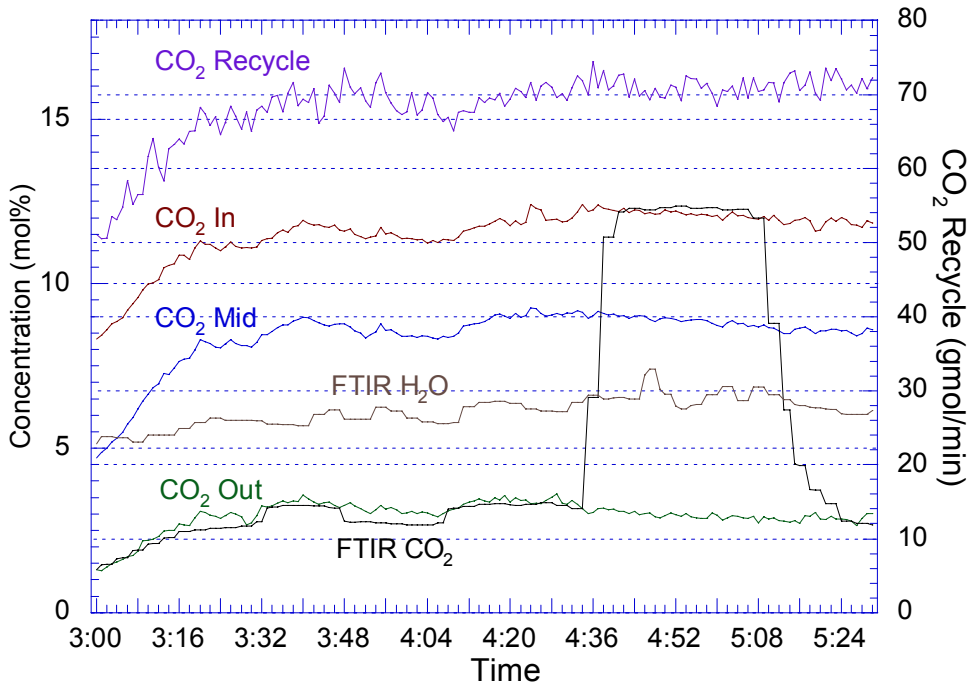

Figure 3-6. Real-time Measurements of CO_2 and H_2O Gas Concentrations in the Absorber and CO_2 Recycle from the Stripper for Campaign 4 (5 m K^+/2.5 m PZ, 1/20/06, 3:00 – 5:30)

The FTIR CO_2 concentrations match the inlet and outlet Vaisala measurements. This is unexpected because the water content for the two analyzers are assumed to be different. The oscillation of the outlet FTIR water concentration appears to trend with the outlet CO_2 concentration, whereas the inlet H_2O concentration does not follow trend of the inlet CO_2 concentration. The FTIR sample point is located 0.6 meters downstream of the steam injection point and the steam may not have completely mixed with the gas and resulted in erratic measurements.

Finally, the plot shows that the CO_2 recycle stream from the stripper trends well with the measurements of CO_2 concentration. However, the CO_2 recycle measurements oscillate excessively. Over the time interval from 4:20 to 5:30 AM, the standard deviation of the CO_2 recycle measurement is ±1.8%. The

CO_2 recycle stream is measured with an annubar that was originally designed for vacuum operation and is oversized for pressure operation. It was concluded that the real-time CO_2 gas measurements are reliable, but the discrepancy between the FTIR and Vaisala measurements should be addressed in future experiments. Also, the outlet FTIR water measurement and CO_2 recycle stream under high flow conditions are reliable.

3.2 LIQUID DENSITY, FLOW RATE AND TEMPERATURE

For each run condition, the real-time process measurements were averaged over the period ten minutes before and after the sample point. In this section, the averaged values of the liquid density, flow rate, and temperatures for Campaign 4 are analyzed. It was assumed that the data for the previous campaigns followed the same trends.

Figure 3-7 compares the densities measured by the Micro Motion® flowmeters for the absorber lean, absorber rich, and stripper lean streams in a parity plot. The figure shows that relative to the absorber lean, for the 5 m K^+/2.5 m PZ and 6.4 m K^+/1.6 m PZ solvents, the stripper lean was on average 0.33% and 0.13% lower, respectively and the absorber rich stream was on average 0.6% higher and 0.04% lower, respectively. The plot also shows that the 5 m K^+/2.5 m PZ density data has more variation than the 6.4 m K^+/1.6 m PZ data. Part of this discrepancy may have been due to the difference in temperature relative to the absorber lean stream.

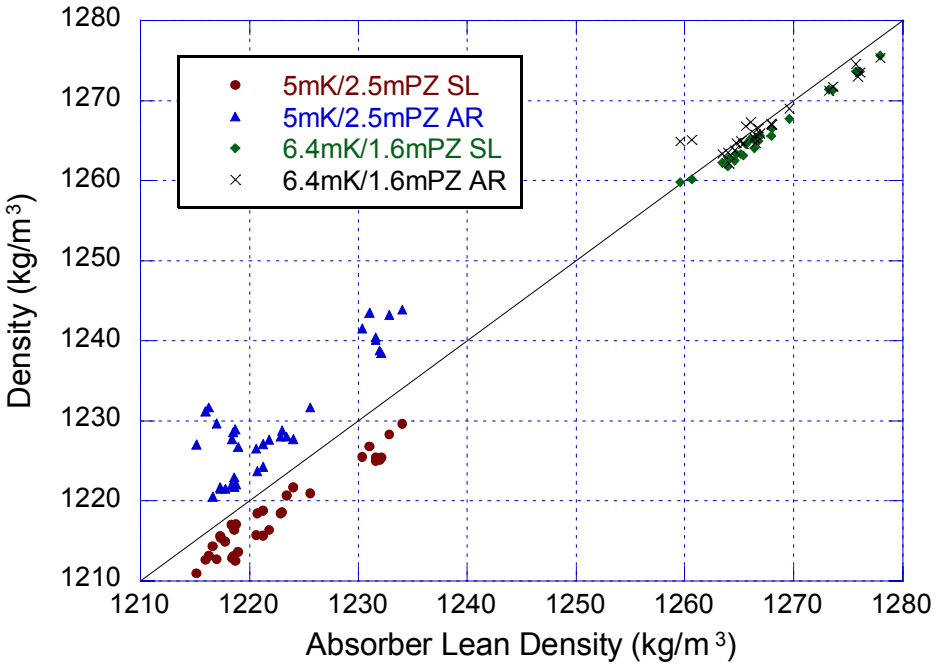

Figure 3-7. Measured Density of Absorber Lean (AL), Absorber Rich (AR), and Stripper Lean (SL) by Micro Motion® Flowmeters of 5 m K^+/2.5 m PZ and 6.4 m K^+/1.6 m PZ for Campaign 4

Figure 3-8 is a plot of the temperature difference for the absorber rich and stripper lean streams relative to the absorber lean stream. The figure shows that for the 5 m K^+/2.5 m PZ solvent, the majority of the stripper lean temperatures are 1 to 2 °C higher than that absorber lean and the difference in temperature for the 6.4 m K^+/1.6 m PZ stripper lean and absorber lean streams are on average less than a 1 °C. The absorber rich temperatures for the 5 m K^+/2.5 m PZ and 6.4 m K^+/1.6 m PZ solvents are typically 4 to 12 °C and 4 to 8 °C higher than the absorber lean streams, respectively. There relative difference in temperature between the absorber lean and rich streams appears to decrease with increasing absorber lean temperatures. Another interpretation is that the liquid outlet temperature remained relatively constant and is independent of the inlet liquid stream temperature.

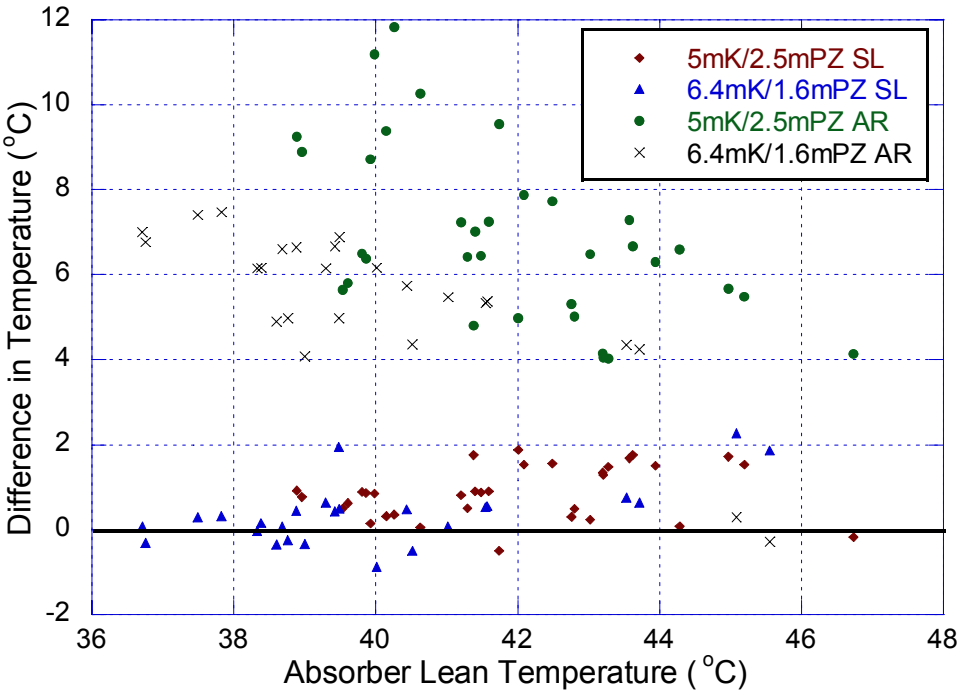

Figure 3-8. Temperatures of Absorber Lean (AL), Stripper Lean (SL), and Absorber Rich (AR) for 5 m K^+/2.5 m PZ and 6.4 m K^+/1.6 m PZ of Campaign 4

The absorber inlet and outlet temperatures are measured by the Micro Motion® flowmeters and Rosemount pH meters at each respective location. Figure 3-9 shows that the temperature measurements by the pH probe for the absorber lean stream are on average consistently lower than that measured by the flowmeter. The absorber lean pH probe is approximately 5 meters downstream of the flowmeter and the temperature is expected to be slightly lower. However, temperature differences of 5 to 7 °C are observed for the absorber lean pH meter and flowmeter, which is unreasonable. The absorber rich pH meter is located a few meters below the absorber sump and the absorber rich flowmeter is located approximately 37 meters downstream of the pH meter. The absorber rich liquid passes through a pump in between the pH probe measurement and the flowmeter measurement. The pump may slightly increase the temperature of the absorber rich stream and this is reflected in the slightly

higher temperatures measured by flowmeter. In both solvent compositions, the flowmeter temperatures are no more than 1 °C higher than the pH probe temperatures. It was concluded that the temperatures measured by absorber inlet and outlet Micro Motion® flowmeters and absorber rich pH meter were reliable, but the absorber lean pH meter temperature measurement are not reliable.

Data analysis of the absorber used the absorber lean Micro Motion® flowmeter and absorber rich pH probe temperature measurements as the absorber inlet and outlet temperatures, respectively. However, the actual liquid temperature entering the absorber may be slightly cooler than the measured temperature because the temperature is measured approximately 22 meters upstream of the inlet nozzle.

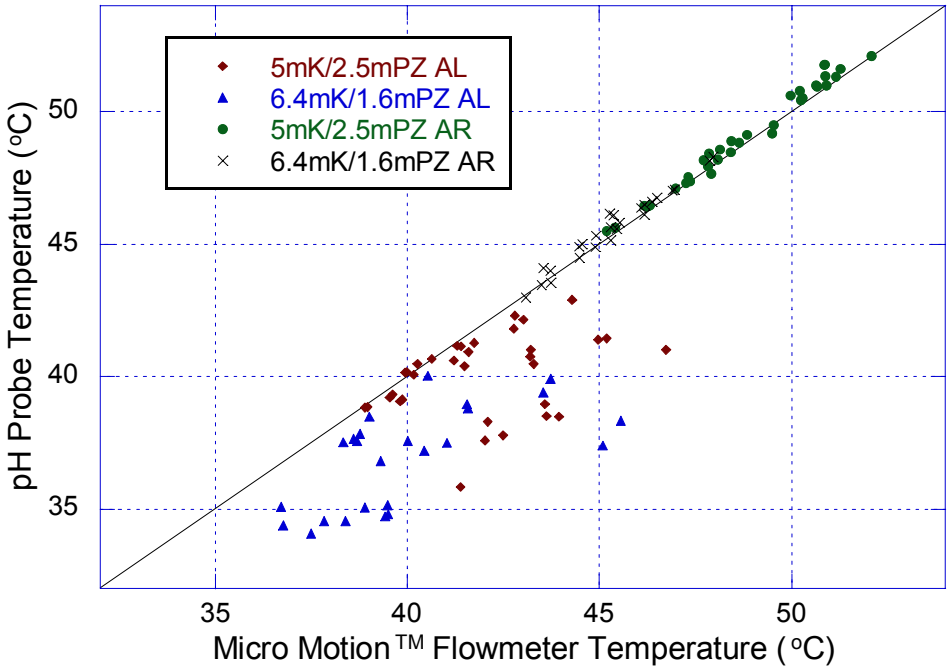

Figure 3-9. Temperature Comparison of Micro Motion® Flowmeters and Rosemount pH Meters for the Absorber Inlet and Outlet of Campaign 4

The Micro Motion® Coriolis flowmeters measure mass flow, density, and temperature. The parameters are then used to calculate the volumetric flow rate. The volumetric flow rate of the absorber lean, absorber rich, and stripper lean streams for Campaign 4 are compared in Figure 3-10. The volumetric flow rates of the stripper lean for the 5 m K^+/2.5 m PZ and 6.4 m K^+/1.6 m PZ solvents are on average, 0.9% lower and 0.3% higher than the absorber lean stream, respectively. The volumetric flow rates of the absorber rich for the 5 m K^+/2.5 m PZ and 6.4 m K^+/1.6 m PZ solvents are on average, 2.4% and 3.3% higher than the absorber lean stream, respectively.

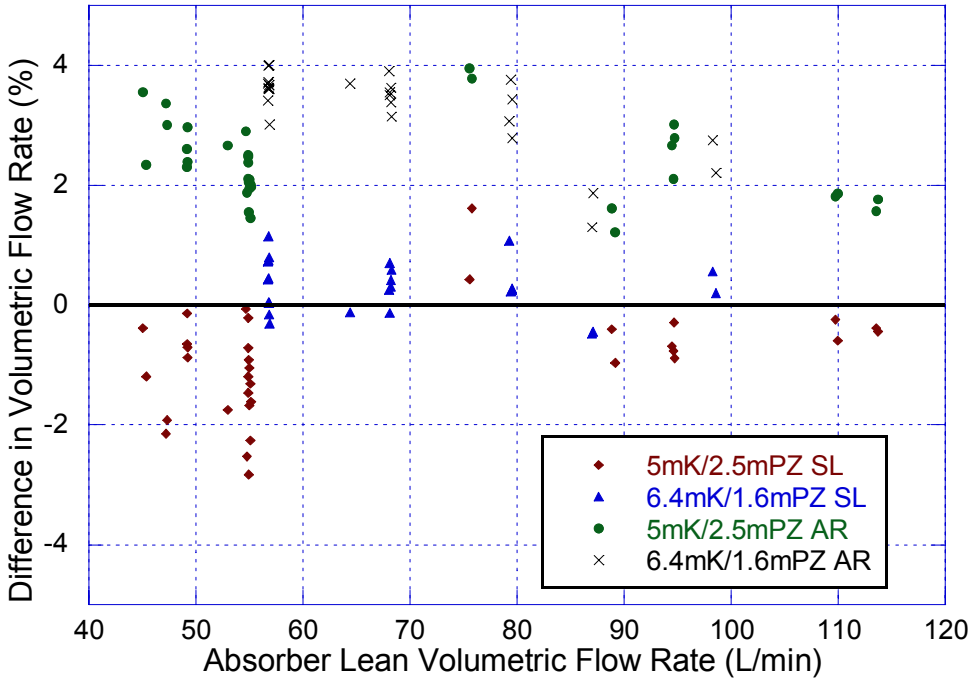

Figure 3-10. Volumetric Flow Rate Comparison of Absorber Lean (AL), Stripper Lean (SL), and Absorber Rich (AR) of 5 m K^+/2.5 m PZ and 6.4 m K^+/1.6 m PZ for Campaign 4

Figure 3-11 illustrates the difference in mass flow rate between the absorber lean, absorber rich, and stripper lean stream of Campaign 4. The mass flow rates of the stripper lean for the 5 m K^+/2.5 m PZ and 6.4 m K^+/1.6 m PZ

solvents are on average, 1.2% lower and 0.2% higher than the absorber lean stream, respectively. The mass flow rates of the absorber rich for the 5 m K^+/2.5 m PZ and 6.4 m K^+/1.6 m PZ solvents are on average, 3.0% and 3.3% higher than the absorber lean streams, respectively.

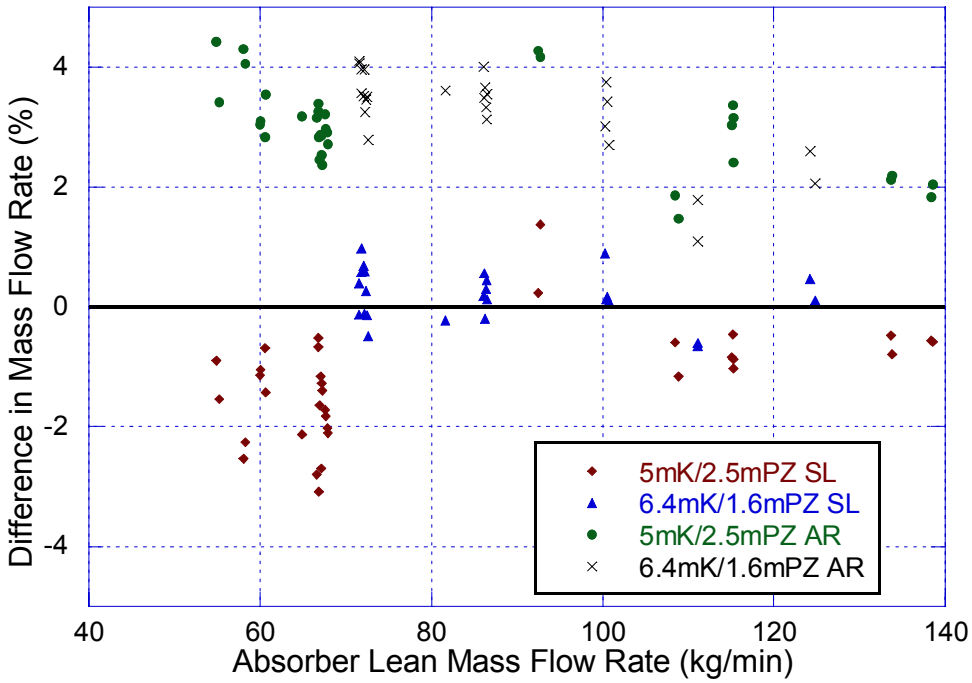

Figure 3-11. Mass Flow Rate of Absorber Lean (AL), Stripper Lean (SL), and Absorber Rich (AR) for 5 m K^+/2.5 m PZ and 6.4 m K^+/1.6 m PZ of Campaign 4

The slightly higher absorber rich mass flow rate is attributed to the absorption of CO_2. It was concluded that the discrepancy between the absorber lean and stripper lean mass flow rates was attributed to fluctuations in liquid flow due to reboiler level control issues and to possible error with the stripper lean density measurement. The figure also shows that about 40% of the 5 m K^+/2.5 m PZ runs were operated at 67 kg/min, with additional points at 55, 60, 90, 109, 115, 134 kg/min. For 6.4 m K^+/1.6 m PZ solvent, approximately 40% of the runs were conducted at 72 kg/min, with additional points at 82, 86, 100, 111, and 125 kg/min.

3.3 LIQUID POTASSIUM AND PIPERAZINE CONCENTRATION

For Campaign 4, the concentration of potassium and piperazine was analyzed using the ion chromatography method developed by this work. The analytical method is detailed in the previous chapter. The concentration of both species were analyzed in the absorber lean, absorber rich, absorber middle, stripper lean, and stripper middle samples. The results of the piperazine and potassium analysis for the 5 m K^+/2.5 m PZ solvent are shown in Figure 3-12. The plot shows that the concentration of both piperazine and potassium for the stripper middle samples are consistently lower than the other four sample locations by approximately 10%.

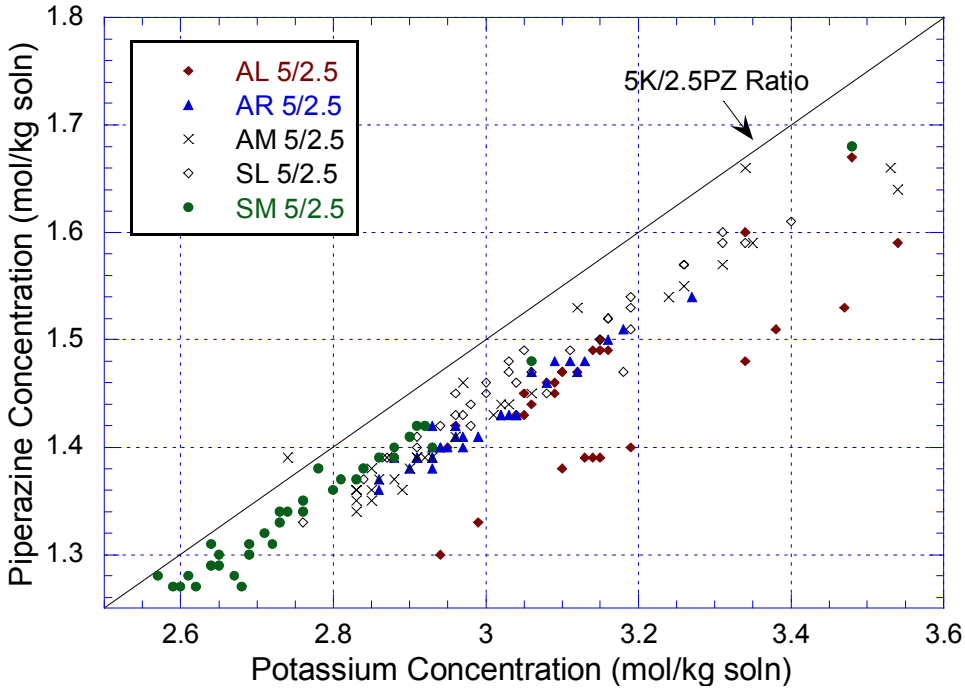

Figure 3-12. Potassium and Piperazine Measurements from Ion Chromatography for 5 m K^+/2.5 m PZ of Campaign 4 for Absorber Lean (AL), Rich (AR), Middle (AM), and Stripper Lean (SL) and Middle (SM)

A similar trend was also observed for the 6.4 m K^+/1.6 m PZ solvent, where the stripper middle samples were 8.5% lower (Figure 3-13). In the stripper,

reflux is continuously added as water to the solvent feed and it is possible that the solvent was being diluted. However, at the same time, there is water loss from the solvent in the form of steam generation, which would concentrate the solvent. At steady state, the evaporated water should be equivalent to amount of reflux that is being returned. The ion chromatograph analysis of the stripper middle was conducted contiguously. Therefore, it is possible that the calibration of analyzer for that set of runs was systemically offset by 10%. The plot also shows that the piperazine concentration for several of the absorber lean points was systematically lower. A more detailed analysis is presented later in this section. A similar plot for the 6.4 m K^+/1.6 m PZ solvent shows that the potassium concentration for the absorber lean points was consistently higher than the other sample points.

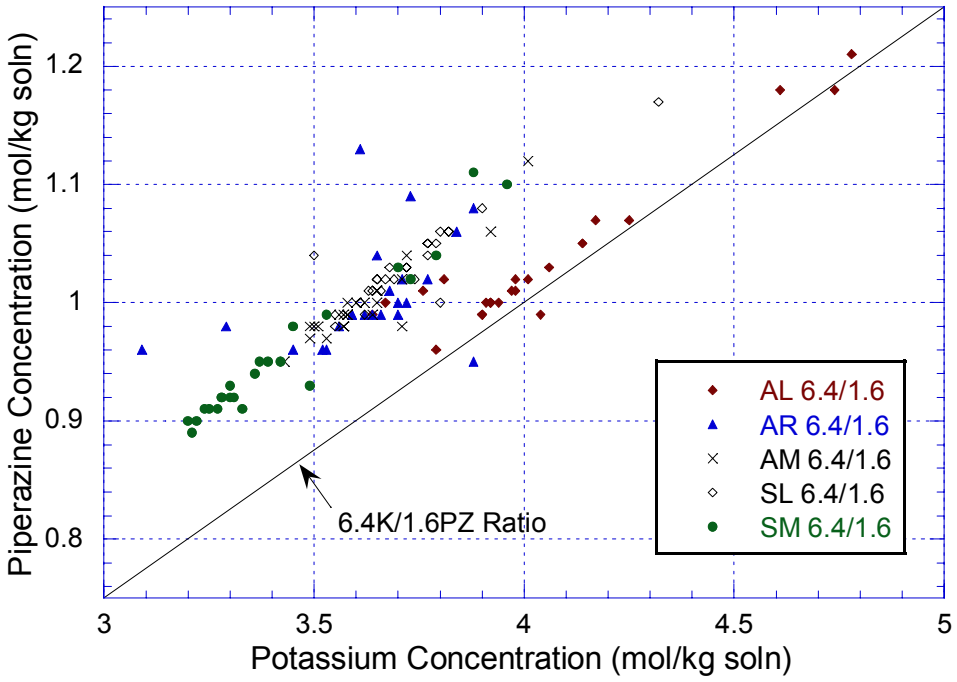

Figure 3-13. Potassium and Piperazine Measurements from Ion Chromatography for 6.4 m K^+/1.6 m PZ of Campaign 4 for Absorber Lean (AL), Rich (AR), Middle (AM), and Stripper Lean (SL) and Middle (SM)

3.3.1 Potassium and Piperazine Concentration Adjustments

A parity plot of the potassium concentrations for the absorber lean, absorber rich and stripper lean streams of Campaign 4 as measured by ion chromatography is shown in Figure 3-14. The plot shows that the potassium concentration of the 5 m K^+/2.5 m PZ absorber lean and stripper lean streams match. However, the absorber rich potassium analysis is consistently lower than the absorber lean stream. The absorber rich stream may have been slightly diluted by the addition of water from the steam injection of the gas pre-heater or the absorption of water from the gas due to condensation. Another possibility is analytical error from the calibration and analysis of the solution on the ion chromatograph. A similar trend is also observed for the piperazine analysis of the 5 m K^+/2.5 m PZ absorber rich solution. The plot was used to identify outliers of the potassium analysis for the 5 m K^+/2.5 m PZ solutions.

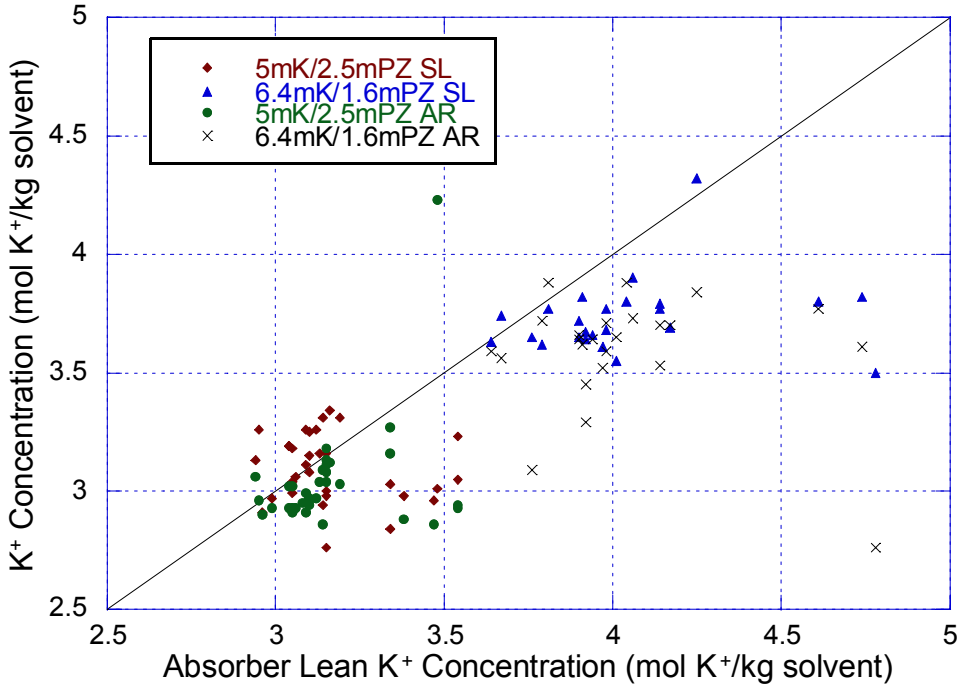

Figure 3-14. Potassium Concentration Comparison of Absorber Lean (AL), Absorber Rich (AR), and Stripper Lean (SL) for Campaign 4

For 6.4 m K^+/1.6 m PZ, the potassium concentration of the absorber lean is consistently higher than the absorber rich and stripper lean. However, the absorber rich and stripper lean potassium values are consistent with each other. The analysis of the piperazine data for the 6.4 m K^+/1.6 m PZ solutions did not demonstrate this trend. Therefore, a correction factor of 0.924 was applied to the measured potassium concentrations of the 6.4 m K^+/1.6 m PZ absorber lean data. The factor was obtained using MS Excel Solver function and setting the target of the average K/PZ mol ratio for the absorber lean equal to 3.61. Figure 3-15 shows the adjusted potassium concentration of the absorber lean points for the 6.4 m K^+/1.6 m PZ solution. The figure was used to identify outliers for the potassium analysis of the 6.4 m K^+/1.6 m PZ solution.

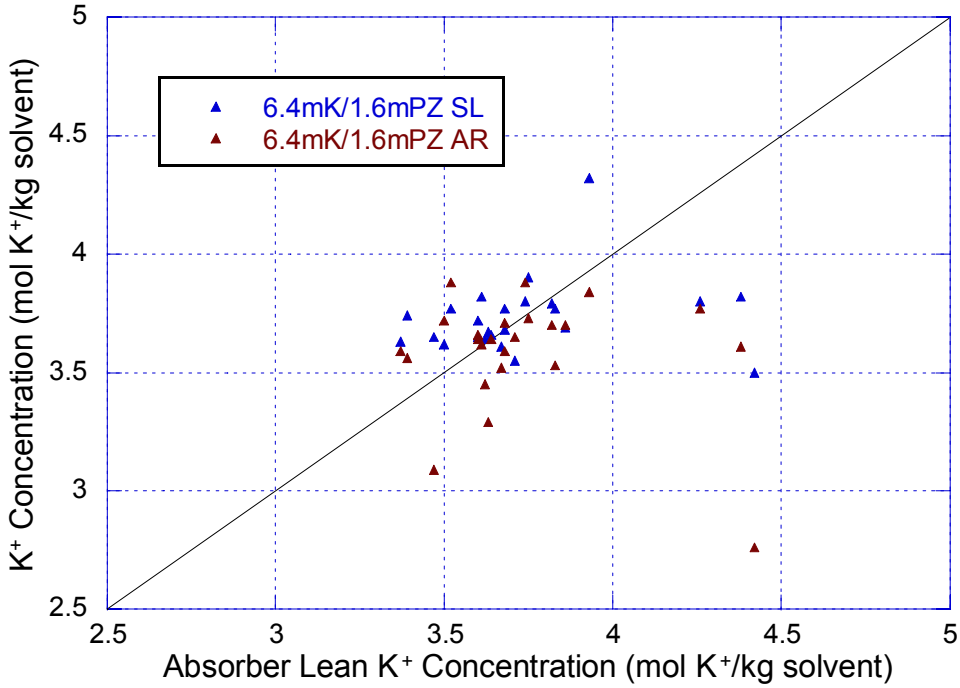

Figure 3-15. Corrected Absorber Lean Potassium Concentrations for 6.4 m K^+/1.6 m PZ of Campaign 4

The 5 m K^+/2.5 m PZ and 6.4 m K^+/1.6 m PZ solutions were analyzed using standards containing piperazine and potassium carbonate at a K^+/PZ ratio

of 2:1, which may have resulted in the possible discrepancies in the IC analysis of the 6.4 m K^+/1.6 m PZ samples. However, analysis of the 6.4 m K^+/1.6 m PZ absorber rich and stripper lean for potassium and piperazine appear to be consistent with each other and do not support this hypothesis. It was concluded that the IC method developed for the analysis of potassium and piperazine could be applied to the analysis of the 6.4 m K^+/1.6 m PZ samples.

The piperazine analysis from the ion chromatograph of the absorber lean, absorber rich and stripper lean solutions for Campaign 4 is shown in Figure 3-16. The piperazine analysis for the 5 m K^+/2.5 m PZ solution shows that the absorber rich values are on average slightly lower than the absorber lean, while the stripper lean values were slightly higher than the absorber lean values. However, corrections were not applied to the measured values because the differences were relatively minor. The piperazine values for the 6.4 m K^+/1.6 m PZ samples appear to be consistent with each other and no corrections were made. The plot was used to eliminate outliers for the piperazine analysis.

Although the absolute values of the piperazine and potassium values may change from sample to sample due to changes in solvent density, the ratio of K^+ to PZ should remain the same. An analysis of the 5 m K^+/2.5 m PZ solution shows that a portion of the absorber lean K^+/PZ was 2.25 instead of 2.1. Closer examination of the piperazine and potassium data indicate that the piperazine concentration for 25% of the data set was 6% lower than the stripper lean and absorber rich piperazine concentration. The piperazine concentrations for those points were adjusted by a factor of 1.068 to give a K^+/PZ ratio of 2.11.

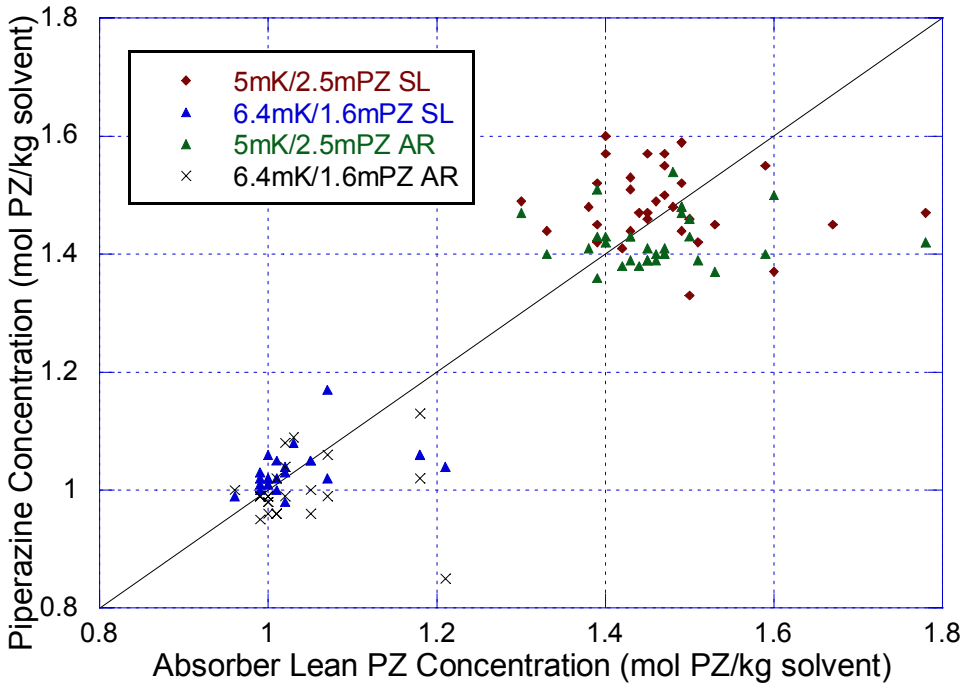

Figure 3-16. Piperazine Concentration of Absorber Lean (AL), Absorber Rich (AR), and Stripper Lean (SL) for Campaign 4

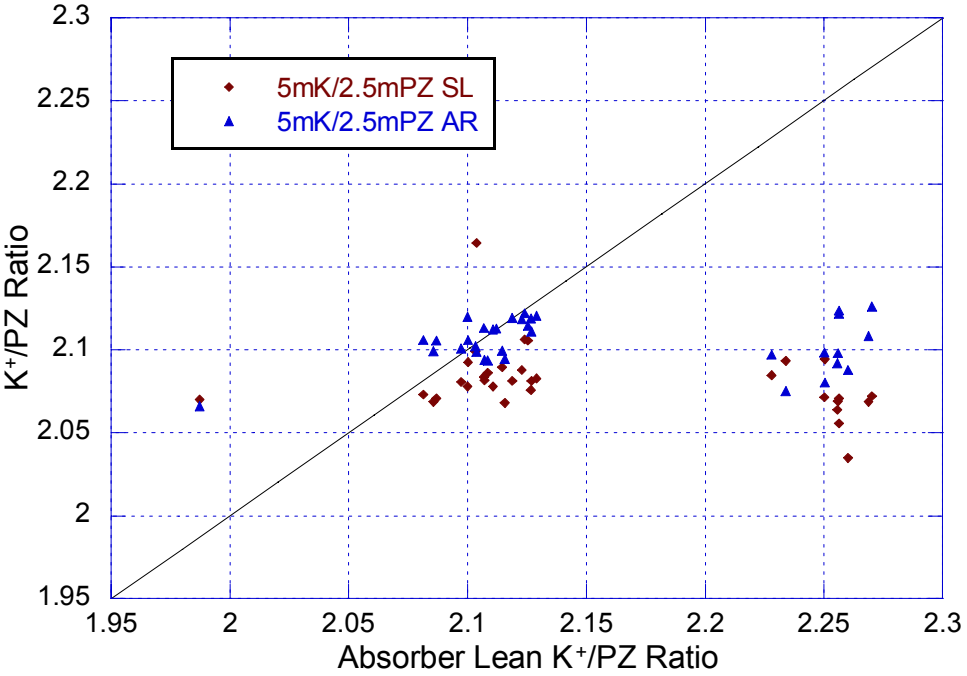

Figure 3-17. K^+/PZ Ratio Comparison Absorber Lean (AL), Absorber Rich (AR) and Stripper Lean (SL) for 5 m K^+/2.5 m PZ of Campaign 4

A similar analysis for the 6.4 m K^+/1.6 m PZ samples shows that the average K^+/PZ ratio for the three solvent streams was approximately 3.6 instead of 4 (Figure 3-18). The stripper lean samples match relatively well with the absorber lean while the absorber rich points are just slightly higher than absorber lean (Figure 3-18). The figure also indicates that some of absorber lean points did not match the absorber rich and stripper lean. Also, some of the absorber rich points appear to be consistently lower than the absorber lean. The outlying points were identified for data analysis.

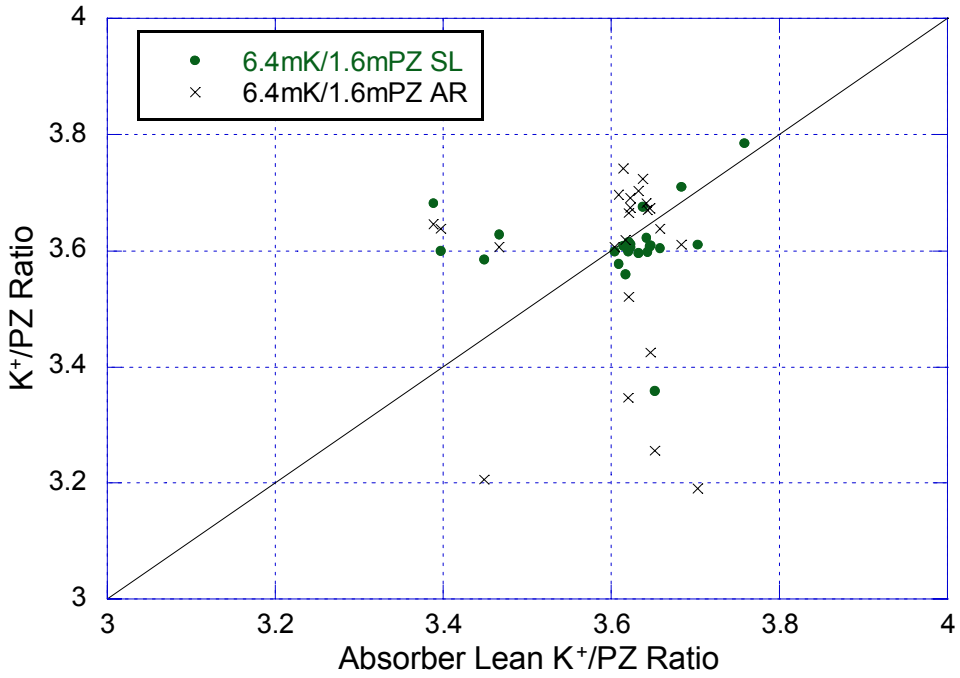

Figure 3-18. K^+/PZ Ratio Comparison Absorber Lean (AL), Absorber Rich (AR) and Stripper Lean (SL) for 6.4 m K^+/1.6 m PZ of Campaign 4

Figure 3-19 shows that the total alkalinity (mol K^+ + 2 mol PZ) of the absorber rich was consistently lower than the absorber lean stream for the 5 m K^+/2.5 m PZ solvent, while the stripper lean points were on average slightly higher than the absorber lean points. For the 6.4 m K^+/1.6 m PZ solvent, the stripper lean values are slightly higher than the absorber lean (Figure 3-20). The

absorber lean and rich measurements are scattered, but consistent with each other. Based on the data analysis, it was concluded that the ion chromatography analysis for piperazine and potassium concentration had a precision of approximately ±10%. In addition, the titration method used in the initial analysis for piperazine and potassium produced results that were consistently lower than the ion chromatography method.

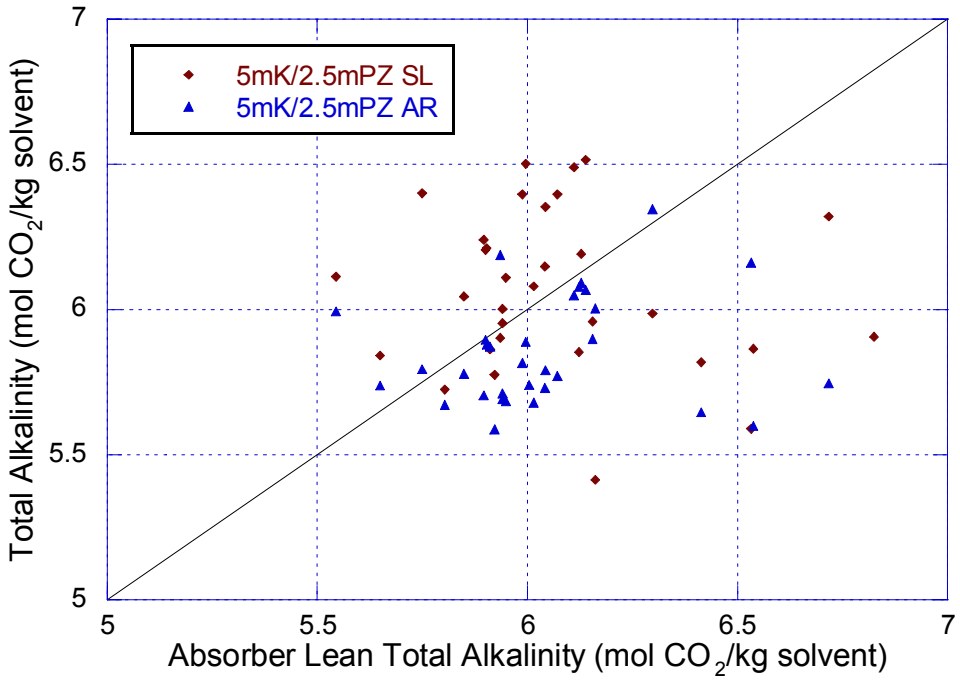

Figure 3-19. Total Alkalinity of Absorber Lean (AL), Absorber Rich (AR) and Stripper Lean (SL) for 5 m K^+/2.5 m PZ of Campaign 4

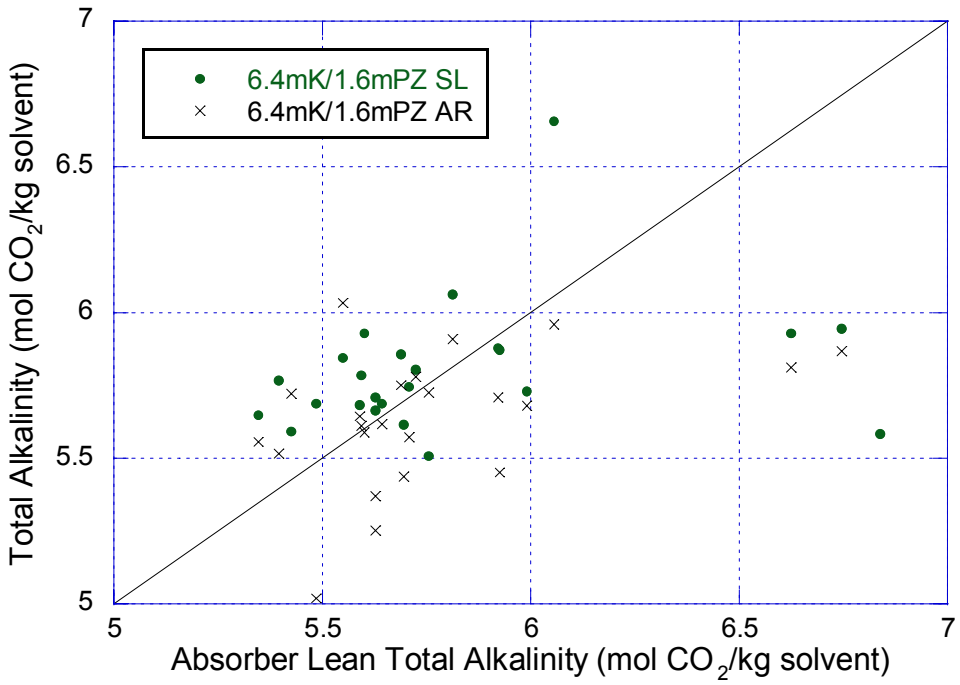

Figure 3-20. Total Alkalinity of Absorber Lean (AL), Absorber Rich (AR) and Stripper Lean (SL) for 6.4 m K^+/1.6 m PZ of Campaign 4

3.4 CO_2 LOADING

An analysis of the CO_2 loading for the absorber lean and stripper lean for Campaign 2 is shown in Figure 3-21. The loading for the two samples should match if the system is at steady state. The parity plot shows that there is some discrepancy between the absorber lean and stripper lean loading data. The absolute average deviation for the CO_2 loading of the two streams is 11.3%. This discrepancy may be related to analytical issues and inconsistencies that were encountered during the loading analysis. It is also possible that the pilot plant was not at steady state and the composition of the stripper lean was different from the absorber lean composition. It is difficult to determine the exact cause because the errore appear to be randomly distributed.

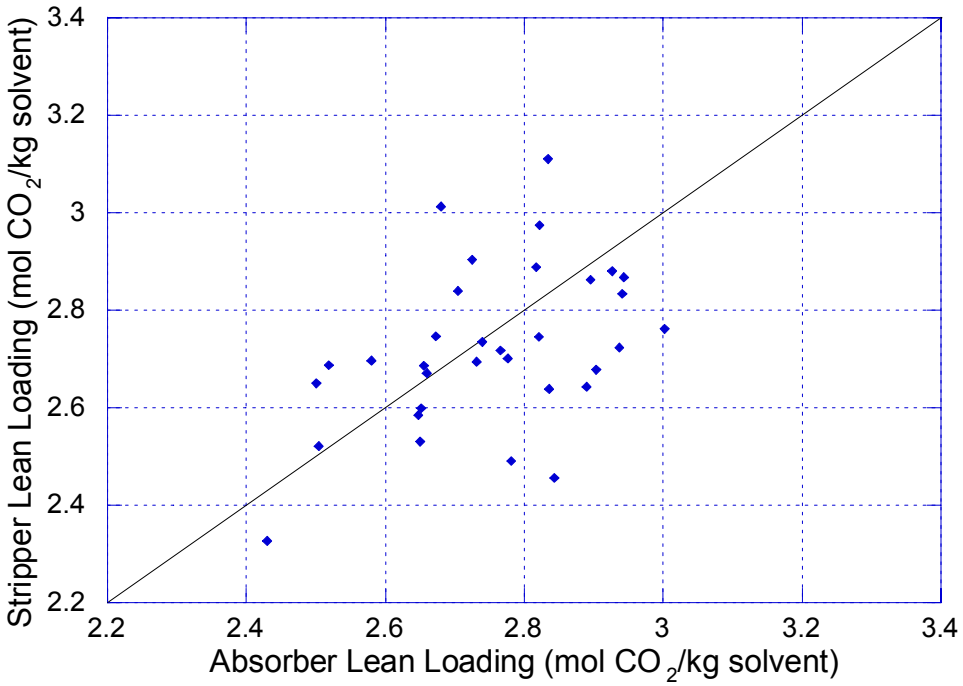

Figure 3-21. Absorber Lean and Stripper Lean CO_2 Loading for 5 m K^+/2.5 m PZ of Campaign 2

Figure 3-22 is a parity plot of CO_2 loading for the absorber lean and stripper lean of Campaign 4. The figure shows that the loading analysis is relatively reliable because the absorber lean and stripper lean loading matched relatively well. The absolute average deviation for the 5 m K^+/2.5 m PZ and 6.4 m K^+/1.6 m PZ solvents are 2.7% and 2.2%, respectively. The plot was used to eliminate outlying absorber lean and stripper lean loading points. The points that had deviations greater than 5% were flagged and eliminated.

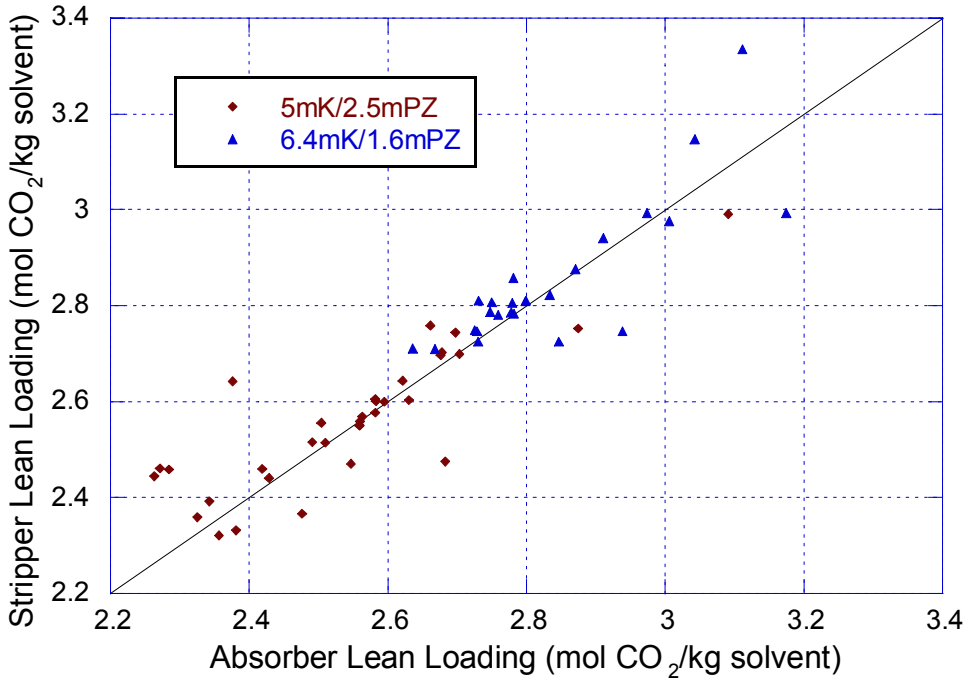

Figure 3-22. Absorber Lean and Stripper Lean Loading for 5 m K^+/2.5 m PZ and 6.4 m K^+/1.6 m PZ of Campaign 4

The capacity of a solvent is defined as the amount of CO_2 that is absorbed per unit mass of solvent. The capacity for the experimental runs was calculated by taking the difference in CO_2 loading between the absorber rich and absorber lean stream. A plot of the absorber lean and absorber rich loading for Campaign 4 shows that the capacity for the 5 m K^+/2.5 m PZ solvent is approximately 50% higher than the 6.4 m K^+/1.6 m PZ solvent (Figure 3-23). The figure also shows that the range of lean loading for the two solvents is completely different. The 5 m K^+/2.5 m PZ solvent was operated at a lower range of lean loading, 2.3 to 2.7 mol CO_2/kg soln and the 6.4 m K^+/1.6 m PZ solvent was operated from 2.6 to 3.2 mol CO_2/kg soln.

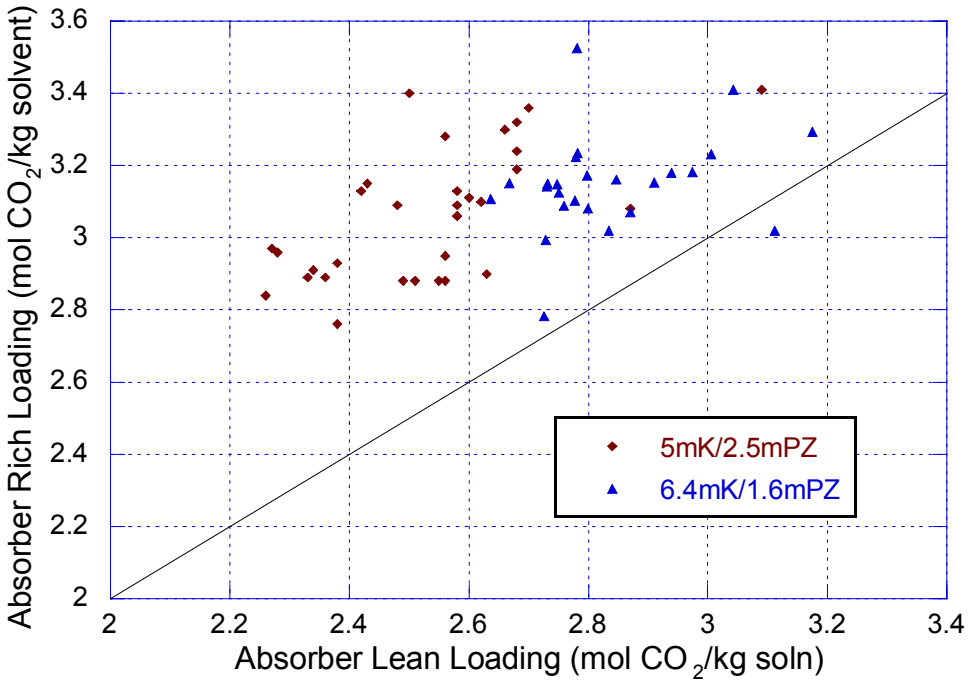

Figure 3-23. Absorber Lean and Absorber Rich Loading Comparison for 5 m K^+/2.5 m PZ and 6.4 m K^+/1.6 m PZ of Campaign 4

Direct correlation of solvent loading to absolute pH values is difficult to measure and often unreliable due to limitations and differences among pH meters. However, indirect measurement of CO_2 loading through pH provides the operator real-time feedback of process conditions and simplifies operation of the plant. The difference between the measured pH values for the absorber lean and absorber rich is plotted against the difference in CO_2 loading of the absorber lean and rich streams, or capacity, of the solvent (Figure 3-24). The figure shows that the liquid capacity for the 5 m K^+/2.5 m PZ solvent correlated well with the ΔpH, whereas there was some scatter with the 6.4 m K^+/1.6 m PZ data. Temperature corrections for the solvent and pH probe were not applied. The automatic temperature compensation function for the pH meter had been disabled. The figure also shows that the 5 m K^+/2.5 m PZ solvent has a capacity that ranges from approximately 0.35 to 0.74 mol CO_2/kg soln, while the 6.4 m

K^+/1.6 m PZ solvent has a capacity that ranges from 0.20 to 0.45 mol CO_2/kg soln. It was assumed that the measured pH values were more reliable than the CO_2 loading analysis. Therefore, the figure shows that the some of the loading measurements for 6.4 m K^+/1.6 m PZ contained significant error. The plot can be used to determine the correct value of the erroneous loading measurements. By taking the difference in pH and knowing at least one of the loading points are accurate, the incorrect loading measurement can be calculated from the capacity plot. This method was not used in the analysis of the pilot plant data.

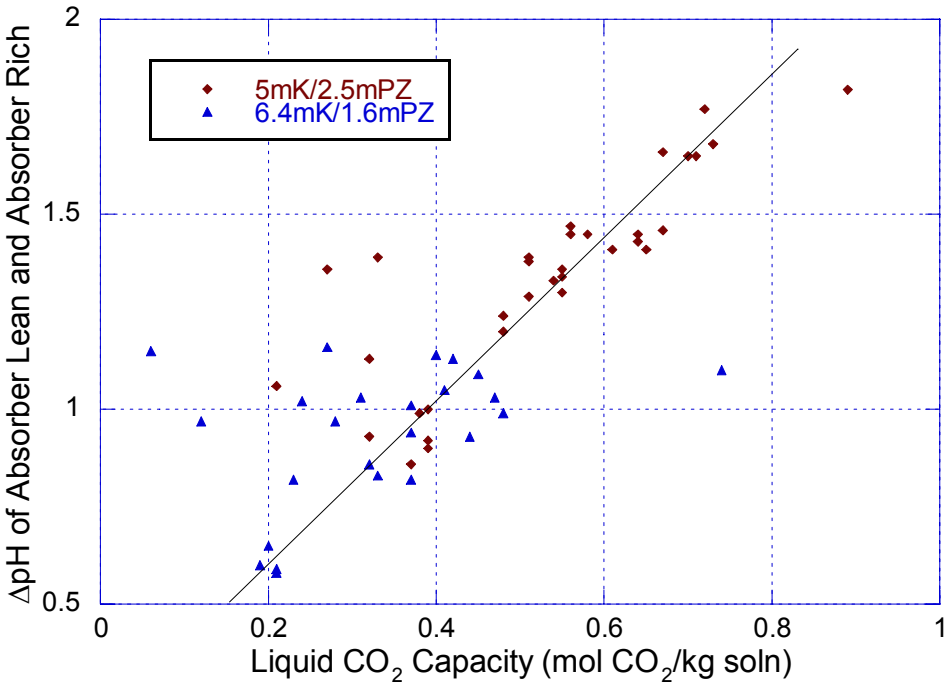

Figure 3-24. Liquid CO_2 Capacity and pH Difference Between Absorber Lean and Rich for 5 m K^+/2.5 m PZ and 6.4 m K^+/1.6 m PZ of Campaign 4

The pH and loading measurements obtained in Campaign 4 are shown in Figure 3-25. The plot shows that the pH decreases with an increase in CO_2 loading of the solution. The figure shows significant scatter and poor correlation of the pH and loading measurements. The correlation of absolute pH measurements with CO_2 loading was difficult to obtain because the water

content was constantly changing throughout the campaigns. Also, due to the high ionic strength of the solvent, the pH measurements may not have been reliable. In addition, the pH meters were only calibrated at the beginning of each campaign. Instrument drift or pH probe degradation over time will affect absolute pH measurements. Finally, the accuracy of the loading measurements will contribute to some of the error.

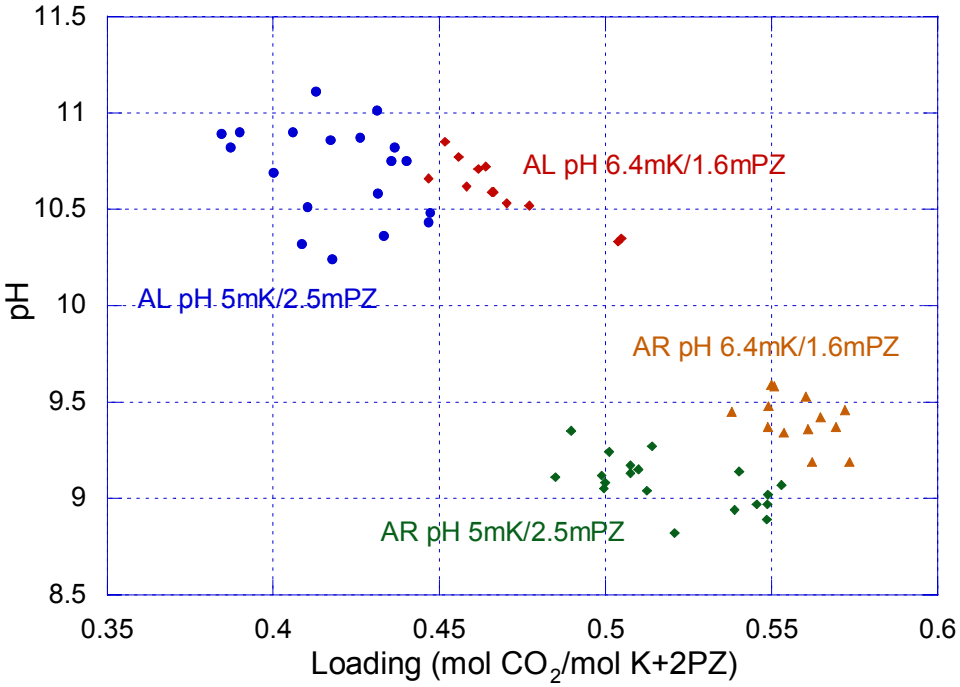

Figure 3-25. Loading and pH Measurements for Absorber Lean (AL) and Absorber Rich (AR) of Campaign 4

3.5 Gas Flow Rate

In the first two campaigns, the gas flow was measured with a Dietrich Standard AN-75 annubar and Ashcroft pressure transmitters in a 20.3 cm diameter PVC pipe. There were some issues with the Ashcroft transmitters and they were eventually replaced with Rosemount 3051 pressure transmitters. The replacement date of the pressure transmitters is unclear, but may have occurred

during Campaign 2. The gas flow rate was verified using a pitot tube traverse in February 2004, before the start of Campaign 1 and was determined to be accurate.

In Campaign 3, the 20.3 cm diameter gas line was replaced with smaller diameter gas lines, 7.6 cm and 10.2 cm schedule 40 PVC pipe and new annubars were installed in each of the gas lines. During the operation of Campaign 3, there were some issues with the gas rate measurement. When the gas flow was shut off, the transmitter still displayed a relatively large flow rate. The gas flow was manually zeroed in DeltaV to correct the offset.

In Campaign 4, the two PVC gas lines were replaced with a single 10.2 cm diameter Schedule 10 stainless steel pipe and the annubar used in the previous campaign was reinstalled. A correction factor for the new inner diameter was applied in DeltaV. The gas flow rate was not re-evaluated after the modifications made in Campaigns 3 and 4. However, packing tests that were performed after Campaigns 3 and 4 showed that the pressure drop measurements were comparable to the vendor values. It was concluded that the real-time gas flow measurements were reliable.

The gas flows for all of the annubars were calibrated for dry air. However, during the operation of the CO_2 capture pilot plant, the composition of the gas contained between 3 to 18% CO_2 and from 2 to 10% H_2O. The molecular weight of the air stream was corrected for the difference in gas composition. The correction term was applied as the square root of the ratio of the two molecular weights of the gases. The correction term reduced the measured gas rate by approximately 3–5%.

3.6 CO_2 Gas Calibration Standards

In the second campaign, it was erroneously concluded that the CO_2 calibration gas cylinders were based on a weight percent instead of volume

percent. If it is assumed that the calibration gases are in weight percent, the material balance for the gas phase matches the liquid phase. When the sales representative of the gas provider was consulted, we were informed that the cylinders were filled gravimetrically and it was initially assumed that the percentages were based on weight. In the MEA campaign, a gas cylinder for 17% was purchased and used to calibrate the CO_2 analyzers. It was assumed that the 17% was in weight percent, which was equivalent to 12 mole percent.

However, after the completion of the Campaign 4, the material balance did not close when a weight based assumption was made. Further investigation into the matter and additional contacts with the manufacturer indicated that the concentrations were volume percent and not mass percent. To further corroborate this, some of the cylinders were tested.

3.7 CO_2 GAS ANALYZER CALIBRATION

The Vaisala and Horiba analyzers are calibrated on a dry basis with Primary Standards for 1%, 4%, 4.9%, 12%, and 16.9 mol% CO_2 purchased from Praxair, Inc. The Vaisala analyzers are located in situ and provide real time CO_2 gas measurements. The Horiba analyzer uses an extractive sampling system. Although calibrations are performed on a dry basis, online Vaisala measurements of CO_2 are taken under wet, sometimes even condensing conditions such as in Campaign 2. The gas stream for the Horiba analyzer, on the other hand, is conditioned and the water is removed prior to analysis.

An analysis of the method, procedure, and results for the calibration of the CO_2 analyzers was performed and a few errors were discovered. In Campaigns 1 and 2, linear calibration curves were used. In Campaigns 3 and 4, a second order polynomial was used to fit the calibration curve. Once the calibration curves are created, the parameters are inputted into the DeltaV process control

system and need to be uploaded into DeltaV in order for the changes to take effect. If the new parameters are not uploaded, DeltaV continues to use the original calibration parameters.

A review of the logged CO_2 gas concentration data found that the calibration parameters for Campaign 2 were not properly updated. A comparison of the process screen printouts and logged data showed that the calibration curve parameters for the outlet CO_2 concentration had not been uploaded and updated after the 11/02/04 calibration. The printout indicated that the 10/27/04 calibration parameters were used for the CO_2 outlet. In addition, it is possible that the inlet calibration curve had also not been updated, which may be significant because the slope of the calibration curve for the Horiba had changed from 1.24 to 1.42. The material balance for Campaign 2 did not close after the pilot plant was reconfigured for vacuum operation, which also corresponds to when the analyzer was recalibrated on 11/02/04.

In addition, it was discovered that the raw signals for the CO_2 concentration were being logged by DeltaV instead of the calibrated values. This error was discovered after the completion of all four pilot plant campaigns when the online process screens were compared to the logged pilot plant data. It was also discovered that the raw signals for the inlet and outlet CO_2 of Campaign 1 were logged instead of the calibrated values. In Campaigns 2 and 4, the calibrated inlet CO_2 concentration had been logged, but the raw signal for the outlet CO_2 concentration was logged. The raw outlet CO_2 concentration for Campaign 3 may have also been logged, but this was not verified. The erroneous inlet and outlet CO_2 concentrations for Campaigns 1, 2 and 4 were updated using the log sheet of the CO_2 calibration curves.

The calibration date and parameters for the CO_2 analyzer calibration curves for Campaigns 1, 2, 3, and 4 are listed in Tables 3-2, 3-3, 3-4, and 3-5,

respectively. The calibration curves for Campaigns 3 and 4 have been refitted to a linear equation instead of a polynomial to facilitate comparison. Three to four calibration points were used to generate the calibration equations, which all had R^2 values greater than 0.999.

Table 3-2. Campaign 1 CO_2 Gas Analyzer Calibration Date and Equations

Date	Time	CO_2 In Vaisala 0–20%	CO_2 Mid Horiba 0–5%	CO_2 Out Vaisala 0–1%
6/15/04		y = 1.0359x + 0.0045	-	-
6/18/04	9:37	y = 1.0234x + 0.0219	y = 0.3087x - 1.193	y = 1.1001x - 0.0154
6/23/04	9:00	y = 1.0555x - 0.0166	y = 0.4278x - 1.7112	y = 1.0373x - 0.0373
6/24/04	7:30	y = 1.0355x + 0.0085	y = 0.4479x - 1.7237	y = 1.0808x - 0.0203

Table 3-3. Campaign 2 CO_2 Gas Analyzer Calibration Date and Equations

Date	Time	CO_2 In Horiba 0–20%	CO_2 Out Vaisala 0–5%
10/24/04		-	y = 1.1534x - 0.0528
10/25/04	16:59	y = 1.2631x - 4.8906	-
10/26/04		y = 1.2342x - 4.7243	-
10/27/04		y = 1.2383x - 4.8413	y = 1.1529x - 0.0305
11/02/04		y = 1.4169x - 5.4974	y = 1.1008x - 0.0562

Table 3-4. Campaign 3 CO_2 Gas Analyzer Calibration Date and Equations

Date	Time	CO_2 In Vaisala 0–20%	CO_2 Mid Horiba 0–20%	CO_2 Out Vaisala 0–5%
2/25/05	15:00	y = 0.9927x - 0.0318	y = 1.5533x - 6.2009	-
2/28/05	-	-	-	y = 1.1079x - 0.0744
3/08/05	17:35	-	y = 1.5675x - 5.7953	-
3/14/05	-	-	-	y = 1.1179x - 0.0508
3/17/05	-	y = 0.9731x - 0.0265	y = 1.5583x - 5.7671	y = 1.1049x - 0.0650
4/05/05	-	y = 0.9731x + 0.0114	y = 1.6127x - 5.9312	y = 1.1988x - 0.0580
4/14/05	-	y = 0.9221x + 0.0531	y = 1.5916x - 5.9856	y = 1.1980x - 0.0752

Table 3-5. Campaign 4 CO_2 Gas Analyzer Calibration Date and Equations

Date	Time	CO_2 In Vaisala 0–20%	CO_2 Mid Horiba 0–20%	CO_2 Out Vaisala 0–5%
11/07/05	12:29	y = 0.9473x - 0.0004	y = 1.5856x - 6.3451	y = 1.2264x - 0.1223
1/10/06	7:55	y = 0.9560x - 0.1172	y = 1.6613x - 6.5822	y = 1.1508x - 0.1399
1/18/06	13:18	y = 0.9443x - 0.0863	y = 1.7545x - 6.7772	y = 1.2164x - 0.1403
FTIR		CO_2 In	-	CO_2 Out
1/10/06	7:55	y = 1.0885x - 2E-05	-	Same

The tables show that the slope of the calibration curve for the 0–5% Horiba analyzer increased by 30% from the 6/18/04 to 6/23/04 calibration, but remained relatively constant in the calibration the on following day. The slope of the high concentration Horiba analyzer (0–20%) steadily increased with each campaign, changing from 1.23 to 1.75. In Campaign 2, the slope changed by approximately 15% for the 11/02/04 calibration. In Campaign 3, the slope for the Horiba remained relatively constant and fluctuated between 1.5 and 1.6. In Campaign 4, the slope increased from 1.66 to 1.75, an increase of 5.4%. The Horiba produces a 4–20mA signal, which should give an offset of 4. The tables show that the intercept of the calibration curve increases from 4.7 to 6.8 over the course of the three campaigns.

In Campaign 1, the slope of the inlet 0–20% Vaisala CO_2 analyzer remained relatively constant, fluctuating between 1.02 and 1.06. In Campaign 2, the inlet 0–20% Vaisala CO_2 analyzer failed at the beginning of the experiments due to excessive moisture in the gas. A new 0–20% Vaisala probe was purchased and installed for Campaign 3. The inlet 0–20% Vaisala CO_2 analyzer was calibrated a total of four times during Campaign 3. At the start of the campaign, the slope the calibration curve was 0.99 and eventually drifted down to 0.92. Prior to the start of Campaign 4, another 0–20% Vaisala probe was purchased. The new probe was installed and the old probe was retained as the backup in

event of another probe failure. In Campaign 4, the inlet Vaisala analyzer was calibrated twice and remained relatively stable. The slope for the calibration equations varied between 0.96 and 0.94 and intercept varied from 0.11 to 0.09.

The outlet 0–5% Vaisala CO_2 analyzer also appeared to remain relatively stable. In Campaign 1, the slope of the calibration curve ranged from 1.04 to 1.10 (~5% difference). In Campaign 2, the slope of the calibration curve also varied by 5%, changing from 1.15 to 1.10. In Campaign 3, the slope of the calibration changed from 1.11 to 1.20, a difference of 10%. In Campaign 4, a new 0–5% Vaisala probe was installed, but the existing transmitter was retained. The slope of the calibration curve was 1.15 at the beginning of the campaign had slightly drifted to 1.22 when the analyzer was recalibrated at the start of the 6.4 m K^+/1.6 m PZ solvent composition change.

In Campaign 4, the FTIR was calibrated at the start of the campaign (1/10/06) with the same CO_2 gas standards used for the Horiba and Vaisala following the same standard procedure. A calibration curve was generated and the parameters were entered into the DeltaV system. The slope of the calibration curve was determined to be 1.09. On 1/23/06, the baseline for the FTIR was re-zeroed. There was some concern with the results of the FTIR calibration. First, the FTIR had previously been calibrated in the laboratory and according some sources, it did not need to be recalibrated once transported into the field. If this is true, this indicates that either the 3 CO_2 gas cylinders used to calibrate the FTIR were all off by 9% or there was a leak in the sample line.

During the analysis of the CO_2 gas concentration, it was found that the response for FTIR and Horiba lagged slightly behind that of the Vaisala analyzers, due to the extractive sampling methods used by both analyzers. At each sample point, the data points 10 minutes before and after were averaged. The amount of time that the FTIR and Horiba data was shifted was evaluated on

a case by case basis. The trend lines for all of the CO_2 gas concentrations were plotted and visually matched. The logged values for the FTIR were shifted by 4 minutes for the data taken on the 10, 11, 12, 18, and 19th. The data taken on the 11th was shifted by 5 minutes. The data for the remaining dates were shifted by 8 minutes. The Horiba data was shifted by 3 minutes for 1/12/06 and by 1 minute for 1/18/06 and 1/19/06. The remaining data points were shifted by 2 minutes. In some cases, some of the FTIR points were deleted from the average because it occurred during the period when the location of the FITR analysis was switched from inlet to outlet or vice versa.

Some possible sources of error for the CO_2 analyzers include differences in the flow rate between the calibration gas and the sampling flow rate once the analyzers were placed into service. If the sample gas rate is different than the calibration flow rate, there may be slight discrepancies with the measured CO_2 concentration. In addition, it is possible that there may have been slight leaks in the sample lines. The Horiba sampling system consists of an initial water knockout, a sample pump, another water knockout and a membrane for further drying. During the operation of the pilot plant, the initial knockout continuously condensed water from the sample gas, which may have contained residual solvent that absorbed CO_2. In addition, a portion of the sample gas is diverted through the second water knockout and the remaining gas is sent to the Horiba analyzer for analysis. A rotameter on the outlet of the Horiba analyzer was used to control the sample gas flow rate. Depending on the conditions in the absorber, there was some variation in sampling gas rate. The rotameter on the outlet of the Horiba needed to be adjusted periodically to maintain a constant sampling gas rate. This may have contributed to some discrepancies in the analysis.

3.8 CO_2 Gas Concentration

Figure 3-26 shows that the inlet CO_2 gas concentration measured by the FTIR and Vaisala analyzers matched. The absolute average deviation for the 5 m K^+/2.5 m PZ and 6.4 m K^+/1.6 m PZ solvents were 1.2% and 1.7%, respectively. The two gas concentrations are measured on a wet basis and are expected to be different because the water content for the two locations should have been different.

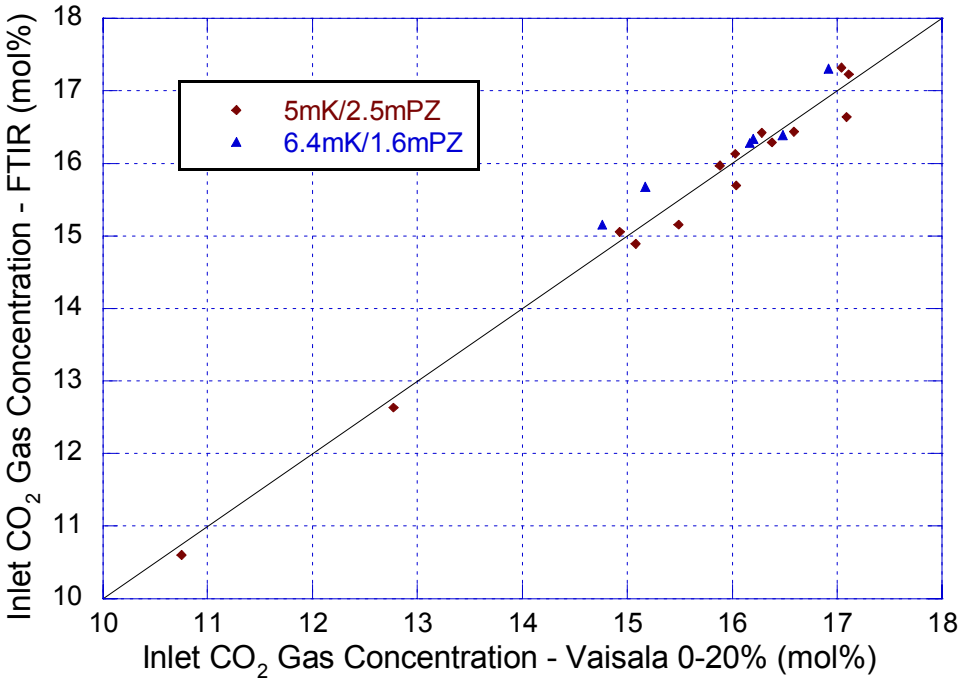

Figure 3-26. Campaign 4 Inlet CO_2 Gas Concentration of Vaisala 0–20% and FTIR (Wet Basis) for 5 m K^+/2.5 m PZ and 6.4 m K^+/1.6 m PZ

Wet and dry CO_2 calibration experiments that were performed on the Vaisala CO_2 analyzers indicated that the sensors were responsive to water vapor pressure. A gas mixture of CO_2 and air was preheated and humidified prior to analysis by the Vaisala. An increase in water vapor results in a proportionate decrease in reading for CO_2 concentration. The water vapor concentration was

adjusted by increasing the temperature and the changes may have partially been a result of the effect of temperature on the Vaisala analyzers.

The inlet Vaisala analyzer is located upstream of the steam injection and was assumed to be at the annubar temperature, which varied between 16 to 27 °C. This results in a saturated water concentration ranging from 1.8 to 3.5 mol%. The FTIR, on the other hand, was analyzed at a gas temperature that was approximately 40 °C, which results in a saturated water concentration of 7.3 mol%.

One possible interpretation of the unexpected discrepancy is that while the steam injection may have heated the gas to 40 °C, the gas may not have been fully saturated. This resulted in water concentrations that are comparable to the conditions at the Vaisala analyzer. Under certain operating conditions, the Vaisala probes may have become wet due to condensing water. A thin paper-like membrane is used in the Vaisala probes to prevent water from contacting the working parts of the probe. However, the membrane is not mechanically sealed and there is a possibility of water leakage. The Vaisala probes are designed to work in non-condensing environments. In Campaign 2, the inlet Vaisala CO_2 analyzer failed because condensing water had penetrated the membrane. It was concluded that the selection of the in situ Vaisala analyzers was useful for real time feedback for use in process control, but may not suitable for accurate measurements of CO_2 in a pilot plant environment, especially under saturated conditions. Finally, the liquid used to feed the steam injector is from the distillate of the stripper condenser. The distillate may contain residual amounts of piperazine, which would have depressed the equilibrium vapor pressure of water.

The outlet CO_2 gas concentration (wet basis) measured by the FTIR and Vaisala analyzers also matched (Figure 3-27). The absolute average deviation for

the 5 m K^+/2.5 m PZ and 6.4 m K^+/1.6 m PZ solvents were 5.7% and 1.3%, respectively. The two measurements of CO_2 are expected to be different because of the water content and gas temperature. The FTIR withdraws the gas sample directly from the head section at the top of the absorber, whereas the Vaisala analyzer, which is located downstream of the FTIR, analyzes a gas stream that has passed through the air cooler, a water knockout and is at a temperature of 10 to 16 °C. However, the equilibrium vapor pressure of water exiting the absorber will be lower than that of pure water because of the presence of potassium carbonate and piperazine.

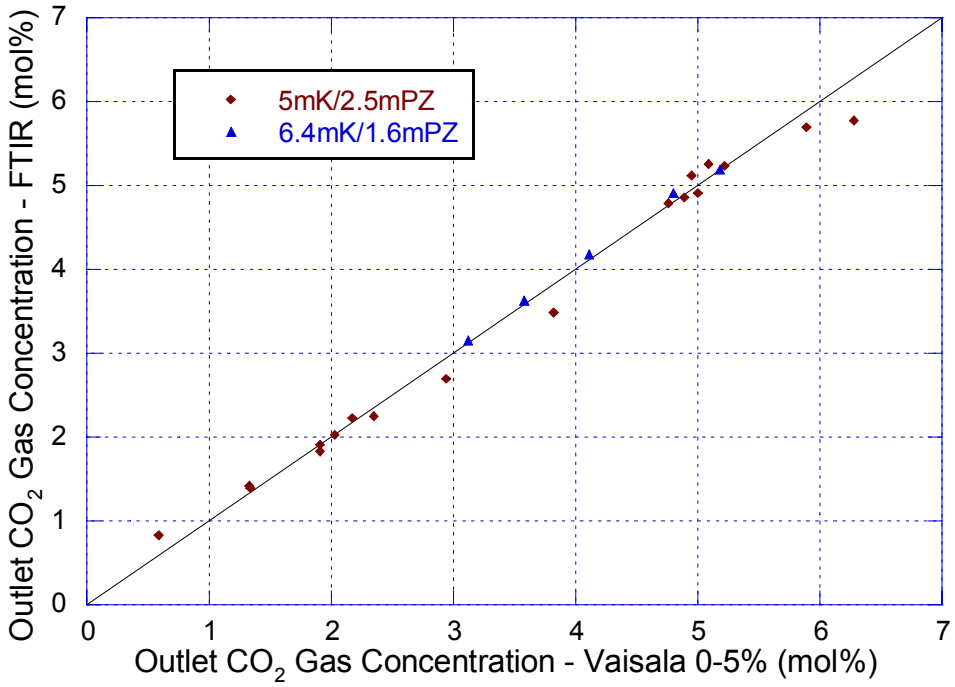

Figure 3-27. Campaign 4 Outlet CO_2 Gas Concentration of Vaisala 0–20% and FTIR (Wet Basis) for 5 m K^+/2.5 m PZ and 6.4 m K^+/1.6 m PZ

The outlet Vaisala analyzer was operated under a slight vacuum (-0.4–1.5 kPag). It is possible that there may have been a slight leak. The diameter of the Vaisala probe was a non-standard metric size and was inserted in the gas pipe using a Swagelok fitting with Teflon ferrules. Although the seal around the

outside of the probe may have been sufficient, it is unknown whether the probe itself was gas–tight. There is a cable that connects the probe to the transmitter and the seal between the probe and cable was probably not designed to be gas–tight. Depending operating conditions and the vacuum pressure a slight leak may have been possible.

3.9 H_2O Gas Concentration

The concentration of water in the gas is important for determining the concentration of CO_2 in the gas. The absorber inlet and outlet water concentration was measured with the FTIR and was used as way to verify assumptions made regarding water content in the gas. The saturated vapor pressure of water calculated at the measured inlet and outlet gas temperatures is plotted against the values obtained by the FTIR (Figure 3-28).

The calculated vapor pressure of water assumes that the solvent is pure water and may not be valid for the outlet gas because the solvent contains piperazine and potassium carbonate. Therefore, the vapor pressure of water for the outlet gas should be slightly depressed. The absolute average deviation of the measured outlet water concentration was 5.5% and 7.9% lower than the calculated values for the 5 m K^+/2.5 m PZ and 6.4 m K^+/1.6 m PZ solvent, respectively. The absolute average deviation of the measured inlet water concentration was 10% and 17.4% lower than the calculated values, for the 5 m K^+/2.5 m PZ and 6.4 m K^+/1.6 m PZ solvent, respectively. The variation of the measured values is most likely due to the close proximity of the FTIR inlet sample port to the steam injection point. The gas was not well mixed at the sample point and resulted in erratic water measurements. In addition, the depressed values may be due to the presence of residual solvent in the distillate.

This was confirmed when the absorber gas preheater had to be shut down to remove solvent residue that had accumulated over time on the reboiler tubes.

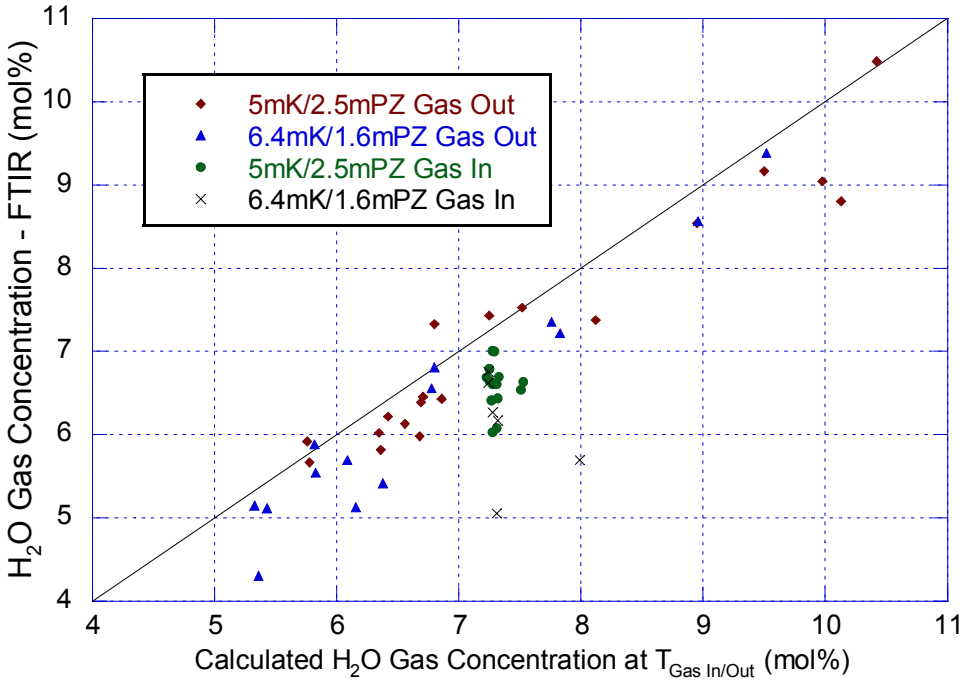

Figure 3-28. Gas Phase H_2O Concentration Measured by FTIR and Calculated Values Assuming Saturation at Measured Inlet and Outlet Gas Temperatures for 5 m K^+/2.5 m PZ and 6.4 m K^+/1.6 m PZ of Campaign 4

The vapor pressure of water over the 5 m K^+/2.5 m PZ solvent was calculated with the Hilliard Aspen Plus® VLE model using a flash calculation from 25 – 60 °C. Figure 3-29 shows that the vapor pressure values predicted by Aspen Plus® are approximately 14% lower than that predicted by the DIPPR equation (Design Institute for Physical Properties (DIPPR), 2006) over pure water. The points that are predicted by the VLE model are fitted to a second order polynomial is given by:

$$P_{H_2O\ AspenPlus} = 8.8518 \times \left(T(^\circ C)\right)^2 - 348.12 \times \left(T(^\circ C)\right) + 6016.7 \qquad (3.1)$$

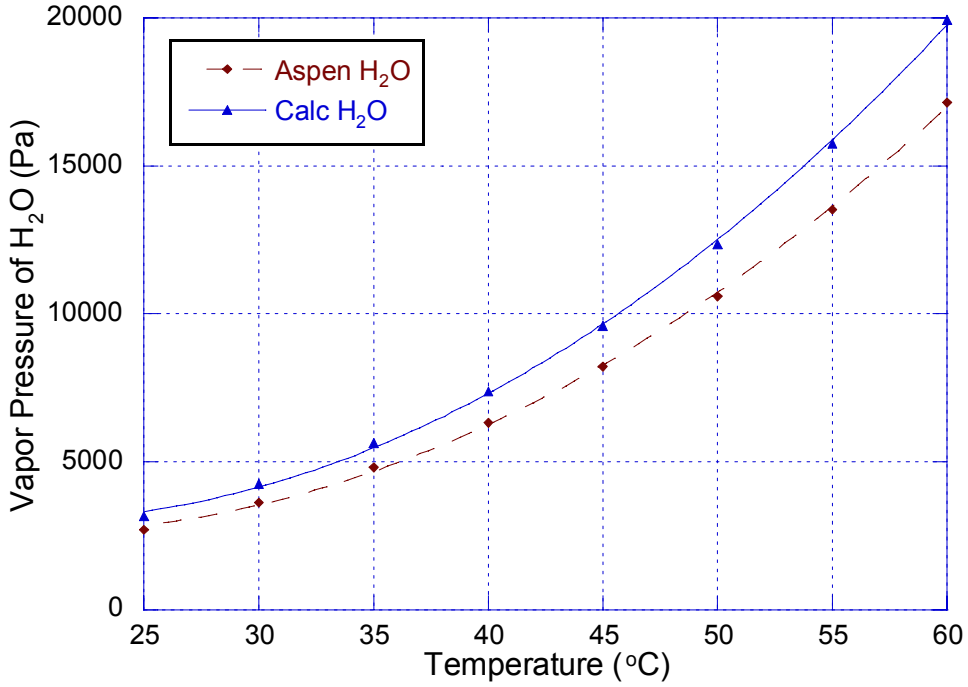

Figure 3-29. Predicted Vapor Pressure of Water Using Hilliard Aspen Plus® VLE Model and Calculated Vapor Pressure over Pure Water

The values measured by the outlet FTIR would most likely correspond to the values predicted by the Aspen Plus® VLE model, but the FTIR values are not as low as that predicted by the simulation. However, the FTIR sample point is approximately 7 meters upstream of the outlet gas temperature measurement, which may have been at a higher temperature. Thus, a higher water vapor pressure would be expected. Also, the measured pressure at the top of the absorber column may not have corresponded to the value at the FTIR sample location and will slightly affect the mole percent reading of the FTIR. Finally, the values of the water vapor pressure predicted by the Aspen Plus® model may not be accurate.

3.10 Gas Phase Impurities

Impurities may accumulate in the gas over time because it is continuously recycled. In Campaign 4, the gas phase concentration of piperazine was

measured with the FTIR. The FTIR measurements showed that the majority of the piperazine measurements were in the 0–20 ppm range for both the inlet and outlet of the absorber and it was concluded that piperazine volatility was insignificant (McLees, 2006). The FTIR measurements also identified an unknown amine, possibly a degradation product, which had a sample spectrum similar to ethylenediamine and ethylamine. During the operation of the 5 m K^+/2.5 m PZ solvent, 10–100 ppm of hexane was detected by the FTIR. When the solvent was changed to 6.4 m K^+/1.6 m PZ, the inlet and outlet hexane concentration increased to 100–1000 ppm. Hexane was used in an extraction experiment in the absorber prior to the start of Campaign 4. In addition, 2–5 ppm of NO_x was measured in the gas. Finally, it is possible that oil from the vacuum pump may have accumulated in gas over time because the gas comes into direct contact with the oil. Aside from hexane, the concentrations of gas phase impurities were negligible. Therefore, gas phase impurities should not affect the liquid composition and the performance of the absorber.

3.11 DATA RECONCILIATION

3.11.1 Stripper Lean Density

The density of the stripper lean measurements for Campaign 4 was adjusted to match the absorber lean measurements. Based on bench-scale density measurements made in Campaign 4, the dependence of temperature of the solvent was correlated and found have an average slope of -0.000542±0.0000095. The measured absorber lean and stripper lean densities were corrected to 40 °C and correlated based on a parity plot. For 5 m K^+/2.5 m PZ solvent, the density was corrected by the following equation:

$$\rho_{CORR,SL} = 1.0343 \cdot \rho_{SL,5K/2.5PZ} - 0.0401 \tag{3.2}$$

For the 6.4 m K^+/1.6 m PZ solvent, the density was corrected by the following equation:

$$\rho_{CORR,SL} = 1.0419 \cdot \rho_{SL,6.4K/1.6PZ} - 0.0515 \quad (3.3)$$

where ρ has units of g/cm^3. The corrected density measurements are enumerated by the following table:

Table 3-6. Campaign 4 Corrected Stripper Lean Density Measurements for 5 m K^+/2.5 m PZ and 6.4 m K^+/1.6 m PZ

Run#	SL Density Original kg/m^3	SL Density Corrected kg/m^3
4.1	1221	1223
4.2.1	1226	1228
4.2.2	1227	1229
4.3.1	1225	1227
4.3.2	1225	1227
4.4.1	1225	1227
4.4.2	1225	1227
4.5.1	1228	1230
4.5.2	1230	1232
4.6.1	1212	1214
4.6.2	1213	1214
4.7.1	1213	1215
4.7.2	1213	1214
4.8	1211	1212
4.9.1	1213	1214
4.9.2	1213	1215
4.10.1	1212	1214
4.10.2	1215	1217
4.11.1	1216	1217
4.11.2	1216	1218
4.12.1	1218	1220
4.12.2	1219	1220
4.13.1	1215	1217
4.13.2	1215	1216
4.14.1	1217	1219
4.14.2	1216	1218
4.15.1	1218	1220
4.15.2	1219	1220
4.16.1	1217	1218
4.16.2	1217	1219
4.17.1	1216	1217
4.17.2	1215	1217
4.18	1221	1223
4.19	1221	1222
4.20.1	1276	1278
4.20.2	1274	1276
4.21.1	1263	1264
4.21.2.	1265	1267
4.22.1	1271	1273
4.22.2	1272	1274
4.23	1274	1276
4.24	1271	1272
4.25	1265	1267
4.26.1	1263	1264
4.26.2	1264	1265
4.27.1	1265	1266
4.27.2	1266	1267
4.28.1	1262	1263
4.28.2	1263	1264
4.29.1	1266	1268
4.29.2	1268	1269
4.30.1	1263	1265
4.30.2	1265	1267
4.31.1	1262	1263
4.31.2	1263	1265
4.32.1	1265	1266
4.32.2	1265	1267
4.33.1	1260	1261
4.33.2	1260	1262

3.11.2 Potassium, Piperazine, and CO_2 Concentration

The adjusted data for the potassium, piperazine, and CO_2 concentration of Campaign 4 are listed in the tables below. The adjustment factor and the corresponding data point are enumerated for the absorber lean and stripper middle samples of the 5 m K^+/2.5 m PZ solution (Table 3-7).

Table 3-7. Adjusted Liquid Analysis Data for Campaign 4 (5 m K^+/2.5 m PZ)

Run#	AK K^+ Adj Factor	AL K^+ Adj mol/kg	AL PZ Adj Factor	AL PZ Adj mol/kg	AL CO_2 Adj Factor	AL CO_2 Adj mol/kg	SM K^+ Adj Factor	SM K^+ Adj mol/kg	SM PZ Adj Factor	SM PZ Adj mol/kg
4.1	-	3.04	-	1.43	-	2.55	1.11	2.90	1.10	1.39
4.2.1	-	3.15	-	1.49	-	2.56	1.11	2.98	1.10	1.43
4.2.2	-	3.16	-	1.49	-	2.50	1.11	3.17	1.10	1.52
4.3.1	-	3.10	-	1.47	-	2.68	1.11	3.20	1.10	1.52
4.3.2	-	3.15	-	1.49	-	2.68	1.11	3.22	1.10	1.55
4.4.1	-	3.15	-	1.50	-	2.66	1.11	3.15	1.10	1.52
4.4.2	0.90	3.13	0.90	1.50	0.90	2.69	1.11	3.23	1.10	1.56
4.5.1	-	3.14	-	1.49	-	2.66	1.11	3.24	1.10	1.56
4.5.2	-	3.15	-	1.50	-	2.70	1.11	3.19	1.10	1.53
4.6.1	-	3.05	-	1.45	-	2.42	1.11	2.87	1.10	1.40
4.6.2	-	3.08	-	1.46	-	2.43	1.11	3.04	1.10	1.47
4.7.1	-	3.12	-	1.47	-	2.34	1.11	2.90	1.10	1.40
4.7.2	-	3.09	-	1.45	-	2.33	1.11	3.14	1.10	1.50
4.8	-	2.96	-	1.42	-	2.26	1.11	2.98	1.10	1.39
4.9.1	-	3.06	-	1.44	-	2.27	1.11	3.02	1.10	1.47
4.9.2	-	3.05	-	1.43	-	2.28	1.11	2.85	1.10	1.40
4.10.1	-	3.04	-	1.43	-	2.63	1.11	3.09	1.10	1.52
4.10.2	-	2.95	-	1.40	-	2.58	1.11	2.94	1.10	1.42
4.11.1	0.88	3.11	0.88	1.40	-	2.60	1.11	3.07	1.10	1.48
4.11.2	-	3.05	-	1.45	-	2.58	1.11	3.12	1.10	1.50
4.12.1	-	3.10	-	1.47	-	2.58	1.11	3.06	1.10	1.47
4.12.2	-	3.09	-	1.46	-	2.62	1.11	3.10	1.10	1.49
4.13.1	1.07	2.94	1.07	1.40	-	2.38	1.11	2.93	1.10	1.41
4.13.2	0.88	2.99	0.93	1.41	-	2.49	1.11	3.02	1.10	1.45
4.14.1	0.88	3.06	0.93	1.43	-	2.56	1.11	2.99	1.10	1.44
4.14.2	1.07	2.99	1.07	1.42	-	2.51	1.11	2.94	1.10	1.41
4.15.1	1.07	3.14	1.07	1.49	-	2.56	1.11	2.96	1.10	1.40
4.15.2	1.07	3.13	1.07	1.48	-	2.56	1.11	3.01	1.10	1.44
4.16.1	0.90	3.19	0.90	1.60	0.90	2.78	1.11	3.87	1.10	1.84
4.16.2	0.90	3.00	0.90	1.44	0.90	2.59	1.11	3.25	1.10	1.53
4.17.1	1.07	3.19	1.07	1.50	-	2.36	1.11	2.93	1.10	1.43
4.17.2	1.07	3.10	1.07	1.47	-	2.38	1.11	2.89	1.10	1.40
4.18	1.07	3.15	1.07	1.49	-	2.48	1.11	3.01	1.10	1.44
4.19	1.07	3.34	1.07	1.58	-	2.68	1.11	3.40	1.10	1.62

The adjustment factor and the corresponding data point for the absorber lean and stripper middle samples of the 6.4 m K^+/1.6 m PZ solution is shown in

Table 3-8. All other data points from the liquid analysis were not corrected and were used directly in the CO_2 material balance and mass transfer performance calculations.

Table 3-8. Adjusted Liquid Analysis Data for Campaign 4 (6.4 m K^+/1.6 m PZ)

Run#	Adj Factor	AL K^+ Adj mol/kg	SM K^+ Adj Factor	SM K^+ Adj mol/kg	SM PZ Adj Factor	SM PZ Adj mol/kg
4.20.1	0.92	3.50	1.09	4.06	1.08	1.10
4.20.2	0.92	3.74	1.09	3.80	1.08	1.01
4.21.1	0.92	3.37	1.09	3.57	1.08	0.99
4.21.2.	0.92	3.39	1.09	3.73	1.08	1.02
4.22.1	0.92	-	1.09	4.31	1.08	1.19
4.22.2	0.92	4.42	1.09	4.22	1.08	1.20
4.23	0.92	4.38	1.09	4.03	1.08	1.11
4.24	0.92	3.93	1.09	4.13	1.08	1.13
4.25	0.92	3.71	1.09	3.53	1.08	0.98
4.26.1	0.92	3.67	1.09	3.56	1.08	0.98
4.26.2	0.92	3.60	1.09	3.49	1.08	0.96
4.27.1	0.92	3.64	1.09	3.76	1.08	1.06
4.27.2	0.92	3.82	1.09	3.58	1.08	1.00
4.28.1	0.92	3.62	1.09	0.00	1.08	0.00
4.28.2	0.92	3.60	1.09	3.69	1.08	1.02
4.29.1	0.92	3.68	1.09	3.65	1.08	1.02
4.29.2	0.92	3.75	1.09	3.59	1.08	1.00
4.30.1	0.92	4.26	1.09	3.48	1.08	0.97
4.30.2	0.92	3.61	1.09	3.51	1.08	0.98
4.31.1	0.92	3.83	1.09	3.54	1.08	0.98
4.31.2	0.92	3.86	1.09	3.61	1.08	1.00
4.32.1	0.92	3.68	1.09	3.63	1.08	0.98
4.32.2	0.92	3.52	1.09	3.84	1.08	1.07
4.33.1	0.92	3.63	1.09	3.67	1.08	1.03
4.33.2	0.92	3.47	1.09	3.59	1.08	1.00

3.12 MATERIAL BALANCE

A material balance for carbon dioxide was performed across the absorber. The rate of carbon dioxide removal was calculated for the gas phase by taking the difference between the inlet and outlet CO_2 gas flow. The CO_2 gas flow was based on the measurements of CO_2 gas concentration, the gas flow rate measured by the annubar, and the calculated water content. The annubar was originally calibrated for air and a density correction was applied to the account for CO_2 and H_2O. The liquid phase CO_2 mass balance was calculated as the difference

between the inlet and outlet CO_2 liquid flow. The molar flow rate of CO_2 in the liquid was calculated from the measured loading and the flow rate and density measured by the Micro Motion® flowmeters for each stream. No adjustments were made to the raw data for the CO_2 material balance calculations.

3.12.1 Campaign 1

The material balance for Campaign 1 indicates that gas side removal of CO_2 was on average 14% higher than the liquid phase (Figure 3-30). In the first campaign, the measurements from the Vaisala analyzer were used for the inlet and outlet CO_2 concentration. The outlet water concentration was assumed to be saturated at the outlet gas temperature and the inlet water concentration was assumed to be saturated at the gas temperature measured downstream of the air cooler. In Campaign 1, samples were taken with Erlenmeyer flasks and it was likely that CO_2 was lost due to flashing. In addition, the analytical method for CO_2 loading was not fully developed at the time, which may have contributed to addition errors in the liquid analysis. However, the error appeared to be systematic, which indicates that the gas or liquid rate or CO_2 gas concentration may be offset. The liquid phase measurements are critical to the CO_2 material balance. If the absorber rich CO_2 loading is increased by 2.5%, the offset is eliminated. For gas–side adjustments, the total gas rate would need to be decreased by 12% to correct the offset.

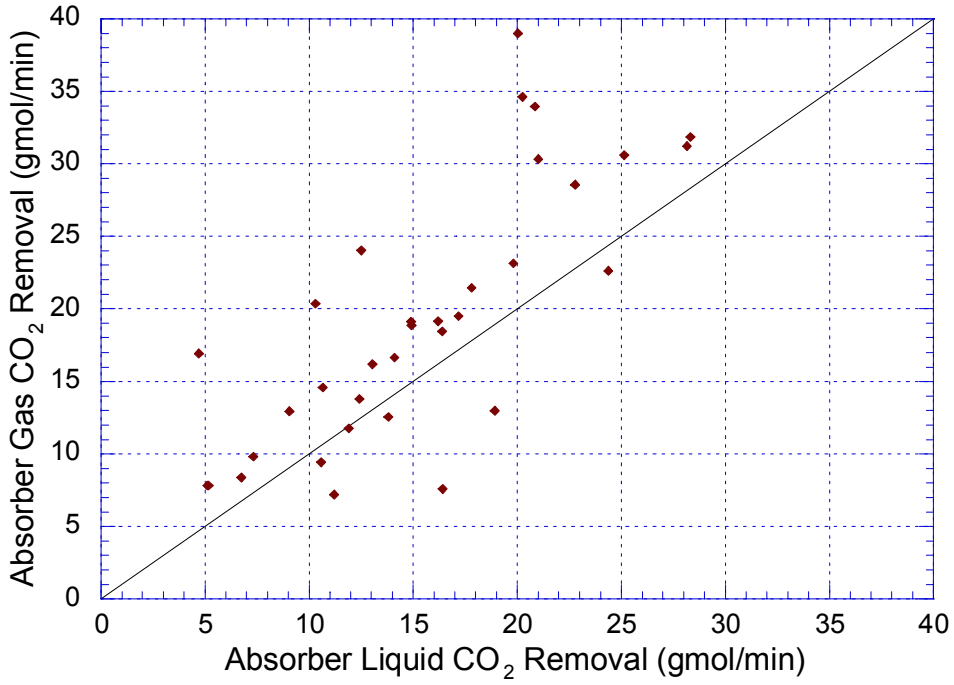

Figure 3-30. Campaign 1 CO_2 Material Balance on Absorber Liquid and Absorber Gas (5 m K^+/2.5 m PZ, Flexipac 1Y)

3.12.2 Campaign 2

The material balance for Campaign 2 is shown in Figure 3-31. The absolute average deviation between and gas and liquid CO_2 material balance was 24.1% and the maximum deviation was 60.1%. In Campaign 2, the inlet and outlet gas was assumed to be saturated at the measured inlet and outlet gas temperatures. During this campaign, the air cooler was not operated and the inlet gas was recycled around the blower in order to increase the inlet gas temperature. Due to the saturated conditions, the inlet Vaisala analyzer failed and was replaced with the Horiba analyzers. In the second campaign, the stripper was first operated at an average pressure of 1.6 bar and one run at 3.4 bar was conducted. The plant was then shut down and reconfigured to operate the stripper in under vacuum. The pilot plant was then shut down again and reconfigured to operate at a stripper pressure of 1.7 bar.

The figure shows that the material balance for the gas and liquid matched relatively well prior to vacuum operation, which is represented by PSTR1 = 1.6 bar and PSTR = 3.4 bar. However, the results for vacuum operation indicated that the gas phase material was consistently higher than the liquid side by approximately 45%. Even after the pilot plant was reconfigured back to pressurized stripping, the material balance was somewhat scattered (PSTR2 = 1.7 bar). During the second set of high pressure runs, the absorber was operated with an inlet CO_2 concentration of 17% because it had initially been assumed that the CO_2 gas calibration standards were in mass percent.

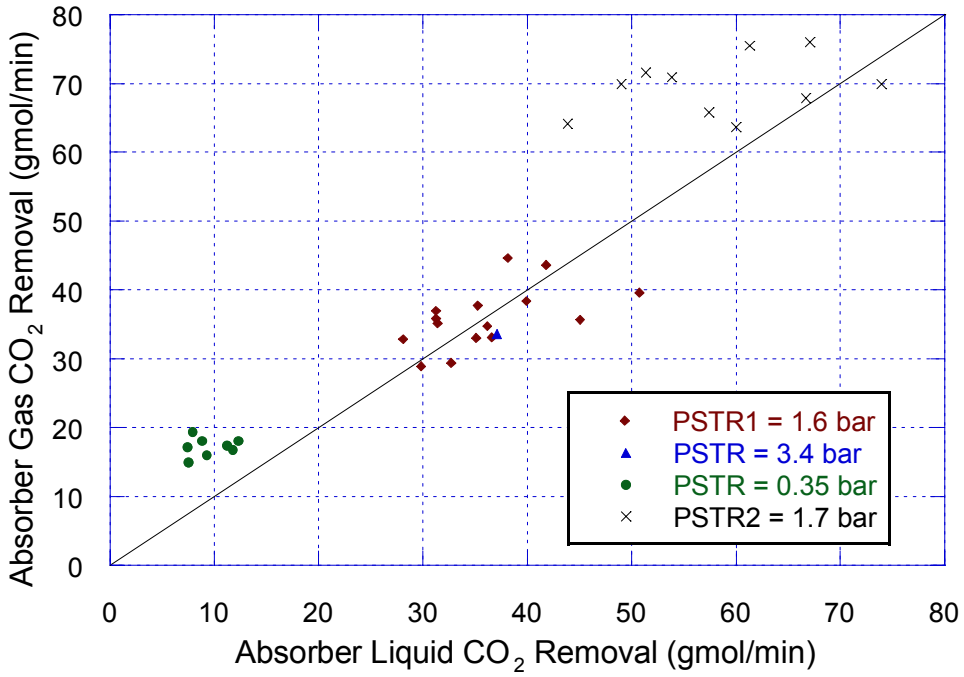

Figure 3-31. Campaign 2 CO_2 Material Balance on Absorber Liquid and Absorber Gas (5 m K^+/2.5 m PZ, Flexipac 1Y)

When the pilot plant was configured to vacuum stripping, all of the CO_2 gas analyzers were calibrated on 11/02/04. In the recalibration, the slope of the inlet Horiba analyzer had increased from 1.24 to 1.42. It is possible that the new calibration was performed incorrectly. However, examination of the Horiba

calibration curves from Campaigns 2, 3, and 4 shows that the slope gradually increased in each campaign. The slope of the outlet Vaisala CO_2 analyzer did not change much, therefore, it was concluded that the CO_2 analyzers were calibrated properly. In the second campaign, sample bombs were used take samples. In the updated loading analysis method, the liquid samples were covered with parafilm and inorganic carbon standards were analyzed every 6 to 10 samples to correct for analyzer drift. Corrections based on the standards to the loading analysis varied between 5 to 10 percent. The liquid sampling and analytical method for liquid CO_2 loading remained consistent throughout the campaign. The IC standards were made on a routine basis and the TOC analyzer used for the loading analysis was calibrated at the beginning of each analytical run. Dilutions to the liquid samples were made on a mass basis.

3.12.3 Campaign 4

A material balance was performed for the absorber gas and absorber liquid for 5 m K^+/2.5 m PZ and 6.4 m K^+/1.6 m PZ solvents of Campaign 4 (Figure 3-32). For 5 m K^+/2.5 m PZ, the absolute average deviation between and gas and liquid CO_2 material balance was 14.0% and the maximum deviation was 52.4%. For 6.4 m K^+/1.6 m PZ, the absolute average deviation between and gas and liquid CO_2 material balance was 10.9% and the maximum deviation was 28.0%. The material balance for the 5 m K^+/2.5 m PZ runs had a systematic offset.

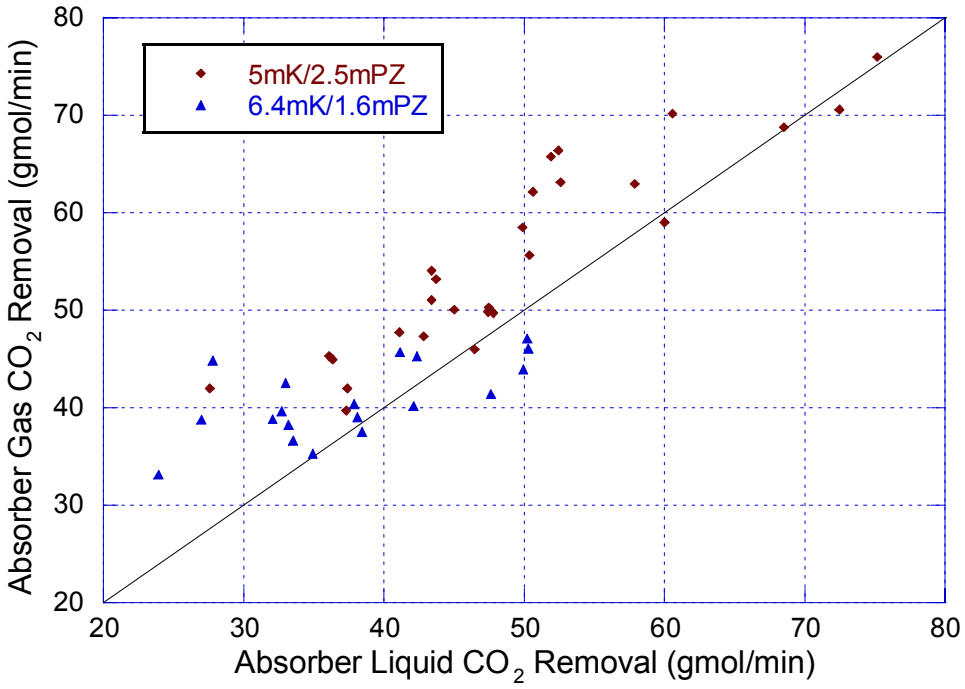

Figure 3-32. Campaign 4 CO_2 Material Balance on Absorber Liquid and Absorber Gas for 5 m K^+/2.5 m PZ and 6.4 m K^+/1.6 m PZ (Flexipac AQ Style 20)

In the fourth campaign, the flow rate of CO_2 gas from the overhead gas accumulator was measured with an annubar. At steady state, the flow of the CO_2 recycle stream should match the CO_2 removal rate in the absorber. The material balance for the absorber gas and CO_2 recycle is shown in Figure 3-33. The material balance assumes the flow was pure CO_2 from the recycle stream. The CO_2 recycle and absorber gas CO_2 of the 6.4 m K^+/1.6 m PZ data match. Although the 5 m K^+/2.5 m PZ data for the CO_2 recycle appears to be reproducible, it is not accurate because the CO_2 recycle annubar was originally specified for vacuum operation. The runs with 6.4 m K^+/1.6 m PZ were conducted under vacuum and a sufficiently high superficial gas velocity was achieved. The CO_2 recycle annubar outputs the flow measurement in terms of standard cubic feet per minute (SCFM). Since the pressure, pressure drop and

temperature at the annubar were not logged, the flow measurement could not be verified at the two stripper conditions.

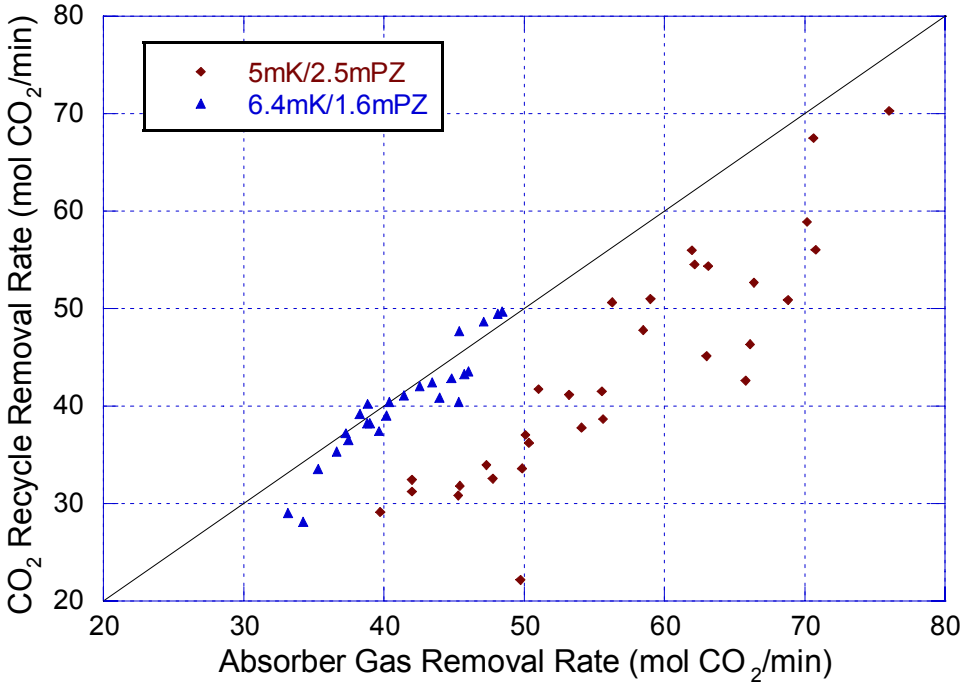

Figure 3-33. Absorber Gas and CO_2 Recycle Material Balance for 5 m K^+/2.5 m PZ and 6.4 m K^+/1.6 m PZ of Campaign 4 Assuming Pure CO_2

However, during the operation of the pilot plant, approximately 150 liters of water was discovered in the overhead gas accumulator where the CO_2 gas was stored and 38 liters of water had to be periodically pumped out each day. If the CO_2 recycle stream is assumed to be saturated with water at the condensate temperature, the CO_2 recycle the material balance for the recycle and absorber gas does not work as well. Since the water content in CO_2 recycle could not be verified, this effect was ignored. It was assumed that water overflowed from the liquid accumulator into the overhead gas accumulator through the alternate gas line.

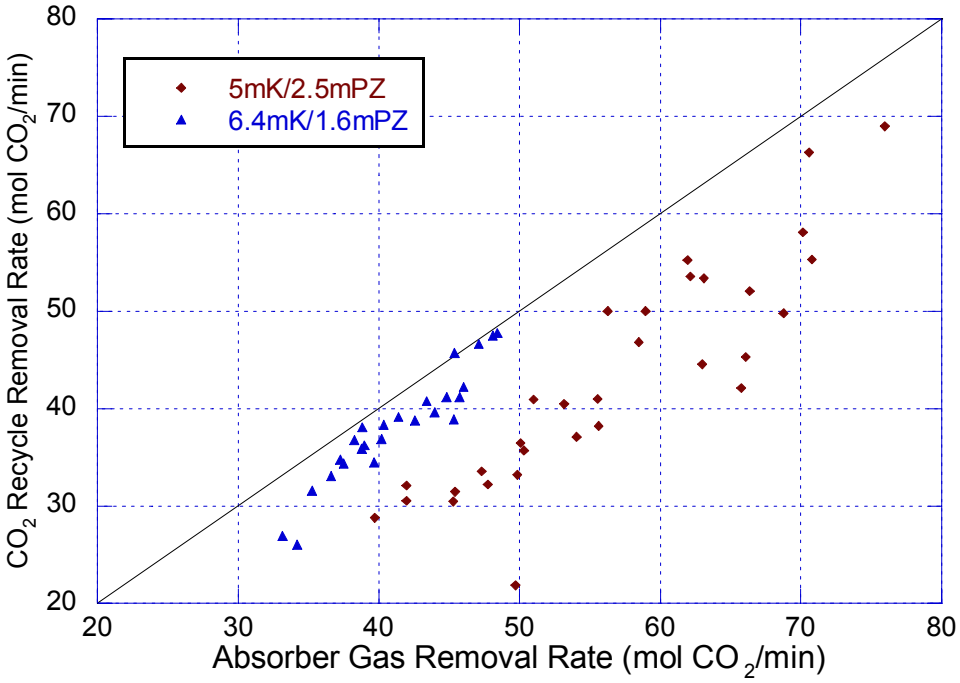

Figure 3-34. CO_2 Recycle and Absorber Gas Material Balance for 5 m K^+/2.5 m PZ and 6.4 m K^+/1.6 m PZ of Campaign 4 Assuming Pure CO_2

Since the material balance for the CO_2 recycle seemed to match the absorber gas flow measurements, it was concluded that there was a systematic error with the liquid-side CO_2 material balance. It was found that a two percent adjustment of the liquid loading measurement or liquid mass flow rate would have accounted for the material balance discrepancy between the absorber gas and liquid CO_2. In addition, some of the liquid loading measurements were adjusted up to 10% based on the analysis of the 100 ppm IC standards used to correct for analyzer drift. An error of 1–2% in the liquid mass flow rate is entirely possible, while an error of 10% in the gas flow measurement is less likely.

The low values of CO_2 in the liquid phase may also indicate there was CO_2 loss during the sample collection, transfer, and analysis process, specifically from the absorber rich samples. It is possible that CO_2 may have flashed when the sample bombs were disengaged from the quick-connects. Also, the syringes

used to extract the sample and to dilute the sample for TOC analysis may have contained trapped air, which would skew the loading results. The auto-sampler for the TOC analyzer also uses a syringe to extract the sample. Additional losses of CO_2 may have occurred when the samples were transferred to the TOC sample vials. The samples were poured into the TOC vials and exposed directly to the air.

3.13 ABSORBER MASS TRANSFER PERFORMANCE

The mass transfer performance of the absorber for Campaigns 1, 2 and 4 was evaluated using the CO_2 material balance obtained in the previous section. The overall gas phase mass transfer coefficient (K_G) was calculated using the following equation:

$$K_G = \frac{N_{CO_2}}{a_{eff} \cdot V_p \cdot \Delta P_{CO_2,lm}} \tag{3.4}$$

where K_G is the overall gas phase mass transfer coefficient with units of gmol/Pa-cm^2-s, N_{CO_2} is the number moles of CO_2 that are absorbed with units of (gmol/min), a_{eff} is the effective interfacial area with units of cm^2/cm^3, and V_p is the volume of packing in units of cm^3. The log mean driving force, $\Delta P_{CO_2,lm}$, has units of Pa and is given by the following equation:

$$\Delta P_{CO_2,lm} = \frac{(P_{CO_2,in} - P^*_{CO_2,in}) - (P_{CO_2,out} - P^*_{CO_2,out})}{\ln\left(\frac{P_{CO_2,in} - P^*_{CO_2,in}}{P_{CO_2,out} - P^*_{CO_2,out}}\right)} \tag{3.5}$$

where $P_{CO_2,in/out}$ is the partial pressure of CO_2 at the inlet and outlet of the absorber and $P^*_{CO_2,in/out}$ is the partial of pressure of CO_2 in equilibrium with the liquid composition at the inlet and outlet of the absorber.

3.13.1 Equilibrium CO_2 Partial Pressure

Recent measurements by Hilliard have shown that the VLE data obtained by Cullinane may not be correct. The Hilliard experimental results indicate that the equilibrium partial pressure of CO_2 was offset by 10% in CO_2 loading or 20 °C in temperature (Figure 3-35). To obtain the correct partial pressure of CO_2, the measured CO_2 loading was multiplied by a factor of 0.9. In this work, it was assumed that the rate data obtained by Cullinane was consistent with the given partial pressures of CO_2, but not with the CO_2 loading.

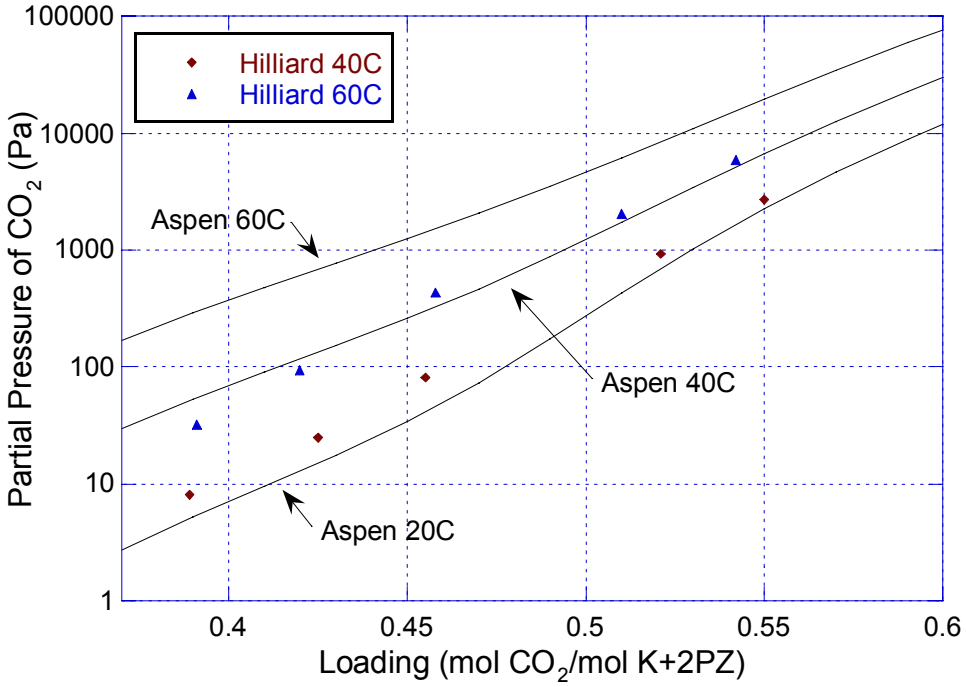

Figure 3-35. Updated Bench-scale Vapor–Liquid Equilibrium Data Measured by Hilliard for 5 m K^+/2.5 m PZ and Aspen Plus® Model Based on Cullinane Data

For the pilot plant mass transfer calculations, the equilibrium partial pressure of CO_2 was obtained through a flash calculation using the Hilliard (2005) K^+/PZ VLE model developed in Aspen Plus®. Since the model was developed based on the Cullinane VLE data, the predicted results were also

incorrect. The molar flow rates of K_2CO_3, PZ, and H_2O were entered into Aspen Plus® flash. The concentration of water was calculated using the measurements of CO_2 loading and the K^+ and PZ concentration from the ion chromatograph. The CO_2 concentration was converted to molality by dividing through by the water concentration and multiplied by 0.9 to account for the VLE error. Since, K_2CO_3 contains one mole of CO_2, the concentration of CO_2 was then adjusted by subtracting half of the calculated potassium carbonate concentration. The equation that was used to calculate the Aspen Plus® input for the flow rate of CO_2 is given by:

$$CO_{2,Aspen} = \frac{[CO_2]\cdot 0.90}{[H_2O]} - \frac{[K_2CO_3]}{2} \tag{3.6}$$

where $CO_{2,Aspen}$ is the CO_2 flow rate with units of mol/hr, $[CO_2]$ is the concentration of the CO_2 in units of mol/kg soln, $[H_2O]$ is the concentration of water in units of kg H_2O/kg soln, and $[K_2CO_3]$ is the concentration of K_2CO_3 in units of mol/kg H_2O.

The concentration of potassium and piperazine measured by ion chromatography indicate that there was a slight difference between the expected concentrations and the actual solution composition. For the flash calculation, the average potassium and piperazine concentration for each campaign composition was used. In Campaign 1, four different solution compositions were used and the concentrations were adjusted accordingly. The difference in solution composition will affect the calculation of the equilibrium partial pressure of CO_2. For example, the IC analysis showed that for Campaign 4, the concentration of potassium was actually 5.9 molal and not 6.4 molal as originally planned. According a flash calculation, for a given loading, the partial pressure of CO_2 for

5.9 m K^+/1.6 m PZ may be 50–100% higher than the 6.4 m K^+/1.6 m PZ (Figure 3-36). The K_g calculation used the 5.9 m K^+/1.6 m PZ solvent formulation.

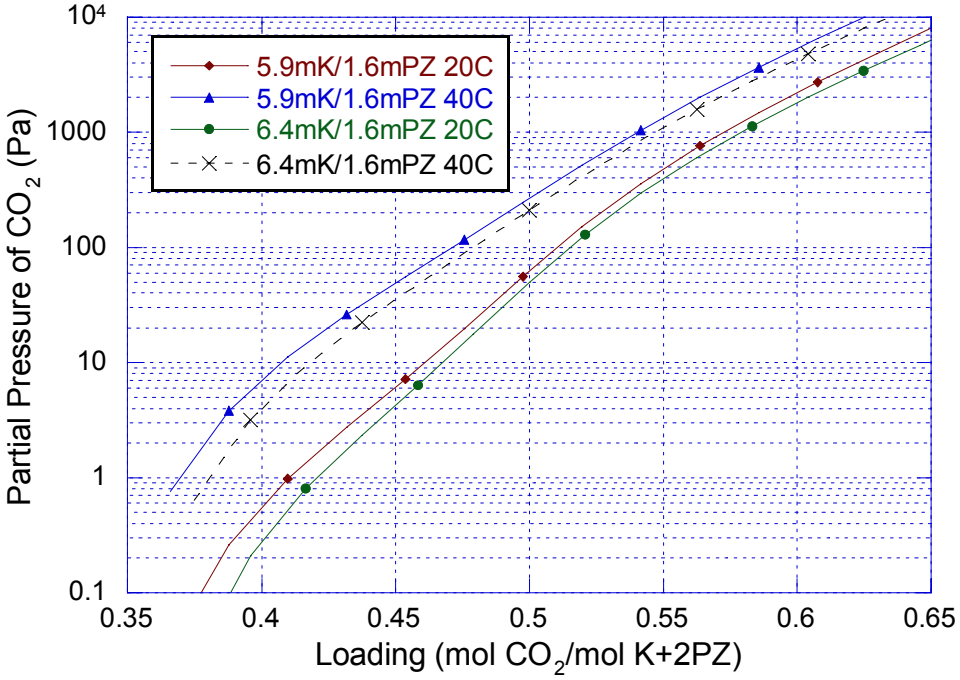

Figure 3-36. Vapor–Liquid Equilibrium Data for 5.9 m K^+/1.6 m PZ and 6.4 m K^+/1.6 m PZ at 20 and 40 °C Generated from Aspen Plus® Model

The following tables list the values that were calculated and entered into the Aspen Plus® flash calculation to determine the partial pressure of CO_2 in equilibrium with the bulk solution. The equilibrium pressure was calculated using the absorber lean solution composition at the top of the column and the absorber rich solution composition at the bottom of the column.

Table 3-9. Campaign 1 Aspen Plus® Input for P_{CO2}* (5 m K^+/2.5 m PZ)

Run#	H_2O	K_2CO_3	PZ	K/PZ	H_2O	Temp Top	Aspen CO_2 Top	Temp Bot	Aspen CO_2 Bot
	kg/kg soln	mol/hr	mol/hr		mol/hr	°C	mol/hr	°C	mol/hr
1.1.1	0.70	1.67	2.26	1.48	55.5	39.33	0.953	29.19	1.255
1.1.2	0.70	1.67	2.26	1.48	55.5	39.11	0.434	28.57	1.232
1.1.3	0.70	1.67	2.26	1.48	55.5	38.90	0.524	28.95	1.298
1.2.1	0.70	1.86	2.06	1.81	55.5	41.50	0.468	32.28	0.888
1.2.2	0.70	1.86	2.06	1.81	55.5	43.16	1.105	32.59	1.053
1.2.3	0.70	1.86	2.06	1.81	55.5	44.46	0.448	32.58	1.094
1.3.1	0.70	1.86	2.06	1.81	55.5	41.02	0.647	38.36	0.976
1.3.2	0.70	1.86	2.06	1.81	55.5	40.67	0.767	38.09	0.910
1.3.3	0.70	1.86	2.06	1.81	55.5	40.42	0.715	38.06	1.192
1.4.1	0.70	1.86	2.06	1.81	55.5	40.01	0.783	39.40	1.173
1.5.1	0.70	1.86	2.06	1.81	55.5	40.08	0.836	38.26	1.073
1.6.1	0.70	1.86	2.06	1.81	55.5	39.53	0.673	44.04	1.268
1.7.1	0.70	1.86	2.06	1.81	55.5	40.05	0.712	39.25	1.374
1.8.1	0.63	2.57	2.58	1.99	55.5	41.16	0.789	29.68	1.894
1.8.2	0.63	2.57	2.58	1.99	55.5	41.48	0.826	29.45	1.421
1.9.1	0.63	2.57	2.58	1.99	55.5	41.49	0.786	31.63	1.947
1.9.2	0.63	2.57	2.58	1.99	55.5	41.55	0.825	31.49	1.538
1.10.1	0.63	2.57	2.58	1.99	55.5	41.58	0.935	30.13	1.464
1.10.2	0.63	2.57	2.58	1.99	55.5	41.52	0.870	29.83	1.569
1.11.1	0.63	2.57	2.58	1.99	55.5	34.63	0.910	22.56	1.759
1.11.2	0.63	2.57	2.58	1.99	55.5	35.39	0.963	22.66	1.542
1.12.1	0.63	2.57	2.58	1.99	55.5	39.81	1.004	34.39	1.465
1.12.2	0.63	2.57	2.58	1.99	55.5	39.64	0.468	34.43	1.567
1.13.1	0.63	2.57	2.58	1.99	55.5	40.49	1.373	38.54	2.051
1.14.1	0.63	2.57	2.58	1.99	55.5	40.26	1.536	41.05	2.346
1.15.1	0.63	2.57	2.58	1.99	55.5	39.59	1.511	39.76	2.193
1.15.2	0.63	2.57	2.58	1.99	55.5	43.23	1.552	40.86	2.288
1.16.1	0.63	2.57	2.58	1.99	55.5	43.34	1.567	38.47	2.309
1.16.2	0.63	2.57	2.58	1.99	55.5	42.48	1.567	38.83	2.317
1.17.1	0.63	2.57	2.58	1.99	55.5	41.34	1.603	38.39	2.282
1.17.2	0.63	2.57	2.58	1.99	55.5	41.22	1.644	38.40	2.357
1.18.1	0.60	2.79	2.67	2.09	55.5	46.24	1.774	43.36	2.799
1.18.2	0.60	2.79	2.67	2.09	55.5	46.05	1.691	43.54	2.765
1.19.1	0.60	2.79	2.67	2.09	55.5	45.27	1.865	40.44	2.787
1.19.2	0.60	2.79	2.67	2.09	55.5	44.84	1.766	39.81	2.704

Table 3-10. Campaign 2 Aspen Plus® Input for P_{CO2}* (5 m K^+/2.5 m PZ)

Run#	H_2O	K_2CO_3	PZ	K/PZ	H_2O	Temp Top	Aspen CO_2 Top	Temp Bot	Aspen CO_2 Bot
	kg/kg soln	mol/hr	mol/hr		mol/hr	°C	mol/hr	°C	mol/hr
2.1.1	0.65	2.29	1.96	2.33	55.5	40.20	1.383	47.44	2.066
2.1.2	0.65	2.29	1.96	2.33	55.5	40.27	1.133	47.16	2.201
2.2.1	0.65	2.29	1.96	2.33	55.5	41.21	1.113	50.51	2.166
2.3.1	0.65	2.29	1.96	2.33	55.5	40.73	1.310	44.74	2.466
2.4.1	0.65	2.29	1.96	2.33	55.5	40.60	1.381	44.59	2.277
2.5.1	0.65	2.29	1.96	2.33	55.5	40.55	1.378	44.61	2.154
2.6.1	0.65	2.29	1.96	2.33	55.5	41.20	1.330	45.93	2.203
2.7.1	0.65	2.29	1.96	2.33	55.5	41.27	1.872	46.41	2.254
2.8.1	0.65	2.29	1.96	2.33	55.5	41.36	1.287	46.64	2.055
2.8.2	0.65	2.29	1.96	2.33	55.5	41.59	1.416	47.77	2.279
2.9.1	0.65	2.29	1.96	2.33	55.5	40.56	1.203	41.84	2.167
2.9.2	0.65	2.29	1.96	2.33	55.5	40.79	1.182	42.34	2.254
2.10.1	0.65	2.29	1.96	2.33	55.5	41.20	1.652	48.00	2.405
2.10.2	0.65	2.29	1.96	2.33	55.5	41.30	1.387	48.19	2.252
2.11.1	0.65	2.29	1.96	2.33	55.5	41.39	1.791	48.45	2.431
2.11.2	0.65	2.29	1.96	2.33	55.5	41.42	1.716	48.56	2.536
2.12.1	0.65	2.29	1.96	2.33	55.5	41.05	1.640	48.38	2.665
2.12.2	0.65	2.29	1.96	2.33	55.5	40.97	1.497	47.97	2.633
2.13.1	0.65	2.29	1.96	2.33	55.5	40.68	1.178	44.97	2.213
2.13.2	0.65	2.29	1.96	2.33	55.5	40.31	1.566	44.12	1.983
2.14.1	0.65	2.29	1.96	2.33	55.5	43.47	-2.285	30.74	-2.285
2.14.2	0.65	2.29	1.96	2.33	55.5	42.52	1.787	30.08	2.402
2.15.1	0.65	2.29	1.96	2.33	55.5	41.90	1.641	34.57	2.195
2.16.1	0.65	2.29	1.96	2.33	55.5	41.98	1.621	34.47	2.242
2.16.2	0.65	2.29	1.96	2.33	55.5	38.78	1.488	31.50	2.040
2.17.1	0.65	2.29	1.96	2.33	55.5	38.99	1.460	29.96	2.081
2.18.1	0.65	2.29	1.96	2.33	55.5	44.79	1.623	37.17	2.014
2.18.2	0.65	2.29	1.96	2.33	55.5	44.81	1.616	37.56	2.090
2.19.1	0.65	2.29	1.96	2.33	55.5	46.99	1.725	40.51	2.428
2.19.2	0.65	2.29	1.96	2.33	55.5	47.82	1.768	42.35	2.159
2.20.1	0.65	2.29	1.96	2.33	55.5	40.11	1.393	47.96	2.051
2.20.2	0.65	2.29	1.96	2.33	55.5	40.08	1.508	48.27	2.471
2.21.1	0.65	2.29	1.96	2.33	55.5	40.10	1.782	48.30	2.600
2.21.2	0.65	2.29	1.96	2.33	55.5	40.86	1.735	50.70	2.428
2.22.1	0.65	2.29	1.96	2.33	55.5	41.77	1.559	51.19	2.273
2.22.2	0.65	2.29	1.96	2.33	55.5	41.08	1.544	50.94	2.348
2.23.1	0.65	2.29	1.96	2.33	55.5	39.86	1.426	47.95	2.464
2.23.2	0.65	2.29	1.96	2.33	55.5	39.82	1.398	47.27	2.160
2.24.1	0.65	2.29	1.96	2.33	55.5	39.68	1.384	47.57	2.270
2.24.2	0.65	2.29	1.96	2.33	55.5	39.65	1.080	47.49	2.021

Table 3-11. Campaign 4 Aspen Plus® Input for P_{CO2}* (5 m K^+/2.5 m PZ)

Run#	H_2O Top kg/kg soln	H_2O Bot kg/kg soln	K_2CO_3 mol/hr	PZ mol/hr	K/PZ	H_2O mol/hr	Temp Top °C	Aspen CO_2 Top mol/hr	Temp Bot °C	Aspen CO_2 Bot mol/hr
4.1	0.65	0.63	2.44	2.32	2.10	55.5	39.93	1.194	48.83	1.710
4.2.1	0.64	0.61	2.44	2.32	2.10	55.5	38.89	1.150	48.56	2.288
4.2.2	0.64	0.60	2.44	2.32	2.10	55.5	38.96	1.055	48.42	2.486
4.3.1	0.63	0.62	2.44	2.32	2.10	55.5	42.09	1.360	50.59	2.224
4.3.2	0.63	0.60	2.44	2.32	2.10	55.5	42.49	1.324	50.78	2.379
4.4.1	0.63	0.61	2.44	2.32	2.10	55.5	43.62	1.299	50.52	2.371
4.4.2	0.63	0.47	2.44	2.32	2.10	55.5	43.94	1.364	50.43	3.605
4.5.1	0.63	0.61	2.44	2.32	2.10	55.5	42.01	1.305	47.08	2.347
4.5.2	0.63	0.61	2.44	2.32	2.10	55.5	41.38	1.354	46.46	2.460
4.6.1	0.65	0.63	2.44	2.32	2.10	55.5	46.73	1.006	51.77	2.146
4.6.2	0.65	0.63	2.44	2.32	2.10	55.5	43.57	0.996	51.75	2.181
4.7.1	0.65	0.64	2.44	2.32	2.10	55.5	45.19	0.844	50.95	1.780
4.7.2	0.65	0.63	2.44	2.32	2.10	55.5	44.97	0.843	50.99	1.740
4.8	0.66	0.64	2.44	2.32	2.10	55.5	43.28	0.839	47.54	1.721
4.9.1	0.66	0.64	2.44	2.32	2.10	55.5	43.20	0.781	47.36	1.898
4.9.2	0.66	0.63	2.44	2.32	2.10	55.5	43.21	0.811	47.30	1.830
4.10.1	0.64	0.64	2.44	2.32	2.10	55.5	44.28	1.322	51.32	1.794
4.10.2	0.65	0.63	2.44	2.32	2.10	55.5	41.74	1.305	51.61	2.070
4.11.1	0.64	0.63	2.44	2.32	2.10	55.5	41.59	1.210	49.13	2.110
4.11.2	0.64	0.63	2.44	2.32	2.10	55.5	41.20	1.245	48.89	2.167
4.12.1	0.64	0.63	2.44	2.32	2.10	55.5	39.81	1.214	46.45	2.046
4.12.2	0.64	0.63	2.44	2.32	2.10	55.5	39.86	1.275	46.41	2.117
4.13.1	0.66	0.63	2.44	2.32	2.10	55.5	41.48	1.017	47.65	1.504
4.13.2	0.65	0.64	2.44	2.32	2.10	55.5	43.02	1.146	49.17	1.801
4.14.1	0.64	0.64	2.44	2.32	2.10	55.5	42.76	1.196	48.19	1.804
4.14.2	0.65	0.64	2.44	2.32	2.10	55.5	42.80	1.171	47.93	1.757
4.15.1	0.64	0.64	2.44	2.32	2.10	55.5	39.54	1.159	45.48	1.909
4.15.2	0.64	0.63	2.44	2.32	2.10	55.5	39.61	1.160	45.61	1.812
4.16.1	0.61	0.61	2.44	2.32	2.10	55.5	41.40	1.480	48.46	2.620
4.16.2	0.64	0.61	2.44	2.32	2.10	55.5	41.29	1.283	48.15	1.954
4.17.1	0.64	0.63	2.44	2.32	2.10	55.5	40.15	0.821	49.49	1.723
4.17.2	0.65	0.63	2.44	2.32	2.10	55.5	40.63	0.918	50.98	1.833
4.18	0.64	0.61	2.44	2.32	2.10	55.5	39.98	1.018	51.31	1.950
4.19	0.62	0.60	2.44	2.32	2.10	55.5	40.26	1.212	52.11	2.141

Table 3-12. Campaign 4 Aspen Plus® Input for P_{CO2}* (6.4 m K^+/1.6 m PZ)

Run#	H_2O Top kg/kg soln	H_2O Bot kg/kg soln	K_2CO_3 mol/hr	PZ mol/hr	K/PZ	H_2O mol/hr	Temp Top °C	Aspen CO_2 Top mol/hr	Temp Bot °C	Aspen CO_2 Bot mol/hr
4.20.1	0.65	0.63	2.90	1.61	3.60	55.5	38.76	1.426	43.53	1.595
4.20.2	0.64	0.63	2.90	1.61	3.60	55.5	38.60	1.217	43.45	1.432
4.21.1	0.66	0.64	2.90	1.61	3.60	55.5	39.00	1.318	42.98	1.440
4.21.2.	0.65	0.64	2.90	1.61	3.60	55.5	40.52	1.354	44.89	1.532
4.22.1	-	0.63	2.90	1.61	3.60	55.5	36.76	-	44.09	1.706
4.22.2	0.59	0.69	2.90	1.61	3.60	55.5	36.71	1.008	43.98	1.951
4.23	0.59	0.62	2.90	1.61	3.60	55.5	37.83	1.136	45.64	1.881
4.24	0.62	0.61	2.90	1.61	3.60	55.5	37.49	1.250	45.31	1.891
4.25	0.64	0.63	2.90	1.61	3.60	55.5	39.48	1.033	44.90	1.497
4.26.1	0.65	0.64	2.90	1.61	3.60	55.5	38.33	1.001	44.47	1.584
4.26.2	0.65	0.64	2.90	1.61	3.60	55.5	38.68	1.072	45.14	1.529
4.27.1	0.65	0.63	2.90	1.61	3.60	55.5	40.01	1.047	46.10	1.717
4.27.2	0.64	0.63	2.90	1.61	3.60	55.5	39.30	0.953	45.57	1.598
4.28.1	0.65	0.64	2.90	1.61	3.60	55.5	38.88	0.994	45.80	1.708
4.28.2	0.65	0.63	2.90	1.61	3.60	55.5	38.39	1.031	45.00	1.546
4.29.1	0.65	0.64	2.90	1.61	3.60	55.5	39.42	0.957	46.36	1.636
4.29.2	0.64	0.62	2.90	1.61	3.60	55.5	39.49	0.926	46.60	1.557
4.30.1	0.62	0.63	2.90	1.61	3.60	55.5	41.02	0.391	46.75	1.449
4.30.2	0.66	0.63	2.90	1.61	3.60	55.5	40.44	0.910	46.50	1.616
4.31.1	0.63	0.64	2.90	1.61	3.60	55.5	41.57	1.022	47.06	1.688
4.31.2	0.63	0.63	2.90	1.61	3.60	55.5	41.55	1.141	47.02	1.604
4.32.1	0.65	0.62	2.90	1.61	3.60	55.5	43.53	1.027	48.14	1.690
4.32.2	0.65	0.60	2.90	1.61	3.60	55.5	43.72	1.139	48.28	2.052
4.33.1	0.65	0.66	2.90	1.61	3.60	55.5	45.55	0.987	46.16	1.604
4.33.2	0.66	0.67	2.90	1.61	3.60	55.5	45.08	1.090	46.08	1.425

3.13.2 Effective Interfacial Area of Packing

In the first two campaigns, Flexipac 1Y structured packing (a_{sp} = 410 m^2/m^3) was used in the absorber and in the final campaign, Flexipac AQ Style 20 structured packing (a_{sp} = 213 m^2/m^3) was used. Effective area measurements for Flexipac 1Y were conducted in the air–water tower and in the carbon steel absorber column that was used in the pilot plant campaigns. The Flexipac AQ Style 20 tests were conducted using the air–water tower system. Experiments for the air–water tower were performed by absorbing CO_2 from ambient air into a solution of 0.1 N NaOH. The air–water PVC column contained 3.05 m of packing and had a diameter of 0.43 m. Experiments with the pilot plant absorber used a solution of 0.1 N KOH. The absorber contained 6.1 m of packing and also had a

diameter of 0.43 m. Effective area measurements have been performed extensively by SRP in the air–water column with numerous packing and are reliable. The air–water measurements for the Flexipac 1Y and AQ packing were used in the evaluation of the mass transfer performance.

Figure 3-37 shows that the Flexipac 1Y effective area measurements in the air–water column were approximately 1.8 times higher than the steel absorber column, while the Flexipac 1Y structured packing has approximately 50% more effective area than Flexipac AQ packing. The effective area measurements were correlated solely as a function of the superficial liquid rate. The effective area (m^2/m^3) for Flexipac 1Y packing in the air–water column was correlated to the following equation:

$$a_{eff,Flexipac1Y-AW} = 1.784 \cdot (\mathrm{L}) + 262.18 \tag{3.7}$$

The effective area for Flexipac AQ Style 20 packing in the air–water column was correlated to the following equation:

$$a_{eff,FlexipacAQ-AW} = 0.569 \cdot (L) + 204.57 \tag{3.8}$$

where, L is the superficial liquid velocity with units of m/hr. The correlations for the effective area do not account for differences in density, surface tension, and viscosity of the potassium carbonate and piperazine solvent, which are dramatically different than of the 0.1 N hydroxide solutions. Preliminary results from the Separations Research Program at the University of Texas at Austin have shown that the interfacial area may increase by 1–1.5 times if the surface tension is reduced by a one-half.

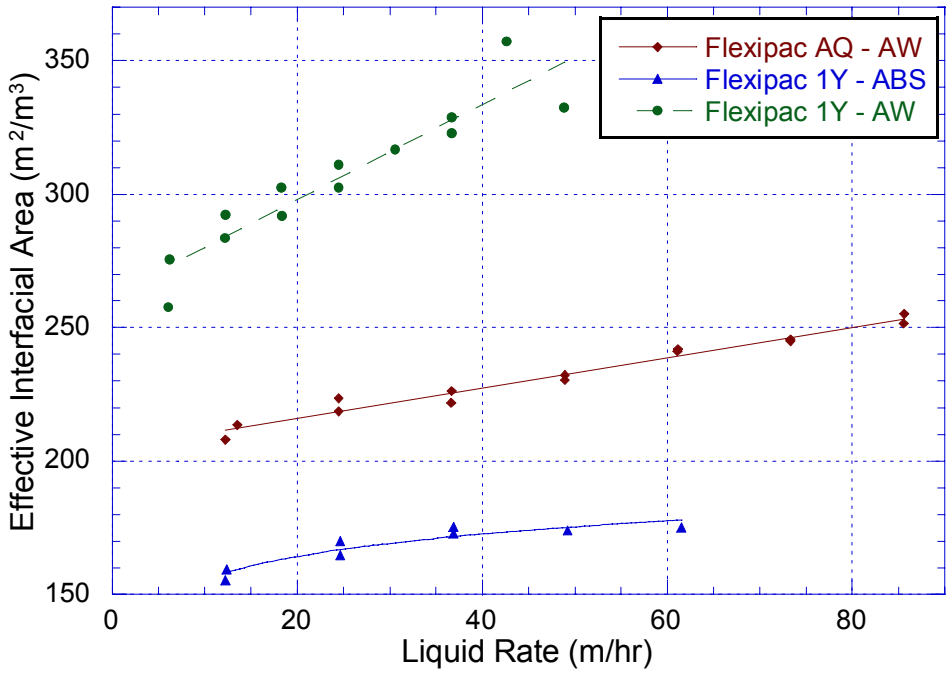

Figure 3-37. Correlation of Effective Interfacial Area for Flexipac 1Y and Flexipac AQ Style 20 from Air–Water (AW) and Absorber Column (ABS) Experiments

3.13.3 K_g Mass Transfer Coefficient

The results of the K_g calculation for Campaigns 1, 2, and 4 are tabulated in Tables 3-13, 3-14, 3-15, and 3-16. Since the gas-side CO_2 removal rates were more consistent than the liquid-side, those values were used as N_{CO2}. However, the gas-side removal rates were also consistently higher than the liquid side by approximately 10% and the K_g results should be interpreted accordingly. An average equilibrium partial pressure of CO_2 was calculated for each K_g based on an arithmetic average of the inlet and outlet equilibrium CO_2 partial pressure. Possible pinch point locations were identified as occurring in the bottom or top of the absorber column. The pinches were identified when the ratio of the equilibrium partial pressure of CO_2 to the bulk CO_2 partial pressure approached one. Outliers were also identified in the table.

Table 3-13. Campaign 1 Results for K_G Calculation

Run#	N_{CO2} gmol/min	Liq Rate m/hr	Eff Intf Area m^2/m^3	P_{CO2} Top Pa	P_{CO2}* Top Pa	P_{CO2} Bot Pa	P_{CO2}* Bot Pa	LMCD Pa	Kgx10^{10} gmol/ Pa-cm^2-s	P_{CO2}* Ave Pa	Comments
1.1.1	14.90	7.84	276.2	178	32	2826	30	897	1.15	31	-
1.1.2	14.65	7.90	276.3	188	1	2783	26	954	1.06	14	-
1.1.3	14.24	7.85	276.2	187	3	2720	34	934	1.06	18	-
1.2.1	8.63	7.84	276.2	5	2	2950	11	418	1.43	7	-
1.2.2	8.46	7.83	276.1	6	76	2901	22	-	-	-	Outlier
1.2.3	8.30	7.83	276.1	7	3	2855	25	444	1.30	14	-
1.3.1	6.34	15.78	290.3	26	8	2223	30	451	0.93	19	-
1.3.2	6.89	15.79	290.4	29	16	2420	23	458	0.99	19	-
1.3.3	6.66	15.76	290.3	32	12	2346	62	477	0.92	37	-
1.4.1	11.04	15.77	290.3	39	16	3883	67	739	0.98	41	-
1.5.1	11.42	14.59	288.2	56	21	2979	43	655	1.16	32	-
1.6.1	18.86	12.29	284.1	330	8	11346	139	3064	0.41	74	Outlier
1.7.1	12.13	7.97	276.4	793	11	11426	124	3939	0.21	67	Outlier
1.8.1	17.18	7.86	276.2	285	6	3333	59	1217	0.98	33	-
1.8.2	17.92	7.91	276.3	230	7	3410	16	1165	1.06	11	-
1.9.1	20.42	7.92	276.3	599	6	3407	85	1584	0.89	45	-
1.9.2	21.22	7.93	276.3	582	7	3495	28	1609	0.91	17	-
1.10.1	11.40	8.02	276.5	47	12	2974	19	657	1.20	16	Top Pinch
1.10.2	10.35	7.80	276.1	32	9	2683	25	555	1.29	17	Top Pinch
1.11.1	7.37	3.90	269.1	245	5	2713	18	1016	0.52	11	Outlier
1.11.2	6.89	3.97	269.3	168	7	2482	10	846	0.58	8	Outlier
1.12.1	12.87	11.04	281.9	359	13	2080	31	957	0.91	22	-
1.12.2	19.95	10.37	280.7	508	0	3329	41	1488	0.91	21	-
1.13.1	34.36	12.26	284.1	1346	46	13878	221	5255	0.44	133	-
1.14.1	26.94	10.98	281.8	1274	69	13139	637	4828	0.38	353	-
1.15.1	26.72	12.41	284.3	1338	61	12312	366	4772	0.38	213	-
1.15.2	25.17	12.42	284.3	957	96	11315	528	3927	0.43	312	-
1.16.1	29.97	12.33	284.2	1978	101	12261	461	5398	0.37	281	-
1.16.2	30.54	12.32	284.2	1968	93	12512	487	5461	0.38	290	-
1.17.1	16.64	8.03	276.5	756	92	11529	422	3708	0.31	257	-
1.17.2	16.82	8.02	276.5	617	100	11527	532	3426	0.34	316	-
1.18.1	27.51	12.31	284.1	498	169	12224	2060	2868	0.65	1114	Top Pinch
1.18.2	28.06	12.28	284.1	521	136	12463	1876	3078	0.61	1006	Top Pinch
1.19.1	16.24	7.90	276.3	668	192	11341	1639	3061	0.37	915	Top Pinch
1.19.2	16.85	7.92	276.3	460	146	11572	1204	2873	0.41	675	Top Pinch

1. LMCD = Log Mean Concentration Difference
2. $P_{CO2,AVE}$* = Average of Inlet and Outlet P_{CO2}*. Plotted against K_g Results.

Table 3-14. Campaign 2 Results for K_G Calculation

Run#	N_{CO2}	Liq Rate	Eff Intf Area	P_{CO2} Top	P_{CO2}* Top	P_{CO2} Bot	P_{CO2}* Bot	LMCD	Kgx10^{10}	P_{CO2}* Ave	Comments
	gmol/min	m/hr	m^2/m^3	Pa	Pa	Pa	Pa	Pa	gmol/ Pa-cm^2-s	Pa	
2.1.1	52.84	12.73	284.9	2261	105	11523	1844	5010	0.71	975	-
2.1.2	50.40	12.73	284.9	2582	47	11410	2949	4917	0.69	1498	-
2.2.1	37.35	12.74	284.9	6109	48	12810	3153	7720	0.32	1600	-
2.3.1	33.22	14.28	287.6	4445	87	11889	6654	4783	0.46	3370	-
2.4.1	37.78	17.45	293.3	3969	108	12460	3363	6110	0.40	1735	-
2.5.1	35.83	17.43	293.3	2962	106	11133	2143	5349	0.44	1125	-
2.6.1	38.43	19.92	297.7	2051	97	10888	2769	4328	0.57	1433	-
2.7.1	39.88	19.96	297.8	2379	603	11616	3423	4196	0.61	2013	-
2.8.1	44.80	20.87	299.4	4388	86	12292	1688	6986	0.41	887	-
2.8.2	43.80	20.79	299.3	4118	132	12013	4035	5753	0.49	2084	-
2.9.1	28.97	13.62	286.5	3702	61	11577	1909	6172	0.31	985	-
2.9.2	29.41	13.57	286.4	3579	58	11627	2724	5802	0.34	1391	-
2.10.1	35.16	18.36	294.9	1934	275	12390	6365	3385	0.67	3320	-
2.10.2	34.81	18.33	294.9	2029	117	12493	3751	4493	0.50	1934	-
2.11.1	32.91	18.30	294.8	1840	454	11963	7128	2760	0.77	3791	-
2.11.2	33.02	18.38	295.0	1997	349	12189	10246	1791	1.19	5298	-
2.12.1	35.62	19.21	296.5	557	261	12590	15545	-	-	7903	Outlier
2.12.2	39.59	19.16	296.4	240	162	12179	13732	-	-	6947	Outlier
2.13.1	33.61	15.96	290.6	2813	57	11876	2719	5331	0.41	1388	-
2.13.2	34.34	15.88	290.5	3186	192	12349	1106	6235	0.36	649	-
2.14.1	15.93	7.76	276.0	784	-	4980	-	-	-	-	Outlier
2.14.2	14.87	7.78	276.1	910	487	4801	2438	1128	0.91	1463	-
2.15.1	18.03	9.43	279.0	738	281	5510	1378	1669	0.74	830	-
2.16.1	18.05	9.30	278.8	626	265	5395	1655	1446	0.86	960	-
2.16.2	19.36	8.54	277.4	513	129	4566	592	1536	0.87	361	-
2.17.1	16.02	8.55	277.4	1148	120	4461	638	2128	0.52	379	-
2.18.1	17.13	12.57	284.6	467	334	4107	782	991	1.16	558	-
2.18.2	16.75	12.47	284.4	419	327	3994	1087	815	1.38	707	-
2.19.1	17.58	15.69	290.2	251	551	4027	4672	-	-	2612	Top Pinch
2.19.2	17.43	15.70	290.2	285	674	4084	1909	-	-	1292	Top Pinch
2.20.1	71.55	32.70	320.5	2141	107	17111	1805	6576	0.65	956	-
2.20.2	69.94	32.66	320.4	1978	155	16931	8103	4440	0.94	4129	-
2.21.1	67.81	35.20	325.0	1259	398	17075	12519	2218	1.80	6458	Outlier
2.21.2	63.64	35.30	325.1	1528	357	17485	7917	3998	0.94	4137	-
2.22.1	75.58	35.18	324.9	2609	212	18737	4759	6568	0.68	2486	-
2.22.2	75.99	35.28	325.1	1928	190	18160	6091	5330	0.84	3141	-
2.23.1	65.95	24.00	305.0	4861	117	17873	7784	7084	0.58	3950	-
2.23.2	64.28	23.90	304.8	4286	106	16938	2560	8254	0.49	1333	-
2.24.1	69.96	24.01	305.0	3686	100	17604	3865	7558	0.58	1983	-
2.24.2	71.01	23.96	304.9	4080	37	18160	1575	8886	0.50	806	-

1. LMCD = Log Mean Concentration Difference
2. $P_{CO2,AVE}$* = Average of Inlet and Outlet P_{CO2}*. Plotted against K_g Results.

Table 3-15. Campaign 4 – 5 m K^+/2.5 m PZ Results for K_G Calculation

Run#	N_{CO2} gmol/min	Liq Rate m/hr	Eff Intf Area m^2/m^3	P_{CO2} Top Pa	P_{CO2}* Top Pa	P_{CO2} Bot Pa	P_{CO2}* Bot Pa	LMCD Pa	Kgx10^{10} gmol/ Pa-cm^2-s	P_{CO2}* Ave Pa	Comment
4.1	41.98	22.51	217.4	641	35	8404	329	2884	1.28	182	-
4.2.1	58.48	20.13	216.0	4184	27	16830	1688	8498	0.61	858	-
4.2.2	58.99	20.15	216.0	5110	20	17761	3174	9020	0.58	1597	-
4.3.1	44.92	20.87	216.5	2712	71	16151	1587	6983	0.57	829	-
4.3.2	45.97	20.96	216.5	2919	66	16773	2604	7061	0.57	1335	-
4.4.1	55.62	23.32	217.8	5327	68	17789	2495	9400	0.52	1282	-
4.4.2	55.54	23.37	217.9	5601	85	17848	97798	-	-	-	Outlier
4.5.1	0.00	23.27	217.8	6949	60	17215	1849	10567	-	955	Outlier
4.5.2	65.77	23.32	217.8	6947	65	18182	2581	10654	0.54	1323	-
4.6.1	50.09	19.26	215.5	2453	36	17219	1365	7144	0.62	701	-
4.6.2	50.32	19.24	215.5	2119	25	17016	1509	6699	0.67	767	-
4.7.1	54.09	23.34	217.9	1398	16	13792	468	5270	0.90	242	-
4.7.2	53.19	23.30	217.8	1074	16	13432	422	4763	0.98	219	-
4.8	51.03	23.27	217.8	1948	13	11291	304	5213	0.86	159	-
4.9.1	63.13	23.18	217.8	5958	10	17138	485	10398	0.53	247	-
4.9.2	62.14	23.23	217.8	5766	11	16761	401	10150	0.54	206	-
4.10.1	45.41	20.89	216.5	5107	78	18170	500	10060	0.40	289	-
4.10.2	45.30	20.90	216.5	5246	58	18224	1085	10000	0.40	572	-
4.11.1	47.75	23.27	217.8	5253	43	15431	1020	9043	0.46	531	-
4.11.2	47.32	23.31	217.8	5549	46	15563	1186	9240	0.45	616	-
4.12.1	39.71	23.29	217.8	4816	37	11605	691	7429	0.47	364	-
4.12.2	41.97	23.28	217.8	5942	44	13064	853	8675	0.42	449	-
4.13.1	70.78	46.46	231.0	5267	22	17976	173	10275	0.57	98	-
4.13.2	70.17	46.56	231.1	4474	41	17063	430	9226	0.63	235	-
4.14.1	66.38	48.12	232.0	3015	46	17895	401	8189	0.67	224	-
4.14.2	63.00	48.02	231.9	2263	43	16637	347	7060	0.74	195	-
4.15.1	49.73	37.59	226.0	2007	30	17319	431	6952	0.61	230	-
4.15.2	49.84	37.64	226.0	2270	30	17607	332	7360	0.57	181	-
4.16.1	61.95	40.14	227.4	6333	93	17113	4944	8877	-	-	Outlier
4.16.2	56.27	40.11	227.4	3883	52	13761	604	7558	0.63	328	-
4.17.1	70.61	40.29	227.5	4956	9	17249	359	9726	0.61	184	-
4.17.2	76.00	40.31	227.5	4352	14	17672	539	9315	0.69	276	-
4.18	68.79	32.39	223.0	1982	19	14632	758	6090	0.97	389	-
4.19	66.08	32.32	223.0	1403	38	13749	1375	4994	-	-	Outlier

1. LMCD = Log Mean Concentration Difference
2. $P_{CO2,AVE}$* = Average of Inlet and Outlet P_{CO2}*. Plotted against K_g Results.

Table 3-16. Campaign 4 – 6.4 m K^+/1.6 m PZ Results for K_G Calculation

Run#	N_{CO2} gmol/min	Liq Rate m/hr	Eff Intf Area m^2/m^3	P_{CO2} Top Pa	P_{CO2}* Top Pa	P_{CO2} Bot Pa	P_{CO2}* Bot Pa	LMCD Pa	Kgx10^{10} gmol/ Pa-cm^2-s	P_{CO2}* Ave Pa	Pinch
4.20.1	38.78	36.72	225.5	5134	121	16308	319	9463	0.35	220	-
4.20.2	38.27	36.89	225.6	5324	54	16373	177	9732	0.33	116	-
4.21.1	39.65	41.79	228.4	3349	82	14795	176	7576	0.44	129	-
4.21.2.	42.55	41.80	228.4	4325	106	16782	279	9006	0.40	193	-
4.22.1	33.15	24.20	218.3	8969	20	18340	492	12891	-	-	Outlier
4.22.2	34.22	24.26	218.4	9081	20	18870	1142	12914	-	-	Outlier
4.23	37.26	24.27	218.4	7769	37	18308	984	11890	0.27	511	-
4.24	36.63	24.24	218.4	7278	56	17652	1001	11288	0.28	528	-
4.25	38.84	27.51	220.2	5577	29	16768	247	10056	0.34	138	-
4.26.1	45.33	33.77	223.8	3718	23	17484	327	8767	0.44	175	-
4.26.2	45.73	33.84	223.8	4259	31	18147	281	9462	0.41	156	-
4.27.1	41.40	29.10	221.1	5338	32	17325	576	9954	0.36	304	-
4.27.2	40.18	29.13	221.2	4958	21	16608	369	9492	0.37	195	-
4.28.1	37.48	24.31	218.4	6429	24	17052	549	10669	0.31	286	-
4.28.2	35.27	24.27	218.4	5206	26	15248	296	9218	0.33	161	-
4.29.1	38.99	24.28	218.4	4412	21	15714	442	8729	0.39	232	-
4.29.2	40.37	24.32	218.4	5121	19	16777	342	9689	0.36	180	-
4.30.1	43.96	29.08	221.1	3244	1	16062	238	7938	0.48	119	-
4.30.2	46.03	29.09	221.1	4148	20	17511	416	9125	0.44	218	-
4.31.1	48.43	33.94	223.9	9008	34	17232	552	12432	0.33	293	-
4.31.2	48.10	33.94	223.9	8822	53	17095	413	12304	0.33	233	-
4.32.1	47.11	29.10	221.1	10050	41	17931	593	13339	0.31	317	-
4.32.2	45.38	29.08	221.1	9563	64	17180	1967	12133	-	-	Outlier
4.33.1	44.82	24.28	218.4	10402	43	17826	391	13592	0.29	217	-
4.33.2	43.42	24.24	218.4	10257	60	17435	209	13406	-	-	Outlier

1. LMCD = Log Mean Concentration Difference
2. $P_{CO2,AVE}$* = Average of Inlet and Outlet P_{CO2}*. Plotted against K_g Results.

Figure 3-38 shows the K_g results for the absorber in Campaign 1. In the first campaign, the four slightly different compositions of the K^+/PZ solvent were used. The four different compositions are differentiated as Run 1, Run 2-7, Run 8-17, and Run 18-19. The figure shows that the first three sets of solvent compositions gave comparable results over an equilibrium CO_2 partial pressure that ranged from 6 to 1000 Pa. The averaged results for each set of runs are also plotted. However, the results for the last run were much higher and not consistent with the other three sets. In Run 18-19, water was removed to further concentrate the solvent and the absorption rate was expected to higher. In addition, the calculated results seemed to indicate that there was a pinch at the

top of the absorber. The figure also shows that the K_g results were lower than the wetted wall column results at 40 °C. This is somewhat unexpected because temperature bulges that ranged from 50 to 70 °C were observed. It is possible that there was some gas film resistance, which would reduce the mass transfer rate. Also, the temperature bulge may have caused the absorber to pinch in the middle of the column.

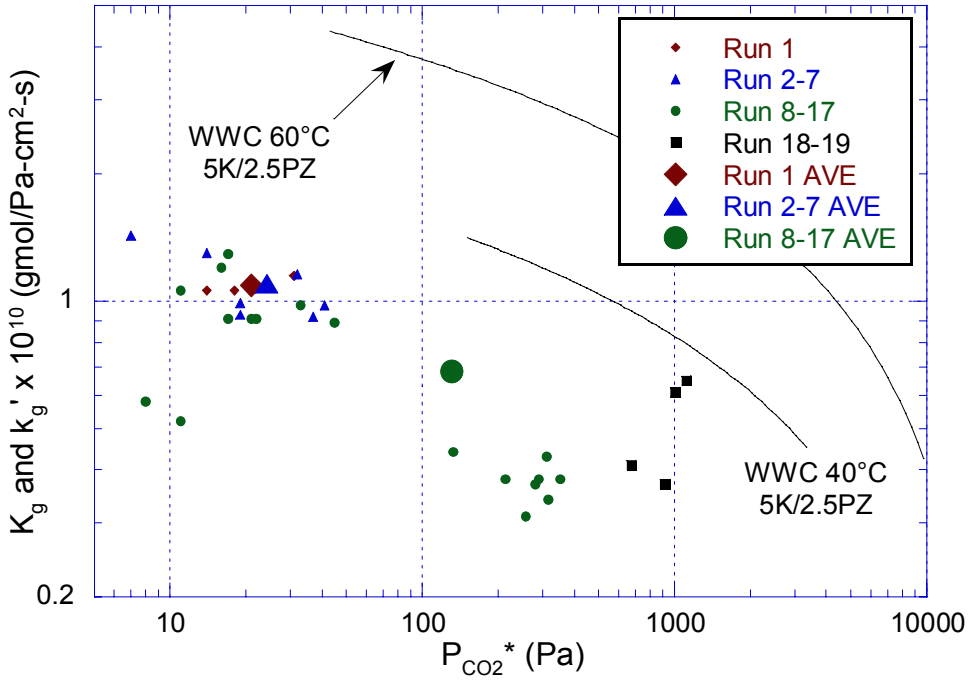

Figure 3-38. Wetted Wall Column Results (k_g') and Absorber (K_g) Results for Campaign 1 (5 m K^+/2.5 m PZ, Flexipac 1Y Structured Packing)

In the second campaign, the absorber was operated over an equilibrium partial pressure that ranged from 200 to 3000 Pa (Figure 3-39). The absorber was operated at three different inlet CO_2 gas concentrations: 5, 12, and 17 mole percent CO_2. The average K_g results for the 5 and 12% run conditions matched the wetted wall column at 40 °C. The 17% case has a slightly higher absorption rate and was in between the 40 and 60 °C wetted wall curves.

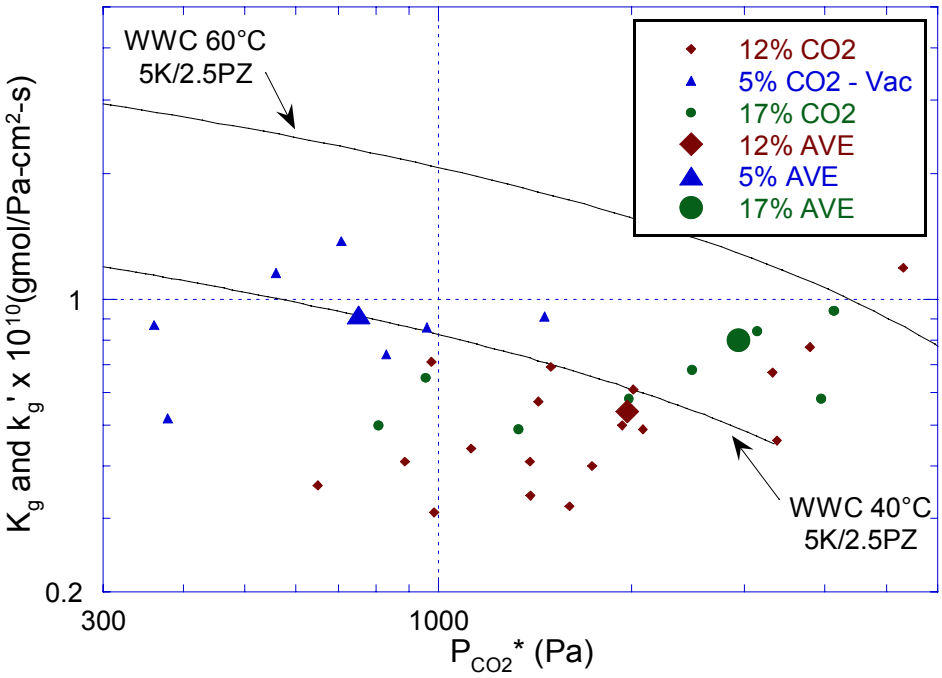

Figure 3-39. Wetted Wall Column Results (k_g') and Absorber (K_g) Results for Campaign 2 (5 m K^+/2.5 m PZ, Flexipac 1Y Structured Packing)

Figure 3-40 shows that in Campaign 4, the 5 m K^+/2.5 m PZ solvent had an absorption rate that is approximately twice that of the 6.4 m K^+/1.6 m PZ solvent. The figure also shows that both solvents had slower absorption rates than the wetted wall column at 40 °C. In addition, the k_g' for the 6.4 m K^+/1.6 m PZ solvent at 40 °C was calculated from the FORTRAN model developed by Cullinane (2005). The FORTRAN model assumes k_l = 0.0004 m/s and k_g = 5.0 x 10^{-9} kmol/Pa-m^2-s. The plot shows that the normalized flux of FORTRAN model for 6.4 m K^+/1.6 m PZ matched the wetted wall column data for the 5 m K^+/2.5 m PZ solvent, which is unexpected.

In the fourth campaign, Flexipac AQ Style 20 structured packing was used, whereas in the first and second campaigns, Flexipac 1Y structured packing was used. When comparing the results from Campaigns 2 and 4, the mass transfer performance was worse with the Flexipac AQ packing. The new packing is

designed to have a lower liquid holdup, which may reduce the mass transfer performance. Also, the effect of bridging between the channels in the packing will be more prevalent with the Flexipac 1Y because it has a more surface area and the channels are narrower. Although the net effect of bridging is to decrease available interfacial area, it may increase the amount of liquid holdup in the packing and provide better mass transfer performance for this system.

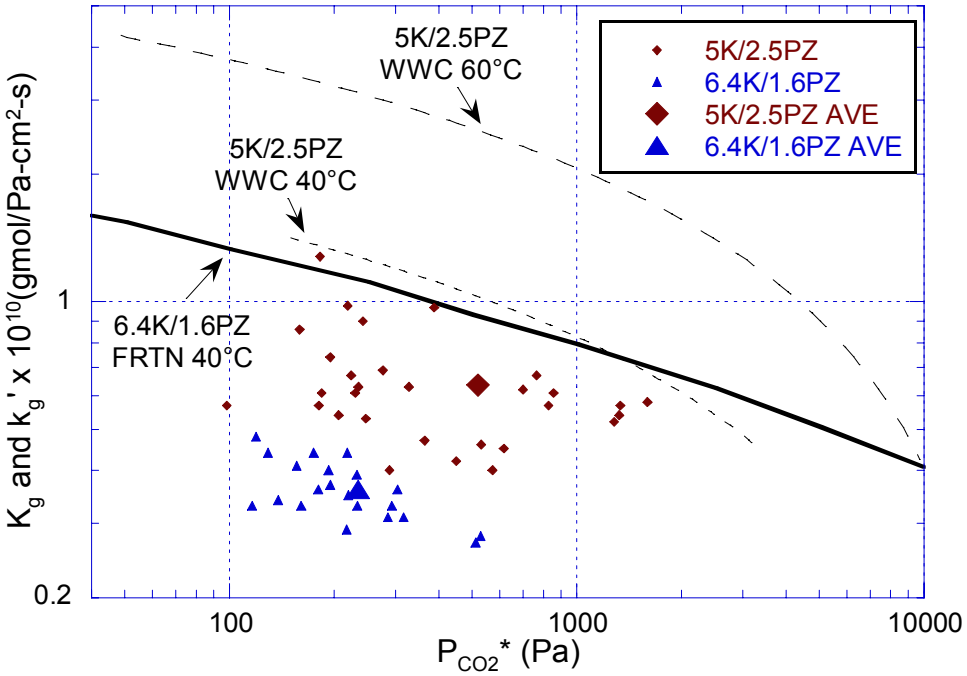

Figure 3-40. Absorber K_g Results for Campaign 4 (5 m K^+/2.5 m PZ and 6.4 m K^+/1.6 m PZ, Flexipac AQ Style 20 Structured Packing), Wetted Wall Column Results (k_g') for 5 m K^+/2.5 m PZ at 40 and 60 °C, and 6.4 m K^+/1.6 m PZ FORTRAN Model Results at 40 °C

The results for all three potassium carbonate and piperazine campaign are compared to the 7 m MEA results from Campaign 3 (Dugas, 2006). The MEA mass transfer coefficient was calculated assuming a 17% inlet CO_2 concentration and was divided by 1.8 because the original calculation used the effective area measurements performed in the metal absorber column and not in the air–water column. Flexipac 1Y structured packing was used in the third campaign.

Figure 3-41 shows that for Flexipac 1Y packing, the 5 m K^+/2.5 m PZ solvent was approximately 2.5 times faster than 7 m MEA when compared with the Campaign 2 results, while the 5 m K^+/2.5 m PZ results from Campaigns 1 and 4 were approximately 1.2 times higher than 7 m MEA. In Campaign 1, differences in solvent composition resulted in a slower absorption rate. In Campaign 4, a less efficient packing (Flexipac AQ Style 20) was used. The K_g analysis also shows that the 5 m K^+/2.5 m PZ solvent has an absorption rate 2 times faster than 6.4 m K^+/1.6 m PZ. Flexipac 1Y structured packing performed 1.8 times better than the Flexipac AQ Style 20 structured packing, even after accounting for the measured values of wetted area. Finally, the K_g results for the 5 m K^+/2.5 m PZ solvent in Campaign 2 matched the performance of the wetted wall column at 40 °C.

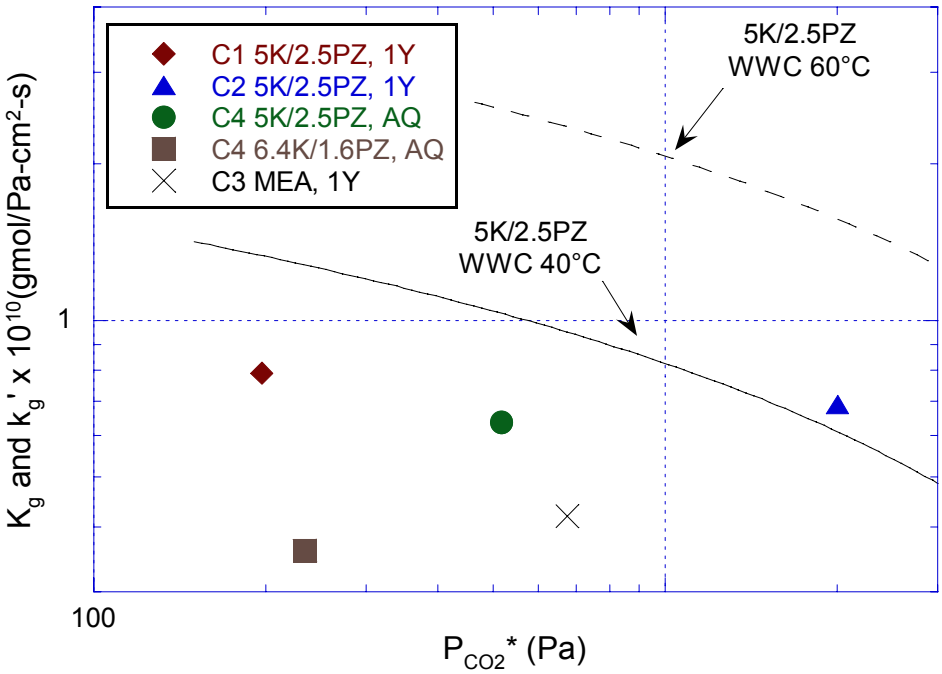

Figure 3-41. Comparison of K_g Results for 5 m K^+/2.5 m PZ, 6.4 m K^+/1.6 m PZ, 7 m MEA, and k_g' of Wetted Wall Column (Cullinane, 2005)

3.14 ABSORBER TEMPERATURE PROFILE

The absorption of CO_2 into piperazine promoted potassium carbonate is an exothermic reaction. One of the advantages of the K^+/PZ solvent is that the heat of absorption is tunable with a composition change. The heat of absorption can be varied from 10 to 20 kcal per mol of CO_2 that is absorbed. The heat that is produced results in an increase in temperatures of the liquid and gas and the transfer of water between the two phases. At the location in the absorber column where the bulk of the CO_2 is absorbed, the temperature profile of the absorber will reach a maximum and produce a temperature bulge. At a high liquid to gas (L/G) ratio, the temperature bulge will be observed towards the bottom of the column and at low L/G ratios, the temperature bulge will be located at the top of the column.

The increase in temperature typically increases the kinetics of the absorption of CO_2, but at the same time will affect the vapor–liquid equilibrium. At high temperatures, the partial pressure of CO_2 in equilibrium with the liquid may begin to approach to the partial pressure of CO_2 in the bulk gas. The lack of a driving force results in a "pinch", where additional CO_2 is not absorbed by the solvent. As a result, the mass transfer performance of the column is reduced. In the operation of a plant, pinch points are typically avoided to maximize the available mass transfer area of the column.

3.14.1 Temperature Sensor Location

The temperature profile of the absorber was characterized with RTDs installed along the length of the column. The RTD sensors are inserted several centimeters into the packing and contact a mixture of gas and liquid. It is almost impossible to surmise whether the temperature of the gas or liquid is being measured. The location of the temperature sensors in absorber are shown in

Figure 3-42. The reference point is given as the bottom of the lower bed of packing. The absorber is divided into two beds of packing, each with a height of 3.05 meters. The two beds of packing are separated by a 1.67 meter section that contains a spool piece where the collector plate and redistributor are located.

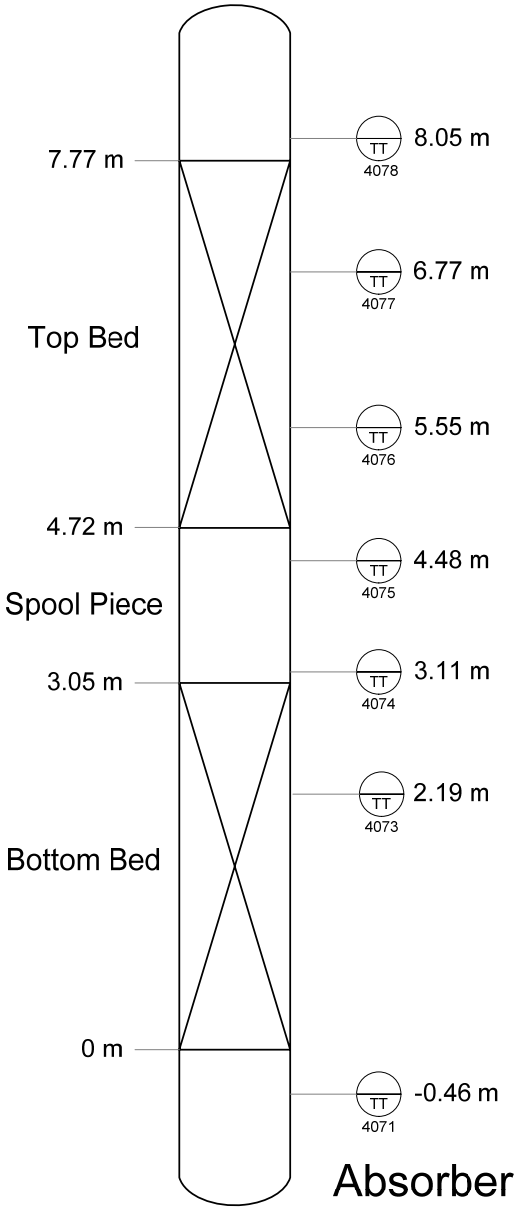

Figure 3-42. Location of Temperature Sensors in Absorber Column

In Campaign 1, the following temperature sensors were used: TT4071, TT7073, TT4076, and TT4078. However, temperature sensor TT4076 was located 6.31 m above the reference point. In the first campaign, the surface temperature of the absorber column was measured with an infrared (IR) temperature sensor to estimate the amount of heat loss from the uninsulated absorber column. The IR measurements were made every 0.15 meters along the length of each packed bed.

3.14.2 Infrared and RTD Measurements

Figure 3-43 illustrates the IR and RTD measurements made on 6/24/04 at 10:45 AM. The gas and liquid flow rates were 8.5 m^3/min and 19.5 L/min, respectively. The inlet CO2 concentration was approximately 12% and the lean loading was 0.53 mol CO_2/(mol K^+ + 2 mol PZ). The figure shows that there is a 2–3 °C difference between the two measurements (TT4073 and TT4076). It can be concluded that the resulting temperature difference is a result of heat loss. A simple heat loss calculation was performed for the just the surface area containing the packing and assuming the thermal conductivity of steel was 43.3 W/m-K and that there was a temperature difference of 2 °C between the inside and outside of the column across the entire length of the column. The heat loss for 6.1 m of the column was estimated to be 51.4 kW, which is in the range of forced

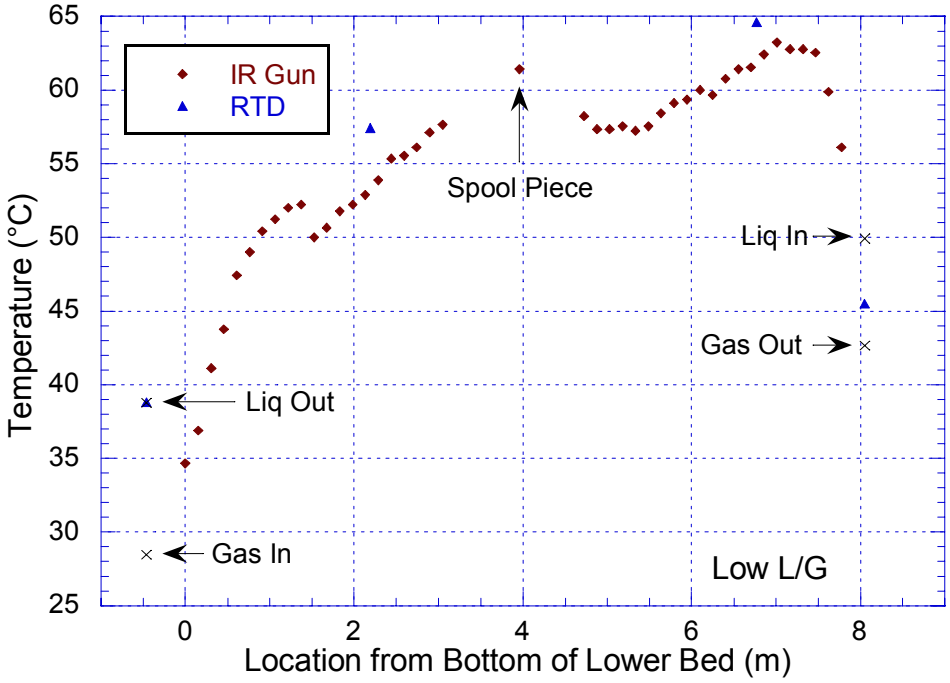

Figure 3-43. Absorber Temperature Profile for Run Performed on 6/24/04 at 10:45 AM (G = 8.5 m³/min, L = 29.5 L/min, CO_2 In = 12%, Lean Ldg = 0.53 mol/Talk)

The figure also shows that there is a drop in temperature of ~2.5 °C at 1.4 meters. The dip in temperature is most likely a result of heat loss from the two support fixtures of the absorber column, which are located in the immediate vicinity. The support fixtures behave as two large fins, conducting and dissipating heat from the absorber column.

An IR temperature measurement taken at middle of the spool piece was 3.8 °C higher than the surrounding measurements made above and below. The higher temperatures indicate that CO_2 is being absorbed in the collector plate or redistributor. However, this is not expected to happen. Future studies should examine this phenomenon in more detail.

Finally, the inlet and outlet temperatures for the gas and liquid are shown. The liquid inlet temperature is about 5 °C higher than top RTD temperature

(TT4078) and the outlet gas temperature is approximately 3 °C lower. Temperature sensor TT4078 is located directly above the distributor and does not contact any liquid. Therefore, TT4078 should be a good indicator of outlet gas temperature. The outlet gas sensor is located approximately 8 meters downstream of the absorber and is expected to be lower than TT4078 because of heat loss. However, during some of the runs, the temperature measurement of TT4078 was actually lower than the gas outlet measurement. It is possible that the probe was not inserted far enough into the column or evaporative cooling from condensation may have skewed the temperature measurement. At the bottom of the column, temperature sensor TT4071 is located 6.3 cm below the inlet gas nozzle and should have intermittent contact with liquid falling down through the packing. In this case, the inlet gas measurement was lower than TT4071 and the outlet liquid temperature matched the RTD measurement. It should be noted that the outlet liquid passes through a pump, a filter and approximately 38 meters of piping before the temperature is measured.

The absorber liquid outlet has two temperature measurements. The outlet pH meter is located 0.9 meters from the absorber outlet and the absorber rich Micro Motion® is located approximately 38 meters downstream of the absorber outlet. The absorber lean Micro Motion® is located 22 meters upstream of the absorber inlet nozzle. The lean pH temperature measurement is located approximately 5 meters downstream of the Micro Motion®.

3.14.3 Temperature Bulge

The location and magnitude of the temperature bulge is dependent upon several factors such as liquid flow rate, liquid to gas flow rate ratio (L/G), inlet CO_2 gas concentration, solvent composition, mass transfer area, and inlet gas and

liquid temperatures. An analysis of the temperature bulge was performed for the three potassium carbonate and piperazine campaigns.

Figure 3-44 shows that the location of the temperature bulge depends on the liquid to gas flow rate ratio (L/G). At low L/G ratios, the temperature bulge will typically be located near the top of the column. As the L/G ratio increases, the temperature bulge will begin to move down towards the bottom of the column and will cease to exist at high liquid rates. At a high L/G ratio, the bulk of the enthalpy is carried out of the column by the high liquid flow rate.

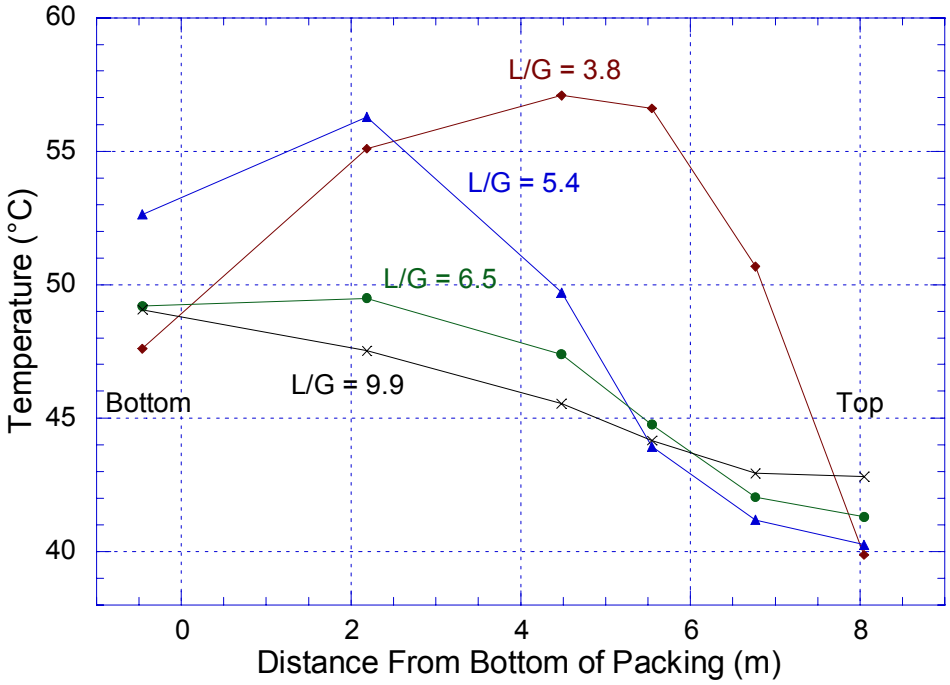

Figure 3-44. Temperature Bulge Location and Magnitude in Absorber (Campaign 4, 5 m K^+/2.5 m PZ, CO_2 In = 17 mol%, L = 93–139 kg/min)

The location of the temperature bulge (T_{max}) was determined based on the RTD measurements. The exact maximum temperature and corresponding location could not be determined because it is not practical to have temperature measurements every 5 cm along the entire length of the column. Figure 3-45 shows that as the L/G ratio increases, the location of T_{max} will move from the top

of the column to the bottom, which was also shown in the previous figure. The plot also shows that at low inlet CO_2 gas concentrations, the temperature bulge will begin to shift down the column at lower L/G ratios. The T_{max} location of the 3–5% inlet CO_2 runs begin to shift at a L/G = 2, while the transition point for the 12% runs occur at L/G = 3.5 and the 17% runs occur at L/G = 4.5.

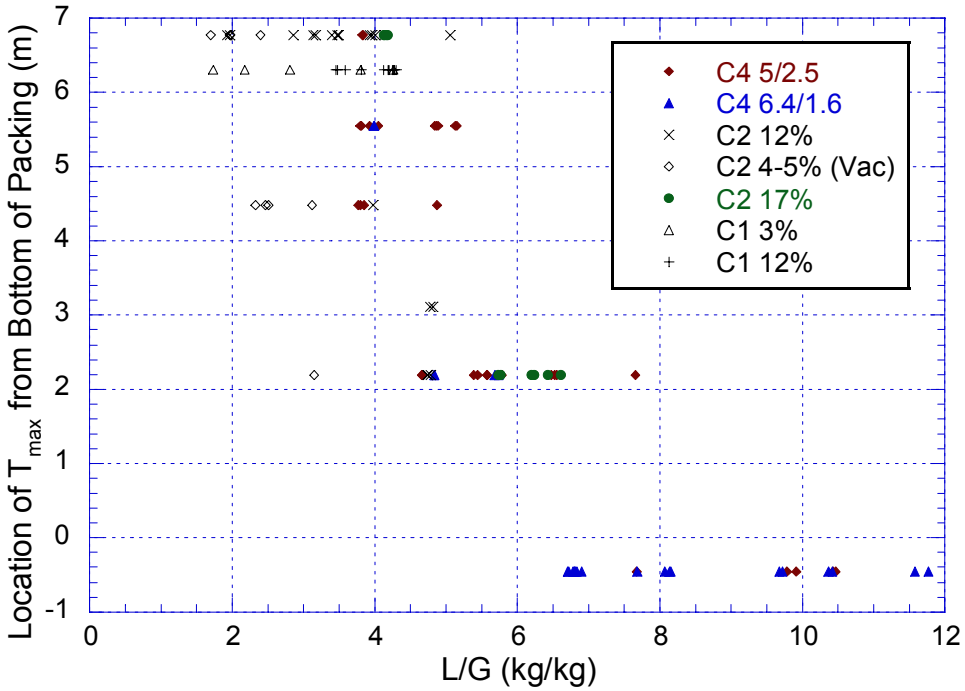

Figure 3-45. Location of Temperature Bulge as a Function of Liquid to Gas Ratio and Inlet CO_2 Gas Concentration for Campaigns 1, 2, and 4

A plot of the T_{max} measurements and L/G ratio illustrates the magnitude of the temperatures that were attained in the three campaigns (Figure 3-46). The figure shows that the maximum temperatures were achieved at an L/G ratio of 4 to 5 kg/kg. The 12% CO_2 data from Campaign 2 also suggests that the temperature bulge passes through a maximum at L/G = 3.5.

The average temperature of the absorber column was calculated by integrating the area under the temperature profile curve and dividing by the height of the column. There were some issues with the TT4078 temperature

measurements located at the top of the absorber (8.05 meters). For the analysis, the highest of the following three temperatures were used as the top temperature: gas out, liquid in or TT4078. At the bottom of the absorber, where TT4071 was located (-0.46 m), the higher of the following two temperatures was used: liquid out or TT4071.

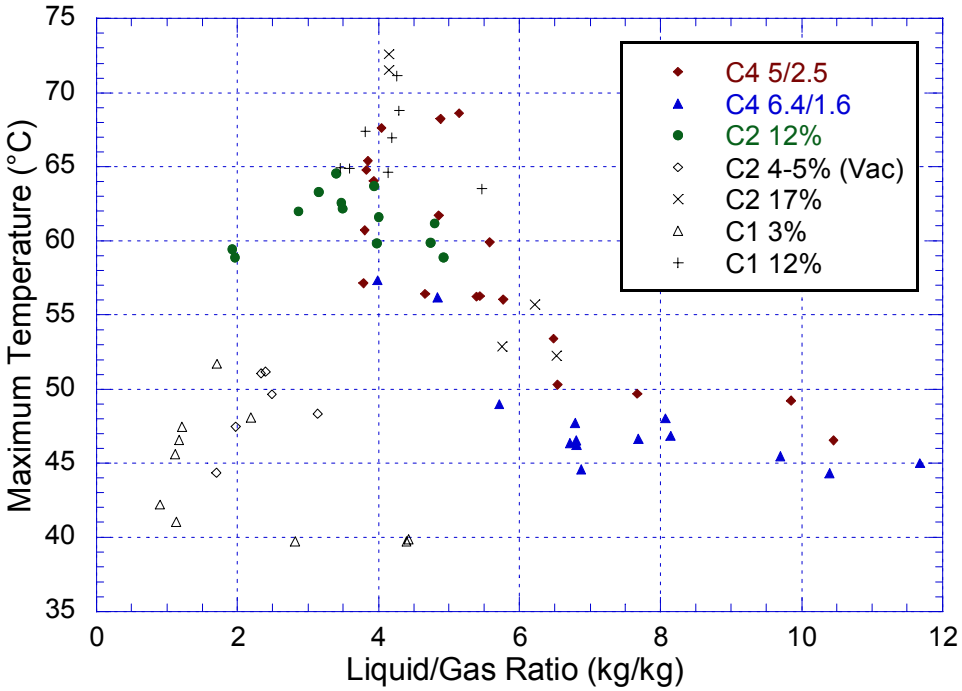

Figure 3-46. Magnitude of Temperature Bulge as a Function of Liquid to Gas Ratio and Inlet CO_2 Gas Concentration for Campaigns 1, 2, and 4

In Campaign 1, only four RTD temperature measurements were available, whereas in Campaigns 2 and 4, there were 7 and 6 RTD measurements, respectively. Therefore, the integrated temperature profiles of Campaign 1 should not be directly compared to those obtained in the other two campaigns because the profile was not characterized as well. Finally, the temperature profile was integrated from the -0.46 m to 8.05 m on the x-axis. The lowest temperature in the profile was used as the reference point for the y-axis as a way of normalizing the difference between top and bottom temperatures, which

varied with each of the runs and were typically the lowest temperatures in the temperature profile.

Table 3-17. Campaign 1 Temperature Profile Analysis

Run#	L/G	L	Temp 8.05 m	Temp 6.31 m	Temp 2.19 m	Temp -0.46 m	T_{max}	T_{max} Loc	T_{ave}	CO_2 Rem Gas-side
	kg/kg	kg/min	°C	°C	°C	°C	°C	m	°C	gmol/min
1.1.1	1.11	21.7	42.6	45.8	39.9	29.2	45.8	6.31	40.6	16.92
1.1.2	1.11	21.7	42.0	45.5	39.5	28.6	45.5	6.31	40.1	16.63
1.1.3	1.12	21.7	42.4	45.6	39.6	29.0	45.6	6.31	40.3	16.17
1.2.1	2.18	21.9	41.5	46.8	46.6	32.9	46.8	6.31	44.0	9.81
1.2.2	2.19	21.9	43.2	48.6	47.3	33.1	48.6	6.31	45.1	9.61
1.2.3	2.20	22.0	44.5	48.8	47.5	33.0	48.8	6.31	45.4	9.44
1.3.1	4.43	43.9	41.0	39.9	37.8	38.4	39.9	6.31	38.9	7.20
1.3.2	4.43	44.0	40.7	40.0	37.7	38.1	40.0	6.31	38.9	7.83
1.3.3	4.43	43.9	40.4	39.7	37.4	38.1	39.7	6.31	38.6	7.57
1.4.1	4.40	43.9	40.0	39.7	37.5	39.4	39.7	6.31	38.8	12.54
1.5.1	2.81	38.1	40.1	39.7	37.3	38.3	39.7	6.31	38.6	12.97
1.6.1	5.60	33.9	39.5	48.2	48.0	44.0	48.2	6.31	46.6	21.43
1.7.1	5.46	22.1	41.5	63.5	51.4	39.2	63.5	6.31	52.7	13.78
1.8.1	1.17	23.0	43.6	46.8	40.9	29.7	46.8	6.31	41.5	19.50
1.8.2	1.17	22.9	43.5	46.3	40.6	29.4	46.3	6.31	41.1	20.34
1.9.1	0.90	22.9	42.1	42.3	36.7	31.6	42.3	6.31	38.4	23.13
1.9.2	0.89	22.9	41.9	42.1	36.8	31.5	42.1	6.31	38.3	24.05
1.10.1	1.73	23.2	42.7	51.6	48.0	30.1	51.6	6.31	45.9	12.95
1.10.2	1.68	22.5	42.7	51.8	48.1	29.8	51.8	6.31	46.0	11.76
1.11.1	1.12	11.4	35.8	40.7	33.9	22.6	40.7	6.31	34.7	8.36
1.11.2	1.13	11.5	36.1	41.4	34.3	22.7	41.4	6.31	35.1	7.82
1.12.1	1.22	32.1	42.9	47.2	41.8	34.4	47.2	6.31	42.6	14.59
1.12.2	1.20	30.0	43.7	47.7	41.7	34.4	47.7	6.31	42.8	22.61
1.13.1	3.59	35.3	49.4	64.9	54.8	38.5	64.9	6.31	55.2	38.98
1.14.1	3.81	30.9	46.2	67.4	57.7	41.0	67.4	6.31	57.3	30.57
1.15.1	4.13	35.6	39.6	61.5	53.0	39.8	61.5	6.31	52.5	30.33
1.15.2	4.13	35.6	44.0	67.7	59.0	40.9	67.7	6.31	57.7	28.57
1.16.1	3.45	35.7	50.8	65.2	57.2	38.5	65.2	6.31	56.4	33.93
1.16.2	3.48	35.8	49.7	64.6	57.4	38.8	64.6	6.31	56.2	34.60
1.17.1	4.18	22.9	48.2	66.8	56.7	38.4	66.8	6.31	56.5	18.89
1.17.2	4.20	22.9	47.7	67.2	57.1	38.4	67.2	6.31	56.7	19.09
1.18.1	4.26	35.9	52.9	71.0	63.5	44.6	71.0	6.31	62.0	31.23
1.18.2	4.25	35.9	53.2	71.3	63.5	46.7	71.3	6.31	62.5	31.86
1.19.1	4.28	23.1	53.7	68.3	59.0	40.4	68.3	6.31	58.8	18.43
1.19.2	4.30	23.2	53.2	69.3	59.0	39.8	69.3	6.31	58.9	19.14

Table 3-18. Campaign 2 Temperature Profile Analysis

Run#	L/G	L	Temp 8.05 m	Temp 6.77 m	Temp 5.55 m	Temp 4.48 m	Temp 3.11 m	Temp 2.19 m	Temp -0.46 m	T_{max}	T_{max} Loc	T_{ave}	CO_2 Rem Gas-side
	kg/kg	kg/min	°C	°C	°C	°C		°C	°C	°C	m	°C	gmol/min
2.1.1	1.93	36.9	49.2	59.7	53.2	52.7	48.3	48.5	49.1	59.7	6.77	51.5	52.74
2.1.2	1.93	37.0	48.8	59.1	52.8	52.4	48.1	48.1	48.8	59.1	6.77	51.1	50.28
2.2.1	1.97	37.0	50.8	58.9	53.1	53.5	49.8	50.0	51.8	58.9	6.77	52.5	37.00
2.3.1	2.86	41.7	44.6	62.0	56.7	57.2	52.3	51.4	45.5	62.0	6.77	53.2	33.09
2.4.1	3.48	51.0	40.9	62.5	58.3	59.2	54.1	54.3	45.4	62.5	6.77	54.3	37.70
2.5.1	3.49	50.8	40.7	62.2	58.4	59.4	54.5	54.5	45.8	62.2	6.77	54.4	35.77
2.6.1	3.98	58.0	41.2	59.3	59.1	59.8	56.6	58.0	47.5	59.8	4.48	55.5	38.39
2.7.1	4.01	58.2	41.3	61.6	60.0	61.0	57.5	58.5	47.7	61.6	6.77	56.4	39.83
2.8.1	3.14	60.6	45.8	63.2	59.1	59.1	57.6	54.7	48.0	63.2	6.77	55.9	44.61
2.8.2	3.17	60.4	46.2	63.4	59.4	59.4	58.1	55.6	48.9	63.4	6.77	56.4	43.60
2.9.1	3.40	39.7	41.1	64.2	58.7	57.3	55.5	53.7	42.7	64.2	6.77	54.0	28.92
2.9.2	3.40	39.6	42.2	64.8	59.1	57.5	55.9	54.0	43.0	64.8	6.77	54.4	29.35
2.10.1	4.74	53.6	41.2	52.2	58.8	58.7	59.1	59.8	48.9	59.8	2.19	55.2	35.12
2.10.2	4.75	53.5	41.3	52.6	59.2	59.0	59.3	59.9	49.7	59.9	2.19	55.5	34.77
2.11.1	4.78	53.3	41.4	55.0	60.6	60.8	61.0	60.7	49.4	61.0	3.11	56.7	32.87
2.11.2	4.82	53.6	41.4	56.0	61.0	61.1	61.4	60.9	50.5	61.4	3.11	57.2	32.98
2.12.1	5.06	56.0	41.0	59.7	59.2	57.3	57.2	57.3	50.5	59.7	6.77	55.6	35.61
2.12.2	4.79	55.7	41.0	52.4	57.0	56.6	56.9	58.1	48.7	58.1	2.19	54.0	39.58
2.13.1	3.96	46.7	40.7	65.0	61.4	62.1	61.5	59.0	45.0	65.0	6.77	57.4	33.57
2.13.2	3.93	46.6	40.3	62.5	59.9	61.0	60.1	57.9	44.1	62.5	6.77	56.1	34.28
2.14.1	1.97	23.2	43.5	48.0	44.1	43.7	36.6	39.7	34.1	48.0	6.77	41.1	15.93
2.14.2	1.98	23.3	42.5	46.9	43.4	43.3	36.2	39.5	33.3	46.9	6.77	40.5	14.87
2.15.1	2.40	28.1	41.9	51.2	49.5	50.6	44.6	46.3	37.0	51.2	6.77	46.1	18.03
2.16.1	2.33	27.4	42.0	50.9	49.8	51.0	45.1	46.7	36.9	51.0	4.48	46.3	18.05
2.16.2	1.70	25.6	38.8	44.8	40.8	41.3	35.6	36.9	34.0	44.8	6.77	38.7	19.35
2.17.1	1.70	25.6	39.0	43.9	40.1	40.7	34.9	36.6	33.0	43.9	6.77	38.1	16.01
2.18.1	2.51	37.3	44.8	45.9	47.5	49.6	43.7	46.7	40.5	49.6	4.48	45.6	17.13
2.18.2	2.47	36.6	44.8	45.7	47.5	49.7	43.9	47.1	40.9	49.7	4.48	45.7	16.74
2.19.1	3.12	46.1	47.0	44.2	44.3	46.9	41.2	46.6	43.6	46.9	4.48	44.8	17.58
2.19.2	3.15	46.2	47.8	46.3	46.5	49.2	44.4	49.8	44.9	49.8	2.19	47.1	17.42
2.20.1	5.73	94.8	40.1	42.5	46.7	51.7	49.3	52.9	49.7	52.9	2.19	48.4	71.52
2.20.2	5.77	94.5	40.1	42.2	45.8	51.4	48.9	52.8	50.1	52.8	2.19	48.2	69.91
2.21.1	6.43	102.2	40.1	40.7	43.4	48.9	47.1	50.8	50.1	50.8	2.19	46.6	67.80
2.21.2	6.61	102.0	40.9	42.3	45.6	51.1	49.9	53.7	52.0	53.7	2.19	48.8	63.62
2.22.1	6.20	101.2	41.8	44.4	49.0	54.0	53.0	56.3	52.4	56.3	2.19	51.1	75.52
2.22.2	6.24	101.9	41.1	42.9	47.2	52.5	51.6	55.1	52.1	55.1	2.19	49.9	75.95
2.23.1	4.17	69.7	41.5	72.1	67.5	67.6	64.7	63.2	49.0	72.1	6.77	62.1	65.79
2.23.2	4.14	69.3	39.8	71.0	67.1	67.4	64.6	62.9	48.6	71.0	6.77	61.6	64.16
2.24.1	4.18	70.0	41.5	72.6	67.6	68.1	65.2	63.8	49.1	72.6	6.77	62.4	69.88
2.24.2	4.13	69.5	42.0	72.5	67.6	68.0	65.0	63.6	49.0	72.5	6.77	62.4	70.91

Table 3-19. Campaign 4 – 5 m K^+/2.5 m PZ Temperature Profile Analysis

Run#	L/G	L	Temp 8.05 m	Temp 6.77 m	Temp 5.55 m	Temp 4.48 m	Temp 2.19 m	Temp -0.46 m	T_{max}	T_{max} Loc	T_{ave}	CO_2 Rem Gas-side
	kg/kg	kg/min	°C	°C	°C	°C	°C	°C	°C	m	°C	gmol/min
4.1	3.85	64.9	42.4	57.1	64.9	65.4	62.1	49.4	65.4	4.48	58.9	42.0
4.2.1	4.05	58.1	45.8	64.8	67.9	64.9	61.3	49.3	67.9	5.55	60.4	58.5
4.2.2	4.05	58.3	46.1	64.9	67.3	64.3	60.5	49.3	67.3	5.55	60.0	59.0
4.3.1	5.75	60.6	42.1	44.3	50.5	52.2	55.7	50.9	55.7	2.19	50.9	44.9
4.3.2	5.79	60.6	42.5	44.8	51.3	52.9	56.3	51.2	56.3	2.19	51.5	46.0
4.4.1	4.87	67.6	43.6	52.7	60.5	61.0	60.9	50.7	61.0	4.48	56.8	55.6
4.4.2	4.84	67.9	43.9	54.1	62.4	62.4	61.5	50.8	62.4	5.55	57.7	55.5
4.5.1	3.81	67.7	45.7	58.4	61.5	59.6	56.7	48.1	61.5	5.55	56.0	-
4.5.2	3.79	67.9	43.6	56.9	59.9	58.1	55.4	47.8	59.9	5.55	54.7	65.8
4.6.1	5.15	55.2	46.7	66.8	69.7	68.4	64.7	52.3	69.7	5.55	63.1	50.1
4.6.2	5.13	54.9	43.6	58.4	67.5	67.3	64.7	51.9	67.5	5.55	61.1	50.3
4.7.1	4.86	67.1	45.2	62.2	68.4	67.5	64.7	51.1	68.4	5.55	61.8	54.1
4.7.2	4.89	66.8	45.0	59.9	68.0	67.8	65.3	51.2	68.0	5.55	61.6	53.2
4.8	3.93	66.9	47.2	62.1	64.1	62.2	58.0	48.2	64.1	5.55	57.9	51.0
4.9.1	3.82	66.6	50.9	65.0	64.2	61.2	57.0	48.0	65.0	6.77	58.1	63.1
4.9.2	3.84	66.8	51.0	64.6	64.0	61.0	56.8	47.9	64.6	6.77	57.9	62.1
4.10.1	5.58	60.0	44.3	49.9	56.7	58.6	60.2	51.3	60.2	2.19	55.3	45.4
4.10.2	5.57	60.0	41.7	46.8	53.4	57.5	59.6	51.0	59.6	2.19	53.8	45.3
4.11.1	4.66	66.8	41.6	46.1	52.2	54.4	56.8	49.6	56.8	2.19	51.9	47.7
4.11.2	4.67	67.1	41.2	45.4	51.3	53.5	56.0	49.4	56.0	2.19	51.2	47.3
4.12.1	3.79	67.2	39.8	49.5	56.3	57.2	55.5	47.6	57.2	4.48	52.6	39.7
4.12.2	3.77	67.2	39.9	50.7	56.6	57.1	55.1	47.6	57.1	4.48	52.7	42.0
4.13.1	7.68	133.7	41.5	42.6	44.8	46.6	48.5	48.8	48.8	-0.46	46.3	70.8
4.13.2	7.66	133.8	43.0	44.1	46.3	48.5	50.5	50.2	50.5	2.19	48.0	70.2
4.14.1	9.79	138.6	42.8	43.1	44.7	46.2	48.1	49.3	49.3	-0.46	46.3	66.4
4.14.2	9.92	138.4	42.8	42.9	44.2	45.6	47.5	49.1	49.1	-0.46	45.9	63.0
4.15.1	10.43	108.5	39.5	39.7	41.0	42.2	44.0	46.5	46.5	-0.46	42.7	49.7
4.15.2	10.47	108.9	39.6	39.8	41.2	42.5	44.1	46.6	46.6	-0.46	42.8	49.8
4.16.1	6.53	115.1	41.4	42.9	46.4	49.2	51.1	49.8	51.1	2.19	48.0	61.9
4.16.2	6.56	115.3	41.3	42.0	44.7	47.4	49.5	49.2	49.5	2.19	46.7	56.3
4.17.1	6.48	115.3	40.1	41.5	45.9	49.9	52.8	51.0	52.8	2.19	48.4	70.6
4.17.2	6.48	115.2	40.6	42.0	46.4	50.8	54.0	51.9	54.0	2.19	49.2	76.0
4.18	5.39	92.7	40.0	41.1	44.5	50.4	56.2	52.2	56.2	2.19	49.4	68.8
4.19	5.44	92.5	40.3	41.2	43.9	49.7	56.3	52.6	56.3	2.19	49.3	66.1

Table 3-20. Campaign 4 – 6.4 m K^+/1.6 m PZ Temperature Profile Analysis

Run#	L/G	L	Temp 8.05 m	Temp 6.77 m	Temp 5.55 m	Temp 4.48 m	Temp 2.19 m	Temp -0.46 m	T_{max}	T_{max} Loc	T_{ave}	CO_2 Rem Gas-side
	kg/kg	kg/min	°C	°C	°C	°C	°C	°C	°C	m	°C	gmol/min
4.20.1	10.43	111.1	38.8	37.7	37.5	40.9	41.4	44.4	44.4	-0.46	40.5	38.8
4.20.2	10.36	111.1	38.6	37.2	38.2	39.8	41.1	44.3	44.3	-0.46	40.2	38.3
4.21.1	11.58	124.2	39.0	38.8	39.2	40.4	41.5	44.3	44.3	-0.46	40.8	39.7
4.21.2.	11.77	124.8	40.5	40.5	41.1	42.4	43.6	45.7	45.7	-0.46	42.7	42.6
4.22.1	6.84	72.2	36.8	37.5	37.6	40.5	41.0	44.5	44.5	-0.46	40.1	33.1
4.22.2	6.91	72.3	36.7	37.6	37.8	40.4	41.0	44.6	44.6	-0.46	40.2	34.2
4.23	6.80	72.5	37.8	39.0	40.2	42.2	43.3	46.5	46.5	-0.46	42.1	37.3
4.24	6.81	72.6	37.5	38.6	40.0	41.6	42.9	46.2	46.2	-0.46	41.7	36.6
4.25	7.69	81.6	39.5	39.8	40.3	42.5	43.5	46.7	46.7	-0.46	42.5	38.8
4.26.1	9.67	100.3	38.3	38.9	39.9	41.6	43.1	45.1	45.1	-0.46	41.7	45.3
4.26.2	9.72	100.7	38.7	39.3	40.6	42.3	43.8	45.8	45.8	-0.46	42.3	45.7
4.27.1	8.14	86.4	40.0	40.9	42.7	44.4	45.8	47.2	47.2	-0.46	44.2	41.4
4.27.2	8.15	86.5	39.3	39.9	41.6	43.4	44.8	46.5	46.5	-0.46	43.2	40.2
4.28.1	6.71	71.8	38.9	40.0	41.9	43.8	45.3	46.8	46.8	-0.46	43.5	37.5
4.28.2	6.72	71.8	38.4	39.0	40.5	42.5	43.8	45.9	45.9	-0.46	42.3	35.3
4.29.1	6.79	72.1	39.4	40.3	42.2	44.4	46.0	47.5	47.5	-0.46	44.1	39.0
4.29.2	6.79	72.2	39.5	40.6	42.7	45.0	46.8	47.9	47.9	-0.46	44.6	40.4
4.30.1	8.07	86.2	41.0	41.2	42.4	44.7	46.2	48.2	48.2	-0.46	44.6	44.0
4.30.2	8.07	86.5	40.4	40.6	42.5	44.5	45.9	47.9	47.9	-0.46	44.3	46.0
4.31.1	5.69	100.5	41.6	42.5	45.4	47.5	49.1	48.7	49.1	2.19	46.7	48.4
4.31.2	5.74	100.4	41.6	42.4	45.1	47.2	48.8	48.7	48.8	2.19	46.5	48.1
4.32.1	4.83	86.1	43.5	45.6	50.7	53.9	55.8	49.9	55.8	2.19	51.4	47.1
4.32.2	4.85	86.2	43.7	45.9	51.3	55.1	56.6	49.9	56.6	2.19	52.0	45.4
4.33.1	3.99	71.6	45.6	54.3	57.8	56.6	53.7	48.1	57.8	5.55	53.4	44.8
4.33.2	3.99	71.5	45.1	52.6	56.9	56.0	53.7	48.2	56.9	5.55	52.9	43.4

The average temperature of the absorber was correlated to the maximum temperature measured in the absorber column (Figure 3-47). The average absorber temperature increased as the maximum temperature increased. The figure also shows the distribution of the integrated temperature profiles among the three campaigns. The plot shows that the highest temperature was achieved with 5 m K^+/2.5 m PZ solvent with the Flexipac 1Y packing and at inlet CO_2 gas concentrations of 12 and 17 mol%.

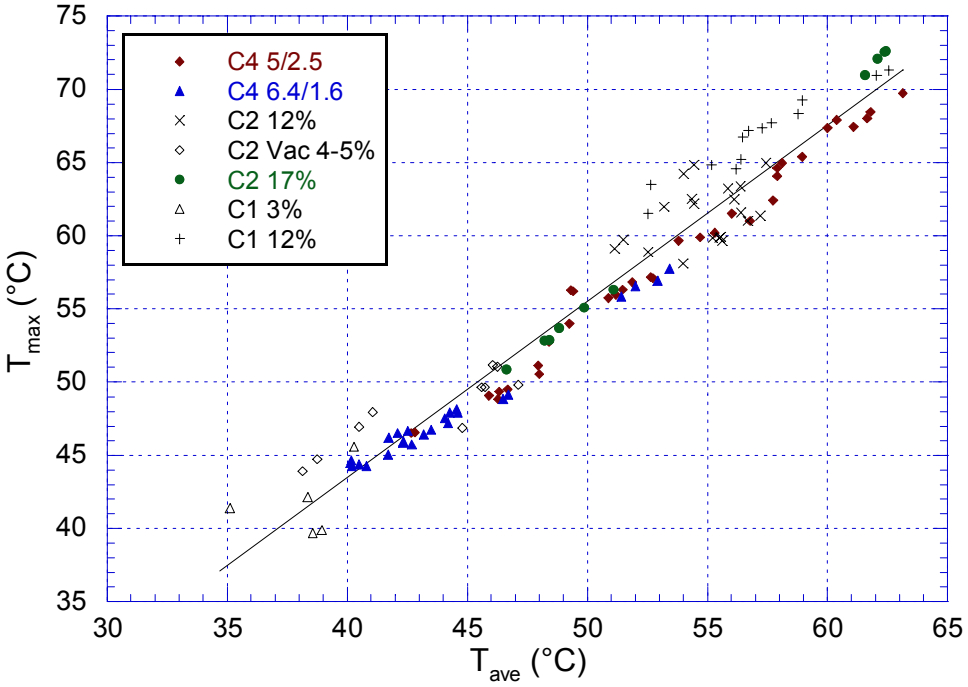

Figure 3-47. Integrated Area of Absorber Temperature Profile and Maximum Temperature Measurements in the Absorber

3.15 PRESSURE DROP

Flexipac AQ Style 20 structured packing has a corrugation angle of 50 degrees. This results in lower liquid holdup, lower pressure drop, and a higher capacity. Flexipac 1Y structured packing has a corrugation angle of 45 degrees, narrower channels, and a higher pressure drop. Figure 3-48 shows the pressure drop data obtained for all three K^+/PZ campaigns. The pressure drop was calculated by taking the square root of the total pressure drop across the absorber column and normalizing by the inlet superficial gas velocity. The total pressure drop was calculated as the sum of the pressure drop for the top (PDT 451) and bottom (PDT 450) packing bed. The figure shows that the Flexipac 1Y packing used in Campaigns 1 and 2 had a higher pressure drop normalized by gas velocity than the Flexipac AQ structured packing used in Campaign 4. The total pressure drop across the column in Campaigns 1 and 2 were comparable, but the

gas rate was typically higher in Campaign 2. The average superficial gas velocity for Campaigns 1 and 2 were 1.06 and 1.43 m/s, respectively.

Analysis of Campaign 1 pressure drop data found that when the ratio for the pressure drop of the bottom bed to top bed exceeded one, the points fell inside the circled region of the figure, where the ratio ranged from 1.1 to 2.2. The majority of the remaining points had bottom to top bed ratios of approximately 0.95. The pressure drop for the low gas flow rate points in Campaign 2 was similar to the high bottom to top bed ratio values of Campaign 1. However in Campaign 2, the threshold for bottom to top bed ratio was 1.4. The low gas rate points of Campaign 2 that fell in the circled region had a bottom to top bed ratio that ranged from 1.8–5.3. It is possible that for some of these points, the bottom bed of the absorber column was foaming. For other points of Campaign 2, the ratio of the pressure drop for the bottom and top bed ranged from 0.9 to 1.4.

Figure 3-49 is a plot of the Flexipac AQ Style 20 packing data for the 5 m K^+/2.5 m PZ and 6.4 m K^+/1.6 m PZ solvent compositions. For a given liquid rate and a gas rate of 0.95 m/s, the figures shows that the 6.4 m K^+/1.6 m PZ solvent has a lower total pressure drop than the 5 m K^+/2.5 m PZ. At a gas rate of 1.59 m/s, both solvents had comparable pressure drop measurements. This is most likely due to temperature bulge effect. When the temperature bulge is large, the density of the gas is much lower and will increase the pressure drop. The 6.4 m K^+/1.6 m PZ has a slower CO_2 absorption rate and does not generate much of temperature bulge at low gas rates (high L/G), which results in a lower pressure drop. At high gas rates (low L/G), the figure suggests that the hydrodynamics of the gas and liquid outweigh the effects of the temperature bulge because the temperature bulge for the 6.4 m K^+/1.6 m PZ solvent were lower than the 5 m K^+/2.5 m PZ solvent. Therefore, column pressure drop designs should account for the temperature bulge.

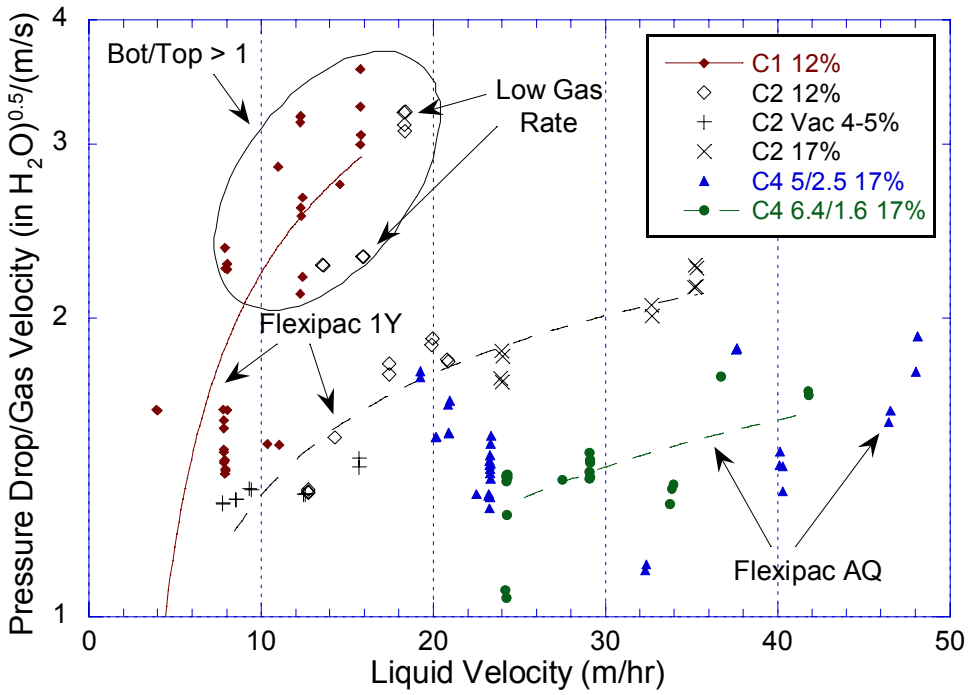

Figure 3-48. Pressure Drop Data of Flexipac 1Y and Flexipac AQ Style 20 for Campaigns 1,2, and 4 (5 m K⁺/2.5 m PZ and 6.4 m K⁺/1.6 m PZ Solvent)

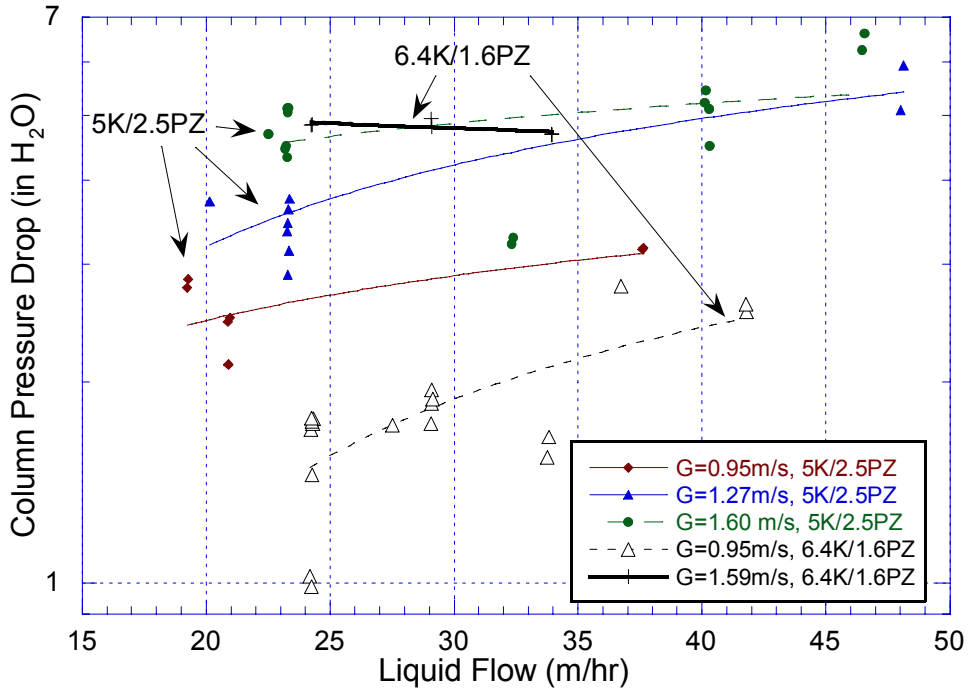

Figure 3-49. Pressure Drop of Flexipac AQ Style 20 for Campaign 4 as a Function of Solvent Composition (5 m K⁺/2.5 m PZ and 6.4 m K⁺/1.6 m PZ)

3.16 STRIPPER HEAT DUTY

In the first two campaigns, the stripper feed was not pre-heated adequately. Therefore, the heat duty obtained for the Campaigns 1 and 2 were not representative. In Campaign 4, a plate and frame cross-exchanger was installed which reduced the approach temperature down to 5–10 °C, relative to the reboiler. However, due to the higher temperatures, the stripper feed would flash at the top of the absorber column in the distributor. It was estimated that the feed entering the distributor was approximately 90–95% gas. In future pilot plant campaigns, a two-phase distributor should be used, which will improve the mass transfer performance in the stripper.

The approximate reboiler heat duty of Campaign 4 is shown in Figure 3-50. The heat duty was calculated based on the steam rate to the reboiler and does not account for heat loss from the stripper. A detailed analysis of stripper performance for the fourth campaign is presented in Oyenekan (2007). The plot shows that reboiler heat duty increases with CO_2 removal efficiency for the 5 m K^+/2.5 m PZ and 6.4 m K^+/1.6 m PZ solvent compositions. However, the 5 m K^+/2.5 m PZ solvent has a slightly lower heat duty for a given CO_2 removal efficiency. This is unexpected because the 6.4 m K^+/1.6 m PZ solvent has a lower heat of absorption than 5 m K^+/2.5 m PZ solvent.

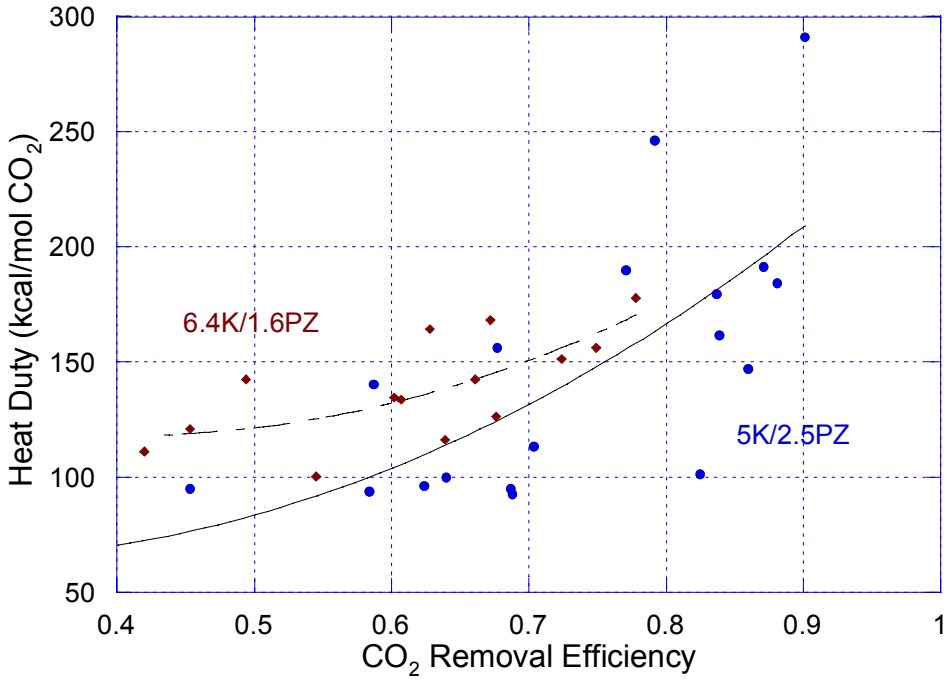

Figure 3-50. Campaign 4 Stripper Performance for 5 m K^+/2.5 m PZ and 6.4 m K^+/1.6 m PZ

3.17 Cross Exchanger Performance

The number of transfer units (NTU) per pass for the Alfa Laval M6-FG plate and frame cross-exchanger was calculated and plotted against the solvent flow rate. The cross-exchanger has a heat transfer area of 14.8 m^2, consists of 99 plates and is arranged for 5 pass flow. Figure 3-51 shows that the NTUs per pass are inversely related to the liquid flow rate. The approach temperatures of the 5 m K^+/2.5 m PZ and the 6.4 m K^+/1.6 m PZ solvent ranged from 6.9 to 8.9 °C and 3.4 to 6.4 °C, respectively. The approach temperature was lower for the 6.4 m K^+/1.6 m PZ because it was operated under vacuum and the stripper temperature profile was much lower. As a result, the NTU dependence is slightly different than the 5 m K^+/2.5 m PZ solvent.

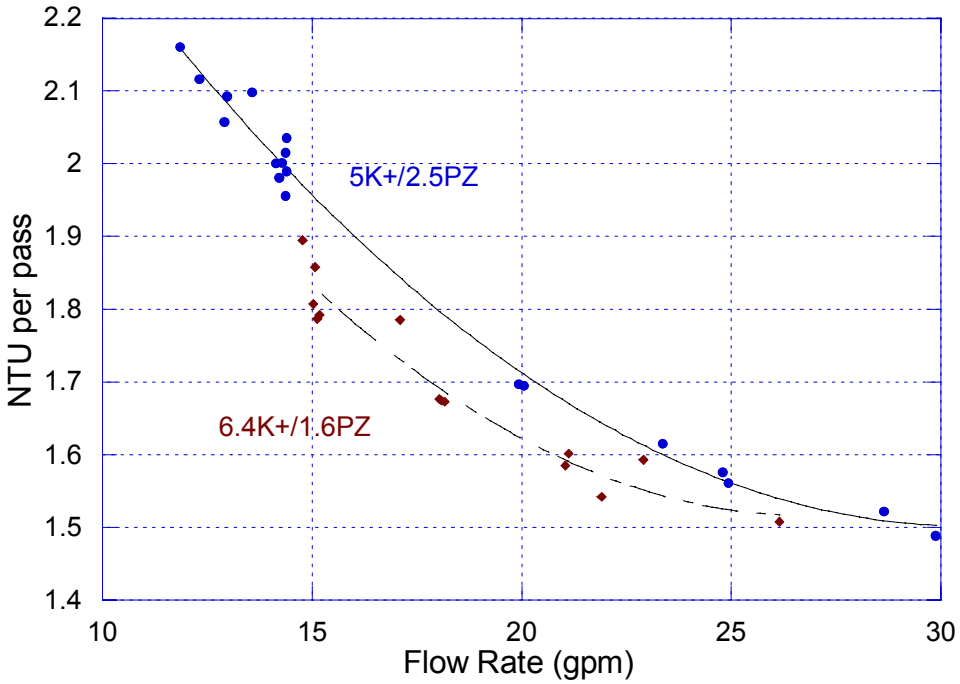

Figure 3-51. Number of Transfer Units for Alfa Laval M6-FG Plate and Frame Cross-Exchanger (Area = 14.8 m², 99 Plates, 5 Pass Flow)

3.18 CONCLUSIONS

The real-time process measurements were reasonably accurate, with the exception of the temperature measurement for the absorber inlet pH meter. The stripper lean mass flowmeter needs to be examined to determine the cause of the oscillating density, temperature, and volumetric flow measurements. The liquid flow measurements demonstrated some oscillation and had a standard deviation between 1 and 4%.

The effective interfacial area of Flexipac 1Y was 30% less than Flexipac AQ Style 20 and the specific dry area of Flexipac 1Y was approximately twice that of the Flexipac AQ packing. Better mass transfer performance was observed with Flexipac 1Y packing, which may due to higher liquid holdup from the inherent design of the packing and possibly from bridging. The K_g for Flexipac 1Y was approximately two times higher than that of Flexipac AQ over the same partial

pressure range. The K_g of the 5 m K^+/2.5 m PZ solvent was approximately three times higher than the 6.4 m K^+/1.6 m PZ solvent. For Flexipac 1Y, the K_g for the 5 m K^+/2.5 m PZ solvent was approximately two times higher than the 7 molal MEA.

Heat loss from the uninsulated absorber column may be significant. The temperature bulge was quantified by integrating the area under the absorber temperature profile and was correlated with the maximum measured temperature. The location of the temperature bulge moves from the top of the column to bottom as the L/G ratio is increased.

The pressure drop normalized by the gas rate was approximately 1.5–2 times higher in the Flexipac 1Y than in Flexipac AQ Style 20, which had steeper corrugation angle. Lower pressure drop was observed with 6.4 m K^+/1.6 m PZ at the lower gas rate because of a low magnitude temperature bulge. However, at high gas rates, the pressure drop will be dictated only by hydraulics.

In future campaigns, it is recommended that the concentration of water in the liquid samples be analyzed. This would help with the interpretation and validation for the liquid analysis of the potassium, piperazine and carbon dioxide concentrations. It is also recommended that quality control and quality assurance for the liquid sampling and liquid analysis of CO_2 loading be verified and validated.

Chapter 4: Rated-Based Absorber Modeling

The thermodynamics and kinetics of potassium carbonate, piperazine, and carbon dioxide were measured in a wetted wall column (Cullinane, 2005). A rigorous thermodynamic model was developed by Cullinane in FORTRAN using the electrolyte non-random two-liquid (NRTL) theory, which predicted vapor–liquid equilibrium (VLE) and speciation for the K_2CO_3-PZ-CO_2-H_2O system. The equilibrium constants and interaction parameters were regressed using experimental data. Cullinane also developed a rigorous kinetic model in FORTRAN that determined the rate constants and diffusion coefficients based on experimental data. Hilliard (2005) developed an Aspen Plus® VLE model with the thermodynamic data of Cullinane. Hilliard used the Data Regression System (DRS) in Aspen Plus® to simultaneously regress the interaction parameters and equilibrium constants for the electrolyte-NRTL model.

In this work, a rate-based model was developed in Aspen Plus® RateSep™ to interpret the results from the pilot plant. The absorber model incorporates the Hilliard (2005) VLE model to predict vapor–liquid equilibrium and component speciation. The absorber model also uses the rate constants developed by Cullinane to predict kinetics. The concentration based rate constants regressed by Cullinane were converted into activity based rates and entered into RateSep™. The absorber model calculates heat and mass transfer and physical properties using correlations that are specified by the user within the Aspen Plus® framework. The absorption of carbon dioxide is an exothermic reaction and

typically results in a temperature bulge in the column. This affects the thermodynamics, kinetics, and physical properties of the solvent.

4.1 THERMODYNAMICS OF POTASSIUM CARBONATE PROMOTED PIPERAZINE

The thermodynamic model for the potassium carbonate, piperazine and carbon dioxide system was originally developed by Cullinane (2005) and extended by Hilliard (2005). Cullinane measure the solubility of carbon dioxide in 0.6–3.6 molal piperazine and 2.5–6.2 molal potassium ion (K^+) from 40 to 110 °C using a wetted wall column. The speciation of piperazine was determined using ^1H NMR. A rigorous thermodynamic model was developed in FORTRAN based on the electrolyte nonrandom two-liquid model (electrolyte-NRTL). Hilliard extended the Cullinane work by creating an electrolyte-NRTL model in Aspen Plus® using the Cullinane data from the wetted wall column. Hilliard simultaneously regressed binary interaction parameters for the K_2CO_3-PZ-CO_2-H_2O system. The VLE model was able to represent the total pressure, CO_2 solubility, and proton NMR speciation for the electrolyte system. However, the simultaneous regression of the interaction parameters by Hilliard did not incorporate heat capacity data for the K_2CO_3-PZ-CO_2-H_2O system because it was not available. Therefore, the temperature dependence of the regressed binary interaction and enthalpy parameters may not have been adequately captured. Recent CO_2 solubility measurements by Hilliard found that the Cullinane VLE data may be offset by 20 °C or shifted by 10% on a CO_2 loading basis. At the time of writing, Hilliard had not updated the VLE Aspen Plus® model with the new data. The original Hilliard (2005) K^+/PZ VLE model was used in this work and a 10% adjustment to the experimental loading was applied.

4.1.1 Reconciliation of Hilliard Aspen Plus® Thermodynamic Model

A non-equilibrium rate-based absorber model for CO_2 absorption into aqueous piperazine and potassium carbonate was developed using Aspen Plus® RateSep™. The model incorporates the Aspen Plus® VLE model that Hilliard (2005) developed for the K_2CO_3-PZ-CO_2-H_2O system. However, the absorber model initially predicted unexpected temperature profiles, which indicated that the heat of absorption for CO_2 was not being correctly predicted by Aspen Plus®. The heat of absorption for the VLE model needed to be reconciled before the absorber modeling work could be continued.

4.1.2 CO_2 Heat of Absorption Inconsistency

An Aspen Plus® flash calculation was used to generate heat duty and vapor–liquid equilibrium data using the Hilliard (2005) VLE model. The flash calculation was performed by absorbing a gas stream of CO_2 into a liquid containing potassium carbonate, piperazine, and CO_2 (Figure 4-1). An outlet vapor fraction of 1.0×10^{-9} was specified and the pressure and temperature of the inlet streams were adjusted to match the flash conditions.

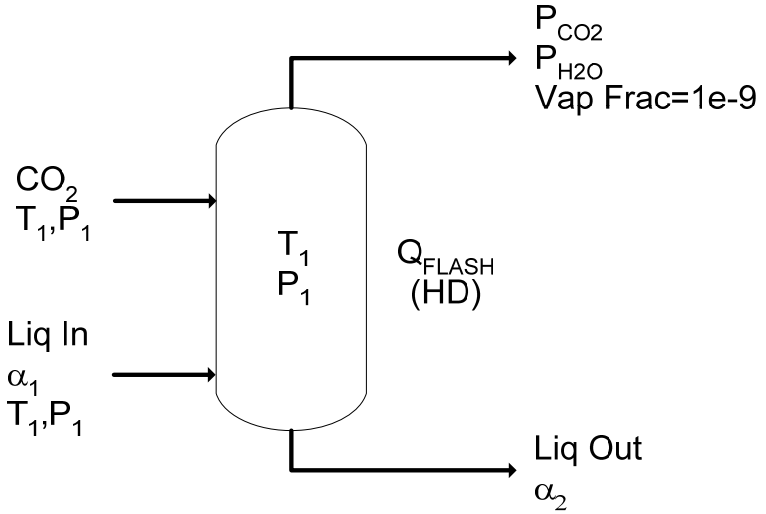

Figure 4-1. Schematic of Aspen Plus® Flash Calculation

The heat duty (HD) from the Aspen Plus® flash calculation represents the heat of absorption of CO_2 into the K^+/PZ solvent. The heat of absorption can also be calculated from the Gibbs–Helmholtz equation using the vapor pressure data generated by the flash calculation and is given by the following equation:

$$\ln \frac{P_{CO_2,T_2}}{P_{CO_2,T_1}} = -\frac{\Delta H_{AB}}{R}\left(\frac{1}{T_2} - \frac{1}{T_1}\right) \tag{4.1}$$

Flash calculations were conducted from 40 to 120 °C at incremental temperatures of 0.1 °C and from 0.45 to 0.55 mol CO_2/(mol K^+ + 2 mol PZ) loading. Using the Gibbs–Helmholtz equation, the heat of absorption was calculated from the vapor pressures generated at T_1 and T_2 (i.e. 40 and 40.1 °C) in equilibrium with the loading of the liquid outlet stream. It was assumed that the difference in loading between the incremental temperatures was negligible because the amount of CO_2 absorbed was extremely small. The heat of absorption calculated from the Gibbs–Helmholtz equation (ΔH-VLE) is expected to match the heat duty generated by the Aspen Plus® flash calculation (ΔH-HD).

Table 4-1 clearly shows that the heat of absorption predicted by Aspen Plus® does not match the VLE predictions. The heat duties generated by Aspen Plus® were not reasonable and in some cases, predicted positive heats of absorption at high loadings. The heat duty calculated by Aspen Plus® is derived from an enthalpy balance using the heats of formation, heat capacities, and heats of vaporization of the various species. However, it appears that Aspen Plus® does not check whether the heat duty is consistent with the other thermodynamic data such as the equilibrium constants and CO_2 vapor pressure. The problem was initially discovered when an Aspen Plus® RateFrac™ absorber model was first developed from the Hilliard VLE model. The absorber model

predicted a negative temperature profile, varying from 40 °C at the top of the column to a negative temperature at the bottom.

Table 4-1. Heat of Absorption Comparison for 5 m K^+/2.5 m PZ

Temp K	P_{CO2} Pa	ΔH-Aspen Plus® Heat Duty kcal/mol	ΔH-Gibbs Helmholtz kcal/mol
313.15	152	-2.45	-17.54
333.15	364	-6.48	-16.07
313.15	2413	49.30	-12.41
333.15	4475	42.43	-12.58

4.1.3 Heat of Formation Adjustment

The liquid heats of formation at 298.15 K were calculated for the four piperazine species (PZH^+, $PZCOO^-$, $PZ(COO^-)_2$, and H^+PZCOO^-) using the parameters from the equilibrium constants and the Van't Hoff equation. The equilibrium equations for the four piperazine species are given below.

$$PZH^+ + H_2O \longleftrightarrow PZ + H_3O^+ \tag{4.2}$$

$$PZ + HCO_3^- \longleftrightarrow PZCOO^- + H_2O \tag{4.3}$$

$$PZCOO^- + HCO_3^- \longleftrightarrow PZ(COO^-)_2 + H_2O \tag{4.4}$$

$$H^+PZCOO^- + PZ \longleftrightarrow PZCOO^- + PZH^+ \tag{4.5}$$

The Van't Hoff equation is given by the following equation:

$$\frac{d\ln K}{d(1/T)} = -\frac{\Delta H_{rxn}}{R} \tag{4.6}$$

The equilibrium constants for the piperazine species in the Hilliard model are in activity based mole-fractions.

Table 4-2. Equilibrium Constants in the Hilliard Aspen Plus® Electrolyte NTRL Model

Eqn No.	Equilibrium Constant	$\ln K_{eq} = A + B/T + C\ln T$		
		A	B	C
4.7	$K_{PZH^+} = \frac{a_{PZ} \cdot a_{H_3O^+}}{a_{PZH^+} \cdot a_{H_2O}}$	481.945	-33448.7	-69.7827
4.8	$K_{PZH^+} = \frac{a_{PZCOO^-} \cdot a_{H_2O}}{a_{PZ} \cdot a_{HCO_3^-}}$	-609.969	36511.7	87.075
4.9	$K_{PZH^+} = \frac{a_{PZ(COO^-)_2} \cdot a_{H_2O}}{a_{PZCOO^-} \cdot a_{HCO_3^-}}$	-251.395	14080.2	36.7818
4.10	$K_{PZH^+} = \frac{a_{PZCOO^-} \cdot a_{PZH^+}}{a_{PZCOO^-} \cdot a_{PZ}}$	-488.753	27752.8	69.7831

The heat of reaction can be calculated by differentiating the K_{eq} equation with respect to 1/T, which results in:

$$\Delta H_{rxn} = (-B + C \cdot T)R \tag{4.11}$$

The heats of formation for the unknown piperazine species can be back-calculated from the known species using the heat of reaction determined from the equilibrium reaction at 298.15 K.

$$\Delta H_{rxn} = H_{f,prod} - H_{f,react} \tag{4.12}$$

For piperazine and water, Aspen Plus® does not list the liquid heat of formation at 298.15 K. Instead, it lists the standard enthalpy of formation of ideal gas at 298.15 K (DHFORM) and the enthalpy of vaporization at the boiling point (DHVLB) and uses this information to extrapolate a liquid heat of formation at 298.15 K (Table 4-3). The heat of formation for water was determined using the DIPPR database and the values for H_3O^+ and HCO_3^- were used directly as entered in Aspen Plus®.

For piperazine, the liquid heat of formation was extrapolated by condensing one mole of piperazine gas into liquid at 298.15 K, using a heater block created in Aspen Plus®. The molar enthalpy from the flash calculation yielded a heat of formation of -8.21 kcal/mol for liquid piperazine at 298.15 K. However, when the value of -8.21 kcal/mol was used to calculate the heats of formation for the corresponding piperazine species, it gave unsatisfactory results. Instead, the heat of formation for liquid piperazine was iteratively adjusted until the heat duty from the flash calculation matched the heat of absorption calculated from the vapor pressures at 298.15 K and a loading of 0.45 mol CO_2/(mol K^+ + 2 mol PZ). In the flash calculation, the amount of gaseous CO_2 to be absorbed was assumed to be 1% of the total CO_2 concentration in the liquid. Later absorber model simulations showed that at each segment (50 segments total) the amount of CO_2 that was absorbed ranged from 0.14 to 1.3% of the total CO_2 liquid concentration. Therefore, 1% was used in order to simplify the flash calculation.

The heats of formation for the PZH^+, $PZCOO^-$, and $PZ(COO^-)_2$ ions were entered into Aspen Plus® as DHAQFM under the DATA4 tab of **Pure Components** in the **Properties** tab. The H^+PZCOO^- ion was given a net zero charge and treated as a molecule in the VLE regression analysis by Hilliard. To maintain this consistency, the ion was treated as an ideal gas molecule and given a zero enthalpy of vaporization. The heat of formation was entered as DHFORM under DATA4 and zero coefficients were entered into the Watson heat of vaporization equation for H^+PZCOO^- under DHVLWT-1 in the **Pure Components** tab of Aspen Plus®. The heat of formation parameters for the 5 m K^+/2.5 m PZ solution is listed in Table 4-3. In order to match the heat duty from Aspen Plus® with the heat of absorption calculated from the Van't Hoff equation for the 6.4 m K^+/1.6 m PZ solution, the heat of formation of liquid piperazine

was adjusted to -6.80 kcal/mol. The calculated DHAQFM parameters for the 6.4 m K^+/1.6 m PZ solution are only approximately 1 kcal/mol higher than the 5 m K^+/2.5 m PZ values and are listed in Table 4-4.

Table 4-3. Heats of Formation Used for 5 m K^+/2.5 m PZ Solution

Species	DHFORM (kcal/mol)	DHVLB (kcal/mol)	DHAQFM (kcal/mol)	$\Delta H_{f,298.15}$ Used (kcal/mol)	Source
H_2O(l)	-57.8	9.717	-	-68.315	DIPPR
H_3O^+	-	-	-68.269	-68.269	Aspen
HCO_3^-	-	-	-165.279	-165.279	Aspen
PZ(l)	3.917	9.999	-	-5.88	Adjusted
PZH^+	-	-	-30.943	-	Calc
$PZCOO^-$	-	-	-123.797	-	Calc
$PZ(COO^-)_2$	-	-	-226.947	-	Calc
H^+PZCOO^-	-135.066	0	-	-	Calc

Table 4-4. Heats of Formation Used for 6.4 m K^+/1.6 m PZ Solution

Species	DHFORM (kcal/mol)	DHVLB (kcal/mol)	DHAQFM (kcal/mol)	$\Delta H_{f,298.15}$ Used (kcal/mol)	Source
H_2O(l)	-57.8	9.717	-	-68.315	DIPPR
H_3O^+	-	-	-68.269	-68.269	Aspen
HCO_3^-	-	-	-165.279	-165.279	Aspen
PZ(l)	3.917	9.999	-	-6.80	Adjusted
PZH^+	-	-	-31.863	-	Calc
$PZCOO^-$	-	-	-124.717	-	Calc
$PZ(COO^-)_2$	-	-	-227.867	-	Calc
H^+PZCOO^-	-135.986	0	-	-	Calc

4.1.4 Heat Capacity Adjustment

The Hilliard (2005) VLE model does not contain heat capacity parameters for the four piperazine species (PZH^+,$PZCOO^-$,$PZ(COO^-)_2$, and H^+PZCOO^-). Hilliard regressed entropy reference values (SO25C) for the four PZ species, which can by used by Aspen Plus® to calculate heat capacities (Hilliard, 2003).

The single parameter SO25C values yielded better results than before, but the heat of absorption still did not match at the higher temperatures and loading. Therefore, multi-parameter heat capacity correlations were regressed for the four piperazine species using the equilibrium constants. From the Van't Hoff equation:

$$-\frac{\Delta H_{rxn}}{R} = \frac{d \ln K_{eq}}{d(1/T)} \tag{4.13}$$

Substituting the equation for the equilibrium constant and differentiating yields:

$$\Delta H_{rxn} = (-B + C \cdot T)R \tag{4.14}$$

Differentiating ΔH_{rxn} and substituting yields the change heat capacity of the equilibrium reaction. If there were four parameters in the equilibrium constant equation, the resulting heat capacity equation would have a dependence on temperature. This would be more representative because the heat capacities of the products and reactants in the equilibrium reactions typically exhibit a temperature dependence.

$$\Delta C_{p,rxn} = \frac{d\Delta H_{rxn}}{dT} = C \cdot R \tag{4.15}$$

Applying the same principles used to calculate the heats of formation, the heat capacities for the unknown piperazine species can be calculated.

$$\Delta C_{P,rxn} = \sum C_{P,prod} - \sum C_{P,reac} \tag{4.16}$$

It was not obvious from the Aspen Plus® property database what was used to calculate the heat capacities of the individual components. A heater block was setup in the Aspen Plus® process flow sheet. PZ and H_2O were entered individually and heated at incremental temperatures ranging from 25 to 120 °C. The heat capacity was calculated from the heat input required to heat the

component by 0.1 °C. The heater block calculated zero heat input for the HCO_3^- and H_3O^+ species, which made sense because they were ions. In Aspen Plus®, under the CPAQ0-1 tab, it lists a single parameter heat capacity for H_3O^+ as 17.98 cal/mol-K and is independent of temperature.

Under **Parameters|Prop-Set**, the heat capacities for the four species were created and used in a sensitivity analysis to determine the C_p values that Aspen Plus® was using. Over the temperature range from 25 to 120 °C, the heat capacity of the PZ and H_2O generated by Aspen Plus® matched the results from the heater block. However, Aspen Plus® generated identical heat capacities for the H_3O^+ and HCO_3^- ions, which varied from 12.6 to 18.9 cal/mol-K over the 25 to 120 °C temperature range, respectively. The heat capacity of the species was regressed in the following two parameter form:

Table 4-5. Regressed Heat Capacity Parameters from Aspen Plus® Property-Set Calculation

Species (cal/mol-K)	$C_P = A + BT$	
	A	B
H_2O	11.84	0.018
H_3O^+	17.98	0.000
HCO_3^-	-7.44	0.066
PZ	19.33	0.089

When the above parameters were used, the heat duty from the Aspen Plus® flash calculation matched to heat of absorption calculated from the CO_2 partial pressure with a 3% error over the temperature range from 25 to 70 °C and up 6% error for the temperature range from 100 to 120 °C (Table 4-6).

Table 4-6. Reconciled Heats of Absorption Results

Temp K	P_{CO2} Pa	ΔH-HD kcal/mol	ΔH-VLE kcal/mol	Diff %
298.15	32	-20.39	-20.39	0.004
313.15	344	-17.19	-16.84	-2.07
333.15	24001	-11.18	-11.32	1.27
343.15	10677	-13.22	-12.85	-2.86
373.15	77922	-11.79	-11.99	1.66
383.15	50817	-10.22	-10.65	4.03
393.25	22704	-7.43	-7.86	5.56

The second CPAQ0-1 parameter for the HCO_3^- species was arbitrarily adjusted to minimize the difference in value for the heat duty and heats of absorption over the 25–70 °C temperature range because the focus of this work is on the absorber. For the 5 m K^+/2.5 m PZ solution, the optimized fit was obtained when the HCO_3^- parameter was changed to 0.45 and resulted in an error of less than 1% (Table 4-7). For the 6.4 m K^+/1.6 m PZ solution, the optimized fit was obtained when the HCO_3^- parameter was adjusted to 1.00 (Table 4-8). More error was observed with the 6.4 m K^+/1.6 m PZ solution, which ranged from 1.3 to 8.8%. Since H^+PZCOO^- has a zero charge and was treated as a molecule, the heat capacity parameters were entered into Aspen Plus® under the ideal gas heat capacity equation (CPIG-1).

Table 4-7. Heat Capacity Constants (CPAQ0-1) for 5 m K^+/2.5 m PZ

Species (cal/mol-K)	$C_P = A + BT$	
	A	B
H_2O	11.84	0.018
H_3O^+	17.98	0.000
HCO_3^-	-7.44	*0.450*
PZ	19.33	0.089
PZH^+	164.05	0.071
PZCOO	172.97	0.521
$PZ(COO^-)_2$	226.74	0.953
$H+PZCOO^-$	179.11	0.503

Table 4-8. Heat Capacity Constants (CPAQ0-1) for 6.4 m K^+/1.6 m PZ

Species (cal/mol-K)	$C_P = A + BT$	
	A	B
H_2O	11.84	0.018
H_3O^+	17.98	0.000
HCO_3^-	-7.44	*1.000*
PZ	19.33	0.089
PZH^+	164.05	0.071
PZCOO	172.97	1.071
$PZ(COO^-)_2$	226.74	2.053
$H+PZCOO^-$	179.11	1.053

Based on a discussion with Dr. Chau-Chyun Chen of Aspen Technologies, an attempt was made to calculated the heat capacity of the HCO_3^- ions using the Criss-Cobble correlation (Criss and Cobble, 1964). The four heat capacity values given by Criss and Cobble at 298.15, 333.15, 373.15, and 423.15 K were regressed into the following three parameter equation:

$$C_p = A + BT + C\ln(T) \tag{4.17}$$

The values for A, B, and C, in units of cal/mol-K, were -47.03, 3.307, and -0.00445, respectively. However, the results were unsatisfactory. It was also

found that the SO25C for HCO_3^- in Aspen Plus® (21.78 cal/mol-K) was somewhat lower than the value regressed from the Criss and Cobble data (27.82 cal/mol-K).

Once the heat capacity parameters for the piperazine ion species were entered into Aspen Plus®, the predicted heat capacity of the solvent was found to be approximately the same as water. Accurate predictions of heat capacity are important for the enthalpy balance across the absorber column, which is manifested in the magnitude and location of the temperature bulge. Hilliard has recently obtained heat capacity data for the potassium carbonate and piperazine system, which was previously unavailable.

CPAQ0-1 parameters for K^+, OH^-, CO_2, HCO_3^-,and CO_3^{2-} were initially regressed using Aspen Plus® DRS and heat capacity data for the K_2CO_3-H_2O, $KHCO_3$-H_2O, and K_2CO_3-PZ-CO_2-H_2O system. Although relatively accurate heat capacity values were predicted for the three solution systems, the heat duty predicted by Aspen Plus® for the absorption of CO_2 was changed and no longer matched the heat of absorption calculated by the Van't Hoff equation using the predicted equilibrium partial pressures of CO_2.

It was found that by adjusting the CPAQ0 parameters for potassium, the heat capacity of the solution could be decreased without affecting the heat of absorption of CO_2 that was reconciled in the previous section. Using the Hilliard heat capacity data for 5 m K^+/2.5 m PZ and the Aspen Plus® DRS regression package, the best fit was found using only the first CPAQ0 parameter. It was found that the heat capacity of the solution could not be adequately represented for the 5 m K^+/2.5 m PZ and 6.4 m K^+/1.6 m PZ solutions with just one value of the CPAQ0 parameter. Therefore, a different value of the CPAQ0/1 parameter was regressed for each solution composition. The CPAQ0/1 parameter for 6.4 m K^+/1.6 m PZ solution was regressed using 6 m K^+/1.2 m PZ data because that was the only data available. The values for the regressed CPAQ0/1 parameters

are shown in Table 4-9. The CPAQ0/1 parameter for the 5 m K^+/2.5 m PZ solution is approximately four times higher than the 6 m K^+/1.2 m PZ solution. The average absolute deviation for the 5 m K^+/2.5 m PZ and 6 m K^+/1.2 m PZ solutions were 2.0 and 2.1%, respectively.

Table 4-9. Aqueous Heat Capacity Parameters for K^+ Regressed using DRS

Parameter	Component	Solution	Value (J/kmol-K)	σ (J/kmol-K)
CPAQ0/1	K^+	5 m K^+/2.5 m PZ	-342374.53	5321.20
CPAQ0/1	K^+	6 m K^+/1.2 m PZ	-121275.25	5837.74

A plot of the experimental and estimated values of heat capacity for the 5 m K^+/2.5 m PZ solution is shown in Figure 4-2. The figure shows that the over the temperature range from 40 to 80 °C, the heat capacity of the solution decreases with loading. Over the temperature range, the estimated heat capacity at a loading of 0.49 mol CO_2/(mol K^+ + 2 mol PZ) was up to 3% lower than the experimental data, while at a loading of 0.55 mol CO_2/(mol K^+ + 2 mol PZ), the estimated heat capacity was up to 3% higher than the experimental data. The figure also shows that the estimated heat capacities increased in value with a rise in temperature.

The results for the 6 m K^+/1.2 m PZ DRS regression are shown in Figure 4-3. The plot shows that the experimental heat capacity values for the 5 m K^+/2.5 m PZ and 6 m K^+/1.2 m PZ solution were approximately the same over the temperature range from 40 to 80 °C. The figure shows that at a loading of 0.43 mol CO_2/(mol K^+ + 2 mol PZ), the estimated heat capacity was up to 5% lower than the experimental values at 80 °C. The predicted heat capacity at the higher loading demonstrated the same increasing trend as the experimental data, but was approximately 1.5% higher in value.

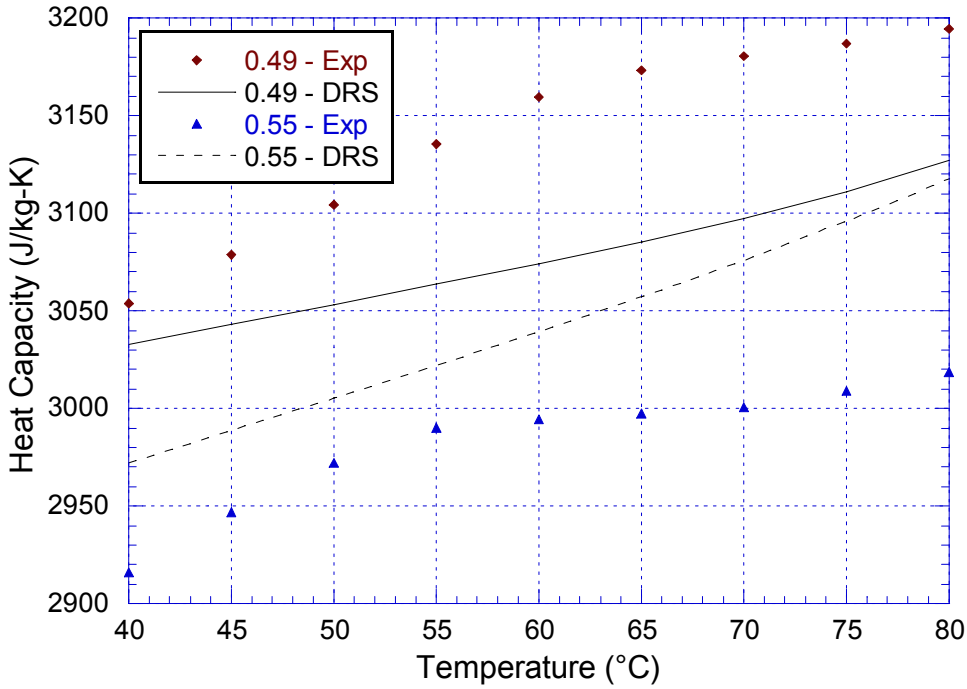

Figure 4-2. DRS Estimated and Experimental Values of Heat Capacity for 5 m K^+/2.5 m PZ at Loading of 0.49 and 0.55 mol CO_2/(mol K^+ + 2 mol PZ)

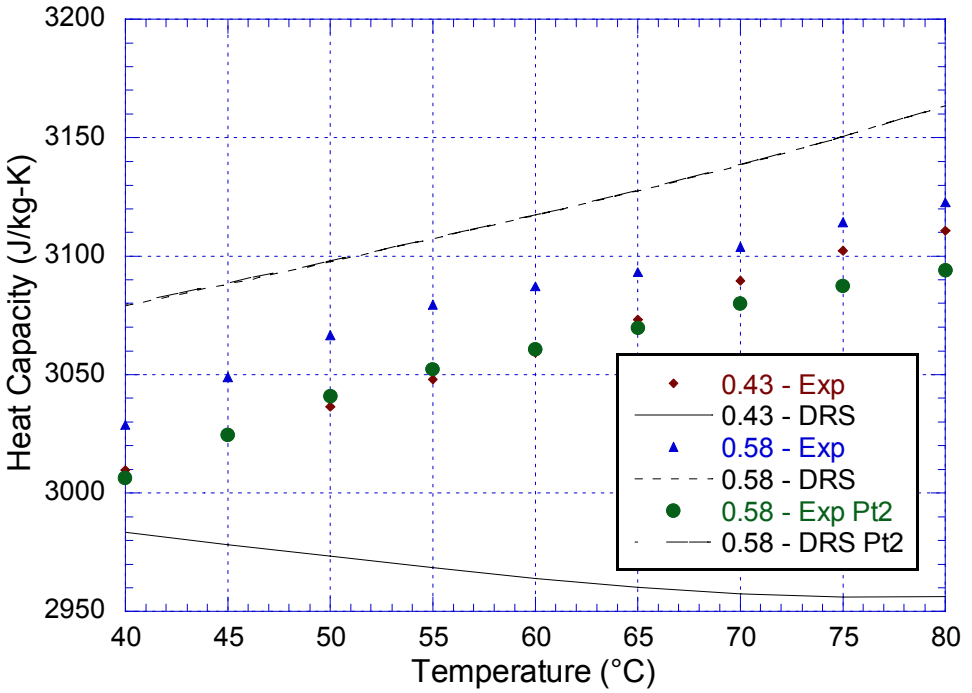

Figure 4-3. DRS Estimated and Experimental Values of Heat Capacity for 6 m K^+/1.2 m PZ at Loading of 0.43 and 0.58 mol CO_2/(mol K^+ + 2 mol PZ)

Differential heat of absorption data for the 5 m K^+/2.5 m PZ and 6 m K^+/1.2 m PZ solutions were available from Hilliard *et al.* (2006). Figure 4-4 shows that the heat of absorption predicted by the Aspen Plus® flash calculation generally matched relatively well with the 40 and 60 °C experimental data over the loading range from 0.45 to 0.7 mol CO_2/(mol K^+ + 2 mol PZ). However, at loadings below 0.45, the experimental data was over-predicted by 20 KJ/mol CO_2 at 40 C and under-predicted by 20 KJ/mol CO_2 at 80 °C. The figure also shows that the experimental data at 80 °C was not consistent with the 40 and 60 °C data and it was concluded that there may have been some errors in the measurement.

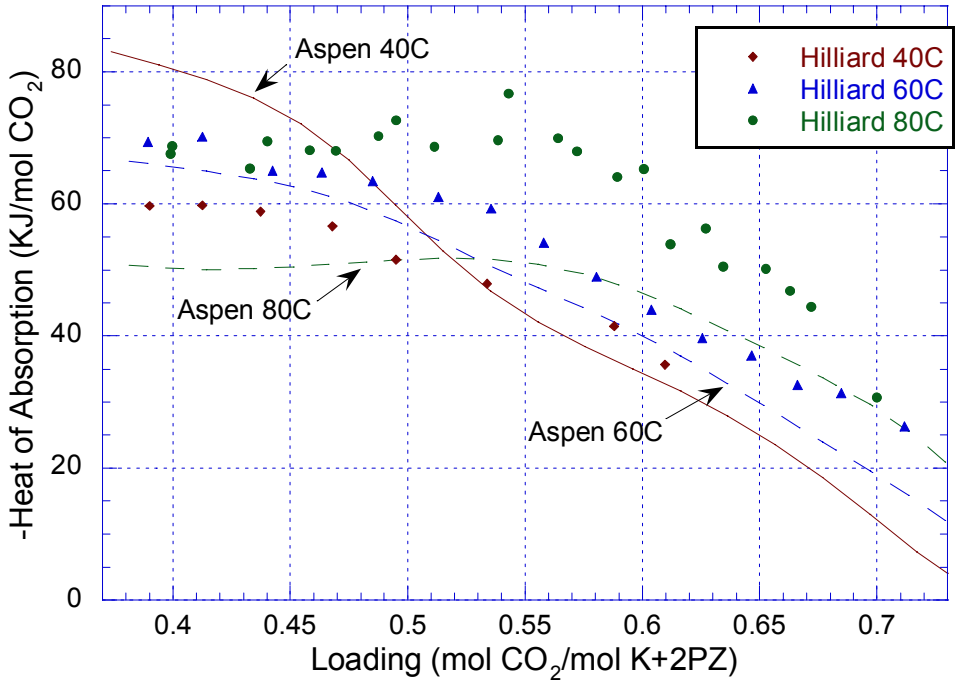

Figure 4-4. Comparison of Differential Heat of Absorption of CO_2 for the 5 m K^+/2.5 m PZ Solution with Aspen Plus® Heat Duty Calculation using Adjusted Heat of Formation and Heat Capacity Parameters

The experimental and Aspen Plus® model results for the 6 m K^+/1.2 m PZ solution are shown in Figure 4-5. The figure shows that Aspen Plus® model

predicted reasonable heat of absorptions over the loading range from 0.51 to 0.68 mol CO_2/(mol K^+ + 2 mol PZ) for temperatures of 40, 60, and 80 °C. However, at a temperature of 40 °C and at the low loading range, the predicted heat of absorption was 50% higher than the experimental data, while at 80 °C, the Aspen Plus® model under-predicted the heat of absorption by approximately 10 KJ/mol CO_2. Since the inlet and outlet of the absorber is typically maintained at 40 °C, it is possible that the temperature profiles predicted by the RateSep™ absorber model will exceed the experimental results even after accounting for heat loss.

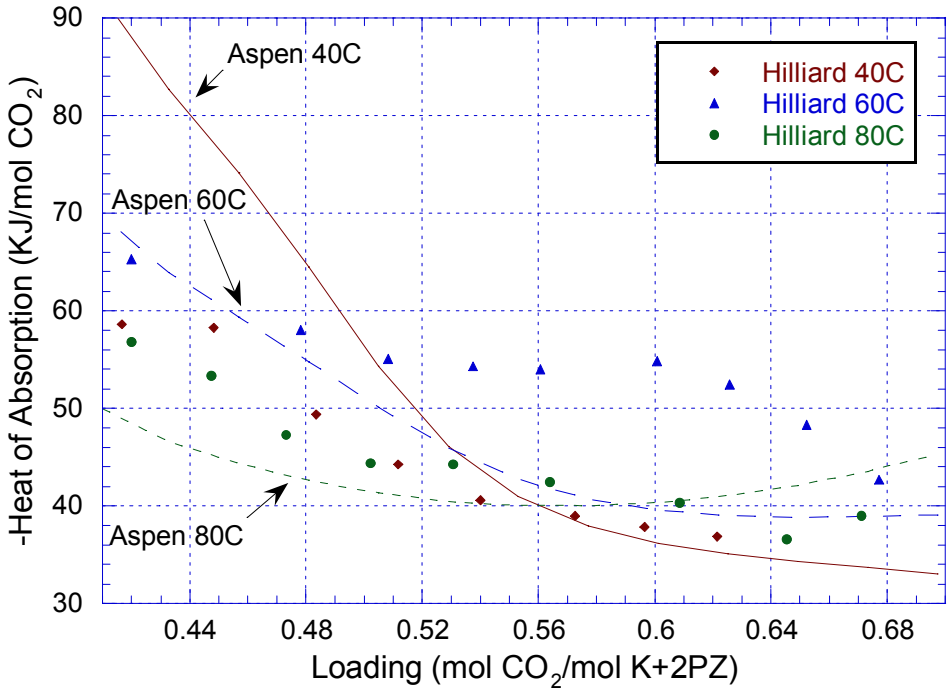

Figure 4-5. Comparison of Differential Heat of Absorption of CO_2 for the 6 m K^+/1.2 m PZ Solution with Aspen Plus® Heat Duty Calculation using Adjusted Heat of Formation and Heat Capacity Parameters

4.1.5 Zwitterion Issues in Aspen Plus®

Aspen Plus® does not account for the existence of net-neutrally charged zwitterions. In the Hilliard (2005) K^+/PZ VLE model, the H^+PZCOO^- ion was given a net charge of zero and was treated as a molecule. This created a number

of issues such as the skewed predictions for the heat of absorption. During the early stages of the reconciliation process, when the charge for the H^+PZCOO^- ion was changed to 0.0001, the heat duties generated by the Aspen Plus® flash calculation gave reasonable trends (Table 4-10). According to communications with Aspen Technologies, when the charge for the H^+PZCOO^- ion is set to zero, the ion is treated as a solvent. When the charge is changed to 0.0001, the ion is treated is as an ionic solute. Therefore, with a near zero charge, the H^+PZCOO^- zwitterion is treated effectively as a "molecular solute." The Aspen Plus® software was originally developed without accounting for zwitterions.

Table 4-10. Heat of Absorption, Charge H+PZCOO- = 0.0001

Temp K	P_{CO2} Pa	ΔH-HD kcal/mol	ΔH-VLE kcal/mol
313.15	168	-31.63	-20.39
323.15	396	-31.31	-15.74
313.15	3315	-17.09	-11.52
323.15	5881	-17.17	-11.68

The use of a 0.0001 charge for H^+PZCOO^- slightly changed the predictions for VLE. The change in charge also affects the diffusivity of the H^+PZCOO^- ion. In Aspen Plus®, the diffusivity is inversely proportional to the charge. This was corrected by inputting the value of 1e-3 in the IONMOB-1 parameter for H^+PZCOO^- (Chen, 2006). If no values for the IONMOB-1 are entered for a certain species, the default value of 5 kmol is used. The heats of formation and heat capacities for the four piperazine ions were calculated from the equilibrium constants following the methods outlined above and entered into Aspen Plus® under the DHFORM and CPAQ0-1 forms. While the heats of absorption were reconciled, attempts to re-regress the vapor–liquid equilibrium constants using a 0.0001 charge did not produce satisfactory results. The method described in the

previous section was used instead to reconcile the heat of absorption in Aspen Plus®.

4.2 KINETICS OF PIPERAZINE AND POTASSIUM CARBONATE

The kinetics for the absorption of carbon dioxide into aqueous potassium carbonate and piperazine were measured by Cullinane (2005) in a wetted wall column (Cullinane, 2005). Experiments were conducted with 0.45–3.6 molal piperazine and 0–3.1 molal potassium carbonate at 25–110 °C. The rate constants for the absorption of CO_2 were regressed using the eddy diffusivity model developed by Bishnoi and Rochelle (2002). The reaction of CO_2 with piperazine was modeled using the "zwitterion" mechanism (Caplow, 1968). Carbon dioxide reacts with the amine to form a neutrally charged intermediate species, followed by the extraction of the proton by a base (Equations 4.18 and 4.19).

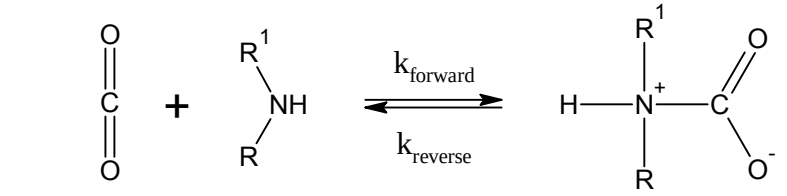

(4.18)

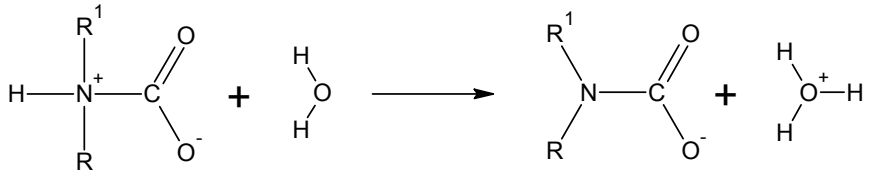

(4.19)

For the zwitterion mechanism, the rate of reaction can be written as (Danckwerts, 1979):

$$r = \frac{[Am][CO_2]}{\frac{1}{k_f} + \frac{k_r}{k_f \sum_b k_{PZ-b}}} \tag{4.20}$$

If we assume that $\sum k_b[b] << k_r$, then the reaction can be re-written as:

$$rate_{CO_2} = \sum_b k_{Am-b}[Am][b][CO_2] \tag{4.21}$$

where

$$k_{Am-b} = \frac{k_f k_b}{k_r} \tag{4.22}$$

The following amine reactions were used in the Cullinane model (2005).

$$PZ + CO_2 + \begin{cases} OH^- \xleftrightarrow{k_{PZ-OH^-}} PZCOO^- + H_2O \\ H_2O \xleftrightarrow{k_{PZ-H_2O}} PZCOO^- + H_3O \\ PZ \xleftrightarrow{k_{PZ-PZ}} PZCOO^- + PZH^+ \\ CO_3^{2-} \xleftrightarrow{k_{PZ-CO_3^{2-}}} PZCOO^- + HCO_3^- \\ PZCOO- \xleftrightarrow{k_{PZ-PZCOO^-}} PZCOO^- + H^+PZCOO^- \end{cases} \tag{4.23}$$

$$PZCOO^- + CO_2 + \begin{cases} H_2O \xleftrightarrow{k_{PZCOO^- - H_2O}} PZ(COO^-)_2 + H_3O \\ PZ \xleftrightarrow{k_{PZCOO^- - PZ}} PZ(COO^-)_2 + PZH^+ \\ CO_3^{2-} \xleftrightarrow{k_{PZCOO^- - CO_3^{2-}}} PZ(COO^-)_2 + HCO_3^- \\ PZCOO- \xleftrightarrow{k_{PZCOO^- - PZCOO^-}} PZ(COO^-)_2 + H^+PZCOO^- \end{cases} \tag{4.24}$$

According to Cullinane, hydroxide reactions were not included in the second set of reactions because the concentration is typically very small when $PZCOO^-$ is present. All of the buffering reactions were considered to be in equilibrium. The reversible rate expressions for CO_2 with PZ and $PZCOO^-$ are given by the following equations:

$$r = \sum_b k_{PZ-b}[b]\left([PZ][CO_2] - \frac{K_w[PZCOO^-]}{K_{PZCOO^-}[OH^-]}\right) \tag{4.25}$$

$$r = \sum_b k_{PZCOO^- - b}[b]\left([PZCOO^-][CO_2] - \frac{K_w[PZ(COO^-)_2]}{K_{PZ(COO^-)_2}[OH^-]}\right) \tag{4.26}$$

The temperature dependence of the rate constants is given by:

$$k^{\infty} = k^{o} \exp\left(\frac{\Delta H_a}{R}\left(\frac{1}{T(K)} - \frac{1}{298.15}\right)\right) \tag{4.27}$$

where k^{o} is the rate constant at 298.15K and ΔH_a is the activation energy. An ionic strength correction is made to the rate constants by:

$$k = k^{\infty} \exp(0.3I) \tag{4.28}$$

where I is the ionic strength of the solution and given by the following:

$$I = \frac{1}{2}\sum_i \left(C_i z_i^2\right) \tag{4.29}$$

where C_i is the molar concentration and the z_i is the charge of the species i.

The catalysis of the formation of bicarbonate ion by hydroxide, piperazine, and piperazine carbamate was also included in the Cullinane model (2005). The reactions that form the bicarbonate ion were included to properly model equilibrium in the boundary layer, but do not affect the CO_2 absorption rate. The three reversible reactions are:

$$CO_2 + OH^- \xleftrightarrow{k_{OH^-}} HCO_3^- \tag{4.30}$$

$$PZ + CO_2 + H_2O \xleftrightarrow{k_{PZ}} PZH^+ + HCO_3^- \tag{4.31}$$

$$PZCOO^- + CO_2 + H_2O \xleftrightarrow{k_{PZCOO^-}} H^+PZCOO^- + HCO_3^- \tag{4.32}$$

The rate expression for bicarbonate formation is given by

$$r = \sum_b k_b [b]\left([CO_2] - \frac{[HCO_3^-]}{K_{HCO_3^-}[OH^-]}\right) \tag{4.33}$$

The rate constant from Pohorecki (1988) for the reaction of CO_2 and OH^- was used. The reaction depends on the ionic strength and is written as

$$\log k_{OH^-} = \log k^{\infty}_{OH^-} + \sum_i \kappa_i I_i \tag{4.34}$$

where

$$\log k_{OH^-}^{\infty} = 11.916 - \frac{2382.0}{T(K)} \tag{4.35}$$

and κ_i is the ion specific parameter and I_i is the ionic strength of species i.

The rates constants for bicarbonate formation by the amines were assumed to be the same as MDEA (Littel, 1991) and is given by:

$$k_{Am}\left(\frac{m^3}{kmol \cdot s}\right) = 1.34 \times 10^9 \exp\left(\frac{-5771.0}{T(K)}\right) \tag{4.36}$$

The rate constant for the amine-catalyzed formation of bicarbonate was corrected for ionic strength using equation 4.28.

4.3 CONVERSION TO ACTIVITY-BASE KINETICS

In Aspen Plus® 2006, the new version of RateSep™ allows the user to enter activities in terms of mole gamma using the power law kinetic expression:

$$r = k\left(\frac{T}{T_0}\right)^n \exp^{\left(\frac{-E}{R}\left(\frac{1}{T}-\frac{1}{T_0}\right)\right)} \prod (x_i \gamma_i)^{\alpha_i} \tag{4.37}$$

where k is the pre-exponential factor independent of temperature, n is the temperature exponent, E is the activation energy, T_o is the reference temperature (298.15K), k is the pre-exponential factor, x_i is reactant species i, γ_i is the activity coefficient, and α_i is the reaction order for the species. Since the equilibrium constants were already activity based, it made sense to implement activity based kinetics within the model as well.

The rate constants developed by Cullinane (2005) use concentration based units and needed to be converted into activity units. A simple algebraic manipulation was performed using the following equation:

$$k_a = \frac{k_c [PZ][CO_2][b]}{(x_{PZ}\gamma_{PZ})(x_{CO_2}\gamma_{CO_2})(x_b\gamma_b)(total\ mol/L)} \tag{4.38}$$

where k_a is the activity base rate constant, k_c is the concentration based rate constant, [*i*] is the concentration of species *i* in units of mol/L, and x_i is the mole fraction and γ_i is the activity coefficient. The last term in the denominator represents the total molar concentration per liter of solvent and was assumed to be constant across the column. For the 5 m K^+/2.5 m PZ solution, a value of 48.38 mol/L was used, which was based on an Aspen Plus® calculation. The value of the total molar concentration for the 6.4 m K^+/1.6 m PZ solution was 51.29 mol/L.

The kinetics developed by Cullinane (2005) contains a correction for ionic strength. However, in Aspen Plus®, this correction cannot be directly implemented. In this work, the ionic strength was assumed to be constant and a correction was applied to *k*, the pre-exponential term of the reaction rate. Figure 4-6 illustrates the loading and temperature dependence of ionic strength for the 5 m K^+/2.5 m PZ solvent. In the pilot plant campaigns, the loading ranged from 0.4 to 0.55 mol CO_2/(mol K^+ + 2mol PZ). In the calculation of the pre-exponential factors, an ionic strength of 5.15 mol/L was used for the 5 m K^+/2.5 m PZ solution, which was calculated at 50 °C and a loading of 0.5 mol CO_2/(mol K^+ + 2mol PZ).

Figure 4-7 illustrates the loading and temperature dependence of ionic strength for the 6.4 m K^+/1.6 m PZ solvent. An ionic strength of 6.90 mol/L, which was calculated at 50 °C and a loading of 0.5 mol CO_2/(mol K^+ + 2 mol PZ), was used for the rate calculation of the 6.4 m K^+/1.6 m PZ solution.

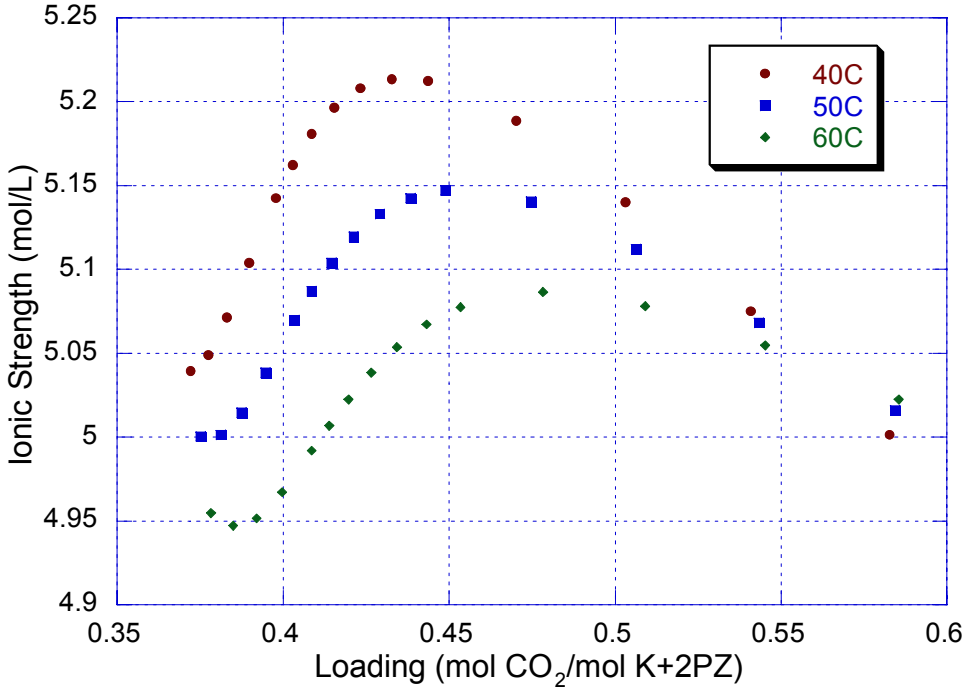

Figure 4-6. Ionic Strength of 5 m K^+/2.5 m PZ Solution from 40 to 60 °C Generated by Aspen Plus® VLE Model

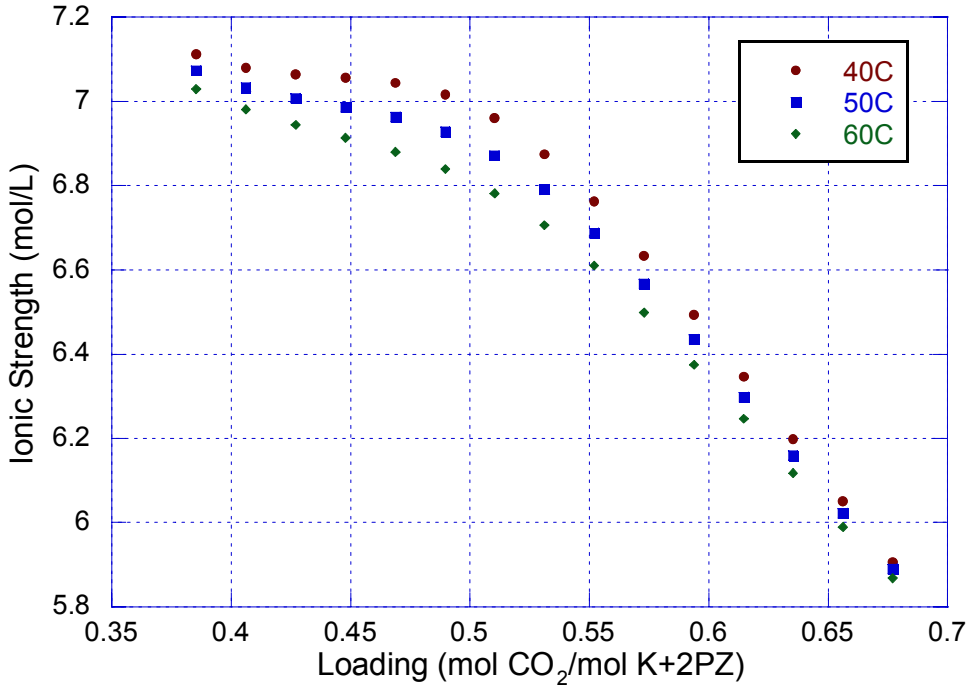

Figure 4-7. Ionic Strength of 6.4 m K^+/1.6 m PZ Solution from 40 to 60 °C Generated by Aspen Plus® VLE Model

The overall rate for the reversible reactions is given by the difference between the forward and reverse rate and is given by the following equations:

$$rate = \sum_b k_{PZ-b}\left(a_{PZ}a_{CO_2}a_b - \frac{a_{PZCOO}a_{Hb}}{K_{PZ-b}} \right)$$
$$rate = \sum_b k_{PZCOO^- -b}\left(a_{PZCOO^-}a_{CO_2}a_b - \frac{a_{PZ(COO^-)2}a_{Hb}}{K_{PZCOO^- -b}} \right) \quad (4.39)$$

where $k_{PZ/PZCOO-b}$ is the forward rate constant in activity units, $K_{PZ/PZCOO-b}$ is the equilibrium constant, and a_i is the activity of the species ($x_i\gamma_i$).

Since the ionic strength of the 6.4 m K^+/1.6 m PZ solution is approximately 40% higher than that of the 5 m K^+/2.5 m PZ solution and the total molar concentration of components were slightly different, two sets of kinetic parameters were calculated and entered into RateSep™. The kinetic parameters for the forward and reverse reactions of the 5 m K^+/2.5 m PZ and 6.4 m K^+/1.6 m PZ solutions are listed in the tables below. The pre-exponential factor for the PZ–H_2O and $PZCOO^-$–H_2O reactions assume a pseudo-first order rate constant with a water concentration 55.55 mol/L (Cullinane, 2005).

Table 4-11. Forward Activity-Based Rate Parameters of 5 m K^+/2.5 m PZ for Piperazine, Piperazine Carbamate, and Bicarbonate Reactions as Entered into Aspen Plus® RATESEP™

Eqn No.	Reaction	$Rate_{for} = k\left(\frac{T}{T_o}\right)^n \exp\left(\frac{-E}{R}\left(\frac{1}{T}-\frac{1}{T_o}\right)\right)$			$E_{a,40°C}$
		k_f x 10^{10}	E_f (KJ/kmol)	n_f	(KJ/kmol)
40	$PZ - H_2O$	0.84	-17619	17.25	26202
41	$PZ - PZCOO$	1.87	-35394	25.70	29898
42	$PZ - PZ$	3.62	-116263	44.43	-3407
43	$PZ - CO_3^{2-}$	39.33	-54002	36.07	37626
44	$PZ - OH$	46.75	-31303	23.83	29229
45	$PZCOO - H_2O$	0.41	63251	-1.47	59507
46	$PZCOO - PZCOO$	1.87	45476	6.98	63202
47	$PZCOO - PZ$	3.63	-35394	25.70	29898
48	$PZCOO - CO_3^{2-}$	19.36	26868	17.35	70931
49	$CO_2 - OH$ (HCO_3^-)	9.30 x 10-4	77495	-3.05	69746
50	$PZ - CO_2$ (HCO_3^-)	2.68 x 10-6	-5086	17.55	39490
51	$PZCOO - CO_2$ (HCO_3^-)	1.98 x 10-6	75784	-1.18	72794

Table 4-12. Reverse Activity-Based Rate Parameters of 5 m K^+/2.5 m PZ for Piperazine, Piperazine Carbamate, and Bicarbonate Reactions as Entered into Aspen Plus® RATESEP™

Eqn No.	Reaction	$Rate_{rev} = k\left(\frac{T}{T_o}\right)^n \exp\left(\frac{-E}{R}\left(\frac{1}{T}-\frac{1}{T_o}\right)\right)$			$E_{a,40°C}$
		k_r	(KJ/kmol)	n_f	(KJ/kmol)
52	$PZ - H_2O$	1.94 x 10^{14}	185406	-33.04	101474
53	$PZ - PZCOO$	2411	214987	-24.59	152526
54	$PZ - PZ$	682	364854	-75.65	172698
55	$PZ - CO_3^{2-}$	7623	252380	-49.70	126125
56	$PZ - OH$	3.52 x 10^{-2}	283511	-48.94	159194
57	$PZCOO - H_2O$	2.37 x 10^{15}	79780	-1.47	76035
58	$PZCOO - PZCOO$	59954	109361	6.98	127088
59	$PZCOO - PZ$	16960	259228	-44.08	147260
60	$PZCOO - CO_3^{2-}$	93182	146755	-18.14	100687
61	$CO_2 - OH$ (HCO_3^-)	3.84 x 10^{-3}	88750	11.25	117337
62	$PZ - CO_2$ (HCO_3^-)	2.77	172473	-15.45	133221
63	$PZCOO - CO_2$ (HCO_3^-)	14.04	22606	35.61	113048

Table 4-13. Forward Activity-Based Rate Parameters of 6.4 m K^+/1.6 m PZ for Piperazine, Piperazine Carbamate, and Bicarbonate Reactions as Entered into Aspen Plus® RATESEP™

Eqn No.	Reaction	$Rate_{for} = k\left(\frac{T}{T_o}\right)^n \exp\left(\frac{-E}{R}\left(\frac{1}{T}-\frac{1}{T_o}\right)\right)$			$E_{a,40°C}$
		k_f x 10^{10}	(KJ/kmol)	n_f	(KJ/kmol)
64	$PZ - H_2O$	1.07	26842	3.15	34850
65	$PZ - PZCOO$	2.23	6050	12.95	38935
66	$PZ - PZ$	3.89	-46093	21.94	9645
67	$PZ - CO_3^{2-}$	38.25	-18707	25.84	46931
68	$PZ - OH$	40.52	7499	12.23	38571
69	$PZCOO - H_2O$	0.59	78985	-5.84	64139
70	$PZCOO - PZCOO$	2.49	58193	3.95	68225
71	$PZCOO - PZ$	4.35	6050	12.95	38935
72	$PZCOO - CO_3^{2-}$	20.98	33436	16.84	76221
73	$CO_2 - OH\ (HCO_3^-)$	1.36 x 10^{-3}	90027	-6.01	90031
74	$PZ - CO_2\ (HCO_3^-)$	3.16 x 10^{-6}	38815	3.70	38815
75	$PZCOO - CO_2\ (HCO_3^-)$	2.60 x 10^{-6}	90958	-5.30	90958

Table 4-14. Reverse Activity-Based Rate Parameters of 6.4 m K^+/1.6 m PZ for Piperazine, Piperazine Carbamate, and Bicarbonate Reactions as Entered into Aspen Plus® RATESEP™

Eqn No.	Reaction	$Rate_{rev} = k\left(\frac{T}{T_o}\right)^n \exp\left(\frac{-E}{R}\left(\frac{1}{T}-\frac{1}{T_o}\right)\right)$			$E_{a,40°C}$
		k_r	E_f (KJ/kmol)	n_f	(KJ/kmol)
76	$PZ - H_2O$	2.47 x 10^{14}	229866	-47.14	110121
77	$PZ - PZCOO$	2888	256430	-37.35	161563
78	$PZ - PZ$	733	435024	-98.13	185750
79	$PZ - CO_3^{2-}$	7413	287674	-59.93	135431
80	$PZ - OH$	0.031	322313	-60.54	168536
81	$PZCOO - H_2O$	3.36 x 10^{15}	95514	-5.84	80668
82	$PZCOO - PZCOO$	80000	122078	3.95	132110
83	$PZCOO - PZ$	20315	300672	-56.84	156297
84	$PZCOO - CO_3^{2-}$	100937	153322	-18.64	105977
85	$CO_2 - OH\ (HCO_3^-)$	5.6 x 10^{-3}	101283	8.29	122347
86	$PZ - CO_2\ (HCO_3^-)$	3.26	216373	-29.30	141941
87	$PZCOO - CO_2\ (HCO_3^-)$	18.44	37780	31.48	117754

4.4 RATE-BASED ABSORBER MODELING USING ASPEN PLUS® RATESEP™

There are several approaches that can be taken to model reactive absorption, which depend upon mass transfer characteristics and the chemical components of the system (Kenig *et al.*, 2001). The simplest approach is to assume equilibrium stages, which does not account for any reactions and gas and liquid film resistance. Reaction kinetics can be added to equilibrium staged models, but do not have any physical basis. If mass transfer resistance and reaction kinetics are accounted for, the modeling approach becomes rate-based. In the simplest non-equilibrium rate-based model, the reaction kinetics is accounted for in the bulk solution and enhancement factors are used to account for the reactions in the film. Finally, in the most rigorous modeling approach, the kinetics in the liquid film is calculated, which is typically performed by discretizing liquid film into various segments, and electrolyte thermodynamics are considered. In the rate-based approach, correlations are needed to fully characterize the mass and heat transfer, hydrodynamics, vapor–liquid equilibrium, and physical properties of the entire system.

A number of rate-based absorber models have been proposed with varying degrees of complexity, which fall into one of the three rate-based modeling categories. Treybal (1969) developed an equilibrium rate-based model for adiabatic absorption and stripping. The model was based on two film theory and took into account mass and heat transfer resistance in the liquid and gas phase. This work was originally developed for the absorption of ammonia into water and was later expanded for multi-component systems. This work was extended to the reactive absorption of CO_2 into MEA (Pandya, 1983). In the Pandya MEA model, equilibrium was not assumed and an enhancement factor was used to quantify the kinetics for the absorption rate of CO_2 and Henry's Law was used to determine vapor–liquid equilibrium. A shooting method algorithm

was proposed to solve the resulting boundary value problem. A number of researchers have further developed and adapted the Pandya MEA model to other amine systems. While the basic framework of the model has remained the same, more rigorous kinetics, vapor–liquid equilibrium, physical properties and mass transfer representations have been incorporated into the model. MEA pilot plants using random and structured packing have been simulated and validated using the non-equilibrium rate-based approach (deMontigny *et al.*, 2006, Escobillana *et al.*, 1991, Pintola *et al.*, 1993, Tontiwachwuthikul *et al.*, 1992). The model has also been adapted to other amine solvents such as 2-amino-2-methyl-1-propanol (AMP) and validated with AMP pilot plant data (Gabrielsen *et al.*, 2006). All of the above models were implemented using FORTRAN or MATLAB.

A non-equilibrium rate-based model for the absorption of CO_2 and H_2S into MEA was implemented in Aspen Plus® RATEFRAC® by Pacheco and Rochelle (1998). The model used Maxwell–Stefan theory for mass transfer and enhancement factor theory to model the kinetics. The electrolyte-NRTL model was used to rigorously model thermodynamics. Freguia (2002) also developed a RATEFRAC® model that used electrolyte-NRTL and an enhancement factor to model the absorption of CO_2 into MEA and validated the model using data from the Bellingham plant designed by Fluor Corporation.

Kucka et al. (2003) developed a non-equilibrium rate-based model that accounted for film reactions without the use of enhancement factors for sour gas absorption into MEA. The model discretizes the liquid film and calculates the reactions in the film and the bulk solution and uses electrolyte-NRTL to model the thermodynamics. They found that the use of 6 non-equidistant film segments could accurately represent 10 equidistant segments. The model was implemented in Aspen Custom Modeler™ and was validated with pilot plant data. More recently, Aspiron (2006) has developed a similar non-equilibrium

rate-based model that included discretized film reactions. The model was implemented on an in-house simulator and the heat transfer model portion was validated with pilot plant data. Finally, a method to optimize the number of film segments and reduce computational time was proposed.

Aspen Plus® RateSep™ was developed based on the work done by Kucka et al. (2003). RateSep™ allows the user to discretize the gas and liquid film and incorporate kinetic reactions within the segments of each film. RateSep™ uses the Maxwell–Stefan theory to solve multi-component mass transfer and can account for electrolyte non-idealities. The model allows the user to divide the column into segments, perform material and energy balances at each segment and integrate across the entire column. The mass and heat transfer coefficients, interfacial area, liquid holdup, and pressure drop can be specified using Aspen supplied correlations. The reaction kinetics can be specified using a power-law form and a number of thermodynamic models are available, including electrolyte-NRTL. The user can also supply custom FORTRAN subroutines if the Aspen supplied mass and transfer and hydrodynamic correlations are not adequate. There are also a number of parameters that can be adjusted or selected, such as four different flow models, reaction and transfer factors, film resistance, and film discretization ratio.

RateSep™ uses a Newton-based simultaneous correction approach to solve the system of equations. In the first pass, the solution obtained from the equilibrium-based mode is used as the initial guess. RateSep™ also provides simple continuation/homotopy method that allows the user to run decreasing homotopy parameters and gradually reach the rate-based solution. The computational time increases with the square of the number of components. In RateSep™, the binary diffusion diffusivities and mass transfer coefficients are

not treated as independent variables. In order to reduce the size of the Jacobian matrix, the mass transfer coefficients are written as follows:

$$k_{i,k,j} = k_j^{\circ} D_{i,k,j}^{\alpha_j} \tag{4.88}$$

where k_j° is a function of flow, temperature, composition and other properties, but independent of the components *i* and *k*. The calculation of the flux and reaction rates depends on the selection of the flow model. In this work, a non-equilibrium rate-based absorber model was developed using Aspen Plus® RateSep™.

4.4.1 Material and Energy Balance

Aspen Plus® RateSep™ performs a material and energy balance, mass transfer, heat transfer, and phase equilibrium calculations for each stage using the two film model. A schematic of the two-film model illustrating the bulk and film parameters for the gas and liquid on stage *j* is shown Figure 4-8. In this work, the model assumes that heat loss to the column is through the liquid and not the gas. The stages are numbered with first stage at the top of the column and the last stage at the bottom of the column.

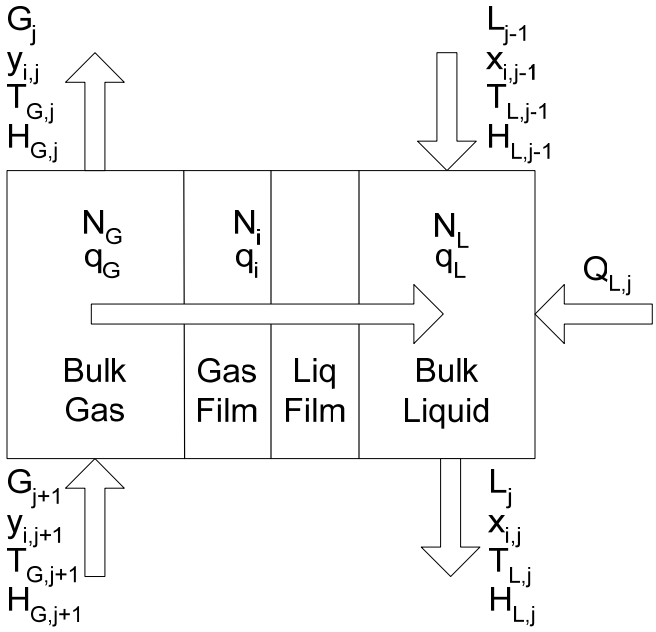

Figure 4-8. Schematic of Two Film Model for Non-Equilibrium Rate-Based Approach of Segment *j*, Neglecting Heat-loss from Gas Phase

The material balance for the bulk gas and liquid is performed using the following equations:

$$L_{j-1}x_{i,j-1} + N_{ij}^{L} + r_{ij}^{L} - L_j x_{ij} = 0 \tag{4.89}$$

$$V_{j+1}y_{i,j+1} - N_{ij}^{V} + r_{ij}^{V} - V_j y_{ij} = 0 \tag{4.90}$$

The material balance equations for the gas and liquid film are:

$$N_{ij}^{I} + r_{ij}^{fL} - N_{ij}^{L} = 0 \tag{4.91}$$

$$N_{ij}^{V} + r_{ij}^{fV} - N_{ij}^{I} = 0 \tag{4.92}$$

The energy balance equations for the bulk gas and liquid are:

$$L_{j-1}H_{j-1}^{L} + Q_j^{L} + q_j^{L} - L_j H_j^{L} = 0 \tag{4.93}$$

$$V_{j+1}H_{j+1}^{V} + Q_j^{V} - q_j^{V} - V_j H_j^{V} = 0 \tag{4.94}$$

The energy balance for the gas and liquid film are:

$$q_j^I - q_j^L = 0 \tag{4.95}$$

$$q_j^V - q_j^I = 0 \tag{4.96}$$

The phase equilibrium at the gas–liquid interface is calculated by:

$$y_{ij}^I - K_{ij} x_{ij}^I = 0 \tag{4.97}$$

Finally, all of the mole fractions in the gas, liquid, bulk, and film must be balanced. The equations that detail how the flux is calculated using the Mixed flow model is enumerated in the appendix. If electrolytes are present, the electrolyte neutrality is satisfied the by adjusting the driving force, $\Delta\phi_j^E\left(\mathbf{x}_j \mathbf{z}_j\right)$, caused by the electric potential in each film region.

4.4.2 Mass Transfer

4.4.2.1 Gas and Liquid Mass Transfer Coefficients

Aspen Plus® RateSep™ provides several built-in correlations for mass transfer and also the option for the user to provide their own correlation or subroutine. These mass transfer models can be used to calculate the gas and liquid mass transfer coefficient and the interfacial area. Most of the packing models are based on empirical and semi-empirical correlations developed mainly through distillation experiments. For structured packing, three models are available: Billet and Schultes (1993), Bravo et al. (1985), and Bravo et al. (1993, 1996). For random packing, three models are also available: Onda et al. (1968), Billet and Schultes (1993), and Bravo and Fair (1982). The user can select from trays, random, or structured packing. The parameters for the correlations are supplied from the Aspen Plus® packing database. Depending on the correlation that is selected, the user may need to input missing packing parameters.

In this work, the Bravo et al. (1993, 1996) correlation was used to calculated the gas and liquid phase mass transfer coefficients for the Flexipac 1Y and Flexipac AQ Style 20 structured packing. Since Flexipac AQ Style 20 resembles the Flexipac 2Y in terms of its physical dimensions and specific area (213 m^2/m^3), Flexipac 2Y was specified as the packing type. RateSep™ uses multi-component Maxwell–Stefan theory to calculate the gas and liquid mass transfer rates. It solves the multi-component Maxwell–Stefan matrix equations using binary mass transfer coefficients (Krishna and Standart, 1976). The binary liquid and vapor phase mass transfer coefficients for the Bravo et al. (1996) model are given by:

$$k_{i,k}^{L} = 2\sqrt{\frac{D_{i,k}^{L} u_{Le}}{\pi S C_E}} \tag{4.98}$$

and

$$k_{i,k}^{V} = 0.54 \frac{D_{i,k}^{V}}{S} \mathrm{Re}_V^{0.8} \, Sc_{V,i,k}^{0.333} \tag{4.99}$$

where $D_{i,k}^{L}$ and $D_{i,k}^{V}$ are the binary liquid and vapor diffusivity, respectively. C_E is correction factor for surface renewal, which has a default value of 0.9 and can be adjusted between 0 and 1. S is the slant height of the corrugation, u_{Le} is the superficial velocity of the liquid, Re_V is the Reynolds number of the vapor and $Sc_{V,i,k}$ is the Schmidt number of the vapor. The details of the correlation are given in the appendix. The mass transfer coefficients depend on gas and liquid flow rates, holdup, physical properties such density, viscosity, surface tension, and on the parameters specific to each packing such as void fraction and material of construction.

4.4.2.2 Effective Interfacial Area

The absorption of CO_2 into aqueous piperazine promoted potassium carbonate occurs by mass transfer with chemical reaction in the boundary layer. The effective interfacial area will be an important factor in modeling, design, and scale-up of CO_2 absorption processes. In the literature, there are a number of different definitions for interfacial area, such as wetted surface area. Although the two are related, in principle, the wetted area includes the liquid surface area in dead zones, whereas the effective interfacial area includes surfaces of drops and jets (Wang *et al.*, 2005). Often times the specific area of the packing is not equivalent to the effective interfacial area due differences in packing material (i.e. steel, plastic, ceramic) and surface treatment (i.e. embossed, gauze), surface tension, viscosity, liquid holdup, hydrodynamics, and gas and liquid flow rates, all of which affects the "wettability" of the packing surface. In the literature, the mass transfer correlations are developed from $k_G a$ and $k_L a$ data and the interfacial area and mass transfer coefficients are then individually separated. In theory, only one correlation should be used to calculate the mass transfer coefficients and the corresponding effective interfacial area of the packing.

In the literature, it has been shown that often these correlations do not predict the correct effective interfacial area for absorption processes. The Separations Research Program (SRP) at the University of Texas at Austin has performed a number of experiments measuring the effective interfacial area of random and structured packing (Lewis *et al.*, 2006, Wilson, 2004). The interfacial area is measured by absorbing carbon dioxide from air into a 0.1 N solution of sodium hydroxide. The experiments are carried out using approximately 3 meters of packing in a pilot scale PVC absorber column with an ID of 0.43 meters, the same diameter as that of the CO_2 capture pilot plant, over a wide range of gas and liquid rates. Since the kinetics for the absorption of CO_2 into sodium

hydroxide is well-characterized, the effective interfacial area can be back-calculated if negligible gas film resistance is assumed. The experiments have shown that many of available models, such as Onda et al., Bravo et al., and Billet and Schultes do not accurately predict the effective interfacial area.

Figure 4-9 shows a plot of the effective interfacial area measured by SRP and that predicted by the Rocha et al. (1996) correlation for Flexipac AQ Style 20 at 2 different gas rates and over of a range of liquid rates. The plot shows that the effective area is independent of gas rate and is a function of the liquid rate. The Rocha, Bravo, Fair (1996) model under-predicts the effective area by approximately 80% when compared to the SRP data. The Rocha, Bravo, Fair results were generated in Aspen Plus® RateSep™ using only air and water, whereas in the SRP system, the addition of 0.1 N NaOH may slightly affect the physical properties of the system and the predicted interfacial area.

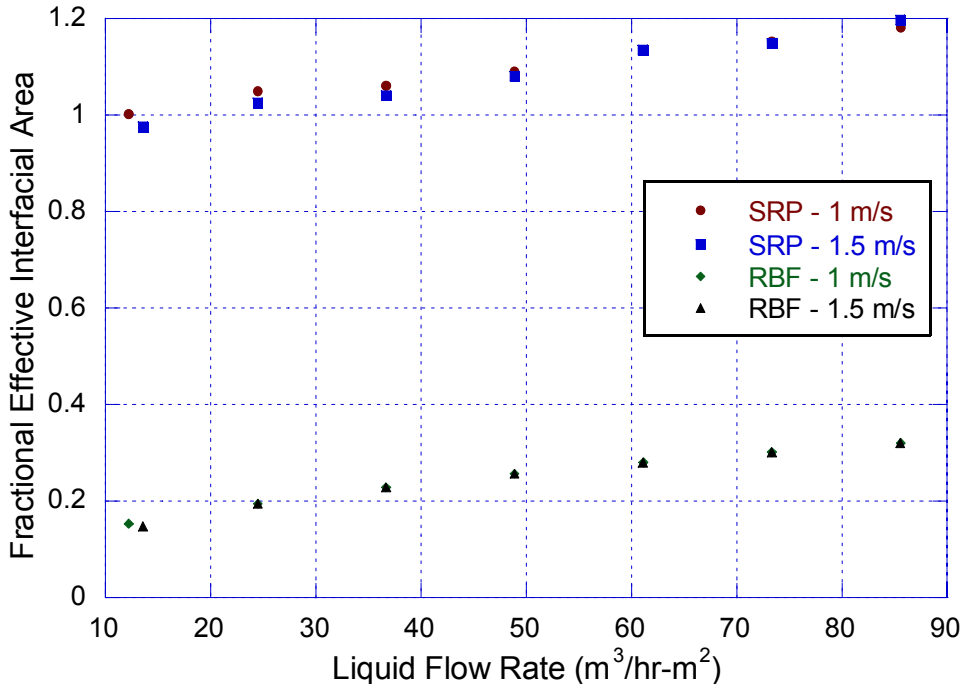

Figure 4-9. Comparison of Effective Area for Flexipac AQ Style 20 (a_p= 213 m^2/m^3) Predicted by the Rocha, Bravo, and Fair Model (1996) and that Measured by SRP

Due to the availability of actual interfacial area measurements in an almost identical setup and the lack of availability of an exact correlation in RateSep™, a correlation dependent only on the superficial liquid velocity was regressed based on the SRP data and used in the absorber simulation. A simple FORTRAN subroutine was written and linked to RateSep™. The equation for the effective interfacial area is given by the following expression:

$$a_{eff} = 0.5694 * (\mathrm{L}) + 204.57 \qquad (4.100)$$

where a_{eff} is the effective interfacial area with units of m^2/m^3 and L is the liquid flow rate in units of m/hr.

In many of the interfacial area models, there are varying degrees of dependence on the viscosity and surface tension. In most of the mass transfer correlations, surface tension has an inverse relationship to the effective interfacial area. A liquid with low surface tension tends to exhibits better wetting characteristics and increases the effective interfacial area (Aspiron, 2005). A number of the interfacial area correlations have exponential surface tension dependencies that vary from -0.15 to -0.95 (Wang *et al.*, 2005). Viscosity is another parameter that may affect the effective interfacial area (Rizzuti *et al.*, 1981). There is some debate as to the effect of viscosity. Some models have a positive exponent of 0.2, whereas other models have -0.13 to -1.0 exponential dependencies on viscosity (Wang *et al.*, 2005). There are also conflicting exponential dependencies for density among the correlations in the literature. In the initial stages of this work, the effect of density, surface tension, and viscosity on the effective interfacial area was not explicitly accounted for. Instead, an interfacial area factor in RateSep™ was adjusted to match the pilot plant data. The effective interfacial area calculated by the FORTRAN area subroutine is multiplied by an area factor, which is then used for the mass transfer calculations.

In the Data-Fit analysis, this method was superceded by another FORTRAN subroutine that set the interfacial area to the specific area of the packing and adjustments were made using the interfacial area factor.

4.4.2.3 Liquid Holdup

Liquid holdup is an important parameter for the calculation of the kinetic reaction rates. In this work, reactions do not occur in the gas phase and only liquid holdup is considered. Liquid holdup is used for the calculation of the reactions in the bulk liquid. For random and structured packing, RateSep™ has several built-in correlations for holdup that the user can select from. Under **RateSep|Holdups|Correlation**, the three correlations for liquid holdup in packing are Billet and Schultes (1993), Stichlmair et al. (1989), and Rocha et al. (1996), which can only be used for structured packing. The user may also select the Percent-Data method, where the liquid percent of the free volume is specified. If the user selects Holdup instead of Correlation, the mass, mole, or volume of holdup for each stage may be specified. RateSep™ provides an adjustable holdup factor that can be used to fit experimental data. In this work, the Percent-Data method was used because it provided a simple and straight-forward method for quantifying of the effect of holdup. An alternative method would have been to select a holdup correlation and adjust the holdup factor to match the pilot plant data.

The holdup that is specified under **Reactions|Holdups** is only used for the initialization of the calculation, but not for the actual calculations of the kinetic reactions. Also, the liquid holdup that is specified in the **RateSep** tab is used only to calculate the kinetic reaction rates. It is not used for the calculation of mass or heat transfer. For example, the Rocha et al. (1996) correlation for mass transfer contains a variable for liquid holdup. However, the correlation

calculates its own liquid holdup according to pressure drop and other parameters and the user specified liquid holdup does not enter into the calculation. The local holdup variable is used only in the correlation itself and not anywhere else (Peng, 2007).

4.4.3 Heat Transfer

The Chilton–Colburn method was used to calculate the heat transfer of the absorber model (Chilton and Colburn, 1934, King, 1980). For the heat transfer calculation, RateSep™ uses the calculated interfacial area as the area for heat transfer. The Chilton–Colburn equation is given by the following:

$$\underline{k}_{av}(Sc)^{2/3} = \frac{h_{tc}}{C_{p,mix}}(\mathrm{Pr})^{2/3} \tag{4.101}$$

where $\underline{k}_{av}$ is the average binary mass transfer coefficient in kmol/sec, which is an unweighted average over all binary mass transfer coefficients, Sc is the Schmidt number and the average binary diffusion coefficient is an unweighted average of all binary diffusivities, h_{tc} is the heat transfer coefficient in Watts/K, $C_{p,mix}$ is the molar heat capacity of the liquid mixture in Joules/kmol-K, and Pr is the Prandtl number. The Schmidt and Prandtl number are given by:

$$Sc = \frac{\eta^l}{\rho^l \underline{D}_{av}} \tag{4.102}$$

$$\mathrm{Pr} = \frac{C_p \eta^l}{\lambda^l} \tag{4.103}$$

Where η^l is the viscosity of the liquid mixture, ρ^l is the density of the liquid, $\underline{D}_{av}$ is the average diffusion coefficient, C_p is the heat capacity of the mixture and λ^l is the thermal conductivity of the liquid mixture.

Under **RateSep Setup|Specifications**, the Chilton–Colburn averaging parameter can be adjusted to weight the average diffusivity and average binary mass transfer coefficients for the calculation of the heat transfer coefficient in Chilton–Colburn analogy. The average diffusivity and average mass transfer coefficient for each stage are calculated by the following equations:

$$\overline{D}_j = \frac{\sum_{i=1}^{nc-1}\sum_{k=i+1}^{nc}\left(x_{ij}+\delta\right)\left(x_{kj}+\delta\right)D_{ikj}}{\sum_{i=1}^{nc-1}\sum_{k=i+1}^{nc}\left(x_{ij}+\delta\right)\left(x_{kj}+\delta\right)} \tag{4.104}$$

and

$$\overline{k}_j = \frac{\sum_{i=1}^{nc-1}\sum_{k=i+1}^{nc}\left(x_{ij}+\delta\right)\left(x_{kj}+\delta\right)k_{ikj}}{\sum_{i=1}^{nc-1}\sum_{k=i+1}^{nc}\left(x_{ij}+\delta\right)\left(x_{kj}+\delta\right)} \tag{4.105}$$

where x is mole fraction of species, nc is the number of components, and δ is the Chilton–Colburn averaging parameter. A large value of the averaging parameter reduces the effect of composition. The default value in RateSep™ is 10^{-4}. An accurate representation of the heat transfer will depend not only on an adequate estimate of the mass transfer coefficient, but on the physical and transport properties as well.

4.4.4 Physical and Transport Properties

The electrolyte-NRTL model in Aspen Plus® uses the following default models to predict the physical and transport properties of the system. For the vapor mixture, the viscosity is determined by the Chapman–Enskog–Brokaw and DIPPR model (Design Institute for Physical Properties (DIPPR), 2006, Reid *et al.*, 1987). Vapor thermal conductivity is calculated using the Stiel–Thodos at low pressure and DIPPR model. Diffusivity in the gas phase is predicted by the

Chapman–Enskog–Wilke–Lee model. The liquid molar volume of the liquid is calculated using the Clarke model and Rackett equation (Chen *et al.*, 1983). The liquid viscosity is calculated by the Andrade and DIPPR models and corrected for the presence of electrolytes using the Jones–Dole model. The diffusivity of each species is determined using the Wilke–Chang model for non-ion components and the Nernst–Hartley model for ions (Horvath, 1985, Wilke and Chang, 1955). Thermal conductivity of the liquid is calculated using the Sato–Riedel and DIPPR models and a correction due to the presence of electrolytes is applied using the Reidel model (Reid *et al.*, 1987). The surface tension of the liquid mixture is calculated by the Hakim–Steinberg–Stiel and DIPPR models and an electrolyte correction is applied using the Onsager–Samaras model (Horvath, 1985).

4.4.4.1 Density

The densities initially predicted by Aspen Plus® for the 5 m K^+/2.5 m PZ solution were approximately 10% lower than the density measurements obtained by Cullinane (2005). The Cullinane density data showed a strong dependence on the potassium concentration, whereas the amine concentration had relatively little impact on the density. The density correlation developed by Cullinane also showed a slight temperature and CO_2 loading dependence. In Aspen Plus®, the electrolyte-NRTL model calculates the density of the potassium carbonate and piperazine solution using the Clarke Aqueous Electrolyte Volume model, which calculates the liquid molar volume for electrolyte solutions (Chen *et al.*, 1983). The model calculates the molar volume of the molecular solvents and adds the contribution from the molar volume of the electrolytes by using the following equation:

$$V_m^l = V_{solv}^l + \sum_{ca} x_{ca} V_{ca} \tag{4.106}$$

where V_m^l is the molar volume of the liquid solution, V_{solv}^l is the molar volume of the liquid solvent, x_{ca} is the mole fraction of the apparent electrolyte *ca*, and V_{ca} is the effective molar volume of the apparent electrolyte *ca*. The liquid molar volume of the solvent is calculated by the following equation:

$$V_{solv}^l = \sum_i x_i V_i^l + \sum_i \sum_j k_{ij} (V_i^l V_j^l)^{0.5} \tag{4.107}$$

where V_i^l is the pure component liquid molar volume of solvent *i* and k_{ij} is the interaction parameter between solvent *i* and solvent *j*. The molar volume of liquid water is calculated from the steam tables. The molar volume of the pure component is calculated using the Rackett, DIPPR, or the IK-CAPE equation. If the RKTZRA parameter is available in the database, the Rackett equation is used. The DIPPR equation is used when the DNLDIP parameter is entered for the component and the IKCAPE equation is used if the parameter VLPO is available. The molar volume contribution of the apparent electrolyte *ca* is calculated by:

$$V_{ca} = V_{ca}^{\infty} + A_{ca} \frac{\sqrt{x_{ca}}}{1+\sqrt{x_{ca}}} \tag{4.108}$$

where V_{ca}^{∞} is the infinite dilution molar volume of the apparent electrolyte *ca* and is entered in Aspen Plus® as VLCLK/1. A_{ca} is the empirical parameter for concentration dependency of the apparent electrolyte *ca* and is entered as VLCLK/2. The mole fraction of the apparent electrolyte *ca* is given by x_{ca}. The temperature dependence of the molar volume of the solution is given by:

$$V_m^l(T) = V_m^l(298K) \frac{\sum_B x_B V_B^{*,l}(T)}{\sum_B x_B V_B^{*,l}(298K)} \tag{4.109}$$

where *B* is any solvent. The temperature dependence of the solution molar volume is equal to the temperature dependence of the mixture molar volume.

The piperazine RKTZRA parameter and cation-anion VLCLK parameters of the K_2CO_3-PZ-CO_2-H_2O system were regressed using Aspen Plus® Data Regression System (DRS). In this work, the pure component Rackett parameter (RKTZRA) for the molar liquid volume of piperazine was regressed. The DIPPR parameters for piperazine, although available, were not entered into the DNLDIP parameter of Aspen Plus®. Initial regression analyses produced the same results when the DNLDIP parameter for piperazine was entered or removed. It appeared that the DNLDIP parameter was overridden by the regressed RKTZRA parameter.

The RKTZRA and VLCLK parameters were simultaneously regressed using density data for the K_2CO_3-H_2O (2–50 wt% K_2CO_3) and $KHCO_3$-H_2O (2–30 wt% $KHCO_3$) system from 25–80 °C (Aseyev and Zaytsev, 1996), density data for K_2CO_3-H_2O, PZ-H_2O, and K_2CO_3-PZ-CO_2-H_2O from 25–70 °C (Cullinane, 2005), and K_2CO_3-PZ-CO_2-H_2O density measurements for 5 m K^+/2.5 m PZ and 6.4 m K^+/1.6 m PZ made by this work. Each of the data sets was given a weight of one for the regression analysis. The tabulated density data used for the regression analysis are listed in the appendix. The DRS results were evaluated based on minimizing the weighted sum of squares and the residual root mean square error. The optimal results of the regression analysis for the RKTZRA and VLCLK parameters are listed in Table 4-15. A parity plot of the DRS estimated values and experimental measurements of density for the K_2CO_3-PZ-CO_2-H_2O system obtained by this work and Cullinane (2005) is shown in Figure 4-10. The absolute average deviation of the Cullinane data set and that measured by this work was 0.33% and 0.32%, respectively.

Table 4-15. DRS Results for Rackett Molar Volume and Clarke Liquid Density Parameters of K_2CO_3-PZ-CO_2-H_2O System

Parameter	Component *i*	Component *j*	Value (SI Units)	σ
RKTZRA/1	PZ		0.2665	0.0014
VLCLK/1	PZH^+	OH^-	-0.4289	0.1825
VLCLK/1	PZH^+	CO_3^{2-}	0.1963	0.1155
VLCLK/1	PZH^+	HCO_3^-	-1.3256	0.2341
VLCLK/2	PZH^+	HCO_3^-	7.4769	1.1085
VLCLK/1	PZH^+	$PZCOO^-$	0.4545	0.0297
VLCLK/1	K^+	OH^-	0.2616	0.0305
VLCLK/2	K^+	OH^-	-1.9636	0.1744
VLCLK/1	K^+	CO_3^{2-}	0.0104	0.0004
VLCLK/2	K^+	CO_3^{2-}	0.1246	0.0016
VLCLK/1	K^+	HCO_3^-	0.0174	0.0005
VLCLK/2	K^+	HCO_3^-	0.0996	0.0025
VLCLK/1	K^+	$PZCOO^-$	0.0011	0.0017
VLCLK/1	K^+	$PZ(COO^-)_2$	0.1210	0.0011

Weighted Sum of Squares: 14.94
Residual Root Mean Square: 0.17

The correlation matrix for the estimated density parameters are listed in the appendix. Plots of the estimated and experimental values of density for the K_2CO_3-H_2O, $KHCO_3$-H_2O and PZ-H_2O systems are shown in the appendix. The simultaneous regression of the Rackett and Clarke density model parameters resulted in an average absolute deviation of 0.07% for the density of the K_2CO_3-H_2O system. The absolute average deviation for the density measurements of the $KHCO_3$-H_2O and PZ-H_2O systems were 0.14 and 0.10%, respectively.

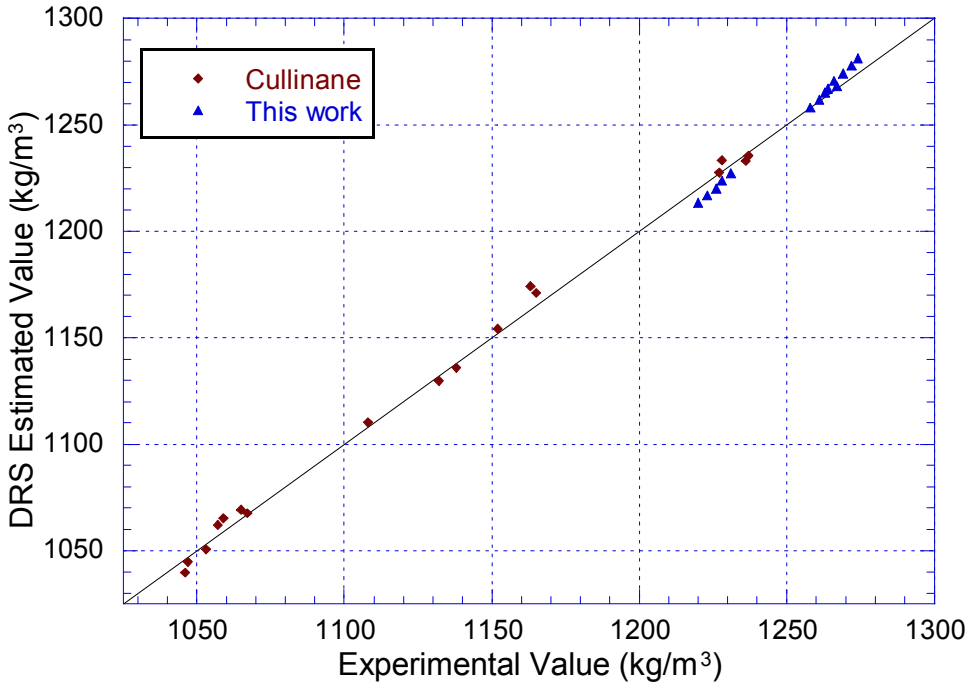

Figure 4-10. DRS Results of Density for the K_2CO_3-PZ-CO_2-H_2O System

4.4.4.2 Viscosity

The liquid viscosity predicted by Aspen Plus® for the potassium carbonate and piperazine solution was approximately 70% lower than the measurements by Cullinane. In Aspen Plus®, the electrolyte-NRTL model calculates the viscosity of the liquid mixture using the modified Andrade equation:

$$\ln \eta^{l} = \sum_{i} f_i \ln \eta_i^{*l} + \sum_{i} \sum_{j} \left(k_{ij} f_i f_j + m_{ij} f_i^2 f_j^2 \right) \tag{4.110}$$

where η_i^{*l} is the pure component viscosity calculated from the Andrade, DIPPR or IK-CAPE equations and f_i is the mole fraction. The binary parameters k_{ij} and m_{ij} are given by:

$$k_{ij} = a_{ij} + \frac{b_{ij}}{T} \tag{4.111}$$

$$m_{ij} = c_{ij} + \frac{d_{ij}}{T} \tag{4.112}$$

The coefficients for the binary parameters a_{ij}, b_{ij}, c_{ij}, and d_{ij} are entered into Aspen Plus® as ANDKIJ/1, ANDKIJ/2, ANDMIJ/1, and ANDMIJ/2, respectively. The default value for the binary parameters is zero. The viscosity correction is applied to the liquid mixture using the Jones–Dole equation, which is given by:

$$\eta^l = \eta_{solv}\left(1 + \sum_{ca} \Delta\eta^l_{ca}\right) \tag{4.113}$$

where η_{solv} is the viscosity of the liquid solvent mixture calculated by the modified Andrade model and $\Delta\eta^l_{ca}$ is the contribution to the viscosity correction due to the apparent electrolyte *ca* (cation–anion). The parameter $\Delta\eta^l_{ca}$ can be calculated by three different equations: Jones–Dole, Breslau–Miller, and Carbonell. If the apparent concentration electrolyte exceeds 0.1 M and the parameters for IONMUB are available, the Breslau–Miller equation is used, which is given by:

$$\Delta\eta^l_{ca} = 2.5V_e c^a_{ca} + 10.05V_e\left(c^a_{ca}\right)^2 \tag{4.114}$$

where c^a_{ca} is the concentration of the apparent electrolyte *ca* and is given by:

$$c^a_{ca} = \frac{x^a_{ca}}{V^l_m} \tag{4.115}$$

where x^a_{ca} is the mole fraction of the apparent electrolyte *ca* and V^l_m is molar volume of the liquid mixture. V_e is the effective volume and for salts involving univalent ions it is given by:

$$V_e = \frac{(B_{ca} - 0.002)}{2.60} \tag{4.116}$$

and for other salts, V_e is given by:

$$V_e = \frac{(B_{ca} - 0.011)}{5.06} \tag{4.117}$$

where B_{ca} is given by:

$$B_{ca} = (b_{c,1} + b_{c,2}T) + (b_{a,1} + b_{a,2}T) \tag{4.118}$$

The b_1 and b_2 Jones–Dole parameters are entered into Aspen Plus® as IONMUB/1 and IONMUB/2, respectively for each ionic species. The b_1 parameter has units of molar volume and b_2 has units of molar volume/temperature. The default value for b_2 is zero. The equations for the Jones–Dole and Carbonell model are listed in the appendix.

The Jones–Dole viscosity model in Aspen Plus® depends on the molar volume of the liquid mixture that is calculated by the Clarke density model. The viscosity parameters were regressed with Aspen Plus® DRS after the density parameters had been fitted. The Andrade parameters for the PZ-H_2O system and the Jones–Dole parameters for the viscosity of the K_2CO_3-PZ-CO_2-H_2O system were simultaneously regressed using viscosity data for the K_2CO_3-H_2O (2–46 wt% K_2CO_3) and $KHCO_3$-H_2O (2–30 wt% $KHCO_3$) system from 25 to 80 °C (Aseyev, 1998) and viscosity data for PZ-H_2O and K_2CO_3-PZ-CO_2-H_2O system from 25 to 70 °C (Cullinane, 2005). Each of the data sets was given a weight of one for the regression analysis. The tabulated viscosity data used for the regression are listed in the appendix. The regressed Andrade binary interaction and IONMUB parameters are shown in Table 4-16.

Table 4-16. DRS Results for Andrade Binary and Jones–Dole Parameters of K_2CO_3-PZ-CO_2-H_2O System

Parameter	Component *i*	Component *j*	Value (SI Units)	σ
ANDKIJ/1	PZ	H_2O	-198.4	24.3
ANDKIJ/2	PZ	H_2O	69824	7775
ANDMIJ/1	PZ	H_2O	4269	970
ANDMIJ/2	PZ	H_2O	-1399414	310498
IONMUB/1	$PZCOO^-$	-	0.7494	0.0367
IONMUB/1	$PZ(COO^-)_2$	-	2.1693	0.0473
IONMUB/1	HCO_3^-	-	0.1892	0.0015
IONMUB/1	OH^-	-	3.0562	0.3863
IONMUB/1	PZH^+	-	-0.7385	0.5003
IONMUB/1	CO_3^{-2}	-	0.6199	0.0026

Weighted Sum of Squares: 12779
Residual Root Mean Square: 5.04

A parity plot of the estimated and experimental values of viscosity for the K_2CO_3-PZ-CO_2-H_2O system measured by Cullinane (2005) is shown in Figure 4-11. The absolute average deviation of the viscosity data was 4.74%. The figure shows that there is significant deviation when the viscosity is larger than 3 centipoises. A similar deviation at high viscosities was also observed in the regressed data for the K_2CO_3-H_2O system, which is shown in the appendix.

The correlation matrix for the estimated viscosity parameters is listed in the appendix. Plots of the estimated and experimental values of viscosity for the K_2CO_3-H_2O, $KHCO_3$-H_2O and PZ-H_2O systems are shown in the appendix. The simultaneous regression of the Andrade and Jones–Dole parameters resulted in an average absolute deviation of 2.68% for the K_2CO_3-H_2O system. The absolute average deviation for the viscosity regression of the $KHCO_3$-H_2O and PZ-H_2O systems were 4.89 and 5.32%, respectively.

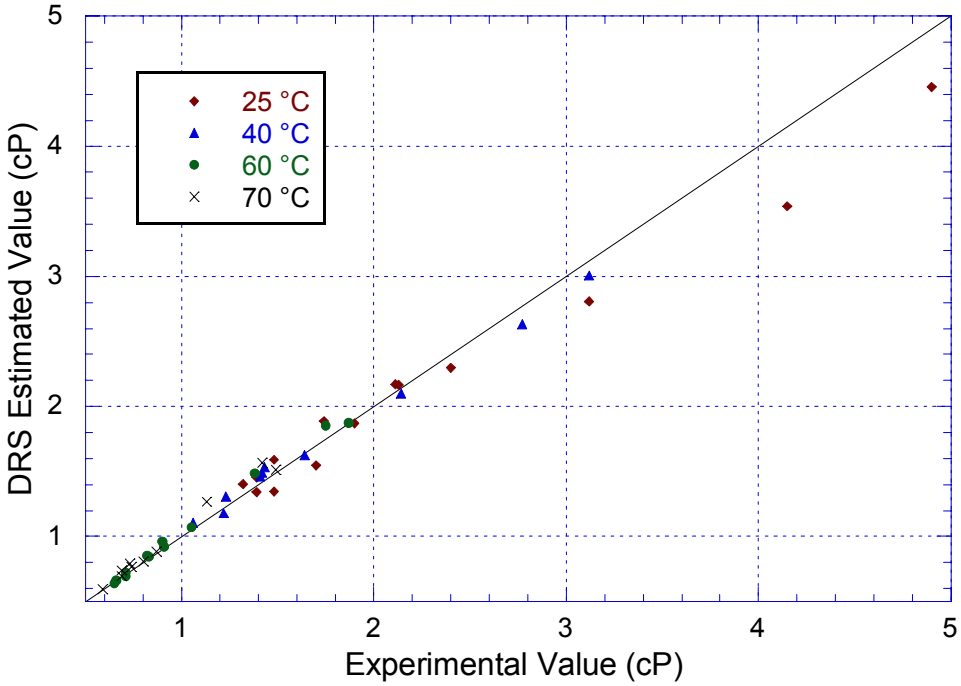

Figure 4-11. DRS Results of Viscosity for K_2CO_3-PZ-CO_2-H_2O System at Various Solution Compositions and Loading at 25 – 70 °C

4.4.4.3 Diffusivity

In the electrolyte-NRTL model, the diffusion coefficients of the molecular species are calculated using the Wilke–Chang model and the effective diffusivity for an ion is calculated using the Nernst–Hartley model. The diffusivities are important parameters for determining the mass transfer and indirectly used to determine the heat transfer coefficient. The Wilke–Chang equation for component *i* is given by:

$$D_i^l = 1.17282x10^{-16}\frac{(\varphi M)^{1/2}T}{\eta^l\left(V_{bi}^{*,l}\right)^{0.6}} \tag{4.119}$$

where

$$\varphi M = \frac{\sum_{j\neq i} x_j \varphi_j M_j}{\sum_{j\neq i} x_j} \tag{4.120}$$

where φ_j is the association factor for the solvent: 2.26 for water, 1.90 for methanol, 1.50 for ethanol, 1.20 for propyl alcohols and n-butanol, and 1.00 for all other solvents, η^l is the mixture viscosity of all non-diffusing components, M_j is the molecular weight of component j and $V_{bi}^{*,l}$ is the liquid molar volume of component i at the normal boiling point. In Aspen Plus®, the liquid mixture viscosity is calculated using the modified Andrade equation and the Jones–Dole electrolyte correction. The liquid molar volume is entered as VB under **Parameters | Pure Component**.

The Nernst–Hartley diffusivity equation for an ion i is given by the following:

$$D_i = \left(\frac{RT}{z_i F^2} \right) \left(l_{i,1} + l_{i,2} T \right) \sum_k x_k \tag{4.121}$$

where F is the Faradays' number and is equal to 9.65 x 10^7 C/kmol, x_k is the mole fraction of any molecular species k, and z_i is the charge of the species. The binary diffusion coefficient of the ion with respect to a molecular species is equal to the effective diffusivity of the ion in the liquid mixture and is given by:

$$D_{i,k} = D_i \tag{4.122}$$

The binary diffusion coefficients of an ion i with respect to an ion j is the arithmetic average of the two diffusivities such that:

$$D_{i,j} = \left(\frac{D_i + D_j}{2} \right) \tag{4.123}$$

In an attempt to reconcile the difference in k_g' calculated by the absorber model and Cullinane (2005), the diffusivity of CO_2 was adjusted by changing the liquid molar volume of CO_2. Even when the maximum VB was entered, the

adjustment was not enough to reconcile the difference in k_g'. It should be noted that Cullinane used different methods to estimate the diffusivities of CO_2 and other components in the system. Cullinane estimated the diffusivity of CO_2 using a correlation developed by Pacheco (1998) that related the diffusivity of N_2O in amine solutions to temperature and viscosity. A modified Wilke–Chang correlation was used to estimate the diffusivities of the amine and other components. The equation is given by:

$$D_{Am}^{\infty} = \frac{1.17 \times 10^{-13} (\xi_{sol} M_{sol})^{0.5} T}{V_{Am}^{0.6} \eta_{sol}} \tag{4.124}$$

where D_{Am}^{∞} is the diffusivity of the amine at infinite dilution in water, V_{Am} is the molar volume, M_{sol} is the molecular weight of the solvent, ξ_{sol} is the solvent specific parameter (2.6 for water), and η_{sol} is the solvent viscosity.

In the Cullinane kinetic model, the diffusion coefficients of all the ions were considered to be equal that of $PZCOO^-$. The estimated molar volume $PZCOO^-$ was 0.1311 m^3/kmol. In addition, Cullinane correlated the diffusivity of the amines to viscosity and found that a correction term was needed during the regression of the kinetic data:

$$D_{Am} = \beta D_{Am}^{\infty} \left(\frac{\eta_w}{\eta_s} \right) \tag{4.125}$$

where β was correlated to be 1.51, η_w is the viscosity of water and η_s is the viscosity of the solvent. The difference in diffusivities may account for some the discrepancies between the RateSep™ model and the kinetic model developed by Cullinane.

4.4.4.4 Surface Tension

Surface tension is a significant parameter in the calculation of effective interfacial area for many of the mass transfer correlations. For electrolyte solutions, the surface tension is calculated using the Onsager–Samara model. The model is given by the following equation:

$$\sigma_{mix} = \sigma_{solv} + \sum_{ca} x_{ca}^{a} \Delta\sigma_{ca} \tag{4.126}$$

where σ_{mix} is the surface tension of the liquid mixture, σ_{solv} is the surface tension of the solvent components in the mixture, x_{ca}^{a} is the mole fraction of apparent electrolyte *ca*, and $\Delta\sigma_{ca}$ is the contribution to surface tension correction due to apparent electrolyte *ca*. The surface tension of the solvent is given by the weighted average equation of the pure components (Reid *et al.*, 1987):

$$(\sigma_{solv})^{r} = \sum_{i} x_i (\sigma_i)^{r} \tag{4.127}$$

where σ_i is the surface tension of the pure component *i* and *r* is an adjustable parameter that can be set to a value of 1, -1, -2, or -3. The default value of *r* is 1. The pure component liquid surface tension can be calculated by the Hakim–Steinberg–Stiel, DIPPR or IK-CAPE models. The electrolyte contribution to surface tension is given by:

$$\Delta\sigma_{ca} = \frac{80.0}{\varepsilon_{solv}} c_{ca}^{a} \log\left\{\frac{1.13\times10^{-13}\left(\varepsilon_{solv}T\right)^{3}}{c_{ca}^{a}}\right\} \tag{4.128}$$

where ε_{solv} is the dielectric constant of the solvent mixture, V_m^l is the liquid molar volume calculated by the Clarke model, and c_{ca}^{a} is the concentration of the apparent electrolyte *ca*.

Surface tension measurements were made by two undergraduate groups taking a senior design class. Both sets of surface tension data showed that the surface tension for the piperazine/potassium carbonate system was between 30 to 50 dynes/cm, which is similar other amine blend systems (Aspiron, 2005). The values predicted by Aspen Plus® were approximately 50% higher and close to the value for water (~70 dynes/cm). Surface tension will dramatically affect the predicted effective interfacial area if the built-in RateSep™ correlations are used. In this work, the subroutine used to calculate interfacial area did not depend on surface tension. It was assumed that the interfacial area factor adjustments in the regression analysis accounted for surface tension effects.

4.4.4.5 Thermal Conductivity

The calculation of the correct thermal conductivity for the liquid mixture is important for evaluating heat transfer coefficients and determining the rate of heat transfer. In the RateSep™ absorber model, the thermal conductivity of the liquid mixture is calculated using the Sato–Riedel model and the Vredeveld mixing rule and adjusted for electrolytes with the Riedel correction. The Sato–Riedel equation is given by the following:

$$\lambda_i^{*,l} = \frac{1.1053152}{M_i^{1/2}} \left(\frac{3 + 20\left(1 - T_{ri}\right)^{2/3}}{3 + 20\left(1 - T_{bri}\right)^{2/3}} \right) \tag{4.129}$$

where,

$$T_{bri} = \frac{T_{bi}}{T_{ci}} \tag{4.130}$$

$$T_{ri} = \frac{T}{T_{ci}} \tag{4.131}$$

where, M_i is the molecular weight, T_{bi} is the normal boiling temperature given by the parameter TB, and T_{ci} is the critical temperature given by the parameter TC. The Vredeveld mixing rule for thermal conductivity is given by:

$$\left(\lambda_{solv}^{l}\right)^{-2} = \sum_{i} w_i \left(\lambda_i^{*,l}\right)^{-2} \tag{4.132}$$

where, w_i is the liquid phase weight fraction of component *i* and $\lambda_i^{*,l}$ is the liquid thermal conductivity of pure component *i*, which is calculated from the Sato–Riedel equation. The Riedel electrolyte correction is given by:

$$\lambda^{l}(T) = \left[\lambda_{solv}^{l}(T = 293) + \sum_{ca} (a_c + a_a) \frac{x_{ca}^{a}}{V_m^{l}} \right] \frac{\lambda_{solv}^{l}(T)}{\lambda_{solv}^{l}(T = 293)} \tag{4.133}$$

where λ_{solv}^{l} is the thermal conductivity of the liquid solvent mixture calculated by the Sato–Riedel model and a_c , a_a are the Riedel ionic coefficients, which are entered into Aspen Plus® as IONDRL.

The IONRDL parameters for the piperazine ion species, PZH^+, $PZCOO^-$, $PZ(COO^-)_2$ and H^+PZCOO^- were not entered into Aspen Plus® because they were unknown. If an IONRDL parameter for a particular species is missing, RateSep™ issues a warning and uses the default value of zero. In addition, the Hilliard (2005) VLE model treats HPZCOO as a molecule. The thermal conductivity is calculated from the molecular weight, critical temperature and normal boiling point using the Sato–Riedel equation. Therefore, the thermal conductivity calculate by RateSep™ may be incorrect. The effects of thermal conductivity for the four piperazine ions were not examined.

4.4.5 RateSep™ Model Specifications

4.4.5.1 Absorber Inputs and Flowsheet

The flowsheet for the RateSep™ absorber model is shown in Figure 4-12. A typical RateSep™ input file is listed in the appendix. The inlet liquid and vapor composition and flow rates were entered on the **Streams** sheet. For the lean liquid feed, the molar flow rates of K_2CO_3, PZ, CO_2, and H_2O were entered based on the values determined from the data analysis of the pilot plant campaigns. The lean stream was not permitted to flash until it reached the lean flash block. This was done to facilitate the regression analysis for Data-Fit. The input for Data-Fit required apparent components. In the lean flash block, the solution speciates into its equilibrium components at a flash temperature that consistent with pilot plant data, which was approximately 313.15 K. The measured vapor flow rates of CO_2, H_2O, N_2 and inlet temperature were entered. The location of the liquid feed was set Stage 1 and the gas feed was set to the last stage using the On-Stage convention for both streams.

In the pilot plant, the packing was divided into 2 separate beds, with a chimney tray and a redistributor in between. In the simulation, the packing was modeled as one continuous bed. It was assumed that there was negligible heat loss and no reactions during the collection and redistribution of the liquid. The packing height was set to 6.096 m and the ID of the column was set to 0.43 m.

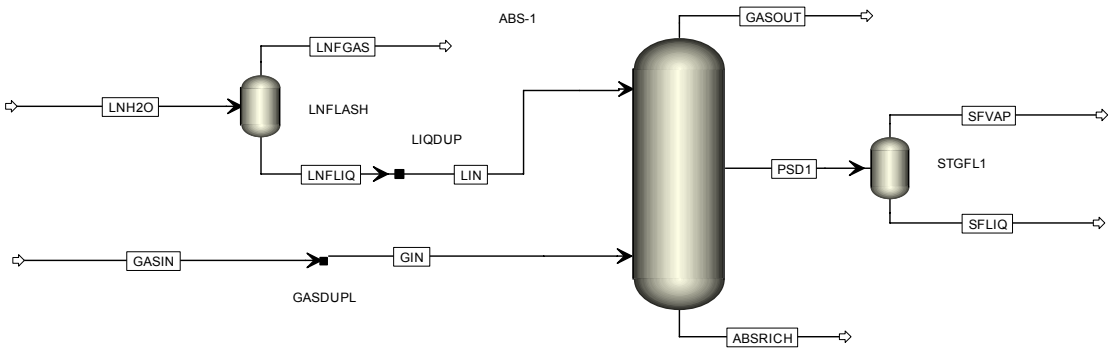

Figure 4-12. Flowsheet for RateSep™ Absorber Model. Pseudostreams for Each Stage were Flashed to Determine $P^*_{CO_2}$ and Create McCabe Thiele Plots

Heat loss to the absorber column was entered under the **Heaters Coolers** tab. The total number of sections was set to the total of segments that were chosen for the simulation. The starting and ending stage values were set to be the same as the section number. A value for the overall column heat loss was assigned to the liquid, which was distributed equally for each segment. It was assumed that the heat loss from the vapor was negligible relative to the liquid. In the MEA modeling by Dugas (2006), the heat loss from the absorber was estimated to be approximately 15,000 watts, which was equivalent to about 25% of the heat loss from the stripper.

4.4.5.2 Kinetic and Equilibrium Reactions

The kinetic equations and corresponding reaction rate parameters derived in the previous section were entered under the **Reactions | Reactions** tab. A total of 24 kinetic rate expressions, which include the 12 forward and 12 reverse reactions developed in the kinetics section, were entered into RateSep™.

$$PZ + CO_2 + H_2O \xleftarrow{k_{PZ-H_2O}} PZCOO^- + H_3O^+ \quad \text{(R.1)}$$

$$PZ + CO_2 + PZCOO^- \xleftarrow{k_{PZ-PZCOO^-}} PZCOO^- + H^+PZCOO^- \quad \text{(R.2)}$$

$$PZ + CO_2 + PZ \xleftarrow{k_{PZ-PZ}} PZCOO^- + PZH^+ \quad \text{(R.3)}$$

$$PZ + CO_2 + CO_3^{2-} \xleftarrow{k_{PZ-CO_3^{2-}}} PZCOO^- + H_3O^+ \quad \text{(R.4)}$$

$$PZ + CO_2 + OH^- \xleftarrow{k_{PZ-OH^-}} PZCOO^- + H_2O \quad \text{(R.5)}$$

$$PZCOO^- + CO_2 + H_2O \xleftarrow{k_{PZCOO^- - H_2O}} PZ(COO^-)_2 + H_3O^+ \quad \text{(R.6)}$$

$$PZCOO^- + CO_2 + PZCOO^- \xleftarrow{k_{PZCOO^- - PZCOO^-}} PZ(COO^-)_2 + H^+PZCOO^- \quad \text{(R.7)}$$

$$PZCOO^- + CO_2 + PZ \xleftarrow{k_{PZCOO^- - PZ}} PZ(COO^-)_2 + PZH^+ \quad \text{(R.8)}$$

$$PZCOO^- + CO_2 + CO_3^- \xleftarrow{k_{PZCOO^- - CO_3^{2-}}} PZ(COO^-)_2 + H_3O^+ \quad \text{(R.9)}$$

$$CO_2 + OH^- \xleftarrow{k_{OH^-}} HCO_3^- \quad \text{(R.10)}$$

$$PZ + CO_2 + H_2O \xleftarrow{k_{PZ}} PZH^+ + HCO_3^- \quad \text{(R.11)}$$

$$PZCOO^- + CO_2 + H_2O \xleftarrow{k_{PZCOO^-}} H^+PZCOO^- + HCO_3^- \quad \text{(R.12)}$$

For the reactions R.1 and R.6, the forward reaction with water was assumed to be pseudo-first order, with a constant water concentration of 55.55 mol/L. In RateSep™, the coefficient for water was set to one and the exponent was set to zero. For reaction R.2, the $PZCOO^-$ species appears as both a reactant and product and could not be entered into Aspen Plus® as such. To solve this problem, the coefficient for $PZCOO^-$ was set to zero, but a value of one was entered into the exponent.

In addition, four equilibrium reactions were entered into RateSep™. The parameters for the equilibrium reactions are derived from Hilliard (2005). The equilibrium constant basis was mole gamma and the temperature approach to equilibrium was set to 0 K.

Eqn No.	Equilibrium Equation	$\ln K_{eq} = A + B/T + C\ln T$		
		A	B	C
E.1	$2 \cdot H_2O \longleftrightarrow H_3O^+ + OH^-$	132.90	-13445.9	-22.48
E.2	$PZH^+ + H_2O \longleftrightarrow PZ + H_3O^+$	481.95	-33448.7	-69.78
E.3	$H^+PZCOO^- + PZ \longleftrightarrow PZCOO^- + PZH^+$	-488.75	27752.8	69.78
E.4	$HCO_3^- + H_2O \longleftrightarrow H_3O^+ + CO_3^{2-}$	216.05	-12431.7	-35.48

4.4.5.3 Number of Stages

An optimization analysis was conducted on the number of segments to determine the minimum number of segments required to adequately model the pilot plant data while maintaining a constant height of packing. Using the inputs from Run 4.5, the number of segments was varied from 5 to 70 and the outlet concentration of CO_2 in the gas phase was recorded. Figure 4-13 shows that the outlet CO_2 gas concentration decreases as the number of segments is increased and the column height remains constant. The plot shows that a minimum is approached at approximately 70 segments. However, due to convergence issues and limitations with computational time, 50 segments were used in this work.

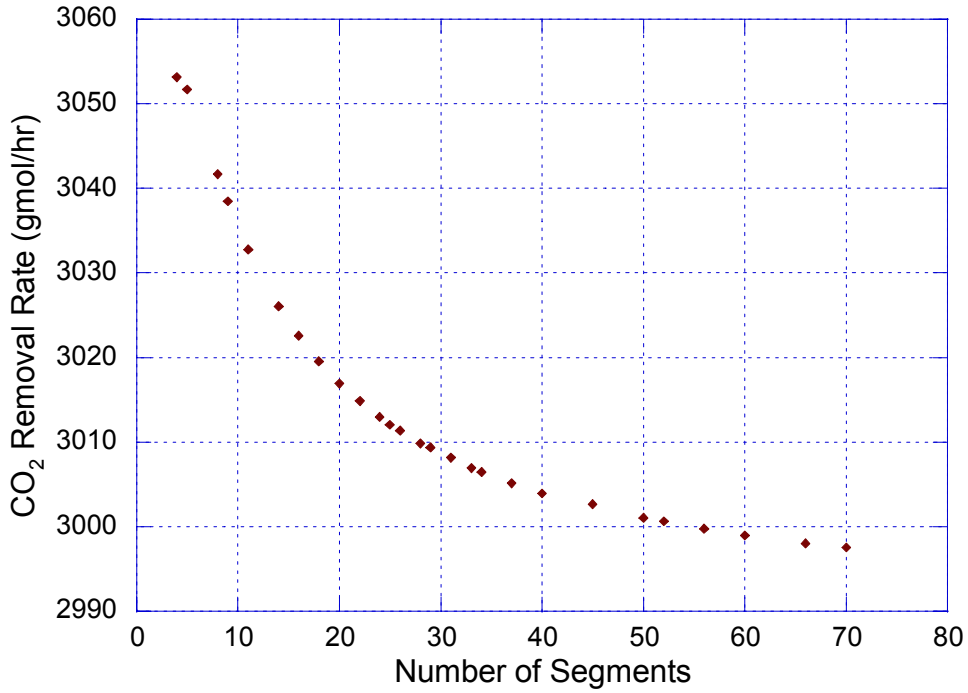

Figure 4-13. Optimization of the Number of Segments (Run 4.5, VPlug-Pavg Flow Model, 7 Film Discretization, Film Ratio = 2)

The temperature profiles corresponding to four different numbers of segments is shown in Figure 4-14. The figure shows that as the number of segments is increased, the temperature bulge becomes larger and in this case,

even shifts further up the column in location. The decrease in absorber performance is mostly likely due to limitations with vapor-liquid equilibrium at the higher temperatures, where the system may begin to pinch. The figure also shows that 50 segments are adequate to properly model the temperature profile.

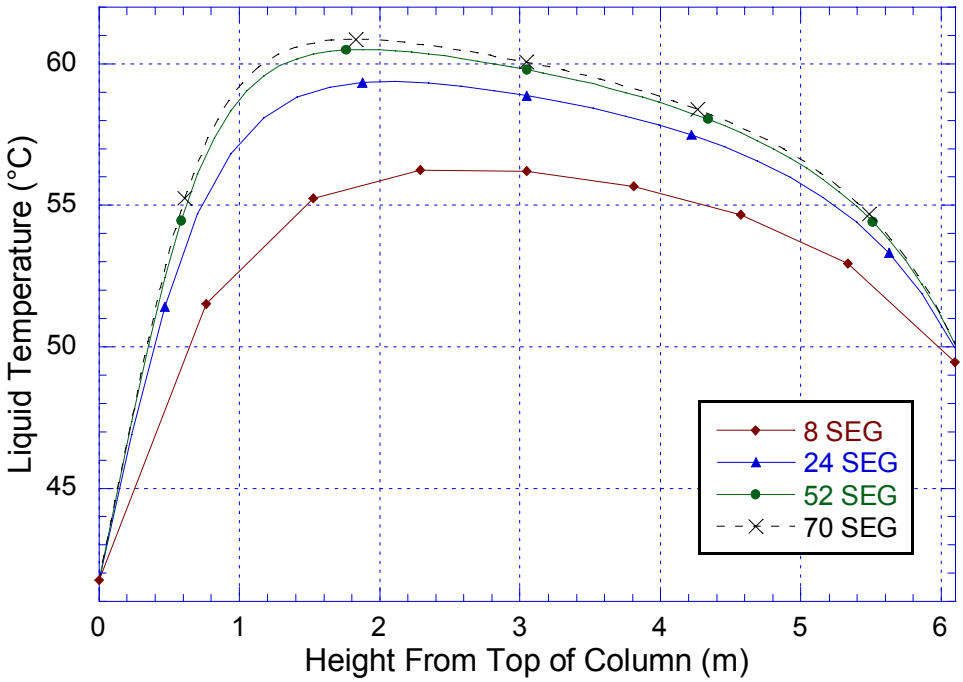

Figure 4-14. Temperature Profile across the Absorber Column Depending on the Number of Stages that are Used

4.4.5.4 Film Discretization

The effect of the number of film segments and the method of film discretization was examined. It has been shown that the discretization of the boundary layer should not be uniformly distributed (Aspiron, 2006, Kucka *et al.*, 2003). Instead, a non-equidistant distribution of the liquid film segments should be used. Thinner films are used in the region where there is the steepest change in the concentration gradient to adequately capture the fast reaction rates and the depletion of reactants (Figure 4-15). For mass transfer with chemical reactions

occurring in the boundary layer, this means using thinner films near the gas–liquid interface and progressively thicker films near the bulk solution.

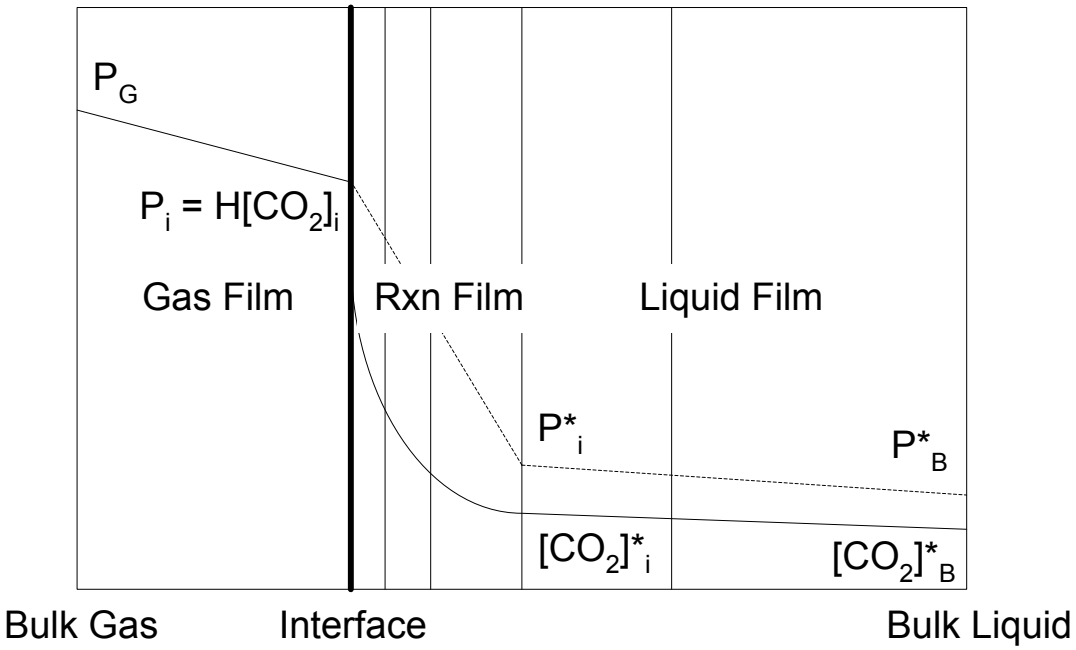

Figure 4-15. Mass Transfer with Chemical Reaction in the Boundary Layer. Thinner Films at the Interface Capture the Rapid Kinetic Reactions

In RateSep™, the user can select the total number of film segments and specify the coordinates the individual film segments. The film discretization ratio can be adjusted by the user to specify the ratio of the thickness of the adjacent discretization region. For example, a film ratio of 2 and 3 film segments results in 4 films segments with a relative thickness ratio of 4:2:1. For the optimization, the number of film segments and film discretization ratio were varied using the inputs from Run 4.5, which were a 5 m K^+/2.5 m PZ solution from Campaign 4. In RateSep™ 2006, the maximum value of the film ratio is 100.

Figure 4-16 shows that most of the reactions occur near the interface because the higher film discretization ratios capture the reactions occurring in the thin film boundary layer near the gas–liquid interface. The plot also shows

that as the film ratio is increased, fewer film discretization points are needed to reach the maximum value of the CO_2 in the outlet gas. However, it also evident that there is some variability with the final outlet CO_2 gas concentration. As the film ratio is increased, the performance of the absorber increases, i.e. when the film ratio is increased from 10 to 100, the final outlet CO_2 gas concentration decreases by 80 gmol/hr, except when the film ratio is equal to 50. It is assumed that the larger number of film segments will result in a more accurate and representative answer and that the use of fewer film segments will reduce the computational time of a simulation.

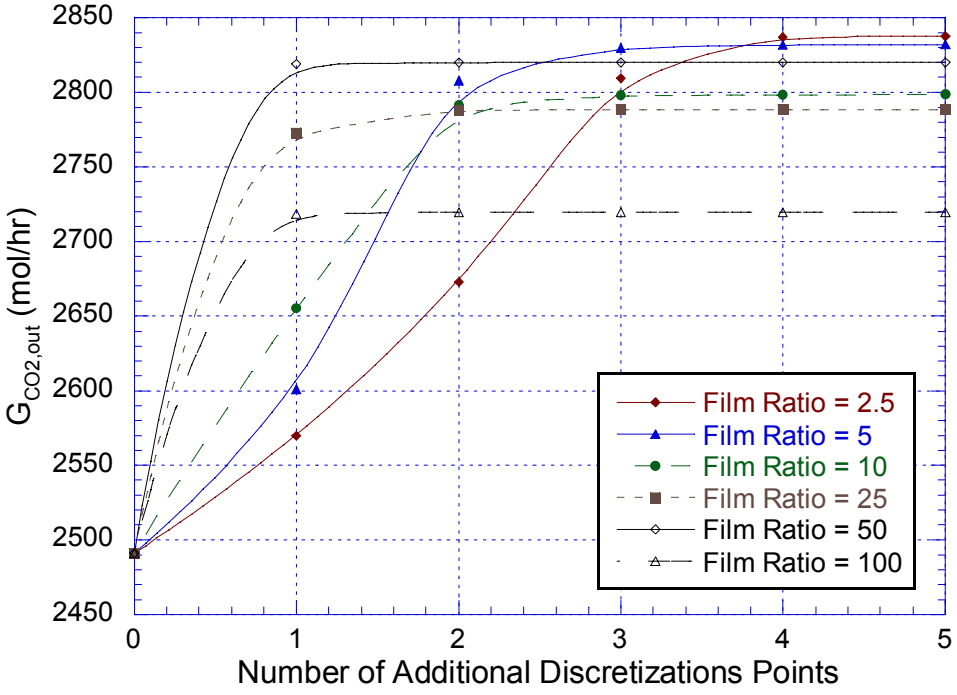

Figure 4-16. Liquid Film Ratio and Number of Discretization Points (5 m K^+/2.5 m PZ, 50 Segments, VPlug-Pavg Flow Model)

Another evaluation of film ratios between 2.5 and 10 is shown Figure 4-17. The figure shows that a film ratio of 2.5 gives the highest outlet CO_2 gas concentration, but requires 5 additional discretization points to attain the final maximum value. The plot shows that a film ratio of six yields a comparable

solution to the 2.5 film ratio, while reducing the number of additional film segments to three. In this work, a film ratio of six and three additional film discretization points (4 film segments) were used to minimize computation time. An optimization analysis was not performed for the 6.4 m K^+/1.6 m PZ solution. A different set of optimized parameters may be needed because the kinetics for 6.4 m K^+/1.6 m PZ are slower than 5 m K^+/2.5 m PZ.

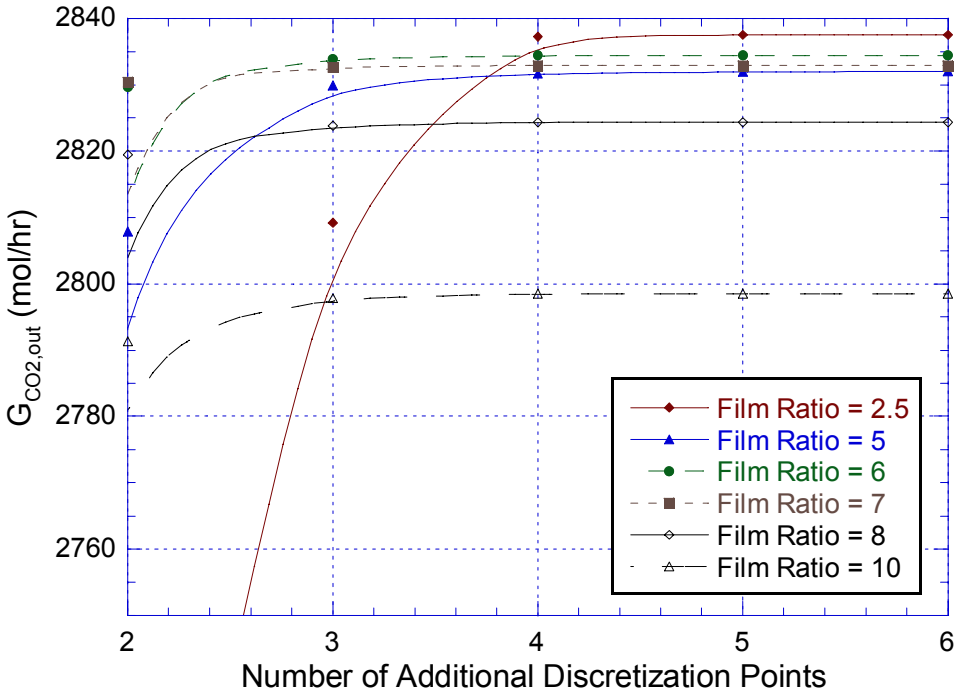

Figure 4-17. Liquid Film Ratio between 2.5 and 10 (5 m K^+/2.5 m PZ, 50 Segments, VPlug-Pavg Flow Model)

4.4.5.5 Flow Model Selection

In RateSep™, there are four different flow models that can be used to determine the bulk properties when the mass and energy fluxes and reactions are calculated for each segment. The four flow models are: Mixed, Countercurrent, VPlug, and VPlug-Pavg. The bulk properties include the mole fraction, temperature, and pressure of gas and liquid, and the bulk gas and liquid rate. In the mixed flow model, the bulk properties of the gas and liquid phase are

assumed to be the same as the condition of the phase leaving the segment. This method is recommended for trays and is the same method used for equilibrium stages. The countercurrent flow model uses the arithmetic average of the inlet and outlet condition for each phase. This method is more accurate for packing, but is more computationally intensive and is recommended when a component less is than 200 ppm (Aspen Technology Inc., 2006). In the VPlug flow model, the outlet conditions are used for the liquid and bulk gas pressure and the average conditions are used for the other vapor properties as in the countercurrent model. For the VPlug-Pavg flow model, the outlet conditions are used for the liquid and the average conditions are used for all of the bulk properties in the vapor phase. The flow models are specified under **Pack Rating|RateSep**.

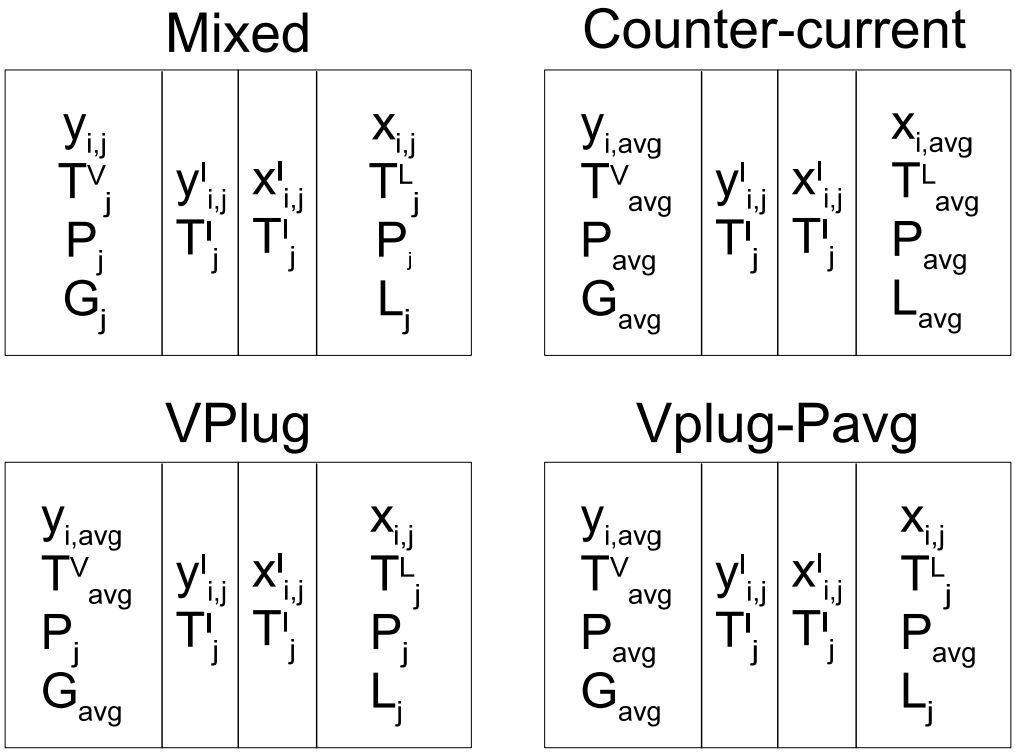

Figure 4-18. Flow Models and Corresponding Bulk Property Specifications Available in RateSep™ for Rate-based Calculations

The effect of flow model selection on absorber performance and the temperature profile is shown in Figure 4-19. The interfacial area factor was adjusted for each flow model until the outlet CO_2 gas concentration was 2623 gmol/hr. The plot shows that the Countercurrent flow model predicts the highest temperature profiles relative to the other models and requires less area to attain the same absorber performance. The VPlug and VPlug-Pavg flow models give the same results and had a slightly lower temperature profile. The Mixed flow model predicted the lowest temperature profile and required the largest amount of interfacial area to achieve the same CO_2 removal rate.

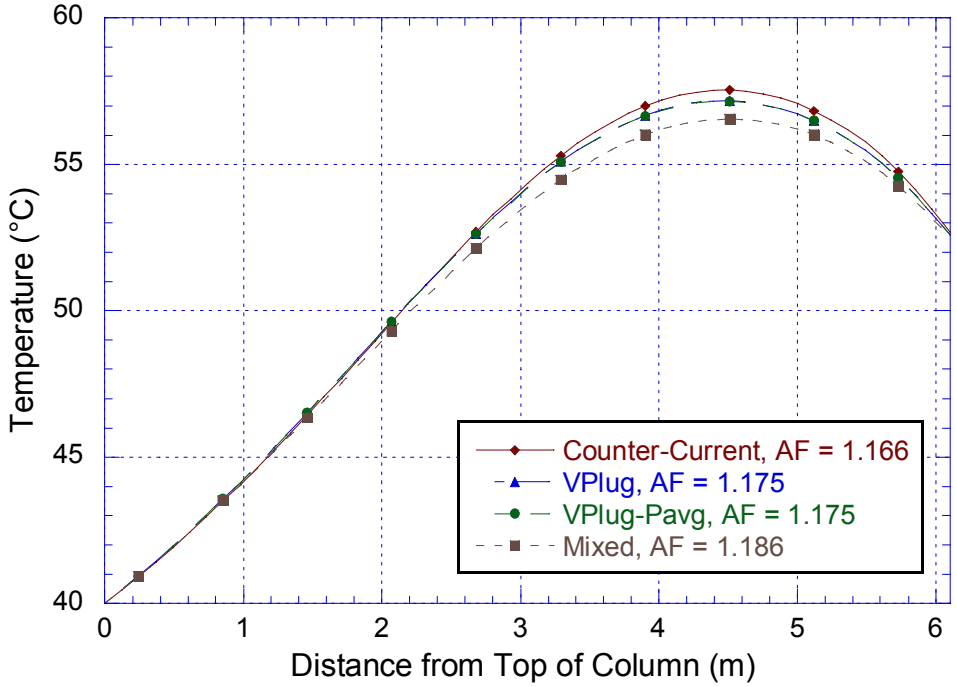

Figure 4-19. Temperature Profile for the Four Flow Models (5 m K^+/2.5 m PZ, Adjusted Area Factor to obtain $G_{CO2,out}$ = 2623 mol/hr)

4.4.5.6 RateSep™ Setup Parameters

There are several additional parameters that can be adjusted within RateSep™ under **RateSep Setup|Specifications**. The Chilton–Colburn averaging parameter can be adjusted to weight the average diffusivity and

average binary mass transfer coefficients for the calculation of the heat transfer coefficient. In addition, the mass transfer flux and reaction rates calculated by RateSep™ for each stage are based on an average of the bulk and film conditions. For fast reactions in the film, the conditions nearer the bulk solution should be weighted more heavily than the interface conditions. The Transfer condition factor determines the weighting factor for the temperature and composition that is used to calculate the mass transfer coefficient. The condition factor is used as follows:

$$C_{avg} = F_{TC} \times C_{bulk} + (1 - F_{TC}) \times C_{\text{int}} \tag{4.134}$$

where C_{avg} is the average condition, C_{bulk} is the bulk condition, C_{int} is the interface condition, and F_{TC} is the Transfer condition factor. The Reaction condition factor is used in the same way, but is used to weight the average conditions for the calculation of the reaction rates in the film. Finally, when the composition or temperature changes dramatically near the top or bottom stage, it is recommended that the Top/Bottom stage condition factor be changed. The default value for all three factors is 0.5. When any of the above conditions apply, it is recommended that the values be set closer to 1 (Aspen Technology Inc., 2006). For highly non-ideal phases, Film non-ideality correction under **Pack Rating|RateSep|Rate Based** may be selected, whereby a correction term is applied to the fugacity. In this work, it was found that using film non-ideality correction slightly increased the removal rate of CO_2 was used and this option was selected.

4.4.6 Rate Data Reconciliation in RateSep™

The kinetic rate constants for the potassium carbonate and piperazine system were derived from the concentration based rate constants regressed by Cullinane from bench-scale wetted wall column experiments (Cullinane, 2005).

Cullinane used the rate constants to develop a FORTRAN model to predict the rate of CO_2 absorption into the piperazine promoted potassium carbonate system. Figure 4-20 shows that the predicted absorption rate for 5 m K^+/2.5 m PZ did not match the wetted wall column data very well beyond P_{CO2}* = 2000 Pa at 40 °C and P_{CO2}* = 4000 Pa at 60 °C. Bench-scale experiments were not conducted for the 6.4 m K^+/1.6 m PZ solvent and were not available for comparison with the FORTRAN rate model predictions. The rate constants used in this work were derived from the Cullinane FORTRAN rate model. Therefore, adjustments to the Aspen Plus® RateSep™ absorber model were made to match the FORTRAN results and not the results from the wetted wall column for the 5 m K^+/2.5 m PZ and 6.4 m K^+/1.6 m PZ solvents.

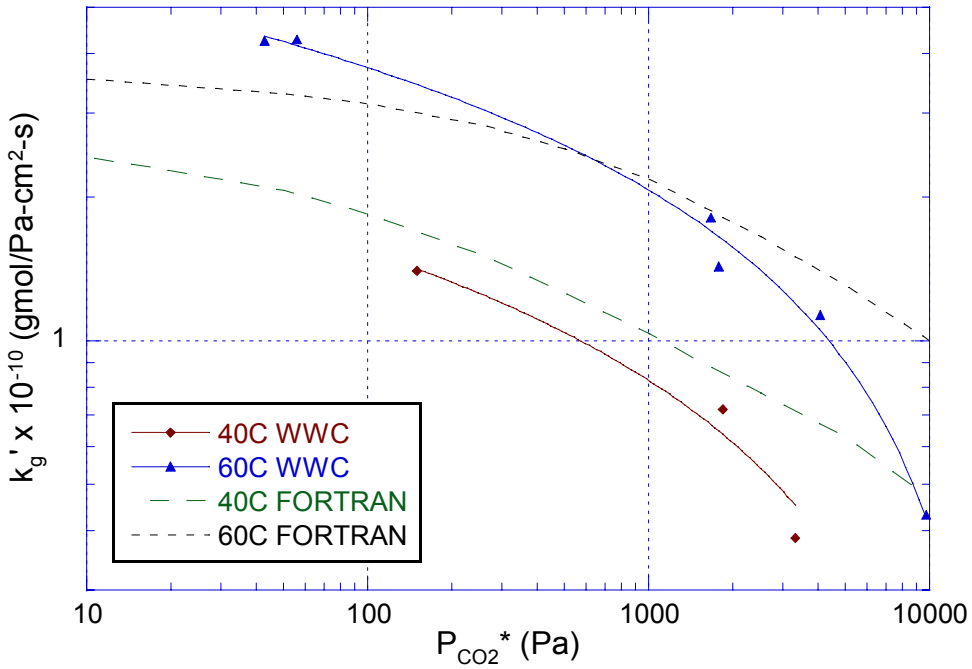

Figure 4-20. Comparison of Wetted Wall Column Data to Predicted Rate Data from Cullinane FORTRAN Model for 5 m K^+/2.5 m PZ (k_l = 0.01 cm/s)

The rate data predicted by the Cullinane (2005) FORTRAN model for 5 m K^+/2.5 m PZ and 6.4 m K^+/1.6 m PZ at 40 and 60 °C is shown in Figure 4-21. The

figure shows that the 5 m K^+/2.5 m PZ solution has rate that is 30–45% higher than the 6.4 m K^+/1.6 m PZ solution.

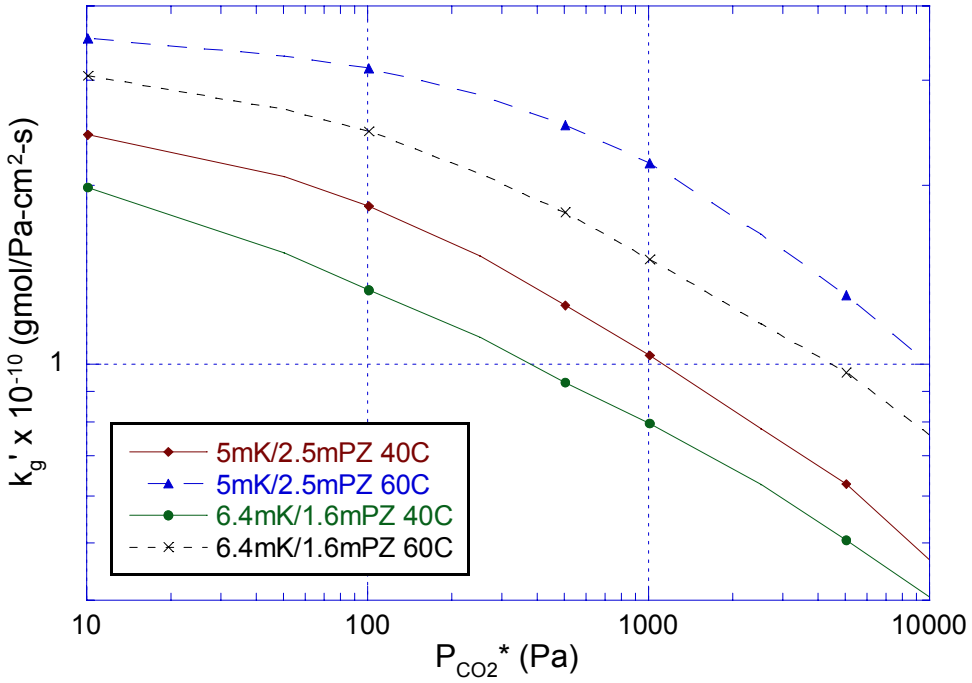

Figure 4-21. Cullinane FORTRAN Rate Data Comparison for 5 m K^+/2.5 m PZ and 6.4 m K^+/1.6 m PZ at 40 and 60 °C (k_l = 0.01 cm/s, P_{CO2}/P_{CO2}^* = 1.01)

The activity based rate constants that were derived earlier in the chapter were entered in Aspen Plus® RateSep™ and the normalized flux, k_g', across a segment of packing was calculated at 40 and 60 °C. The absorber diameter and height were set to 42.7 and 3 cm, respectively. The number of stages was set to two (minimum) and Flexipac 2Y and the counter-current flow model was used. In the Aspen Plus® flow sheet, a pseudo stream was taken from each segment and flashed at the inlet liquid temperature to determine the equilibrium partial pressure of CO_2 of the solution. The potassium carbonate, piperazine, and water concentration of the solution was maintained constant while the inlet CO_2 concentration was varied. The k_g' was calculated taking the flux of CO_2 calculated by RateSep™ and dividing the interfacial area calculated by RateSep™

for the segment and the CO_2 partial pressure driving force and is given by the following equation:

$$k_g' = \frac{N_{CO_2}}{Area \cdot (P_{CO_2,\inf} - P_{CO_2}^*)} \tag{4.135}$$

where N_{CO_2} is the flux of CO_2 at each segment calculated by RateSep™ under **Interface Profiles|Mass Transfer|CO_2**. *Area* is the interfacial area calculated for each segment under **Interface Profiles|Interfacial Area.** $P_{CO_2,\inf}$ is the partial pressure of CO_2 at the interface, which is calculated from y_{CO2} under the **Interface Profiles|Compositions|Vapor** tab and $P_{CO_2}^*$ is calculated from the flash calculation of the pseudo stream at the specified inlet liquid temperature of 40 or 60 °C. It was assumed that the Cullinane (2005) kinetics were consistent with the Aspen Plus® VLE model and no attempts were made to correct for the VLE deviations observed by Hilliard.

The RateSep™ rates were five times faster than the Cullinane (2005) FORTRAN model and the wetted wall column results. The Cullinane FORTRAN model assumes that all of the ions have the same diffusion coefficient as $PZCOO^-$ and use the Wilke–Chang correlation to estimate the diffusivity. Cullinane also applied a correction term of 1.51 to the ionic diffusivities. In RateSep™, the diffusivities of the ion species were not assumed to be the same and the Nernst–Hartley equation was used to calculate diffusivities. Adjustments were made to the density and viscosity model in Aspen Plus®, which slightly affect the predicted diffusivities. The diffusivities predicted by Aspen Plus® were reasonable and do not appear to be source of the discrepancy.

The reverse kinetic reactions for Cullinane assume that there is no change in activity coefficient and water concentration from the gas–liquid interface to the bulk solution, whereas RateSep™ calculates the activities of each species across

the film. The Cullinane model uses eddy diffusivity theory, which has a square root dependence, to model the mass transfer. RateSep™ uses two-film theory, which does not have square root dependence. Finally, the Henry's constant for CO_2 and the activity coefficients are calculated differently. The Aspen Plus® activity coefficient (Gamus) for CO_2 varies by a factor of five over a temperature range from 25 to 65 °C.

To account for this discrepancy, the pre-exponential factor for the forward and reverse kinetic reactions were multiplied by a factor of 0.2. The predicted k_g' results for the 5 m K^+/2.5 m PZ solution are shown in Figure 4-22. The k_l for both models was approximately 0.01 cm/s. The pre-exponential factors in RateSep™ were adjusted until the FORTRAN and RateSep™ predictions matched for the 60 °C points. The predicted RateSep™ points at 40 °C were approximately 40% lower than the FORTRAN points at 40 °C. It was assumed that a more accurate representation of absorber performance was achieved at the higher temperatures.

The activity-based kinetics calculated for the 6.4 m K^+/1.6 m PZ solution was entered into RateSep™ and a similar k_g' analysis was performed. The pre-exponential factors for the 6.4 m K^+/1.6 m PZ reactions were also multiplied by a factor of 0.2. Figure 4-23 shows that at low partial pressures of CO_2 and a temperature of 60 °C, the predicted RateSep™ k_g' is 40% higher than the FORTRAN model, while at partial pressures greater than 2500 Pa, the normalized flux is lower than the FORTRAN model. The RateSep™ 40 °C curve is consistently lower than the FORTRAN values. Finally, the figure shows that at partial pressures beyond 1000 Pa, a precipitous drop occurs, similar to that observed in the wetted wall column data (Cullinane, 2002). This trend was not captured by the FORTRAN model or by the RateSep™ model for the 5 m K^+/2.5 m PZ solution.

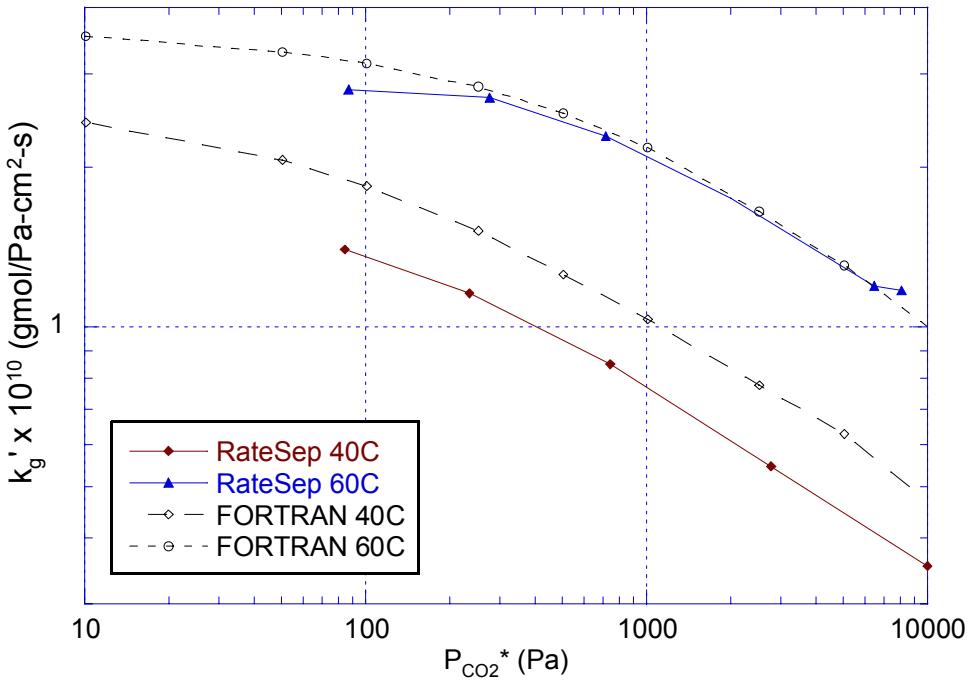

Figure 4-22. Normalized Flux of CO_2 Predicted by RateSep™ for 5 m K^+/2.5 m PZ Solution at 40 and 60 °C ($k_{l,FORTRAN}$ = 0.01 cm/s, $k_{l,RateSep}$ = 0.1-0.15 cm/s)

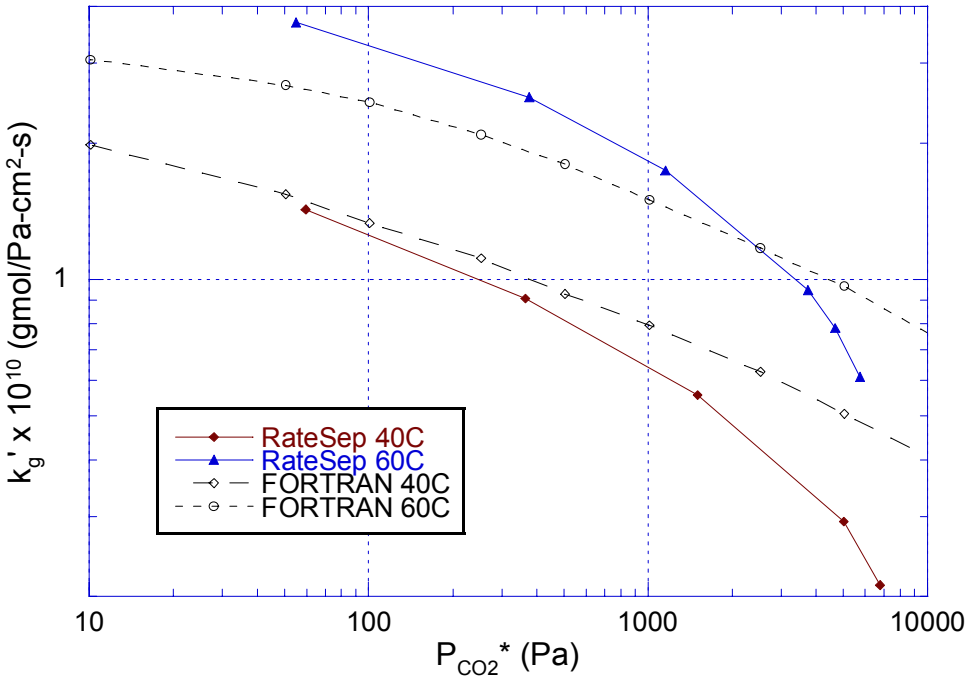

Figure 4-23. Normalized Flux of CO_2 Predicted by RateSep™ for 6.4 m K^+/1.6 m PZ at 40 and 60 °C ($k_{l,FORTRAN}$ = 0.01 cm/s, $k_{l,RateSep}$ = 0.1-0.15 cm/s)

4.4.7 RateSep™ Convergence

The convergence of RateSep™ was facilitated by providing estimates to the top and bottom stages of the absorber (Aspen Technology Inc., 2006). The Aspen Plus® help file recommended that the temperature be under-estimated for the top stage and over-estimated for the bottom by a few degrees. In the RateSep™ simulations, the top stage temperature was set to 38 °C and the bottom stage was set 2 degrees higher the liquid outlet temperature of the pilot plant. In addition, under **RadFrac|Convergence**, Absorber=YES was selected. The inlet gas and liquid streams were specified using the ON-STAGE feed convention.

4.5 SUMMARY

A rate-based absorber model was developed in Aspen Plus® RateSep™ for the potassium carbonate and piperazine system. Activity-based kinetic parameters for the 5 m K^+/2.5 m PZ and 6.4 m K^+/1.6 m PZ solution were derived from the Cullinane (2005) rate model. The heat of absorption predicted by Aspen Plus® was corrected by calculating the heat of formation and heat capacity parameters of the piperazine ions from the equilibrium equations. Density and viscosity parameters for the potassium carbonate and piperazine solution were regressed using Aspen Plus® DRS. The pre-exponential factors for the kinetic reactions of the 5 m K^+/2.5 m PZ and 6.4 m K^+/1.6 m PZ solution were adjusted by a factor of 0.2. The optimal number of segments was determined to be approximately 70 segments, but only 50 segments were used in the simulations to reduce the computational time. A film ratio of six and three film segments were used to optimize the simulation process. Aspen Plus® Data-Fit was used to reconcile the pilot plant data and validate the RateSep™ absorber model. The results are presented in the next chapter.

Chapter 5: Absorber Modeling Results and Data Reconciliation

Aspen Plus® Data-Fit was used to perform the simultaneous regression of the interfacial area factor and absorber heat loss and the reconciliation of pilot plant data from Campaigns 2 and 4. The mole component flow rates, inlet and outlet temperatures for the gas and liquid, and the temperature profile across the column were used as the parameters for Data-Fit. Sensitivity analyses were performed to determine which parameters from the experimental data set should be adjusted by Data-Fit. The lean loading for the experimental data points from the pilot plant were adjusted downward by 10% due some inconsistencies with the Hilliard (2005) VLE model. The validated RateSep™ absorber model was used to analyze of absorber design and performance.

5.1 ASPEN PLUS® DATA-FIT

In Aspen Plus®, the simulation models can be fitted to plant and laboratory data using the Data-Fit regression package. Data-Fit is located under **Model Analysis Tools|Data Fit**. It can be used to fit the data to a simulation model by adjusting the model input parameters. Data-Fit can be also used to simultaneously reconcile the measured data. Data-Fit performs a least squares fit between the measured data and model predictions.

Data-Fit can be used to fit either measured point data or profile data. When profile data is provided, Data-Fit performs a regression analysis of the coefficients for a kinetic model from the bench-scale data. When point data is provided, Data-Fit can fit a simulation model to plant data, reconcile plant data

to match the model, estimate missing measurements, and identify poor measurements. In this work, Data-Fit was used to simultaneously reconcile pilot plant data and validate the absorber model.

The data set to be regressed must first be entered under **Data Fit|Data Set** before a regression case can be specified. In the first row of Data Set, the type of data is specified: Input or Result variable. In the second row, the standard deviation for each measurement is specified. The standard deviation can be entered as an absolute value or as a percentage. For an Input variable, if a zero standard deviation is specified, the measurement is not adjusted by Data-Fit and used as an exact measurement. For values greater than zero, the measurement is adjusted along with the results to match the fitted model. For a Result variable, the standard deviation that is specified must be greater than zero. If a zero standard deviation is specified, it is not included in the regression.

Point data is entered in the row below the standard deviation specification. If measurements for Result variables are not available, it can be left blank and Data-Fit will estimate it. In this work, the molar flow rates of the apparent components for the liquid and vapor phases were entered (Figure 5-1). The inlet temperature and pressure for the gas and liquid streams were also entered. In addition, the temperature profile across the absorber and the outlet liquid temperature was specified. Standard deviations were assigned to each of the input values.

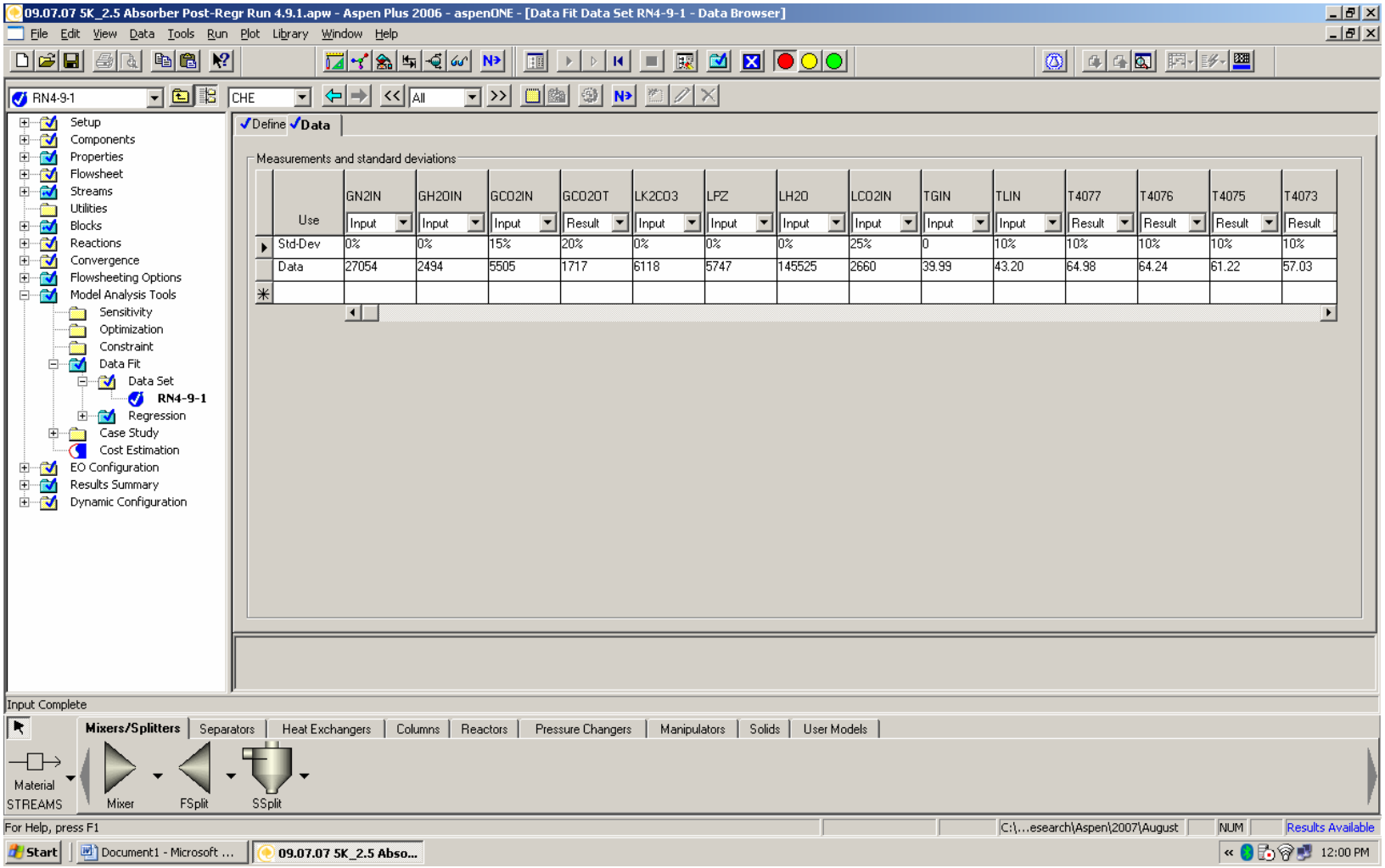

Figure 5-1. Example of Input for Aspen Plus® Data Fit.

After the data set has been specified, the Data-Fit regression case can be setup. Both point and profile data can be regressed in the same case. The regression case requires the input of an estimated parameter or a reconciled input where the standard deviation is greater than zero. Data-Fit can be used to estimate an unlimited number of parameters. The numerical formulation for the least squares regression analysis that Data-Fit performs is given by:

$$\underset{X_p, X_{ri}}{Min} \frac{1}{2} \sum_{i=1}^{N_{sets}} \left(W_i \times \left(\sum_{j=1}^{N_{\exp i}} (\omega_1 + \omega_2) \right) \right) \tag{5.1}$$

where

$$\omega_1 = \sum_{l=1}^{N_{ri}} \left(\frac{X_{mri} - X_{ri}}{\sigma_{X_{mri}}} \right)^2 \tag{5.2}$$

$$\omega_2 = \sum_{m=1}^{N_{rr}} \left(\frac{X_{mrr} - X_{rr}}{\sigma_{X_{mrr}}} \right)^2 \tag{5.3}$$

where N_{sets} is the number of data sets specified on the **Regression|Specification** sheet, $N_{\exp i}$ is the number of experiments in data set *i*, N_{ri} is the number of reconciled input variables, N_{rr} is the number of measured results variables, W_i is the weight for data set *i* specified under **Regression|Specification**, X_p is the vector of varied parameters, X_{mri} is the measured values of the reconciled input variables, X_{ri} is the calculated values of the reconciled input variables, X_{mrr} is the measured values of the results variables, X_{rr} is the calculated values of the results variables, and σ_X is the standard deviation specified for the measured variables. Adjustments made to X_p and X_{ri} variables are subject to the specified lower and upper bounds. The lower and upper bounds are calculated by the following equations:

$$Lower\ Bound = MV - (F_B \times \sigma) \tag{5.4}$$

$$Upper\ Bound = MV + (F_B \times \sigma) \tag{5.5}$$

where MV is the measured value, F_B is the bound factor, and σ is the standard deviation. The bound factor has a default value of 10, but can be changed in the **Regression|Convergence** sheet. The reconciled input variables are adjusted to minimize the error of the sum of squares for each experimental point independently.

The Data-Fit problem is considered converged when either the absolute function tolerance, relative function tolerance or X convergence tolerance are satisfied. In the first case, Data-Fit is converged when the objective function value reaches a value that is less than the absolute function. In the second case, the problem converges when the optimizer predicts a maximum possible function reduction of at most the relative function times the absolute value of the function value at the start of the current iteration and if in the last step, no more than twice the predicted function decrease was achieved. Finally, when a step change has a relative change in X less than or equal to the X convergence tolerance and if the step change decreases the objective function by no more than twice the predicted objective function decrease, Data-Fit converges. The default values for the absolute function, relative function, X convergence tolerances are 0.01, 0.002, and 0.002, respectively. Additional Data-Fit convergence parameters can also be specified in the **Regression|Advanced** sheet, but in most cases, is not necessary to change the default parameters (Aspen Technology Inc., 2006).

The sequence for the Data-Fit regression is as follows: Aspen Plus® executes the base-case simulation; the Data-Fit loop is run until it converges or fails to converge; the base-case values of fitted parameters are replaced with the regressed values and the base-case is re-run. After the Data-Fit regression is

executes, it outputs the follow results: chi-square statistics for the fit, final estimates and standard deviations for the estimated parameters, a table of measured values, estimated values, and normalized residues for the data sets, and a table of iteration history of the function results, the varying results and reconciled inputs.

5.2 VAPOR–LIQUID EQUILIBRIUM ADJUSTMENT

Recent CO_2 solubility measurements by Hilliard have found that the vapor–liquid equilibrium data for CO_2 and piperazine/potassium carbonate reported by Cullinane may be incorrect. The vapor pressure of CO_2 reported by Cullinane was higher than Hilliard data. Experimental data from Hilliard shows that the Cullinane VLE data was shifted by approximately 10%on a loading basis or offset by 20 °C on a temperature basis (Figure 5-2).

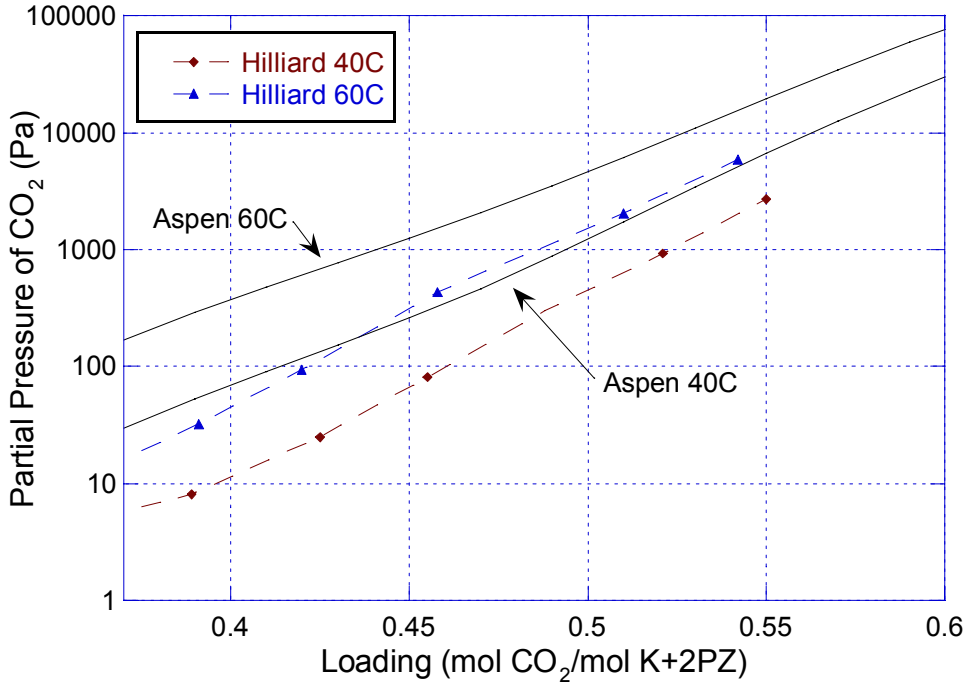

Figure 5-2. Comparison of Hilliard Experimental VLE Data for 5 m K^+/2.5 m PZ at 40 and 60 °C with the Hilliard (2005) Aspen Plus® VLE Model

The Hilliard (2005) K^+/PZ VLE model used in the RateSep™ model was based on the Cullinane VLE data. In this work, the new Hilliard data was assumed to correctly represent the potassium carbonate and piperazine system. Updating the Hilliard (2005) VLE model with the new data is not in the scope of this work. Instead, the experimental loading data from the pilot plant was adjusted downward by 10% to compensate for the errors. Figure 5-3 shows that the results predicted by the Hilliard (2005) Aspen Plus® VLE model and the Hilliard experimental data are more consistent when the loading is shifted downward by 10%.

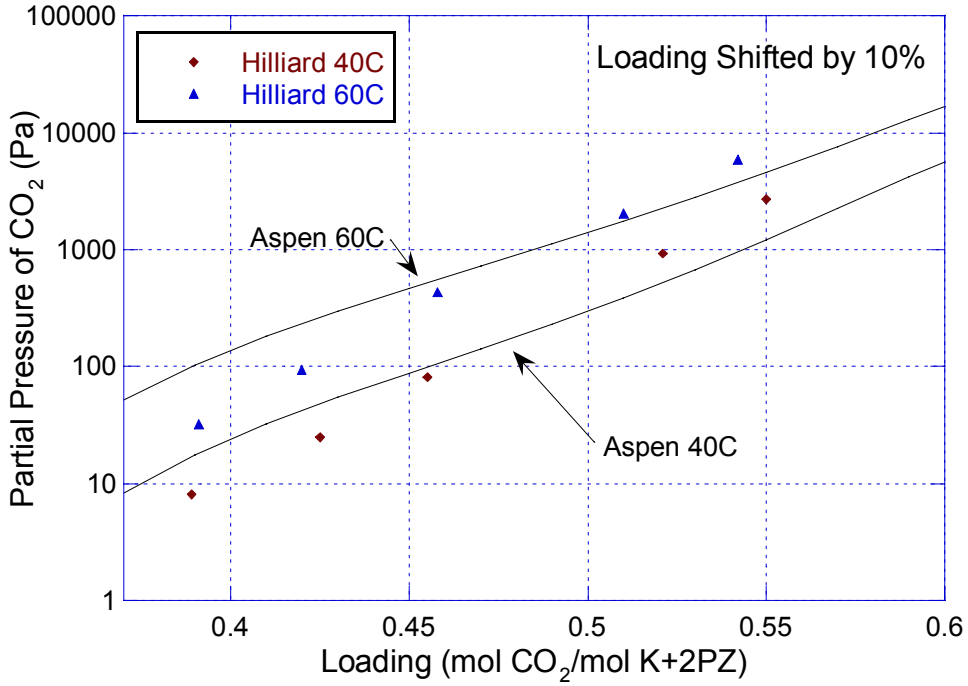

Figure 5-3. Results of Hilliard (2005) Aspen Plus® VLE Model with 10% Loading Adjustment for 5 m K^+/2.5 m PZ VLE Data at 40 and 60 °C

5.3 RATESEP™ SENSITIVITY RESULTS

The Aspen Plus® Data-Fit regression package allows the user to assign standard deviations to each point in the data set. In order to expedite and simply the Data-Fit regression process, a sensitivity analysis was performed to

determine which input variables should be set as constants (standard deviation = zero) and which should be included in the data reconciliation process (non-zero standard deviation). A sensitivity analysis was performed for the following variables: inlet gas and liquid temperatures, inlet gas concentrations of carbon dioxide and water, inlet liquid concentrations piperazine and potassium carbonate, lean loading, heat-loss, effective interfacial area factor, and liquid holdup. The effect of each parameter was quantified based on the variation of the absorber CO_2 removal efficiency. The temperature profile was also plotted to quantify the enthalpy effects on the absorber.

In order to simplify the modeling effort, a value of heat loss was assigned to the entire column for the liquid phase. In Aspen Plus®, the column heat loss is divided by the total number of stages and the same value is assigned to each stage. It should be noted that in the pilot plant, the heat loss will not be distributed evenly across the column due to temperature differences, sections where the column does not contain any packing, and from structural elements on the column such as the support fins, which will enhance heat transfer. The default conditions for each parameter, unless otherwise noted, are listed in Table 5-1. The gas and liquid temperature profile for the base case RateSep™ absorber model simulation is plotted in Figure 5-4.

Table 5-1. Input Specifications of RateSep™ Absorber Model for Sensitivity Analysis (Run 4.4.1 – Campaign 4, 5 m K^+/2.5 m PZ)

Parameter	Value
Inlet CO_2 Gas	16.3 mol%
Inlet H_2O Gas	7.0 mol%
Gas Flow	27,800 mol/hr
K_2CO_3	2.5 molal
PZ	2.5 molal
CO_2 Loading	0.405 mol CO_2/(mol K+ + 2 mol PZ)
Liquid Flow	158,700 mol/hr
$T_{Gas\ In}$	40 °C
$T_{Liquid\ In}$	40 °C
Column ID	0.43 m
Packing Type	Flexipac 2Y
Specific Area of Packing	225 m^2/m^3
Height of Packing	6.096 m
Intf Area Model	Rocha-Bravo-Fair 1992
Packing Area Factor	2.7 (161 m^2/m^3)
Heat Loss	15,000 W
Liquid Holdup	1% Free Volume

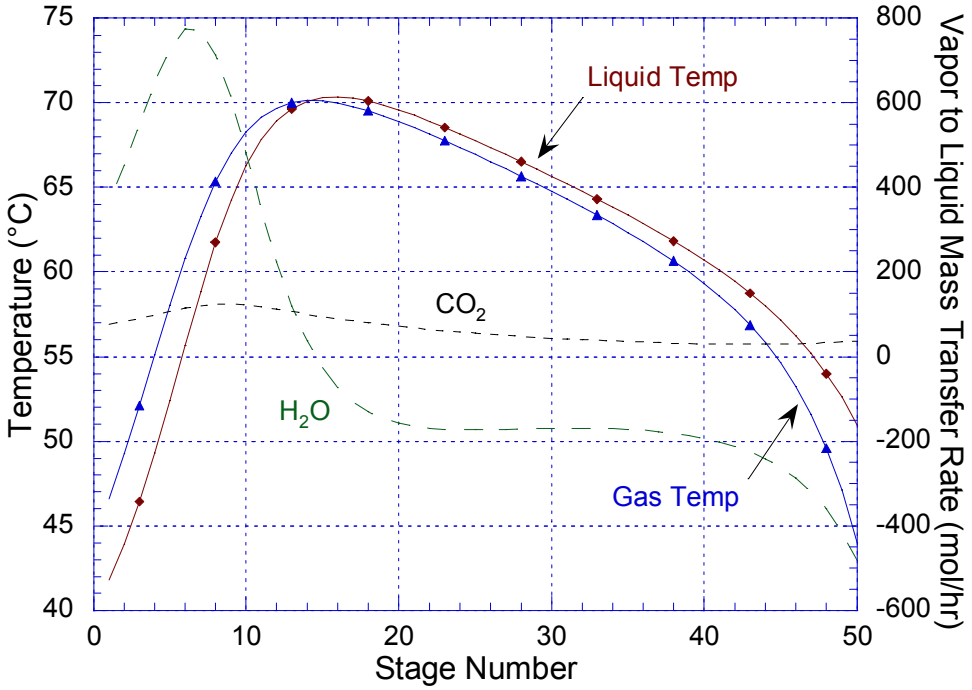

Figure 5-4. Gas and Liquid Temperature Profile and Vapor Phase Mass Transfer Rate of CO_2 and H_2O for Base Case of Sensitivity Analysis (Positive for Mass Transfer from Vapor to Liquid, Top of Absorber = Stage No. 1)

Figure 5-5 is a McCabe–Thiele plot of the base case RateSep™ absorber sensitivity analysis. The mole fraction of CO_2 in the vapor phase calculated by RateSep™ was converted to a CO_2 partial pressure and used as the operating line. The equilibrium line was generated by taking a pseudo-stream at each stage and performing a flash calculation at the liquid temperature of the corresponding stage. The partial pressure of CO_2 calculated by pseudo-stream flash block was used as the equilibrium line. The figure shows that the operating line approaches 70% of equilibrium near stage 30.

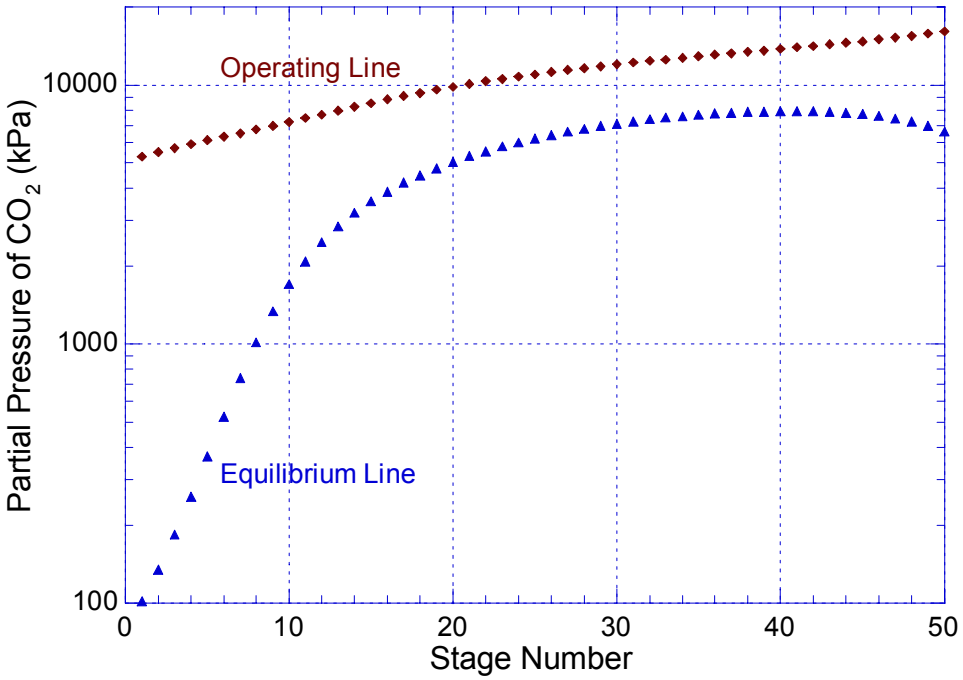

Figure 5-5. McCabe–Thiele Plot for Base Case of Sensitivity Analysis (Top of Absorber = Stage No. 1)

The liquid composition across the absorber column for the base case sensitivity analysis is shown in Figure 5-6. The figure shows that the concentration of CO_3^{2-} and $PZCOO^-$ decreases by approximately one-third from the top to the bottom of the column. While the concentration of HCO_3^- and $PZ(COO^-)_2$ both increase by a factor of three from the top to the bottom of the

column. The concentration of piperazine decreases by a factor of 7 across the column to almost zero at the bottom of the column and H^+PZCOO^- increases by a factor of 4.5. The concentration of PZH^+ remains low and relatively constant across the entire absorber column. The reaction with PZ and CO_3^{2-} will dominate the lean end of the column and reaction with $PZCOO^-$ and CO_3^{2-} will dominate the rich end.

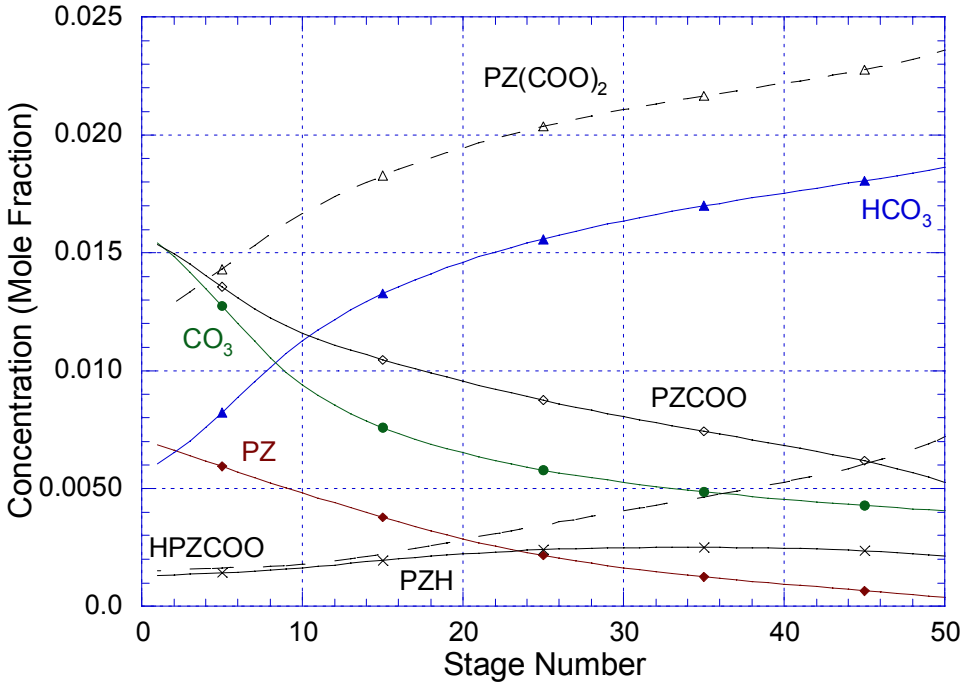

Figure 5-6. Liquid Composition for Base Case of Sensitivity Analysis (Top of Absorber = Stage No. 1)

A sensitivity analysis was performed on the absorber column heat loss. The column heat loss for the liquid phase was varied between 0 to 40,000 watts. Figure 5-7 shows that the CO_2 removal efficiency increases by approximately 0.05 as the heat loss increases from 0 to 40,000 watts. The improvement in performance with increased heat loss is most likely due to a pinch point in the absorber, where a maximum would occur at the highest temperatures with zero heat loss.

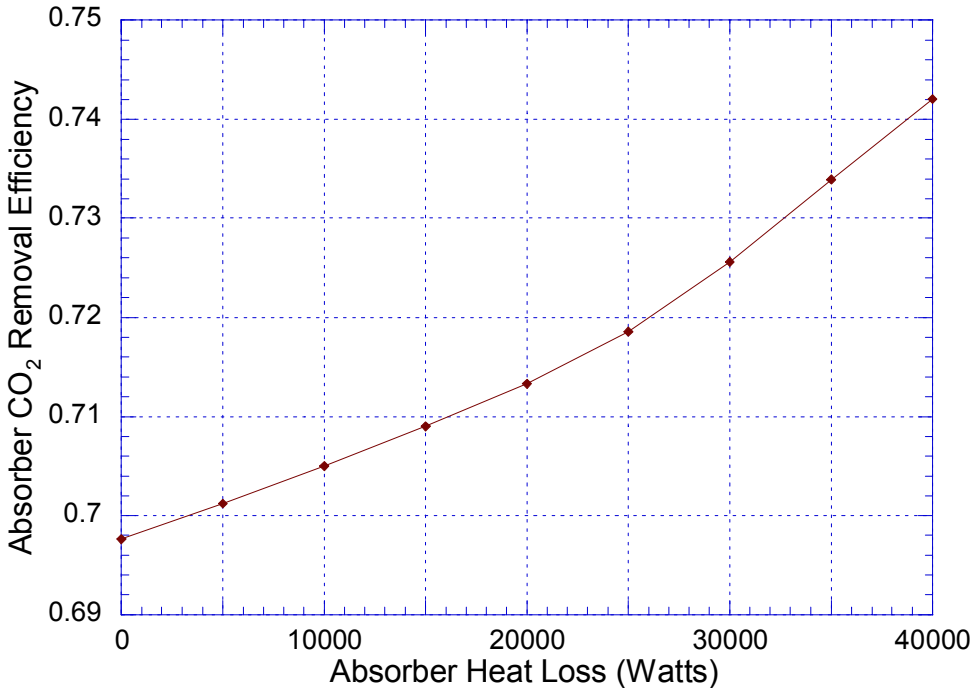

Figure 5-7. Absorber Performance with Heat Loss Adjustment (5 m K^+/2.5 m PZ, Loading = 0.40, Area Factor = 2.7, Holdup = 1% Free Volume)

The temperature profile for several values of heat loss is shown in Figure 5-8. The figure shows that with no heat loss, the maximum temperature bulge is attained, reaching approximately 72 °C. As the heat loss increases, the magnitude of the temperature bulge decreases and the location of the maximum temperature moves from the top of the column towards the bottom. Dugas (2006) assumed that the heat loss from the absorber was 25% of the stripper heat loss, which was determined to be approximately 15,000 W.

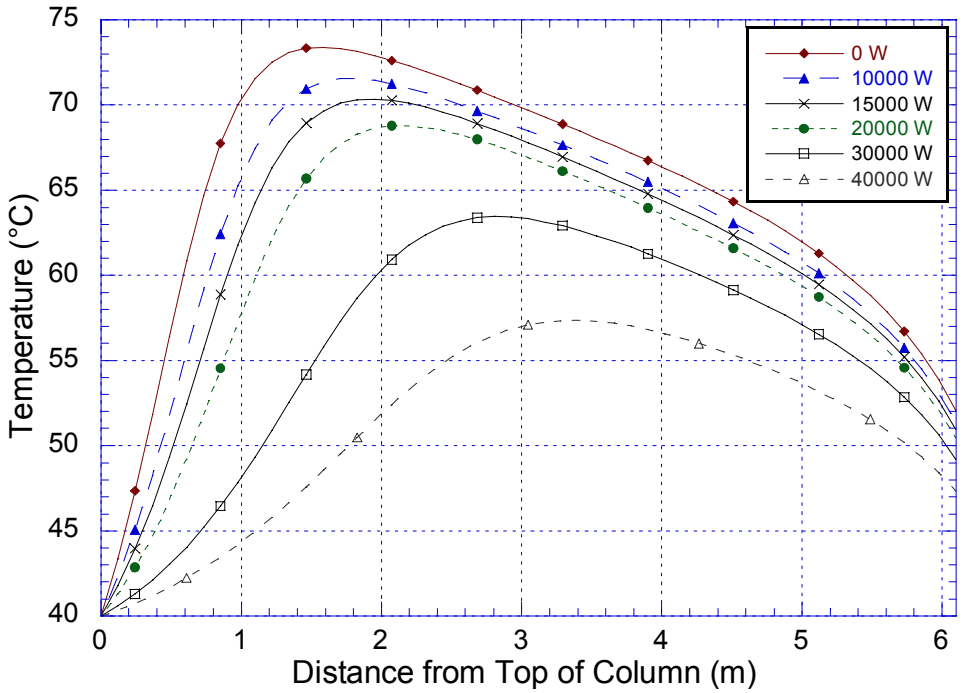

Figure 5-8. Effect of Heat Loss on Absorber Liquid Temperature Profile (5 m K^+/2.5 m PZ, Loading = 0.40, Area Factor = 2.7, Holdup = 1% Free Volume)

The liquid heat capacity initially predicted by RateSep™ was approximately 25 cal/mol-K. Preliminary attempts to reconcile the temperature profile of the pilot plant absorber column were unsuccessful. Once heat capacity data became available, the data was used to regress heat capacity parameters for potassium. The results of the DRS regression fit for liquid heat capacity are given in the previous chapter. The corrected heat capacity is approximately 17–18 cal/mol-K. At a heat capacity of 17.1 cal/mol-K, the maximum temperature is approximately 70 °C and located in the upper third of the column (Figure 5-9). As the value of the liquid heat capacity increases, the magnitude of the temperature bulge decreases and the location moves down the absorber column. The correct prediction of liquid heat capacity is required to properly model the temperature profile.

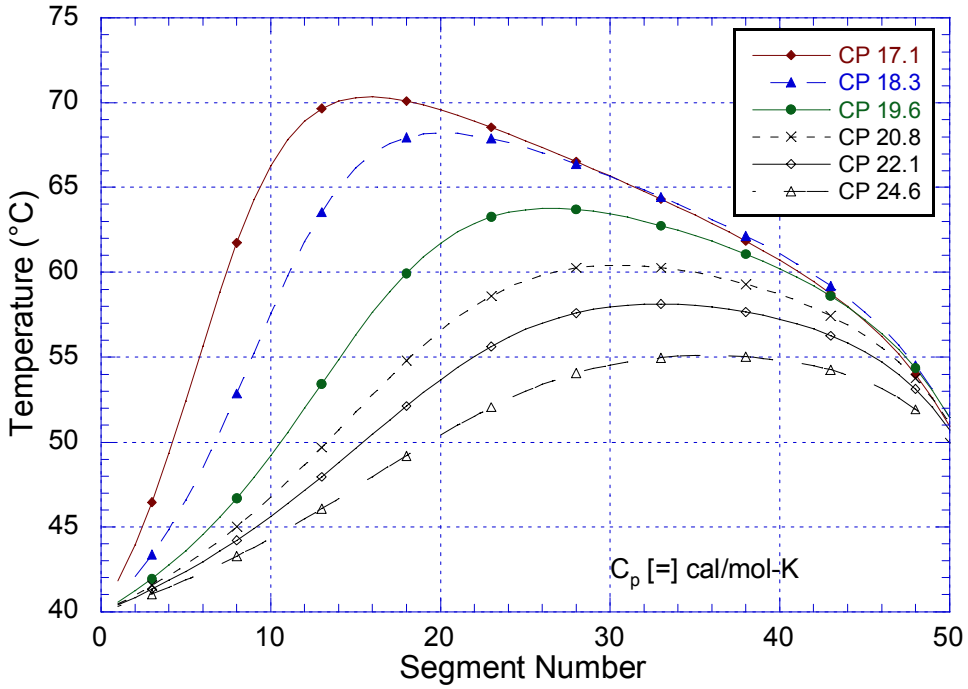

Figure 5-9. Effect of Liquid Heat Capacity on Liquid Temperature Profile (5 m K^+/2.5 m PZ, Loading = 0.40, Area Factor = 2.7, Holdup = 1% Free Volume)

Although the value of the liquid heat capacity has a profound effect on the temperature profile, it only has a minor effect on absorber performance (Figure 5-10). The figure shows that the when the liquid heat capacity changes from 18 to 25 cal/mol-K, the CO_2 removal rate increases from 0.706 to 0.735. In the preliminary attempts to match the pilot plant data, the CO_2 removal rates could be matched relatively well, but the temperature profile could not be fitted properly.

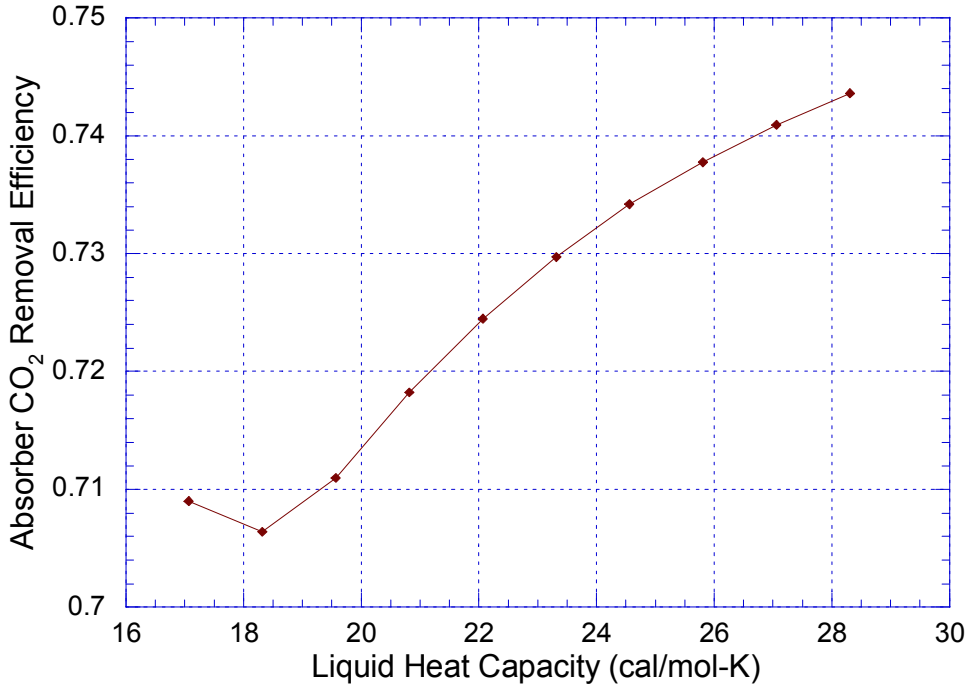

Figure 5-10. Effect of Liquid Heat Capacity on Absorber Performance (5 m K^+/2.5 m PZ, Loading = 0.40, Area Factor = 2.7, Heat Loss = 15,000 W)

A sensitivity analysis was performed on the effective interfacial area by adjusting the interfacial area factor in RateSep™. The Rocha–Bravo–Fair (1996) model for Flexipac 2Y structured packing was used in the analysis. It should be noted that the predictions from the Rocha–Bravo–Fair model do not match the effective area data obtained by UT SRP. Figure 5-11 shows that as the interfacial area factor increases from 0.5 to 5, the CO_2 removal efficiency approaches a maximum near at approximately 75%. The effective interfacial area is related the kinetic reaction rates in the film layer.

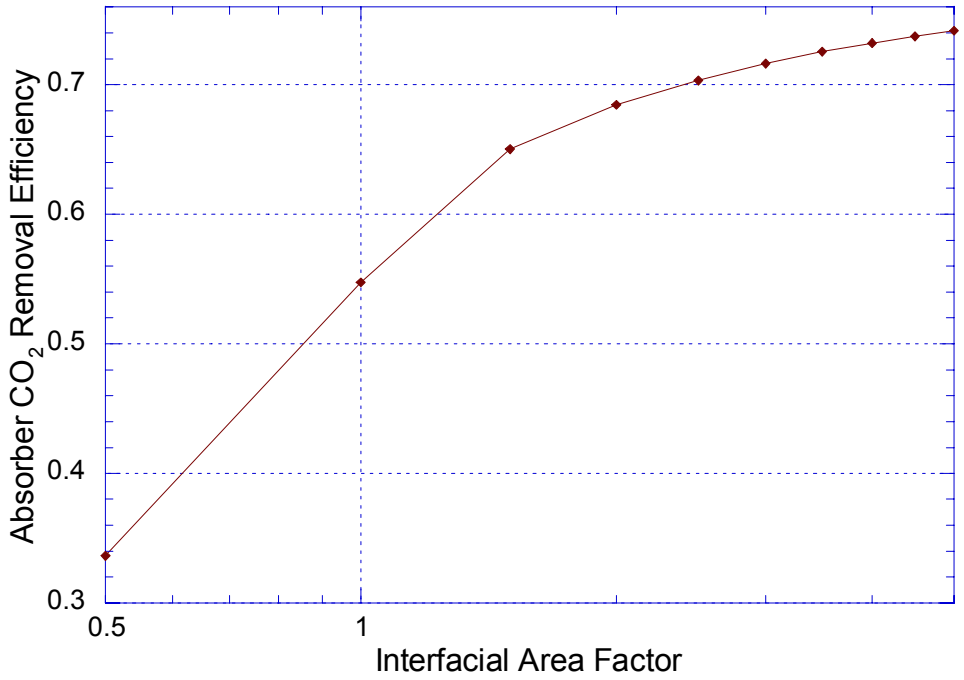

Figure 5-11. Effect of Interfacial Area on Absorber Performance (5 m K^+/2.5 m PZ, Loading = 0.40, Holdup = 1%, Heat Loss = 15,000 W)

As the area factor increases from 0.5 to 5, the location of the temperature bulge moves from the bottom of the column and to the top of the column (Figure 5-12). An increase in interfacial area results in more absorption of CO_2 and an increase in magnitude of the maximum temperature. The maximum temperature for an area factor was approximately 45 °C. An area factor of five results in a maximum temperature of 73 °C. These results show that the effective interfacial area is important for determining absorber performance and obtaining the correct temperature profile for modeling purposes.

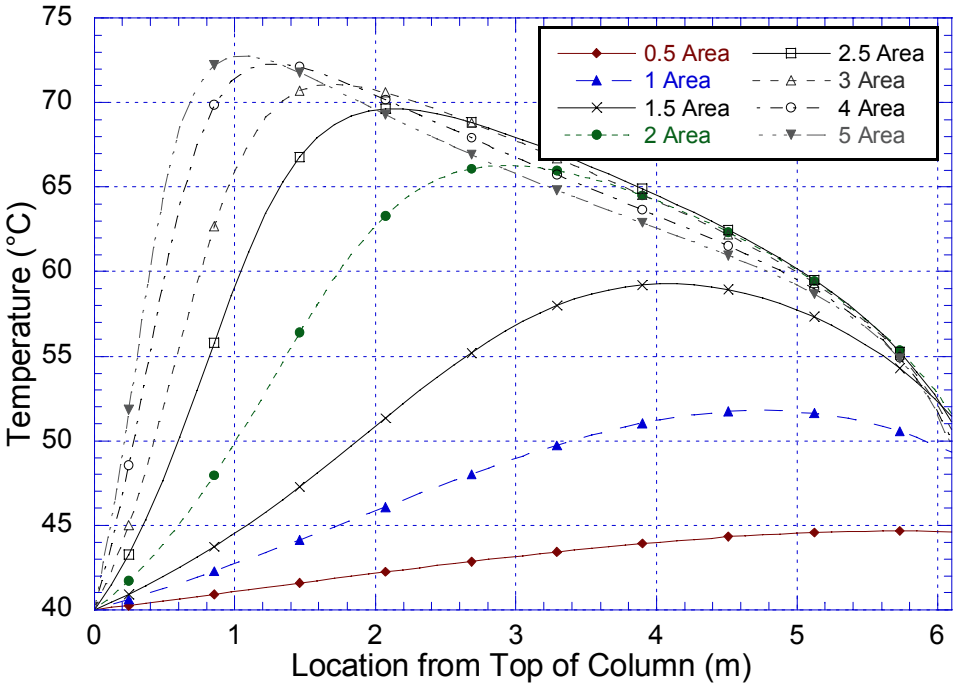

Figure 5-12. Effect of Interfacial Area on Absorber Liquid Temperature Profile (5 m K^+/2.5 m PZ, Loading = 0.40, Holdup = 1%, Heat Loss = 15,000 W)

A sensitivity analysis was performed on the liquid holdup of the absorber column. The liquid holdup controls the amount of reaction in the bulk solution. In a packed column, the liquid holdup is expected to be approximately 3–5%. Figure 5-13 shows that as the liquid holdup is varied between 3 and 5% of free volume, the absorber performance increases from approximately 71.7 to 72.4%, which is insignificant. However, the liquid holdup analysis was performed at a point where increases to the wetted area had approached a plateau and additional wetted area had a minor affect on CO_2 removal.

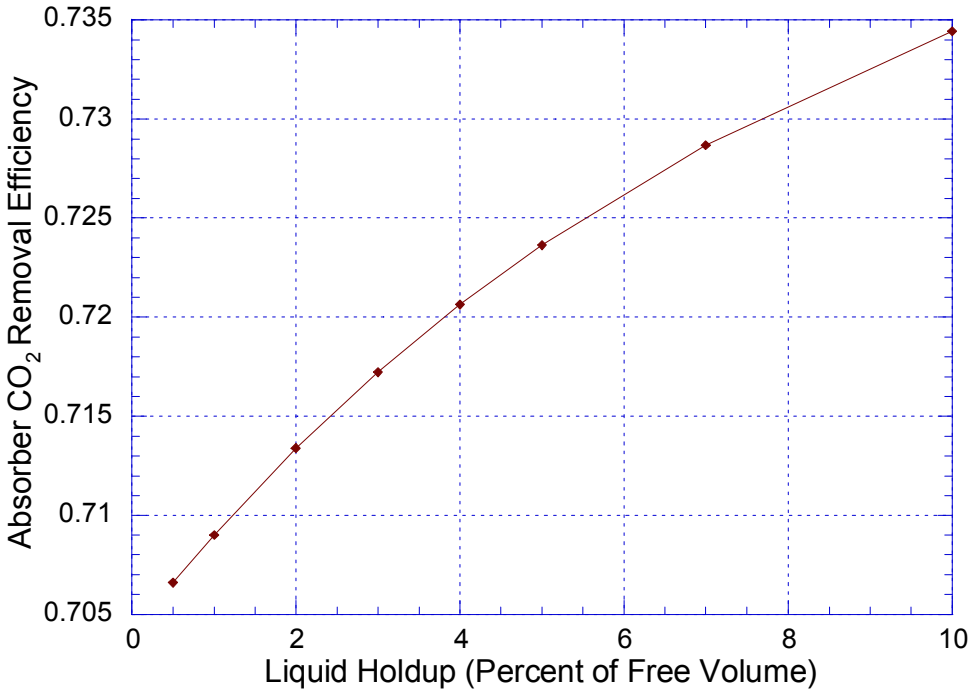

Figure 5-13. Effect of Liquid Holdup on Absorber Performance (5 m K^+/2.5 m PZ, Loading = 0.40, Area Factor = 2.7, Heat Loss = 15,000 W)

Figure 5-14 shows that the temperature profile of the absorber is not affected by the value of the liquid holdup. According to Aspen Plus®, a small liquid holdup typically allows RateSep™ to converge easier. Since the absorber performance only increased marginally from 1 to 3% and did not affect the temperature profile, a liquid holdup of one percent by free volume was used in the simulations.

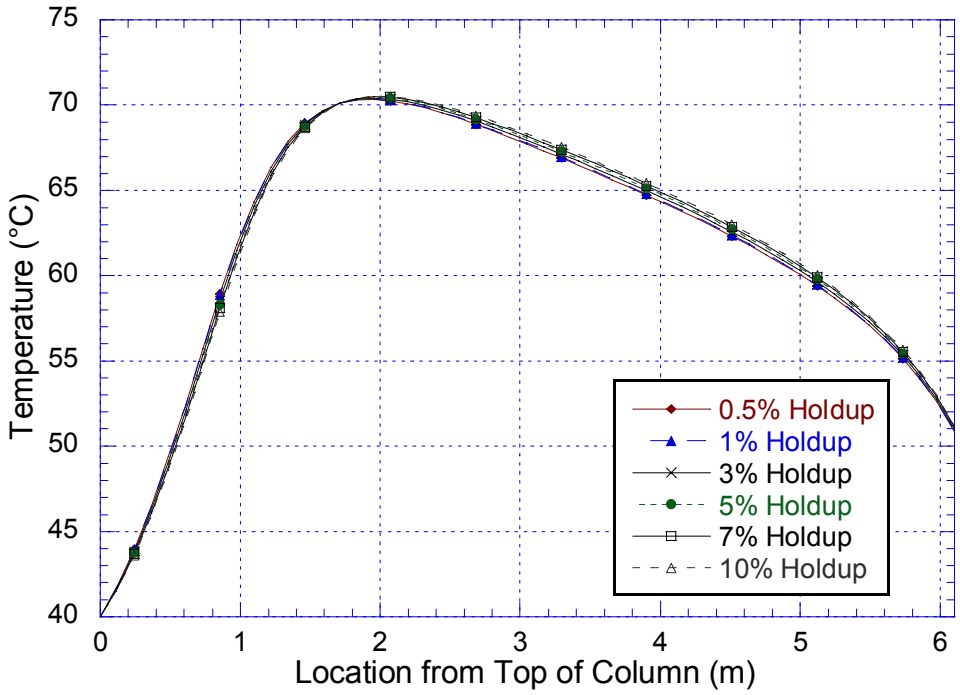

Figure 5-14. Effect of Liquid Holdup on Absorber Liquid Temperature Profile (5 m K^+/2.5 m PZ, Loading = 0.40, Area Factor = 2.7, Heat Loss = 15,000 W)

Figure 5-15 shows that the lean loading of the absorber is another critical parameter for determining absorber performance. As the lean loading increases from 0.38 to 0.50 mol CO_2/(mol K^+ + 2 mol PZ), the CO_2 removal efficiency dramatically decreases from approximately 85 to 25%. In the absorber model, the lean loading was shifted downward by 10% to account for the measurement errors in the vapor–liquid equilibrium of the potassium carbonate and piperazine system discovered by Hilliard.

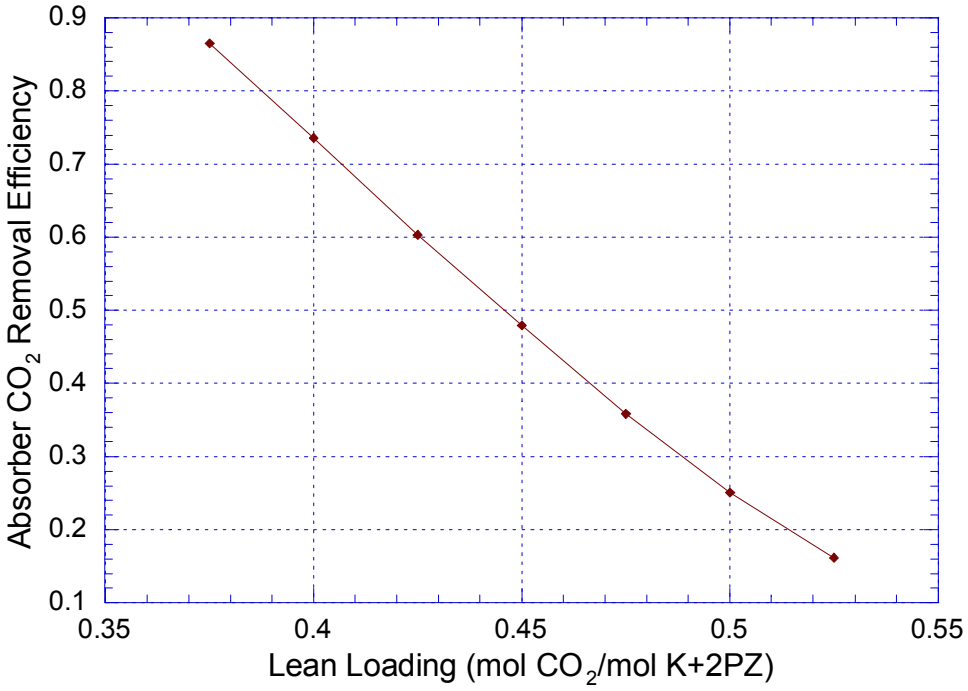

Figure 5-15. Effect of Lean Loading on Absorber Performance (5 m K^+/2.5 m PZ, Area Factor = 2.7, Holdup = 1%, Heat Loss = 15,000 W)

A lean solution will absorb more CO_2 than a richer solution. The absorption of CO_2 into the liquid results in a pronounced temperature bulge in the absorber (Figure 5-16). At a lean loading of 0.38 mol CO_2/(mol K^+ + 2 mol PZ), the temperature profile reaches a maximum of 75 °C. A lean loading of 0.45 mol CO_2/(mol K^+ + 2 mol PZ) results in a maximum temperature of 54 °C. The figure also shows that when the amount of CO_2 that is absorbed decreases, the location of the temperature bulge moves from the top of the column towards the bottom.

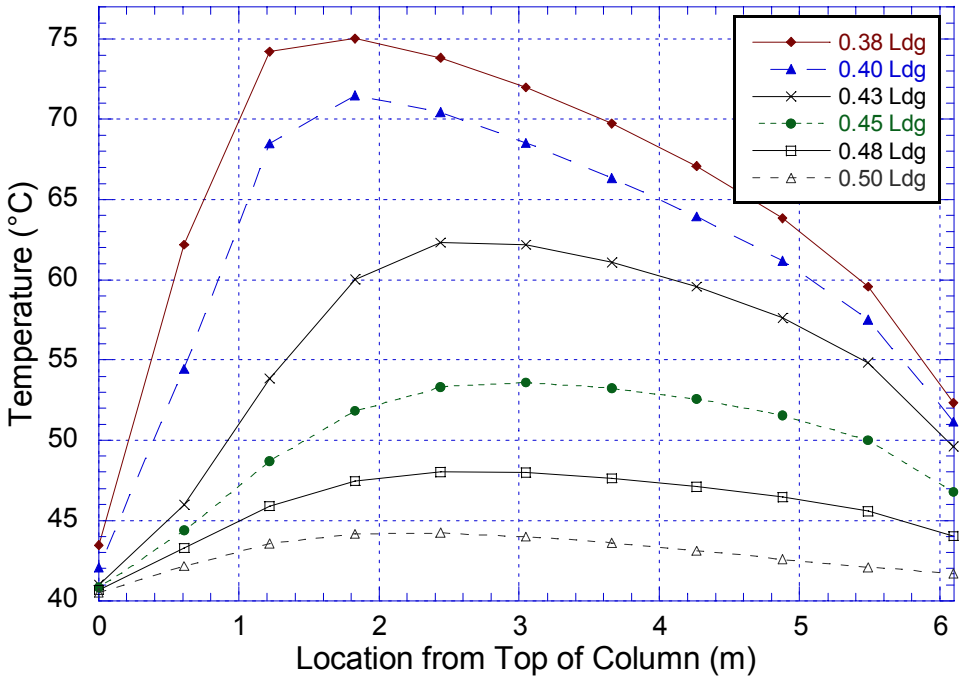

Figure 5-16. Effect of Lean Loading on Absorber Liquid Temperature Profile (5 m K^+/2.5 m PZ, Area Factor = 2.7, Holdup = 1%, Heat Loss = 15,000 W)

Figure 5-17 shows that as the concentration of piperazine and potassium carbonate is increased, the CO_2 removal rate in the absorber increases. The plot shows that absorber performance is more sensitive to changes in the piperazine concentration. When the concentration of piperazine increases from 2.4 to 2.5 mol PZ/kg H_2O, the CO_2 removal rate increases from 67 to 71%. For K_2CO_3, a concentration change from 2.4 to 2.5 mol K_2CO_3/kg H_2O, increases the removal efficiency from 69 to 71%. The results of the ion chromatograph analysis for piperazine and potassium concentration had a precision of approximately ±10%, which may contribute additional errors in the modeling process.

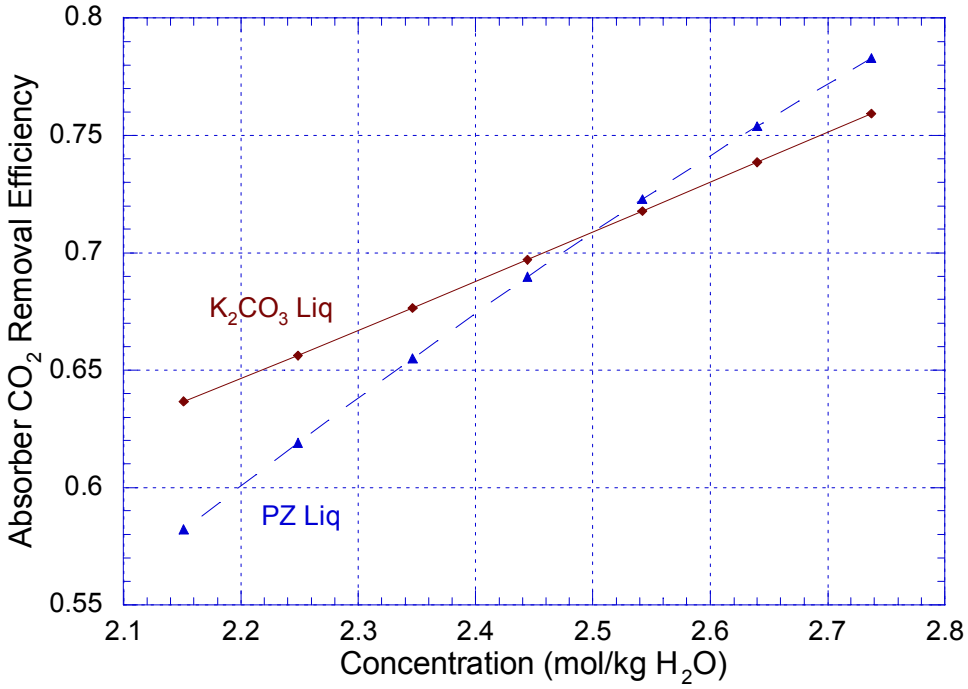

Figure 5-17. Effect of Piperazine and Potassium Carbonate Concentration on Absorber Performance (5 m K^+/2.5 m PZ, Area Factor = 2.7, Holdup = 1%, Heat Loss = 15,000 W)

The temperature profiles of the absorber for the various concentrations of piperazine are shown in Figure 5-18. The figure shows that as the concentration of piperazine increases from 2.15 to 2.74 mol PZ/kg H_2O, the maximum of the temperature bulge increases from 63 to 73 °C. The location of the temperature bulge also slightly moves up the column with an increase in piperazine concentration due to an increased CO_2 absorption rate.

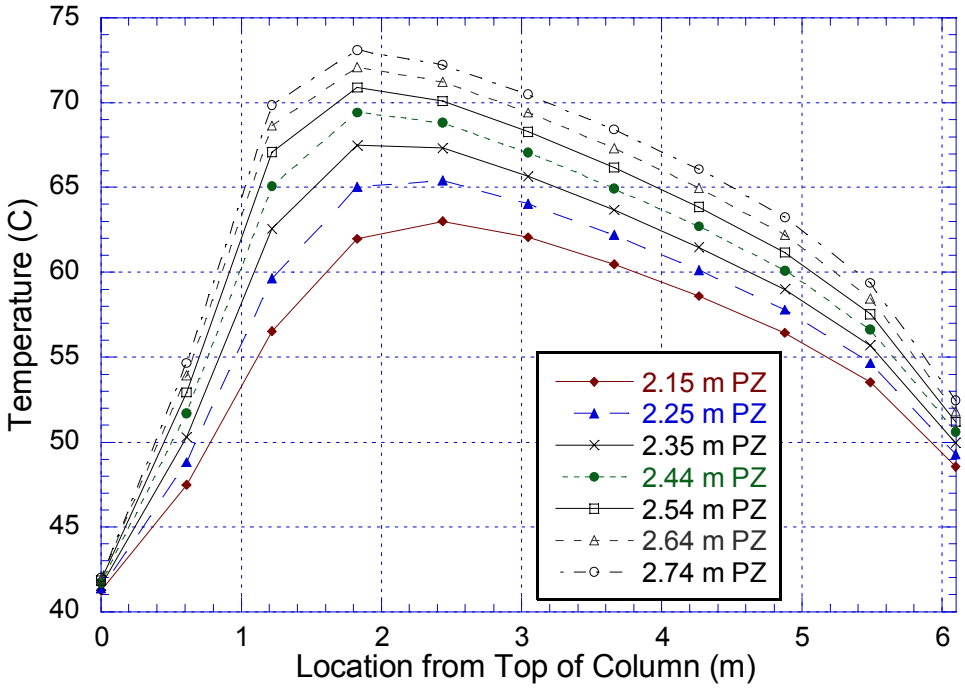

Figure 5-18. Effect of Piperazine Concentration on Absorber Liquid Temperature Profile (5 m K^+/2.5 m PZ, Area Factor = 2.7, Holdup = 1%, Heat Loss = 15,000 W)

The absorber temperature profiles for several concentrations of potassium carbonate are shown in Figure 5-19. The figure shows that as the concentration of potassium carbonate increases from 4.30 to 5.48 mol K^+/kg H_2O, the magnitude of the temperature bulge increases from 66 to 73 °C. The location of the temperature bulge also slightly moves up the column from 2.5 m to 1.8 m. The increase in the temperature bulge indicates an increase in CO_2 absorption rate.

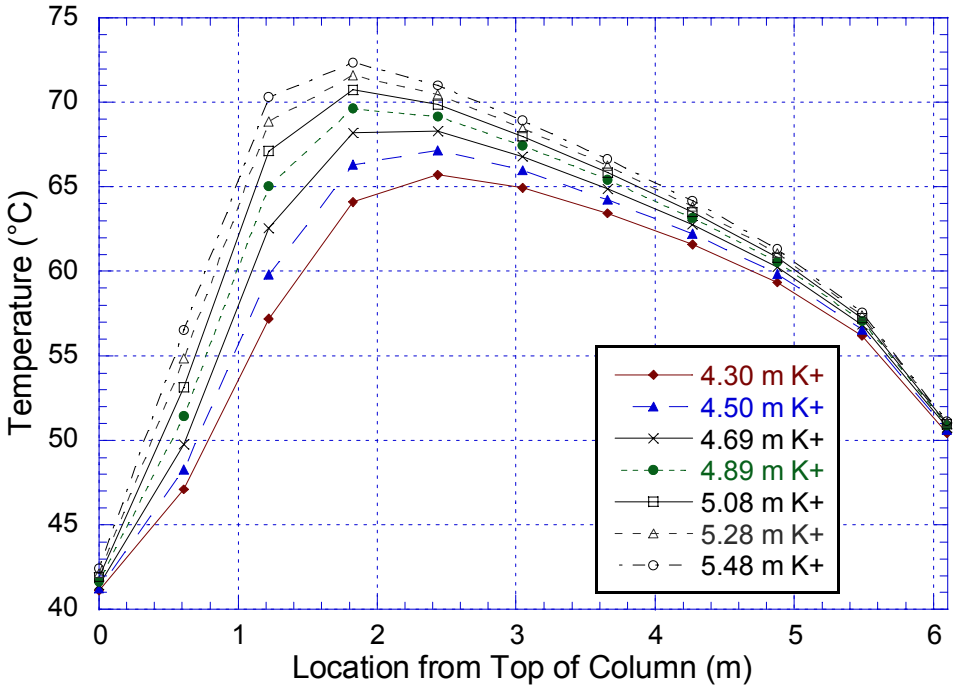

Figure 5-19. Effect of Potassium Concentration on Absorber Liquid Temperature Profile (5 m K^+/2.5 m PZ, Area Factor = 2.7, Holdup = 1%, Heat Loss = 15,000 W)

The effect of inlet CO_2 and H_2O gas concentration on CO_2 removal in the absorber was examined (Figure 5-20). The figure shows that the inlet water gas concentration has a slight effect on absorber performance. The figure also shows that as the inlet CO_2 gas concentration increases from 1 to 5%, the CO_2 removal efficiency reaches a maximum. As the inlet gas concentration increases from 10 to 20% CO_2, the removal efficiency drops precipitously from 91 to 59%.

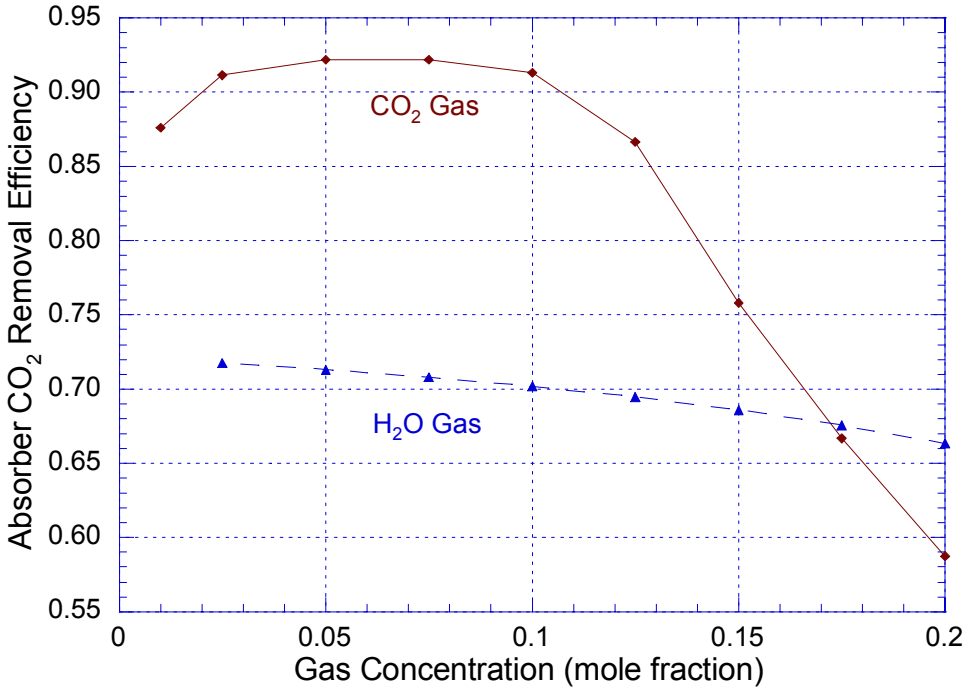

Figure 5-20. Effect of Inlet CO_2 and H_2O Gas Concentration on Absorber Performance (5 m K^+/2.5 m PZ, Loading = 0.40, Area Factor = 2.7, Holdup = 1%, Heat Loss = 15,000 W)

The effect of inlet water gas concentration on the absorber temperature profile is shown in Figure 5-21. The figure shows that as the inlet water concentration decreases, the outlet liquid temperature also decreases. The decrease in outlet liquid temperature is due to evaporative cooling as the inlet gas becomes saturated with water from the outlet liquid, which is at a higher temperature. A higher inlet water concentration in the gas also seems result in a slightly hotter temperature profile throughout the absorber column.

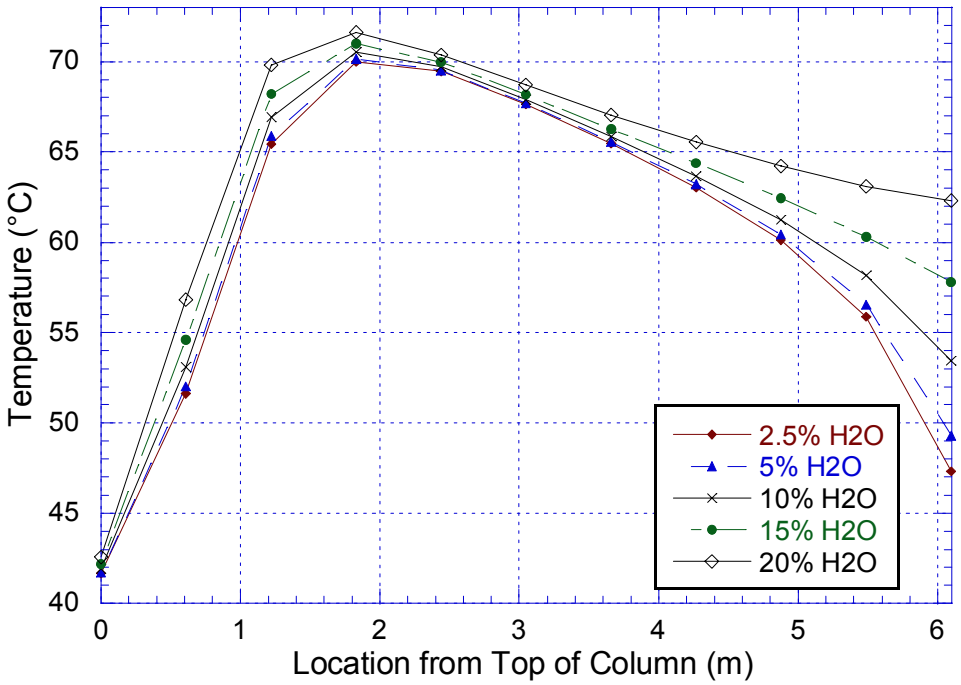

Figure 5-21. Effect of Inlet H_2O Gas Concentration on Absorber Liquid Temperature Profile (5 m K^+/2.5 m PZ, Loading = 0.40, Area Factor = 2.7, Holdup = 1%, Heat Loss = 15,000 W)

Figure 5-22 shows that the inlet CO_2 gas concentration has a profound affect on the temperature profile. For an inlet CO_2 concentration between 1 and 7.5%, the temperature in the absorber is at times below the inlet gas and liquid temperatures of 40 °C, which is unexpected. It is possible that heat of absorption generated by Aspen Plus® at these conditions is incorrect. These conditions also corresponded to the maximum CO_2 removal efficiency observed in the previous graph. It is possible that instead of CO_2 being absorbed, it is being desorbed, which may result in a negative heat of absorption and generates the depressed temperature profile. The plot also shows that there is a large change in the shape and magnitude of the temperature profile when the inlet CO_2 gas concentration increases from 12.5 to 15 mol% CO_2. At 12.5% CO_2, the temperature bulge is located near the bottom of the column and reaches a maximum of at 61 °C. At

15% CO_2, the temperature bulge moves into the top half of the column and reaches a maximum of 70 °C. The rapid rise of the temperature bulge may result in a pinch in the absorber and the drastic reduction in performance as the CO_2 concentration increases from 10 to 20 mol% CO_2.

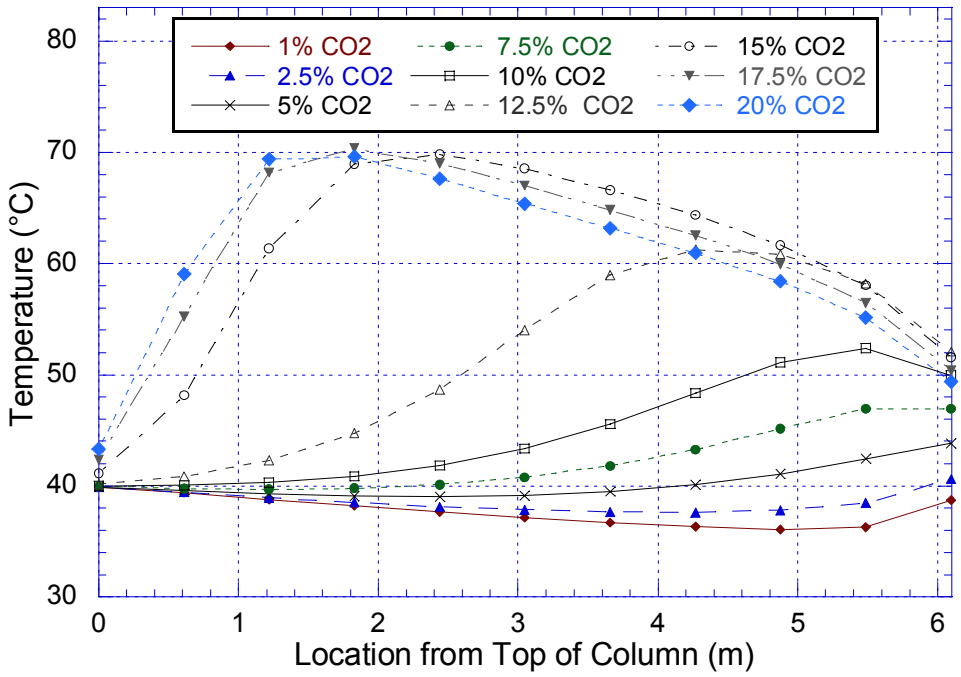

Figure 5-22. Effect of Inlet CO_2 Gas Concentration (mol%) on Absorber Liquid Temperature Profile (5 m K^+/2.5 m PZ, Loading = 0.40Area Factor = 2.7, Holdup = 1%, Heat Loss = 15,000 W)

Figure 5-23 illustrates the effect of inlet gas and liquid temperature on absorber performance. The plot shows that the inlet gas temperature has a minimal affect on CO_2 removal efficiency. As the inlet gas temperature increases from 30 to 60 °C, the removal rate decreases from 71 to 70.5%. The inlet liquid temperature demonstrates an unexpected trend. As the inlet liquid temperature increases from 30 to 38 °C, the CO_2 removal efficiency decreases from 73% and reaches a minimum at 70.7%. From 38 to 60 °C, the CO_2 removal efficiency

increases to 72.8%. The inlet liquid temperature of the absorber was maintained at approximately 40 °C in all of the pilot plant campaigns.

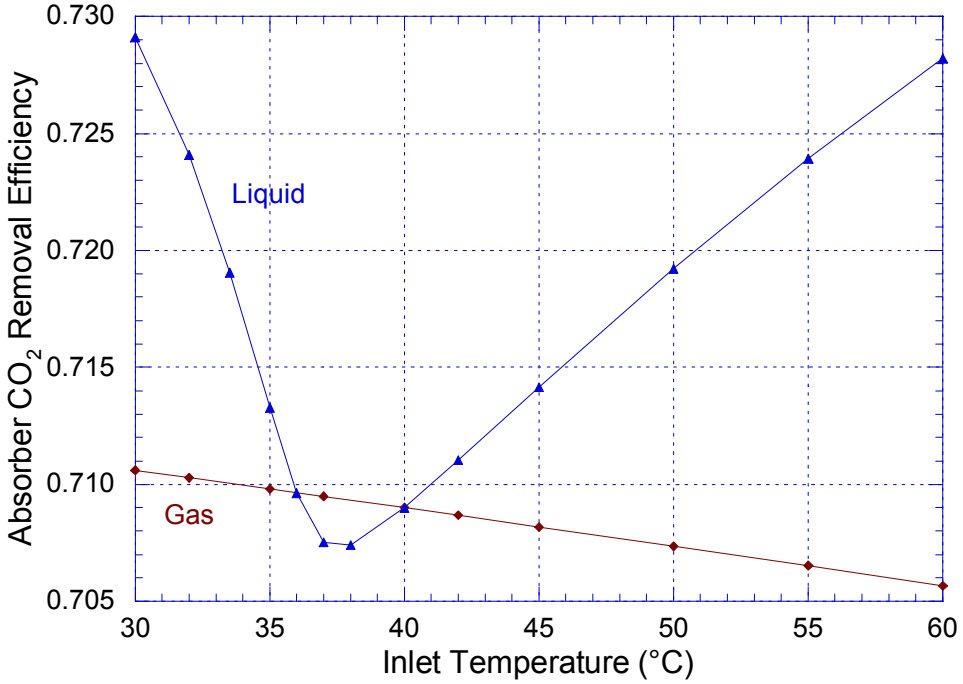

Figure 5-23. Effect of Inlet Gas and Liquid Temperature on Absorber Performance (5 m K^+/2.5 m PZ, Loading = 0.40, Area Factor = 2.7, Holdup = 1%, Heat Loss = 15,000 W)

An increase inlet liquid temperature to the absorber dramatically affects the temperature profile (Figure 5-24). An inlet liquid temperature of 30 °C results in a temperature bulge location near the bottom of the column. As the inlet liquid temperature increases, the location of the temperature bulge moves up the column. The figure shows that at 38 °C, the largest temperature difference (~30 °C) between the inlet liquid and maximum of the temperature bulge occurs, which also corresponds to the minimum in CO_2 removal efficiency observed in the previous plot. The minimum is most likely due to the possible pinching in the absorber at the elevated temperatures. Finally, it is observed that the outlet liquid temperature for all of the cases approach 50 °C, with the

exception of the 30 and 35 °C points. The inlet gas temperature was 40 °C and was assumed to be saturated with water.

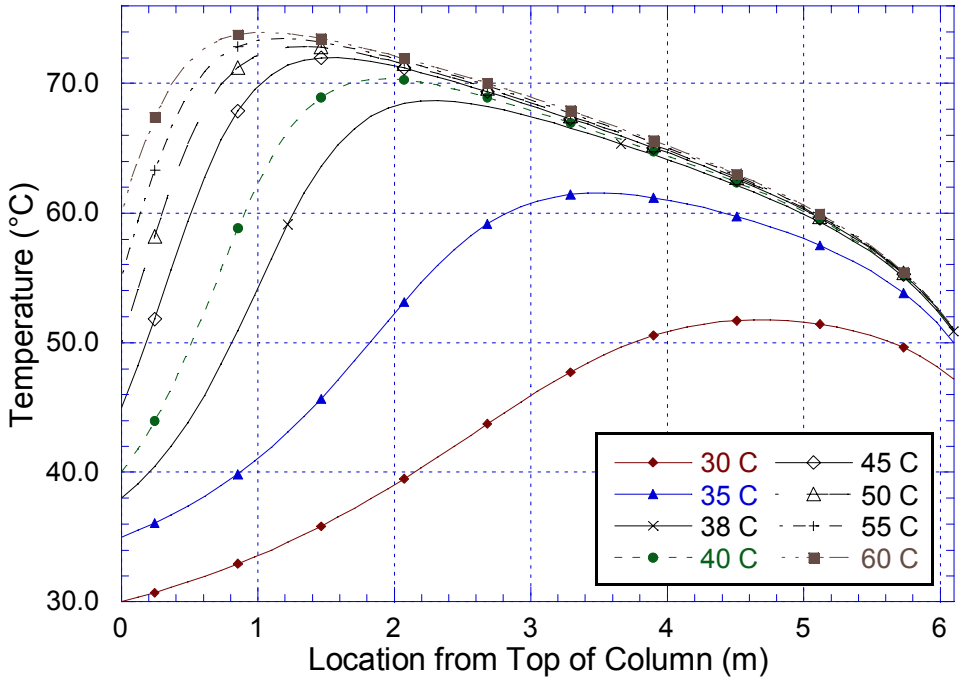

Figure 5-24. Effect of Inlet Liquid Temperature on Absorber Liquid Temperature Profile (5 m K^+/2.5 m PZ, Loading = 0.40, Area Factor = 2.7, Holdup = 1%, Heat Loss = 15,000 W)

Figure 5-25 shows that the absorber temperature profile is affected by the inlet gas temperature. The temperature profile remains essentially the same when the inlet gas temperature is varied from 30 to 60 °C. The maximum of the temperature bulge was approximately 70 °C and was located in the top half of the absorber column. This is consistent with the slight change in the CO_2 removal efficiency observed in Figure 5-23.

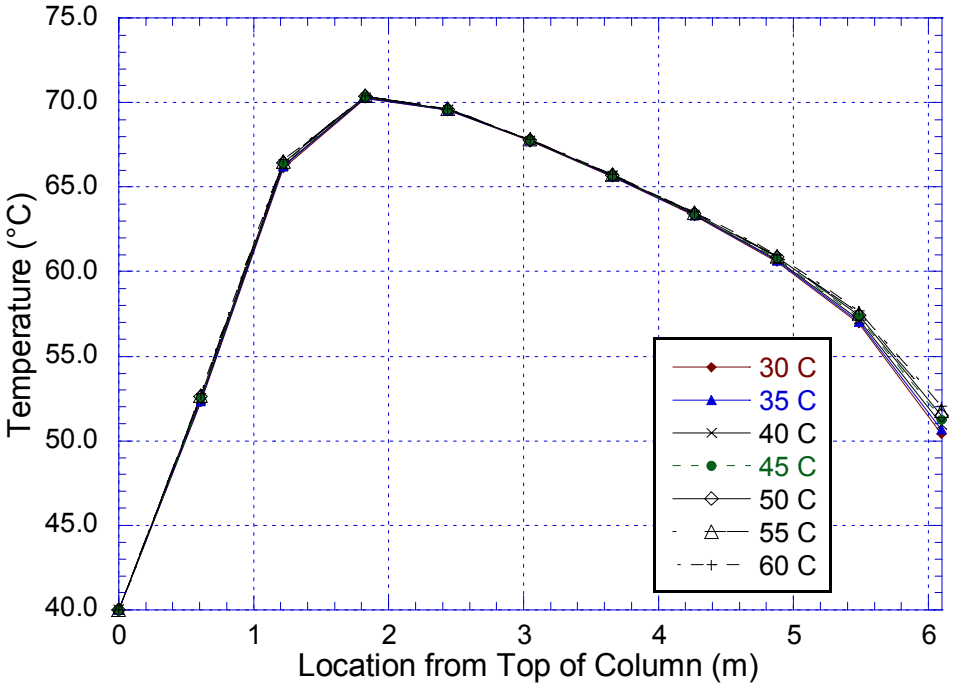

Figure 5-25. Effect of Inlet Gas Temperature on Absorber Liquid Temperature Profile (5 m K^+/2.5 m PZ, Loading = 0.40, Area Factor = 2.7, Holdup = 1%, Heat Loss = 15,000 W)

5.4 DATA-FIT RESULTS

A total of 93 pilot plant runs from Campaigns 2 and 4 were used to validate the absorber model and to reconcile experimental measurements from the pilot plant. Aspen Plus® Data-Fit was used to regress the interfacial area factor and overall absorber column heat loss for the RateSep™ absorber model. The measured lean loading from the pilot plant data was shifted downward by 10%. A value for standard deviation was assigned to the inlet and outlet CO_2 gas concentration, inlet liquid CO_2 concentration, inlet and outlet temperatures, and the temperature profile across the column. The parameters were selected based on the results from the sensitivity analysis. This allowed Data-Fit to make adjustments and reconcile the pilot plant data. Each pilot plant data set was

regressed individually by Data-Fit. The results of all 93 Data-Fit regression runs are tabulated in the appendix.

5.4.1 Pilot Plant Data Reconciliation

It was assumed that the measured CO_2 gas concentrations were more reliable than the CO_2 loading measurements. The inlet and outlet CO_2 gas concentrations were assigned a starting standard deviation of 5%. In this work, it was assumed that the inlet water concentration was saturated at the measured inlet gas temperature, which was typically 40 °C. However, the sensitivity analysis of water vapor concentration showed that it only slightly affects the CO_2 removal rate. The standard deviation for the nitrogen and water in the gas were given a standard deviation of zero.

The sensitivity analysis showed that CO_2 lean loading has the most profound affect on absorber performance and that the concentration of piperazine and potassium carbonate only had slightly affect on CO_2 removal rate. Due to the issues with the Hilliard (2005) K^+/PZ VLE model and the possibility that the experimental CO_2 loading measurements were not as reliable, the starting standard deviation for the inlet liquid CO_2 concentration was set to 15%. In addition, the standard deviation for piperazine, potassium carbonate, and water was assigned a value of zero. Finally, the standard deviation for the temperatures of the inlet and outlet gas and liquid and temperature profile were set to a starting value of 5%. If the Data-Fit convergence criteria were not met, the standard deviation for the parameter with the highest residual was increased.

The Data-Fit results of Campaign 2 for the CO_2 gas concentration shows that the regression analysis made only minor adjustments (Figure 5-26). The absolute average deviation for the inlet and outlet CO_2 gas concentration for Campaigns 2 and 4 were less than 2% (Table 5-2). The ΔCO_2 Gas was calculated

as the difference between the inlet and outlet CO_2 gas concentration. The absolute average deviation of ΔCO_2 Gas between the experimental and Data-Fit values was between 1.1 to 2.2%.

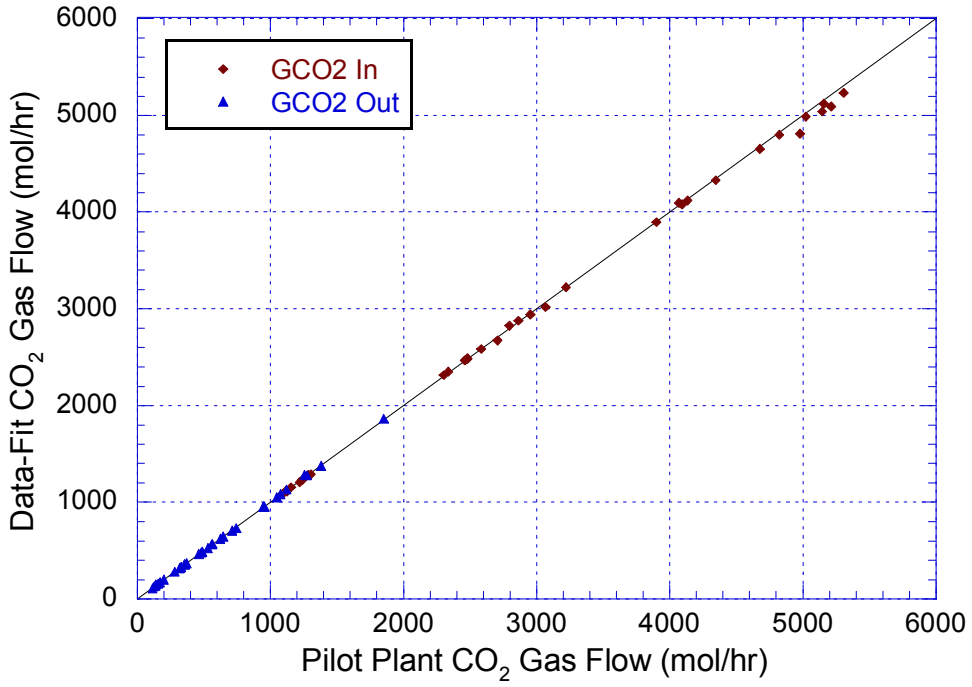

Figure 5-26. Campaign 2 Data-Fit Regression Results for Inlet and Outlet CO_2 Gas Concentration (Entered into RateSep™ as Flow Rate)

Table 5-2. Data-Fit Results for Inlet and Outlet CO_2 Gas Concentration of Campaigns 2 and 4

Campaign	Solvent (m)	Inlet CO_2 Gas		Outlet CO_2 Gas		ΔCO_2 Gas
	K^+/PZ	AAD (%)	Max (%)	AAD (%)	Max (%)	AAD (%)
2	5/2.5	0.72	3.35	0.52	6.25	1.05
4	5/2.5	1.45	6.69	0.68	2.09	2.17
4	6.4/1.6	0.56	2.26	0.35	1.25	1.14

A parity plot of the experimental and regressed lean loadings for Campaigns 2 and 4 is shown in Figure 5-27. The experimental liquid CO_2 loading measurements were adjusted downward by 10%. The figure shows that a relatively good fit was obtained for the Campaign 4 pilot plant data. However,

for Campaign 2, the plot shows that the even with the 10% adjustment, the experimental lean loadings were still slightly higher than the values reconciled by Data-Fit.

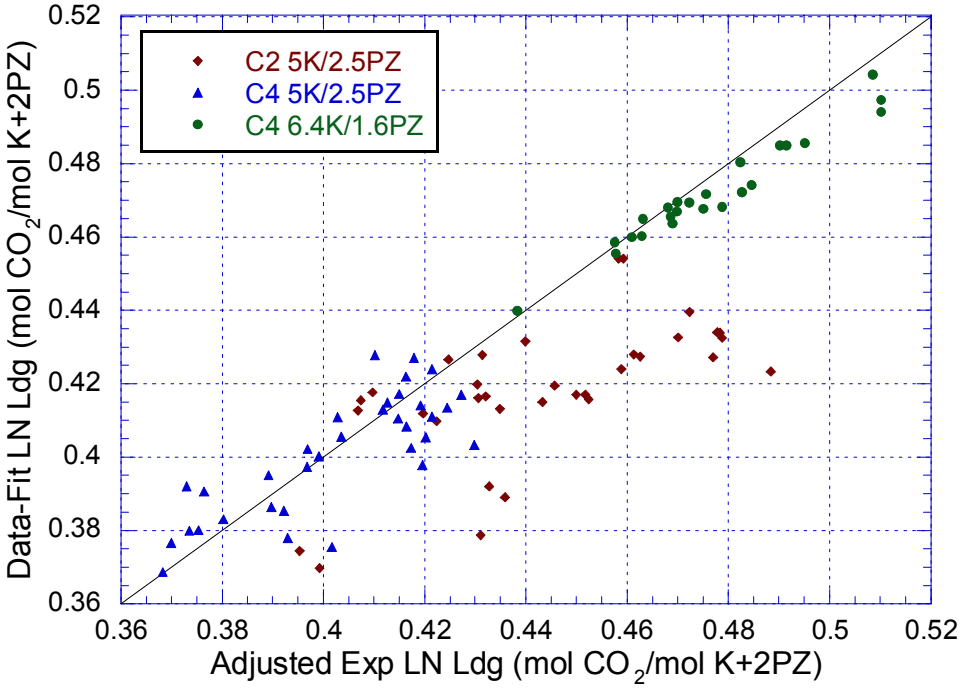

Figure 5-27. Campaign 2 and 4 Data-Fit Results for Lean Loading

In the Data-Fit analysis, the values for rich loading were not entered into the data set in order to expedite convergence. The values of rich loading were calculated by Data-Fit based on the lean loading, gas phase material balance and the temperature profile. The experimental measurements of rich loading were adjusted downward by 10% to account for the VLE correction suggested by Hilliard and compared to the values regressed by Data-Fit. Figure 5-28 shows that the Data-Fit values of rich loading were systematically higher than the pilot plant measurements for Campaign 4 by approximately 10%. The rich loading data for Campaign 2 had less deviation and did not exhibit this offset. The figure also suggests that the experimental results for rich loading were too low. It is possible that there was a loss of CO_2 from the rich liquid samples during the

sample collection process due to flashing. There may have also been additional CO_2 losses during sample dilution and sample transfer for the TOC analysis. The samples were poured by hand into the TOC vials. The direct contact with the air and the agitation may have resulted in additional losses of CO_2 from the liquid samples.

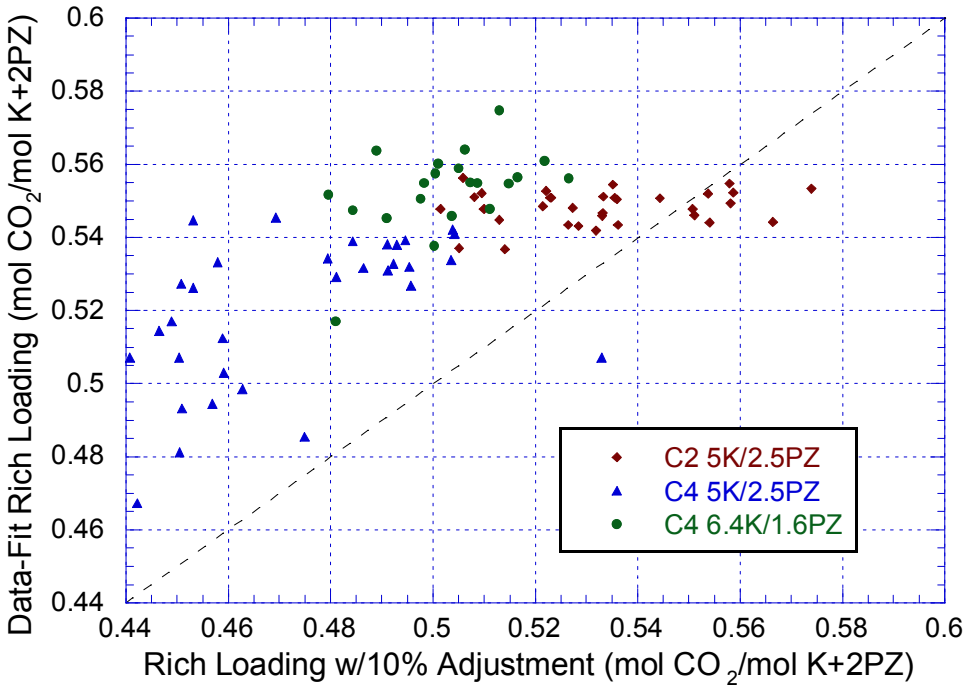

Figure 5-28. Campaign 2 and 4 Data-Fit Results for Rich Loading

Table 5-3 lists the average absolute deviation and maximum deviation for the Data-Fit and experimental pilot plant results of lean and rich loading. The absolute average deviation between the experimental and Data-Fit values of the lean and rich loadings for Campaign 2 was approximately the same. For Campaign 4, the AAD of the rich loading was consistently higher than the lean loading. Also, the ΔCO_2 Liquid was calculated as the difference between in the lean and rich CO_2 mole flow rate as entered into Aspen Plus®. The AAD results for the two campaigns ranged from 17.1 to 28.6%.

Table 5-3. Data-Fit Results for Lean and Rich Loading of Campaigns 2 and 4

Campaign	Solvent (m)	Lean Loading		Rich Loading		ΔCO_2 Liq
	K^+/PZ	AAD (%)	Max (%)	AAD (%)	Max (%)	AAD (%)
2	5/2.5	5.87	13.3	3.89	9.96	28.6
4	5/2.5	2.14	6.54	10.6	20.2	17.1
4	6.4/1.6	1.07	3.15	10.1	15.3	26.4

An energy balance in the form of a temperature profile was used to fit the absorber model parameters regressed by Data-Fit. This included pilot plant data for the inlet and outlet liquid temperatures and the inlet gas temperature. Also, temperatures corresponding to RTD measurements from TT4077, TT4076, TT4075, and TT4073 were used in the data set. The standard deviation for the temperature inlet and outlet gas and liquid temperatures were assigned a starting value of 2% and increased accordingly to attain the convergence. The standard deviations for the four temperatures in the column were assigned a starting standard deviation of 5% and increased when the convergence criteria was not met. A higher standard deviation was used for the temperature profile because of possible inaccuracies with the predicted heat of absorption and liquid heat capacity. In the majority of the cases, Data-Fit was able to fit the temperature profile to within 2 °C. Figure 5-29 shows the Data-Fit temperature profile results of Run 4.5.1 from Campaign 4.

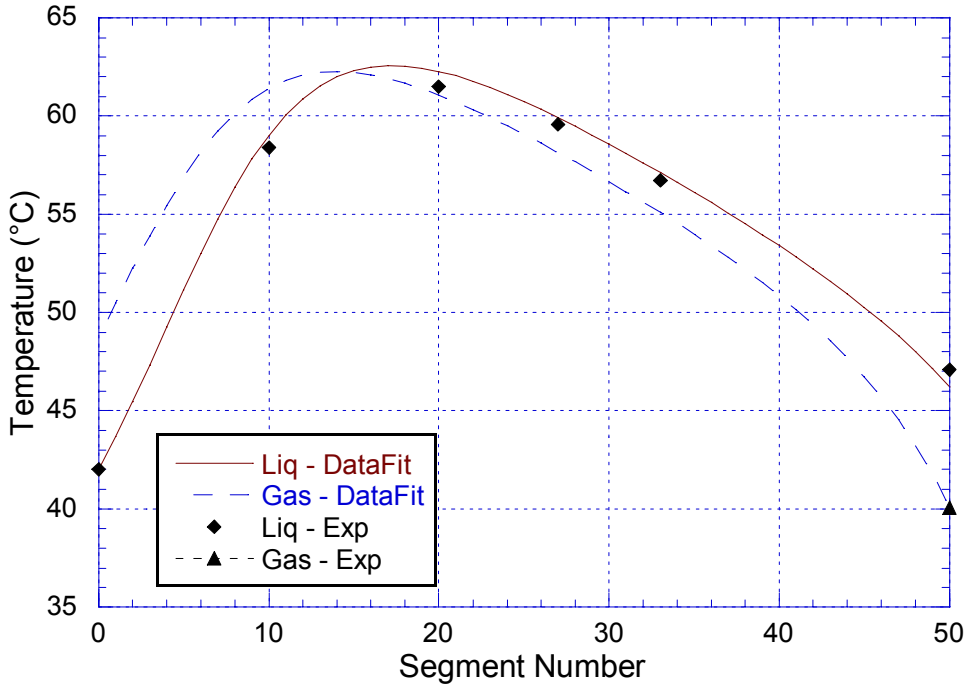

Figure 5-29. Campaign 4 - Run 4.5.1 Data-Fit Results for Temperature Profile

5.4.2 Interfacial Area and Heat Loss Parameters

The interfacial area for each run was obtained by adjusting the interfacial area factor to obtain the optimized fit. In the Campaign 4 Data-Fit regression, the interfacial area was calculated by the Rocha–Bravo–Fair model, which resulted in slightly different values of interfacial area across the column due to changing physical properties and temperatures. The true interfacial area was obtained by multiplying the average of the predicted areas by the interfacial area factor regressed by Data-Fit. For the regression analysis of Campaign 2, the predicted interfacial area was set to the specific area of the packing, which did not vary across column. The true interfacial area was calculated by multiplying the specific area with the regressed area factor.

The Data-Fit regression results for the effective interfacial of the pilot plant runs for Campaign 2 are shown in Figure 5-30. Campaign 2 was conducted with 5 m K^+/2.5 m PZ and Flexipac 1Y (a_{sp} = 410 m^2/m^3) structured packing in the

absorber. In Campaign 2, the stripper was first operated at 1.6 bar and then reconfigured for vacuum operation and the absorber was operated at lower gas and liquid rates. The pilot plant was then reconfigured back to pressure operation in the stripper and operated at higher liquid and gas rates. The plot shows that the majority of the regressed values for the interfacial area were between 150 and 300 m^2/m^3, with an average value of 240 m^2/m^3. The effective area obtained by the air–water experiments in the PVC column with 3 m of packing was approximately 300 m^2/m^3, while air–water experiments in the actual absorber column with 6.1 m of packing was approximately half of the PVC column with a value of 160 m^2/m^3.

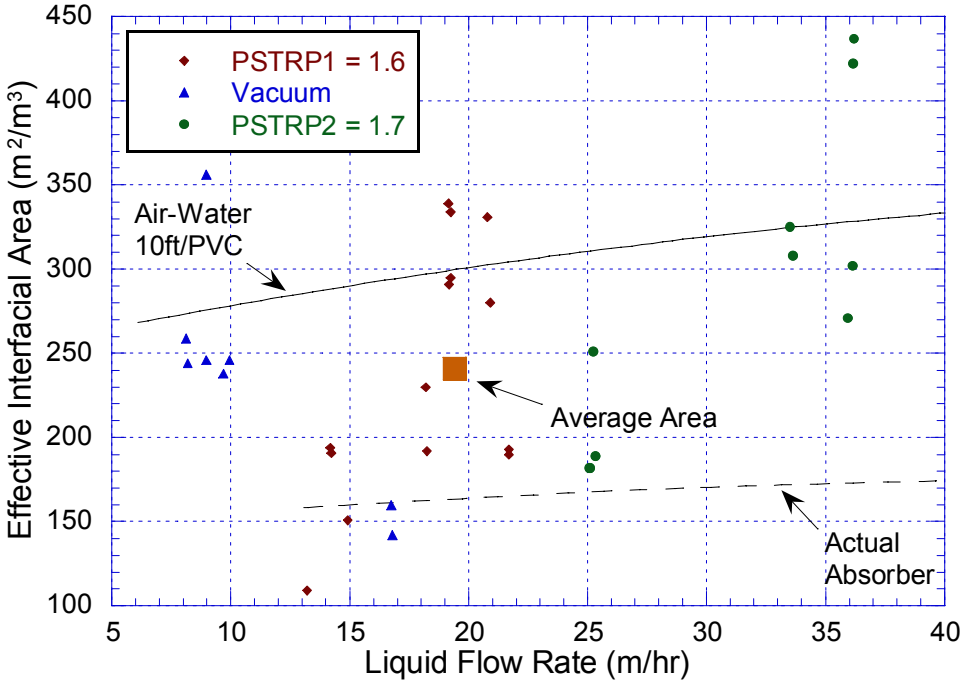

Figure 5-30. Data-Fit Results for Effective Interfacial Area of Campaign 2 (5 m K^+/2.5 m PZ, Flexipac 1Y - Specific Area = 410 m^2/m^3)

The low values of interfacial area for the experiments in the 6.1 m absorber tower may be due to issues with the setup of the column such as the maldistribution of gas and liquid and possible issues with the collector plate,

distributor, or redistributor. In addition, the density, viscosity, and surface tension of the potassium carbonate/piperazine solution are very different than a 0.1 N NaOH solution, which also affects the wetting properties of the packing.

The regressed values of interfacial area for the fourth campaign are shown in Figure 5-31. In Campaign 4, Flexipac AQ Style 20 (a_{sp} = 213 m^2/m^3) structured packing was used in the absorber column. Air–water experiments performed in the 3 m PVC column showed that the effective area was approximately 220 m^2/m^3, which was about the same as the specific area. The average value of the regressed interfacial areas for the 5 m K^+/2.5 m PZ and 6.4 m K^+/1.6 m PZ solution were 136 and 110 m^2/m^3, respectively. The values of effective area for the two solvent compositions were approximately same, which was expected if the kinetics were properly modeled. A summary of the different values of effective interfacial area is given in Table 5-4.

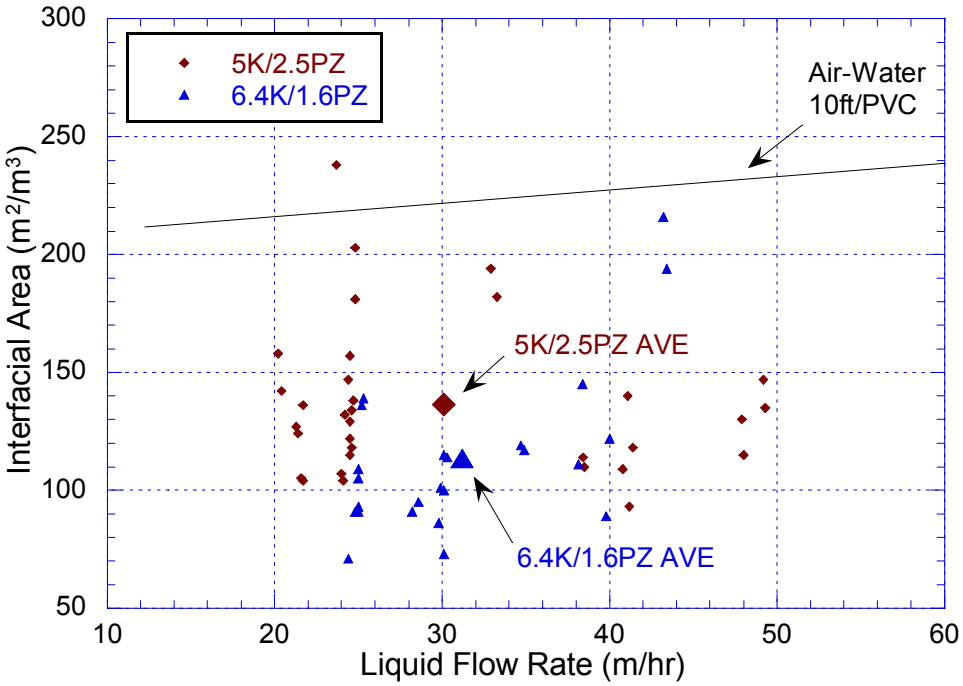

Figure 5-31. Data-Fit Results for Effective Interfacial Area of Campaign 4 (5 m K^+/2.5 m PZ, 6.4 m K^+/1.6 m PZ, Flexipac AQ – Specific Area = 213 m^2/m^3)

Table 5-4. Summary of Effective Interfacial Area Results for Flexipac 1Y and Flexipac AQ Style 20 Structured Packing

Packing	Specific Area m^2/m^3	Air-Water m^2/m^3	Absorber m^2/m^3	Data-Fit m^2/m^3
Flexipac 1Y	410	300	160	240
Flexipac AQ Style 20	213	220	-	110, 136

At high lean loadings, some of the interfacial areas and heat losses regressed by Data-Fit were unreasonable. It is possible that at those conditions, a pinch existed in the column. When the absorber is pinched, Data-Fit was forced to increase the interfacial area in order to satisfy the removal requirements. Consequently, a large heat loss was needed to offset the large interfacial area.

Heat loss to the entire column in the liquid phase was regressed by Data-Fit to match the temperature profile for each pilot plant run. The regressed value of heat loss was divided by the total number of segments in the column. Thus, the same value of heat loss was assigned to each segment. This approach may not be completely accurate because more heat loss is expected at the higher temperatures of the temperature bulge. However, it simplifies the regression process greatly.

The overall liquid heat loss across the absorber column was adjusted by Data-Fit to match the temperature profile within the specified standard deviation and regression tolerances. The Data-Fit results for the absorber column heat loss of Campaigns 2 and 4 are presented in Figure 5-32. The average column temperature for each pilot plant run was calculated by integrating the values of the temperature profile reconciled by Data-Fit. The plot shows that for the 6.4 m K^+/1.6 m PZ solution, the average temperature and heat loss was approximately 44.0 °C and 10,400 Watts, respectively. For the 5 m K^+/2.5 m PZ solution, the average heat losses were 27,600 and 28,700 Watts for the Flexipac AQ Style 20

and Flexipac 1Y packing, respectively. The average temperature was 52.3 and 50.7 °C for the Flexipac AQ Style 20 and Flexipac 1Y packing, respectively. This suggests that the heat loss values were based on the characteristics of the solvent and not on the interfacial area of the packing because approximately the same value of heat loss was regressed for two different packing using the same solvent. Recent measurements by SRP showed that the heat loss was approximately 12,000 W. Water was fed at a constant temperature of 51.7 °C to the top of the absorber and the water temperature exiting the absorber was record. The ambient temperature was approximately 24 °C.

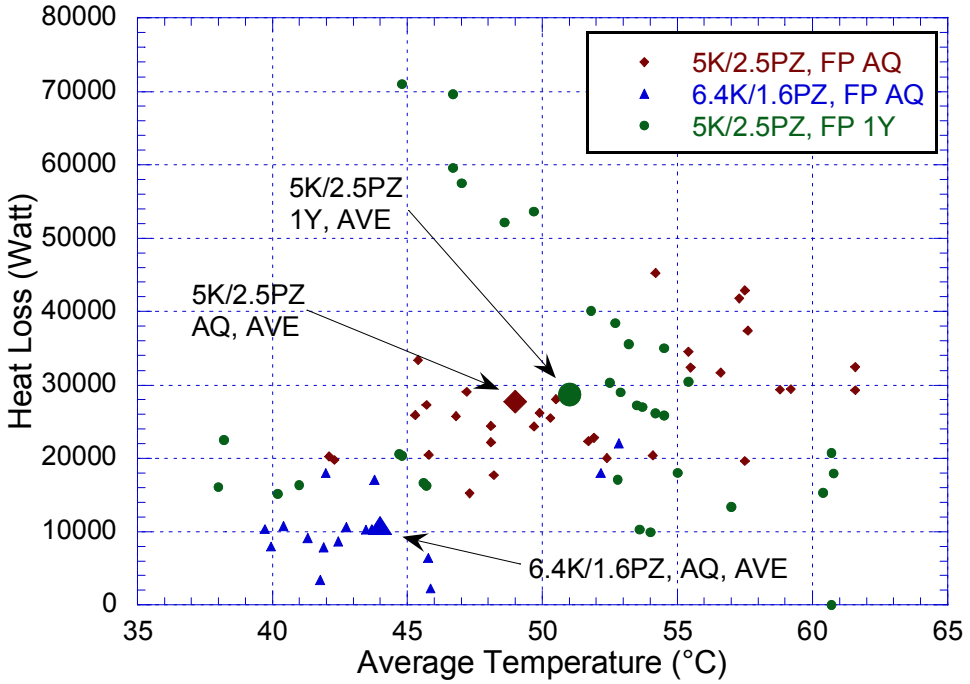

Figure 5-32. Data-Fit Results for Heat Loss of Campaign 2 (5 m K^+/2.5 m PZ, Flexipac 1Y) and Campaign 4 (5 m K^+/2.5 m PZ, 6.4 m K^+/1.6 m PZ, Flexipac AQ)

A calculation was performed to determine whether the regressed heat loss was due to actual heat loss or from flawed predictions for the heat of absorption. The heat transfer coefficient was calculated for a 5 m K^+/2.5 m PZ base case

which assumed the following: heat loss of 28,000 Watts, average column temperature of 50 °C, ambient temperature of 15 °C, and a surface area of 9.9 m^2, which is approximately 1.2 times the area for a 6.1 m column height and 0.43 m inner diameter. The calculation for the 6.4 m K^+/1.6 m PZ base case assumed a heat loss of 10,000 and an average column temperature of 44 °C. The heat transfer coefficient was calculated to be 81 and 35 W/m^2-K for 5 m K^+/2.5 m PZ and 6.4 m K^+/1.6 m PZ, respectively. For natural convection, the heat transfer coefficient is typically 1–20 W/m^2-K, while forced convection ranges from 50 to 250 W/m^2-K. It is unlikely that forced convection was responsible for the heat loss from absorber column. It was concluded that the heat of absorption was not adequately predicted in the RateSep™ model.

5.4.3 Absorber Pinch Analysis

The K_g analysis for Campaign 2 identified Run 2.19 as a pinch point. Run 2.12 was as identified as an outlier because the calculated equilibrium partial pressure was higher than the CO_2 gas concentration. This point could also be interpreted as a pinch point. The Data-Fit regression analysis for Run 2.12 and Run 2.19 did not converge and indicates that these two runs were pinched.

For high values of lean loading, Data-Fit regressed large values of interfacial area and may indicate a pinch in the absorber column. When the column is pinched, a large interfacial area is required to achieve the target CO_2 removal efficiency. In Run 2.18.1 and Run 2.18.2, Data-Fit regressed an interfacial area of 553 and 606 m^2/m^3, respectively. The lean loading for Run 2.18 was 0.45 mol CO_2/(mol K^+ + 2 mol PZ), which was the highest lean loading in Campaign 2. In Run 4.21.1 and Run 4.21.2, Data-Fit regressed an interfacial area of 215 and 160 m^2/m^3, respectively. Run 4.21 had a lean loading of 0.50 mol

CO_2/(mol K^+ + 2 mol PZ), which was also the highest value of lean loading for the 6.4 m K^+/1.6 m PZ solution.

5.5 ABSORBER DESIGN/OPTIMIZATION

The validated absorber model was used to determine whether the design of an absorber column for the K^+/PZ system should have a large diameter and short height or a small diameter and tall height. The analysis was performed with the 5 m K^+/2.5 m PZ solution and two gas rates, 8.5 and 14.2 m^3/min or 300 and 500 cfm, respectively. The interfacial area of the packing was based on the Data-Fit results of the Flexipac AQ packing. The interfacial area was set equal to the specific area of Flexipac 2Y (225 m^2/m^3) and an area factor of 0.6 was used. The corrugation angle of the packing was also adjusted to 50 degrees. The absorber column pressure drop was calculated using the model provided by the vendor to Aspen Plus®. The predicted pressure drop was lower than the pressure drop measured in the pilot plant. In addition, no heat loss was assumed for this analysis. This may slightly the affect the results, but the same trends should predicted. The inner diameter of the column was varied and the gas and liquid flow rate was kept constant for each case. Aspen Plus® Design Spec was used to adjust the packing height to attain 90% CO_2 removal.

Table 5-5. Input Specifications of RateSep™ Absorber Model for Absorber Design/Optimization

Parameter	Value
Inlet CO_2 Gas	12 mol%
Inlet H_2O Gas	7.4 mol%
Gas Flow	8.5 & 14.2 m^3/min
K_2CO_3	2.5 molal
PZ	2.5 molal
CO_2 Loading	0.40 mol CO_2/(mol K^+ + 2 mol PZ)
Liquid Flow	82.1 L/min
$T_{Gas\ In}$	40 °C
$T_{Liquid\ In}$	40 °C
Column ID	Variable
Packing Type	Flexipac 2Y
Specific Area of Packing	225 m^2/m^3
Height of Packing	Variable
Intf Area Model	$a_{intf} = a_{specific}$
Packing Area Factor	0.6 (161 m^2/m^3)
Heat Loss	-
Liquid Holdup	1% Free Volume

Figure 5-33 shows the results of the absorber column design analysis. The volume of packing was normalized by the gas flow rate. The plot shows that as the gas velocity increases, the amount of packing needed decreases. One tradeoff associated with decreasing column diameter is that the pressure drop across the column increases and results in a higher energy cost to operate the blower. Another tradeoff is that at low gas velocities, the gas may be poorly distributed.

The energy associated with the absorber column pressure drop was calculated assuming a blower with an efficiency of 70%. At 90% flood and a L/G of 6.2 kg/kg, the column pressure drop was 15.3 inches of H_2O. At these conditions, the energy requirement associated with column pressure drop was calculated to be 1.3 kJ/gmol CO_2 removed and corresponded to a volume of packing or residence time of 4.7 seconds. If the column is operated at 64% of flooding, the column pressure drop decreases to 3.3 inches of H_2O. The energy requirement is reduced by 80% to 0.27 kJ/mol CO_2 and the volume of packing increases by 5.9% to 4.8 seconds. A large energy savings associated with

pressure drop can be achieved by using slightly more packing and a larger diameter column. However, as the diameter of the column continues to be increased, the law of diminishing returns begins to affect the savings on pressure drop. In addition, practical construction considerations may limit the design diameter of the column.

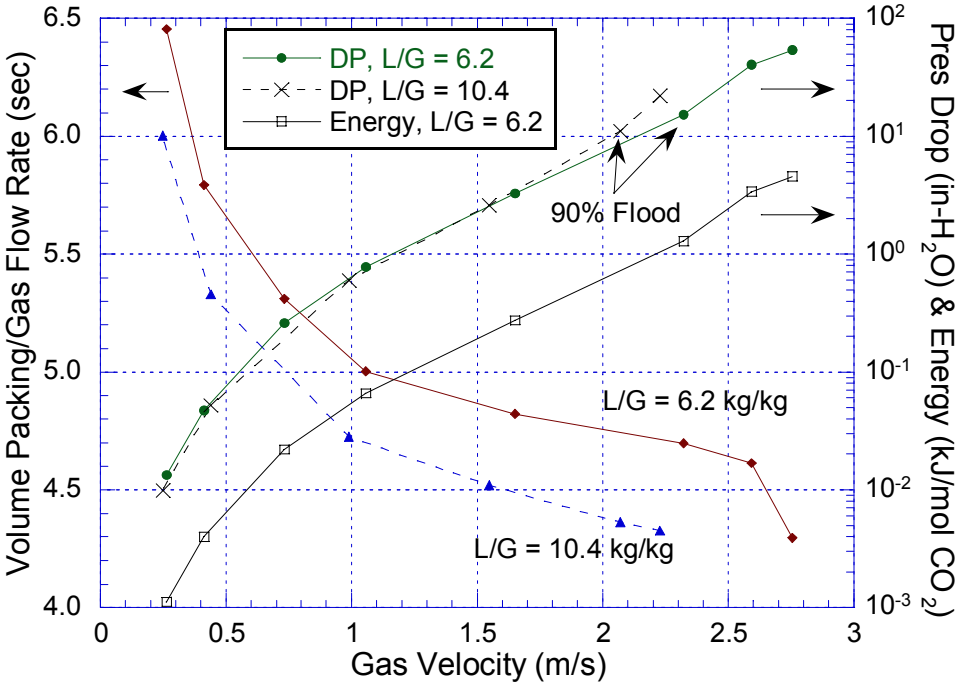

Figure 5-33. Absorber Diameter and Pressure Drop Optimization Analysis (5 m K^+/2.5 m PZ, No Heat Loss, Flexipac AQ, 0.4 LDG, 90% CO_2 Removal)

5.6 Absorber Performance Analysis

The effect of varying the CO_2 lean loading with a constant 90% CO_2 removal rate was examined. This analysis was performed for the 5 m K^+/2.5 m PZ and 6.4 m K^+/1.6 m PZ solutions. A gas rate of 8.5 m^3/min (300 cfm) and packing heights of 5 and 6 meters were used. The absorber packing was modeled assuming Flexipac AQ Style 20 and implemented in RateSep™ by setting the interfacial area equal to the specific area of Flexipac 2Y and using an interfacial area factor of 0.6, which was equivalent to 135 m^2/m^3. Zero heat loss

and 1% liquid holdup were used in the analysis. The liquid flow rate was adjusted using Aspen Plus® Design Spec to achieve 90% CO_2 removal. Table 5-6 summarizes the parameters that were used for the performance analysis in RateSep™ with the validated absorber model.

Table 5-6. Input Specifications of RateSep™ Model for Absorber Performance Analysis

Parameter	Value
Inlet CO_2 Gas	12 mol%
Inlet H_2O Gas	7.4 mol%
Gas Flow	8.5 m^3/min
K_2CO_3	2.5 & 3.2 molal
PZ	2.5 & 1.6 molal
CO_2 Loading	Variable
Liquid Flow	Variable
$T_{Gas\ In}$	40 °C
$T_{Liquid\ In}$	40 °C
Column ID	0.43 m
Packing Type	Flexipac 2Y
Interfacial Area	161 m^2/m^3
Packing Height	5 & 6 m
CO_2 Removal	90%
Heat Loss	-
Liquid Holdup	1% Free Volume

The lean loading entered into RateSep™ was shifted downward by 10% to be consistent with the Hilliard experimental VLE data. The equilibrium partial pressures of CO_2 that are plotted in the following figures represent the corrected VLE. The rich loadings were adjusted to represent the corrected VLE. It was assumed that the liquid capacity for CO_2 was constant. Therefore, the corrected rich loading was calculated by adding the difference between rich and lean loading (capacity) from the RateSep™ run to the starting value of lean loading.

Figure 5-34 shows the results of the runs for the 5 m K^+/2.5 m PZ solution for packing heights of 5 and 6 meters. As the lean loading increases, the magnitude of the rich loading decreases and approaches the value of the lean

loading. However, near a loading of 0.44 mol CO_2/(mol K^+ + 2 mol PZ), the curve for a packed height of 6 m exhibits a local minimum and then a local maximum before continuing to decrease downward.

It appears that the local minimum corresponds to the point where the temperature bulge is located at the middle of the absorber column. For the runs with 5 meters of packing, the local minimum occurs at lower lean loading, but exhibits a plateau instead before continuing to decrease. The local minimum also corresponds to the point where the temperature bulge is located in the middle of the column.

The plot also shows the magnitude of the maximum temperature (T_{max}) for each lean loading condition. At low lean loadings and a packing height of 6 m, the maximum temperature slowly decreases from 69.5 °C and reaches a maximum of 73 °C, before dropping precipitously as the lean loading continues to increase. The precipitous decrease in magnitude of the maximum temperature occurs at approximately the same lean loading of the local minimum in the loading analysis. A similar temperature maximum was observed for the 5 m packing height, where the drop in maximum temperature corresponded to a plateau in rich loading change.

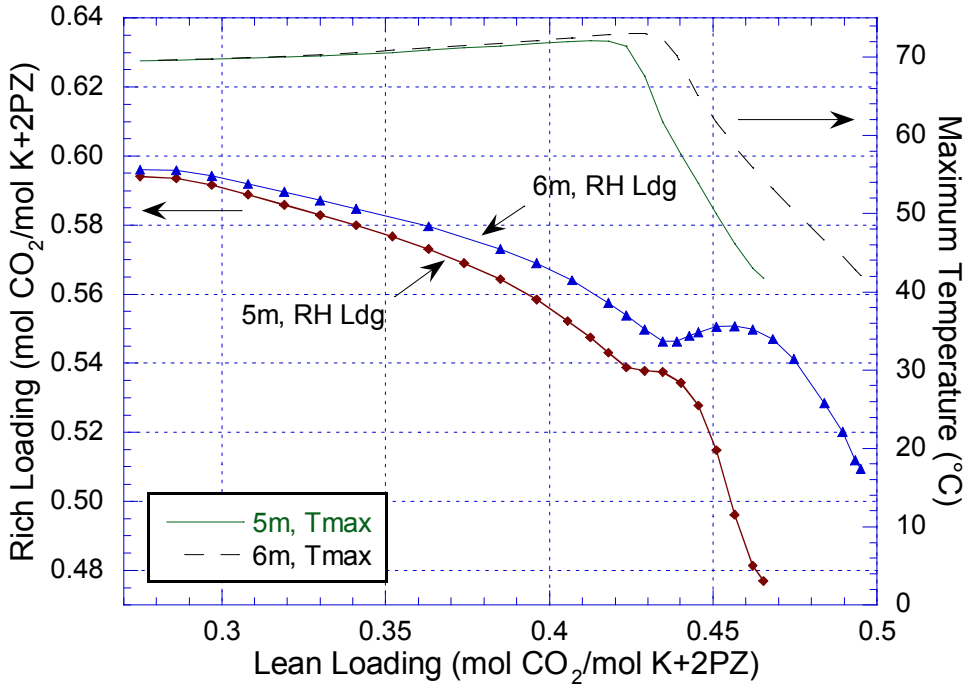

Figure 5-34. Lean and Rich Loadings for 5 m K^+/2.5 m PZ at Constant 90% CO_2 Removal (Packing Height: 5 & 6 m, No Heat Loss, 300 cfm, Flexipac AQ)

Similar results were obtained when the same analysis was performed for the 6.4 m K^+/1.6 m PZ solution. In Figure 5-35, at a lean loading of 0.485 mol CO_2/(mol K^+ + 2 mol PZ), the slope of the curve for the 6 meter packing height changes, approaches a local minimum and then begins to decrease. As in the 5 m K^+/2.5 m PZ solution, the local minimum corresponds to where the temperature bulge occurs in the middle of absorber column. For a packing height of 5 meters, the inflection point occurs at a lean loading of 0.476 mol CO_2/(mol K^+ + 2 mol PZ). As with the 5 m K^+/2.5 m PZ solution, the line where the maximum temperature decreases precipitously corresponds to the same point where a local minimum for the rich loading curve is observed. An examination of the plot shows that the local minimum of both packing heights corresponds to the point where the location of T_{max} finally transitions to the last segment.

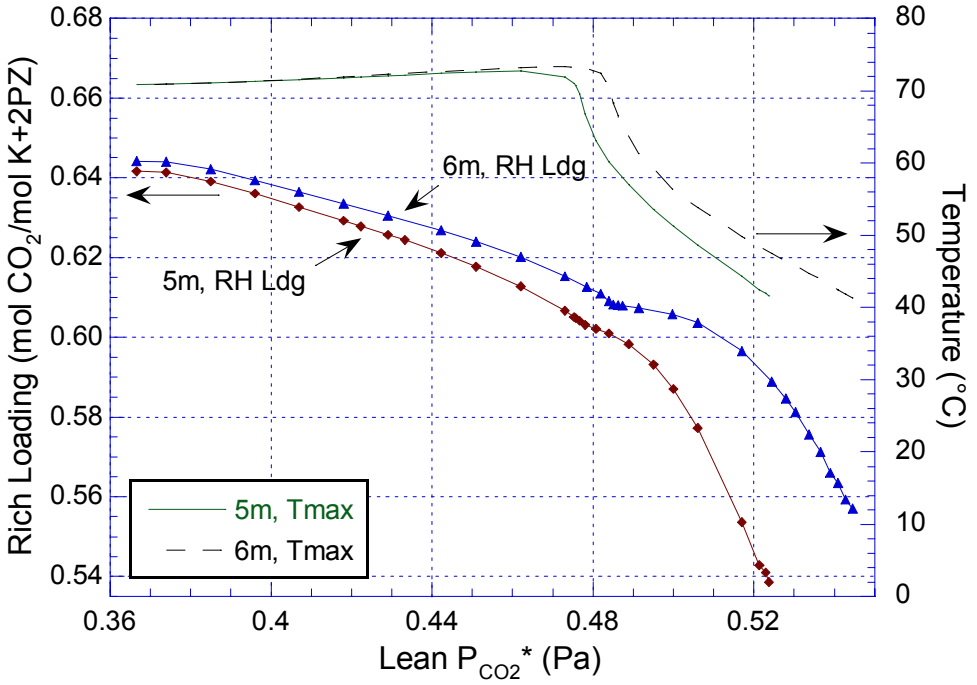

Figure 5-35. Lean and Rich Loadings for 6.4 m K^+/1.6 m PZ at Constant 90% CO_2 Removal (Packing Height: 5 & 6 m, No Heat Loss, 300 cfm, Flexipac AQ)

A plot of the CO_2 solvent capacity for the 5 m K^+/2.5 m PZ and 6.4 m K^+/1.6 m PZ solutions is shown in Figure 5-36. The capacity was calculated by taking the difference between the lean and rich loading and normalizing by the inlet liquid mass flow rate. The lean loading was converted to equilibrium partial pressure of CO_2 so that the two solvents could be compared on the same basis. The figure shows that over an equilibrium partial pressure range from 0.001 to 10 Pa, 5 m K^+/2.5 m PZ has a capacity that approximately 0.3 mol CO_2/kg solvent higher than 6.4 m K^+/1.6 m PZ, which is equivalent of being 15 to 25% higher. Between 50 and 100 Pa, the difference in capacity decreases to 0.2 mol CO_2/kg solvent due to the inflection point of the 5 m K^+/2.5 m PZ solvent and thereafter increases back to 0.3 mol CO_2/kg solvent. Beyond 100 Pa, the capacity of 5 m K^+/2.5 m PZ is almost twice that of the 6.4 m K^+/1.6 m PZ solvent.

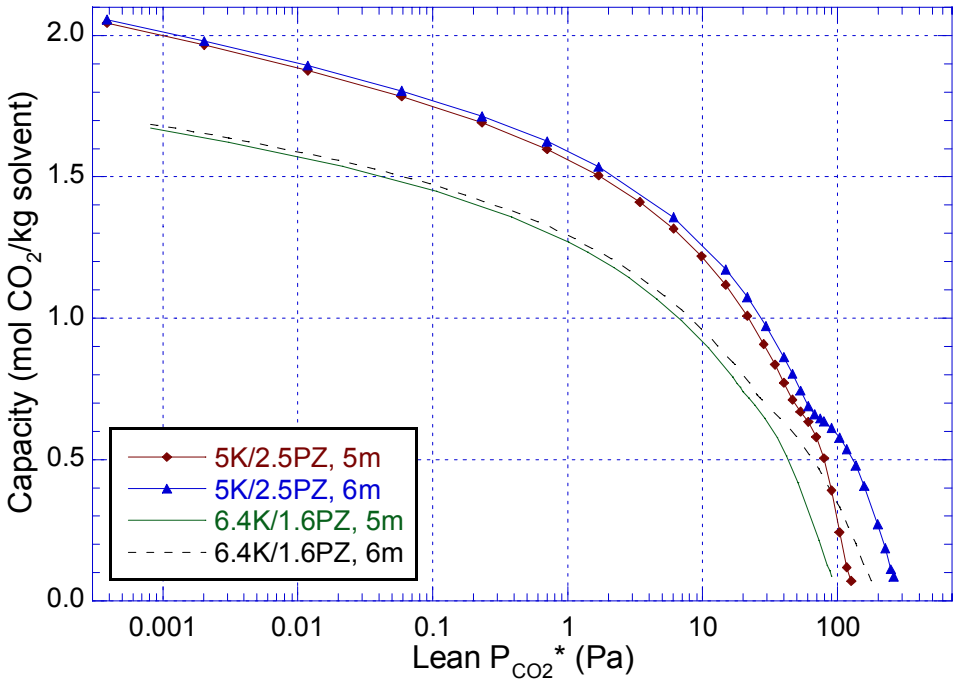

Figure 5-36. Capacity of 5 m K^+/2.5 m PZ and 6.4 m K^+/1.6 m PZ at 90% CO_2 Removal (Packing Height: 5 & 6 m, No Heat Loss, 300 cfm, Flexipac AQ)

The magnitude and location of the temperature bulge in the absorber column for the 5 m K^+/2.5 m PZ solution is shown in Figure 5-37. The figure shows that for both packing heights, the location of the maximum temperature bulge occurs in the upper half of the absorber column. For a packed height of 6 m, the maximum temperature occurs on segment 15. For 5 meters of packing, it occurs on segment 17. The figure also shows that once the temperature bulge moves from the top to the middle of the absorber column, the magnitude of the temperature bulge drops precipitously and quickly moves down to the bottom of the column. When the location of the temperature bulge is on the last segment, the magnitude of the maximum approaches a temperature of 41 °C. Finally, the plot shows that at high lean loadings, a high liquid flow rate is needed to achieve 90%CO_2 removal. It also suggests that the sharp drop in maximum temperature is not a direct result of high liquid flow rates.

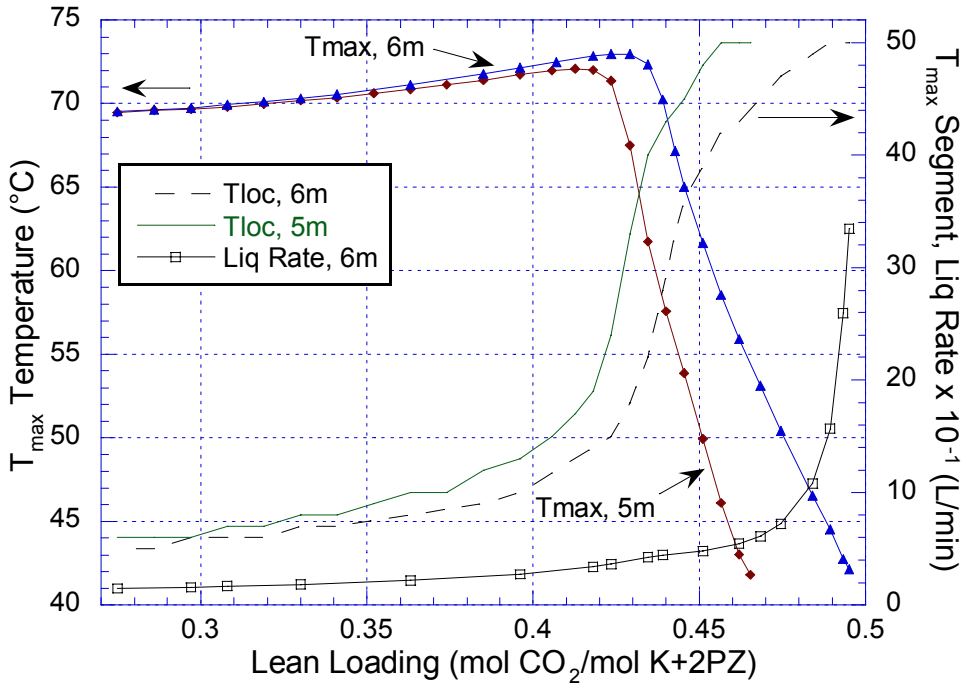

Figure 5-37. Location and Magnitude of Temperature Bulge in the Absorber Column (5 m K^+/2.5 m PZ, Packing Height: 5 & 6 m, 90% Removal)

The magnitude and location of the maximum temperature of the absorber column for the 6.4 m K^+/1.6 m PZ solution is shown in Figure 5-38. Examination of the plot along with Figure 5-35 shows that the local minimum for the loading plots of both packing heights corresponds to the point where the location of the T_{max} finally transitions to the segment 50. As with the 5 m K^+/2.5 m PZ solution, an inflection point for the temperature bulge location occurs at the middle of the column (segment 25). The same decrease in magnitude of the temperature bulge is observed once the location of the temperature bulge moves beyond the middle of the column.

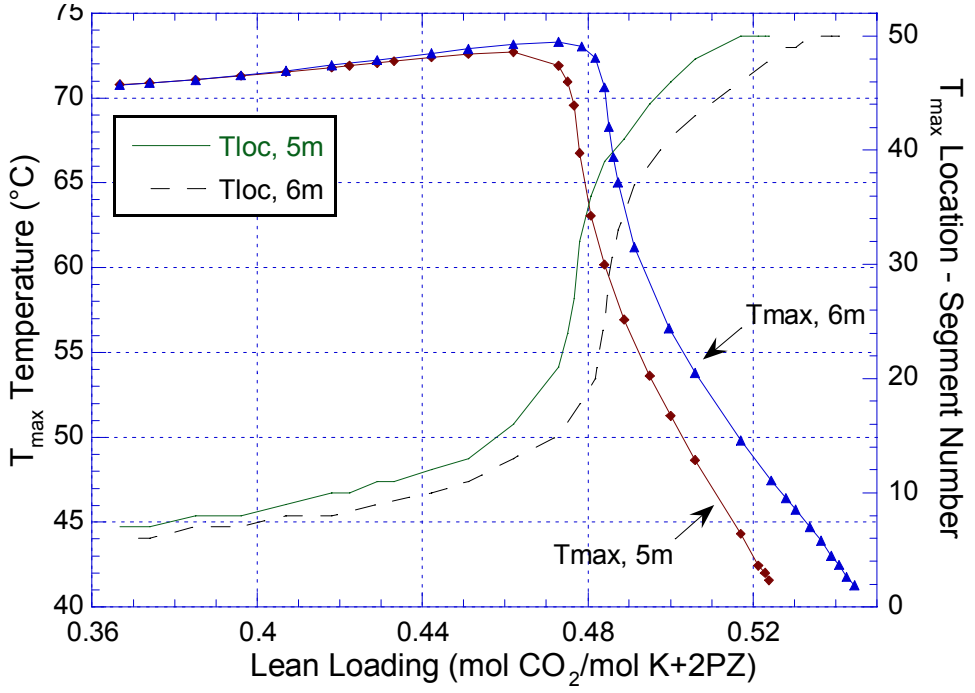

Figure 5-38. Location and Magnitude of Temperature Bulge in the Absorber Column (6.4 m K^+/1.6 m PZ, Packing Height: 5 & 6.1 m, 90% Removal)

McCabe–Thiele diagrams were generated for the local minimum and maximum points observed in Figure 5-34 for the 5 m K^+/2.5 m PZ solution. Figure 5-39 is the McCabe–Thiele diagram for an inlet lean loading of 0.424 mol CO_2/(mol K^+ + 2 mol PZ) (P_{CO2}* = 46.0 Pa), which is where the maximum temperature bulge occurs. The plot shows that the driving force is well distributed across the absorber column. However, at the top of the column, the difference in CO_2 partial pressure between the equilibrium and operating line is greater than an order of magnitude. Also, the location of the temperature bulge occurs in the upper third of the absorber column.

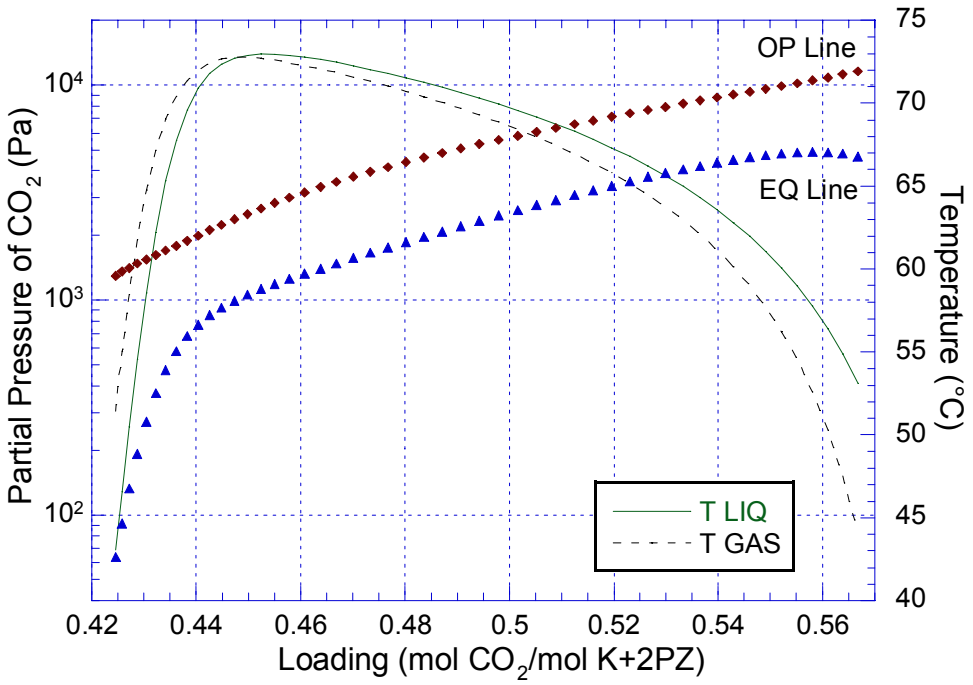

Figure 5-39. McCabe–Thiele Diagram and Temperature Profile for 0.424 Lean Loading (5 m K^+/2.5 m PZ, 6 m Packing Height, Liquid Rate = 36.5 L/min)

Figure 5-40 illustrates the McCabe Thiele plot at a lean loading of 0.439 mol CO_2/(mol K^+ + 2 mol PZ) (P_{CO2}* = 67.5 Pa) for 5 m K^+/2.5 m PZ and a packing height of 6 meters. This loading corresponds to the local minimum observed in Figure 5-34 and is also the point where the temperature bulge is located in the middle of the column on stage 28. The figure shows that the shape of the equilibrium line has changed in the upper half of the column. The CO_2 driving force is larger in the top half of the column than in the bottom. Also, the temperature bulge is located in the upper third of column on segment 14.

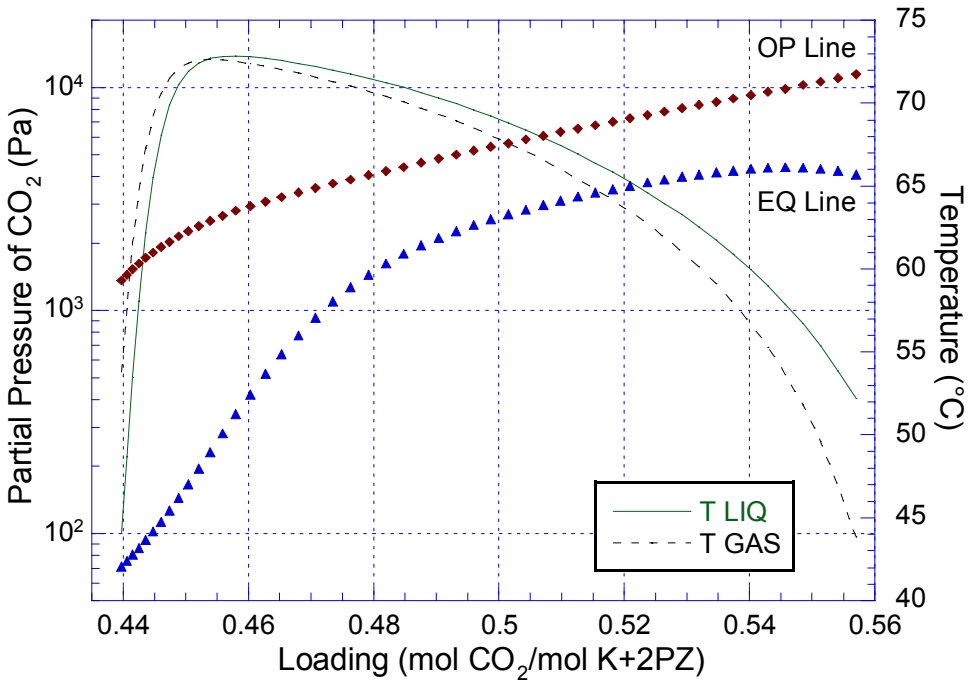

Figure 5-40. McCabe–Thiele Diagram and Temperature Profile for 0.439 Lean Loading (5 m K^+/2.5 m PZ, 6 m Packing Height, Liquid Rate = 44.4 L/min)

The McCabe Thiele diagram for the local maximum, which occurs at 0.451 mol CO_2/(mol K^+ + 2 mol PZ) (P_{CO2}* = 90.2 Pa) lean loading in Figure 5-34, shows that the driving force approaches a pinch near the rich end of the column (Figure 5-41). Near the top of the column, the loading of the top 10 segments do not change much, which may indicate a pinch. However, a large CO_2 partial pressure driving force is present, which indicates otherwise. The figure shows that the temperature bulge has shifted to the bottom half of the column on segment 39, with only a slight increase in liquid rate and lean loading. The magnitude of the maximum for temperature bulge is also approximately 10 °C lower than the previous two figures. This suggests that the location of the temperature bulge is not completely dictated by the liquid to gas rate ratio. Also, the temperature bulge tends to be located either at the top or bottom of column and not at the middle.

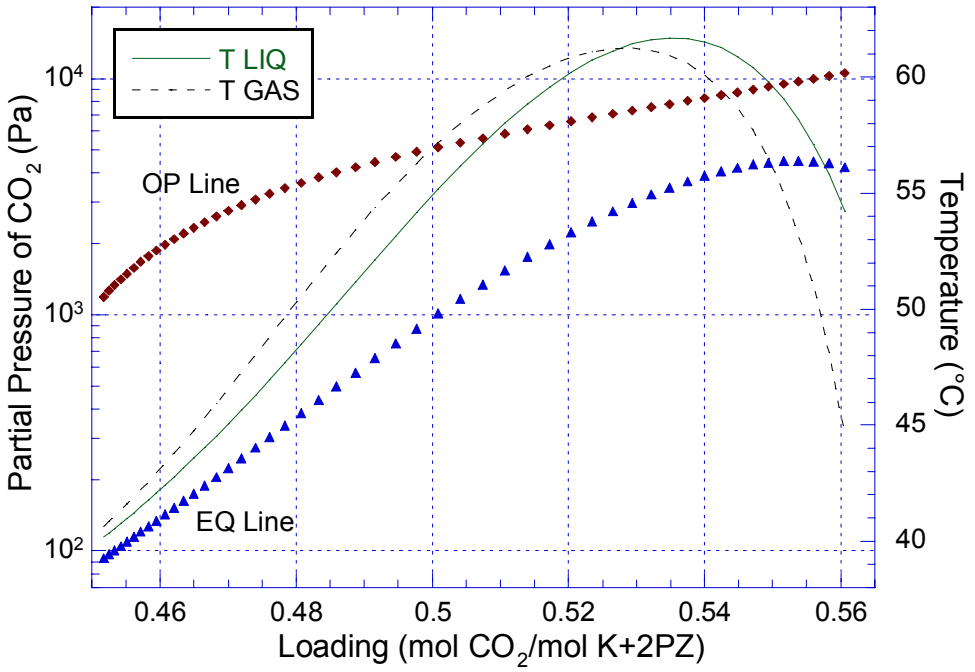

Figure 5-41. McCabe–Thiele Diagram and Temperature Profile for 0.451 Lean Loading (5 m K^+/2.5 m PZ, 6 m Packing Height, Liquid Rate = 47.9 L/min)

A McCabe Thiele plot for a 6.4 m K^+/1.6 m PZ solution, packing height of 5 m, and a lean loading of 0.476 mol CO_2/(mol K^+ + 2 mol PZ) (P_{CO2}* = 18.3 Pa) is shown in Figure 5-42. The 0.476 loading corresponds to the point where the location of the liquid temperature bulge is located in the middle of the column on segment 25. It is also approximately the same location where the slope of the lean and rich curve in Figure 5-35 changes. The plot shows that the operating line has comparable CO_2 partial pressures with the 5 m K^+/2.5 m PZ at the inlet and outlet of the column (1,000–10,000 Pa). However, the P_{CO2} of the equilibrium line at the lean end of the column is two orders of magnitude smaller than the 5 m K^+/2.5 m PZ solution. At the rich end of absorber, the equilibrium partial pressure of CO_2 for the 6.4 m K^+/1.6 m PZ is lower by about 1000 Pa than the 5 m K^+/2.5 m PZ. The figure shows that at the rich end, the CO_2 partial pressure driving force is much lower than at the top of the column.

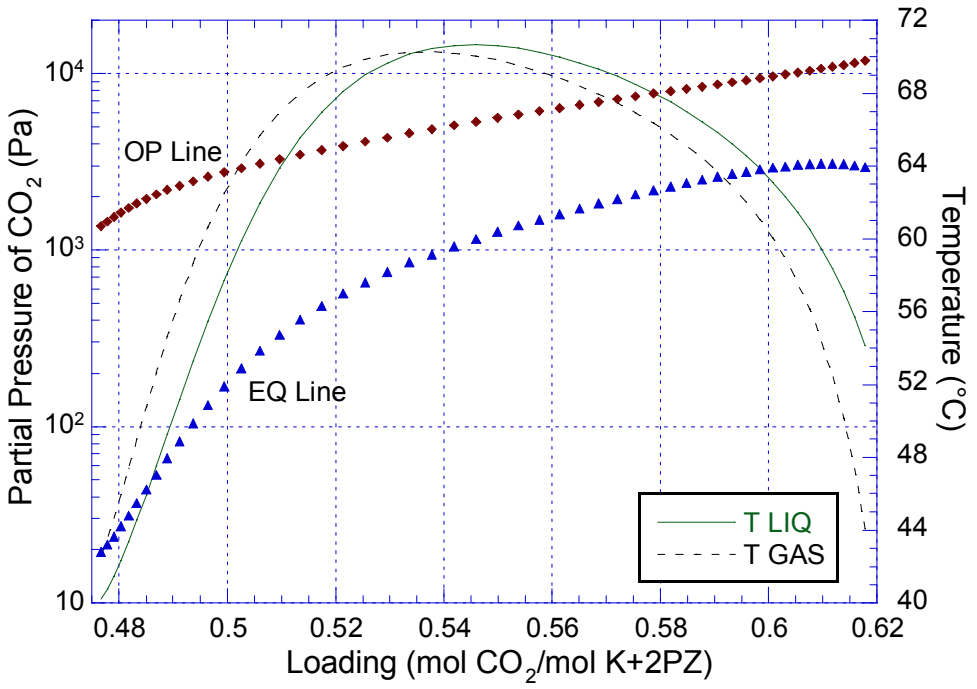

Figure 5-42. McCabe–Thiele Diagram and Temperature Profile for 0.476 Lean Loading (6.4 m K^+/1.6 m PZ, 5 m Packing Height, Liquid Rate = 36.8 L/min)

5.7 CONCLUSIONS

Aspen Plus® Data-Fit was successfully used to regress the effective interfacial area for the Flexipac 1Y and Flexipac AQ Style 20 and overall column heat loss for the 5 m K^+/2.5 m PZ and 6.4 m K^+/1.6 m PZ solutions. Ninety-three pilot plant data runs were used in the regression analysis and each run was independently regressed in Data-Fit.

The interfacial wetted area regressed by Data-Fit was less than the air–water measurements. The average interfacial area of Flexipac 1Y (a_{sp} = 410 m^2/m^3) structured packing was 240 m^2/m^3, which was 80% of the value measured by the air–water column and 59% of the specific area. The average interfacial area of Flexipac AQ Style 20 (a_{sp} = 213 m^2/m^3) structured packing for 5 m K^+/2.5 m PZ was 136 m^2/m^3, which was 56% of the air–water measurement and 52% of the specific area. The average interfacial area of Flexipac AQ for 6.4

m K^+/1.6 m PZ was 110 m^2/m^3, which was 67% of the air–water measurement and 64% of the specific area. The same interfacial area was obtained for Flexipac AQ even when two different solvents were used.

The average heat losses regressed by Data-Fit for 5 m K^+/2.5 m PZ were 27,600 and 28,700 Watts for the Flexipac AQ Style 20 and Flexipac 1Y packing, respectively. The average heat loss for 6.4 m K^+/1.6 m PZ was 10,400 Watts. For both solvents, the heat transfer coefficient was found to be in the range of forced convection, which is unlikely to have occurred in the pilot plant. Therefore, it was concluded that the heat of absorption for CO_2 was not adequately predicted in the RateSep™ absorber model.

The pilot plant data was successfully reconciled by Data-Fit. The maximum absolute average deviation of the inlet and outlet CO_2 gas concentration was 1.45 and 0.68%, respectively. The maximum deviations of the inlet and outlet CO_2 gas concentration was 6.7 and 6.3%, respectively. The maximum absolute average deviation for the lean and rich loadings was 5.87 and 10.6, respectively. The maximum deviations of the lean and rich loadings were 13.3 and 20.2%, respectively.

A sensitivity analysis showed that liquid heat capacity is important for obtaining the correct shape of the temperature profile. If the heat capacity was incorrect, the location of the temperature bulge cannot be simultaneously fitted to match the pilot plant material balance. Absorber performance is most sensitive to lean loading and interfacial area. Both parameters affect the magnitude and location of the temperature bulge. Piperazine concentration has a secondary affect on absorber performance. Heat loss, liquid holdup, potassium carbonate concentration, inlet water vapor concentration, and inlet liquid and vapor temperatures all have a minor affect on absorber performance. The magnitude and location of the temperature bulge is sensitive to the value of heat

loss. Inlet water vapor concentration impacts the temperature profile in the bottom half of the absorber column.

The absorber design analysis showed that a tradeoff exists between column diameter, pressure drop, and volume of packing. The analysis showed that if the column is operated at 64% of flooding instead of 90%, the column pressure drop reduces from 15.3 to 3.3 inches of H_2O. The energy requirement is reduced by 80% to 0.27 kJ/mol CO_2 and the volume of packing only increases by 5.9%. A large energy savings associated with pressure drop in the absorber can be achieved by using slightly more packing and a larger diameter column.

The absorber performance analysis showed that at the inflection point of the rich loading, the temperature bulge is located at the middle of the absorber column. The magnitude of the temperature bulge decreases dramatically when the location moves form the middle to the bottom of the column. At the top of the absorber column, the magnitude of the maximum temperature of the bulge remains relatively constant. The analysis also showed that over an equilibrium CO_2 partial pressure of 0.001 to 200 Pa and 90% CO_2 removal, the 5 m K^+/2.5 m PZ solution has a capacity that is 15–100% higher than 6.4 m K^+/1.6 m PZ.

Chapter 6: Conclusions and Recommendations

6.1 SUMMARY

Wetted wall column measurements showed that the absorption of CO_2 into aqueous piperazine promoted potassium bicarbonate was 1–1.5 times faster than 7 m MEA (Cullinane, 2005). Four pilot plant campaigns were conducted to validate the bench-scale results and evaluate the commercial viability of the solvent. A distillation/extraction pilot plant was extensively modified and converted into an absorber/stripper system. In the first and second campaign, the pilot plant was conducted with the 5 m K^+/2.5 m PZ solvent and 6.1 meters of Flexipac 1Y structured packing in the absorber. The stripper contained 14 sieve trays and 6.1 meters of IMTP #40 random packing in the first and second campaigns, respectively. In the third campaign, 7 m MEA was tested to establish a base case that could be used as comparison with the K^+/PZ solvent. In the first half of the campaign, Flexipac 1Y and IMTP #40 were used in the absorber and stripper, respectively. In the second half of the campaign, the two packing were switched. In the fourth campaign, the 5 m K^+/2.5 m PZ and 6.4 m K^+/1.6 m PZ solvents were tested with 6.1 meters of Flexipac AQ structured packing in both the absorber and stripper. The quality of the pilot plant data was evaluated and a preliminary analysis of absorber performance was completed.

Absorber modeling efforts were undertaken to better characterize the pilot plant results from the absorber, evaluate packing performance, and develop a design and optimization tool for the piperazine promoted potassium carbonate

system. The absorber model was developed in Aspen Plus® RateSep™ and incorporated the Hilliard (2005) VLE model for K^+/PZ. The kinetics developed by Cullinane (2005) was converted into activity based rates and were entered into RateSep™. The heat of absorption predicted by Aspen Plus® was adjusted and made consistent with the Gibbs–Helmholtz equation. Aspen Plus® parameters for liquid heat capacity, density, and viscosity were regressed using Aspen Plus® DRS. Optimization of the total number of segments and film discretization was performed. A sensitivity analysis was performed to evaluate the effects of various parameters on absorber performance and the temperature profile. Aspen Plus® Data-Fit was used to simultaneously regress interfacial area and heat loss parameters and to reconcile pilot plant data. The lean loadings from the pilot plant data were shifted down by 10% to account for the VLE discrepancy discovered by Hilliard for Data-Fit regression analysis. The validated absorber model used to quantify the tradeoffs associated with the absorber design.

6.2 CONCLUSIONS

6.2.1 Pilot Plant

The operation of an absorber/stripper pilot plant for CO_2 capture using aqueous piperazine promoted potassium carbonate was successfully demonstrated. The pilot plant was operated for three campaigns. For the last two campaigns, the plant was operated continuously for 10 days, 24 hours a day. Greater than 90% CO_2 removal rate was achieved with the 5 m K^+/2.5 m PZ solvent using Flexipac 1Y and Flexipac AQ Style 20 structured packing in the absorber column.

The effective interfacial area measured by the PVC air-water column for Flexipac 1Y structured packing was 50% higher than Flexipac AQ Style 20 structured packing. The specific area of Flexipac 1Y was approximately twice

that of the Flexipac AQ packing. Better mass transfer performance was observed with Flexipac 1Y packing, which may be due to higher liquid holdup resulting from the geometry of the packing and from bridging.

An evaluation of absorber mass transfer performance using the raw pilot plant data found that the 5 m K^+/2.5 m PZ solvent is approximately two times faster than the 7 m MEA solvent and three times faster than the 6.4 m K^+/1.6 m PZ solvent. For 5 m K^+/2.5 m PZ and Flexipac 1Y packing, the average K_g was 6.9 x 10^{-9} gmol/Pa-cm^2-s at an equilibrium partial pressure of 2000 Pa. For 7 m MEA and Flexipac 1Y packing, the average K_g was 4.2 x 10^{-9} gmol/Pa-cm^2-s at an equilibrium partial pressure of 670 Pa. For 5 m K^+/2.5 m PZ and Flexipac AQ packing, the average K_g was 6.3 x 10^{-9} gmol/Pa-cm^2-s at an equilibrium partial pressure of 520 Pa. For 6.4 m K^+/1.6 m PZ and Flexipac 1Y packing, the average K_g was 3.6 x 10^{-9} gmol/Pa-cm^2-s at an equilibrium partial pressure of 230 Pa.

The operation of the pilot plant showed that the location of the temperature bulge moves from the top of the column to bottom as the liquid to gas flow rate ratio is increased. The pressure drop normalized by the gas rate was approximately 1.5–2 times higher in the Flexipac 1Y than in Flexipac AQ Style 20, which had steeper corrugation angle. Lower pressure drop was observed with 6.4 m K^+/1.6 m PZ at the lower gas rate because of a low magnitude temperature bulge. However, at high gas rates, the pressure bulge will be dictated only by hydraulics.

The carbon dioxide material balance across the absorber column for Campaign 1 indicates that gas side removal of CO_2 was on average approximately 14% higher than the liquid phase. For Campaign 2, the absolute average deviation between and gas and liquid CO_2 material balance was 24.1% and the maximum deviation was 60.1%. The material balance of the fourth campaign found that for 5 m K^+/2.5 m PZ, the absolute average deviation

between and gas and liquid CO_2 material balance was 14.0% and the maximum deviation was 52.4%. For 6.4 m K^+/1.6 m PZ, the absolute average deviation between and gas and liquid CO_2 material balance was 10.9% and the maximum deviation was 28.0%. It was found that if the absorber gas flow is adjusted by downward by 10% or the absorber rich CO_2 loading is increased by 2%, the systematic offset could be eliminated.

The liquid phase CO_2 material balance was consistently lower than the gas phase, which may indicate the loss of CO_2 during the sample collection, transfer, and analysis process. It is possible that residual amounts of CO_2 may have flashed when the sample bombs were disengaged from the quick-connects. Also, the syringes used to extract the sample and to dilute the sample for TOC analysis may have contained trapped air, which would skew the loading results. The auto-sampler for the TOC analyzer also uses a syringe to extract the sample. Additional losses of CO_2 may have occurred when the samples were transferred to the TOC sample vials. The samples were poured into the TOC vials and exposed directly to the air. Finally, the TOC analyzer exhibited a significant amount of drift. Corrections up to 10% were made with IC standards and may have contributed to additional errors in the liquid loading analysis.

No observable corrosion was detected with the corrosions coupons over the course of each campaign. No detectable degradation products were observed with the potassium carbonate/piperazine solvent during the three campaigns. Foaming occurred in the absorber during the first two campaigns. In Campaign 4, foaming occurred in the stripper. It was found that the DOW Corning Q2-3183A antifoam worked well for the piperazine and potassium carbonate system. Flashing feed to the stripper in the fourth campaign may have contributed to poor stripper performance.

6.2.2 RateSep™ Absorber Model

Using pilot plant data for Campaigns 2 and 4, the Aspen Plus® Data-Fit regression analysis found that the effective interfacial wetted area was less than the air–water measurements. The average interfacial area of Flexipac 1Y (a_{sp} = 410 m^2/m^3) structured packing was 240 m^2/m^3, which was 80% of the value measured by the air–water column and 59% of the specific area. The average interfacial area of Flexipac AQ Style 20 (a_{sp} = 213 m^2/m^3) structured packing for 5 m K^+/2.5 m PZ was 136 m^2/m^3, which was 56% of the air–water measurement and 52% of the specific area. The average interfacial area of Flexipac AQ for 6.4 m K^+/1.6 m PZ was 110 m^2/m^3, which was 67% of the air–water measurement and 64% of the specific area. Essentially the same interfacial area was obtained for Flexipac AQ even when two different solvents were used, which shows that the kinetics for two different solvents were correctly modeled.

The average heat losses regressed by Data-Fit for 5 m K^+/2.5 m PZ were 27,600 and 28,700 Watts for the Flexipac AQ Style 20 and Flexipac 1Y packing, respectively, while the regressed average heat loss for 6.4 m K^+/1.6 m PZ was 10,400 Watts. The heat loss results show that the Data-Fit regression analysis was consistent for the each of the solvents. A simple calculation of the heat transfer coefficient found that the heat loss was consistent with forced convection. This is unlikely to have occurred under the run conditions. It was concluded that the CO_2 heat of absorption may not have been adequately predicted by the RateSep™ absorber model.

The absorber design analysis suggests that a large energy savings associated with pressure drop in the absorber can be achieved by using slightly more packing and a slightly larger diameter column (lower gas velocity). The absorber performance analysis showed that that at the inflection point of the rich loading, the temperature bulge is located at the middle of the absorber column,

and that the magnitude of the temperature bulge decreases dramatically when the location moves form the middle to the bottom of the column. At the top of the absorber column, the magnitude of the maximum temperature of the bulge remains relatively constant. The analysis also showed that the 5 m K^+/2.5 m PZ solution has a capacity that is 15–100% higher than 6.4 m K^+/1.6 m PZ.

The Data-Fit results implicitly show that bench-scale kinetic and vapor–liquid equilibrium and air–water measurements in the PVC column cannot directly be used in RateSep™ to model CO_2 capture with potassium carbonate/piperazine in an absorber column. In this work, the kinetics was adjusted by a factor of 0.2 and the regressed average effective area was 56–80% of the air–water measurements. In addition, the vapor–liquid equilibrium model (Hilliard, 2005) used this work was regressed based on inconsistent bench-scale data and experimental loading data needed to be adjusted by 10%.

Pilot plant data was successfully reconciled by Data-Fit. The maximum absolute average deviation of the inlet and outlet CO_2 gas concentration of Campaign 4 was 1.45 and 0.68%, respectively. The maximum deviations of the inlet and outlet CO_2 gas concentration was 6.7 and 6.3%, respectively. The maximum absolute average deviation for the lean and rich loadings of Campaign 4 was 5.87 and 10.6, respectively. The maximum deviations of the lean and rich loadings were 13.3 and 20.2%, respectively. Data reconciliation by Data-Fit indicated that the experimental rich loadings were low by 10%. Data-Fit adjustments to the inlet and outlet gas phase CO_2 concentration were consistent with the pilot plant measurements.

Liquid heat capacity and CO_2 heat of absorption is important for modeling the profile temperature of an absorber column. If the heat capacity is incorrect, the location of the temperature bulge cannot be simultaneously fitted to match the pilot plant material balance. Absorber performance is most sensitive to lean

loading and interfacial area, which affect the magnitude and location of the temperature bulge. Piperazine concentration has a secondary affect on absorber performance. Heat loss, liquid holdup, potassium carbonate concentration, inlet water vapor concentration, and inlet liquid and vapor temperatures all have a minor affect on absorber performance. The magnitude and location of the temperature bulge is sensitive to the value of heat loss. Inlet water vapor concentration impacts the temperature profile in the bottom half of the absorber column.

Heat capacity and heat of formation for the four piperazine ions ($PZCOO^-$, H^+PZCOO^-, $PZ(COO^-)_2$, and PZH^+) were calculated from the derivative of the corresponding equilibrium reactions. This was used to reconcile the Aspen Plus® heat duty derived from a flash calculation with the heat of absorption calculated by the Gibbs–Helmholtz equation using vapor–liquid equilibrium data.

This work has shown that all of the predictions by Aspen Plus® must be verified with experimental data. While the Aspen Plus® models are comprehensive and allow for custom tuning, more often than not, the default parameters are incorrect and give erroneous results. Accurate predictions of the physical and transport properties are just as important as the thermodynamics and kinetics. In many cases, the calculation of the latter depends upon the former.

6.2.3 Data-Fit and Approximate K_g Analysis

The rigorous Data-Fit analysis accounts for the temperature bulge and the non-linear driving force across the absorber column, whereas the approximate K_g rate analysis does not. The regressed Data-Fit results for the effective interfacial areas were approximately 20% lower for Flexipac 1Y structured packing and two times lower for Flexipac AQ Style 20 structured packing. In the Data-Fit analysis,

the kinetic rates had been adjusted to match the Cullinane wetted wall column results. In the K_g analysis of the pilot plant data, the results for the 5 m K^+/2.5 m PZ data from Campaigns 1 and 4 were approximately four times slower than the 60 °C wetted wall column results. The approximate analysis used the interfacial area results obtained by SRP in the air-water column with 0.1 N NaOH. While the results from the rigorous Data-Fit analysis showed marked improvements were made over the approximate analysis, additional work is still needed to properly model the interfacial area, kinetics, and temperature bulge. However, the approximate analysis is needed because it allows direct comparison of the K^+/PZ mass transfer results with MEA and the analysis is more transparent than the rigorous analysis. The approximate analysis also validates the rigorous analysis because both analyses show that the absorption rate for 5 m K^+/2.5 m PZ is faster than 6.4 m K^+/1.6 m PZ.

6.2.4 K^+/PZ and MEA as Solvents for CO_2 Capture

The selection of a solvent for CO_2 capture should not depend solely on absorber and stripper performance of an absorber, but also on solvent operability. The bench and pilot scale work for the aqueous piperazine promoted potassium carbonate has shown that the 5 m K^+/2.5 m PZ solvent has a CO_2 absorption rate that is 1–1.5 times faster than 7 m MEA. However, the pilot plant experiments show that the heat duty requirement for desorption of CO_2 from the stripper may be slightly higher than MEA. From an operational viewpoint, the MEA pilot plant campaign went much smoother than the K^+/PZ campaigns. Solubility issues with the potassium carbonate/piperazine campaigns resulted in periodic losses of critical instrumentation such reboiler level and column sump level due to lines being plugged with solids. Complete shutdown of the pilot plant also occurred on several occasions. The cost of piperazine is also approximately 5

times higher than MEA. However, the K^+/PZ system has ability to be "tuned" and further optimization of solvent and process configuration may show that it can be competitive with MEA.

6.3 RECOMMENDATIONS

6.3.1 Pilot Plant

The pilot plant should be operated at a constant run condition until a satisfactory material balance is obtained, before moving onto the next run condition. In all three of the K^+/PZ campaigns, the CO_2 material balance for the gas phase was systematically higher than the liquid phase. Although the liquid sampling methods and loading analysis methods were greatly improved over the course of the four campaigns, additional development and testing is recommended to improve the material balance.

A more accurate method of online loading measurement should be developed and online process instrumentation should be installed both upstream and downstream of the absorber feed tank. This will allow the operator to know how much steam to provide to the reboiler and better control the lean loading. During the operation of the pilot plant, the lean loading in the solvent was often unknown because real time analysis was not available and often it was unclear whether the desired lean loading condition had been attained. The difficulty of discerning lean loading was also compounded by the lack of direct feedback of the solvent loading entering the absorber feed tank, water losses, and solubility issues. Controlling and maintaining a constant lean leading to the absorber column was often a challenge because there was no indictor or measurement of the loading of the feed to the absorber feed tank and accurate real time analysis of the lean loading to the absorber column was not available. For the K^+/PZ

campaigns, pH meters were installed at the absorber inlet and outlet and only provided approximate real time analysis of the loading.

The ability to have real-time analysis of the liquid loading, composition, and water content should be implemented in the next pilot plant campaign. Water losses and solubility issues resulted in liquid compositions that were constantly changing. Attempts to correlate loading with pH and density were unsuccessful for the K^+/PZ system, which made it difficult to maintain constant conditions and made continuous operation difficult.

A metering pump that continuously adds antifoam to the solvent should be installed in future pilot plant campaigns. During the pilot plant campaigns, foaming occurred in the absorber in the first two campaigns and in the fourth campaign, it occurred in the stripper. This resulted in poor performance and upsets in pilot plant operation. Antifoam was periodically added to the system to rectify this problem. However, antifoam is typically designed for once through systems. In the pilot plant campaigns, the solvent was continuously re-circulated and over time the antifoam lost its efficacy. The effects of antifoam and its degradation products on the performance of the K^+/PZ solvent are unknown and should be studied.

A two phase distributor should be used at the top of the stripper column to account for the flashing feed. In all three K^+/PZ campaigns, the performance of the stripper was limited due to a flashing feed at the top of the stripper. The control valve was moved directly to upstream of the stripper inlet and two pumps were used in series to pressurize the feed, but the problem remained unresolved.

The gas line from the condenser to the overhead gas phase accumulator should be enlarged instead of the allowing the CO_2 gas to flow through the liquid accumulator. Maintaining the water balance in the system was critical for

the potassium carbonate and piperazine solvent. Since the solvent was operated near its solubility limit, water losses resulted in plugged filters, plugged instrument lines, loss of level measurements, and wreaked havoc on the pilot plant. In the fourth campaign, a significant amount of water was found in the overhead accumulator. It was surmised that the water was being entrained through the liquid accumulator.

The heat loss for the absorber column should be measured and correlated. Since, the temperature of the absorber column affects the vapor–liquid equilibrium, kinetics, physical properties, and ultimately CO_2 removal performance, it is recommended that heat loss measurements be conducted. Another possibility would be to insulate the absorber column. The heat loss measurements could be compared to the values calculated by the RateSep™ absorber model in this work.

The degradation of piperazine via oxidative and thermal degradation should be thoroughly studied. Since, the cost of piperazine is five times higher than MEA, additional losses of piperazine from degradation may make it cost prohibitive. Long term corrosion studies with the potassium carbonate/piperazine system should be studied. Vanadium oxide was added to the solvent as a corrosion inhibitor based on the suggestion from a vendor.

6.3.2 RateSep™ Absorber Model

The Hilliard (2005) Aspen Plus® vapor–liquid equilibrium model should be regressed with newly available heat capacity data, which may resolve issues with heat of absorption and liquid heat capacity. While significant improvements were made to the predicted heats of absorption and liquid heat capacity in Aspen Plus®, the experimental data and Data-Fit results both show that it was not properly modeled over the range of absorber conditions. The

Hilliard (2005) VLE model used in this work was regressed without liquid heat capacity data because it was not available at the time, which resulted in missing parameters and inconsistencies. Proper heat of absorption and liquid heat capacity models are needed to fit the temperature profile of the absorber.

A secondary and related issue is that Aspen Plus® does not account for zwitterions. One recommendation is to regress the potassium carbonate and piperazine VLE model with a small charge for the HPZCOO species. H^+PZCOO^- is an ion that has a net zero charge. In this work, the net zero charge was retained and the ion was treated as a molecule. It was also found that by giving the ion a small charge (0.0001), Aspen Plus® would treat it as an ion. However, this also changed the VLE predicted by the Hilliard (2005) model because it was regressed assuming a zero charge.

The Aspen Plus® VLE model should be regressed with the updated vapor–liquid equilibrium data for K^+/PZ. Recent measurements by Hilliard have found that the vapor–liquid equilibrium from Cullinane may be systematically offset by 10%. In this work, the RateSep™ model used the Hilliard (2005) VLE model, which was regressed based on the Cullinane data.

The discrepancy between the mass transfer rates from wetted wall column and RateSep™ should be resolved. When the Cullinane (2005) kinetics for K^+/PZ was transformed from concentration to activity based rates and translated into RateSep™, the mass transfer rates (k_g') were found to be five times faster than that measured in the wetted wall column. It is possible that the kinetics do not have the strong ionic strength dependence that was concluded by Cullinane. Also, it possible that the optimal temperature and loading range was not selected when the parameter for gamma were regressed.

The optimization analysis for the number of stages and the film discretization in RateSep™ should be conducted for the 6.4 m K^+/1.6 m PZ

solution. The optimization analysis was performed for the 5 m K^+/2.5 m PZ solvent and the results were used for the 6.4 m K^+/1.6 m PZ solvent. Since, 6.4 m K^+/1.6 m PZ has slower CO_2 absorption rate, this may affect the film ratio and the number of film discretization that should be used.

The effects of k_g and k_l on mass transfer rates should be examined. A FORTRAN subroutine could be written to address this issue because the mass transfer models provided by RateSep™ only allow for limited adjustments.

The effects of density, viscosity, and surface tension should be further studied and new effective area model should be proposed. The Data-Fit results for interfacial area suggest that the air–water measurements are dramatically affected by the physical properties of the solvent.

Experimental data for surface tension and thermal conductivity for the potassium carbonate/piperazine solution should be obtained and used to fit the parameters in Aspen Plus®. This work has shown that missing parameters in Aspen Plus® will result in erroneous predictions. While corrections to density and viscosity predictions in Aspen Plus® were addressed in this work, surface tension and thermal conductivity were not. Surface tension will affect the prediction of interfacial area of packing and thermal conductivity will be important for heat and mass transfer.

Appendix A: Campaign 1 Raw Pilot Plant Data and DeltaV Process Control Graphics

Table A-1. Campaign 1 Raw Absorber Data

	ABS LEAN	ABS LEAN	ABS LEAN	ABS LEAN	ABS RICH	ABS RICH	ABS RICH	ABS RICH	GAS	GAS	GAS	Cool	GAS
	FLOW	DEN	TEMP	pH	FLOW	DEN	TEMP	pH	FLOW	IN	OUT	TEMP	PRESS
Time	FT403	FT403	TT403	AI403	FT200	FT200	TT200	AI401	FI900	TT400	TT404	TT412	PT900
	(GPM)	(LB/FT^3)	(F)	(pH)	(GPM)	(LB/FT^3)	(F)	(pH)	(ACFM)	(F)	(F)	(F)	(PSIA)
6/16/2004 15:30	5.01	71.51	102.80	11.40	4.85	73.27	84.54	9.70	600.69	101.85	108.75	69.89	0.15
6/16/2004 16:15	5.00	71.53	102.39	11.50	4.95	73.23	83.42	10.00	599.64	99.82	107.61	68.78	0.14
6/16/2004 17:00	5.00	71.60	102.02	11.60	4.88	73.32	84.12	10.00	599.77	101.87	108.34	69.35	0.14
6/17/2004 11:30	4.97	72.60	106.70	11.60	4.91	73.69	90.11	10.00	300.05	82.44	103.66	57.41	0.04
6/17/2004 12:15	4.98	72.59	109.68	11.50	4.87	73.71	90.65	10.60	300.20	84.21	107.22	58.19	0.04
6/17/2004 13:00	4.99	72.55	112.02	11.40	4.87	73.75	90.65	10.50	300.08	84.97	109.33	58.11	0.04
6/17/2004 16:15	9.96	72.72	105.83	11.40	9.90	73.15	101.04	10.50	299.88	91.22	103.13	58.87	0.14
6/17/2004 16:45	9.96	72.75	105.20	11.21	9.93	73.20	100.56	10.79	299.86	91.84	102.71	58.44	0.15
6/17/2004 17:15	9.95	72.76	104.76	11.23	9.90	73.21	100.50	10.77	299.47	91.89	101.69	58.18	0.16
6/17/2004 18:33	9.94	72.81	104.02	11.30	9.91	73.37	102.92	10.70	299.83	91.62	100.34	58.38	0.18
6/17/2004 19:13	8.63	72.80	104.15	11.30	9.74	73.31	100.87	10.70	407.75	92.15	100.58	59.98	0.20
6/18/2004 15:30	7.69	72.74	103.15	10.70	7.79	73.68	111.27	9.20	179.50	92.22	60.51	60.51	0.07
6/21/2004 16:45	5.02	72.60	104.09	10.60	5.02	73.89	102.65	9.60	120.24	90.06	106.78	60.17	0.01
6/22/2004 17:45	5.02	75.33	106.09	10.90	4.87	77.06	85.42	9.60	600.24	99.71	110.54	70.80	0.14
6/22/2004 18:30	5.01	75.36	106.66	11.00	4.95	77.21	85.01	9.60	599.89	99.75	110.34	70.17	0.14
6/22/2004 19:30	5.01	75.31	106.67	11.00	4.97	77.15	88.93	9.60	800.34	116.41	107.76	74.42	0.25
6/22/2004 20:15	5.01	75.34	106.79	11.00	4.97	77.13	88.68	9.70	800.27	115.33	107.33	74.04	0.25
6/22/2004 21:15	5.08	75.40	106.84	11.00	5.02	76.91	86.24	9.70	399.99	83.17	108.79	61.29	0.07
6/22/2004 22:00	4.93	75.41	106.74	11.20	4.90	76.95	85.69	10.10	399.83	81.79	108.81	61.27	0.07
6/23/2004 8:15	2.49	75.69	94.33	11.20	2.43	77.46	72.61	10.10	300.15	74.42	96.46	55.06	0.04
6/23/2004 9:00	2.51	75.59	95.70	11.20	2.49	77.49	72.79	10.10	299.65	75.42	97.05	55.16	0.04
6/23/2004 14:30	7.00	75.60	103.66	10.60	6.90	76.96	93.91	9.40	840.43	126.88	109.14	76.99	0.31
6/23/2004 15:15	6.54	75.62	103.36	10.60	6.52	77.01	93.98	9.40	790.76	124.05	110.64	76.82	0.28
6/23/2004 17:30	7.69	75.62	104.88	10.90	7.75	77.16	101.37	9.80	287.85	87.24	120.84	61.25	0.07
6/23/2004 18:15	6.73	75.66	104.48	11.10	7.09	76.95	105.89	9.40	236.92	85.34	115.17	57.96	0.09
6/24/2004 9:00	7.74	75.92	103.26	11.10	7.88	77.05	103.57	9.40	248.96	76.40	95.51	55.89	0.05
6/24/2004 9:30	7.74	75.77	109.82	10.80	7.89	77.05	105.55	9.40	249.66	77.99	111.26	56.70	0.08
6/24/2004 10:30	7.77	75.68	110.02	10.80	7.75	77.29	101.24	9.40	299.87	81.27	123.53	61.04	0.11
6/24/2004 11:00	7.79	75.72	108.46	11.10	7.72	77.25	101.89	9.60	299.53	83.68	121.42	60.75	0.12
6/24/2004 12:15	4.98	75.77	106.41	11.04	5.13	77.36	101.10	9.47	159.65	80.18	118.81	56.02	0.02
6/24/2004 12:30	4.99	75.76	106.20	10.90	5.10	77.35	101.12	9.40	159.46	80.10	117.89	56.24	0.02
6/24/2004 16:00	7.72	76.71	115.24	10.80	7.78	78.17	110.04	9.30	249.64	92.64	127.31	60.43	0.11
6/24/2004 16:15	7.73	76.67	114.90	10.80	7.73	78.15	110.37	9.30	250.59	93.51	127.75	60.86	0.11
6/24/2004 17:00	4.97	76.70	113.48	11.00	4.98	78.48	104.79	9.20	160.71	91.19	128.62	59.23	0.03
6/24/2004 17:30	4.99	76.67	112.71	11.00	4.98	78.46	103.67	9.20	160.16	89.72	127.68	58.93	0.02

Table A-2. Campaign 1 Raw Absorber Data – Continued

	PRESSURE	PRESSURE	BED	BED	BED	BED	CO_2	CO_2	CO_2
	DRP	DRP	TEMP	TEMP	TEMP	TEMP	IN	MID	OUT
Time	PDT450	PDT451	TT4078	TT4076	TT4073	TT4071	AI400	AI406	AI404
	(in H_2O)	(in H_2O)	(F)	(F)	(F)	(F)	(mol%)	(mol%)	(mol%)
6/16/2004 15:30	3.27	3.07	106.83	114.51	103.82	82.46	2.89	1.71	0.16
6/16/2004 16:15	2.54	3.09	105.21	113.81	103.03	81.57	2.84	1.69	0.17
6/16/2004 17:00	2.90	3.05	106.16	114.05	103.24	82.22	2.78	1.70	0.17
6/17/2004 11:30	0.75	0.99	98.35	116.33	115.83	91.30	2.97	0.18	0.00
6/17/2004 12:15	0.81	0.99	102.19	119.40	117.14	91.64	2.92	0.18	0.01
6/17/2004 13:00	0.55	1.01	104.61	119.85	117.46	91.47	2.88	0.19	0.01
6/17/2004 16:15	3.79	2.71	100.57	103.81	100.01	100.91	2.25	0.17	0.02
6/17/2004 16:45	3.68	3.11	100.21	104.07	99.94	99.66	2.45	0.26	0.03
6/17/2004 17:15	4.29	3.43	99.38	103.48	99.25	98.09	2.37	0.21	0.03
6/17/2004 18:33	5.34	3.80	98.03	103.51	99.54	102.88	3.92	0.70	0.04
6/17/2004 19:13	5.70	4.26	98.09	103.47	99.19	98.32	3.00	0.43	0.05
6/18/2004 15:30	1.61	0.84	98.34	118.70	118.39	99.71	11.72	5.84	0.32
6/21/2004 16:45	0.59	0.29	102.27	146.27	124.48	98.00	11.62	5.41	0.73
6/22/2004 17:45	2.90	3.09	107.30	116.28	105.56	84.43	3.39	1.43	0.26
6/22/2004 18:30	2.91	3.09	107.04	115.36	104.99	84.44	3.47	1.23	0.21
6/22/2004 19:30	4.90	5.28	105.60	108.05	98.05	88.85	3.58	1.79	0.56
6/22/2004 20:15	4.93	5.31	104.98	107.85	98.32	88.56	3.66	1.72	0.54
6/22/2004 21:15	1.63	1.73	103.86	124.89	118.46	85.59	2.98	0.54	0.04
6/22/2004 22:00	1.63	1.74	103.91	125.29	118.53	85.29	2.68	0.54	0.03
6/23/2004 8:15	0.91	0.98	92.28	105.33	93.06	70.01	2.71	1.54	0.23
6/23/2004 9:00	0.91	0.97	92.72	106.55	93.67	70.54	2.48	1.39	0.16
6/23/2004 14:30	6.10	6.64	106.21	117.00	107.32	93.81	2.25	1.83	0.33
6/23/2004 15:15	5.41	5.85	107.54	117.86	107.02	93.26	3.58	2.14	0.47
6/23/2004 17:30	1.62	1.21	115.67	148.75	130.62	97.57	13.99	2.77	1.20
6/23/2004 18:15	2.45	1.03	107.97	153.30	135.83	100.16	13.22	1.46	1.15
6/24/2004 9:00	1.30	1.00	89.48	142.75	127.45	96.95	12.30	0.12	1.26
6/24/2004 9:30	2.11	1.27	100.72	153.90	138.25	97.03	11.30	1.61	0.88
6/24/2004 10:30	2.75	1.69	115.52	149.44	134.93	98.60	12.23	0.11	1.74
6/24/2004 11:00	2.82	1.79	113.63	148.24	135.28	100.45	12.51	0.00	1.75
6/24/2004 12:15	0.50	0.51	113.33	152.17	134.11	99.27	11.59	0.85	0.68
6/24/2004 12:30	0.47	0.52	112.13	152.89	134.83	101.00	11.59	0.68	0.55
6/24/2004 16:00	3.33	1.59	119.27	159.74	146.22	112.36	12.40	0.64	0.43
6/24/2004 16:15	3.40	1.52	120.05	160.41	146.37	116.03	12.65	0.61	0.45
6/24/2004 17:00	0.61	0.49	125.63	155.01	138.19	98.47	11.55	0.56	0.58
6/24/2004 17:30	0.52	0.48	124.16	156.68	138.14	98.06	11.76	0.81	0.40

Table A-3. Campaign 1 Raw Stripper Data

	ACCUMULATOR	COLUMN	COLUMN	REBOILER	REBOILER	COLUMN	PRESSURE	PRESSURE	STRP	STRP	STRP
	LEVEL	LEVEL	LEVEL	LEVEL	DUTY	PRESSURE	DROP (LOW)	DROP (HIGH)	REFLUX	RETURN	RETURN
Time	LC203	LC201	LT206	LT204	QIC202	PT215	PDT250	PDT251	FT203	FT201	FT201
	(in)	(in)	(in)	(in)	(MMBTU/hr)	(PSIA)	(in H_2O)	(in H_2O)	(GPM)	(GPM)	(F)
6/16/2004 15:30	12.80	6.48	6.50	4.92	0.85	19.98	5.96	15.29	1.20	4.80	104.83
6/16/2004 16:15	12.80	6.50	6.50	5.19	0.850	20.12	5.96	15.24	1.06	4.63	104.69
6/16/2004 17:00	12.80	6.51	6.50	5.47	0.850	20.08	5.96	15.05	1.03	4.66	104.93
6/17/2004 11:30	13.00	8.50	8.51	7.21	0.828	16.92	5.96	22.46	0.83	4.93	124.20
6/17/2004 12:15	13.00	8.52	8.51	8.13	0.819	17.02	5.96	22.07	0.81	4.82	123.59
6/17/2004 13:00	13.00	8.49	8.49	8.53	0.814	17.07	5.96	21.72	0.82	4.81	113.80
6/17/2004 16:15	12.50	9.99	10.00	6.48	0.751	16.36	5.96	18.63	0.58	9.82	105.08
6/17/2004 16:45	12.50	10.00	9.98	6.68	0.749	15.39	5.96	17.90	0.46	9.81	105.07
6/17/2004 17:15	12.50	10.27	10.28	6.91	0.750	20.68	5.96	15.63	0.23	10.48	103.96
6/17/2004 18:33	12.50	10.06	10.04	7.82	0.750	19.63	5.96	14.91	0.29	9.50	104.82
6/17/2004 19:13	12.50	10.12	10.13	7.48	0.750	22.98	5.96	14.45	0.22	10.16	104.79
6/18/2004 15:30	12.50	8.14	8.15	6.04	1.00	16.79	5.96	25.21	1.77	7.60	104.00
6/21/2004 16:45	12.50	10.13	10.13	7.16	1.000	16.58	5.96	18.82	1.27	4.91	103.55
6/22/2004 17:45	8.00	11.98	11.98	11.90	0.998	15.70	5.96	19.57	0.54	4.58	109.83
6/22/2004 18:30	8.00	11.94	11.94	11.19	0.925	15.88	5.96	18.47	0.39	4.67	109.75
6/22/2004 19:30	8.00	12.02	12.03	10.81	0.925	15.96	5.96	18.47	0.39	5.14	110.51
6/22/2004 20:15	8.00	12.06	12.06	10.69	0.925	15.84	5.96	18.36	0.39	5.01	109.90
6/22/2004 21:15	8.00	12.05	12.05	10.53	0.899	17.12	5.96	18.51	0.32	4.92	110.47
6/22/2004 22:00	8.00	12.10	12.09	10.41	0.719	16.94	5.40	15.66	0.24	5.88	110.61
6/23/2004 8:15	8.00	9.99	9.98	6.71	0.708	16.40	5.96	24.44	0.01	0.67	102.50
6/23/2004 9:00	8.00	14.46	14.46	12.95	0.687	17.64	5.96	14.59	-0.01	2.45	113.72
6/23/2004 14:30	9.50	-2.49	-2.50	-2.00	1.100	16.08	5.96	44.13	0.57	7.03	105.12
6/23/2004 15:15	9.50	-2.50	-2.50	-1.87	1.099	16.70	5.96	44.12	0.57	6.61	105.02
6/23/2004 17:30	9.50	-2.51	-2.51	-1.15	1.150	18.52	5.96	46.45	0.51	7.52	107.07
6/23/2004 18:15	9.50	-2.52	-2.52	-1.33	0.745	19.40	5.96	50.30	0.34	6.36	106.71
6/24/2004 9:00	15.00	14.14	14.13	8.83	1.148	21.61	5.96	19.44	0.29	7.53	120.16
6/24/2004 9:30	15.00	14.12	14.13	8.31	1.152	22.62	5.96	19.62	0.43	7.52	119.86
6/24/2004 10:30	15.00	13.73	13.74	7.00	1.148	18.96	5.96	18.91	0.43	7.47	108.09
6/24/2004 11:00	15.00	13.49	13.50	6.34	1.150	20.17	5.96	18.95	0.45	7.44	107.89
6/24/2004 12:15	17.00	13.78	13.78	9.03	1.201	21.49	5.96	19.33	0.49	4.44	108.04
6/24/2004 12:30	17.00	13.79	13.77	9.53	1.201	21.15	5.96	19.32	0.49	4.54	107.93
6/24/2004 16:00	22.50	13.05	13.05	10.67	1.101	22.58	5.96	18.62	0.38	7.55	115.28
6/24/2004 16:15	22.50	13.02	13.01	10.63	1.100	21.97	5.96	18.47	0.38	7.52	115.05
6/24/2004 17:00	22.50	12.76	12.75	10.54	1.100	24.72	5.96	18.05	0.38	4.96	115.24
6/24/2004 17:30	22.50	12.87	12.85	11.02	1.100	24.68	5.96	18.17	0.38	5.14	115.32

Table A-4. Campaign 1 Raw Stripper Data – Continued

	TOP	TOP MID	BOT MID	BOT	CONDENS	VAPOR	BOT LIQ TO	VAP TO	ORG. OUT	CW	CW	CW
	TEMP	TEMP	TEMP	TEMP	RETURN	INLET	REB	CONDEN	(COND)	INLET	OUTLET	FLOW
Time	T20710	T2073	T2074	T2071	T203	T208	T219	T216	T225	T224	T226	FT205
	(F)	(F)	(F)	(F)	(F)	(F)	(F)	(F)	(F)	(F)	(F)	(GPM)
6/16/2004 15:30	218.88	230.44	231.37	232.69	218.30	235.84	235.17	207.55	92.00	49.65	55.19	209.65
6/16/2004 16:15	219.77	230.87	231.78	233.13	222.32	237.22	236.26	207.94	90.24	49.40	54.22	209.67
6/16/2004 17:00	219.48	230.94	231.85	233.18	220.54	235.79	235.69	207.70	91.96	49.16	54.79	209.85
6/17/2004 11:30	199.81	222.37	223.30	224.65	242.51	224.05	227.61	199.14	73.89	48.43	52.52	209.66
6/17/2004 12:15	200.36	222.64	223.51	224.85	241.07	224.91	227.88	199.70	72.54	48.41	52.91	209.69
6/17/2004 13:00	203.46	222.83	223.69	225.04	240.51	225.64	227.89	199.99	74.16	48.38	53.41	209.71
6/17/2004 16:15	193.88	220.93	221.82	223.29	233.10	224.63	225.96	198.05	63.17	49.00	52.67	204.40
6/17/2004 16:45	194.54	217.68	218.59	220.13	230.42	220.62	221.36	193.98	63.65	49.17	52.14	204.63
6/17/2004 17:15	218.33	232.66	233.72	235.19	238.72	235.58	235.66	199.42	64.13	49.34	50.69	204.48
6/17/2004 18:33	212.24	229.63	230.69	232.31	238.83	232.69	233.61	196.75	65.34	49.45	51.60	204.55
6/17/2004 19:13	218.88	238.26	239.36	240.87	244.58	241.58	242.67	201.97	65.97	48.66	51.12	204.54
6/18/2004 15:30	214.67	222.79	223.74	225.19	231.11	230.74	227.60	199.48	98.46	51.88	61.29	204.91
6/21/2004 16:45	208.82	220.76	221.68	223.10	255.67	223.47	225.99	197.39	105.62	50.48	56.61	197.52
6/22/2004 17:45	212.57	219.80	220.66	222.22	218.63	223.90	226.44	196.59	116.54	51.36	59.28	196.75
6/22/2004 18:30	212.65	220.59	221.39	222.99	216.12	224.23	227.02	197.10	113.16	51.09	58.31	196.67
6/22/2004 19:30	212.63	220.57	221.37	223.00	216.68	224.16	227.08	196.88	110.35	50.74	58.04	196.92
6/22/2004 20:15	212.26	220.10	220.94	222.53	217.11	223.69	226.67	196.37	112.09	50.47	57.56	196.84
6/22/2004 21:15	216.84	224.23	225.10	226.65	220.66	227.45	230.89	200.03	111.27	50.06	57.07	196.78
6/22/2004 22:00	214.67	223.11	224.06	225.61	217.48	226.82	230.57	199.29	108.58	49.27	55.97	196.66
6/23/2004 8:15	216.72	220.90	221.84	223.19	254.04	226.02	228.23	195.28	90.25	49.32	54.61	196.20
6/23/2004 9:00	220.74	224.94	225.80	227.18	254.80	230.21	232.04	198.74	87.64	49.57	54.09	205.36
6/23/2004 14:30	212.12	221.44	222.29	223.86	259.03	223.68	227.24	196.44	113.00	51.59	59.84	207.40
6/23/2004 15:15	214.13	223.51	224.40	226.01	259.44	225.61	228.87	199.47	113.28	51.58	59.55	207.39
6/23/2004 17:30	215.85	229.05	229.96	231.60	258.77	230.99	234.71	203.26	83.37	51.55	59.25	207.29
6/23/2004 18:15	206.01	226.83	229.81	232.03	252.04	232.79	237.53	205.39	84.74	50.82	56.95	207.15
6/24/2004 9:00	221.96	237.21	238.21	239.70	281.39	237.66	242.47	205.03	81.16	50.99	58.10	207.84
6/24/2004 9:30	223.24	239.83	240.81	242.21	281.24	241.08	246.18	209.25	84.89	51.20	58.47	208.00
6/24/2004 10:30	216.90	230.25	231.21	232.73	275.56	231.79	235.99	201.64	83.82	51.30	59.70	208.08
6/24/2004 11:00	220.00	233.63	234.59	236.06	277.78	234.96	239.44	204.77	84.03	51.35	59.66	208.12
6/24/2004 12:15	221.93	236.48	237.37	238.79	282.56	239.23	243.38	209.88	107.43	51.65	58.74	208.03
6/24/2004 12:30	220.61	235.56	236.49	237.90	281.37	238.59	242.63	208.98	108.15	51.75	58.53	207.95
6/24/2004 16:00	224.70	240.93	241.88	243.35	265.35	242.55	247.11	211.50	108.26	51.95	59.25	207.90
6/24/2004 16:15	224.27	239.51	240.49	241.94	264.09	241.55	245.75	210.76	108.52	51.90	59.06	207.97
6/24/2004 17:00	235.50	245.46	246.36	247.77	269.71	247.51	251.92	217.23	114.78	51.82	59.12	208.22
6/24/2004 17:30	235.31	245.35	246.19	247.66	270.93	247.85	252.36	217.33	116.52	51.74	59.52	208.17

Table A-5. Campaign 1 Absorber Temperature Profile Results from Infrared Temperature Gun

Location of Bed	Ht From Bed Bot (ft)	Run 1.7.1 6/21/04 16:00 (°F)	Run 1.9.2 6/22/04 20:00 (°F)	Run 1.10.2 6/22/04 21:45 (°F)	Run 1.14.1 6/23/04 18:00 (°F)	Run 1.16.2 6/24/04 10:45 (°F)
Top	10.0	110.4	103.6	108.4	123.4	133.0
	9.5	118.8	104.6	110.8	133.8	139.8
	9.0	133.0	105.4	114.2	143.6	144.6
	8.5	142.2	105.2	115.6	148.4	145.0
	8.0	145.8	106.0	117.0	149.4	145.0
	7.5	148.6	105.0	117.8	151.4	145.8
	7.0	148.6	103.4	118.2	151.2	144.4
	6.5	147.2	103.0	118.2	149.4	142.8
	6.0	145.8	102.6	118.8	148.6	142.6
	5.5	144.8	102.2	118.6	147.2	141.4
	5.0	142.6	102.4	118.8	146.0	139.4
	4.5	140.8	102.2	120.2	145.8	140.0
	4.0	138.2	101.2	120.8	143.4	138.8
	3.5	135.8	100.4	120.8	141.6	138.4
	3.0	133.6	99.6	120.2	140.6	137.2
	2.5	130.8	98.8	119.2	139.0	135.6
	2.0	128.6	98.2	117.6	137.4	135.0
	1.5	126.2	98.0	117.2	136.4	135.6
	1.0	124.2	98.2	117.8	135.6	135.2
	0.5	122.8	99.8	118.0	135.4	135.2
	0.0	118.8	101.0	119.4	136.2	136.8
Bottom	10.0	126.6	97.8	118.8	136.6	135.8
	9.5	126.4	97.4	118.4	136.2	134.8
	9.0	125.4	96.6	118.2	135.4	133.0
	8.5	124.6	96.0	118.6	134.8	132.0
	8.0	126.0	95.6	118.4	134.2	131.6
	7.5	125.8	95.0	117.4	132.0	129.0
	7.0	124.6	94.0	117.2	130.6	127.2
	6.5	123.8	93.0	116.4	129.2	126.0
	6.0	122.0	92.2	114.8	127.6	125.2
	5.5	120.6	91.8	112.8	128.2	123.2
	5.0	118.0	91.2	109.2	126.2	122.0
	4.5	121.4	91.4	110.2	122.4	126.0
	4.0	121.2	91.8	108.2	130.0	125.6
	3.5	120.2	91.4	106.6	128.4	124.2
	3.0	119.2	90.2	105.8	127.2	122.8
	2.5	117.6	90.0	102.4	124.4	120.2
	2.0	112.8	89.6	97.2	118.4	117.4
	1.5	108.9	89.0	93.8	111.4	110.8
	1.0	105.8	89.0	90.2	108.2	106.0
	0.5	98.6	90.0	85.4	101.2	98.4
	0.0	96.4	89.2	82.2	98.8	94.4

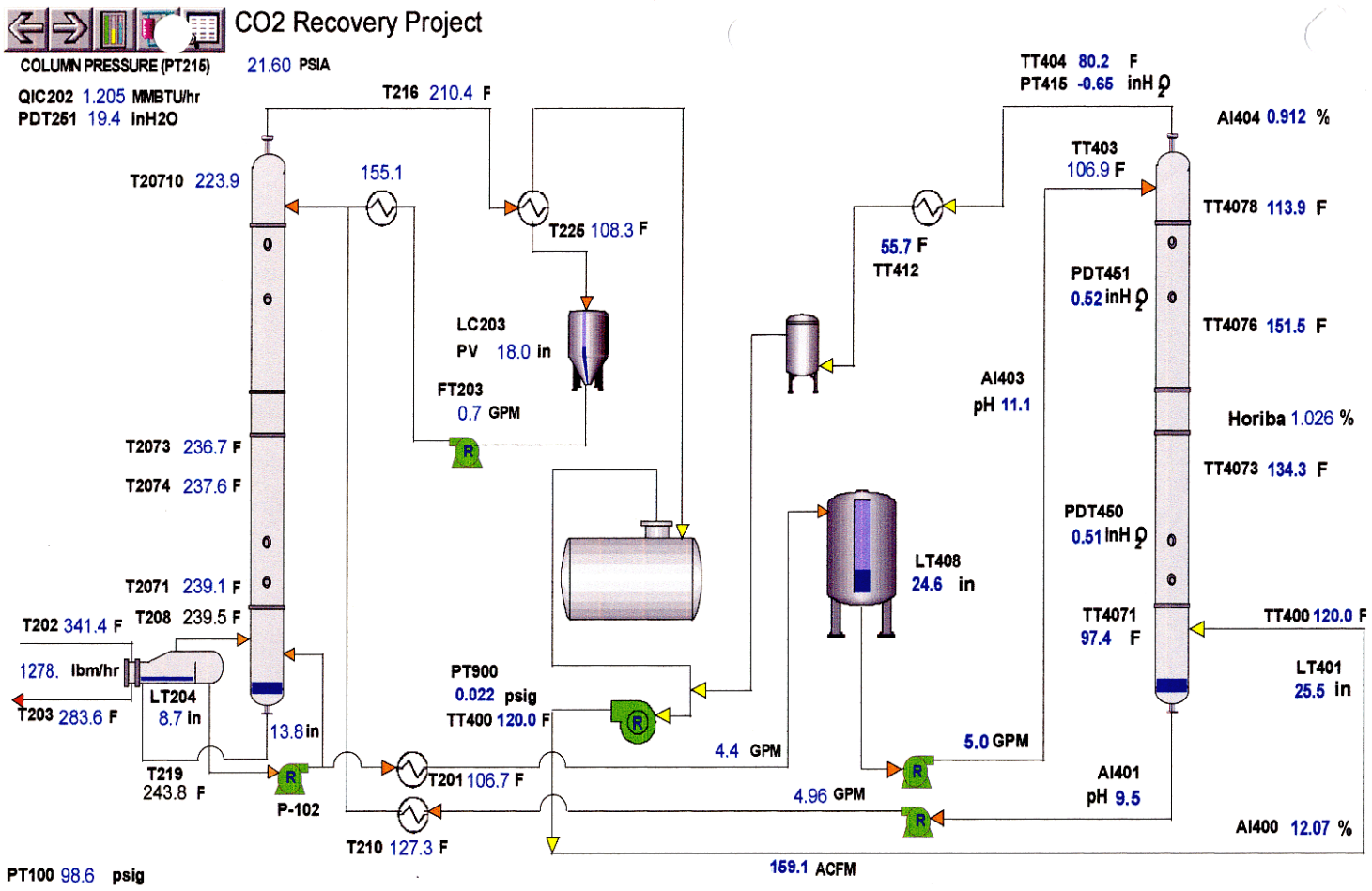

Figure A-1. Campaign 1 DeltaV Overall Process View

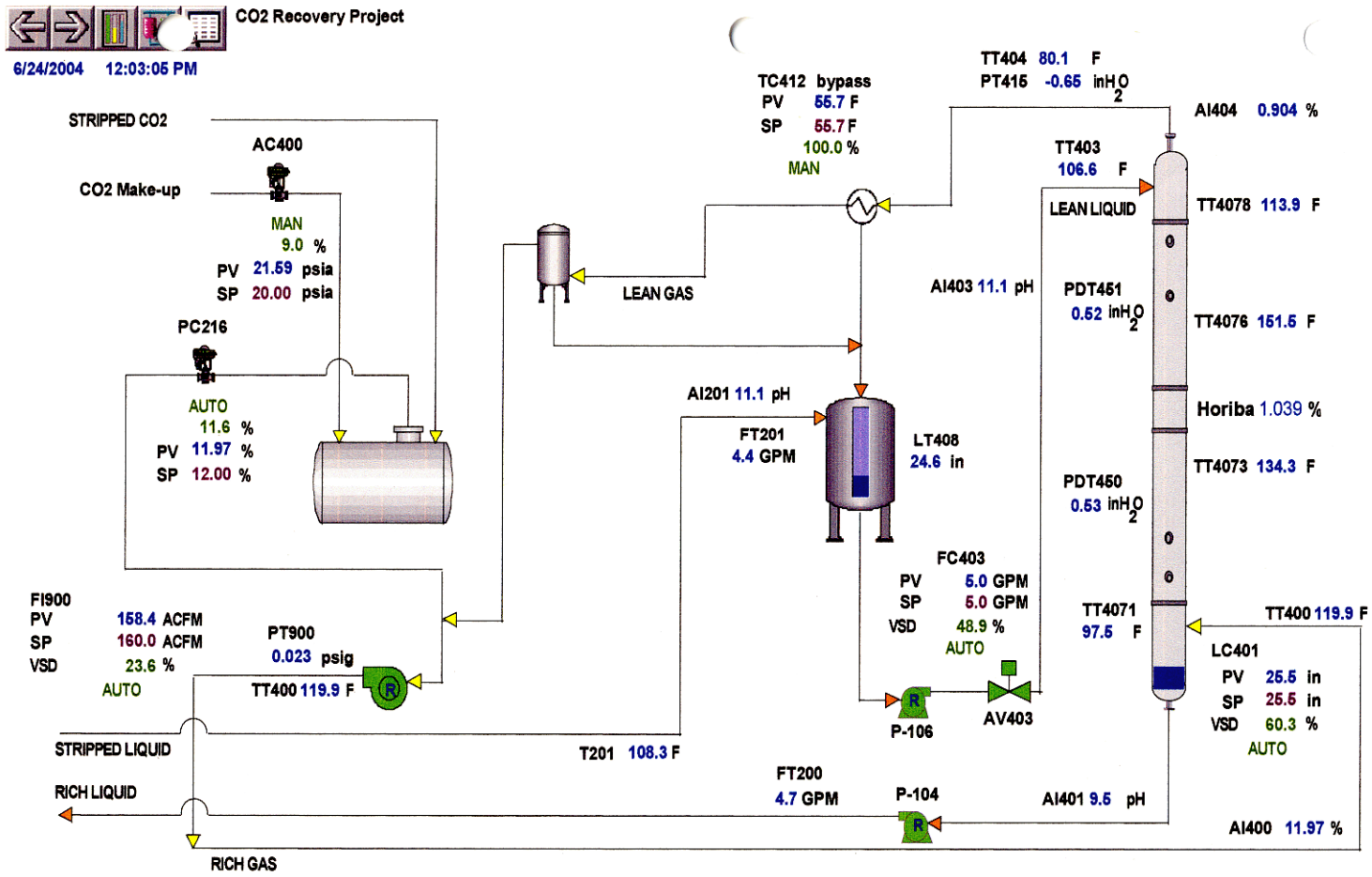

Figure A-2. Campaign 1 DeltaV Absorber Side Process View

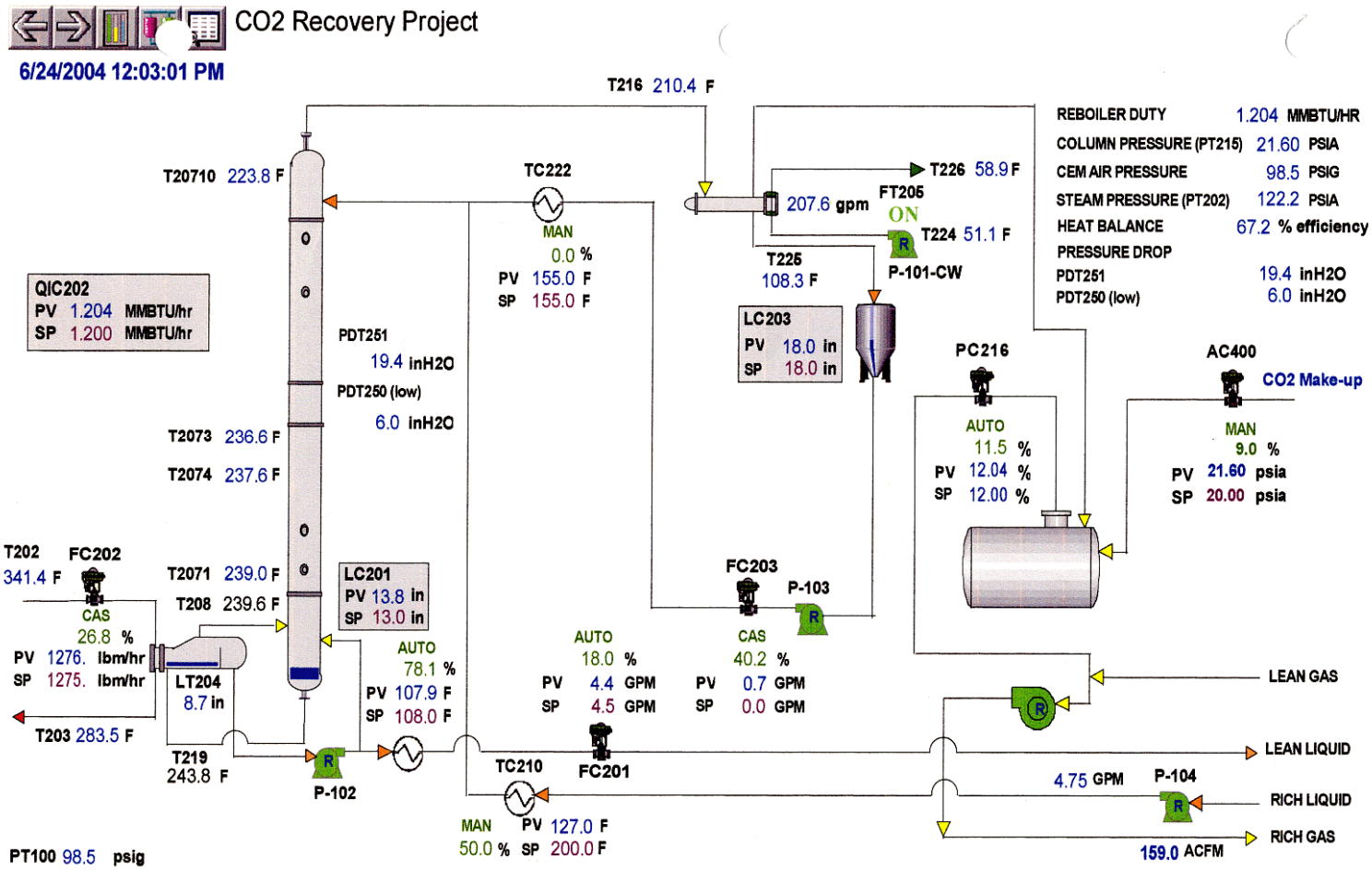

Figure A-3. Campaign 1 DeltaV Stripper Side Process View

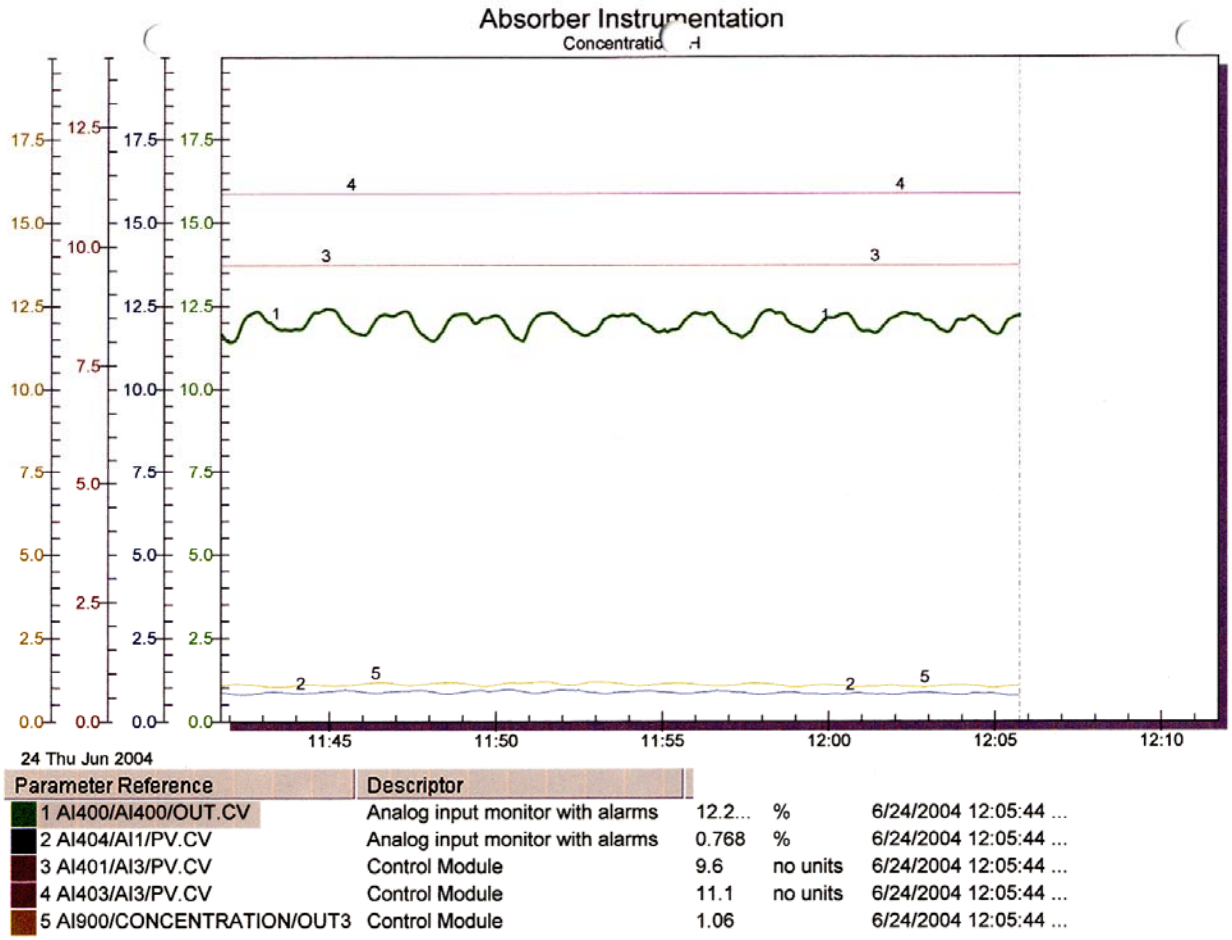

Figure A-4. Campaign 1 DeltaV Instrumentation History View

Appendix B: Campaign 2 Raw Pilot Plant Data and DeltaV Process Control Graphics

Table B-1. Campaign 2 Raw Absorber Data

	ABS LEAN	ABS LEAN	ABS LEAN	ABS LEAN	ABS RICH	ABS RICH	ABS RICH	ABS RICH	GAS	GAS	GAS	COOL	GAS
	FLOW	DEN	TEMP	pH	FLOW	DEN	TEMP	pH	FLOW	IN	OUT	TEMP	PRES
Time	FT403	FT403	TT403	AI403	FT200	FT200	TT200	AI401	FI900	T404	TT400	TT412	PT900
	(GPM)	(LB/FT^3)	(F)	(pH)	(GPM)	(LB/FT^3)	(F)	(pH)	(ACFM)	(F)	(F)	(F)	(PSIA)
10/26/04 10:35	7.97	76.44	104.37	11.15	8.05	77.51	117.39	-	599.67	120.42	120.47	118.26	0.38
10/26/04 11:00	7.99	76.46	104.48	11.09	8.04	77.41	116.88	-	599.74	120.85	119.85	117.65	0.39
10/26/04 14:45	7.96	76.56	106.18	10.96	8.08	77.41	122.92	-	599.60	129.95	123.44	121.68	0.40
10/27/04 0:15	8.98	76.57	105.32	10.65	9.00	77.38	112.53	-	450.58	115.21	112.28	110.03	0.34
10/27/04 2:30	10.97	76.60	105.07	10.62	11.01	77.34	112.27	-	449.72	114.12	105.69	102.68	0.40
10/27/04 3:30	10.93	76.63	104.99	10.63	11.02	77.32	112.30	-	449.49	116.10	105.17	102.26	0.43
10/27/04 6:00	12.48	76.66	106.16	10.59	12.60	77.24	114.68	-	450.25	116.93	101.54	98.53	0.44
10/27/04 7:00	12.52	76.67	106.28	10.60	12.62	77.26	115.54	-	449.92	118.67	103.02	100.06	0.45
10/27/04 12:00	13.05	76.59	106.45	10.61	13.24	77.28	115.94	-	599.58	123.49	114.35	112.24	0.54
10/27/04 13:00	13.01	76.60	106.87	10.58	13.17	77.25	117.99	-	600.11	127.73	115.22	113.42	0.55
10/28/04 4:15	8.55	76.55	105.01	10.62	8.60	77.45	107.31	-	349.75	97.08	105.93	102.47	0.20
10/28/04 5:15	8.53	76.55	105.42	10.64	8.56	77.47	108.21	-	350.49	99.40	108.02	104.80	0.20
10/28/04 13:40	11.54	76.68	106.16	10.61	11.59	77.29	118.40	-	350.16	116.89	101.50	98.60	0.38
10/28/04 14:55	11.50	76.69	106.34	10.62	11.59	77.29	118.75	-	349.08	118.72	102.07	99.26	0.39
10/28/04 16:35	11.46	76.71	106.49	10.61	11.59	77.29	119.20	-	349.97	124.12	102.69	100.07	0.44
10/28/04 17:15	11.52	76.72	106.55	10.61	11.63	77.30	119.42	-	349.47	124.64	103.25	100.50	0.43
10/28/04 19:15	12.04	76.74	105.89	10.63	12.16	77.35	119.09	-	350.22	139.73	99.39	96.50	0.91
10/28/04 20:15	11.96	76.75	105.74	10.67	12.17	77.37	118.35	-	350.68	118.22	99.30	96.34	0.80
10/29/04 5:45	10.02	76.79	105.22	10.62	10.07	77.53	112.94	-	349.60	92.24	102.65	99.29	0.20
10/29/04 6:45	10.00	76.81	104.57	10.62	10.00	77.58	111.42	-	349.74	89.59	99.70	96.63	0.20
11/2/2004 20:32	4.99	76.58	110.24	10.41	4.78	77.80	87.34	-	349.89	84.74	100.80	95.10	0.13
11/2/2004 21:45	5.02	76.62	108.54	10.42	4.77	77.75	86.15	-	349.98	82.77	98.17	92.67	0.14
11/3/04 0:30	6.05	76.70	107.43	10.41	5.83	77.56	94.23	-	349.92	85.76	97.92	92.87	0.13
11/3/04 1:30	5.89	76.81	107.56	10.44	5.82	77.65	94.04	-	350.06	85.09	97.04	91.91	0.13
11/3/04 5:15	5.49	76.87	101.80	10.47	5.27	77.74	88.70	-	449.68	91.39	96.04	91.44	0.28
11/3/04 6:15	5.49	76.93	102.19	10.48	5.27	77.91	85.94	-	449.92	89.04	94.73	89.67	0.28
11/3/04 11:30	8.06	76.28	112.63	10.25	7.77	76.97	98.91	-	449.83	96.25	102.25	97.94	0.28
11/3/04 12:30	7.91	76.30	112.65	10.25	7.79	76.97	99.61	-	450.22	97.87	102.57	98.42	0.28
11/3/04 15:45	9.97	76.27	116.58	10.21	9.79	76.82	104.92	-	449.97	99.25	104.86	100.05	0.30
11/3/04 16:45	9.98	76.27	118.07	10.21	9.79	76.77	108.23	-	449.97	103.48	107.27	102.90	0.31
11/4/04 6:00	20.43	76.53	104.19	10.57	20.74	76.96	118.34	-	499.84	116.76	97.27	93.64	0.58
11/4/04 7:30	20.37	76.53	104.14	10.57	20.77	76.95	118.89	-	499.99	121.49	97.40	94.04	0.61
11/4/04 10:15	22.03	76.51	104.18	10.55	22.30	76.89	118.94	-	500.42	137.10	96.49	92.65	0.73
11/4/04 11:15	22.00	76.45	105.55	10.52	22.46	76.82	123.26	-	500.28	147.82	100.54	97.11	0.74
11/4/04 13:30	21.92	76.13	107.18	10.48	22.39	76.58	124.14	-	499.88	121.11	102.73	99.64	0.48
11/4/04 15:15	22.01	76.35	105.94	10.55	22.41	76.74	123.69	-	499.98	120.41	101.59	98.58	0.48
11/4/04 21:15	15.01	76.61	103.75	10.69	15.21	77.22	118.30	-	500.23	107.54	106.68	104.63	0.38
11/4/04 23:00	14.92	76.59	103.68	10.68	15.18	77.21	117.08	-	500.04	105.89	103.56	101.16	0.39
11/5/04 3:45	15.05	76.72	103.42	10.82	15.19	77.39	117.63	-	500.07	107.06	106.65	103.70	0.42
11/5/04 4:45	14.93	76.73	103.37	10.82	15.25	77.42	117.48	-	500.05	106.74	107.62	104.71	0.42

Table B-2. Campaign 2 Raw Absorber Data – Continued

	PRES DRP	PRES DRP	ABS PRESS	BED TEMP	BED TEMP	BED TEMP	BED TEMP	BED TEMP	BED TEMP	BED TEMP	CO_2 IN	CO_2 MID	CO_2 OUT
Time	PDT450	PDT451	PT415	TT4078	TT4077	TT4076	TT4075	TT4074	TT4073	TT4071	AI400	AI406	AI404
	(in H_2O)	(in H_2O)	(in H_2O)	(F)	(F)	(F)	(F)	(F)	(F)	(F)	(mol%)	(mol%)	(mol%)
10/26/04 10:35	3.19	3.45	-	114.02	139.54	127.84	126.91	118.88	119.27	120.30	11.09	-	2.08
10/26/04 11:00	3.24	3.51	-	113.46	138.41	127.04	126.26	118.51	118.64	119.86	10.97	-	2.36
10/26/04 14:45	3.23	3.50	-	117.97	137.97	127.64	128.23	121.67	122.03	125.23	12.31	-	5.38
10/27/04 0:15	2.29	2.52	3.77	102.70	143.54	134.12	135.05	126.10	124.52	113.84	11.47	-	4.04
10/27/04 2:30	3.35	3.05	3.97	97.69	144.57	136.98	138.55	129.38	129.75	113.67	11.97	-	3.65
10/27/04 3:30	3.53	3.24	4.13	97.44	143.88	137.05	138.86	130.03	130.11	114.43	10.68	-	2.74
10/27/04 6:00	4.09	3.34	4.02	96.23	138.72	138.41	139.71	133.81	136.32	117.43	10.43	-	1.92
10/27/04 7:00	4.15	3.47	4.01	96.95	142.89	139.98	141.77	135.42	137.34	117.88	11.12	-	2.22
10/27/04 12:00	5.83	6.42	1.24	103.73	145.81	138.44	138.32	135.67	130.53	118.44	11.70	-	4.01
10/27/04 13:00	5.96	6.51	1.17	105.08	146.05	138.93	138.90	136.59	132.05	120.00	11.43	-	3.76
10/28/04 4:15	5.31	1.03	2.12	96.60	147.64	137.65	135.10	131.92	128.73	108.78	11.27	-	3.50
10/28/04 5:15	5.38	1.01	2.13	98.20	148.71	138.29	135.48	132.56	129.28	109.32	11.32	-	3.38
10/28/04 13:40	7.96	4.09	2.50	96.68	126.04	137.80	137.72	138.39	139.72	120.10	11.92	-	1.88
10/28/04 14:55	8.09	4.27	2.50	97.62	126.70	138.54	138.11	138.72	139.89	121.43	12.01	-	1.96
10/28/04 16:35	8.46	4.84	2.75	97.81	131.03	141.02	141.44	141.81	141.17	121.00	11.47	-	1.79
10/28/04 17:15	8.48	4.82	2.72	97.94	132.81	141.76	142.03	142.43	141.55	122.83	11.68	-	1.93
10/28/04 19:15	9.57	28.33	-7.05	94.95	139.40	138.53	135.16	135.04	135.18	122.82	11.70	-	0.61
10/28/04 20:15	9.50	33.21	-7.07	94.10	126.25	134.69	133.95	134.42	136.58	119.68	11.40	-	0.31
10/29/04 5:45	3.10	3.47	-1.47	95.56	148.93	142.61	143.84	142.73	138.23	112.16	11.57	-	2.69
10/29/04 6:45	3.11	3.44	-1.45	93.95	144.44	139.76	141.77	140.11	136.26	110.71	12.02	-	3.05
11/2/2004 20:32	1.02	1.12	1.41	93.41	118.32	111.34	110.72	97.82	103.51	93.30	4.87	-	0.78
11/2/2004 21:45	1.03	1.13	1.44	90.93	116.50	110.18	110.00	97.09	103.17	91.96	4.69	-	0.89
11/3/04 0:30	1.11	1.18	1.13	89.85	124.12	121.12	123.02	112.30	115.36	98.67	5.39	-	0.73
11/3/04 1:30	1.11	1.19	1.15	89.00	123.62	121.55	123.87	113.18	116.08	98.47	5.28	-	0.63
11/3/04 5:15	1.75	1.89	3.66	88.61	112.55	105.49	106.39	96.10	98.50	93.26	4.42	-	0.51
11/3/04 6:15	1.75	1.89	3.65	87.20	111.06	104.26	105.31	94.88	97.82	91.43	4.32	-	1.10
11/3/04 11:30	1.81	1.94	3.47	94.83	114.60	117.56	121.36	110.62	115.99	104.95	3.98	-	0.48
11/3/04 12:30	1.81	1.96	3.48	95.33	114.28	117.44	121.39	111.08	116.80	105.59	3.87	-	0.44
11/3/04 15:45	2.17	2.10	3.44	98.08	111.55	111.66	116.36	106.09	115.88	110.43	3.90	-	0.29
11/3/04 16:45	2.20	2.26	3.48	100.57	115.33	115.65	120.60	111.93	121.67	112.87	3.95	-	0.33
11/4/04 6:00	5.85	4.33	5.09	90.93	108.42	116.14	125.05	120.78	127.20	121.55	16.25	-	2.00
11/4/04 7:30	6.16	4.62	5.23	91.86	107.98	114.40	124.58	120.09	127.11	122.11	16.04	-	1.85
11/4/04 10:15	7.67	5.70	5.71	90.41	105.35	110.11	120.00	116.70	123.51	122.13	16.05	-	1.19
11/4/04 11:15	7.73	5.77	5.54	94.08	108.22	114.08	123.98	121.75	128.62	125.65	16.43	-	1.43
11/4/04 13:30	6.85	4.79	0.42	99.17	111.87	120.22	129.21	127.35	133.36	126.34	17.91	-	2.47
11/4/04 15:15	6.91	4.80	0.42	98.38	109.26	116.95	126.54	124.83	131.13	125.71	17.35	-	1.84
11/4/04 21:15	3.59	3.82	2.27	96.20	161.77	153.48	153.66	148.45	145.78	120.28	17.19	-	4.49
11/4/04 23:00	3.68	3.86	2.28	93.89	159.77	152.71	153.33	148.29	145.24	119.50	16.29	-	3.98
11/5/04 3:45	4.04	4.31	2.35	93.24	162.70	153.66	154.54	149.31	146.85	120.39	16.89	-	3.42
11/5/04 4:45	4.10	4.43	2.33	93.67	162.58	153.70	154.40	149.08	146.48	120.15	17.42	-	3.77

Table B-3. Campaign 2 Raw Stripper Data

	ACC	COLUMN	COLUMN	REBOILER	REBOILER	COLUMN	PRES	PRES	STR	STR	STR	STR
	LEVEL	LEVEL	LEVEL	LEVEL	DUTY	PRESSURE	DRP (LO)	DRP (HI)	REFLUX	RETURN	RETURN	RETURN
Time	LC203	LC201	LT206	LT204	QIC202	PT215	PDT250	PDT251	FT203	FT201	FT201	FT201
	(in)	(in)	(in)	(in)	(MMBTU/hr)	(psia)	(in H_2O)	(in H_2O)	(GPM)	(GPM)	(F)	(LB/FT^3)
10/26/04 10:35	15.00	11.48	11.47	13.41	1.49	23.26	5.12	4.94	1.71	8.05	108.0	-
10/26/04 11:00	15.00	10.94	10.93	12.31	1.56	22.31	5.65	5.60	1.82	8.00	108.0	-
10/26/04 14:45	15.00	14.04	14.03	14.44	1.73	23.38	5.95	6.75	2.01	7.89	108.0	-
10/27/04 0:15	15.00	10.16	10.14	7.85	0.82	23.44	1.64	1.41	0.45	8.78	108.0	-
10/27/04 2:30	15.00	10.52	10.49	6.52	0.92	23.20	2.35	2.13	0.40	10.61	108.1	-
10/27/04 3:30	15.00	10.50	10.49	6.95	0.92	22.54	2.59	2.36	0.41	10.63	107.9	-
10/27/04 6:00	15.00	10.50	10.51	6.36	0.98	23.47	3.36	3.14	0.41	12.22	107.9	-
10/27/04 7:00	15.00	10.51	10.51	6.87	0.98	23.84	3.69	3.47	0.43	12.24	108.0	-
10/27/04 12:00	15.00	10.50	10.50	5.63	1.09	22.35	4.88	4.69	0.59	12.79	107.9	-
10/27/04 13:00	15.00	10.49	10.49	5.82	1.09	22.25	5.40	5.26	0.60	12.75	108.0	-
10/28/04 4:15	15.00	10.49	10.48	7.88	0.69	26.23	0.31	0.04	0.15	8.25	110.1	-
10/28/04 5:15	15.00	10.51	10.49	7.34	0.64	24.92	0.31	0.05	0.13	8.28	110.0	-
10/28/04 13:40	15.00	10.50	10.50	6.80	1.04	22.41	4.01	3.81	0.59	11.18	108.0	-
10/28/04 14:55	15.00	10.50	10.50	6.89	1.04	22.43	4.42	4.24	0.58	11.16	107.9	-
10/28/04 16:35	15.00	10.52	10.51	6.95	1.04	22.00	4.94	4.72	0.71	11.25	108.0	-
10/28/04 17:15	15.00	10.51	10.50	6.88	1.04	21.99	5.13	4.95	0.71	11.21	108.0	-
10/28/04 19:15	15.00	10.51	10.50	6.67	1.14	23.06	5.31	5.14	0.71	11.76	108.0	-
10/28/04 20:15	15.00	10.49	10.49	6.57	1.25	23.05	5.95	6.70	0.87	11.72	108.0	-
10/29/04 5:45	15.00	10.53	10.50	6.18	0.89	49.32	0.62	0.35	0.00	9.7	108.02	-
10/29/04 6:45	15.00	10.49	10.49	6.11	0.89	49.77	0.53	0.26	0.01	9.7	108.01	-
11/2/2004 20:32	14.00	12.46	12.48	12.00	0.47	4.61	0.82	0.62	0.37	5.6	119.42	-
11/2/2004 21:45	14.00	11.97	11.97	9.94	0.47	4.51	0.91	0.70	0.40	4.7	119.13	-
11/3/04 0:30	14.00	11.70	11.70	9.91	0.53	5.25	1.30	1.11	0.50	5.8	113.49	-
11/3/04 1:30	14.00	11.91	11.92	10.63	0.52	5.25	1.26	1.06	0.45	5.6	113.26	-
11/3/04 5:15	14.00	11.77	11.79	10.48	0.45	4.78	0.99	0.78	0.40	4.9	114.01	-
11/3/04 6:15	14.00	12.17	12.16	10.71	0.45	4.78	0.97	0.78	0.37	5.1	111.08	-
11/3/04 11:30	14.00	11.35	11.34	10.75	0.54	5.12	2.42	2.13	0.49	7.7	121.20	-
11/3/04 12:30	14.00	11.37	11.36	11.19	0.56	5.04	2.79	2.46	0.50	7.6	120.77	-
11/3/04 15:45	14.00	11.53	11.50	12.21	0.64	5.24	4.88	4.65	0.68	9.7	123.37	-
11/3/04 16:45	14.00	11.11	11.11	11.92	0.64	5.24	5.12	4.90	0.71	9.7	123.38	-
11/4/04 6:00	14.00	12.06	12.05	11.15	1.45	25.31	4.82	4.65	0.14	20.0	103.91	-
11/4/04 7:30	14.00	15.10	15.09	13.28	1.44	24.67	4.81	3.33	0.24	20.0	104.03	-
11/4/04 10:15	14.00	12.34	12.33	9.97	1.55	25.91	5.96	5.73	0.15	21.3	104.38	-
11/4/04 11:15	14.00	11.84	11.84	11.27	1.55	26.62	5.96	6.53	0.28	22.0	105.12	-
11/4/04 13:30	14.00	11.88	11.89	7.40	1.54	27.04	5.22	5.05	0.20	22.0	106.30	-
11/4/04 15:15	14.00	12.74	12.76	10.40	1.55	26.72	5.96	8.36	0.31	21.2	105.63	-
11/4/04 21:15	14.00	12.15	12.15	12.14	1.36	23.86	4.06	3.81	0.74	15.0	103.92	-
11/4/04 23:00	14.00	11.81	11.82	10.84	1.34	23.39	4.31	4.07	0.68	15.0	103.97	-
11/5/04 3:45	14.40	11.90	11.87	12.95	1.80	24.47	5.96	11.52	1.38	14.60	103.9	-
11/5/04 4:45	14.40	12.15	12.19	13.16	1.80	24.71	5.96	11.95	1.36	14.77	104.0	-

Table B-4. Campaign 2 Raw Stripper Data – Continued

	TOP	TOP MID	TOP BOT	BOT TOP	BOT MID	BOT	CONDENS	VAPOR	BOT LIQ	VAP TO	ORG. OUT
	TEMP	TEMP	TEMP	TEMP	TEMP	TEMP	RETURN	INLET	TO REB	CONDEN	(COND)
Time	T20710	T2079	T2078	T2074	T2073	T2071	T203	T208	T219	T216	T225
	(F)	(F)	(F)	(F)	(F)	(F)	(F)	(F)	(F)	(F)	(F)
10/26/04 10:35	233.7	239.26	241.6	241.97	242.68	243.75	274.41	244.53	247.34	215.50	131.88
10/26/04 11:00	232.1	236.83	239.1	239.44	240.28	241.27	273.69	242.47	244.79	213.56	130.09
10/26/04 14:45	235.2	239.55	241.9	242.02	242.81	243.79	279.08	247.05	247.26	216.36	125.58
10/27/04 0:15	222.1	239.32	241.5	241.63	243.54	244.31	264.30	247.47	246.87	204.64	80.00
10/27/04 2:30	215.9	237.83	240.9	241.13	242.96	243.93	266.87	247.56	246.18	197.56	78.28
10/27/04 3:30	216.0	236.29	239.3	239.57	241.41	242.24	266.02	244.91	244.61	198.19	79.04
10/27/04 6:00	217.3	238.20	241.3	241.86	243.33	244.51	268.18	246.51	246.78	199.84	79.77
10/27/04 7:00	218.0	238.84	242.2	242.81	244.35	245.50	269.48	247.63	247.79	200.80	79.52
10/27/04 12:00	214.1	234.50	238.3	239.26	240.79	242.07	268.26	244.79	244.26	200.59	84.38
10/27/04 13:00	215.0	233.98	238.4	238.92	240.50	241.73	267.33	244.63	244.03	201.77	86.71
10/28/04 4:15	215.4	245.04	247.2	247.86	249.80	251.30	270.56	253.32	253.28	194.38	70.43
10/28/04 5:15	210.1	241.87	244.1	244.77	246.82	248.17	267.14	250.26	250.44	190.70	70.20
10/28/04 13:40	217.7	235.50	239.1	239.54	241.00	242.11	264.71	244.87	244.43	203.87	86.02
10/28/04 14:55	218.1	235.35	239.0	239.53	240.99	242.19	264.19	244.91	244.51	204.00	86.30
10/28/04 16:35	219.4	234.40	238.0	238.42	240.00	241.12	262.99	243.72	243.43	205.43	89.31
10/28/04 17:15	219.7	234.22	237.5	238.22	239.82	241.01	262.86	243.91	243.36	205.69	89.83
10/28/04 19:15	220.4	236.87	240.5	241.05	242.63	243.77	266.95	246.90	246.12	207.06	89.98
10/28/04 20:15	222.3	237.62	240.6	241.27	242.73	243.76	268.77	246.15	246.41	208.90	97.28
10/29/04 5:45	162.69	203.7	278.37	282.29	287.59	288.37	308.23	292.60	290.98	149.65	67.03
10/29/04 6:45	154.54	194.7	275.22	281.08	288.13	288.84	309.14	293.17	291.62	136.49	67.25
11/2/2004 20:32	153.12	160.9	162.86	162.73	163.64	165.01	195.48	164.27	165.26	138.16	61.82
11/2/2004 21:45	152.39	160.4	162.33	161.80	162.72	164.07	195.54	163.34	164.41	137.94	62.74
11/3/04 0:30	157.77	166.6	168.46	168.37	169.41	170.74	206.94	170.28	170.96	144.06	70.27
11/3/04 1:30	158.01	165.9	167.89	168.39	169.43	170.74	202.06	169.74	171.00	143.45	67.02
11/3/04 5:15	154.06	162.9	165.01	164.11	165.26	166.58	186.00	166.19	166.75	139.71	63.03
11/3/04 6:15	153.58	162.8	164.76	164.12	165.33	166.63	184.06	165.82	166.79	138.56	61.90
11/3/04 11:30	157.73	165.6	167.70	167.39	168.56	169.64	196.57	168.42	170.11	143.11	68.54
11/3/04 12:30	156.28	165.3	167.23	166.71	167.97	169.16	196.36	167.42	169.35	143.14	71.32
11/3/04 15:45	160.87	166.3	168.73	168.91	170.20	171.20	212.41	169.56	171.88	145.69	80.63
11/3/04 16:45	162.06	166.6	168.88	169.06	170.33	171.34	209.20	169.79	172.06	146.60	83.87
11/4/04 6:00	189.46	241.2	244.12	245.26	246.98	248.20	282.73	245.10	249.07	173.28	67.35
11/4/04 7:30	194.56	239.4	243.06	244.01	245.62	246.96	282.02	246.57	247.72	181.30	72.13
11/4/04 10:15	174.46	242.3	245.34	246.39	248.47	250.00	286.47	248.04	250.86	158.90	66.61
11/4/04 11:15	187.95	243.4	246.79	248.02	249.92	251.59	287.59	249.02	252.37	172.62	71.42
11/4/04 13:30	182.15	244.0	248.03	248.84	250.78	252.26	290.38	255.87	253.10	168.64	73.67
11/4/04 15:15	185.76	243.9	247.85	248.15	250.18	251.69	287.88	251.13	252.63	171.64	74.17
11/4/04 21:15	218.16	239.5	242.06	243.28	244.31	245.66	277.75	243.65	246.39	204.49	91.87
11/4/04 23:00	216.19	238.5	241.79	242.17	243.18	244.59	278.13	242.77	245.33	202.23	90.30
11/5/04 3:45	228.7	241.14	244.9	245.16	246.45	247.51	289.85	247.42	248.88	210.83	112.54
11/5/04 4:45	229.5	241.47	245.7	245.77	247.00	248.03	289.78	247.82	249.42	211.33	111.51

Table B-5. Campaign 2 Raw Stripper Data – Continued

	CW	CW	CW	FEED	REFLUX	STEAM	STEAM	STEAM	HEAT	PRE-HEAT
	INLET	OUTLET	FLOW	TEMP	TEMP	PRES	FLOW	TEMP	BALANCE	
Time	T224	T226	FT205	TT210	TT222	PT202	FC202	T202	HB202	TC210
	(F)	(F)	(GPM)	(F)	(F)	(PSIA)	(LB/HR)	(F)	%	%
10/26/04 10:35	58.21	65.33	202.58	177.20	128.15	120.52	1560.22	340.98	-	-
10/26/04 11:00	56.77	64.99	202.44	176.76	127.22	120.54	1637.56	340.49	74.53	-
10/26/04 14:45	55.01	64.57	202.48	176.40	128.51	119.00	1827.07	339.48	75.48	-
10/27/04 0:15	50.77	51.98	201.79	171.09	127.52	128.47	850.09	346.34	74.89	13.15
10/27/04 2:30	51.34	53.08	201.76	164.32	127.11	126.86	956.14	345.45	77.42	13.36
10/27/04 3:30	51.64	53.20	201.66	163.29	123.75	123.25	954.60	342.30	77.64	13.44
10/27/04 6:00	52.46	54.09	201.66	169.32	123.77	121.83	1019.97	341.77	79.06	22.00
10/27/04 7:00	52.51	54.27	201.53	170.04	124.22	121.68	1019.78	341.80	79.32	22.00
10/27/04 12:00	53.08	55.28	201.96	168.29	121.88	120.89	1134.81	341.36	77.65	22.00
10/27/04 13:00	53.10	55.46	201.95	170.28	122.55	120.93	1137.39	341.34	77.83	22.00
10/28/04 4:15	49.50	50.36	201.47	171.73	135.90	129.82	719.75	347.14	74.18	14.00
10/28/04 5:15	49.88	50.79	201.42	172.36	139.90	128.84	664.47	346.66	75.16	14.00
10/28/04 13:40	51.14	53.78	201.21	168.00	121.12	121.76	1075.05	341.90	76.82	14.00
10/28/04 14:55	51.21	53.81	201.19	168.82	122.69	121.42	1075.24	341.84	76.71	14.00
10/28/04 16:35	51.00	53.88	201.27	175.47	121.31	121.13	1075.33	341.46	74.75	28.00
10/28/04 17:15	50.97	53.77	201.27	176.22	123.07	121.38	1074.78	341.89	75.00	28.00
10/28/04 19:15	51.66	54.49	201.27	172.68	116.06	121.01	1192.08	341.52	75.27	20.19
10/28/04 20:15	52.24	55.55	201.46	171.94	112.71	120.44	1308.63	340.91	75.70	20.34
10/29/04 5:45	50.79	50.78	201.32	165.60	190.39	128.64	970.03	345.98	87.61	12.87
10/29/04 6:45	50.86	50.80	201.07	164.02	185.32	127.82	969.96	345.56	88.78	12.90
11/2/2004 20:32	45.89	47.51	202.24	101.64	113.96	131.41	449.48	347.52	68.35	6.50
11/2/2004 21:45	46.05	47.68	202.06	108.76	108.77	131.14	449.81	347.47	67.09	6.60
11/3/04 0:30	46.53	48.58	202.11	119.96	108.82	133.74	520.33	348.83	70.02	7.00
11/3/04 1:30	46.75	48.71	202.26	119.37	112.09	133.79	500.35	348.89	70.62	7.00
11/3/04 5:15	46.35	47.52	202.08	119.71	114.41	132.54	425.11	347.98	65.44	7.00
11/3/04 6:15	46.62	47.20	201.96	116.23	115.65	132.72	425.36	348.09	63.70	7.49
11/3/04 11:30	47.27	49.09	202.54	130.97	113.81	132.30	524.73	348.33	68.86	8.80
11/3/04 12:30	47.17	49.18	202.49	132.21	114.47	132.90	544.48	348.78	69.45	9.00
11/3/04 15:45	47.33	50.34	202.55	147.47	107.79	131.93	625.08	347.91	68.43	11.31
11/3/04 16:45	46.97	50.87	202.83	150.79	109.83	132.21	624.99	348.13	70.08	11.53
11/4/04 6:00	54.18	55.00	201.96	158.22	141.14	121.05	1538.28	339.77	83.11	30.00
11/4/04 7:30	54.90	55.41	202.11	158.82	134.36	120.51	1530.50	339.82	84.09	30.00
11/4/04 10:15	56.34	56.77	201.91	157.76	135.67	118.05	1649.74	338.56	86.46	100.00
11/4/04 11:15	56.98	57.65	201.95	160.68	144.30	118.36	1649.78	338.72	86.67	100.00
11/4/04 13:30	57.08	57.59	202.15	160.17	165.74	119.12	1650.05	339.30	85.90	20.00
11/4/04 15:15	56.93	57.76	201.98	159.54	154.70	119.48	1650.44	339.30	86.87	20.00
11/4/04 21:15	53.92	57.11	202.24	168.38	119.48	121.67	1434.79	340.44	77.74	100.00
11/4/04 23:00	53.92	57.08	202.20	167.28	118.96	121.44	1410.84	340.53	77.12	100.00
11/5/04 3:45	57.20	63.54	202.62	166.66	115.88	118.00	1929.74	338.04	76.86	100.00
11/5/04 4:45	57.14	62.85	202.67	166.34	115.21	118.28	1929.73	338.10	76.26	100.00

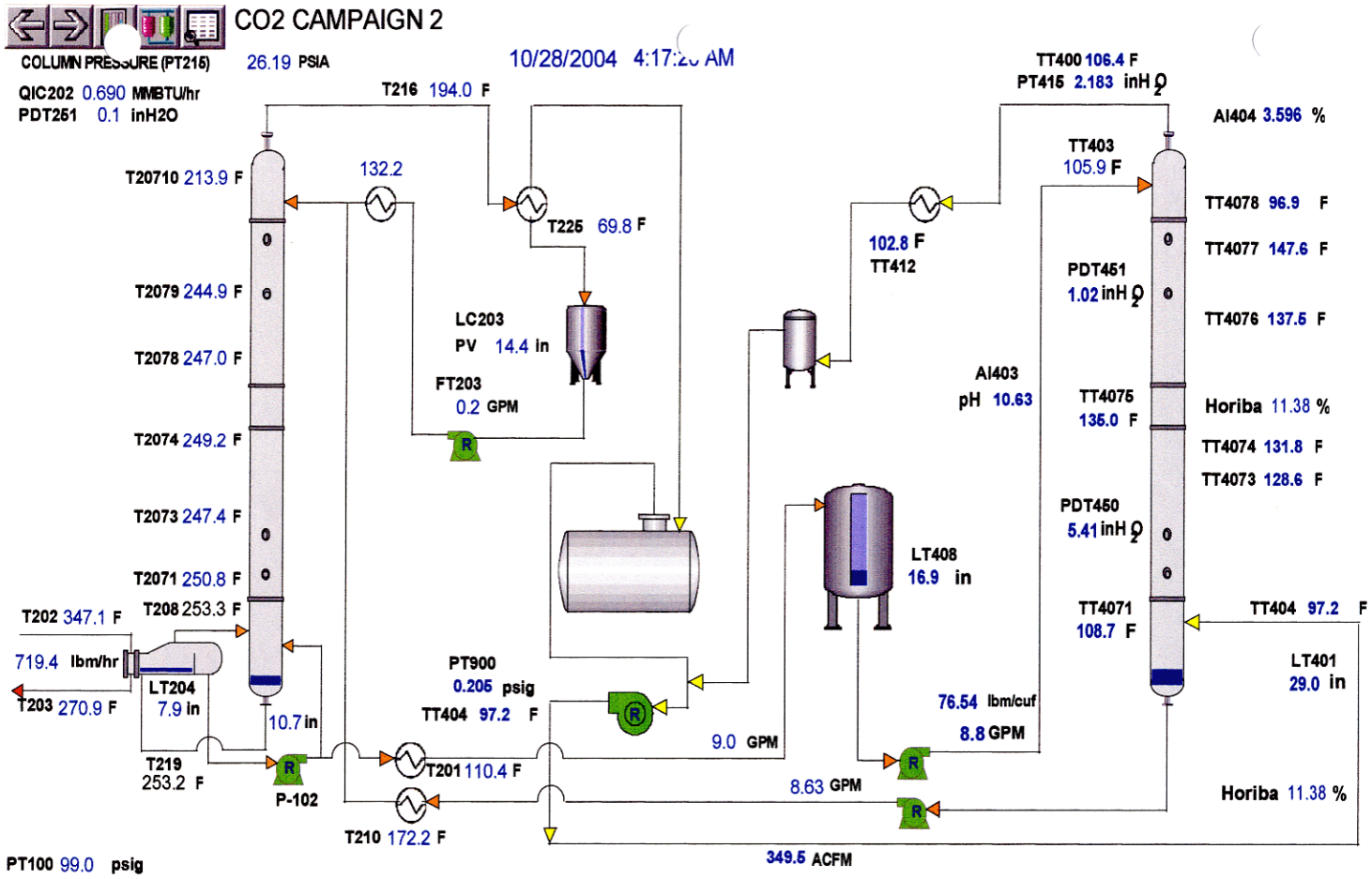

Figure B-1. Campaign 2 DeltaV Overall Process View

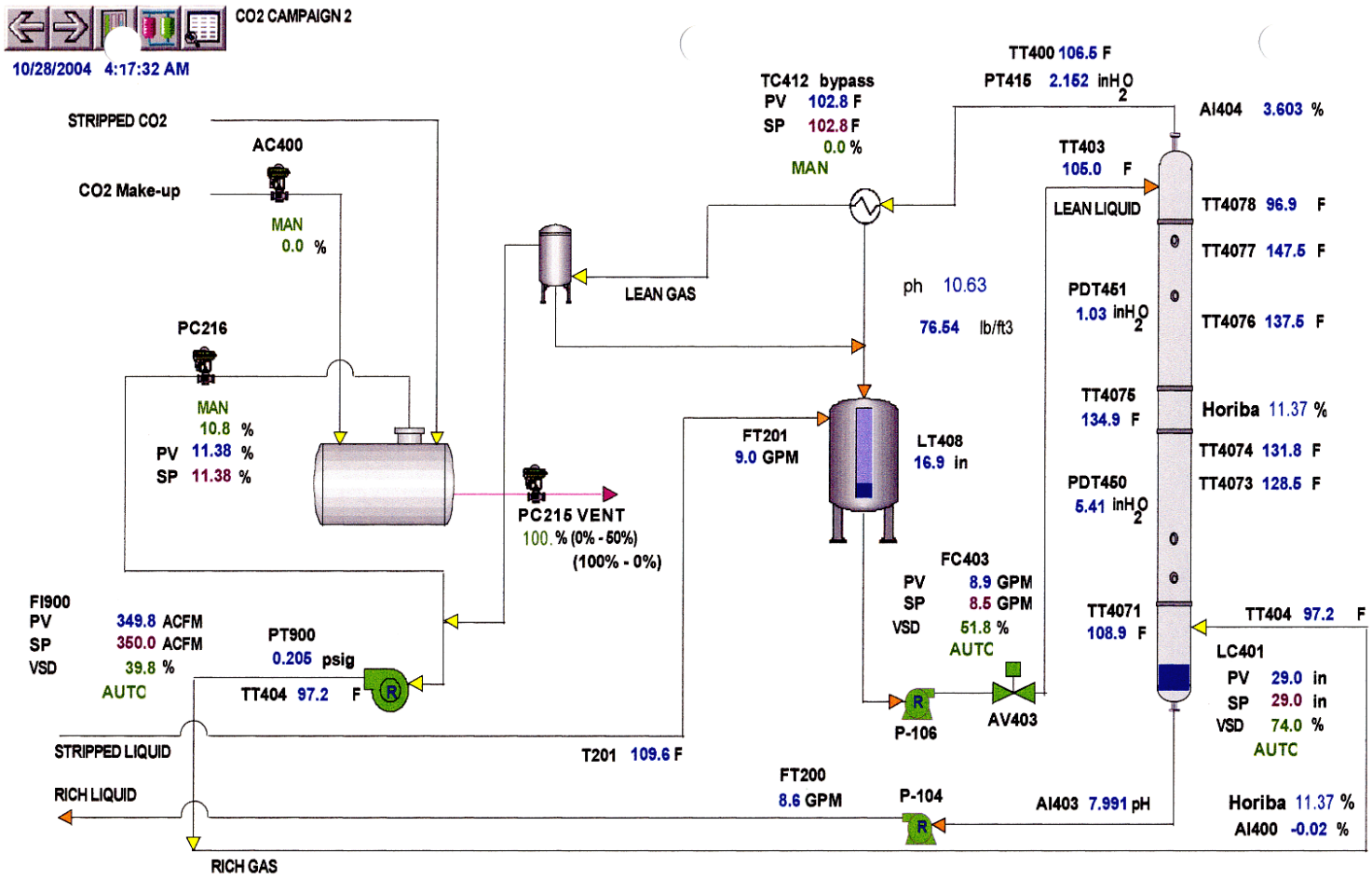

Figure B-2. Campaign 2 DeltaV Absorber Side Process View

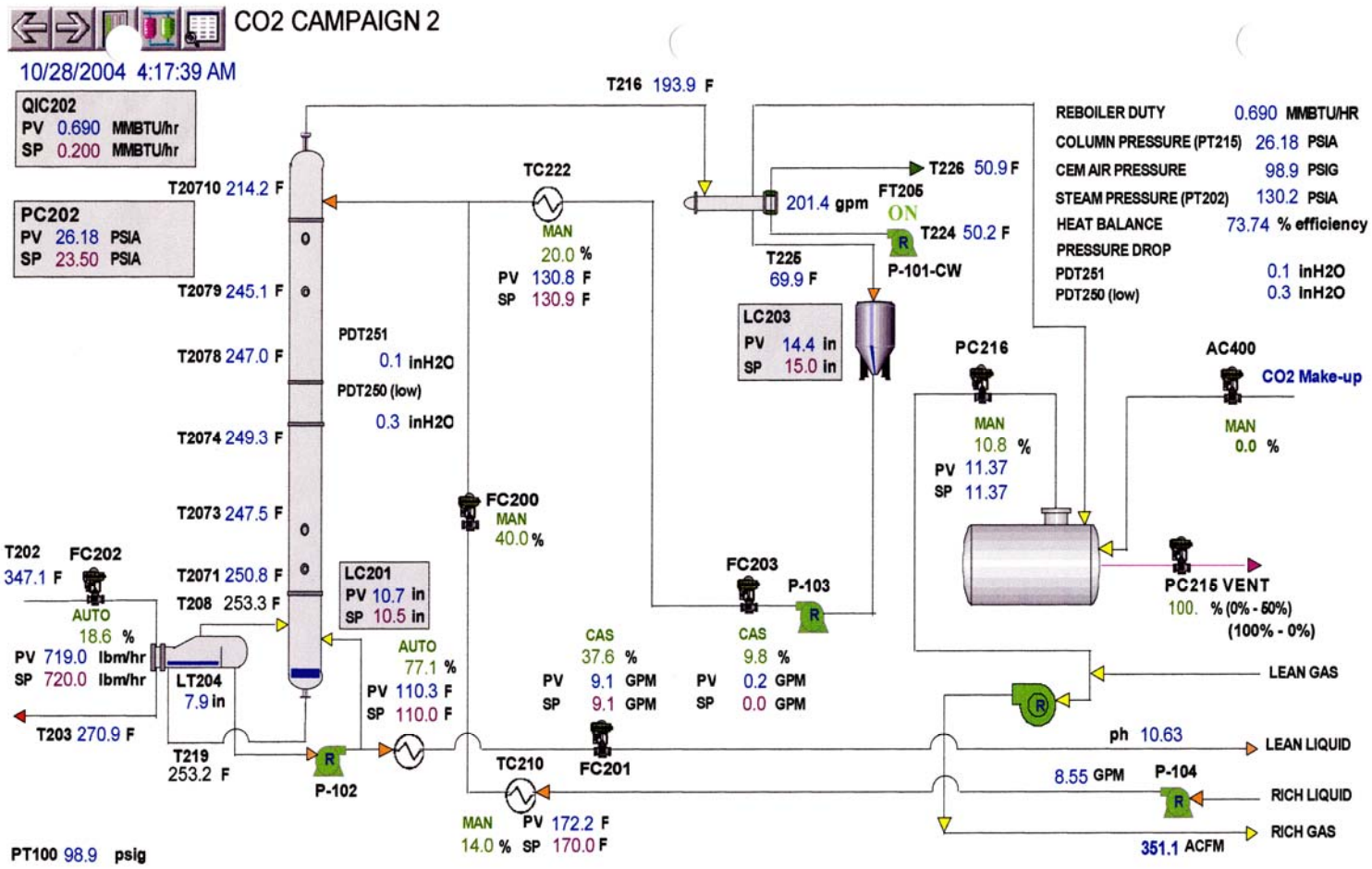

Figure B-3. Campaign 2 DeltaV Stripper Side Process View

Appendix C: Campaign 4 Raw Pilot Plant Data and DeltaV Process Control Graphics

Table C-1. Campaign 4 Raw Absorber Data for 5 m K^+/2.5 m PZ

	ABS LEAN	ABS LEAN	ABS LEAN	ABS LEAN	ABS LEAN	ABS RICH	ABS RICH	ABS RICH	ABS RICH	ABS RICH	GAS	ANNUBAR	GAS	GAS	Cool GAS
	FLOW	DEN	TEMP	pH	pH TEMP	FLOW	DEN	TEMP	pH	pH TEMP	FLOW	TEMP	IN	OUT	TEMP
Time	FT403	FT403	TT403	AI403	AI403-T	FT200	FT200	TT200	AI401	AI401-T	FT900	TT407	TT406	TT400	TT412
	(GPM)	(LB/FT^3)	(F)	(pH)	(F)	(GPM)	(LB/FT^3)	(F)	(pH)	(F)	(ACFM)	(F)	(F)	(F)	(F)
1/10/06 15:28	13.99	76.51	103.87	11.01	104.29	14.36	76.90	119.54	9.62	119.89	500	82.32	103.90	108.27	61.49
1/10/06 21:04	12.47	76.81	102.00	11.07	101.91	12.89	77.51	118.64	9.30	119.41	400	61.95	103.88	114.50	56.80
1/10/06 21:58	12.50	76.85	102.13	11.07	101.95	12.88	77.63	118.13	9.25	119.15	400	61.72	104.21	115.01	56.68
1/11/06 12:00	12.99	76.92	107.77	10.68	100.93	13.29	77.32	121.96	9.31	123.07	300	72.16	105.15	100.60	52.10
1/11/06 13:01	13.00	76.91	108.48	10.70	100.02	13.39	77.34	122.38	9.28	123.40	300	75.14	105.07	101.62	53.08
1/11/06 15:59	14.50	76.89	110.52	10.69	101.30	14.86	77.42	122.52	9.26	122.93	400	79.24	103.97	107.32	54.41
1/11/06 17:28	14.57	76.89	111.10	10.71	101.28	14.86	77.44	122.44	9.25	122.78	400	74.19	103.99	108.27	53.28
1/11/06 21:19	14.50	76.97	107.61	10.72	99.66	14.81	77.62	116.57	9.27	116.75	500	67.56	104.17	114.30	53.20
1/11/06 22:29	14.53	77.04	106.49	10.73	96.50	14.83	77.66	115.13	9.27	115.62	500	65.16	103.96	110.48	51.95
1/12/06 6:28	11.99	75.98	116.12	10.88	105.82	12.27	76.77	123.55	9.23	125.18	300	64.55	104.10	116.10	54.07
1/12/06 7:25	11.90	76.08	110.42	10.92	102.13	12.32	76.72	123.54	9.25	125.15	300	64.88	103.91	104.81	54.40
1/12/06 14:04	14.55	76.07	113.34	10.86	106.58	14.84	76.70	123.21	9.39	123.71	400	77.43	104.03	112.77	57.56
1/12/06 15:00	14.49	76.06	112.94	10.87	106.53	14.85	76.65	123.15	9.42	123.78	400	81.37	104.19	110.16	58.57
1/12/06 17:07	14.55	75.86	109.91	10.91	104.87	14.76	76.61	117.16	9.47	117.56	500	80.54	103.82	116.99	60.05
1/12/06 18:03	14.46	75.91	109.76	10.92	105.38	14.73	76.86	117.24	9.27	117.26	500	76.67	103.99	123.56	60.06
1/12/06 18:31	14.52	75.93	109.78	10.91	105.84	14.74	76.90	117.06	9.25	117.14	500	76.05	103.98	123.79	60.03
1/12/06 22:22	13.00	76.10	111.71	10.51	109.22	13.31	76.58	123.58	9.15	124.37	300	64.23	103.93	103.65	50.56
1/12/06 23:21	12.99	76.20	107.13	10.53	106.27	13.33	76.57	124.30	9.14	124.90	300	63.40	103.94	101.47	50.01
1/13/06 2:06	14.44	76.24	106.86	10.53	105.65	14.86	76.61	119.91	9.25	120.44	400	61.56	104.11	97.39	48.69
1/13/06 3:03	14.50	76.28	106.16	10.53	105.11	14.85	76.64	119.17	9.24	119.99	400	59.79	103.94	96.14	48.20
1/13/06 5:12	14.53	76.34	103.65	10.55	102.31	14.81	76.66	115.34	9.35	115.61	500	61.85	104.17	100.60	49.47
1/13/06 5:49	14.51	76.35	103.75	10.55	102.43	14.81	76.71	115.23	9.31	115.54	500	61.44	104.20	101.44	49.67
1/18/06 17:10	28.99	76.03	106.67	10.34	104.72	29.52	76.26	118.26	9.33	117.76	500	78.63	104.03	101.17	54.37
1/18/06 17:45	29.05	75.96	109.43	10.33	107.85	29.59	76.20	121.09	9.33	120.51	500	76.34	103.90	103.89	54.27
1/19/06 10:27	30.04	76.09	108.97	10.31	107.26	30.57	76.29	118.53	9.37	118.74	400	70.81	104.13	100.00	52.48
1/19/06 12:20	30.00	76.08	109.04	10.31	108.14	30.47	76.27	118.08	9.44	118.28	400	76.05	103.83	100.60	53.90
1/19/06 13:56	23.48	76.21	103.18	10.35	102.60	23.86	76.39	113.32	9.45	113.86	300	79.30	103.96	95.90	53.94
1/19/06 15:10	23.55	76.24	103.30	10.34	102.78	23.84	76.43	113.75	9.42	114.10	300	79.46	103.93	96.02	53.95
1/19/06 19:35	24.95	76.08	106.51	10.47	106.04	25.61	76.34	119.14	9.34	119.24	500	70.82	104.03	100.68	53.42
1/19/06 21:03	24.99	76.06	106.32	10.47	106.11	25.52	76.28	117.88	9.41	118.67	501	69.29	104.10	99.23	53.47
1/20/06 4:13	25.02	76.00	104.27	10.70	104.13	25.72	76.27	121.15	9.37	121.09	501	67.43	103.98	98.91	56.84
1/20/06 5:13	25.01	76.00	105.14	10.69	105.20	25.76	76.26	123.62	9.35	123.77	499	66.51	104.11	100.19	56.96
1/20/06 13:30	20.01	76.38	103.96	10.87	104.33	20.77	76.66	124.09	9.46	124.36	500	79.66	104.88	99.08	59.93
1/20/06 14:34	19.96	76.42	104.47	10.88	104.85	20.75	76.65	125.76	9.50	125.80	500	84.17	104.76	100.72	60.89

Table C-2. Campaign 4 Raw Absorber Data for 5 m K^+/2.5 m PZ – Continued

	GAS	PRESSURE	PRESSURE	ABS	BED	BED	BED	BED	BED	BED	COLUMN	CO_2	CO_2	CO_2	FTIR	FTIR
	PRESS	DRP	DRP	PRESS	TEMP	TEMP	TEMP	TEMP	TEMP	TEMP	LEVEL	IN	MID	OUT	CO_2	H_2O
Time	PT900	PDT450	PDT451	PT415	TT4078	TT4077	TT4076	TT4075	TT4073	TT4071	LT401	AI400	AI406	AI404	AI408	AI408
	(PSIA)	(in H_2O)	(in H_2O)	(in H_2O)	(F)	(F)	(F)	(F)	(F)	(F)	(in)	(mol%)	(mol%)	(mol%)	(mol%)	(mol%)
1/10/06 15:28	0.02	2.34	2.35	-5.8	100.4	134.8	148.9	149.7	143.8	121.0	24.7	7.98	3.61	0.59	0.83	-
1/10/06 21:04	0.02	2.00	1.71	-4.1	105.9	148.7	154.2	148.8	142.4	120.8	25.6	16.28	12.72	4.08	-	9.05
1/10/06 21:58	0.01	1.99	1.72	-4.3	106.9	148.8	153.2	147.8	140.9	120.8	25.6	17.19	14.06	5.00	4.91	8.81
1/11/06 12:00	0.03	1.47	0.99	-2.6	93.4	111.7	122.8	126.0	132.3	123.7	26.1	15.49	10.43	2.60	15.16	6.64
1/11/06 13:01	0.02	1.50	0.99	-2.7	95.0	112.7	124.4	127.3	133.4	124.2	25.9	16.04	10.94	2.81	15.70	6.54
1/11/06 15:59	0.01	2.05	1.57	-4.2	101.0	126.8	140.9	141.8	141.5	123.3	25.8	16.95	13.03	5.22	5.24	7.38
1/11/06 17:28	0.02	2.11	1.64	-4.2	101.9	129.4	144.3	144.3	142.8	123.5	25.3	17.09	13.27	5.49	16.64	6.61
1/11/06 21:19	0.02	2.62	2.49	-6.2	107.4	137.1	142.7	139.3	134.1	118.6	24.8	16.59	13.92	6.89	16.44	6.44
1/11/06 22:29	0.02	2.65	2.48	-6.2	103.6	134.5	139.8	136.6	131.7	118.0	25.0	17.55	15.08	6.89	9.03	8.54
1/12/06 6:28	0.02	1.69	1.15	-3.0	107.7	152.2	157.5	155.1	148.5	126.1	25.0	16.63	11.45	2.35	2.25	10.49
1/12/06 7:25	0.02	1.69	1.07	-3.0	98.4	137.1	153.4	153.2	148.5	125.4	24.8	16.43	10.88	2.03	2.03	7.53
1/12/06 14:04	0.01	1.74	1.39	-4.0	106.4	144.0	155.2	153.5	148.4	123.9	25.5	13.17	7.79	1.33	1.42	9.17
1/12/06 15:00	0.00	1.59	1.30	-3.8	104.1	139.8	154.5	154.0	149.6	124.1	25.5	12.77	6.92	1.01	12.63	6.70
1/12/06 17:07	0.00	2.14	2.19	-5.9	110.6	143.7	147.3	144.0	136.4	118.8	24.8	10.75	7.16	1.89	10.60	6.79
1/12/06 18:03	0.01	2.16	2.29	-5.9	117.4	149.0	147.6	142.2	134.6	118.3	24.7	16.38	13.29	5.89	16.29	7.00
1/12/06 18:31	0.01	2.18	2.31	-5.9	117.5	148.3	147.1	141.8	134.2	118.2	24.6	16.03	13.02	5.70	16.13	7.01
1/12/06 22:22	0.01	1.28	0.84	-2.2	98.8	121.9	134.0	137.6	140.3	124.3	25.0	17.56	13.68	4.95	5.12	7.43
1/12/06 23:21	0.01	1.32	0.80	-2.3	97.1	116.2	128.1	135.5	139.4	123.7	25.0	17.62	13.76	5.09	5.26	7.33
1/13/06 2:06	0.01	1.87	1.49	-3.6	92.5	115.1	126.0	129.8	134.3	121.2	25.0	14.93	11.61	5.13	15.06	6.08
1/13/06 3:03	0.01	1.92	1.54	-3.7	91.3	113.8	124.4	128.3	132.8	121.0	25.0	15.08	11.96	5.42	14.89	6.41
1/13/06 5:12	0.01	2.59	2.45	-6.2	94.3	121.1	133.3	134.9	131.9	117.7	24.9	11.23	9.06	4.76	4.79	6.39
1/13/06 5:49	0.02	2.62	2.50	-6.2	95.0	123.2	133.9	134.8	131.2	117.7	24.9	12.64	10.50	5.89	5.70	6.43
1/18/06 17:10	0.04	3.32	2.93	-6.4	97.3	108.6	112.6	115.9	119.2	119.9	30.1	17.11	12.89	5.21	17.23	6.03
1/18/06 17:45	0.04	3.52	3.09	-6.6	100.0	111.3	115.4	119.4	122.9	122.3	30.0	16.28	11.93	4.43	16.42	6.65
1/19/06 10:27	0.04	3.08	2.86	-5.5	95.3	109.6	112.5	115.1	118.6	120.8	30.4	17.16	11.11	2.94	2.70	6.13
1/19/06 12:20	0.04	2.73	2.36	-5.0	96.3	109.3	111.5	114.0	117.5	120.3	30.1	15.88	9.18	2.19	15.97	6.69
1/19/06 13:56	0.02	1.76	1.40	-3.0	91.7	103.5	105.8	108.0	111.1	115.7	29.6	16.49	9.08	1.91	1.83	5.92
1/19/06 15:10	0.03	1.80	1.36	-3.1	92.0	103.7	106.1	108.5	111.4	115.8	30.4	16.76	9.52	2.17	2.23	5.67
1/19/06 19:35	0.02	3.04	2.40	-6.3	96.1	109.2	115.6	120.5	124.0	121.6	30.4	16.44	13.18	6.28	5.78	6.46
1/19/06 21:03	0.01	2.88	2.33	-6.1	95.4	107.7	112.5	117.3	121.1	120.5	30.1	13.24	9.70	3.82	3.49	6.22
1/20/06 4:13	0.01	2.94	2.16	-6.0	93.3	106.7	114.6	121.8	127.0	123.8	30.0	16.62	12.67	4.89	4.86	6.02
1/20/06 5:13	0.01	2.60	1.90	-5.2	94.8	107.7	115.6	123.4	129.2	125.4	29.8	17.04	12.54	4.27	17.32	6.61
1/20/06 13:30	0.00	1.95	1.33	-4.3	94.5	105.9	112.0	122.7	133.2	126.0	30.0	13.94	8.57	1.91	1.91	5.82
1/20/06 14:34	0.00	1.92	1.28	-4.4	96.2	106.1	111.1	121.5	133.3	126.7	29.5	13.04	7.07	1.34	1.39	5.98

Table C-3. Campaign 4 Raw Stripper Data for 5 m K^+/2.5 m PZ

	STR RETURN	STR RETURN	STR RETURN	STR RETURN	STR RETURN	STR RETURN	STR RETURN	STR RETURN	STR RETURN	COLUMN PRESSURE	PRES DRP (LO)	PRES DRP (HI)
Time	FT201	FT201	FT201	FT203	FT203	FT203	FT204	FT204	FT204	PT215	PDT250	PDT251
	(GPM)	(F)	(LB/FT^3)	(GPM)	(F)	(LB/FT^3)	(GPM)	(F)	(LB/FT^3)	(PSIA)	(in H_2O)	(in H_2O)
1/10/06 15:28	13.74	104.12	76.22	2.72	128.85	61.08	0.16	126.21	61.82	23.49	5.96	15.36
1/10/06 21:04	12.20	103.65	76.51	2.35	128.04	61.70	0.20	123.97	62.47	23.50	5.96	14.52
1/10/06 21:58	12.26	103.51	76.59	2.36	127.73	61.85	0.10	120.82	62.68	23.50	5.96	15.52
1/11/06 12:00	12.98	110.52	76.50	0.67	101.06	61.62	0.16	100.41	62.05	23.50	4.12	4.21
1/11/06 13:01	12.89	111.28	76.48	0.66	103.06	61.58	0.15	102.12	62.02	23.50	4.43	4.54
1/11/06 15:59	14.33	113.70	76.47	0.72	104.21	61.55	0.21	103.47	62.00	23.50	5.96	6.74
1/11/06 17:28	14.33	113.79	76.50	0.71	103.00	61.57	0.12	101.52	62.04	23.50	5.96	7.15
1/11/06 21:19	14.29	110.99	76.68	0.56	99.61	61.67	0.18	99.13	62.09	23.50	5.96	7.33
1/11/06 22:29	14.29	109.65	76.77	0.49	94.56	61.78	0.30	93.82	62.15	23.50	5.96	7.19
1/12/06 6:28	11.85	115.79	75.71	1.61	113.94	61.52	0.11	110.19	62.14	23.50	5.96	13.63
1/12/06 7:25	11.85	113.45	75.70	1.56	114.05	61.52	0.14	110.25	62.15	23.49	5.96	15.03
1/12/06 14:04	14.22	116.10	75.73	2.05	122.92	61.25	0.11	120.20	61.94	23.51	5.96	15.46
1/12/06 15:00	14.46	116.03	75.72	2.08	122.79	61.31	0.08	120.39	61.99	23.50	5.96	11.31
1/12/06 17:07	14.36	112.56	75.60	2.24	125.79	61.14	0.18	123.11	61.86	23.51	5.38	8.84
1/12/06 18:03	14.10	112.18	75.70	2.12	124.84	61.18	0.29	122.62	61.89	23.51	5.96	11.20
1/12/06 18:31	14.11	112.09	75.73	2.12	123.58	61.24	0.17	121.22	61.93	23.50	5.96	12.11
1/12/06 22:22	12.91	111.86	75.77	0.47	100.18	61.69	0.09	98.85	62.13	23.50	5.36	5.53
1/12/06 23:21	12.91	106.22	75.90	0.49	102.58	61.64	0.09	100.77	62.11	23.50	5.82	6.03
1/13/06 2:06	14.43	108.47	75.89	0.41	95.41	61.79	0.17	93.66	62.19	23.50	5.96	7.36
1/13/06 3:03	14.40	107.62	75.94	0.39	93.09	61.85	0.11	91.16	62.23	23.50	5.96	7.49
1/13/06 5:12	14.38	105.25	76.07	0.33	94.82	61.82	0.16	94.20	62.19	23.50	5.96	7.92
1/13/06 5:49	14.38	105.31	76.07	0.33	94.73	61.82	0.22	94.21	62.19	23.50	5.96	8.13
1/18/06 17:10	28.92	108.24	75.85	0.79	103.78	61.61	0.15	103.01	62.07	23.51	5.96	9.78
1/18/06 17:45	28.87	109.85	75.81	0.80	104.18	61.61	0.15	102.97	62.08	23.50	5.96	12.27
1/19/06 10:27	29.90	109.51	75.98	0.64	95.45	61.80	0.13	94.76	62.17	23.50	5.96	13.62
1/19/06 12:20	29.89	109.93	75.94	0.68	98.06	61.75	0.11	97.39	62.14	23.51	5.96	14.47
1/19/06 13:56	23.38	104.09	76.06	0.49	100.05	61.70	0.08	99.16	62.10	23.51	5.96	8.55
1/19/06 15:10	23.33	104.42	76.09	0.42	100.53	61.67	0.07	99.10	62.10	23.50	5.96	9.27
1/19/06 19:35	24.77	108.14	75.96	0.77	100.95	61.72	0.19	99.85	62.16	23.50	5.96	12.01
1/19/06 21:03	24.80	107.21	75.98	0.79	98.60	61.77	0.18	97.29	62.19	23.50	5.96	9.70
1/20/06 4:13	24.80	104.83	75.89	1.81	114.89	61.45	0.15	112.34	62.06	23.50	5.96	11.09
1/20/06 5:13	24.93	105.22	75.88	1.93	118.93	61.36	0.26	116.98	62.00	23.50	5.96	12.42
1/20/06 13:30	20.34	105.49	76.21	2.56	128.57	61.13	0.13	127.00	61.84	23.51	5.96	12.70
1/20/06 14:34	20.04	105.10	76.27	2.65	132.35	61.02	0.14	130.62	61.77	23.49	5.96	15.53

Table C-4. Campaign 4 Raw Stripper Data for 5 m K^+/2.5 m PZ – Continued

	TOP	TOP MID	TOP BOT	BOT TOP	BOT MID	BOT	COLUMN	ACC	REBOILER	OVHD	COND	CW	CW	CW	CO_2	VAPORIZER
	TEMP	TEMP	TEMP	TEMP	TEMP	TEMP	LEVEL	LEVEL	LEVEL	VAPOR	LIQ	INLET	OUTLET	FLOW	FLOW	LEVEL
Time	T20710	T2078	T2076	T2075	T2073	T2071	LT206	LC203	LT204	TT216	T225	T224	T226	FT205	FT216	LT802
	(F)	(F)	(F)	(F)	(F)	(F)	(in)	(in)	(in)	(F)	(F)	(F)	(F)	(GPM)	(SCFM)	(in)
1/10/06 15:28	239.38	240.3	242.96	243.5	241.01	244.74			247.28	236.2	123.7	57.1	72.9	221	26.51	-
1/10/06 21:04	236.83	238.1	242.87	243.5	241.08	244.98	274.41	242.80	244.88	235.7	127.1	54.9	68.4	222	40.54	-
1/10/06 21:58	236.43	237.0	242.98	243.5	241.23	245.15	279.36	246.46	247.11	235.3	128.6	54.8	67.8	222	43.27	-
1/11/06 12:00	222.82	232.0	239.80	240.1	241.26	244.10	264.27	247.67	247.41	227.0	66.8	48.1	52.3	241	9.83	39.03
1/11/06 13:01	222.48	232.1	239.96	240.1	241.09	244.07	267.04	247.45	246.16	226.6	68.5	48.6	52.8	242	13.26	39.80
1/11/06 15:59	223.40	234.6	241.21	241.1	242.34	244.39	266.03	244.96	244.62	226.2	82.7	49.3	54.1	242	32.82	37.99
1/11/06 17:28	223.58	235.5	241.27	241.6	242.98	244.41	268.09	246.72	247.34	226.1	80.8	48.9	53.6	242	35.22	37.89
1/11/06 21:19	222.58	234.9	240.52	241.3	242.89	244.36	269.47	247.62	247.87	224.6	67.6	48.5	52.7	242	35.03	37.75
1/11/06 22:29	221.43	232.9	239.76	240.7	241.90	244.34	268.26	245.06	244.22	223.4	59.1	47.9	51.7	242	36.13	37.49
1/12/06 6:28	235.60	236.4	242.12	242.7	241.67	244.36	267.17	243.69	243.99	233.1	101.1	51.5	60.2	244	31.40	38.03
1/12/06 7:25	235.90	234.6	242.20	242.7	241.54	244.48	270.63	253.28	253.50	233.1	100.8	51.9	60.4	244	30.75	38.12
1/12/06 14:04	237.05	236.3	242.26	242.6	239.47	244.61	267.32	250.17	250.63	234.0	113.1	53.4	64.4	244	32.05	37.76
1/12/06 15:00	237.48	238.9	242.18	242.4	240.10	244.12	264.71	244.80	244.69	233.6	116.4	53.8	65.0	244	34.94	38.06
1/12/06 17:07	237.85	240.5	242.17	242.3	240.43	243.71	264.20	245.40	244.78	233.9	120.2	54.2	66.3	244	35.40	37.59
1/12/06 18:03	236.19	239.4	242.26	242.5	240.58	244.10	262.97	244.19	243.64	233.0	125.9	54.0	65.7	244	46.13	37.62
1/12/06 18:31	235.75	239.0	242.28	242.5	240.45	244.20	262.86	243.91	243.37	233.3	126.0	54.1	65.6	244	46.27	37.76
1/12/06 22:22	221.04	229.5	238.04	239.3	239.38	243.15	266.93	247.28	246.18	222.7	57.8	47.4	50.6	242	26.96	38.02
1/12/06 23:21	221.53	230.0	238.03	239.1	239.52	243.18	268.75	246.30	246.44	222.9	57.7	47.3	50.6	241	26.12	38.37
1/13/06 2:06	220.69	229.7	237.05	238.1	240.01	243.38	308.18	292.53	290.89	222.3	55.2	46.5	49.6	241	27.63	37.59
1/13/06 3:03	220.26	229.0	236.72	237.9	240.32	243.41	309.13	293.21	291.60	221.4	53.6	46.4	49.5	241	28.78	37.49
1/13/06 5:12	222.19	230.1	235.54	236.6	239.89	243.28	194.46	164.25	165.71	223.4	54.6	46.7	49.8	241	24.69	37.25
1/13/06 5:49	221.36	229.9	236.24	237.2	240.49	243.49	193.71	163.79	164.79	222.3	54.1	46.9	49.9	241	27.52	37.33
1/18/06 17:10	222.06	230.6	237.03	238.3	240.87	243.32	206.08	170.39	171.24	224.1	89.4	49.7	55.6	210	47.55	38.01
1/18/06 17:45	222.79	231.4	237.52	238.7	241.12	243.70	201.94	169.45	171.11	224.3	89.7	49.9	55.4	210	49.95	38.07
1/19/06 10:27	221.53	230.5	235.60	236.6	239.92	243.48	184.20	166.20	166.65	222.3	84.7	49.2	53.7	213	44.70	37.96
1/19/06 12:20	222.62	232.0	236.28	237.1	240.05	243.42	183.55	165.94	166.45	223.4	82.0	49.5	54.2	213	38.28	38.04
1/19/06 13:56	219.83	228.1	234.05	234.8	238.74	242.79	196.51	168.29	170.21	222.2	61.0	48.6	51.9	212	18.78	38.32
1/19/06 15:10	218.31	226.2	232.44	233.1	237.98	242.87	196.92	167.48	169.41	220.6	58.8	48.3	51.4	213	28.50	38.48
1/19/06 19:35	222.48	229.2	237.68	238.7	240.66	243.84	212.75	169.43	171.72	224.7	86.4	49.6	55.2	213	47.48	38.17
1/19/06 21:03	223.16	230.9	237.91	239.0	240.73	243.58	210.78	169.93	172.05	225.8	87.7	49.7	55.4	213	42.98	37.90
1/20/06 4:13	234.75	237.9	240.91	241.5	241.65	244.22	283.09	245.36	249.40	230.5	125.3	54.3	65.7	214	57.28	37.69
1/20/06 5:13	235.37	238.6	241.08	241.8	241.63	244.37	281.76	246.42	247.36	231.1	127.8	54.8	66.8	214	59.64	37.90
1/20/06 13:30	238.27	240.5	242.46	242.9	241.14	244.66	286.46	248.06	250.99	234.1	137.6	55.9	71.1	214	43.15	38.05
1/20/06 14:34	238.66	240.9	242.75	243.1	241.61	245.01	287.58	249.17	252.44	234.6	139.3	56.5	72.2	214	39.33	37.99

Table C-5. Campaign 4 Raw Stripper Data for 5 m K^+/2.5 m PZ – Continued

	REBOILER	STEAM	STEAM	COND	STM ANNUBAR	BOT LIQ	VAPOR	BOT	BOT	FEED	FEED	TRIM	STRP
	DUTY	FLOW	TEMP	RETURN	PRES	TO REB	INLET	PROD	PROD	INLET	OUTLET	TEMP	FEED
Time	QIC202	FC202	T202	T203		T209	T208	TT215	TT212	TT200	TT217	TT210	TT211
	(MMBTU/HR)	(LB/HR)	(F)	(F)	(PSIA)	(F)	(F)	(F)	(F)	(F)	(F)	(F)	(F)
1/10/06 15:28	2.138	2224.1	333.8	261.4	116.9	244.9	245.5	245.7	127.9	119.5	231.2	230.2	227.7
1/10/06 21:04	1.887	1967.5	335.2	264.7	119.1	245.2	246.5	246.0	127.1	118.6	231.6	230.8	229.0
1/10/06 21:58	1.850	1933.1	335.8	266.7	120.1	245.4	246.6	246.1	126.9	118.1	231.9	231.1	228.9
1/11/06 12:00	0.827	854.4	341.8	259.1	127.4	243.7	244.2	243.6	131.2	122.0	231.2	229.7	226.6
1/11/06 13:01	0.829	855.8	341.7	258.8	127.3	243.7	244.1	243.5	131.2	122.4	230.6	228.8	226.2
1/11/06 15:59	0.950	981.4	341.6	259.7	127.4	244.1	242.3	243.8	131.6	122.5	230.6	229.2	226.5
1/11/06 17:28	0.935	965.8	342.0	260.0	127.6	244.0	242.2	244.0	131.6	122.4	230.7	229.6	227.1
1/11/06 21:19	0.875	903.7	342.7	259.6	129.2	244.2	243.9	244.1	126.2	116.6	229.9	228.7	226.0
1/11/06 22:29	0.864	890.8	342.9	258.5	129.7	243.9	243.8	243.7	124.8	115.1	229.3	227.5	224.9
1/12/06 6:28	1.425	1482.1	338.4	263.7	122.5	244.3	245.1	244.4	131.7	123.5	231.5	229.6	226.0
1/12/06 7:25	1.399	1453.9	338.3	263.4	122.3	244.4	245.5	244.5	131.6	123.5	231.3	229.6	226.0
1/12/06 14:04	1.732	1806.7	336.2	265.7	119.5	244.2	242.9	244.8	131.9	123.2	230.7	229.6	226.7
1/12/06 15:00	1.748	1824.0	336.0	265.5	119.5	243.8	242.2	244.4	132.3	123.2	231.0	229.8	226.6
1/12/06 17:07	1.873	1951.5	334.9	263.7	118.0	243.4	243.7	244.3	127.1	117.2	230.3	229.2	226.7
1/12/06 18:03	1.818	1899.9	335.6	267.2	119.2	243.9	243.3	244.7	126.4	117.2	229.8	228.8	226.0
1/12/06 18:31	1.818	1901.6	335.7	267.9	119.3	243.9	243.5	244.7	126.2	117.1	229.7	228.7	226.2
1/12/06 22:22	0.693	712.4	342.7	256.2	129.7	242.5	243.1	242.5	132.6	123.6	230.0	228.7	225.6
1/12/06 23:21	0.682	701.9	343.6	256.6	131.0	242.6	243.1	242.7	133.5	124.3	230.3	229.0	226.8
1/13/06 2:06	0.740	761.0	343.1	255.5	130.5	242.6	242.9	242.4	129.6	119.9	229.2	227.3	223.8
1/13/06 3:03	0.740	759.6	344.1	255.4	132.3	242.7	242.9	242.4	128.8	119.2	228.9	226.6	223.1
1/13/06 5:12	0.700	719.0	343.3	255.6	131.2	242.6	242.8	242.5	125.4	115.3	228.4	227.0	223.9
1/13/06 5:49	0.699	718.6	344.4	255.6	133.0	242.7	242.8	242.7	125.4	115.2	228.6	227.1	224.2
1/18/06 17:10	1.227	1271.5	340.2	261.4	125.3	242.0	240.6	241.9	131.7	118.3	226.2	226.0	224.6
1/18/06 17:45	1.219	1265.4	338.8	262.3	123.0	242.3	241.1	242.3	134.0	121.1	226.7	226.4	225.2
1/19/06 10:27	1.150	1192.3	339.1	261.7	123.9	242.2	240.0	241.8	132.1	118.5	225.9	225.6	224.1
1/19/06 12:20	1.149	1191.4	339.1	261.4	123.8	242.2	240.0	241.8	131.8	118.1	225.8	225.5	223.9
1/19/06 13:56	0.884	912.0	341.9	258.1	128.0	241.2	244.2	240.6	126.4	113.3	225.2	224.6	222.9
1/19/06 15:10	0.860	886.5	341.9	257.2	128.1	241.0	243.8	240.4	126.6	113.7	225.1	224.6	222.8
1/19/06 19:35	1.199	1243.8	338.8	261.9	123.6	242.6	240.0	242.2	131.5	119.1	226.4	226.1	224.7
1/19/06 21:03	1.225	1271.3	338.9	262.4	123.6	242.3	240.3	241.9	130.4	117.9	225.9	224.9	223.3
1/20/06 4:13	1.853	1951.3	334.9	273.7	118.8	243.2	245.4	243.5	133.2	121.1	227.3	227.0	225.9
1/20/06 5:13	1.871	1971.9	335.4	274.9	119.5	243.4	246.4	244.0	135.8	123.6	228.3	228.3	227.1
1/20/06 13:30	2.175	2266.6	333.2	263.1	115.9	244.0	244.9	244.2	135.6	124.1	229.8	229.3	227.2
1/20/06 14:34	2.193	2288.9	331.4	263.4	113.4	244.4	245.4	244.8	136.6	125.8	229.8	229.5	227.9

Table C-6. Campaign 4 Raw Absorber Data for 6.4 m K^+/1.6 m PZ

	ABS LEAN	ABS LEAN	ABS LEAN	ABS LEAN	ABS LEAN	ABS RICH	ABS RICH	ABS RICH	ABS RICH	ABS RICH	GAS	ANNUBAR	GAS	GAS	Cool GAS
	FLOW	DEN	TEMP	pH	pH TEMP	FLOW	DEN	TEMP	pH	pH TEMP	FLOW	TEMP	IN	OUT	TEMP
Time	FT403	FT403	TT403	AI403	AI403-T	FT200	FT200	TT200	AI401	AI401-T	FT900	TT407	TT406	TT400	TT412
	(GPM)	(LB/FT^3)	(F)	(pH)	(F)	(GPM)	(LB/FT^3)	(F)	(pH)	(F)	(ACFM)	(F)	(F)	(F)	(F)
1/23/06 18:40	22.98	79.78	101.77	10.25	100.11	23.27	79.62	110.73	9.67	110.36	300	66.10	106.05	93.35	50.00
1/23/06 21:40	23.01	79.64	101.49	10.28	99.79	23.44	79.57	110.29	9.69	110.21	300	65.13	105.96	93.91	49.89
1/24/06 7:38	25.95	78.92	102.19	10.37	101.28	26.67	78.80	109.53	9.77	109.37	300	61.56	105.98	91.85	53.48
1/24/06 9:00	26.04	79.07	104.94	10.30	104.08	26.61	78.95	112.80	9.65	112.80	300	68.88	106.03	95.42	53.03
1/24/06 11:30	14.98	79.49	98.16	10.29	93.90	15.49	79.36	110.35	9.46	111.35	300	72.59	106.15	92.84	49.99
1/24/06 12:25	15.01	79.51	98.08	10.28	95.16	15.55	79.39	110.70	9.46	111.16	300	77.29	107.01	93.68	50.97
1/24/06 19:37	15.00	79.67	100.09	10.50	94.21	15.56	79.50	113.53	9.53	114.14	300	68.33	106.99	94.09	52.24
1/24/06 20:34	15.04	79.65	99.48	10.50	93.36	15.49	79.48	112.81	9.53	113.56	300	66.97	106.98	93.50	51.85
1/25/06 4:58	17.01	79.09	103.07	10.57	95.25	17.64	79.03	112.04	9.60	112.83	300	68.09	107.10	91.46	53.60
1/25/06 15:00	20.94	79.00	100.99	10.52	99.54	21.58	78.95	112.07	9.69	112.05	300	80.69	101.67	98.21	57.12
1/25/06 16:00	21.01	79.06	101.63	10.52	99.62	21.60	79.00	113.51	9.66	113.26	300	82.01	103.96	99.38	56.91
1/25/06 21:00	18.02	79.07	104.02	10.51	99.61	18.63	79.02	115.12	9.58	114.98	300	68.62	104.02	97.85	53.50
1/25/06 22:04	18.02	79.16	102.74	10.54	98.28	18.67	79.11	113.81	9.60	114.02	300	67.92	104.07	96.36	53.31
1/26/06 0:58	15.01	78.91	101.98	10.56	95.12	15.61	78.88	113.96	9.51	114.45	300	64.74	104.13	95.27	52.11
1/26/06 2:00	15.01	78.95	101.09	10.57	94.21	15.55	78.90	112.19	9.56	113.00	300	63.13	104.07	93.54	51.66
1/26/06 5:32	15.02	79.16	102.95	10.70	94.49	15.56	79.10	114.95	9.57	115.45	300	66.79	103.94	95.62	54.59
1/26/06 6:32	15.01	79.26	103.09	10.69	94.64	15.61	79.22	115.47	9.55	115.88	300	67.06	103.76	96.06	54.55
1/26/06 10:00	18.00	78.98	105.84	10.68	99.53	18.63	78.97	115.67	9.64	116.16	300	64.53	103.96	96.32	55.79
1/26/06 11:00	18.03	79.08	104.79	10.70	98.99	18.60	79.07	115.12	9.71	115.70	300	65.13	103.78	94.74	55.80
1/26/06 15:00	21.01	78.88	106.82	10.57	101.84	21.73	78.87	116.51	9.54	116.71	500	69.97	103.80	101.12	57.16
1/26/06 16:00	20.98	78.96	106.80	10.57	102.15	21.77	78.95	116.40	9.56	116.63	500	74.46	104.28	101.20	57.41
1/26/06 19:00	17.97	79.01	110.35	10.51	102.94	18.67	79.09	118.17	9.43	118.66	500	66.42	103.91	105.60	54.13
1/26/06 19:50	17.99	79.04	110.69	10.53	103.87	18.63	79.12	118.32	9.44	118.91	500	66.28	103.76	105.91	54.98
1/27/06 0:30	15.02	78.63	113.99	10.53	100.99	15.57	78.97	113.46	9.38	115.08	501	63.70	103.62	112.63	54.32
1/27/06 1:30	14.99	78.70	113.15	10.52	99.30	15.54	78.98	113.65	9.38	114.95	501	62.85	104.19	110.50	53.44

Table C-7. Campaign 4 Raw Absorber Data for 6.4 m K^+/1.6 m PZ – Continued

	GAS	PRESSURE	PRESSURE	ABS	BED	BED	BED	BED	BED	BED	COLUMN	CO_2	CO_2	CO_2	FTIR	FTIR
	PRESS	DRP	DRP	PRESS	TEMP	TEMP	TEMP	TEMP	TEMP	TEMP	LEVEL	IN	MID	OUT	CO_2	H_2O
Time	PT900	PDT450	PDT451	PT415	TT4078	TT4077	TT4076	TT4075	TT4073	TT4071	LT401	AI400	AI406	AI404	AI408	AI408
	(PSIA)	(in H_2O)	(in H_2O)	(in H_2O)	(F)	(F)	(F)	(F)	(F)	(F)	(in)	(mol%)	(mol%)	(mol%)	(mol%)	(mol%)
1/23/06 18:40	0.02	1.35	1.43	-2.5	87.9	99.9	99.6	105.5	106.6	111.9	25.6	15.72	11.02	4.98	-	-
1/23/06 21:40	0.09	1.50	6.07	-5.8	89.1	98.9	100.7	103.7	106.0	111.7	18.5	15.73	11.02	5.26	-	-
1/24/06 7:38	0.02	1.52	1.09	-2.5	85.2	101.9	102.5	104.7	106.6	111.7	17.8	14.32	9.20	3.23	-	-
1/24/06 9:00	0.02	1.51	1.04	-2.5	87.6	104.9	106.0	108.4	110.5	114.3	17.5	16.15	10.98	4.19	-	-
1/24/06 11:30	0.01	0.53	0.49	-1.5	85.5	99.4	99.7	104.8	105.8	112.1	17.7	17.60	14.72	7.32	8.78	3.99
1/24/06 12:25	0.01	0.53	0.46	-1.5	86.1	99.6	100.0	104.7	105.8	112.4	17.6	18.02	15.08	7.32	8.88	4.31
1/24/06 19:37	0.00	0.77	0.68	-1.8	89.1	102.1	104.3	107.9	109.9	115.8	18.4	17.64	14.24	7.32	7.60	5.12
1/24/06 20:34	0.00	0.84	0.85	-2.1	88.4	101.5	104.1	106.9	109.2	115.2	18.7	17.03	13.63	7.31	7.13	5.15
1/25/06 4:58	0.00	1.01	0.72	-2.1	84.5	103.6	104.6	108.6	110.2	116.0	17.0	16.17	12.43	5.41	16.28	5.70
1/25/06 15:00	0.00	0.99	0.55	-1.9	92.3	101.9	103.8	106.9	109.6	113.1	16.7	16.64	11.37	3.58	3.63	5.13
1/25/06 16:00	0.01	1.05	0.60	-2.0	92.4	102.8	105.1	108.1	110.8	114.5	16.6	17.24	12.18	4.11	4.18	5.42
1/25/06 21:00	0.00	1.12	0.74	-2.2	92.4	105.7	108.9	111.9	114.5	117.0	17.3	16.69	12.58	5.18	5.19	5.70
1/25/06 22:04	0.00	1.13	0.76	-2.2	91.4	103.8	106.8	110.1	112.6	115.6	17.5	16.01	11.93	4.80	4.91	5.55
1/26/06 0:58	0.00	1.02	0.71	-2.1	90.2	103.9	107.4	110.8	113.5	116.2	16.9	16.48	13.22	6.24	16.39	6.17
1/26/06 2:00	0.00	1.04	0.73	-2.0	88.7	102.2	105.0	108.4	110.9	114.7	16.9	14.76	11.47	5.04	15.16	5.06
1/26/06 5:32	-0.01	1.02	0.73	-2.2	90.0	104.5	107.9	111.9	114.7	117.6	17.0	15.17	11.30	4.27	15.68	6.27
1/26/06 6:32	-0.01	1.05	0.71	-2.2	90.3	105.0	108.9	113.0	116.2	118.3	17.1	16.20	12.41	4.96	16.34	6.76
1/26/06 10:00	0.00	1.06	0.68	-2.1	91.1	106.1	108.3	112.5	115.2	118.7	17.1	15.53	10.55	3.12	3.16	5.89
1/26/06 11:00	0.00	1.18	0.76	-2.2	89.7	105.1	108.4	112.0	114.6	118.2	17.4	16.92	12.22	4.01	17.31	6.62
1/26/06 15:00	0.02	2.50	2.18	-5.3	95.3	108.5	113.7	117.5	120.5	119.6	16.6	16.56	14.58	7.32	8.86	6.56
1/26/06 16:00	0.02	2.51	2.18	-5.4	95.1	108.3	113.2	117.0	119.9	119.6	16.3	16.37	14.27	7.32	8.68	6.81
1/26/06 19:00	0.01	2.58	2.23	-5.9	98.9	114.1	123.3	129.0	132.5	121.7	17.2	17.29	15.83	7.32	9.92	7.36
1/26/06 19:50	0.01	2.64	2.30	-6.1	99.4	114.6	124.4	131.2	133.8	121.9	17.2	16.57	14.99	7.32	9.44	7.22
1/27/06 0:30	0.00	2.45	2.40	-6.5	105.6	129.7	136.0	133.9	128.7	118.6	17.1	17.24	16.54	7.32	10.28	9.39
1/27/06 1:30	-0.01	2.46	2.37	-6.6	103.2	126.6	134.5	132.8	128.7	118.7	17.1	16.88	16.11	7.32	10.14	8.57

Table C-8. Campaign 4 Raw Stripper Data for 6.4 m K^+/1.6 m PZ

	STR RETURN	STR RETURN	STR RETURN	STR RETURN	STR RETURN	STR RETURN	STR RETURN	STR RETURN	STR RETURN	COLUMN PRESSURE	PRES DRP (LO)	PRES DRP (HI)
Time	FT201	FT201	FT201	FT203	FT203	FT203	FT204	FT204	FT204	PT215	PDT250	PDT251
	(GPM)	(F)	(LB/FT^3)	(GPM)	(F)	(LB/FT^3)	(GPM)	(F)	(LB/FT^3)	(PSIA)	(in H_2O)	(in H_2O)
1/23/06 18:40	22.87	101.32	79.64	1.16	92.88	61.73	0.07	91.23	62.13	5.11	5.96	8.43
1/23/06 21:40	22.91	100.86	79.51	1.25	92.42	62.65	0.06	90.91	63.04	5.16	5.35	6.08
1/24/06 7:38	26.10	101.58	78.84	1.72	96.36	61.98	0.11	93.61	62.42	5.14	5.96	20.88
1/24/06 9:00	26.09	104.04	78.99	1.70	95.89	63.84	0.09	93.48	64.34	5.08	5.96	20.80
1/24/06 11:30	15.09	97.60	79.37	0.62	93.57	61.78	0.05	93.31	62.16	5.11	2.82	2.81
1/24/06 12:25	15.07	98.21	79.37	0.66	94.71	61.69	0.07	94.63	62.07	5.10	3.06	3.07
1/24/06 19:37	15.01	100.66	79.52	1.43	97.15	61.66	0.07	95.27	62.11	5.11	5.96	6.53
1/24/06 20:34	14.99	99.99	79.51	1.38	96.36	61.68	0.10	94.39	62.13	5.10	5.96	6.70
1/25/06 4:58	16.99	106.55	79.01	2.43	102.72	65.23	0.09	99.31	65.77	5.21	5.96	18.06
1/25/06 15:00	21.16	100.94	78.86	1.98	108.68	61.57	0.06	106.08	62.14	7.51	5.96	19.43
1/25/06 16:00	21.07	101.75	78.92	1.94	108.39	61.63	0.05	106.70	62.16	7.50	5.96	19.54
1/25/06 21:00	18.10	102.44	78.97	1.70	104.67	61.68	0.09	102.14	62.21	7.50	5.96	11.07
1/25/06 22:04	18.07	103.89	79.01	1.66	104.56	61.62	0.07	102.17	62.15	7.50	5.96	11.08
1/26/06 0:58	15.18	102.77	78.77	1.39	102.53	61.61	0.09	100.40	62.11	7.50	5.96	6.99
1/26/06 2:00	15.12	101.37	78.82	1.24	101.08	61.62	0.09	97.92	62.14	7.50	5.96	6.52
1/26/06 5:32	15.14	103.72	79.07	2.10	108.05	62.15	0.04	104.75	62.75	7.50	5.96	12.63
1/26/06 6:32	15.02	103.98	79.14	2.12	107.62	62.27	0.08	104.18	62.84	7.49	5.96	15.44
1/26/06 10:00	18.12	105.99	78.87	2.22	113.11	61.40	0.08	107.46	62.08	10.99	5.96	12.33
1/26/06 11:00	18.14	105.62	78.97	2.21	111.91	61.46	0.08	106.64	62.12	11.00	5.96	16.10
1/26/06 15:00	21.07	107.82	78.80	1.88	107.38	61.56	0.21	104.69	62.12	11.00	5.96	16.00
1/26/06 16:00	21.03	107.74	78.87	1.87	107.73	61.54	0.23	105.87	62.08	11.00	5.96	17.49
1/26/06 19:00	18.02	111.70	78.95	1.45	102.39	61.62	0.21	100.26	62.13	11.00	5.96	8.99
1/26/06 19:50	17.96	111.82	78.98	1.47	103.32	61.59	0.24	101.09	62.11	11.00	5.96	9.26
1/27/06 0:30	14.99	117.35	78.65	1.04	95.54	61.76	0.18	93.66	62.19	11.00	4.99	5.18
1/27/06 1:30	15.05	117.24	78.68	1.03	93.58	61.80	0.25	92.22	62.21	10.99	5.09	5.27

Table C-9. Campaign 4 Raw Stripper Data for 6.4 m K^+/1.6 m PZ – Continued

	TOP	TOP MID	TOP BOT	BOT TOP	BOT MID	BOT	COLUMN	ACC	REBOILER	OVHD	COND	CW	CW	CW	CO_2	VAPORIZER
	TEMP	TEMP	TEMP	TEMP	TEMP	TEMP	LEVEL	LEVEL	LEVEL	VAPOR	LIQ	INLET	OUTLET	FLOW	FLOW	LEVEL
Time	T20710	T2078	T2076	T2075	T2073	T2071	LT206	LC203	LT204	TT216	T225	T224	T226	FT205	FT216	LT802
	(F)	(F)	(F)	(F)	(F)	(F)	(in)	(in)	(in)	(F)	(F)	(F)	(F)	(GPM)	(SCFM)	(in)
1/23/06 18:40	164.79	166.7	168.65	169.0	170.34	171.74	14.99	5.96	11.59	160.2	83.7	48.3	55.6	217	32.47	37.70
1/23/06 21:40	160.82	163.4	165.54	166.2	169.20	171.55	12.03	6.08	8.19	158.1	85.0	48.6	56.1	217	33.26	37.54
1/24/06 7:38	165.70	168.8	170.73	170.8	173.05	175.16	17.02	5.84	13.84	162.8	97.3	53.0	63.4	216	31.78	37.42
1/24/06 9:00	164.44	168.2	170.25	170.3	172.65	174.90	16.99	5.60	13.63	162.3	97.3	52.3	61.9	216	35.65	37.46
1/24/06 11:30	161.17	162.8	166.74	166.6	165.41	169.43	17.00	5.71	12.64	157.0	56.0	47.7	51.7	215	24.59	37.74
1/24/06 12:25	161.60	162.8	166.89	166.7	165.80	169.52	16.98	5.84	12.37	157.2	57.4	48.4	52.6	215	23.88	37.69
1/24/06 19:37	165.64	167.3	168.33	168.7	167.33	171.00	16.98	6.23	13.49	161.8	87.7	50.9	59.6	216	31.56	37.64
1/24/06 20:34	165.55	167.2	168.27	168.7	166.90	170.95	17.00	6.30	13.63	161.7	85.8	50.6	59.0	216	29.99	37.57
1/25/06 4:58	165.44	170.0	171.24	171.1	170.31	174.92	15.99	5.89	14.13	163.6	106.4	53.1	64.4	220	34.13	37.69
1/25/06 15:00	182.41	185.9	187.22	187.3	188.40	190.39	16.00	5.55	13.40	179.6	104.6	53.9	65.7	215	34.28	38.01
1/25/06 16:00	181.91	185.5	187.03	187.2	188.12	190.30	16.01	5.42	13.50	179.3	104.8	53.7	65.2	215	36.68	37.90
1/25/06 21:00	181.74	184.3	185.49	186.1	184.51	188.30	15.97	6.17	12.99	178.8	98.7	52.2	62.2	216	34.85	38.14
1/25/06 22:04	181.81	184.3	185.52	186.1	184.47	188.34	15.97	6.08	12.93	178.7	97.0	52.0	61.8	218	33.11	37.90
1/26/06 0:58	181.05	183.0	184.61	185.1	183.63	187.03	16.01	6.02	12.96	177.2	89.5	50.7	59.0	218	30.98	38.11
1/26/06 2:00	180.98	182.3	184.50	184.9	183.62	186.89	16.00	6.00	12.91	176.8	89.2	50.2	57.7	218	28.44	38.23
1/26/06 5:32	181.86	184.4	185.93	186.1	183.29	188.36	16.01	6.20	14.00	179.7	105.8	53.4	65.3	218	32.44	38.11
1/26/06 6:32	181.29	185.3	186.59	186.7	184.42	189.05	15.99	5.99	13.98	179.6	107.1	53.5	65.4	218	34.30	38.23
1/26/06 10:00	200.60	203.0	204.04	204.3	202.28	206.36	16.01	5.73	13.70	196.9	115.6	54.5	67.3	219	34.68	38.43
1/26/06 11:00	200.39	202.9	204.76	204.9	203.68	207.04	16.02	5.80	13.82	197.1	115.9	54.5	67.3	218	36.93	38.22
1/26/06 15:00	199.41	202.5	204.10	204.5	203.52	206.88	15.98	6.34	14.04	195.7	112.8	54.1	65.7	218	42.16	38.42
1/26/06 16:00	199.31	201.9	204.14	204.4	203.80	206.91	15.98	6.25	13.61	195.7	112.3	53.8	65.5	218	41.97	38.67
1/26/06 19:00	198.21	200.8	202.89	203.4	200.95	205.56	16.00	6.08	13.41	194.2	101.9	50.9	60.0	220	41.27	38.39
1/26/06 19:50	198.46	200.9	203.17	203.7	200.92	205.68	15.99	6.09	13.44	194.4	102.1	51.7	60.9	220	40.45	38.60
1/27/06 0:30	196.90	198.4	202.17	202.4	202.00	204.68	15.99	5.96	13.67	192.0	89.1	50.2	57.1	222	36.34	39.06
1/27/06 1:30	196.85	198.2	202.23	202.4	201.36	204.67	15.99	5.98	13.62	191.9	88.7	49.6	56.5	221	36.00	38.22

Table C-10. Campaign 4 Raw Stripper Data for 6.4 m K^+/1.6 m PZ – Continued

	REBOILER	STEAM	STEAM	COND	STM ANNUBAR	BOT LIQ	VAPOR	BOT	BOT	FEED	FEED	TRIM	STRP
	DUTY	FLOW	TEMP	RETURN	PRES	TO REB	INLET	PROD	PROD	INLET	OUTLET	TEMP	FEED
Time	QIC202	FC202	T202	T203		T209	T208	TT215	TT212	TT200	TT217	TT210	TT211
	(MMBTU/HR)	(LB/HR)	(F)	(F)	(PSIA)	(F)	(F)	(F)	(F)	(F)	(F)	(F)	(F)
1/23/06 18:40	1.068	1006.3	342.4	169.2	129.5	170.2	171.0	170.6	116.6	110.7	162.9	163.1	162.3
1/23/06 21:40	1.074	1015.3	343.3	173.6	131.4	170.0	171.5	170.5	116.2	110.3	162.7	162.9	162.3
1/24/06 7:38	1.463	1381.6	338.0	168.8	123.0	173.6	175.9	174.4	116.2	109.5	165.5	165.6	164.8
1/24/06 9:00	1.386	1304.7	339.0	166.6	123.8	173.2	175.6	174.0	119.2	112.8	165.8	165.8	164.9
1/24/06 11:30	0.624	587.8	342.4	168.7	128.1	167.8	168.4	168.0	115.2	110.4	161.4	161.2	160.1
1/24/06 12:25	0.646	608.9	342.2	169.1	127.8	167.9	168.5	168.2	115.4	110.7	161.5	161.5	160.4
1/24/06 19:37	1.172	1100.4	344.0	166.8	131.6	170.0	172.1	171.0	118.2	113.5	164.2	164.1	163.2
1/24/06 20:34	1.150	1079.5	344.2	166.3	132.2	169.9	172.0	170.7	117.5	112.8	163.8	163.7	162.8
1/25/06 4:58	1.583	1493.0	337.0	167.5	121.1	173.1	175.7	174.5	116.9	112.0	166.3	165.9	164.4
1/25/06 15:00	1.573	1521.0	338.2	193.1	122.2	189.0	191.3	189.8	119.7	112.1	179.8	179.9	179.1
1/25/06 16:00	1.535	1481.7	338.7	191.9	122.8	188.9	191.2	189.7	120.8	113.5	179.8	179.9	179.2
1/25/06 21:00	1.367	1329.0	339.2	199.4	123.8	186.8	189.0	187.5	121.8	115.1	178.5	178.6	177.9
1/25/06 22:04	1.350	1306.8	339.4	195.0	124.1	186.8	189.0	187.5	120.7	113.8	178.3	178.3	177.6
1/26/06 0:58	1.164	1119.4	341.7	189.4	127.7	185.6	187.5	186.3	120.2	114.0	177.6	177.5	176.5
1/26/06 2:00	1.076	1029.3	342.5	184.4	129.0	185.4	187.3	185.8	118.5	112.2	177.0	176.8	175.8
1/26/06 5:32	1.573	1519.9	336.7	192.0	120.6	187.0	189.5	188.1	121.1	114.9	179.1	178.9	177.9
1/26/06 6:32	1.577	1521.3	337.4	190.7	121.4	187.7	190.0	188.8	121.5	115.5	179.7	179.4	178.4
1/26/06 10:00	1.768	1750.0	336.1	215.1	119.8	204.7	206.9	205.6	124.1	115.7	194.3	193.9	192.7
1/26/06 11:00	1.793	1776.8	335.9	216.5	119.5	205.3	207.6	206.2	123.6	115.1	194.8	194.3	192.8
1/26/06 15:00	1.682	1664.4	336.4	214.7	119.9	205.2	207.0	205.9	125.3	116.5	194.2	193.9	192.8
1/26/06 16:00	1.683	1663.1	336.8	214.4	120.3	205.2	207.0	205.9	125.2	116.4	194.2	193.9	192.7
1/26/06 19:00	1.378	1368.0	338.0	219.3	122.3	204.0	206.1	204.7	126.0	118.2	193.7	193.3	192.2
1/26/06 19:50	1.388	1374.0	337.2	216.1	121.2	204.2	206.3	204.8	126.1	118.3	193.7	193.2	192.1
1/27/06 0:30	1.123	1104.9	339.0	210.9	123.8	203.3	205.2	203.3	120.9	113.5	192.3	191.6	189.6
1/27/06 1:30	1.125	1112.7	339.2	216.1	124.2	203.2	205.2	203.3	121.1	113.7	192.3	191.6	189.5

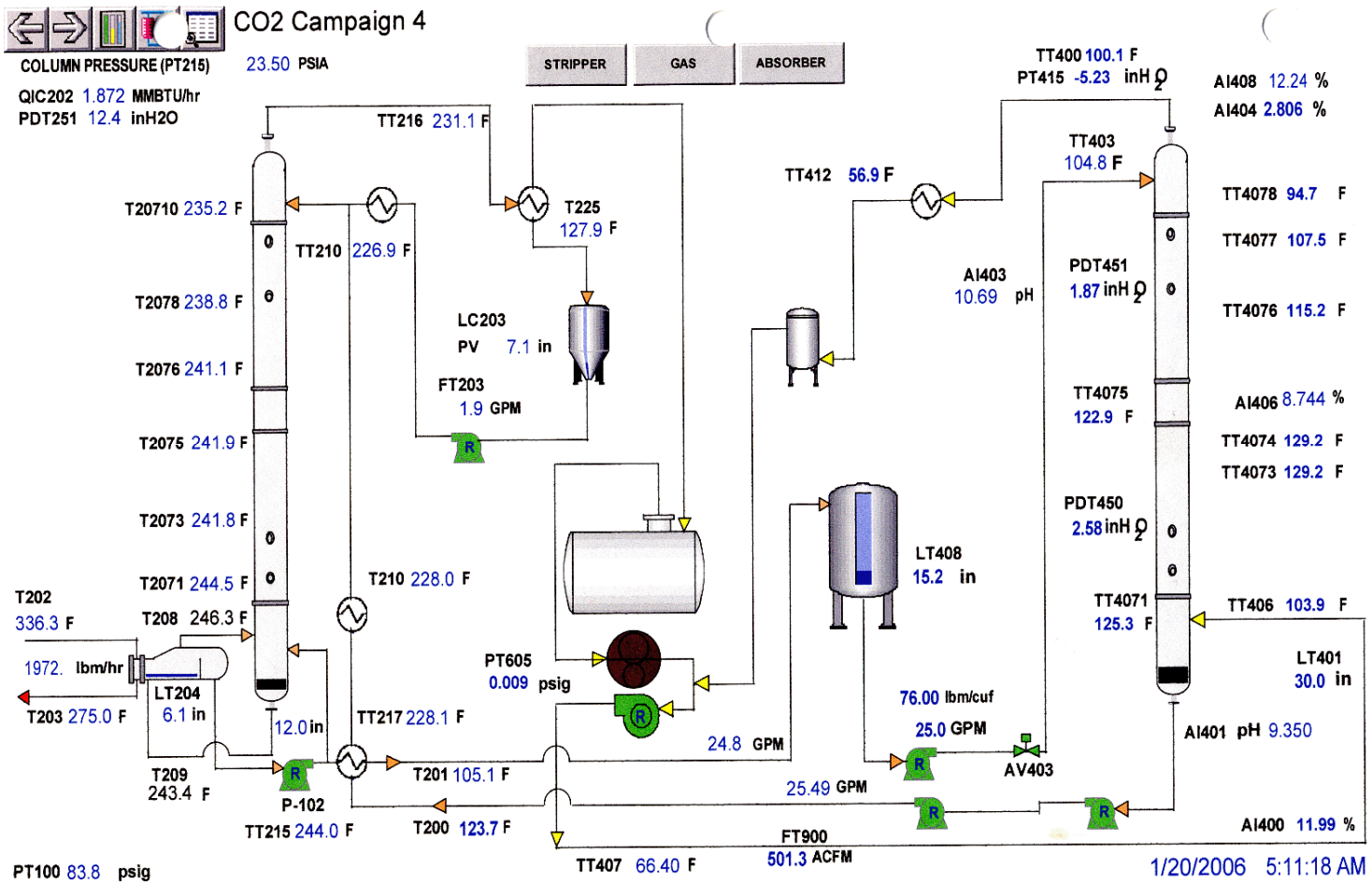

Figure C-1. Campaign 4 DeltaV Overall Process View

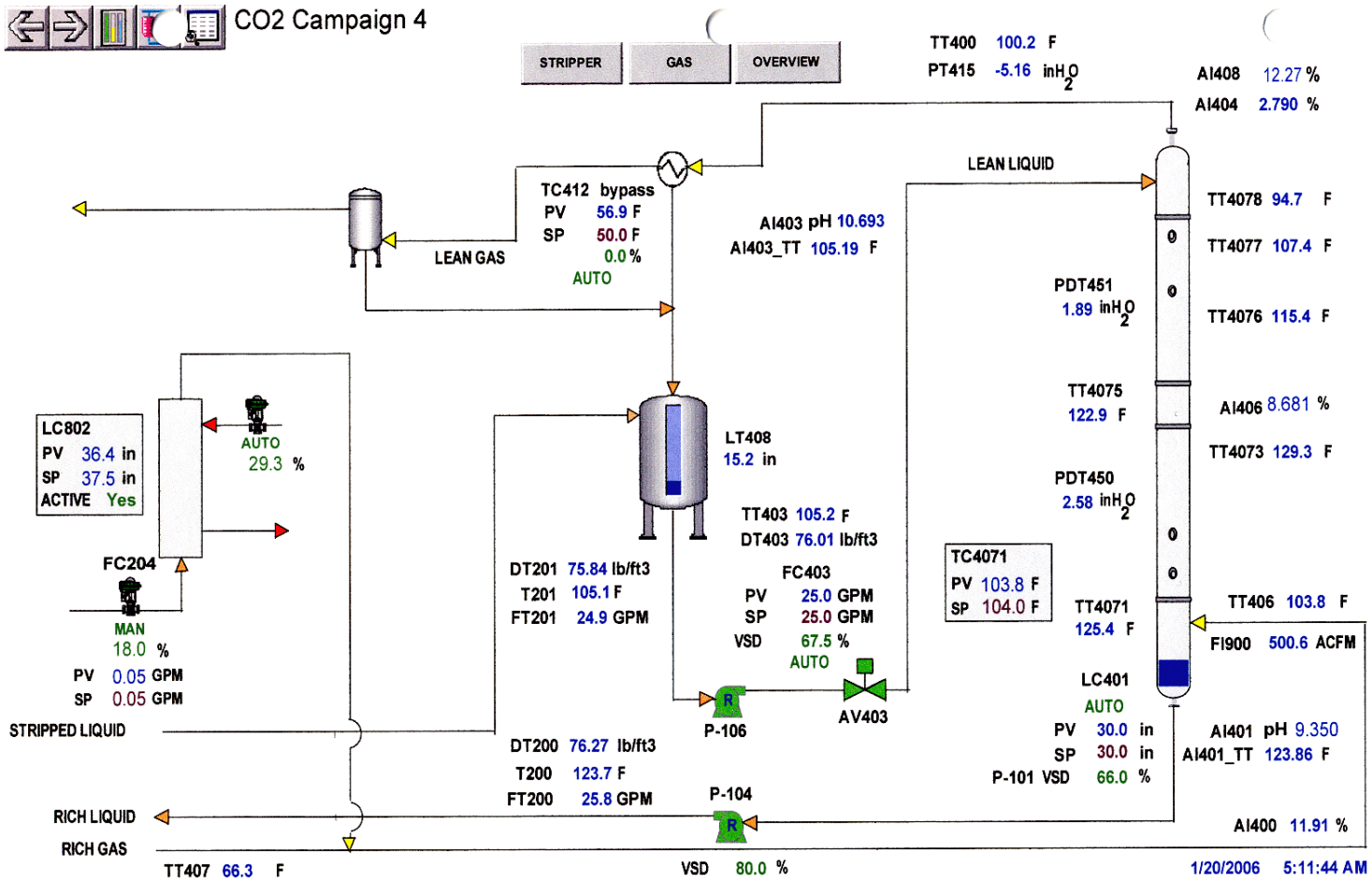

Figure C-2. Campaign 4 DeltaV Absorber Side Process View

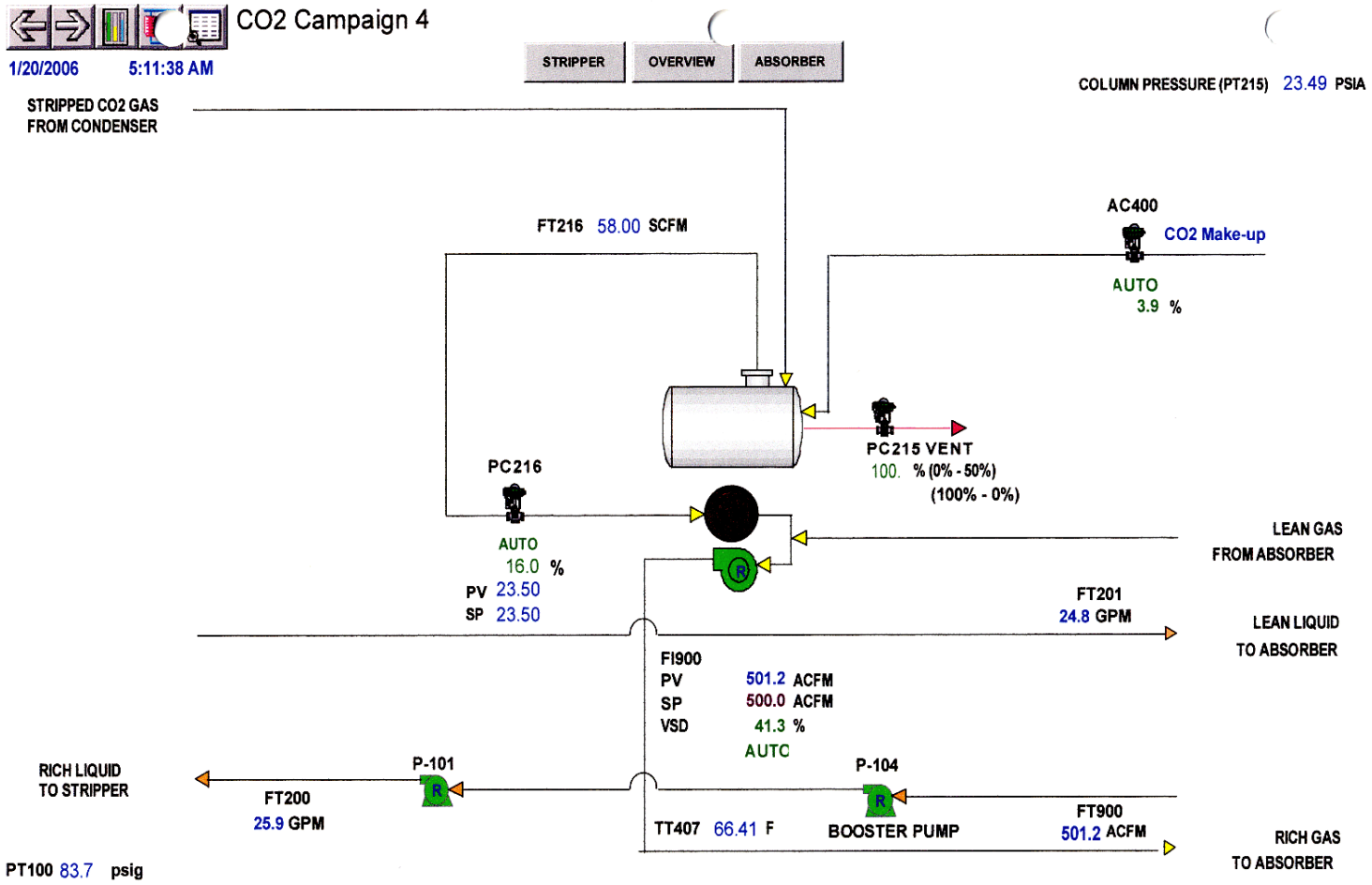

Figure C-3. Campaign 4 DeltaV CO_2 Recycle Process View

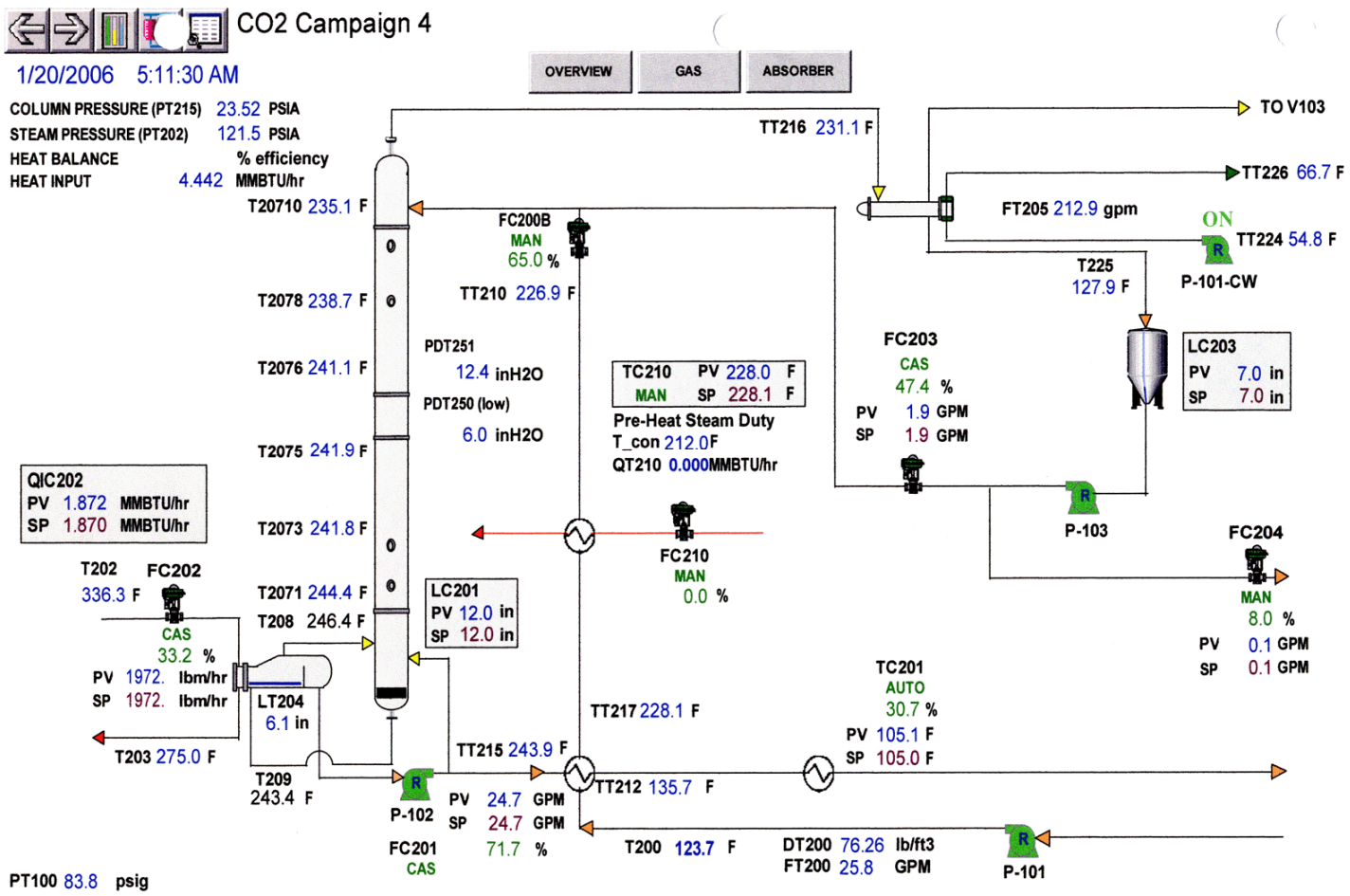

Figure C-4. Campaign 4 DeltaV Stripper Side Process View

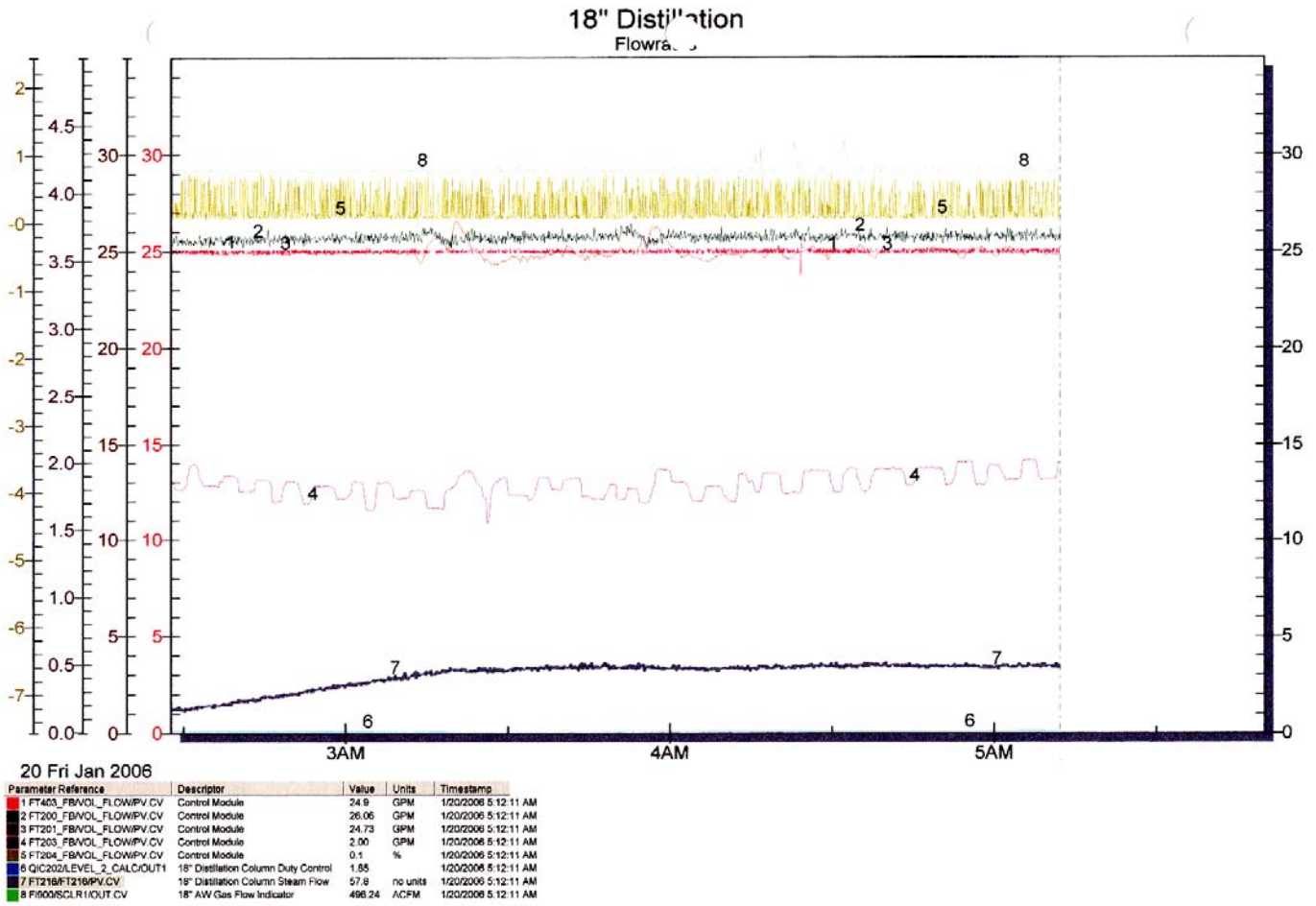

Figure C-5. Campaign 4 DeltaV Gas and Liquid Flow Rate History View

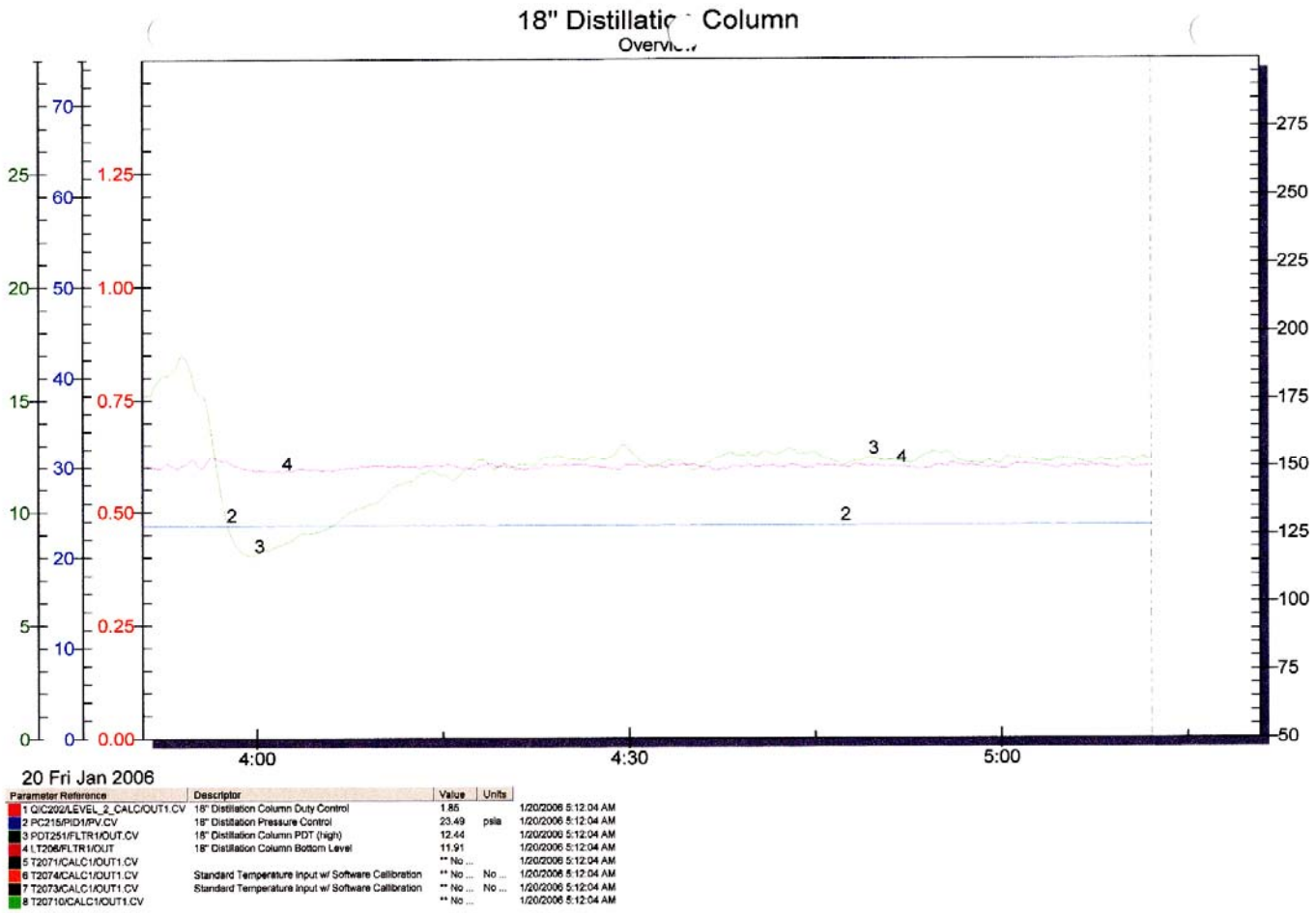

Figure C-6. Campaign 4 DeltaV Stripper Process Instrumentation History View

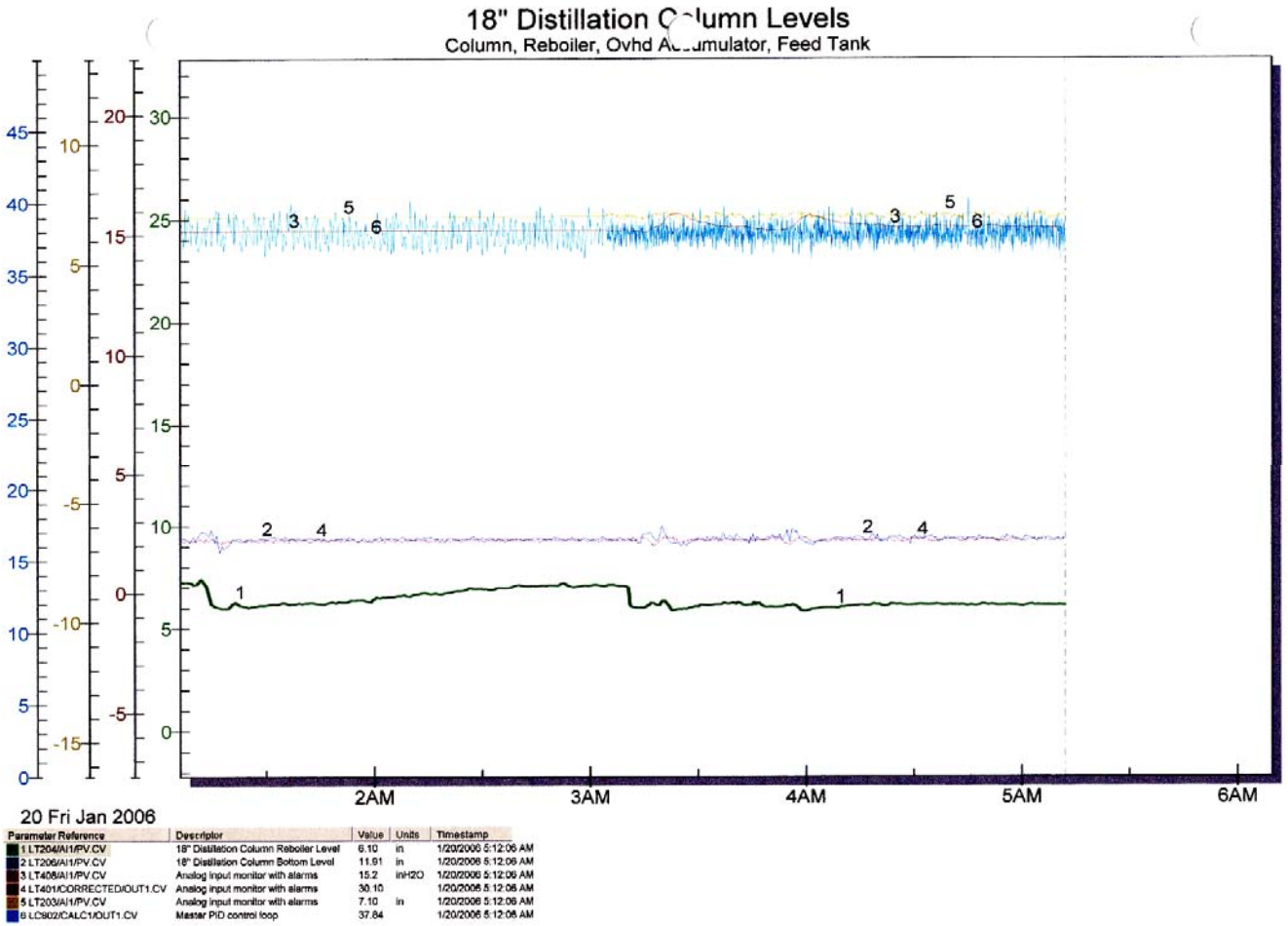

Figure C-7. Campaign 4 DeltaV Stripper Level and Pressure History View

Appendix D: Physical and Transport Property Data Used for DRS Regression

The kinematic viscosity measured by Cullinane (2005) was converted to dynamic viscosity using the values predicted by the density correlation:

$$\rho = 1.130 + 0.0537\left[K^+\right] - 1.204\times10^{-3}\left[K^+\right]^2 + 1.882\times10^{-3}\left[PZ\right] - 0.442\times10^{-3}T + 9.010\times10^{-3}\alpha \quad \text{(D.1)}$$

where ρ density has units of g/cm^3, [i] is the concentration of the species in molality, T is the temperature in Kelvin, and α is the loading in mol CO_2/(mol K + mol PZ).

D.1 Density Data

Table D-1. Density Data for Aqueous PZ (Cullinane, 2005)

Temp K	[PZ] mole/kg H_2O	ρ_{meas} g/cm^3
298.15	0.5	0.999
298.15	1.0	1.001
298.15	1.5	1.003
298.15	1.8	1.004
313.15	0.5	0.994
313.15	1.0	0.996
313.15	1.5	0.997
313.15	1.8	0.999

Table D-2. Density Data for Aqueous K^+ (Cullinane, 2005)

Temp K	$[K^+]$ mole/kg H_2O	Loading	ρ_{meas} g/cm^3
298.15	1.5	0.950	1.085
298.15	3.0	0.950	1.159
298.15	3.0	0.850	1.154
298.15	6.0	0.500	1.283
298.15	12.0	0.500	1.466
313.15	1.5	0.950	1.087
313.15	3.0	0.950	1.152
313.15	3.0	0.850	1.152
313.15	6.0	0.500	1.275
313.15	12.0	0.500	1.461

Loading = mol CO_2^{tot}/(mol K^+)

Table D-3. Density Data for K^+/PZ Mixtures (Cullinane, 2005)

Temp K	$[K^+]$ mole/kg H_2O	[PZ] mole/kg H_2O	Loading	ρ_{meas} g/cm^3
298.15	1.0	1.0	0.250	1.053
298.15	1.0	1.0	0.500	1.067
298.15	1.0	2.5	0.286	1.065
298.15	2.5	2.5	0.500	1.138
298.15	3.0	0.3	0.455	1.152
298.15	3.0	0.3	0.909	1.163
298.15	3.0	0.9	0.769	1.165
298.15	5.0	2.5	0.667	1.237
313.15	1.0	1.0	0.250	1.047
313.15	1.0	1.0	0.500	1.059
313.15	1.0	2.5	0.143	1.046
313.15	1.0	2.5	0.285	1.057
313.15	2.5	2.5	0.250	1.108
313.15	2.5	2.5	0.500	1.132
313.15	5.0	0.5	0.455	1.228
313.15	5.0	0.5	0.909	1.236
313.15	5.0	2.5	0.667	1.227

Loading = mol CO_2^{tot}/(mol K + mol PZ)

Table D-4. Density Data for K^+/PZ Mixtures (This Work)

Temp K	[K^+] mole/kg H_2O	[PZ] mole/kg H_2O	Loading	ρ_{meas} g/cm^3
314.05	5.0	2.5	0.500	1.231
317.45	5.0	2.5	0.500	1.229
319.25	5.0	2.5	0.500	1.228
322.45	5.0	2.5	0.500	1.227
324.55	5.0	2.5	0.500	1.226
327.15	5.0	2.5	0.500	1.224
329.05	5.0	2.5	0.500	1.223
331.85	5.0	2.5	0.500	1.221
333.75	5.0	2.5	0.500	1.220
313.75	6.4	1.6	0.399	1.268
317.35	6.4	1.6	0.399	1.267
320.15	6.4	1.6	0.399	1.265
322.75	6.4	1.6	0.399	1.263
324.15	6.4	1.6	0.399	1.262
327.15	6.4	1.6	0.399	1.261
328.95	6.4	1.6	0.399	1.260
332.55	6.4	1.6	0.399	1.258
334.05	6.4	1.6	0.399	1.257
313.95	6.4	1.6	0.602	1.274
316.45	6.4	1.6	0.602	1.273
319.05	6.4	1.6	0.602	1.272
321.85	6.4	1.6	0.602	1.270
324.15	6.4	1.6	0.602	1.269
327.05	6.4	1.6	0.602	1.267
328.95	6.4	1.6	0.602	1.266
332.05	6.4	1.6	0.602	1.264
333.75	6.4	1.6	0.602	1.264

Loading = mol CO_2^{tot}/(mol K + 2 mol PZ)

Table D-5. Density Data for K_2CO_3-H_2O (kg/m³), (Aseyev and Zaytsev, 1996)

K_2CO_3	x-K_2CO_3	Temperature (°C)											
wt%	Mole	25	30	35	40	45	50	55	60	65	70	75	80
2	0.002653	1013.4	1011.7	1009.9	1008.0	1005.9	1003.6	1001.3	998.8	996.1	993.4	990.5	987.7
4	0.005402	1031.2	1029.4	1027.4	1025.4	1023.2	1020.8	1018.4	1015.8	1013.2	1010.4	1007.6	1004.8
6	0.008251	1049.4	1047.4	1045.4	1043.2	1040.9	1038.5	1036.0	1033.4	1030.7	1028.0	1025.2	1022.4
8	0.011207	1068.0	1065.9	1063.7	1061.5	1059.1	1056.7	1054.1	1051.5	1048.8	1046.0	1043.3	1040.5
10	0.014276	1086.9	1084.7	1082.5	1080.2	1077.7	1075.2	1072.6	1070.0	1067.2	1064.5	1061.7	1058.9
12	0.017464	1106.1	1103.9	1101.5	1099.1	1096.7	1094.1	1091.5	1088.8	1086.1	1083.3	1080.5	1077.7
14	0.020778	1125.7	1123.3	1120.9	1118.5	1116.0	1113.4	1110.7	1108.0	1105.3	1102.5	1099.7	1096.9
16	0.024226	1145.6	1143.2	1140.7	1138.2	1135.6	1133.0	1130.3	1127.6	1124.8	1122.1	1119.3	1116.4
18	0.027816	1165.8	1163.3	1160.8	1158.3	1155.7	1153.0	1150.3	1147.6	1144.8	1142.0	1139.2	1136.4
20	0.031558	1186.4	1183.9	1181.4	1178.8	1176.1	1173.4	1170.7	1167.9	1165.2	1162.3	1159.5	1156.7
22	0.035460	1207.4	1204.8	1202.2	1199.6	1196.9	1194.2	1191.5	1188.7	1185.9	1183.1	1180.2	1177.4
24	0.039534	1228.7	1226.1	1223.5	1220.8	1218.1	1215.4	1212.6	1209.8	1207.0	1204.1	1201.3	1198.4
26	0.043791	1250.3	1247.7	1245.1	1242.4	1239.6	1236.8	1234.0	1231.2	1228.4	1225.6	1222.7	1219.9
28	0.048244	1272.3	1269.6	1267.0	1264.2	1261.5	1258.7	1255.8	1253.0	1250.2	1247.3	1244.5	1241.6
30	0.052907	1294.6	1291.9	1289.2	1286.4	1283.6	1280.8	1278.0	1275.2	1272.3	1269.5	1266.6	1263.8
32	0.057794	1317.3	1314.5	1311.8	1309.0	1306.2	1303.3	1300.5	1297.7	1294.8	1292.0	1289.1	1286.3
34	0.062922	1340.2	1337.5	1334.7	1331.9	1329.1	1326.2	1323.4	1320.5	1317.7	1314.8	1312.0	1309.1
36	0.068311	1363.5	1360.8	1358.0	1355.1	1352.3	1349.4	1346.6	1343.7	1340.9	1338.0	1335.1	1332.3
38	0.073979	1387.2	1384.4	1381.6	1378.7	1375.9	1373.0	1370.2	1367.3	1364.4	1361.6	1358.7	1355.8
40	0.079949	1411.2	1408.4	1405.5	1402.7	1399.8	1396.9	1394.1	1391.2	1388.3	1385.4	1382.5	1379.6
42	0.086247	1435.6	1432.7	1429.9	1427.0	1424.1	1421.3	1418.4	1415.5	1412.6	1409.7	1406.8	1403.9
44	0.092900	1460.4	1457.5	1454.6	1451.8	1448.9	1446.0	1443.2	1440.3	1437.4	1434.4	1431.5	1428.6
46	0.099938	1485.6	1482.7	1479.8	1477.0	1474.1	1471.2	1468.3	1465.4	1462.5	1459.6	1456.6	1453.7
48	0.107397	1511.2	1508.3	1505.4	1502.5	1499.6	1496.7	1493.9	1491.0	1488.0	1485.1	1482.1	1479.1
50	0.115314	1537.0	1534.1	1531.2	1528.3	1525.5	1522.6	1519.7	1516.8	1513.8	1510.9	1507.9	1504.9

Table D-6. Density Data for $KHCO_3$-H_2O (kg/m^3), (Aseyev and Zaytsev, 1996)

$KHCO_3$	x-$KHCO_3$	Temperature (°C)											
wt%	mole	25	30	35	40	45	50	55	60	65	70	75	80
2	0.003659	1011.5	1009.5	1007.4	1005.4	1002.9	1000.5	998.1	995.6	992.8	990.0	987.2	984.4
4	0.007441	1027.9	1025.6	1023.2	1020.9	1018.3	1015.7	1013.1	1010.5	1007.6	1004.7	1001.8	998.9
6	0.011355	1043.9	1041.4	1038.8	1036.2	1033.5	1030.8	1028.1	1025.3	1022.4	1019.4	1016.4	1013.4
8	0.015405	1059.5	1056.8	1054.1	1051.4	1048.5	1045.7	1042.9	1040.1	1037.0	1033.9	1030.8	1027.8
10	0.019601	1075.1	1072.2	1069.4	1066.5	1063.6	1060.6	1057.7	1054.8	1051.6	1048.4	1045.3	1042.1
12	0.023949	1090.3	1087.3	1084.4	1081.4	1078.4	1075.4	1072.4	1069.4	1066.1	1062.9	1059.6	1056.4
14	0.028458	1105.4	1102.4	1099.4	1096.3	1093.2	1090.1	1087.0	1084.0	1080.6	1077.3	1074.0	1070.6
16	0.033137	1120.5	1117.4	1114.3	1111.2	1108.0	1104.9	1101.7	1098.5	1095.1	1091.7	1088.3	1084.9
18	0.037997	1135.5	1132.3	1129.2	1126.0	1122.8	1119.6	1116.4	1113.1	1109.6	1106.1	1102.7	1099.2
20	0.043047	1150.4	1147.3	1144.1	1140.9	1137.6	1134.3	1131.0	1127.7	1124.1	1120.6	1117.0	1113.4
22	0.048299	1165.5	1162.3	1159.0	1155.8	1152.4	1149.1	1145.7	1142.4	1138.7	1135.1	1131.4	1127.8
24	0.053766	1180.6	1177.3	1174.0	1170.7	1167.3	1163.9	1160.4	1157.0	1153.3	1149.6	1145.9	1142.1
26	0.059461	1195.5	1192.5	1189.1	1185.8	1182.3	1178.8	1175.3	1171.8	1168.0	1164.2	1160.4	1156.6
28	0.065398	-	-	1204.4	1200.9	1197.3	1193.7	1190.2	1186.6	1182.7	1178.8	1174.9	1171.1
30	0.071594	-	-	-	1216.1	1212.4	1208.7	1205.0	1201.4	1197.4	1193.5	1189.5	1185.5

D.2 VISCOSITY DATA

Table D-7. Viscosity Data for Aqueous PZ (cP), (Cullinane, 2005)

x-PZ	x-H_2O	Temperature (°C)			
mole	mole	25	40	60	70
0.008927	0.991073	1.09	0.78	0.54	0.45
0.017696	0.982304	1.28	0.91	0.60	0.51
0.026311	0.973689	1.52	1.03	0.68	0.57
0.031409	0.968591	1.66	1.13	0.73	0.60

Table D-8. Viscosity Data for K^+/PZ Mixtures (cP), (Cullinane, 2005)

x-K_2CO_3	x-PZ	x-CO_2	x-H_2O	Temperature (°C)			
mole	mole	mole	mole	25	40	60	70
0.025637	0	0.025637	0.948726	1.32	-	-	-
0.043097	0	0	0.956903	1.90	-	-	-
0.004405	0.017618	0	0.977977	1.39	0.66	-	-
0.004385	0.017541	0.004403	0.973671	1.39	0.65	-	-
0.008546	0.034183	0.008546	0.948726	2.11	1.41	0.91	0.74
0.00877	0.017541	0	0.973689	1.48	1.06	0.71	0.59
0.008694	0.017388	0.008694	0.965223	1.48	-	0.71	-
0.008619	0.034477	0	0.956903	2.13	1.42	0.9	0.73
0.017388	0.017388	0	0.965223	1.74	1.23	0.83	0.69
0.017091	0.017091	0.017091	0.948726	1.70	1.22	0.82	0.69
0.016804	0.033608	0.016804	0.932784	2.40	1.64	1.05	0.87
0.025858	0.017239	0	0.956903	-	1.43	-	0.8
0.028704	0.057408	0.028704	0.885184	4.90	3.12	1.87	1.49
0.032515	0.032515	0.032515	0.902454	3.12	2.14	1.38	1.13
0.039677	0.039677	0.039677	0.88097	4.15	2.77	1.75	1.42

Table D-9. Viscosity Data for K_2CO_3-H_2O (kg/m³), (Aseyev and Zaytsev, 1996)

K_2CO_3	x-K_2CO_3	Temperature (°C)											
wt%	mole	25	30	35	40	45	50	55	60	65	70	75	80
2	0.002653	0.928	0.839	0.763	0.701	0.647	0.599	0.533	0.509	0.467	0.432	0.404	0.377
4	0.005402	0.974	0.881	0.804	0.738	0.680	0.629	0.582	0.539	0.498	0.461	0.428	0.400
6	0.008251	1.014	0.924	0.848	0.780	0.718	0.662	0.613	0.569	0.528	0.489	0.454	0.424
8	0.011207	1.053	0.969	0.894	0.825	0.760	0.700	0.647	0.600	0.558	0.519	0.482	0.450
10	0.014276	1.104	1.012	0.934	0.864	0.799	0.737	0.682	0.632	0.588	0.547	0.510	0.477
12	0.017464	1.160	1.059	0.977	0.906	0.840	0.778	0.721	0.670	0.622	0.579	0.539	0.505
14	0.020778	1.228	1.115	1.026	0.953	0.886	0.823	0.765	0.711	0.660	0.614	0.573	0.537
16	0.024226	1.289	1.183	1.093	1.014	0.943	0.877	0.815	0.757	0.704	0.655	0.610	0.571
18	0.027816	1.376	1.269	1.172	1.086	1.010	0.939	0.872	0.811	0.755	0.704	0.656	0.612
20	0.031558	1.481	1.369	1.265	1.172	1.089	1.012	0.940	0.875	0.816	0.762	0.710	0.662
22	0.035460	1.613	1.485	1.370	1.269	1.179	1.097	1.020	0.949	0.884	0.824	0.769	0.718
24	0.039534	1.758	1.613	1.486	1.376	1.278	1.189	1.106	1.028	0.956	0.891	0.831	0.777
26	0.043791	1.906	1.748	1.612	1.493	1.387	1.291	1.202	1.118	1.038	0.966	0.900	0.842
28	0.048244	2.063	1.893	1.746	1.618	1.503	1.399	1.302	1.212	1.127	1.050	0.980	0.916
30	0.052907	2.230	2.050	1.893	1.755	1.630	1.516	1.411	1.313	1.333	1.136	1.057	0.988
32	0.057794	2.415	2.228	2.059	1.908	1.771	1.649	1.537	1.432	1.329	1.227	1.134	1.056
34	0.062922	2.611	2.412	2.232	2.071	1.924	1.784	1.653	1.537	1.43	1.323	1.219	1.135
36	0.068311	2.828	2.613	2.419	2.247	2.087	1.930	1.782	1.654	1.544	1.438	1.333	1.242
38	0.073979	3.072	2.832	2.619	2.431	2.257	2.085	1.920	1.781	1.668	1.565	1.463	1.368
40	0.079949	3.391	3.094	2.847	2.639	2.453	2.277	2.111	1.961	1.829	1.712	1.604	1.503
42	0.086247	3.861	3.450	3.138	2.895	2.686	2.495	2.317	2.151	2.001	1.871	1.755	1.648
44	0.092900	4.593	3.983	3.553	3.239	2.985	2.764	2.564	2.378	2.208	2.058	1.927	1.818
46	0.099938	5.642	4.751	4.133	3.701	3.367	3.089	2.849	2.638	2.449	2.277	2.120	1.981

Table D-10. Density Data for $KHCO_3$-H_2O (kg/m^3), (Aseyev and Zaytsev, 1996)

$KHCO_3$	x-$KHCO_3$	Temperature (°C)											
wt%	mole	25	30	35	40	45	50	55	60	65	70	75	80
2	0.003659	0.932	0.832	0.750	0.681	0.622	0.571	0.528	0.490	0.457	0.429	0.404	0.383
4	0.007441	0.970	0.867	0.784	0.713	0.652	0.598	0.550	0.509	0.473	0.443	0.417	0.396
6	0.011355	1.008	0.902	0.815	0.740	0.676	0.620	0.571	0.530	0.494	0.463	0.436	0.412
8	0.015405	1.047	0.941	0.851	0.772	0.702	0.643	0.594	0.552	0.517	0.486	0.459	0.434
10	0.019601	1.084	0.980	0.889	0.807	0.734	0.672	0.620	0.576	0.539	0.508	0.484	0.463
12	0.023949	1.123	1.021	0.927	0.842	0.767	0.702	0.647	0.601	0.563	0.533	0.508	0.488
14	0.028458	1.162	1.058	0.963	0.877	0.802	0.736	0.679	0.631	0.592	0.561	0.535	0.513
16	0.033137	1.202	1.097	1.000	0.914	0.838	0.771	0.712	0.663	0.623	0.590	0.562	0.537
18	0.037997	1.241	1.136	1.040	0.954	0.877	0.809	0.749	0.698	0.655	0.620	0.588	0.559
20	0.043047	1.282	1.178	1.084	0.998	0.920	0.849	0.787	0.733	0.687	0.649	0.615	0.583
22	0.048299	1.324	1.219	1.124	1.039	0.962	0.891	0.827	0.770	0.721	0.679	0.643	0.611
24	0.053766	1.366	1.260	1.165	1.081	1.005	0.935	0.870	0.810	0.758	0.713	0.674	0.640
26	0.059461	1.409	1.300	1.206	1.123	1.049	0.980	0.914	0.853	0.799	0.750	0.708	0.670
28	0.065398	-	-	1.247	1.168	1.096	1.028	0.961	0.898	0.841	0.790	0.743	0.700
30	0.071594	-	-	-	1.211	1.143	1.076	1.007	0.942	0.884	0.830	0.779	0.730

Appendix E: Aspen Plus® DRS Regression Results

Data for the Aspen Plus® Data Regression System was inputted as mole fractions for each the components. The apparent component concentration approach was used for the regression analysis. The conversion factor that was used for water was 55.5093 mole H_2O/kg H_2O. Final model parameters were selected based on the smallest residual root mean square error value that could be obtained through the regression analysis. Also, the degree of correlation between any two parameters was evaluated by observing the values for the off-diagonal elements of the matrix in the Regression Results| Correlations sheet. For parameters that are independent, the correlation coefficient is zero, whereas 1 or -1 means a high degree correlation. However, asymmetric binary parameters for activity coefficient models are highly correlated, where both the *ij* and *ji* parameters are needed to fit the data (Aspen Technology Inc., 2006).

E.1 Density Results

The DRS results of the simultaneous density regression analysis for the K_2CO_3-H_2O, $KHCO_3$-H_2O, and PZ-H_2O systems are shown in this section. The correlation matrix of the regressed parameters for density is shown in Table E-1. The matrix shows that there is a high degree of correlation of between 4 sets of parameters, which are in bold and italicized. However, removal of these parameters in resulted higher residual errors and the parameters were not removed.

Table E-1. Parameter Correlation Matrix of Liquid Density for the K_2CO_3-PZ-H_2O-CO_2 System

Parameter	1	2	3	4	5	6	7	8	9	10	11	12	13	14
1	1.00													
2	-0.84	1.00												
3	0.16	-0.13	1.00											
4	0.03	-0.03	-0.55	1.00										
5	-0.04	0.03	0.53	***-0.99***	1.00									
6	-0.23	0.19	-0.62	0.00	0.01	1.00								
7	-0.64	0.53	-0.12	0.00	0.01	0.19	1.00							
8	0.44	-0.36	0.10	-0.01	0.01	-0.18	***-0.92***	1.00						
9	0.56	-0.47	0.07	0.02	-0.02	-0.08	-0.64	0.40	1.00					
10	-0.54	0.45	-0.08	-0.01	0.02	0.10	0.72	-0.56	***-0.97***	1.00				
11	0.02	-0.02	0.07	-0.16	0.17	-0.02	-0.02	0.01	0.00	0.00	1.00			
12	-0.03	0.02	-0.07	0.16	-0.18	0.02	0.02	-0.01	0.00	0.00	***-0.99***	1.00		
13	-0.65	0.54	-0.49	0.26	-0.23	0.08	0.38	-0.20	-0.42	0.38	-0.05	0.05	1.00	
14	0.22	-0.19	-0.43	0.14	-0.21	0.37	-0.12	0.06	0.14	-0.13	-0.01	0.01	-0.22	1.00

A plot of the estimated and experimental values of density for the K_2CO_3-H_2O system is shown in Figure E-1. The average absolute deviation was 0.07% and the root mean square error was 0.09%. The figure shows that the density of potassium carbonate was well predicted by the regressed parameters over the range of 2–50 wt% K_2CO_3 and from 25 to 80 °C.

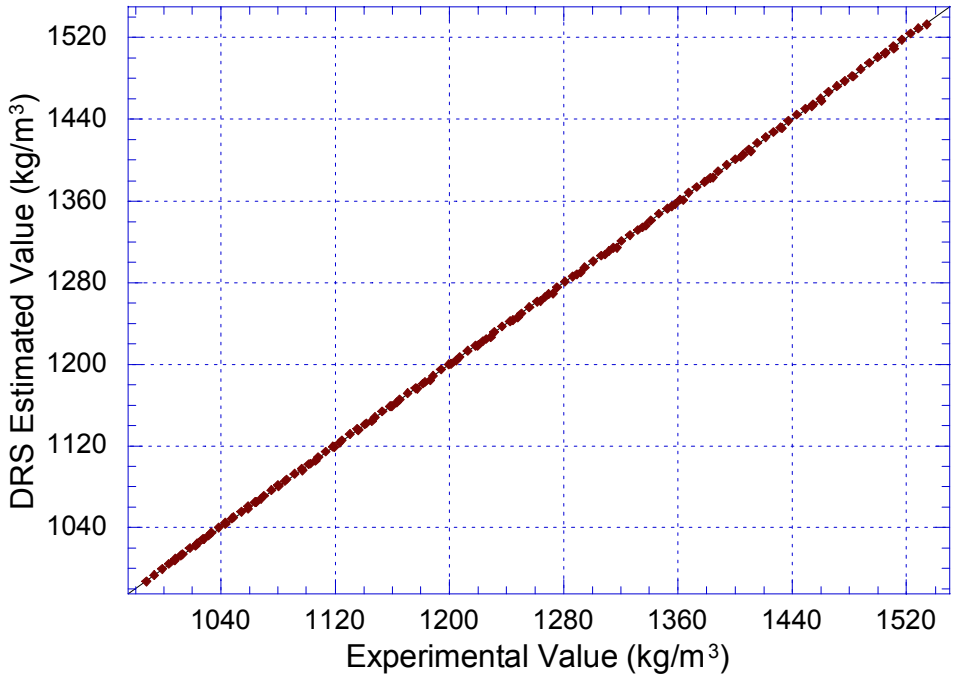

Figure E-1. DRS Results for Density of K_2CO_3-H_2O System

A plot of the estimated and experimental values of density for the $KHCO_3$-H_2O system is shown in Figure E-2. The average absolute deviation was 0.14% and the root mean square error was 0.18%. The figure shows that the density of potassium bicarbonate was well correlated with the regressed parameters over the range of 2–30 wt% $KHCO_3$ and from 25 to 80 °C. However, the plot shows that there was a slight systematic deviation within each set of data points. Within each data set, the predictions of density at the lower temperatures appeared to be systematically off.

A plot of the estimated and experimental values of density for the PZ-H_2O system is shown in Figure E-3. The average absolute deviation was 0.10% and the root mean square error was 0.11%. The figure shows that the density of piperazine was well correlated with the regressed parameters over the range of 0.5–1.8 molal piperazine and from 25 to 40 °C.

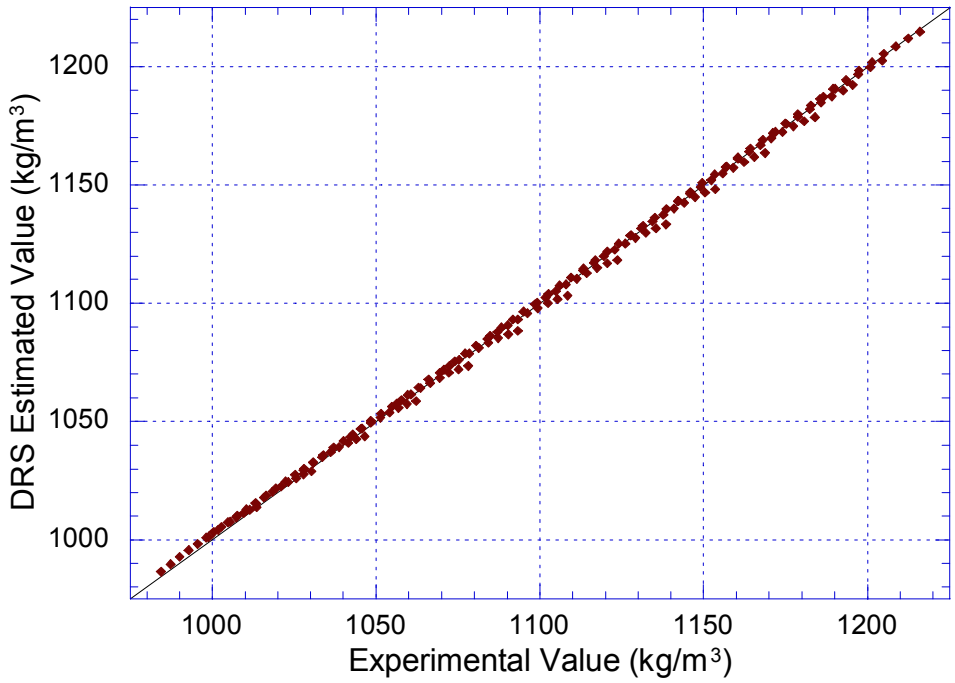

Figure E-2. DRS Results for Density of $KHCO_3$-H_2O System

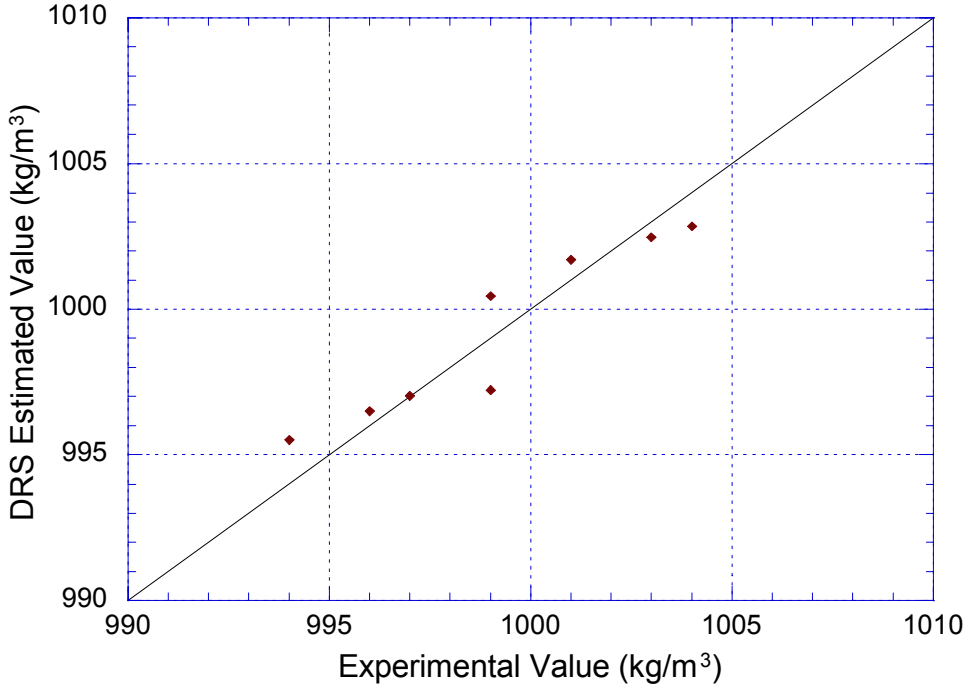

Figure E-3. DRS Results for Density of PZ-H_2O System

E.2 VISCOSITY RESULTS

The DRS results of the simultaneous viscosity regression analysis for the K_2CO_3-H_2O, $KHCO_3$-H_2O, and PZ-H_2O systems are presented. The correlation matrix of the regressed parameters for viscosity is shown in Table E-2. The matrix shows that there is a high degree of correlation of between the four binary interaction parameters for the Andrade equation, which is expected per the Aspen Plus® help file.

Table E-2. Parameter Correlation Matrix of Liquid Viscosity for the K_2CO_3-PZ-H_2O-CO_2 System

Parameter	1	2	3	4	5	6	7	8	9	10
1	1.00									
2	-0.09	1.00								
3	0.00	-0.02	1.00							
4	0.18	-0.11	0.00	1.00						
5	-0.58	-0.38	-0.01	0.18	1.00					
6	-0.10	0.06	-0.01	-0.59	-0.10	1.00				
7	0.08	-0.06	0.00	-0.02	-0.10	0.01	1.00			
8	-0.10	0.07	0.00	-0.01	0.07	0.01	***-1.00***	1.00		
9	-0.09	0.07	0.00	-0.01	0.08	0.01	***-0.96***	***0.96***	1.00	
10	0.10	-0.07	0.00	0.02	-0.06	-0.01	***0.95***	***-0.96***	***-1.00***	1.00

The DRS results for the regression of K_2CO_3-H_2O viscosity is plotted in Figure E-4. The average absolute deviation was 2.68% and the root mean square error was 3.98%. The figure shows that the viscosity of potassium carbonate was well predicted by the regressed parameters over the range of 2–50 wt% K_2CO_3 and from 25 to 80 °C up to a value of 3.2 cP. At high viscosities, which were typically at low temperatures and high K_2CO_3 concentrations, the viscosities were under predicted by up to 20%.

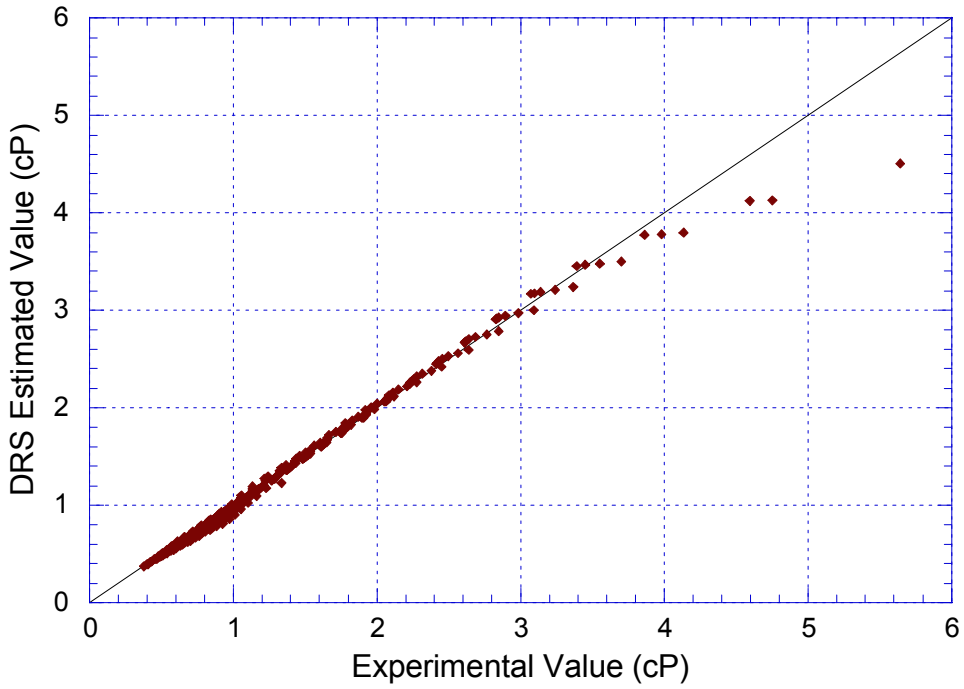

Figure E-4. DRS Results for Viscosity of K_2CO_3-H_2O System

The DRS results for the regression of $KHCO_3$-H_2O viscosity is presented in Figure E-5. The average absolute deviation was 4.89% and the root mean square error was 5.89%. The figure shows that the viscosity of potassium bicarbonate was not as well predicted by the regressed parameters over the range of 2–30wt% K_2CO_3 and from 25 to 80 °C. The predicted liquid viscosity was reasonable up to 0.65 cP. At higher viscosities, a difference of 5–15% was consistently observed between the experimental and regressed data.

Figure E-6 shows that the DRS parameters consistently under predict the viscosity of the PZ-H_2O system. The average absolute deviation of the regressed values was 5.32% and the root mean square error was 5.72%. The viscosity parameters were regressed using data for 0.5–1.8 molal piperazine from 25 to 70 °C. Predicted values of piperazine viscosity should reasonable over the same range of conditions.

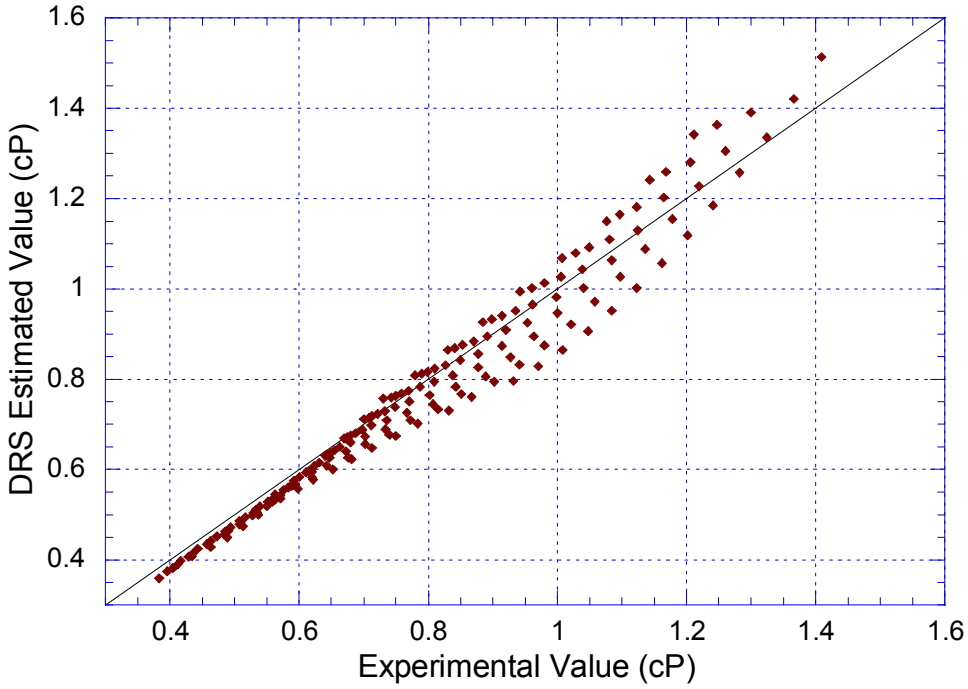

Figure E-5. DRS Results for Viscosity of $KHCO_3$-H_2O System

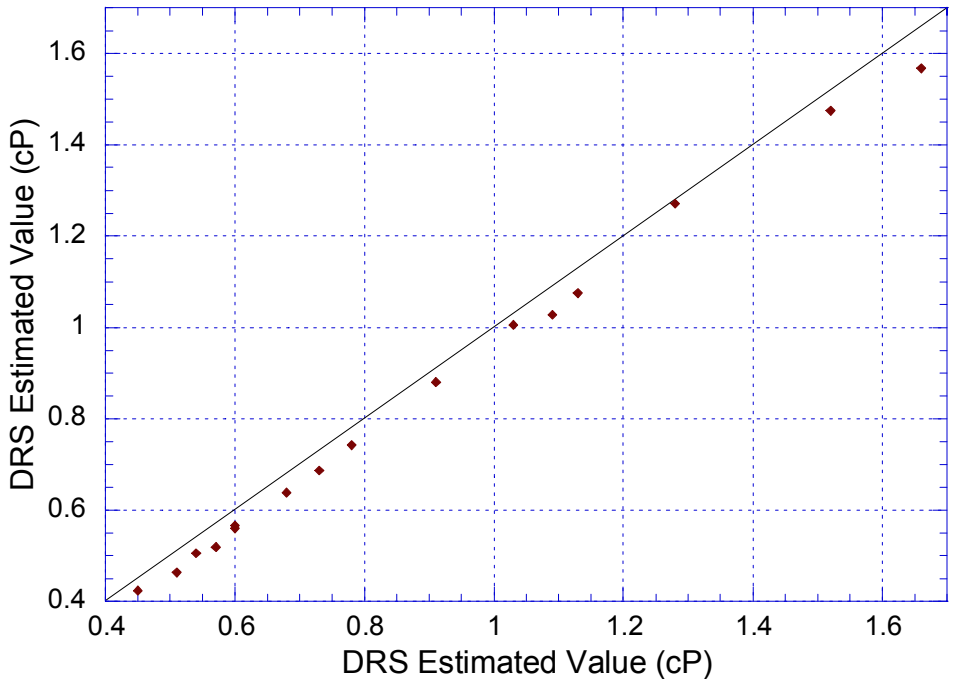

Figure E-6. DRS Results for Viscosity of PZ-H_2O System

Appendix F:Aspen Plus® Data-Fit Regression Results – Campaign 2

Table F-1. Run 2.2 Data-Fit Results

Vary No.	Initial Value	Est Value	Stnd Dev	95% Conf Int Low Limit	95% Conf Int Up Limit
1	0.26	0.26	0.13	0.10	0.52
2	40079	40079	17427	5923	50000

	Var Name	Units	Meas Val	Est Val	Meas σ	Est σ	Norm Residue
1	GN2IN	MOL/HR	29174				
2	GH2OIN	MOL/HR	5745				
3	GCO2IN	MOL/HR	4095	4080	205	193	-0.075
4	GCO2OT	MOL/HR	1854	1862	93	92	0.083
5	LK2CO3	MOL/HR	3301				
6	LPZ	MOL/HR	2835				
7	LH2O	MOL/HR	80026				
8	LCO2IN	MOL/HR	1598	1237	479.4	180	-0.753
9	TGIN	C	54.42				
10	TLIN	C	41.21	41.24	2.06	2.06	0.013
11	T4077	C	58.87	55.65	5.89	5.48	-0.546
12	T4076	C	53.13	53.09	5.31	3.39	-0.007
13	T4075	C	51.64	50.99	7.75	4.37	-0.084
14	T4073	C	50.02	50.23	7.50	4.05	0.028
15	TLOUT	C	50.51	54.91	2.53	0.84	1.742
16	RHLDG			0.551			
17	LCO2RH	MOL/HR		6755			
18	LNLDG			0.370			
19	AVELIQ	SQM		0.00052			
20	AVEGAS	CUM/SEC		0.277			
21	AREA	SQM		1.90			
22	AVAREA	SQM	29174				

Table F-2. Run 2.3 Data-Fit Results

Vary No.	Initial Value	Est Value	Stnd Dev	95% Conf Int Low Limit	95% Conf Int Up Limit
1	0.36	0.36	0.37	0.10	1.09
2	17058	17058	30841	5000	50000

	Var Name	Units	Meas Val	Est Val	Meas σ	Est σ	Norm Residue
1	GN2IN	MOL/HR	23689				
2	GH2OIN	MOL/HR	2927				
3	GCO2IN	MOL/HR	3069	3018	460	398	-0.111
4	GCO2OT	MOL/HR	1076	1088	215	208	0.056
5	LK2CO3	MOL/HR	3724				
6	LPZ	MOL/HR	3198				
7	LH2O	MOL/HR	90288				
8	LCO2IN	MOL/HR	2124	1948	637.2	350	-0.276
9	TGIN	C	46.23				
10	TLIN	C	40.73	40.85	8.15	8.14	0.015
11	T4077	C	61.97	61.07	9.30	8.97	-0.096
12	T4076	C	56.74	57.21	8.51	3.81	0.055
13	T4075	C	54.76	53.58	8.21	4.85	-0.144
14	T4073	C	51.4	50.82	7.71	5.02	-0.075
15	TLOUT	C	44.74	47.52	6.71	2.24	0.414
16	RHLDG			0.549			
17	LCO2RH	MOL/HR		7602			
18	LNLDG			0.410			
19	AVELIQ	SQM		0.00059			
20	AVEGAS	CUM/SEC		0.225			
21	AREA	SQM		2.64			
22	AVAREA	SQM	23689				

Table F-3. Run 2.4 Data-Fit Results

Vary No.	Initial Value	Est Value	Stnd Dev	95% Conf Int Low Limit	95% Conf Int Up Limit
1	0.46	0.46	0.18	0.11	0.81
2	29000	29000	12169	5149	50000

	Var Name	Units	Meas Val	Est Val	Meas σ	Est σ	Norm Residue
1	GN2IN	MOL/HR	23707				
2	GH2OIN	MOL/HR	2832				
3	GCO2IN	MOL/HR	3223	3225	161	155	0.016
4	GCO2OT	MOL/HR	956	955	48	48	-0.012
5	LK2CO3	MOL/HR	4550				
6	LPZ	MOL/HR	3907				
7	LH2O	MOL/HR	110299				
8	LCO2IN	MOL/HR	2734	2486	546.8	143	-0.453
9	TGIN	C	45.62				
10	TLIN	C	40.6	40.67	2.03	2.03	0.036
11	T4077	C	62.54	61.11	6.25	6.09	-0.229
12	T4076	C	58.32	58.27	5.83	2.06	-0.008
13	T4075	C	56.65	54.32	5.67	2.76	-0.412
14	T4073	C	54.31	51.10	5.43	3.00	-0.591
15	TLOUT	C	44.59	46.39	2.23	1.41	0.805
16	RHLDG			0.550			
17	LCO2RH	MOL/HR		9306			
18	LNLDG			0.416			
19	AVELIQ	SQM		0.00073			
20	AVEGAS	CUM/SEC		0.226			
21	AREA	SQM		3.36			
22	AVAREA	SQM	23707				

Table F-4. Run 2.5 Data-Fit Results

Vary No.	Initial Value	Est Value	Stnd Dev	95% Conf Int Low Limit	95% Conf Int Up Limit
1	0.54	0.54	0.18	0.18	0.90
2	30250	30250	10890	8906	50000

	Var Name	Units	Meas Val	Est Val	Meas σ	Est σ	Norm Residue
1	GN2IN	MOL/HR	23950				
2	GH2OIN	MOL/HR	2996				
3	GCO2IN	MOL/HR	2863	2875	143	139	0.082
4	GCO2OT	MOL/HR	713	712	36	36	-0.042
5	LK2CO3	MOL/HR	4536				
6	LPZ	MOL/HR	3895				
7	LH2O	MOL/HR	109956				
8	LCO2IN	MOL/HR	2721	2543	544.2	126	-0.326
9	TGIN	C	46.72				
10	TLIN	C	40.55	40.65	2.03	2.03	0.047
11	T4077	C	62.16	60.46	6.22	6.09	-0.274
12	T4076	C	58.36	57.77	5.84	1.87	-0.101
13	T4075	C	56.92	53.76	5.69	2.61	-0.555
14	T4073	C	54.5	50.47	5.45	2.96	-0.739
15	TLOUT	C	44.61	46.84	2.23	1.49	1.000
16	RHLDG			0.548			
17	LCO2RH	MOL/HR		9246			
18	LNLDG			0.420			
19	AVELIQ	SQM		0.00072			
20	AVEGAS	CUM/SEC		0.224			
21	AREA	SQM		4.01			
22	AVAREA	SQM	23950				

Table F-5. Run 2.6 Data-Fit Results

Vary No.	Initial Value	Est Value	Stnd Dev	95% Conf Int Low Limit	95% Conf Int Up Limit
1	0.79	0.79	0.17	0.45	1.13
2	38399	38349	7122	24389	50000

	Var Name	Units	Meas Val	Est Val	Meas σ	Est σ	Norm Residue
1	GN2IN	MOL/HR	24017				
2	GH2OIN	MOL/HR	3071				
3	GCO2IN	MOL/HR	2797	2825	140	135	0.200
4	GCO2OT	MOL/HR	491	490	25	25	-0.035
5	LK2CO3	MOL/HR	5179				
6	LPZ	MOL/HR	4447				
7	LH2O	MOL/HR	125556				
8	LCO2IN	MOL/HR	2997	3034	599.4	118	0.062
9	TGIN	C	47.18				
10	TLIN	C	41.2	41.38	2.06	2.05	0.087
11	T4077	C	59.29	58.92	5.93	5.92	-0.062
12	T4076	C	59.12	58.66	5.91	2.24	-0.078
13	T4075	C	58.2	54.58	5.82	2.64	-0.621
14	T4073	C	54.31	51.21	5.43	2.79	-0.571
15	TLOUT	C	44.59	46.95	2.23	1.45	1.058
16	RHLDG			0.548			
17	LCO2RH	MOL/HR		10548			
18	LNLDG			0.427			
19	AVELIQ	SQM		0.00083			
20	AVEGAS	CUM/SEC		0.223			
21	AREA	SQM		5.78			
22	AVAREA	SQM	24017				

Table F-6. Run 2.7 Data-Fit Results

Vary No.	Initial Value	Est Value	Stnd Dev	95% Conf Int Low Limit	95% Conf Int Up Limit
1	0.67	0.67	0.18	0.32	1.02
2	35000	35000	8004	19313	50000

	Var Name	Units	Meas Val	Est Val	Meas σ	Est σ	Norm Residue
1	GN2IN	MOL/HR	23607				
2	GH2OIN	MOL/HR	3211				
3	GCO2IN	MOL/HR	2954	2944	148	145	-0.066
4	GCO2OT	MOL/HR	561	561	28	28	0.012
5	LK2CO3	MOL/HR	5199				
6	LPZ	MOL/HR	4464				
7	LH2O	MOL/HR	126028				
8	LCO2IN	MOL/HR	4240	2984	848	131	-1.481
9	TGIN	C	48.15				
10	TLIN	C	41.27	41.44	2.06	2.06	0.082
11	T4077	C	61.61	61.07	6.16	6.14	-0.087
12	T4076	C	59.99	60.39	6.00	2.30	0.067
13	T4075	C	59.22	56.55	5.92	2.91	-0.451
14	T4073	C	58.52	53.32	5.85	3.12	-0.888
15	TLOUT	C	46.41	48.67	2.32	1.38	0.975
16	RHLDG			0.547			
17	LCO2RH	MOL/HR		10564			
18	LNLDG			0.423			
19	AVELIQ	SQM		0.00083			
20	AVEGAS	CUM/SEC		0.225			
21	AREA	SQM		4.88			
22	AVAREA	SQM	23607				

Table F-7. Run 2.8.1 Data-Fit Results

Vary No.	Initial Value	Est Value	Stnd Dev	95% Conf Int Low Limit	95% Conf Int Up Limit
1	0.45	0.45	0.18	0.10	0.81
2	35553	35553	17102	5000	50000

	Var Name	Units	Meas Val	Est Val	Meas σ	Est σ	Norm Residue
1	GN2IN	MOL/HR	30722				
2	GH2OIN	MOL/HR	4857				
3	GCO2IN	MOL/HR	4071	4098	204	195	0.134
4	GCO2OT	MOL/HR	1383	1378	69	69	-0.076
5	LK2CO3	MOL/HR	5410				
6	LPZ	MOL/HR	4646				
7	LH2O	MOL/HR	131157				
8	LCO2IN	MOL/HR	3031	2874	606.2	187	-0.259
9	TGIN	C	50.83				
10	TLIN	C	41.36	41.43	2.07	2.07	0.033
11	T4077	C	63.23	59.75	6.32	6.06	-0.550
12	T4076	C	59.13	57.29	5.91	2.01	-0.311
13	T4075	C	58.33	53.74	5.83	2.91	-0.788
14	T4073	C	54.74	50.88	5.47	3.50	-0.705
15	TLOUT	C	46.64	50.80	2.33	1.30	1.786
16	RHLDG			0.548			
17	LCO2RH	MOL/HR		11012			
18	LNLDG			0.412			
19	AVELIQ	SQM		0.00086			
20	AVEGAS	CUM/SEC		0.291			
21	AREA	SQM		3.32			
22	AVAREA	SQM	30722				

Table F-8. Run 2.8.2 Data-Fit Results

Vary No.	Initial Value	Est Value	Stnd Dev	95% Conf Int Low Limit	95% Conf Int Up Limit
1	0.47	0.47	0.27	0.10	1.00
2	30460	30460	22130	5000	50000

	Var Name	Units	Meas Val	Est Val	Meas σ	Est σ	Norm Residue
1	GN2IN	MOL/HR	30240				
2	GH2OIN	MOL/HR	5436				
3	GCO2IN	MOL/HR	3902	3894	390	363	-0.021
4	GCO2OT	MOL/HR	1274	1278	127	126	0.029
5	LK2CO3	MOL/HR	5396				
6	LPZ	MOL/HR	4633				
7	LH2O	MOL/HR	130809				
8	LCO2IN	MOL/HR	3327	2891	831.75	318	-0.524
9	TGIN	C	53.18				
10	TLIN	C	41.59	41.62	2.08	2.08	0.015
11	T4077	C	63.36	62.05	6.34	6.22	-0.207
12	T4076	C	59.41	59.22	5.94	3.33	-0.033
13	T4075	C	58.75	56.01	8.81	4.57	-0.311
14	T4073	C	55.58	53.63	8.34	5.14	-0.234
15	TLOUT	C	47.77	53.95	4.78	1.31	1.294
16	RHLDG			0.543			
17	LCO2RH	MOL/HR		10895			
18	LNLDG			0.413			
19	AVELIQ	SQM		0.00086			
20	AVEGAS	CUM/SEC		0.291			
21	AREA	SQM		3.36			
22	AVAREA	SQM	30240				

Table F-9. Run 2.9.1 Data-Fit Results

Vary No.	Initial Value	Est Value	Stnd Dev	95% Conf Int Low Limit	95% Conf Int Up Limit
1	0.45	0.45	0.63	0.10	1.20
2	10300	10300	27350	5000	50000

	Var Name	Units	Meas Val	Est Val	Meas σ	Est σ	Norm Residue
1	GN2IN	MOL/HR	19538				
2	GH2OIN	MOL/HR	1366				
3	GCO2IN	MOL/HR	2482	2487	124	121	0.042
4	GCO2OT	MOL/HR	744	736	149	142	-0.050
5	LK2CO3	MOL/HR	3544				
6	LPZ	MOL/HR	3043				
7	LH2O	MOL/HR	85913				
8	LCO2IN	MOL/HR	1855	1959	463.75	165	0.224
9	TGIN	C	36.16				
10	TLIN	C	40.56	40.55	2.03	2.03	-0.003
11	T4077	C	64.24	64.37	6.42	5.29	0.020
12	T4076	C	58.69	59.47	5.87	4.40	0.133
13	T4075	C	56.39	55.77	8.46	4.14	-0.073
14	T4073	C	53.74	52.91	8.06	3.97	-0.103
15	TLOUT	C	41.84	42.05	4.18	2.25	0.051
16	RHLDG			0.551			
17	LCO2RH	MOL/HR		7255			
18	LNLDG			0.418			
19	AVELIQ	SQM		0.00057			
20	AVEGAS	CUM/SEC		0.189			
21	AREA	SQM		3.33			
22	AVAREA	SQM	19538				

Table F-10. Run 2.9.2 Data-Fit Results

Vary No.	Initial Value	Est Value	Stnd Dev	95% Conf Int Low Limit	95% Conf Int Up Limit
1	0.46	0.46	0.68	0.10	1.20
2	9840	9874	29007	5000	50000

	Var Name	Units	Meas Val	Est Val	Meas σ	Est σ	Norm Residue
1	GN2IN	MOL/HR	19420				
2	GH2OIN	MOL/HR	1464				
3	GCO2IN	MOL/HR	2478	2484	124	121	0.048
4	GCO2OT	MOL/HR	713	705	143	137	-0.058
5	LK2CO3	MOL/HR	3534				
6	LPZ	MOL/HR	3034				
7	LH2O	MOL/HR	85665				
8	LCO2IN	MOL/HR	1818	1922	454.5	159	0.229
9	TGIN	C	37.45				
10	TLIN	C	40.79	40.78	2.04	2.04	-0.003
11	T4077	C	64.84	64.80	6.48	5.24	-0.006
12	T4076	C	59.05	59.75	5.91	4.63	0.119
13	T4075	C	56.68	56.01	8.50	4.17	-0.079
14	T4073	C	54.05	53.14	8.11	3.93	-0.112
15	TLOUT	C	42.34	42.79	4.23	2.16	0.107
16	RHLDG			0.551			
17	LCO2RH	MOL/HR		7235			
18	LNLDG			0.415			
19	AVELIQ	SQM		0.00056			
20	AVEGAS	CUM/SEC		0.189			
21	AREA	SQM		3.38			
22	AVAREA	SQM	19420				

Table F-11. Run 2.10.1 Data-Fit Results

Vary No.	Initial Value	Est Value	Stnd Dev	95% Conf Int Low Limit	95% Conf Int Up Limit
1	0.70	0.70	0.17	0.37	1.03
2	27001	27206	6345	14770	39642

	Var Name	Units	Meas Val	Est Val	Meas σ	Est σ	Norm Residue
1	GN2IN	MOL/HR	18228				
2	GH2OIN	MOL/HR	2378				
3	GCO2IN	MOL/HR	2466	2469	123	121	0.024
4	GCO2OT	MOL/HR	357	357	18	18	-0.002
5	LK2CO3	MOL/HR	4791				
6	LPZ	MOL/HR	4114				
7	LH2O	MOL/HR	116141				
8	LCO2IN	MOL/HR	3448	2822	1724	102	-0.363
9	TGIN	C	47.16				
10	TLIN	C	41.2	41.34	2.06	2.05	0.069
11	T4077	C	52.25	51.92	5.23	5.11	-0.064
12	T4076	C	58.78	60.66	5.88	2.78	0.320
13	T4075	C	58.92	58.03	5.89	2.94	-0.152
14	T4073	C	59.84	55.39	5.98	2.98	-0.743
15	TLOUT	C	48	49.18	2.40	1.44	0.491
16	RHLDG			0.546			
17	LCO2RH	MOL/HR		9724			
18	LNLDG			0.427			
19	AVELIQ	SQM		0.00076			
20	AVEGAS	CUM/SEC		0.174			
21	AREA	SQM		5.14			
22	AVAREA	SQM	18228				

Table F-12. Run 2.10.2 Data-Fit Results

Vary No.	Initial Value	Est Value	Stnd Dev	95% Conf Int Low Limit	95% Conf Int Up Limit
1	0.69	0.69	0.17	0.35	1.03
2	26955	26976	6407	14418	39534

	Var Name	Units	Meas Val	Est Val	Meas σ	Est σ	Norm Residue
1	GN2IN	MOL/HR	18014				
2	GH2OIN	MOL/HR	2489				
3	GCO2IN	MOL/HR	2459	2465	123	120	0.050
4	GCO2OT	MOL/HR	370	370	19	18	-0.007
5	LK2CO3	MOL/HR	4773				
6	LPZ	MOL/HR	4099				
7	LH2O	MOL/HR	115721				
8	LCO2IN	MOL/HR	2881	2817	1440.5	101	-0.044
9	TGIN	C	48.18				
10	TLIN	C	41.3	41.42	2.07	2.05	0.056
11	T4077	C	52.61	52.43	5.26	5.16	-0.034
12	T4076	C	59.19	60.64	5.92	2.61	0.245
13	T4075	C	59.12	57.98	5.91	2.98	-0.193
14	T4073	C	59.94	55.37	5.99	3.10	-0.762
15	TLOUT	C	48.19	49.79	2.41	1.49	0.662
16	RHLDG			0.546			
17	LCO2RH	MOL/HR		9686			
18	LNLDG			0.428			
19	AVELIQ	SQM		0.00076			
20	AVEGAS	CUM/SEC		0.173			
21	AREA	SQM		5.07			
22	AVAREA	SQM	18014				

Table F-13. Run 2.11.1 Data-Fit Results

Vary No.	Initial Value	Est Value	Stnd Dev	95% Conf Int Low Limit	95% Conf Int Up Limit
1	0.83	0.83	0.26	0.32	1.20
2	26100	26100	5797	14737	37463

	Var Name	Units	Meas Val	Est Val	Meas σ	Est σ	Norm Residue
1	GN2IN	MOL/HR	17797				
2	GH2OIN	MOL/HR	2885				
3	GCO2IN	MOL/HR	2305	2313	115	113	0.068
4	GCO2OT	MOL/HR	331	330	17	17	-0.087
5	LK2CO3	MOL/HR	4760				
6	LPZ	MOL/HR	4088				
7	LH2O	MOL/HR	115404				
8	LCO2IN	MOL/HR	3713	2892	742.6	100	-1.105
9	TGIN	C	51.18				
10	TLIN	C	41.39	41.80	2.07	2.05	0.196
11	T4077	C	55.01	54.22	5.50	5.48	-0.143
12	T4076	C	60.57	60.26	6.06	2.90	-0.051
13	T4075	C	60.9	57.44	6.09	3.09	-0.568
14	T4073	C	60.65	54.98	6.07	3.09	-0.935
15	TLOUT	C	48.45	51.64	2.42	1.31	1.317
16	RHLDG			0.544			
17	LCO2RH	MOL/HR		9626			
18	LNLDG			0.432			
19	AVELIQ	SQM		0.00076			
20	AVEGAS	CUM/SEC		0.171			
21	AREA	SQM		5.90			
22	AVAREA	SQM	17797				

Table F-14. Run 2.11.2 Data-Fit Results

Vary No.	Initial Value	Est Value	Stnd Dev	95% Conf Int Low Limit	95% Conf Int Up Limit
1	0.82	0.82	0.26	0.30	1.20
2	25800	25800	5860	14314	37286

	Var Name	Units	Meas Val	Est Val	Meas σ	Est σ	Norm Residue
1	GN2IN	MOL/HR	17673				
2	GH2OIN	MOL/HR	2919				
3	GCO2IN	MOL/HR	2338	2348	117	115	0.082
4	GCO2OT	MOL/HR	357	355	18	18	-0.085
5	LK2CO3	MOL/HR	4784				
6	LPZ	MOL/HR	4108				
7	LH2O	MOL/HR	115984				
8	LCO2IN	MOL/HR	3576	2909	715.2	102	-0.932
9	TGIN	C	51.46				
10	TLIN	C	41.42	41.81	2.07	2.06	0.189
11	T4077	C	56.01	55.28	5.60	5.58	-0.130
12	T4076	C	60.98	60.45	6.10	2.94	-0.087
13	T4075	C	61.24	57.58	6.12	3.09	-0.597
14	T4073	C	60.86	55.15	6.09	3.07	-0.938
15	TLOUT	C	48.56	51.92	2.43	1.32	1.384
16	RHLDG			0.544			
17	LCO2RH	MOL/HR		9677			
18	LNLDG			0.432			
19	AVELIQ	SQM		0.00076			
20	AVEGAS	CUM/SEC		0.170			
21	AREA	SQM		5.82			
22	AVAREA	SQM	17673				

Table F-15. Run 2.13.1 Data-Fit Results

Vary No.	Initial Value	Est Value	Stnd Dev	95% Conf Int Low Limit	95% Conf Int Up Limit
1	0.34	0.34	0.16	0.10	0.66
2	13238	13352	8647	5000	30301

	Var Name	Units	Meas Val	Est Val	Meas σ	Est σ	Norm Residue
1	GN2IN	MOL/HR	19752				
2	GH2OIN	MOL/HR	1184				
3	GCO2IN	MOL/HR	2583	2587	129	126	0.034
4	GCO2OT	MOL/HR	566	566	28	28	0.000
5	LK2CO3	MOL/HR	4168				
6	LPZ	MOL/HR	3579				
7	LH2O	MOL/HR	101043				
8	LCO2IN	MOL/HR	2135	2225	427	177	0.211
9	TGIN	C	33.47				
10	TLIN	C	40.68	40.71	2.03	2.03	0.015
11	T4077	C	64.96	64.16	6.50	6.36	-0.122
12	T4076	C	61.45	64.60	6.15	2.41	0.513
13	T4075	C	61.83	61.83	9.27	3.16	0.000
14	T4073	C	59.02	58.89	5.90	3.49	-0.022
15	TLOUT	C	44.97	44.11	4.50	2.48	-0.191
16	RHLDG			0.543			
17	LCO2RH	MOL/HR		8412			
18	LNLDG			0.412			
19	AVELIQ	SQM		0.00067			
20	AVEGAS	CUM/SEC		0.196			
21	AREA	SQM		2.48			
22	AVAREA	SQM	19752				

Table F-16. Run 2.13.2 Data-Fit Results

Vary No.	Initial Value	Est Value	Stnd Dev	95% Conf Int Low Limit	95% Conf Int Up Limit
1	0.37	0.37	0.17	0.10	0.70
2	18000	18000	6506	5248	30752

	Var Name	Units	Meas Val	Est Val	Meas σ	Est σ	Norm Residue
1	GN2IN	MOL/HR	19797				
2	GH2OIN	MOL/HR	1094				
3	GCO2IN	MOL/HR	2706	2675	135	133	-0.230
4	GCO2OT	MOL/HR	645	647	32	32	0.061
5	LK2CO3	MOL/HR	4161				
6	LPZ	MOL/HR	3573				
7	LH2O	MOL/HR	100868				
8	LCO2IN	MOL/HR	2837	2269	567.4	152	-1.001
9	TGIN	C	32				
10	TLIN	C	40.31	40.32	2.02	2.01	0.005
11	T4077	C	62.47	62.68	6.25	6.19	0.034
12	T4076	C	59.87	62.59	5.99	3.21	0.454
13	T4075	C	60.52	59.35	9.08	3.70	-0.129
14	T4073	C	57.92	56.25	5.79	3.54	-0.288
15	TLOUT	C	44.12	42.08	4.41	1.75	-0.462
16	RHLDG			0.548			
17	LCO2RH	MOL/HR		8469			
18	LNLDG			0.416			
19	AVELIQ	SQM		0.00067			
20	AVEGAS	CUM/SEC		0.193			
21	AREA	SQM		2.80			
22	AVAREA	SQM	19797				

Table F-17. Run 2.14.1 Data-Fit Results

Vary No.	Initial Value	Est Value	Stnd Dev	95% Conf Int Low Limit	95% Conf Int Up Limit
1	0.62	0.62	0.18	0.26	0.98
2	16297	16297	4595	7292	25302

	Var Name	Units	Meas Val	Est Val	Meas σ	Est σ	Norm Residue
1	GN2IN	MOL/HR	22009				
2	GH2OIN	MOL/HR	962				
3	GCO2IN	MOL/HR	1127	1115	56	55	-0.205
4	GCO2OT	MOL/HR	171	171	9	9	0.045
5	LK2CO3	MOL/HR	2069				
6	LPZ	MOL/HR	1777				
7	LH2O	MOL/HR	50170				
8	LCO2IN	MOL/HR	1600	1217	320	55	-1.197
9	TGIN	C	29.3				
10	TLIN	C	43.47	43.50	2.17	2.17	0.014
11	T4077	C	47.96	47.60	4.80	4.43	-0.075
12	T4076	C	44.08	45.28	4.41	1.82	0.273
13	T4075	C	40.15	41.73	4.02	1.79	0.394
14	T4073	C	39.73	38.12	3.97	2.31	-0.405
15	TLOUT	C	30.74	30.55	1.54	1.02	-0.125
16	RHLDG			0.550			
17	LCO2RH	MOL/HR		4229			
18	LNLDG			0.427			
19	AVELIQ	SQM		0.00032			
20	AVEGAS	CUM/SEC		0.174			
21	AREA	SQM		4.52			
22	AVAREA	SQM	22009				

Table F-18. Run 2.14.2 Data-Fit Results

Vary No.	Initial Value	Est Value	Stnd Dev	95% Conf Int Low Limit	95% Conf Int Up Limit
1	0.59	0.59	0.20	0.20	0.97
2	15179	15179	3890	7555	22802

	Var Name	Units	Meas Val	Est Val	Meas σ	Est σ	Norm Residue
1	GN2IN	MOL/HR	22193				
2	GH2OIN	MOL/HR	906				
3	GCO2IN	MOL/HR	1093	1083	55	54	-0.176
4	GCO2OT	MOL/HR	201	202	10	10	0.108
5	LK2CO3	MOL/HR	2083				
6	LPZ	MOL/HR	1789				
7	LH2O	MOL/HR	50507				
8	LCO2IN	MOL/HR	1622	1277	324.4	60	-1.063
9	TGIN	C	28.21				
10	TLIN	C	42.52	42.54	2.13	2.12	0.012
11	T4077	C	46.94	46.51	4.69	4.28	-0.092
12	T4076	C	43.43	44.34	4.34	1.90	0.210
13	T4075	C	39.75	41.09	3.98	1.85	0.338
14	T4073	C	39.54	37.81	3.95	2.33	-0.437
15	TLOUT	C	30.08	29.93	1.50	0.96	-0.096
16	RHLDG			0.548			
17	LCO2RH	MOL/HR		4241			
18	LNLDG			0.434			
19	AVELIQ	SQM		0.00033			
20	AVEGAS	CUM/SEC		0.175			
21	AREA	SQM		4.26			
22	AVAREA	SQM	22193				

Table F-19. Run 2.15 Data-Fit Results

Vary No.	Initial Value	Est Value	Stnd Dev	95% Conf Int Low Limit	95% Conf Int Up Limit
1	0.57	0.57	0.20	0.17	0.97
2	16600	16600	3544	9653	23547

	Var Name	Units	Meas Val	Est Val	Meas σ	Est σ	Norm Residue
1	GN2IN	MOL/HR	21791				
2	GH2OIN	MOL/HR	991				
3	GCO2IN	MOL/HR	1241	1232	62	61	-0.144
4	GCO2OT	MOL/HR	160	160	8	8	0.033
5	LK2CO3	MOL/HR	2514				
6	LPZ	MOL/HR	2158				
7	LH2O	MOL/HR	60935				
8	LCO2IN	MOL/HR	1797	1485	359.4	81	-0.868
9	TGIN	C	29.87				
10	TLIN	C	41.9	41.94	2.10	2.09	0.019
11	T4077	C	51.18	50.97	5.12	4.68	-0.041
12	T4076	C	49.51	50.77	4.95	2.22	0.254
13	T4075	C	47.59	48.39	4.76	2.31	0.169
14	T4073	C	46.31	45.49	4.63	2.70	-0.177
15	TLOUT	C	34.57	34.07	1.73	1.04	-0.292
16	RHLDG			0.543			
17	LCO2RH	MOL/HR		5076			
18	LNLDG			0.428			
19	AVELIQ	SQM		0.00040			
20	AVEGAS	CUM/SEC		0.180			
21	AREA	SQM		4.28			
22	AVAREA	SQM	21791				

Table F-20. Run 2.16 Data-Fit Results

Vary No.	Initial Value	Est Value	Stnd Dev	95% Conf Int Low Limit	95% Conf Int Up Limit
1	0.57	0.57	0.17	0.24	0.90
2	16216	16216	3863	8644	23788

	Var Name	Units	Meas Val	Est Val	Meas σ	Est σ	Norm Residue
1	GN2IN	MOL/HR	21874				
2	GH2OIN	MOL/HR	971				
3	GCO2IN	MOL/HR	1219	1210	61	60	-0.151
4	GCO2OT	MOL/HR	136	136	7	7	0.024
5	LK2CO3	MOL/HR	2448				
6	LPZ	MOL/HR	2102				
7	LH2O	MOL/HR	59353				
8	LCO2IN	MOL/HR	1728	1409	345.6	81	-0.923
9	TGIN	C	29.49				
10	TLIN	C	41.98	42.02	2.10	2.10	0.018
11	T4077	C	50.9	50.56	5.09	4.51	-0.067
12	T4076	C	49.75	50.88	4.98	2.12	0.227
13	T4075	C	48.07	48.92	4.81	1.82	0.177
14	T4073	C	46.71	46.22	4.67	2.36	-0.106
15	TLOUT	C	34.47	34.05	1.72	1.34	-0.243
16	RHLDG			0.542			
17	LCO2RH	MOL/HR		4930			
18	LNLDG			0.424			
19	AVELIQ	SQM		0.00038			
20	AVEGAS	CUM/SEC		0.180			
21	AREA	SQM		4.15			
22	AVAREA	SQM	21874				

Table F-21. Run 2.17.1 Data-Fit Results

Vary No.	Initial Value	Est Value	Stnd Dev	95% Conf Int Low Limit	95% Conf Int Up Limit
1	0.84	0.84	0.18	0.48	1.20
2	22466	22466	4934	12795	32137

	Var Name	Units	Meas Val	Est Val	Meas σ	Est σ	Norm Residue
1	GN2IN	MOL/HR	28172				
2	GH2OIN	MOL/HR	1511				
3	GCO2IN	MOL/HR	1303	1289	195	195	-0.070
4	GCO2OT	MOL/HR	142	151	21	21	0.417
5	LK2CO3	MOL/HR	2284				
6	LPZ	MOL/HR	1961				
7	LH2O	MOL/HR	55369				
8	LCO2IN	MOL/HR	1480	1240	592	59	-0.406
9	TGIN	C	33				
10	TLIN	C	38.78	38.79	3.88	3.87	0.002
11	T4077	C	44.75	44.28	4.48	4.13	-0.106
12	T4076	C	40.83	42.38	4.08	1.97	0.380
13	T4075	C	38.47	38.42	5.77	2.65	-0.008
14	T4073	C	36.94	34.21	5.54	3.71	-0.494
15	TLOUT	C	31.5	31.99	3.15	1.62	0.156
16	RHLDG			0.551			
17	LCO2RH	MOL/HR		4677			
18	LNLDG			0.415			
19	AVELIQ	SQM		0.00036			
20	AVEGAS	CUM/SEC		0.219			
21	AREA	SQM		6.21			
22	AVAREA	SQM	28172				

Table F-22. Run 2.17.2 Data-Fit Results

Vary No.	Initial Value	Est Value	Stnd Dev	95% Conf Int Low Limit	95% Conf Int Up Limit
1	0.59	0.59	0.30	0.10	1.18
2	16096	16064	9011	5000	33726

	Var Name	Units	Meas Val	Est Val	Meas σ	Est σ	Norm Residue
1	GN2IN	MOL/HR	28427				
2	GH2OIN	MOL/HR	1410				
3	GCO2IN	MOL/HR	1284	1285	321	288	0.002
4	GCO2OT	MOL/HR	323	323	97	96	0.000
5	LK2CO3	MOL/HR	2288				
6	LPZ	MOL/HR	1965				
7	LH2O	MOL/HR	55472				
8	LCO2IN	MOL/HR	1454	1383	581.6	257	-0.122
9	TGIN	C	31.69				
10	TLIN	C	38.99	39.04	5.85	5.85	0.008
11	T4077	C	43.92	43.43	6.59	6.00	-0.074
12	T4076	C	40.15	40.96	6.02	2.90	0.135
13	T4075	C	37.83	37.92	5.67	3.11	0.015
14	T4073	C	36.56	35.03	5.48	4.06	-0.278
15	TLOUT	C	29.96	32.05	4.49	1.50	0.465
16	RHLDG			0.545			
17	LCO2RH	MOL/HR		4633			
18	LNLDG			0.432			
19	AVELIQ	SQM		0.00036			
20	AVEGAS	CUM/SEC		0.221			
21	AREA	SQM		4.29			
22	AVAREA	SQM	28427				

Table F-23. Run 2.18.1 Data-Fit Results

Vary No.	Initial Value	Est Value	Stnd Dev	95% Conf Int Low Limit	95% Conf Int Up Limit
1	1.33	1.33	0.85	0.10	1.50
2	20535	20559	4068	12586	28532

	Var Name	Units	Meas Val	Est Val	Meas σ	Est σ	Norm Residue
1	GN2IN	MOL/HR	27910				
2	GH2OIN	MOL/HR	1746				
3	GCO2IN	MOL/HR	1156	1156	58	58	-0.008
4	GCO2OT	MOL/HR	128	128	13	13	0.007
5	LK2CO3	MOL/HR	3328				
6	LPZ	MOL/HR	2857				
7	LH2O	MOL/HR	80672				
8	LCO2IN	MOL/HR	2352	2289	588	121	-0.107
9	TGIN	C	35.69				
10	TLIN	C	44.79	44.81	2.24	2.24	0.007
11	T4077	C	45.89	45.59	4.59	3.95	-0.065
12	T4076	C	47.53	48.18	4.75	2.34	0.136
13	T4075	C	46.66	47.18	7.00	2.83	0.074
14	T4073	C	46.66	45.06	7.00	4.54	-0.228
15	TLOUT	C	37.17	37.71	3.72	2.38	0.145
16	RHLDG			0.537			
17	LCO2RH	MOL/HR		6643			
18	LNLDG			0.454			
19	AVELIQ	SQM		0.00052			
20	AVEGAS	CUM/SEC		0.226			
21	AREA	SQM		9.64			
22	AVAREA	SQM	27910				

Table F-24. Run 2.18.2 Data-Fit Results

Vary No.	Initial Value	Est Value	Stnd Dev	95% Conf Int Low Limit	95% Conf Int Up Limit
1	1.45	1.45	0.96	0.10	1.50
2	20282	20284	3746	12942	27626

	Var Name	Units	Meas Val	Est Val	Meas σ	Est σ	Norm Residue
1	GN2IN	MOL/HR	27827				
2	GH2OIN	MOL/HR	1832				
3	GCO2IN	MOL/HR	1119	1119	56	56	-0.005
4	GCO2OT	MOL/HR	115	115	12	11	0.009
5	LK2CO3	MOL/HR	3268				
6	LPZ	MOL/HR	2806				
7	LH2O	MOL/HR	79216				
8	LCO2IN	MOL/HR	2299	2248	574.75	117	-0.089
9	TGIN	C	36.6				
10	TLIN	C	44.81	44.82	2.24	2.24	0.006
11	T4077	C	45.71	45.36	4.57	3.96	-0.077
12	T4076	C	47.47	48.28	4.75	2.30	0.171
13	T4075	C	46.8	47.35	7.02	2.94	0.078
14	T4073	C	47.11	45.18	7.07	4.73	-0.273
15	TLOUT	C	37.56	38.32	3.76	2.28	0.204
16	RHLDG			0.537			
17	LCO2RH	MOL/HR		6518			
18	LNLDG			0.454			
19	AVELIQ	SQM		0.00051			
20	AVEGAS	CUM/SEC		0.225			
21	AREA	SQM		10.56			
22	AVAREA	SQM	27827				

Table F-25. Run 2.20.1 Data-Fit Results

Vary No.	Initial Value	Est Value	Stnd Dev	95% Conf Int Low Limit	95% Conf Int Up Limit
1	0.73	0.73	0.16	0.43	1.04
2	57441	57441	12042	33839	80000

	Var Name	Units	Meas Val	Est Val	Meas σ	Est σ	Norm Residue
1	GN2IN	MOL/HR	24863				
2	GH2OIN	MOL/HR	3348				
3	GCO2IN	MOL/HR	4822	4799	241	236	-0.094
4	GCO2OT	MOL/HR	530	530	27	26	0.007
5	LK2CO3	MOL/HR	8468				
6	LPZ	MOL/HR	7271				
7	LH2O	MOL/HR	205277				
8	LCO2IN	MOL/HR	5133	4645	1026.6	212	-0.476
9	TGIN	C	47.09				
10	TLIN	C	40.11	40.27	2.01	1.92	0.079
11	T4077	C	42.46	41.44	4.25	1.53	-0.241
12	T4076	C	46.74	46.95	4.67	3.65	0.044
13	T4075	C	50.51	51.09	5.05	3.03	0.115
14	T4073	C	52.89	51.80	5.29	2.69	-0.207
15	TLOUT	C	47.96	48.07	2.40	2.04	0.044
16	RHLDG			0.552			
17	LCO2RH	MOL/HR		17382			
18	LNLDG			0.417			
19	AVELIQ	SQM		0.00134			
20	AVEGAS	CUM/SEC		0.228			
21	AREA	SQM		5.37			
22	AVAREA	SQM	24863				

Table F-26. Run 2.20.2 Data-Fit Results

Vary No.	Initial Value	Est Value	Stnd Dev	95% Conf Int Low Limit	95% Conf Int Up Limit
1	0.78	0.78	0.16	0.46	1.10
2	59531	59531	12161	35695	80000

	Var Name	Units	Meas Val	Est Val	Meas σ	Est σ	Norm Residue
1	GN2IN	MOL/HR	24475				
2	GH2OIN	MOL/HR	3803				
3	GCO2IN	MOL/HR	4677	4654	234	230	-0.099
4	GCO2OT	MOL/HR	481	481	24	24	0.012
5	LK2CO3	MOL/HR	8439				
6	LPZ	MOL/HR	7247				
7	LH2O	MOL/HR	204596				
8	LCO2IN	MOL/HR	5542	4719	1108.4	204	-0.742
9	TGIN	C	49.72				
10	TLIN	C	40.08	40.26	2.00	1.92	0.089
11	T4077	C	42.21	41.21	4.22	1.57	-0.237
12	T4076	C	45.78	46.53	4.58	3.71	0.165
13	T4075	C	50.19	50.33	5.02	2.86	0.027
14	T4073	C	52.84	50.76	5.28	2.62	-0.393
15	TLOUT	C	48.27	48.65	2.41	2.05	0.159
16	RHLDG			0.552			
17	LCO2RH	MOL/HR		17326			
18	LNLDG			0.419			
19	AVELIQ	SQM		0.00133			
20	AVEGAS	CUM/SEC		0.223			
21	AREA	SQM		5.67			
22	AVAREA	SQM	24475				

Table F-27. Run 2.21.1 Data-Fit Results

Vary No.	Initial Value	Est Value	Stnd Dev	95% Conf Int Low Limit	95% Conf Int Up Limit
1	1.04	1.04	0.34	0.37	1.20
2	71000	71000	25489	21041	80000

	Var Name	Units	Meas Val	Est Val	Meas σ	Est σ	Norm Residue
1	GN2IN	MOL/HR	22753				
2	GH2OIN	MOL/HR	5708	5523.895	1141.6	1103.622	-0.16127
3	GCO2IN	MOL/HR	4350	4328	218	215	-0.103
4	GCO2OT	MOL/HR	282	283	42	42	0.016
5	LK2CO3	MOL/HR	9127				
6	LPZ	MOL/HR	7837				
7	LH2O	MOL/HR	221265				
8	LCO2IN	MOL/HR	7083	5598	1416.6	226	-1.048
9	TGIN	C	58.39				
10	TLIN	C	40.1	40.28	2.01	1.93	0.091
11	T4077	C	40.75	40.04	4.08	1.58	-0.175
12	T4076	C	43.39	44.29	4.34	3.90	0.208
13	T4075	C	47.97	46.85	7.20	3.06	-0.156
14	T4073	C	50.84	46.43	7.63	3.99	-0.578
15	TLOUT	C	48.3	49.67	4.83	4.12	0.283
16	RHLDG			0.553			
17	LCO2RH	MOL/HR		18771			
18	LNLDG			0.434			
19	AVELIQ	SQM		0.00144			
20	AVEGAS	CUM/SEC		0.204			
21	AREA	SQM		7.63			
22	AVAREA	SQM	22753				

Table F-28. Run 2.21.2 Data-Fit Results

Vary No.	Initial Value	Est Value	Stnd Dev	95% Conf Int Low Limit	95% Conf Int Up Limit
1	1.00	1.00	0.41	0.20	1.20
2	69376	69553	31396	8017	80000

	Var Name	Units	Meas Val	Est Val	Meas σ	Est σ	Norm Residue
1	GN2IN	MOL/HR	21027				
2	GH2OIN	MOL/HR	7452	6936.383	1490.4	1408.787	0.34596
3	GCO2IN	MOL/HR	4135	4119	414	402	-0.039
4	GCO2OT	MOL/HR	317	317	48	47	-0.001
5	LK2CO3	MOL/HR	9105				
6	LPZ	MOL/HR	7819				
7	LH2O	MOL/HR	220732				
8	LCO2IN	MOL/HR	6882	5773	1720.5	357	-0.645
9	TGIN	C	64.35				
10	TLIN	C	40.86	41.54	4.09	3.67	0.165
11	T4077	C	42.34	41.96	4.23	2.35	-0.089
12	T4076	C	45.6	46.63	4.56	4.16	0.226
13	T4075	C	50.48	48.07	7.57	3.13	-0.318
14	T4073	C	53.68	47.08	8.05	4.43	-0.820
15	TLOUT	C	50.7	53.53	5.07	4.25	0.558
16	RHLDG			0.552			
17	LCO2RH	MOL/HR		18680			
18	LNLDG			0.440			
19	AVELIQ	SQM		0.00144			
20	AVEGAS	CUM/SEC		0.193			
21	AREA	SQM		7.36			
22	AVAREA	SQM	21027				

Table F-29. Run 2.22.1 Data-Fit Results

Vary No.	Initial Value	Est Value	Stnd Dev	95% Conf Int Low Limit	95% Conf Int Up Limit
1	0.65	0.65	0.11	0.43	0.86
2	53656	53621	14627	24953	60000

	Var Name	Units	Meas Val	Est Val	Meas σ	Est σ	Norm Residue
1	GN2IN	MOL/HR	23643				
2	GH2OIN	MOL/HR	3750				
3	GCO2IN	MOL/HR	5158	5121	258	253	-0.145
4	GCO2OT	MOL/HR	623	624	31	31	0.032
5	LK2CO3	MOL/HR	9035				
6	LPZ	MOL/HR	7758				
7	LH2O	MOL/HR	219034				
8	LCO2IN	MOL/HR	6135	4971	1227	231	-0.949
9	TGIN	C	49.5				
10	TLIN	C	41.77	41.89	2.09	1.99	0.057
11	T4077	C	44.37	43.70	4.44	1.88	-0.151
12	T4076	C	49.01	49.69	4.90	3.82	0.140
13	T4075	C	53.49	53.88	5.35	3.12	0.073
14	T4073	C	56.31	54.73	5.63	2.83	-0.281
15	TLOUT	C	51.19	51.34	2.56	2.16	0.057
16	RHLDG			0.551			
17	LCO2RH	MOL/HR		18500			
18	LNLDG			0.417			
19	AVELIQ	SQM		0.00143			
20	AVEGAS	CUM/SEC		0.223			
21	AREA	SQM		4.73			
22	AVAREA	SQM	23643				

Table F-30. Run 2.22.2 Data-Fit Results

Vary No.	Initial Value	Est Value	Stnd Dev	95% Conf Int Low Limit	95% Conf Int Up Limit
1	0.72	0.72	0.12	0.49	0.95
2	52377	52115	14380	23929	60000

	Var Name	Units	Meas Val	Est Val	Meas σ	Est σ	Norm Residue
1	GN2IN	MOL/HR	23916				
2	GH2OIN	MOL/HR	3686				
3	GCO2IN	MOL/HR	5022	4986	251	247	-0.145
4	GCO2OT	MOL/HR	463	464	23	23	0.025
5	LK2CO3	MOL/HR	9101				
6	LPZ	MOL/HR	7815				
7	LH2O	MOL/HR	220626				
8	LCO2IN	MOL/HR	6120	5006	1224	225	-0.910
9	TGIN	C	49.12				
10	TLIN	C	41.08	41.19	2.05	1.94	0.054
11	T4077	C	42.92	42.28	4.29	1.73	-0.150
12	T4076	C	47.19	47.65	4.72	3.50	0.097
13	T4075	C	52.04	52.45	5.20	3.27	0.080
14	T4073	C	55.07	53.97	5.51	2.81	-0.200
15	TLOUT	C	50.94	50.96	2.55	2.19	0.009
16	RHLDG			0.551			
17	LCO2RH	MOL/HR		18629			
18	LNLDG			0.417			
19	AVELIQ	SQM		0.00144			
20	AVEGAS	CUM/SEC		0.221			
21	AREA	SQM		5.26			
22	AVAREA	SQM	23916				

Table F-31. Run 2.23.1 Data-Fit Results

Vary No.	Initial Value	Est Value	Stnd Dev	95% Conf Int Low Limit	95% Conf Int Up Limit
1	0.59	0.59	0.46	0.10	1.20
2	4	4	23	0	50

	Var Name	Units	Meas Val	Est Val	Meas σ	Est σ	Norm Residue
1	GN2IN	MOL/HR	25110				
2	GH2OIN	MOL/HR	2596				
3	GCO2IN	MOL/HR	5214	5091	521	501	-0.236
4	GCO2OT	MOL/HR	1257	1281	126	125	0.188
5	LK2CO3	MOL/HR	6228				
6	LPZ	MOL/HR	5348				
7	LH2O	MOL/HR	150983				
8	LCO2IN	MOL/HR	3865	2780	1352.75	411	-0.802
9	TGIN	C	41.96				
10	TLIN	C	39.86	39.90	3.99	3.99	0.011
11	T4077	C	72.09	72.86	7.21	5.96	0.107
12	T4076	C	67.49	67.21	6.75	5.18	-0.042
13	T4075	C	66.14	63.77	13.23	4.90	-0.179
14	T4073	C	63.21	61.23	9.48	4.42	-0.209
15	TLOUT	C	47.95	49.11	4.80	2.88	0.242
16	RHLDG			0.555			
17	LCO2RH	MOL/HR		12828			
18	LNLDG			0.389			
19	AVELIQ	SQM		0.00100			
20	AVEGAS	CUM/SEC		0.283			
21	AREA	SQM		4.38			
22	AVAREA	SQM	25110				

Table F-32. Run 2.23.2 Data-Fit Results

Vary No.	Initial Value	Est Value	Stnd Dev	95% Conf Int Low Limit	95% Conf Int Up Limit
1	0.42	0.42	0.58	0.10	1.20
2	15300	15300	66980	-4000	50000

	Var Name	Units	Meas Val	Est Val	Meas σ	Est σ	Norm Residue
1	GN2IN	MOL/HR	25591				
2	GH2OIN	MOL/HR	2483				
3	GCO2IN	MOL/HR	4980	4813	747	686	-0.223
4	GCO2OT	MOL/HR	1123	1133	168	168	0.057
5	LK2CO3	MOL/HR	6187				
6	LPZ	MOL/HR	5313				
7	LH2O	MOL/HR	149987				
8	LCO2IN	MOL/HR	3765	2829	1506	638	-0.621
9	TGIN	C	41.05				
10	TLIN	C	39.82	39.84	3.98	3.98	0.006
11	T4077	C	70.98	71.72	10.65	10.44	0.070
12	T4076	C	67.06	67.44	10.06	4.20	0.038
13	T4075	C	66.01	63.90	9.90	5.18	-0.213
14	T4073	C	62.91	60.90	9.44	5.05	-0.213
15	TLOUT	C	47.27	48.52	4.73	2.55	0.265
16	RHLDG			0.553			
17	LCO2RH	MOL/HR		12702			
18	LNLDG			0.392			
19	AVELIQ	SQM		0.00100			
20	AVEGAS	CUM/SEC		0.278			
21	AREA	SQM		3.17			
22	AVAREA	SQM	25591				

Table F-33. Run 2.24.1 Data-Fit Results

Vary No.	Initial Value	Est Value	Stnd Dev	95% Conf Int Low Limit	95% Conf Int Up Limit
1	0.45	0.47	0.36	0.10	1.18
2	21128	17932	44348	5000	50000

	Var Name	Units	Meas Val	Est Val	Meas σ	Est σ	Norm Residue
1	GN2IN	MOL/HR	25320				
2	GH2OIN	MOL/HR	2562				
3	GCO2IN	MOL/HR	5147	5042	257	248	-0.408
4	GCO2OT	MOL/HR	949	955	47	47	0.124
5	LK2CO3	MOL/HR	6252				
6	LPZ	MOL/HR	5369				
7	LH2O	MOL/HR	151570				
8	LCO2IN	MOL/HR	3767	2549	753.4	231	-1.617
9	TGIN	C	41.7				
10	TLIN	C	39.68	39.71	1.98	1.98	0.017
11	T4077	C	72.61	72.50	7.26	4.06	-0.015
12	T4076	C	67.59	68.52	6.76	2.06	0.137
13	T4075	C	66.63	64.63	6.66	2.87	-0.300
14	T4073	C	63.81	61.23	6.38	2.35	-0.405
15	TLOUT	C	47.57	48.48	2.38	1.22	0.383
16	RHLDG			0.555			
17	LCO2RH	MOL/HR		12877			
18	LNLDG			0.378			
19	AVELIQ	SQM		0.00101			
20	AVEGAS	CUM/SEC		0.279			
21	AREA	SQM		3.29			
22	AVAREA	SQM	25320				

Table F-34. Run 2.24.2 Data-Fit Results

Vary No.	Initial Value	Est Value	Stnd Dev	95% Conf Int Low Limit	95% Conf Int Up Limit
1	0.44	0.44	0.42	0.10	1.20
2	20720	20720	60177	5000	50000

	Var Name	Units	Meas Val	Est Val	Meas σ	Est σ	Norm Residue
1	GN2IN	MOL/HR	25169				
2	GH2OIN	MOL/HR	2536				
3	GCO2IN	MOL/HR	5310	5236	266	250	-0.278
4	GCO2OT	MOL/HR	1049	1052	52	52	0.056
5	LK2CO3	MOL/HR	6202				
6	LPZ	MOL/HR	5326				
7	LH2O	MOL/HR	150350				
8	LCO2IN	MOL/HR	2912	2428	582.4	263	-0.830
9	TGIN	C	41.52				
10	TLIN	C	39.65	39.67	1.98	1.98	0.009
11	T4077	C	72.54	72.58	7.25	6.12	0.005
12	T4076	C	67.61	68.34	6.76	2.64	0.107
13	T4075	C	66.52	64.33	6.65	3.65	-0.329
14	T4073	C	63.6	60.88	6.36	3.23	-0.427
15	TLOUT	C	47.49	48.24	2.37	1.67	0.314
16	RHLDG			0.556			
17	LCO2RH	MOL/HR		12814			
18	LNLDG			0.374			
19	AVELIQ	SQM		0.00100			
20	AVEGAS	CUM/SEC		0.278			
21	AREA	SQM		3.18			
22	AVAREA	SQM	25169				

Appendix G: Aspen Plus® Data-Fit Regression Results – Campaign 4

Table G-1. Run 4.1 Data-Fit Results

Vary No.	Initial Value	Est Value	Stnd Dev	95% Conf Int Low Limit	95% Conf Int Up Limit
1	4.18	4.18	1.98	1	5
2	19610	19610	12318	5000	43754

	Var Name	Units	Meas Val	Est Val	Meas σ	Est σ	Norm Residue
1	GN2IN	MOL/HR	30027				
2	GH2OIN	MOL/HR	2607				
3	GCO2IN	MOL/HR	2712	2712.5	135.6	134.74	0.0037
4	GCO2OT	MOL/HR	194	194.0	9.7	9.70	-0.0005
5	LK2CO3	MOL/HR	5922				
6	LPZ	MOL/HR	5573				
7	LH2O	MOL/HR	139594				
8	LCO2IN	MOL/HR	3200	3215	800	554	0.018
9	TGIN	C	39.94				
10	TLIN	C	39.93	39.91	2.00	1.98	-0.011
11	T4077	C	57.13	57.25	5.71	5.61	0.021
12	T4076	C	64.93	64.73	6.49	1.20	-0.031
13	T4075	C	65.38	64.20	6.54	0.74	-0.18
14	T4073	C	62.1	62.74	6.21	0.71	0.10
15	TLOUT	C	48.83	48.86	2.44	1.77	0.014
16	RHLDG			0.51			
17	LCO2RH	MOL/HR	1	11658	11659		
18	LNLDG			0.40			
19	AVELIQ	SQM		0.00094			
20	AVEGAS	CUM/SEC		0.29			
21	AREA	SQM		4.14			
22	AVAREA	SQM		4.17			

Table G-2. Run 4.2.1 Data-Fit Results

Vary No.	Initial Value	Est Value	Stnd Dev	95% Conf Int Low Limit	95% Conf Int Up Limit
1	2.30	2.30	0.37	1.57	3.03
2	29445	29445	9477	10869	48020

	Var Name	Units	Meas Val	Est Val	Meas σ	Est σ	Norm Residue
1	GN2IN	MOL/HR	22587				
2	GH2OIN	MOL/HR	2006				
3	GCO2IN	MOL/HR	4492	4474	225	221	-0.080
4	GCO2OT	MOL/HR	983	987	98	98	0.041
5	LK2CO3	MOL/HR	5481				
6	LPZ	MOL/HR	5193				
7	LH2O	MOL/HR	122979				
8	LCO2IN	MOL/HR	3095	2534	1238	233	-0.453
9	TGIN	C	39.94				
10	TLIN	C	38.89	38.88	1.94	1.94	-0.004
11	T4077	C	64.82	64.88	3.24	3.20	0.019
12	T4076	C	67.89	67.71	3.39	1.15	-0.054
13	T4075	C	64.86	64.87	3.24	1.56	0.003
14	T4073	C	61.31	61.66	3.07	1.83	0.115
15	TLOUT	C	48.56	48.17	2.43	1.40	-0.160
16	RHLDG			0.539			
17	LCO2RH	MOL/HR		11502			
18	LNLDG			0.375			
19	AVELIQ	SQM		0.00084			
20	AVEGAS	CUM/SEC		0.238			
21	AREA	SQM		2.20			
22	AVAREA	SQM		2.21			

Table G-3. Run 4.2.2 Data-Fit Results

Vary No.	Initial Value	Est Value	Stnd Dev	95% Conf Int Low Limit	95% Conf Int Up Limit
1	2.25	2.25	0.32	1.62	2.88
2	29361	29361	7584	14497	44225

	Var Name	Units	Meas Val	Est Val	Meas σ	Est σ	Norm Residue
1	GN2IN	MOL/HR	22312				
2	GH2OIN	MOL/HR	1901				
3	GCO2IN	MOL/HR	4737	4723	95	93	0.0037
4	GCO2OT	MOL/HR	1198	1204	60	59	-0.0005
5	LK2CO3	MOL/HR	5526				
6	LPZ	MOL/HR	5203				
7	LH2O	MOL/HR	123801				
8	LCO2IN	MOL/HR	2906	2584	435.9	127	0.018
9	TGIN	C	40.12				
10	TLIN	C	38.96	38.96	0.78	0.78	-0.011
11	T4077	C	64.87	65.02	3.24	3.21	0.021
12	T4076	C	67.35	67.28	3.37	1.21	-0.031
13	T4075	C	64.34	64.19	3.22	1.56	-0.18
14	T4073	C	60.51	60.88	3.03	1.77	0.10
15	TLOUT	C	48.42	47.57	2.42	1.29	0.014
16	RHLDG			0.542			
17	LCO2RH	MOL/HR		11629			
18	LNLDG			0.378			
19	AVELIQ	SQM		0.00085			
20	AVEGAS	CUM/SEC		0.238			
21	AREA	SQM		2.15			
22	AVAREA	SQM		2.17			

Table G-4. Run 4.3.1 Data-Fit Results

Vary No.	Initial Value	Est Value	Stnd Dev	95% Conf Int Low Limit	95% Conf Int Up Limit
1	2.44	2.44	1.34	1.00	5.00
2	24367	24367	23566	5000	50000

	Var Name	Units	Meas Val	Est Val	Meas σ	Est σ	Norm Residue
1	GN2IN	MOL/HR	16686				
2	GH2OIN	MOL/HR	1568				
3	GCO2IN	MOL/HR	3157	3065	789	707	-0.117
4	GCO2OT	MOL/HR	462	465	116	115	0.030
5	LK2CO3	MOL/HR	5628				
6	LPZ	MOL/HR	5360				
7	LH2O	MOL/HR	128009				
8	LCO2IN	MOL/HR	3700	3460	1480	699	-0.162
9	TGIN	C	40.64				
10	TLIN	C	42.09	42.27	4.21	3.80	0.042
11	T4077	C	44.26	44.10	6.64	3.03	-0.023
12	T4076	C	50.45	48.89	7.57	4.25	-0.207
13	T4075	C	52.23	53.38	7.83	5.30	0.147
14	T4073	C	55.72	56.02	8.36	4.87	0.036
15	TLOUT	C	50.59	50.15	5.06	4.67	-0.088
16	RHLDG			0.532			
17	LCO2RH	MOL/HR		11689			
18	LNLDG			0.414			
19	AVELIQ	SQM		0.00086			
20	AVEGAS	CUM/SEC		0.155			
21	AREA	SQM		2.35			
22	AVAREA	SQM		2.38			

Table G-5. Run 4.3.2 Data-Fit Results

Vary No.	Initial Value	Est Value	Stnd Dev	95% Conf Int Low Limit	95% Conf Int Up Limit
1	2.34	2.33	1.43	1.00	5.00
2	25494	25564	23457	5000	50000

	Var Name	Units	Meas Val	Est Val	Meas σ	Est σ	Norm Residue
1	GN2IN	MOL/HR	16406				
2	GH2OIN	MOL/HR	1529				
3	GCO2IN	MOL/HR	3248	3141	812	712	-0.132
4	GCO2OT	MOL/HR	490	497	123	121	0.054
5	LK2CO3	MOL/HR	5726				
6	LPZ	MOL/HR	5413				
7	LH2O	MOL/HR	127461				
8	LCO2IN	MOL/HR	3612	3498	1444.8	684	-0.079
9	TGIN	C	40.59				
10	TLIN	C	42.49	42.83	4.25	3.54	0.081
11	T4077	C	44.85	44.79	4.49	2.63	-0.014
12	T4076	C	51.33	49.73	5.13	3.01	-0.311
13	T4075	C	52.94	54.14	5.29	3.62	0.227
14	T4073	C	56.34	56.55	5.63	3.47	0.038
15	TLOUT	C	50.78	50.32	5.08	4.55	-0.091
16	RHLDG			0.533			
17	LCO2RH	MOL/HR		11866			
18	LNLDG			0.414			
19	AVELIQ	SQM		0.00086			
20	AVEGAS	CUM/SEC		0.154			
21	AREA	SQM		2.24			
22	AVAREA	SQM		2.26			

Table G-6. Run 4.4.1 Data-Fit Results

Vary No.	Initial Value	Est Value	Stnd Dev	95% Conf Int Low Limit	95% Conf Int Up Limit
1	1.96	1.96	1.03	1.00	3.98
2	31361	31361	26872	5000	50000

	Var Name	Units	Meas Val	Est Val	Meas σ	Est σ	Norm Residue
1	GN2IN	MOL/HR	21304				
2	GH2OIN	MOL/HR	1951				
3	GCO2IN	MOL/HR	4532	4296	906	698	-0.260
4	GCO2OT	MOL/HR	1195	1220	239	232	0.103
5	LK2CO3	MOL/HR	6394				
6	LPZ	MOL/HR	6089				
7	LH2O	MOL/HR	141934				
8	LCO2IN	MOL/HR	3961	3858	1188.3	547	-0.087
9	TGIN	C	39.98				
10	TLIN	C	43.62	44.07	4.36	4.20	0.103
11	T4077	C	52.65	51.66	5.27	4.09	-0.188
12	T4076	C	60.49	60.75	6.05	4.36	0.043
13	T4075	C	61	62.45	6.10	3.23	0.237
14	T4073	C	60.86	60.66	6.09	3.59	-0.033
15	TLOUT	C	50.52	49.70	5.05	3.82	-0.162
16	RHLDG			0.534			
17	LCO2RH	MOL/HR		13325			
18	LNLDG			0.411			
19	AVELIQ	SQM		0.00097			
20	AVEGAS	CUM/SEC		0.215			
21	AREA	SQM		2.00			
22	AVAREA	SQM		2.04			

Table G-7. Run 4.4.2 Data-Fit Results

Vary No.	Initial Value	Est Value	Stnd Dev	95% Conf Int Low Limit	95% Conf Int Up Limit
1	2.01	2.01	1.18	1.00	4.31
2	31699	31699	26219	5000	50000

	Var Name	Units	Meas Val	Est Val	Meas σ	Est σ	Norm Residue
1	GN2IN	MOL/HR	21592				
2	GH2OIN	MOL/HR	1876				
3	GCO2IN	MOL/HR	4610	4479	692	610	-0.190
4	GCO2OT	MOL/HR	1277	1298	255	248	0.084
5	LK2CO3	MOL/HR	6383				
6	LPZ	MOL/HR	6134				
7	LH2O	MOL/HR	142384				
8	LCO2IN	MOL/HR	4138	3766	1241.4	621	-0.299
9	TGIN	C	40				
10	TLIN	C	43.94	43.98	4.39	4.34	0.009
11	T4077	C	54.09	53.67	8.11	6.51	-0.052
12	T4076	C	62.39	62.77	9.36	5.74	0.041
13	T4075	C	62.39	63.32	9.36	3.58	0.100
14	T4073	C	61.53	61.59	9.23	4.10	0.006
15	TLOUT	C	50.43	49.64	5.04	4.20	-0.156
16	RHLDG			0.532			
17	LCO2RH	MOL/HR		13326			
18	LNLDG			0.405			
19	AVELIQ	SQM		0.00098			
20	AVEGAS	CUM/SEC		0.222			
21	AREA	SQM		2.02			
22	AVAREA	SQM		2.05			

Table G-8. Run 4.5.1 Data-Fit Results

Vary No.	Initial Value	Est Value	Stnd Dev	95% Conf Int Low Limit	95% Conf Int Up Limit
1	2.07	2.07	0.52	1.06	3.08
2	34511	34511	14865	5376	50000

	Var Name	Units	Meas Val	Est Val	Meas σ	Est σ	Norm Residue
1	GN2IN	MOL/HR	27700				
2	GH2OIN	MOL/HR	2428				
3	GCO2IN	MOL/HR	5662	5462	566	475	-0.354
4	GCO2OT	MOL/HR	2073	2102	207	203	0.141
5	LK2CO3	MOL/HR	6367				
6	LPZ	MOL/HR	6040				
7	LH2O	MOL/HR	142522				
8	LCO2IN	MOL/HR	3988	3622	797.6	469	-0.459
9	TGIN	C	40.09				
10	TLIN	C	42.01	42.02	2.10	2.09	0.005
11	T4077	C	58.4	58.27	5.84	5.52	-0.023
12	T4076	C	61.52	62.24	6.15	2.38	0.117
13	T4075	C	59.59	60.14	5.96	2.31	0.093
14	T4073	C	56.74	57.44	5.67	2.53	0.124
15	TLOUT	C	47.08	46.46	2.35	1.84	-0.261
16	RHLDG			0.538			
17	LCO2RH	MOL/HR		13349			
18	LNLDG			0.403			
19	AVELIQ	SQM		0.00097			
20	AVEGAS	CUM/SEC		0.281			
21	AREA	SQM		2.09			
22	AVAREA	SQM		2.12			

Table G-9. Run 4.5.2 Data-Fit Results

Vary No.	Initial Value	Est Value	Stnd Dev	95% Conf Int Low Limit	95% Conf Int Up Limit
1	2.20	2.20	0.53	1.16	3.24
2	45249	45249	15242	15375	50000

	Var Name	Units	Meas Val	Est Val	Meas σ	Est σ	Norm Residue
1	GN2IN	MOL/HR	27493				
2	GH2OIN	MOL/HR	2506				
3	GCO2IN	MOL/HR	6004	5687	600	500	-0.528
4	GCO2OT	MOL/HR	2058	2100	206	201	0.202
5	LK2CO3	MOL/HR	6422				
6	LPZ	MOL/HR	6124				
7	LH2O	MOL/HR	142058				
8	LCO2IN	MOL/HR	4107	3562	821.4	472	-0.663
9	TGIN	C	39.98				
10	TLIN	C	41.38	41.40	2.07	2.07	0.009
11	T4077	C	56.94	56.60	5.69	5.37	-0.060
12	T4076	C	59.89	61.18	5.99	2.25	0.215
13	T4075	C	58.12	59.02	5.81	2.21	0.155
14	T4073	C	55.38	56.17	5.54	2.57	0.143
15	TLOUT	C	46.46	45.65	2.32	1.84	-0.349
16	RHLDG			0.541			
17	LCO2RH	MOL/HR		13568			
18	LNLDG			0.398			
19	AVELIQ	SQM		0.00097			
20	AVEGAS	CUM/SEC		0.278			
21	AREA	SQM		2.22			
22	AVAREA	SQM		2.25			

Table G-10. Run 4.6.1 Data-Fit Results

Vary No.	Initial Value	Est Value	Stnd Dev	95% Conf Int Low Limit	95% Conf Int Up Limit
1	2.64	2.64	0.49	1.68	3.61
2	31782	31714	5495	20944	42484

	Var Name	Units	Meas Val	Est Val	Meas σ	Est σ	Norm Residue
1	GN2IN	MOL/HR	16749				
2	GH2OIN	MOL/HR	1461				
3	GCO2IN	MOL/HR	3424	3420	68	68	-0.064
4	GCO2OT	MOL/HR	419	420	21	21	0.032
5	LK2CO3	MOL/HR	5050				
6	LPZ	MOL/HR	4793				
7	LH2O	MOL/HR	119534				
8	LCO2IN	MOL/HR	2671	2537	400.65	119	-0.334
9	TGIN	C	40.06				
10	TLIN	C	46.73	46.74	0.93	0.93	0.015
11	T4077	C	66.79	66.65	3.34	3.29	-0.043
12	T4076	C	69.72	70.81	3.49	1.04	0.314
13	T4075	C	68.38	68.41	3.42	1.55	0.007
14	T4073	C	64.73	65.37	3.24	1.90	0.198
15	TLOUT	C	51.77	50.44	2.59	1.47	-0.515
16	RHLDG			0.538			
17	LCO2RH	MOL/HR		10587			
18	LNLDG			0.385			
19	AVELIQ	SQM		0.00081			
20	AVEGAS	CUM/SEC		0.183			
21	AREA	SQM		2.44			
22	AVAREA	SQM		2.48			

Table G-11. Run 4.6.2 Data-Fit Results

Vary No.	Initial Value	Est Value	Stnd Dev	95% Conf Int Low Limit	95% Conf Int Up Limit
1	2.93	2.93	0.51	1.94	3.92
2	33920	33920	4332	25430	42410

	Var Name	Units	Meas Val	Est Val	Meas σ	Est σ	Norm Residue
1	GN2IN	MOL/HR	16772				
2	GH2OIN	MOL/HR	1480				
3	GCO2IN	MOL/HR	3380	3376	68	67	-0.060
4	GCO2OT	MOL/HR	361	362	18	18	0.039
5	LK2CO3	MOL/HR	5080				
6	LPZ	MOL/HR	4810				
7	LH2O	MOL/HR	118259				
8	LCO2IN	MOL/HR	2629	2564	394.35	102	-0.164
9	TGIN	C	39.95				
10	TLIN	C	43.57	43.63	0.87	0.87	0.070
11	T4077	C	58.37	58.12	2.92	2.87	-0.086
12	T4076	C	67.46	69.84	3.37	1.13	0.704
13	T4075	C	67.33	67.94	3.37	1.70	0.180
14	T4073	C	64.75	64.86	3.24	2.01	0.033
15	TLOUT	C	51.75	49.98	2.59	1.27	-0.683
16	RHLDG			0.539			
17	LCO2RH	MOL/HR		10664			
18	LNLDG			0.387			
19	AVELIQ	SQM		0.00080			
20	AVEGAS	CUM/SEC		0.178			
21	AREA	SQM		2.74			
22	AVAREA	SQM		2.78			

Table G-12. Run 4.7.1 Data-Fit Results

Vary No.	Initial Value	Est Value	Stnd Dev	95% Conf Int Low Limit	95% Conf Int Up Limit
1	3.10	3.10	1.05	1.04	5.00
2	32462	32441	13818	5358	50000

	Var Name	Units	Meas Val	Est Val	Meas σ	Est σ	Norm Residue
1	GN2IN	MOL/HR	22646				
2	GH2OIN	MOL/HR	1961				
3	GCO2IN	MOL/HR	3566	3599	357	344	0.092
4	GCO2OT	MOL/HR	320	320	32	32	0.007
5	LK2CO3	MOL/HR	6288				
6	LPZ	MOL/HR	5936				
7	LH2O	MOL/HR	144825				
8	LCO2IN	MOL/HR	2830	3295	1132	435	0.411
9	TGIN	C	40.02				
10	TLIN	C	45.19	45.30	2.26	2.24	0.048
11	T4077	C	62.21	61.81	6.22	6.12	-0.065
12	T4076	C	68.44	69.76	6.84	1.38	0.192
13	T4075	C	67.47	68.58	6.75	1.60	0.164
14	T4073	C	64.66	66.32	6.47	2.16	0.257
15	TLOUT	C	50.95	50.91	2.55	2.22	-0.017
16	RHLDG			0.526			
17	LCO2RH	MOL/HR		12862			
18	LNLDG			0.392			
19	AVELIQ	SQM		0.00099			
20	AVEGAS	CUM/SEC		0.236			
21	AREA	SQM		3.11			
22	AVAREA	SQM		3.15			

Table G-13. Run 4.7.2 Data-Fit Results

Vary No.	Initial Value	Est Value	Stnd Dev	95% Conf Int Low Limit	95% Conf Int Up Limit
1	2.73	2.73	1.12	1.00	4.92
2	29244	29244	21723	5000	50000

	Var Name	Units	Meas Val	Est Val	Meas σ	Est σ	Norm Residue
1	GN2IN	MOL/HR	22480				
2	GH2OIN	MOL/HR	1936				
3	GCO2IN	MOL/HR	3435	3480	515	488	0.088
4	GCO2OT	MOL/HR	243	245	61	60	0.036
5	LK2CO3	MOL/HR	6187				
6	LPZ	MOL/HR	5818				
7	LH2O	MOL/HR	145124				
8	LCO2IN	MOL/HR	2824	2938	706	626	0.162
9	TGIN	C	40.1				
10	TLIN	C	44.97	46.30	6.75	6.08	0.197
11	T4077	C	59.92	59.42	5.99	5.83	-0.083
12	T4076	C	68.04	69.08	6.80	2.77	0.153
13	T4075	C	67.79	68.96	6.78	1.73	0.172
14	T4073	C	65.31	67.33	6.53	1.65	0.309
15	TLOUT	C	50.99	52.24	5.10	2.67	0.245
16	RHLDG			0.514			
17	LCO2RH	MOL/HR		12349			
18	LNLDG			0.380			
19	AVELIQ	SQM		0.00098			
20	AVEGAS	CUM/SEC		0.233			
21	AREA	SQM		2.71			
22	AVAREA	SQM		2.73			

Table G-14. Run 4.8 Data-Fit Results

Vary No.	Initial Value	Est Value	Stnd Dev	95% Conf Int Low Limit	95% Conf Int Up Limit
1	3.50	3.25	1.59	1.00	5.00
2	37393	33807	23704	5000	50000

	Var Name	Units	Meas Val	Est Val	Meas σ	Est σ	Norm Residue
1	GN2IN	MOL/HR	29024				
2	GH2OIN	MOL/HR	2540				
3	GCO2IN	MOL/HR	3640	3754	546	493	0.208
4	GCO2OT	MOL/HR	578	575	116	115	-0.029
5	LK2CO3	MOL/HR	5948				
6	LPZ	MOL/HR	5704				
7	LH2O	MOL/HR	147616				
8	LCO2IN	MOL/HR	2825	3156	847.5	557	0.390
9	TGIN	C	39.9				
10	TLIN	C	43.28	43.46	4.33	4.30	0.042
11	T4077	C	62.05	61.14	9.31	8.92	-0.097
12	T4076	C	64.06	64.75	9.61	2.88	0.071
13	T4075	C	62.22	63.09	9.33	3.17	0.093
14	T4073	C	57.98	60.72	8.70	3.91	0.315
15	TLOUT	C	47.54	47.67	4.75	3.18	0.027
16	RHLDG			0.527			
17	LCO2RH	MOL/HR		12283			
18	LNLDG			0.391			
19	AVELIQ	SQM		0.00098			
20	AVEGAS	CUM/SEC		0.286			
21	AREA	SQM		3.24			
22	AVAREA	SQM		3.28			

Table G-15. Run 4.9.1 Data-Fit Results

Vary No.	Initial Value	Est Value	Stnd Dev	95% Conf Int Low Limit	95% Conf Int Up Limit
1	2.33	2.32	0.78	1.00	3.85
2	42828	42506	19458	5000	50000

	Var Name	Units	Meas Val	Est Val	Meas σ	Est σ	Norm Residue
1	GN2IN	MOL/HR	27054				
2	GH2OIN	MOL/HR	2494				
3	GCO2IN	MOL/HR	5505	5687	826	599	0.220
4	GCO2OT	MOL/HR	1717	1688	343	328	-0.084
5	LK2CO3	MOL/HR	6118				
6	LPZ	MOL/HR	5747				
7	LH2O	MOL/HR	145525				
8	LCO2IN	MOL/HR	2660	2819	665	512	0.240
9	TGIN	C	39.99				
10	TLIN	C	43.2	43.26	4.32	4.31	0.014
11	T4077	C	64.98	64.62	6.50	6.33	-0.056
12	T4076	C	64.24	64.73	6.42	2.45	0.076
13	T4075	C	61.22	61.51	6.12	3.05	0.047
14	T4073	C	57.03	58.21	5.70	3.50	0.207
15	TLOUT	C	47.36	46.36	4.74	2.38	-0.212
16	RHLDG			0.545			
17	LCO2RH	MOL/HR		12936			
18	LNLDG			0.377			
19	AVELIQ	SQM		0.00098			
20	AVEGAS	CUM/SEC		0.284			
21	AREA	SQM		2.32			
22	AVAREA	SQM		2.34			

Table G-16. Run 4.9.2 Data-Fit Results

Vary No.	Initial Value	Est Value	Stnd Dev	95% Conf Int Low Limit	95% Conf Int Up Limit
1	2.38	2.38	0.80	1.00	3.96
2	41750	41761	20106	5000	50000

	Var Name	Units	Meas Val	Est Val	Meas σ	Est σ	Norm Residue
1	GN2IN	MOL/HR	27250				
2	GH2OIN	MOL/HR	2391				
3	GCO2IN	MOL/HR	5398	5546	810	598	0.183
4	GCO2OT	MOL/HR	1670	1648	334	320	-0.066
5	LK2CO3	MOL/HR	6108				
6	LPZ	MOL/HR	5744				
7	LH2O	MOL/HR	146256				
8	LCO2IN	MOL/HR	2746	2899	686.5	516	0.223
9	TGIN	C	39.99				
10	TLIN	C	43.21	43.29	4.32	4.31	0.017
11	T4077	C	64.61	64.25	6.46	6.30	-0.056
12	T4076	C	63.96	64.53	6.40	2.39	0.089
13	T4075	C	60.98	61.35	6.10	2.98	0.060
14	T4073	C	56.78	58.08	5.68	3.45	0.229
15	TLOUT	C	47.3	45.99	4.73	2.48	-0.277
16	RHLDG			0.545			
17	LCO2RH	MOL/HR		12905			
18	LNLDG			0.380			
19	AVELIQ	SQM		0.00098			
20	AVEGAS	CUM/SEC		0.284			
21	AREA	SQM		2.38			
22	AVAREA	SQM		2.40			

Table G-17. Run 4.10.1 Data-Fit Results

Vary No.	Initial Value	Est Value	Stnd Dev	95% Conf Int Low Limit	95% Conf Int Up Limit
1	1.89	1.88	1.31	1.00	4.45
2	20416	20402	25104	5000	50000

	Var Name	Units	Meas Val	Est Val	Meas σ	Est σ	Norm Residue
1	GN2IN	MOL/HR	16517				
2	GH2OIN	MOL/HR	1416				
3	GCO2IN	MOL/HR	3606	3365	902	692	-0.267
4	GCO2OT	MOL/HR	882	900	221	214	0.084
5	LK2CO3	MOL/HR	5463				
6	LPZ	MOL/HR	5146				
7	LH2O	MOL/HR	128323				
8	LCO2IN	MOL/HR	3603	3385	900.75	621	-0.242
9	TGIN	C	39.96				
10	TLIN	C	44.28	44.52	4.43	3.98	0.054
11	T4077	C	49.95	49.45	5.00	2.93	-0.100
12	T4076	C	56.65	56.49	5.67	3.98	-0.028
13	T4075	C	58.65	59.58	5.87	3.41	0.158
14	T4073	C	60.18	59.90	6.02	3.13	-0.046
15	TLOUT	C	51.32	50.63	5.13	4.41	-0.134
16	RHLDG			0.533			
17	LCO2RH	MOL/HR		11313			
18	LNLDG			0.417			
19	AVELIQ	SQM		0.00086			
20	AVEGAS	CUM/SEC		0.164			
21	AREA	SQM		1.80			
22	AVAREA	SQM		1.83			

Table G-18. Run 4.10.2 Data-Fit Results

Vary No.	Initial Value	Est Value	Stnd Dev	95% Conf Int Low Limit	95% Conf Int Up Limit
1	1.88	1.88	0.61	1.00	3.07
2	19971	19971	6723	6794	33149

	Var Name	Units	Meas Val	Est Val	Meas σ	Est σ	Norm Residue
1	GN2IN	MOL/HR	16556				
2	GH2OIN	MOL/HR	1420				
3	GCO2IN	MOL/HR	3627	3617	73	72	-0.135
4	GCO2OT	MOL/HR	909	913	45	45	0.088
5	LK2CO3	MOL/HR	5313				
6	LPZ	MOL/HR	5043				
7	LH2O	MOL/HR	130068				
8	LCO2IN	MOL/HR	3589	3040	538.35	229	-1.020
9	TGIN	C	39.97				
10	TLIN	C	41.74	41.78	0.83	0.81	0.044
11	T4077	C	46.78	46.28	2.34	0.85	-0.215
12	T4076	C	53.41	53.77	2.67	1.80	0.136
13	T4075	C	57.52	58.13	2.88	1.72	0.214
14	T4073	C	59.65	59.35	2.98	1.55	-0.101
15	TLOUT	C	51.61	50.52	2.58	2.14	-0.421
16	RHLDG			0.534			
17	LCO2RH	MOL/HR		11066			
18	LNLDG			0.404			
19	AVELIQ	SQM		0.00086			
20	AVEGAS	CUM/SEC		0.163			
21	AREA	SQM		1.81			
22	AVAREA	SQM		1.83			

Table G-19. Run 4.11.1 Data-Fit Results

Vary No.	Initial Value	Est Value	Stnd Dev	95% Conf Int Low Limit	95% Conf Int Up Limit
1	1.86	1.84	0.58	1.00	2.98
2	28066	27805	6771	14535	41075

	Var Name	Units	Meas Val	Est Val	Meas σ	Est σ	Norm Residue
1	GN2IN	MOL/HR	23060				
2	GH2OIN	MOL/HR	2023				
3	GCO2IN	MOL/HR	4138	4132	83	82	-0.072
4	GCO2OT	MOL/HR	1273	1277	64	63	0.063
5	LK2CO3	MOL/HR	6239				
6	LPZ	MOL/HR	5600				
7	LH2O	MOL/HR	143103				
8	LCO2IN	MOL/HR	3742	3492	561.3	374	-0.446
9	TGIN	C	40.06				
10	TLIN	C	41.59	41.61	0.83	0.81	0.029
11	T4077	C	46.14	45.81	2.31	0.95	-0.141
12	T4076	C	52.23	52.03	2.61	1.62	-0.075
13	T4075	C	54.35	55.37	2.72	1.63	0.375
14	T4073	C	56.84	56.25	2.84	1.24	-0.207
15	TLOUT	C	49.13	48.49	2.46	1.80	-0.260
16	RHLDG			0.532			
17	LCO2RH	MOL/HR		12586			
18	LNLDG			0.411			
19	AVELIQ	SQM		0.00095			
20	AVEGAS	CUM/SEC		0.217			
21	AREA	SQM		1.83			
22	AVAREA	SQM		1.85			

Table G-20. Run 4.11.2 Data-Fit Results

Vary No.	Initial Value	Est Value	Stnd Dev	95% Conf Int Low Limit	95% Conf Int Up Limit
1	1.78	1.80	0.52	1.00	2.81
2	26074	26244	6401	13699	38789

	Var Name	Units	Meas Val	Est Val	Meas σ	Est σ	Norm Residue
1	GN2IN	MOL/HR	23117				
2	GH2OIN	MOL/HR	1955				
3	GCO2IN	MOL/HR	4192	4188	84	83	-0.050
4	GCO2OT	MOL/HR	1353	1356	68	67	0.042
5	LK2CO3	MOL/HR	6136				
6	LPZ	MOL/HR	5834				
7	LH2O	MOL/HR	143474				
8	LCO2IN	MOL/HR	3832	3642	574.8	349	-0.331
9	TGIN	C	39.97				
10	TLIN	C	41.2	41.22	0.82	0.80	0.021
11	T4077	C	45.42	45.24	2.27	0.89	-0.080
12	T4076	C	51.32	51.07	2.57	1.57	-0.096
13	T4075	C	53.49	54.40	2.67	1.60	0.341
14	T4073	C	55.99	55.51	2.80	1.44	-0.172
15	TLOUT	C	48.89	48.34	2.44	1.84	-0.224
16	RHLDG			0.527			
17	LCO2RH	MOL/HR		12611			
18	LNLDG			0.408			
19	AVELIQ	SQM		0.00096			
20	AVEGAS	CUM/SEC		0.217			
21	AREA	SQM		1.80			
22	AVAREA	SQM		1.81			

Table G-21. Run 4.12.1 Data-Fit Results

Vary No.	Initial Value	Est Value	Stnd Dev	95% Conf Int Low Limit	95% Conf Int Up Limit
1	2.50	2.49	1.97	1.00	5.00
2	20574	22151	36870	5000	50000

	Var Name	Units	Meas Val	Est Val	Meas σ	Est σ	Norm Residue
1	GN2IN	MOL/HR	30351				
2	GH2OIN	MOL/HR	2636				
3	GCO2IN	MOL/HR	3922	4000	1177	961	0.066
4	GCO2OT	MOL/HR	1539	1531	462	439	-0.017
5	LK2CO3	MOL/HR	6248				
6	LPZ	MOL/HR	5941				
7	LH2O	MOL/HR	142996				
8	LCO2IN	MOL/HR	3752	4182	1876	829	0.229
9	TGIN	C	40.09				
10	TLIN	C	39.81	39.93	5.97	5.88	0.020
11	T4077	C	49.52	49.10	7.43	6.34	-0.056
12	T4076	C	56.29	56.77	8.44	5.54	0.056
13	T4075	C	57.19	57.28	8.58	4.35	0.011
14	T4073	C	55.48	55.92	8.32	5.34	0.053
15	TLOUT	C	46.45	46.58	6.97	4.61	0.019
16	RHLDG			0.529			
17	LCO2RH	MOL/HR		12899			
18	LNLDG			0.428			
19	AVELIQ	SQM		0.00097			
20	AVEGAS	CUM/SEC		0.284			
21	AREA	SQM		2.50			
22	AVAREA	SQM		2.55			

Table G-22. Run 4.12.2 Data-Fit Results

Vary No.	Initial Value	Est Value	Stnd Dev	95% Conf Int Low Limit	95% Conf Int Up Limit
1	2.26	2.26	0.88	1.00	3.99
2	22821	22821	11969	5000	46279

	Var Name	Units	Meas Val	Est Val	Meas σ	Est σ	Norm Residue
1	GN2IN	MOL/HR	29799				
2	GH2OIN	MOL/HR	2628				
3	GCO2IN	MOL/HR	4405	4409	220	216	0.020
4	GCO2OT	MOL/HR	1887	1887	189	185	-0.001
5	LK2CO3	MOL/HR	6231				
6	LPZ	MOL/HR	5894				
7	LH2O	MOL/HR	142745				
8	LCO2IN	MOL/HR	3902	4123	1170.6	338	0.189
9	TGIN	C	40.11				
10	TLIN	C	39.86	39.91	1.99	1.98	0.023
11	T4077	C	50.68	50.14	5.07	4.09	-0.106
12	T4076	C	56.61	57.22	5.66	3.11	0.108
13	T4075	C	57.1	57.28	5.71	2.10	0.032
14	T4073	C	55.1	55.70	5.51	2.37	0.109
15	TLOUT	C	46.41	46.36	2.32	1.99	-0.023
16	RHLDG			0.531			
17	LCO2RH	MOL/HR		12874			
18	LNLDG			0.427			
19	AVELIQ	SQM		0.00097			
20	AVEGAS	CUM/SEC		0.285			
21	AREA	SQM		2.26			
22	AVAREA	SQM		2.31			

Table G-23. Run 4.13.1 Data-Fit Results

Vary No.	Initial Value	Est Value	Stnd Dev	95% Conf Int Low Limit	95% Conf Int Up Limit
1	1.53	1.53	0.59	1.00	2.69
2	33381	31287	50937	5000	50000

	Var Name	Units	Meas Val	Est Val	Meas σ	Est σ	Norm Residue
1	GN2IN	MOL/HR	26664				
2	GH2OIN	MOL/HR	2326				
3	GCO2IN	MOL/HR	5733	5738	860	853	0.005
4	GCO2OT	MOL/HR	1486	1487	223	223	0.006
5	LK2CO3	MOL/HR	11771				
6	LPZ	MOL/HR	11193				
7	LH2O	MOL/HR	293989				
8	LCO2IN	MOL/HR	6561	6608	2296.35	2256	0.021
9	TGIN	C	40.02				
10	TLIN	C	41.48	41.73	6.22	3.91	0.041
11	T4077	C	42.57	42.79	6.39	3.82	0.035
12	T4076	C	44.76	44.56	6.71	3.03	-0.030
13	T4075	C	46.63	46.23	6.99	3.28	-0.057
14	T4073	C	48.45	47.86	7.27	4.25	-0.081
15	TLOUT	C	47.65	48.64	7.15	5.20	0.138
16	RHLDG			0.493			
17	LCO2RH	MOL/HR		22630			
18	LNLDG			0.400			
19	AVELIQ	SQM		0.00191			
20	AVEGAS	CUM/SEC		0.241			
21	AREA	SQM		2.00			
22	AVAREA	SQM		2.00			

Table G-24. Run 4.13.2 Data-Fit Results

Vary No.	Initial Value	Est Value	Stnd Dev	95% Conf Int Low Limit	95% Conf Int Up Limit
1	1.72	1.72	0.77	1.00	3.23
2	29046	29046	26071	5000	50000

	Var Name	Units	Meas Val	Est Val	Meas σ	Est σ	Norm Residue
1	GN2IN	MOL/HR	27197				
2	GH2OIN	MOL/HR	2350				
3	GCO2IN	MOL/HR	5488	5498	823	819	0.012
4	GCO2OT	MOL/HR	1278	1281	192	191	0.017
5	LK2CO3	MOL/HR	12001				
6	LPZ	MOL/HR	11309				
7	LH2O	MOL/HR	290576				
8	LCO2IN	MOL/HR	7198	7252	2159.4	2141	0.025
9	TGIN	C	39.94				
10	TLIN	C	43.02	43.17	4.30	3.82	0.034
11	T4077	C	44.08	44.20	6.61	2.77	0.019
12	T4076	C	46.33	46.13	6.95	2.75	-0.029
13	T4075	C	48.54	47.97	7.28	3.40	-0.079
14	T4073	C	50.53	49.74	7.58	4.26	-0.105
15	TLOUT	C	49.17	49.75	4.92	3.01	0.118
16	RHLDG			0.503			
17	LCO2RH	MOL/HR		23448			
18	LNLDG			0.413			
19	AVELIQ	SQM		0.00190			
20	AVEGAS	CUM/SEC		0.247			
21	AREA	SQM		2.24			
22	AVAREA	SQM		2.25			

Table G-25. Run 4.14.1 Data-Fit Results

Vary No.	Initial Value	Est Value	Stnd Dev	95% Conf Int Low Limit	95% Conf Int Up Limit
1	1.76	1.76	0.32	1.14	2.38
2	27289	27289	12704	5000	50000

	Var Name	Units	Meas Val	Est Val	Meas σ	Est σ	Norm Residue
1	GN2IN	MOL/HR	21811				
2	GH2OIN	MOL/HR	1902				
3	GCO2IN	MOL/HR	4661	4661	93	93	-0.001
4	GCO2OT	MOL/HR	678	680	68	68	0.035
5	LK2CO3	MOL/HR	12740				
6	LPZ	MOL/HR	11866				
7	LH2O	MOL/HR	297530				
8	LCO2IN	MOL/HR	7684	7794	1152.6	1128	0.095
9	TGIN	C	40.07				
10	TLIN	C	42.76	42.81	0.86	0.80	0.060
11	T4077	C	43.11	43.29	2.16	0.68	0.085
12	T4076	C	44.75	44.50	2.24	0.81	-0.113
13	T4075	C	46.17	45.86	2.31	1.07	-0.133
14	T4073	C	48.11	47.38	2.41	1.37	-0.304
15	TLOUT	C	48.19	49.19	2.41	1.54	0.415
16	RHLDG			0.498			
17	LCO2RH	MOL/HR		24527			
18	LNLDG			0.418			
19	AVELIQ	SQM		0.00196			
20	AVEGAS	CUM/SEC		0.195			
21	AREA	SQM		2.35			
22	AVAREA	SQM		2.35			

Table G-26. Run 4.14.2 Data-Fit Results

Vary No.	Initial Value	Est Value	Stnd Dev	95% Conf Int Low Limit	95% Conf Int Up Limit
1	1.92	1.92	0.32	1.29	2.54
2	25903	25903	12590	5000	50000

	Var Name	Units	Meas Val	Est Val	Meas σ	Est σ	Norm Residue
1	GN2IN	MOL/HR	21893				
2	GH2OIN	MOL/HR	1882				
3	GCO2IN	MOL/HR	4287	4287	86	86	-0.002
4	GCO2OT	MOL/HR	506	508	51	50	0.033
5	LK2CO3	MOL/HR	12434				
6	LPZ	MOL/HR	11796				
7	LH2O	MOL/HR	299649				
8	LCO2IN	MOL/HR	7566	7666	1134.9	1109	0.088
9	TGIN	C	39.91				
10	TLIN	C	42.8	42.86	0.86	0.78	0.065
11	T4077	C	42.93	43.11	2.15	0.69	0.085
12	T4076	C	44.16	44.04	2.21	0.76	-0.053
13	T4075	C	45.55	45.23	2.28	0.98	-0.142
14	T4073	C	47.51	46.63	2.38	1.32	-0.369
15	TLOUT	C	47.93	48.87	2.40	1.68	0.393
16	RHLDG			0.493			
17	LCO2RH	MOL/HR		23899			
18	LNLDG			0.415			
19	AVELIQ	SQM		0.00196			
20	AVEGAS	CUM/SEC		0.191			
21	AREA	SQM		2.56			
22	AVAREA	SQM		2.56			

Table G-27. Run 4.15.1 Data-Fit Results

Vary No.	Initial Value	Est Value	Stnd Dev	95% Conf Int Low Limit	95% Conf Int Up Limit
1	1.65	1.69	0.59	1.00	2.85
2	25701	25200	16626	5000	50000

	Var Name	Units	Meas Val	Est Val	Meas σ	Est σ	Norm Residue
1	GN2IN	MOL/HR	16093				
2	GH2OIN	MOL/HR	1393				
3	GCO2IN	MOL/HR	3311	3302	331	330	-0.026
4	GCO2OT	MOL/HR	328	332	66	65	0.054
5	LK2CO3	MOL/HR	10217				
6	LPZ	MOL/HR	9692				
7	LH2O	MOL/HR	229882				
8	LCO2IN	MOL/HR	5822	6141	2328.8	2249	0.137
9	TGIN	C	39.98				
10	TLIN	C	39.54	39.86	1.98	1.75	0.160
11	T4077	C	39.72	39.78	3.97	1.43	0.014
12	T4076	C	40.99	40.37	4.10	1.37	-0.152
13	T4075	C	42.24	41.31	4.22	1.53	-0.221
14	T4073	C	43.96	42.53	4.40	1.75	-0.326
15	TLOUT	C	45.48	46.05	2.27	2.00	0.249
16	RHLDG			0.485			
17	LCO2RH	MOL/HR		19328			
18	LNLDG			0.411			
19	AVELIQ	SQM		0.00153			
20	AVEGAS	CUM/SEC		0.136			
21	AREA	SQM		2.07			
22	AVAREA	SQM		2.07			

Table G-28. Run 4.15.2 Data-Fit Results

Vary No.	Initial Value	Est Value	Stnd Dev	95% Conf Int Low Limit	95% Conf Int Up Limit
1	1.57	1.57	0.19	1.19	1.95
2	19757	19757	9910	5000	39181

	Var Name	Units	Meas Val	Est Val	Meas σ	Est σ	Norm Residue
1	GN2IN	MOL/HR	16013				
2	GH2OIN	MOL/HR	1381				
3	GCO2IN	MOL/HR	3360	3359	67	67	-0.016
4	GCO2OT	MOL/HR	370	371	19	18	0.037
5	LK2CO3	MOL/HR	10217				
6	LPZ	MOL/HR	9691				
7	LH2O	MOL/HR	231145				
8	LCO2IN	MOL/HR	5853	5933	877.95	868	0.091
9	TGIN	C	39.96				
10	TLIN	C	39.61	39.72	0.79	0.74	0.133
11	T4077	C	39.83	39.94	1.99	0.63	0.053
12	T4076	C	41.18	40.80	2.06	0.73	-0.186
13	T4075	C	42.52	41.92	2.13	0.93	-0.282
14	T4073	C	44.11	43.29	2.21	1.17	-0.372
15	TLOUT	C	45.61	46.88	2.28	1.55	0.558
16	RHLDG			0.481			
17	LCO2RH	MOL/HR		19159			
18	LNLDG			0.406			
19	AVELIQ	SQM		0.00153			
20	AVEGAS	CUM/SEC		0.137			
21	AREA	SQM		1.93			
22	AVAREA	SQM		1.92			

Table G-29. Run 4.16.1 Data-Fit Results

Vary No.	Initial Value	Est Value	Stnd Dev	95% Conf Int Low Limit	95% Conf Int Up Limit
1	1.49	1.49	0.82	1.00	3.09
2	25709	25709	16419	5000	50000

	Var Name	Units	Meas Val	Est Val	Meas σ	Est σ	Norm Residue
1	GN2IN	MOL/HR	27500				
2	GH2OIN	MOL/HR	2421				
3	GCO2IN	MOL/HR	5581	5617	558	554	0.065
4	GCO2OT	MOL/HR	1864	1870	280	277	0.022
5	LK2CO3	MOL/HR	11007				
6	LPZ	MOL/HR	11078				
7	LH2O	MOL/HR	235588				
8	LCO2IN	MOL/HR	7382	7630	1845.5	1699	0.134
9	TGIN	C	40.02				
10	TLIN	C	41.4	41.47	2.07	1.94	0.036
11	T4077	C	42.89	43.37	4.29	1.57	0.111
12	T4076	C	46.45	46.08	4.65	1.86	-0.080
13	T4075	C	49.16	48.26	4.92	2.36	-0.183
14	T4073	C	51.13	50.03	5.11	2.71	-0.216
15	TLOUT	C	48.46	49.10	2.42	1.70	0.263
16	RHLDG			0.507			
17	LCO2RH	MOL/HR		22400			
18	LNLDG			0.423			
19	AVELIQ	SQM		0.00162			
20	AVEGAS	CUM/SEC		0.254			
21	AREA	SQM		1.88			
22	AVAREA	SQM		1.89			

Table G-30. Run 4.16.2 Data-Fit Results

Vary No.	Initial Value	Est Value	Stnd Dev	95% Conf Int Low Limit	95% Conf Int Up Limit
1	1.96	1.96	0.74	1.00	3.41
2	20439	20439	18359	5000	50000

	Var Name	Units	Meas Val	Est Val	Meas σ	Est σ	Norm Residue
1	GN2IN	MOL/HR	28983				
2	GH2OIN	MOL/HR	2526				
3	GCO2IN	MOL/HR	4550	4562	455	453	0.027
4	GCO2OT	MOL/HR	1173	1173	117	117	0.003
5	LK2CO3	MOL/HR	10381				
6	LPZ	MOL/HR	9949				
7	LH2O	MOL/HR	247548				
8	LCO2IN	MOL/HR	6759	6856	1351.8	1264	0.072
9	TGIN	C	40.05				
10	TLIN	C	41.29	41.26	2.06	1.83	-0.017
11	T4077	C	42.03	42.64	4.20	1.62	0.145
12	T4076	C	44.75	44.82	4.48	1.66	0.016
13	T4075	C	47.39	46.82	4.74	2.09	-0.121
14	T4073	C	49.49	48.67	4.95	2.56	-0.166
15	TLOUT	C	48.15	48.51	2.41	1.87	0.148
16	RHLDG			0.507			
17	LCO2RH	MOL/HR		20620			
18	LNLDG			0.424			
19	AVELIQ	SQM		0.00163			
20	AVEGAS	CUM/SEC		0.256			
21	AREA	SQM		2.42			
22	AVAREA	SQM		2.44			

Table G-31. Run 4.17.1 Data-Fit Results

Vary No.	Initial Value	Est Value	Stnd Dev	95% Conf Int Low Limit	95% Conf Int Up Limit
1	1.30	1.29	0.15	1.01	1.58
2	15600	15124	7753	5000	30320

	Var Name	Units	Meas Val	Est Val	Meas σ	Est σ	Norm Residue
1	GN2IN	MOL/HR	27746				
2	GH2OIN	MOL/HR	2385				
3	GCO2IN	MOL/HR	5686	5685	114	114	-0.008
4	GCO2OT	MOL/HR	1449	1463	145	144	0.097
5	LK2CO3	MOL/HR	11025				
6	LPZ	MOL/HR	10393				
7	LH2O	MOL/HR	246642				
8	LCO2IN	MOL/HR	4753	4767	712.95	713	0.020
9	TGIN	C	39.99				
10	TLIN	C	40.15	40.15	0.80	0.75	-0.004
11	T4077	C	41.51	42.33	2.08	0.68	0.394
12	T4076	C	45.92	45.72	2.30	0.91	-0.089
13	T4075	C	49.88	48.86	2.49	1.31	-0.409
14	T4073	C	52.76	51.71	2.64	1.69	-0.399
15	TLOUT	C	49.49	51.92	2.47	1.09	0.982
16	RHLDG			0.467			
17	LCO2RH	MOL/HR		20014			
18	LNLDG			0.369			
19	AVELIQ	SQM		0.00164			
20	AVEGAS	CUM/SEC		0.254			
21	AREA	SQM		1.63			
22	AVAREA	SQM		1.61			

Table G-32. Run 4.17.2 Data-Fit Results

Vary No.	Initial Value	Est Value	Stnd Dev	95% Conf Int Low Limit	95% Conf Int Up Limit
1	1.65	1.65	1.01	1.00	3.62
2	17735	17735	53277	5000	50000

	Var Name	Units	Meas Val	Est Val	Meas σ	Est σ	Norm Residue
1	GN2IN	MOL/HR	27547				
2	GH2OIN	MOL/HR	2492				
3	GCO2IN	MOL/HR	5813	5912	2035	1983	0.049
4	GCO2OT	MOL/HR	1253	1258	439	435	0.010
5	LK2CO3	MOL/HR	10707				
6	LPZ	MOL/HR	10182				
7	LH2O	MOL/HR	248446				
8	LCO2IN	MOL/HR	5179	5295	2330.55	2300	0.050
9	TGIN	C	40.06				
10	TLIN	C	40.63	40.62	6.09	4.49	-0.001
11	T4077	C	42.04	42.72	6.31	3.54	0.108
12	T4076	C	46.43	46.29	6.96	3.23	-0.021
13	T4075	C	50.75	49.92	7.61	4.06	-0.109
14	T4073	C	54	53.42	8.10	5.66	-0.072
15	TLOUT	C	50.98	52.83	7.65	3.79	0.241
16	RHLDG			0.495			
17	LCO2RH	MOL/HR		20658			
18	LNLDG			0.383			
19	AVELIQ	SQM		0.00165			
20	AVEGAS	CUM/SEC		0.255			
21	AREA	SQM		2.07			
22	AVAREA	SQM		2.06			

Table G-33. Run 4.18 Data-Fit Results

Vary No.	Initial Value	Est Value	Stnd Dev	95% Conf Int Low Limit	95% Conf Int Up Limit
1	2.66	2.78	0.98	1.00	4.69
2	23556	24647	8549	7891	41403

	Var Name	Units	Meas Val	Est Val	Meas σ	Est σ	Norm Residue
1	GN2IN	MOL/HR	27786				
2	GH2OIN	MOL/HR	2472				
3	GCO2IN	MOL/HR	4688	4718	469	427	0.063
4	GCO2OT	MOL/HR	560	559	84	81	-0.017
5	LK2CO3	MOL/HR	8771				
6	LPZ	MOL/HR	8274				
7	LH2O	MOL/HR	197451				
8	LCO2IN	MOL/HR	4498	4695	899.6	771	0.219
9	TGIN	C	40.49				
10	TLIN	C	39.98	39.84	2.00	1.46	-0.071
11	T4077	C	41.07	41.08	2.05	1.25	0.006
12	T4076	C	44.45	44.77	2.22	1.10	0.142
13	T4075	C	50.37	50.22	2.52	1.76	-0.061
14	T4073	C	56.23	56.18	2.81	2.28	-0.019
15	TLOUT	C	51.31	52.01	2.57	1.18	0.273
16	RHLDG			0.517			
17	LCO2RH	MOL/HR		17625			
18	LNLDG			0.395			
19	AVELIQ	SQM		0.00132			
20	AVEGAS	CUM/SEC		0.251			
21	AREA	SQM		3.19			
22	AVAREA	SQM		3.19			

Table G-34. Run 4.19 Data-Fit Results

Vary No.	Initial Value	Est Value	Stnd Dev	95% Conf Int Low Limit	95% Conf Int Up Limit
1	2.98	2.93	1.11	1.00	5.00
2	22099	21468	11392	5000	43795

	Var Name	Units	Meas Val	Est Val	Meas σ	Est σ	Norm Residue
1	GN2IN	MOL/HR	27756				
2	GH2OIN	MOL/HR	2486				
3	GCO2IN	MOL/HR	4359	4392	654	573	0.051
4	GCO2OT	MOL/HR	394	393	79	75	-0.008
5	LK2CO3	MOL/HR	9261				
6	LPZ	MOL/HR	8783				
7	LH2O	MOL/HR	189428				
8	LCO2IN	MOL/HR	5063	5249	1012.6	800	0.183
9	TGIN	C	40.42				
10	TLIN	C	40.26	40.16	2.01	1.45	-0.048
11	T4077	C	41.18	41.07	2.06	1.20	-0.055
12	T4076	C	43.93	44.26	2.20	1.10	0.148
13	T4075	C	49.71	49.52	2.49	1.73	-0.078
14	T4073	C	56.28	56.07	2.81	2.40	-0.073
15	TLOUT	C	52.11	52.75	2.61	1.59	0.245
16	RHLDG			0.513			
17	LCO2RH	MOL/HR		18495			
18	LNLDG			0.402			
19	AVELIQ	SQM		0.00131			
20	AVEGAS	CUM/SEC		0.248			
21	AREA	SQM		3.38			
22	AVAREA	SQM		3.39			

Table G-35. Run 4.20.1 Data-Fit Results

Vary No.	Initial Value	Est Value	Stnd Dev	95% Conf Int Low Limit	95% Conf Int Up Limit
1	2.11	2.11	4.21	1.00	5.00
2	8663	8663	41235	5000	40000

	Var Name	Units	Meas Val	Est Val	Meas σ	Est σ	Norm Residue
1	GN2IN	MOL/HR	16649				
2	GH2OIN	MOL/HR	1533				
3	GCO2IN	MOL/HR	3300	3289	660	657	-0.017
4	GCO2OT	MOL/HR	747	748	149	149	0.004
5	LK2CO3	MOL/HR	12704				
6	LPZ	MOL/HR	7499				
7	LH2O	MOL/HR	272216				
8	LCO2IN	MOL/HR	7912	7262	4747.2	3679	-0.137
9	TGIN	C	41.13				
10	TLIN	C	40.52	40.16	4.05	3.59	-0.089
11	T4077	C	40.5	40.80	6.08	2.58	0.050
12	T4076	C	41.11	41.93	6.17	2.70	0.133
13	T4075	C	42.43	42.81	6.36	3.13	0.060
14	T4073	C	43.62	43.54	6.54	3.31	-0.012
15	TLOUT	C	44.89	44.49	4.49	3.90	-0.090
16	RHLDG			0.557			
17	LCO2RH	MOL/HR		22524			
18	LNLDG			0.495			
19	AVELIQ	SQM		0.00172			
20	AVEGAS	CUM/SEC		0.146			
21	AREA	SQM		2.62			
22	AVAREA	SQM		2.67			

Table G-36. Run 4.20.2 Data-Fit Results

Vary No.	Initial Value	Est Value	Stnd Dev	95% Conf Int Low Limit	95% Conf Int Up Limit
1	1.54	1.54	2.11	1.00	5.00
2	7640	8519	73158	5000	40000

	Var Name	Units	Meas Val	Est Val	Meas σ	Est σ	Norm Residue
1	GN2IN	MOL/HR	17003				
2	GH2OIN	MOL/HR	1510				
3	GCO2IN	MOL/HR	3254	3249	651	643	-0.008
4	GCO2OT	MOL/HR	957	949	287	287	-0.027
5	LK2CO3	MOL/HR	12456				
6	LPZ	MOL/HR	6629				
7	LH2O	MOL/HR	236926				
8	LCO2IN	MOL/HR	6254	6054	3127	2998	-0.064
9	TGIN	C	41.09				
10	TLIN	C	38.6	37.54	5.79	4.74	-0.183
11	T4077	C	37.15	38.22	7.43	2.84	0.144
12	T4076	C	38.17	39.32	7.63	2.80	0.151
13	T4075	C	39.82	40.18	5.97	2.89	0.060
14	T4073	C	41.14	40.92	6.17	3.04	-0.035
15	TLOUT	C	43.45	42.51	6.52	5.37	-0.144
16	RHLDG			0.545			
17	LCO2RH	MOL/HR		20814			
18	LNLDG			0.485			
19	AVELIQ	SQM		0.00151			
20	AVEGAS	CUM/SEC		0.148			
21	AREA	SQM		1.82			
22	AVAREA	SQM		1.85			

Table G-37. Run 4.21.1 Data-Fit Results

Vary No.	Initial Value	Est Value	Stnd Dev	95% Conf Int Low Limit	95% Conf Int Up Limit
1	3.01	3.05	5.00	2.00	4.00
2	10780	11029	54138	5000	15000

	Var Name	Units	Meas Val	Est Val	Meas σ	Est σ	Norm Residue
1	GN2IN	MOL/HR	17449				
2	GH2OIN	MOL/HR	1608				
3	GCO2IN	MOL/HR	2979	2972	447	444	-0.017
4	GCO2OT	MOL/HR	600	600	90	90	0.001
5	LK2CO3	MOL/HR	12539				
6	LPZ	MOL/HR	7383				
7	LH2O	MOL/HR	272319				
8	LCO2IN	MOL/HR	7722	7554	2316.6	2077	-0.073
9	TGIN	C	41.1				
10	TLIN	C	39	38.42	5.85	4.51	-0.099
11	T4077	C	38.83	38.92	5.82	3.22	0.016
12	T4076	C	39.19	39.92	5.88	2.70	0.124
13	T4075	C	40.39	40.70	6.06	3.05	0.051
14	T4073	C	41.45	41.31	6.22	3.43	-0.022
15	TLOUT	C	42.98	42.32	6.45	4.74	-0.102
16	RHLDG			0.564			
17	LCO2RH	MOL/HR		22465			
18	LNLDG			0.504			
19	AVELIQ	SQM		0.00172			
20	AVEGAS	CUM/SEC		0.148			
21	AREA	SQM		3.75			
22	AVAREA	SQM		3.82			

Table G-38. Run 4.21.2 Data-Fit Results

Vary No.	Initial Value	Est Value	Stnd Dev	95% Conf Int Low Limit	95% Conf Int Up Limit
1	2.65	2.27	4.14	2.00	4.00
2	8801	8490	41771	5000	15000

	Var Name	Units	Meas Val	Est Val	Meas σ	Est σ	Norm Residue
1	GN2IN	MOL/HR	16649				
2	GH2OIN	MOL/HR	1533				
3	GCO2IN	MOL/HR	3300	3281	660	655	-0.028
4	GCO2OT	MOL/HR	747	747	299	299	0.002
5	LK2CO3	MOL/HR	12704				
6	LPZ	MOL/HR	7499				
7	LH2O	MOL/HR	272216				
8	LCO2IN	MOL/HR	7912	7393	3560.4	2864	-0.146
9	TGIN	C	41.13				
10	TLIN	C	40.52	40.12	4.05	3.57	-0.099
11	T4077	C	40.5	40.81	6.08	2.62	0.051
12	T4076	C	41.11	41.98	6.17	2.71	0.141
13	T4075	C	42.43	42.87	6.36	3.09	0.069
14	T4073	C	43.62	43.59	6.54	3.26	-0.005
15	TLOUT	C	44.89	44.44	4.49	3.84	-0.100
16	RHLDG			0.560			
17	LCO2RH	MOL/HR		22631			
18	LNLDG			0.497			
19	AVELIQ	SQM		0.00172			
20	AVEGAS	CUM/SEC		0.146			
21	AREA	SQM		2.79			
22	AVAREA	SQM		2.84			

Table G-39. Run 4.22.2 Data-Fit Results

Vary No.	Initial Value	Est Value	Stnd Dev	95% Conf Int Low Limit	95% Conf Int Up Limit
1	1.19	1.19	1.49	1.00	4.11
2	10391	10391	32367	5000	40000

	Var Name	Units	Meas Val	Est Val	Meas σ	Est σ	Norm Residue
1	GN2IN	MOL/HR	15811				
2	GH2OIN	MOL/HR	1495				
3	GCO2IN	MOL/HR	3616	3581	542	533	-0.065
4	GCO2OT	MOL/HR	1563	1576	391	388	0.033
5	LK2CO3	MOL/HR	9590				
6	LPZ	MOL/HR	5252				
7	LH2O	MOL/HR	141211				
8	LCO2IN	MOL/HR	5000	4807	1500	1386	-0.129
9	TGIN	C	41.67				
10	TLIN	C	36.71	35.93	5.51	4.44	-0.141
11	T4077	C	37.56	37.43	5.63	2.96	-0.023
12	T4076	C	37.77	39.22	5.67	2.70	0.256
13	T4075	C	40.37	40.34	6.06	2.97	-0.005
14	T4073	C	40.98	41.15	6.15	3.39	0.028
15	TLOUT	C	43.98	42.69	6.60	4.63	-0.195
16	RHLDG			0.553			
17	LCO2RH	MOL/HR		16407			
18	LNLDG			0.485			
19	AVELIQ	SQM		0.00097			
20	AVEGAS	CUM/SEC		0.141			
21	AREA	SQM		1.22			
22	AVAREA	SQM		1.25			

Table G-40. Run 4.23 Data-Fit Results

Vary No.	Initial Value	Est Value	Stnd Dev	95% Conf Int Low Limit	95% Conf Int Up Limit
1	1.55	1.55	1.92	1.00	5.00
2	3400	3400	29265	100	40000

	Var Name	Units	Meas Val	Est Val	Meas σ	Est σ	Norm Residue
1	GN2IN	MOL/HR	16312				
2	GH2OIN	MOL/HR	1532				
3	GCO2IN	MOL/HR	3597	3532	719	694	-0.091
4	GCO2OT	MOL/HR	1361	1372	340	339	0.033
5	LK2CO3	MOL/HR	9522				
6	LPZ	MOL/HR	5144				
7	LH2O	MOL/HR	175448				
8	LCO2IN	MOL/HR	5000	4721	1500	1282	-0.186
9	TGIN	C	41.66				
10	TLIN	C	37.83	37.46	3.78	3.48	-0.098
11	T4077	C	38.96	39.18	5.84	2.44	0.038
12	T4076	C	40.16	41.26	6.02	2.78	0.183
13	T4075	C	42.17	42.62	6.33	3.09	0.072
14	T4073	C	43.3	43.63	6.50	3.21	0.051
15	TLOUT	C	45.64	44.71	4.56	3.63	-0.204
16	RHLDG			0.559			
17	LCO2RH	MOL/HR		16397			
18	LNLDG			0.485			
19	AVELIQ	SQM		0.00113			
20	AVEGAS	CUM/SEC		0.147			
21	AREA	SQM		1.62			
22	AVAREA	SQM		1.65			

Table G-41. Run 4.24 Data-Fit Results

Vary No.	Initial Value	Est Value	Stnd Dev	95% Conf Int Low Limit	95% Conf Int Up Limit
1	1.39	1.42	1.83	1.00	5.00
2	8918	9406	29414	5000	40000

	Var Name	Units	Meas Val	Est Val	Meas σ	Est σ	Norm Residue
1	GN2IN	MOL/HR	16516				
2	GH2OIN	MOL/HR	1579				
3	GCO2IN	MOL/HR	3483	3404	871	834	-0.090
4	GCO2OT	MOL/HR	1285	1295	386	384	0.026
5	LK2CO3	MOL/HR	8551				
6	LPZ	MOL/HR	4643				
7	LH2O	MOL/HR	150152				
8	LCO2IN	MOL/HR	4236	3959	1694	1457	-0.163
9	TGIN	C	41.66				
10	TLIN	C	37.49	37.10	4.50	3.90	-0.086
11	T4077	C	38.61	38.67	5.79	2.78	0.011
12	T4076	C	40.05	40.75	6.01	2.82	0.116
13	T4075	C	41.6	42.12	6.24	3.18	0.083
14	T4073	C	42.87	43.13	6.43	3.47	0.040
15	TLOUT	C	45.31	44.35	5.44	4.21	-0.176
16	RHLDG			0.555			
17	LCO2RH	MOL/HR		14639			
18	LNLDG			0.475			
19	AVELIQ	SQM		0.00098			
20	AVEGAS	CUM/SEC		0.147			
21	AREA	SQM		1.43			
22	AVAREA	SQM		1.46			

Table G-42. Run 4.25 Data-Fit Results

Vary No.	Initial Value	Est Value	Stnd Dev	95% Conf Int Low Limit	95% Conf Int Up Limit
1	1.50	1.49	1.09	1.00	3.62
2	18047	17828	21005	5000	40000

	Var Name	Units	Meas Val	Est Val	Meas σ	Est σ	Norm Residue
1	GN2IN	MOL/HR	16670				
2	GH2OIN	MOL/HR	1596				
3	GCO2IN	MOL/HR	3307	3281	661	650	-0.040
4	GCO2OT	MOL/HR	976	976	195	195	-0.001
5	LK2CO3	MOL/HR	9074				
6	LPZ	MOL/HR	5012	5046.369	751.8	732	0.046
7	LH2O	MOL/HR	174887				
8	LCO2IN	MOL/HR	4163	4081	1041	989	-0.079
9	TGIN	C	41.72				
10	TLIN	C	39.48	39.30	1.97	1.83	-0.093
11	T4077	C	39.76	40.02	3.98	1.47	0.065
12	T4076	C	40.34	41.39	4.03	1.71	0.260
13	T4075	C	42.54	42.42	4.25	2.10	-0.027
14	T4073	C	43.46	43.26	4.35	2.45	-0.046
15	TLOUT	C	44.9	44.38	4.49	3.01	-0.117
16	RHLDG			0.547			
17	LCO2RH	MOL/HR		15460			
18	LNLDG			0.466			
19	AVELIQ	SQM		0.00112			
20	AVEGAS	CUM/SEC		0.146			
21	AREA	SQM		1.54			
22	AVAREA	SQM		1.57			

Table G-43. Run 4.26.1 Data-Fit Results

Vary No.	Initial Value	Est Value	Stnd Dev	95% Conf Int Low Limit	95% Conf Int Up Limit
1	1.82	1.82	1.06	1.00	3.91
2	8674	8674	7681	5000	23729

	Var Name	Units	Meas Val	Est Val	Meas σ	Est σ	Norm Residue
1	GN2IN	MOL/HR	15978				
2	GH2OIN	MOL/HR	1270				
3	GCO2IN	MOL/HR	3331	3331	500	489	0.000
4	GCO2OT	MOL/HR	612	607	92	92	-0.049
5	LK2CO3	MOL/HR	11040				
6	LPZ	MOL/HR	6098				
7	LH2O	MOL/HR	216418				
8	LCO2IN	MOL/HR	5006	5001	1501.8	1487	-0.003
9	TGIN	C	38.71				
10	TLIN	C	38.33	38.13	5.75	5.75	-0.035
11	T4077	C	38.85	39.04	5.83	2.96	0.033
12	T4076	C	39.89	40.56	5.98	2.89	0.112
13	T4075	C	41.59	41.87	6.24	2.95	0.045
14	T4073	C	43.13	43.06	6.47	3.03	-0.011
15	TLOUT	C	44.47	44.62	6.67	2.41	0.022
16	RHLDG			0.548			
17	LCO2RH	MOL/HR		18774			
18	LNLDG			0.468			
19	AVELIQ	SQM		0.00138			
20	AVEGAS	CUM/SEC		0.138			
21	AREA	SQM		2.06			
22	AVAREA	SQM		2.09			

Table G-44. Run 4.26.2 Data-Fit Results

Vary No.	Initial Value	Est Value	Stnd Dev	95% Conf Int Low Limit	95% Conf Int Up Limit
1	1.78	1.78	1.59	1.00	4.89
2	7857	8123	21665	5000	40000

	Var Name	Units	Meas Val	Est Val	Meas σ	Est σ	Norm Residue
1	GN2IN	MOL/HR	15777				
2	GH2OIN	MOL/HR	1344				
3	GCO2IN	MOL/HR	3440	3440	172	171	-0.001
4	GCO2OT	MOL/HR	696	695	104	104	-0.006
5	LK2CO3	MOL/HR	10891				
6	LPZ	MOL/HR	6013				
7	LH2O	MOL/HR	218482				
8	LCO2IN	MOL/HR	5000	4980	1500	1480	-0.013
9	TGIN	C	39.98				
10	TLIN	C	38.68	38.54	3.87	2.71	-0.037
11	T4077	C	39.31	39.41	5.90	3.16	0.016
12	T4076	C	40.59	41.04	6.09	3.33	0.073
13	T4075	C	42.25	42.38	6.34	3.15	0.021
14	T4073	C	43.8	43.56	6.57	2.71	-0.037
15	TLOUT	C	45.14	45.04	4.51	3.36	-0.022
16	RHLDG			0.551			
17	LCO2RH	MOL/HR		18616			
18	LNLDG			0.469			
19	AVELIQ	SQM		0.00138			
20	AVEGAS	CUM/SEC		0.138			
21	AREA	SQM		2.00			
22	AVAREA	SQM		2.03			

Table G-45. Run 4.27.1 Data-Fit Results

Vary No.	Initial Value	Est Value	Stnd Dev	95% Conf Int Low Limit	95% Conf Int Up Limit
1	1.63	1.71	1.16	1.00	3.99
2	10330	9693	17513	5000	40000

	Var Name	Units	Meas Val	Est Val	Meas σ	Est σ	Norm Residue
1	GN2IN	MOL/HR	16524				
2	GH2OIN	MOL/HR	1423				
3	GCO2IN	MOL/HR	3408	3402	341	308	-0.019
4	GCO2OT	MOL/HR	924	924	139	137	-0.003
5	LK2CO3	MOL/HR	9444				
6	LPZ	MOL/HR	5181				
7	LH2O	MOL/HR	186794				
8	LCO2IN	MOL/HR	4468	4353	1340.4	1054	-0.086
9	TGIN	C	40.01				
10	TLIN	C	40.01	39.90	2.00	1.67	-0.054
11	T4077	C	40.92	41.17	4.09	2.13	0.062
12	T4076	C	42.72	43.13	4.27	2.32	0.096
13	T4075	C	44.42	44.57	4.44	2.29	0.033
14	T4073	C	45.84	45.68	4.58	2.16	-0.035
15	TLOUT	C	46.1	46.00	2.31	2.12	-0.043
16	RHLDG			0.556			
17	LCO2RH	MOL/HR		16275			
18	LNLDG			0.472			
19	AVELIQ	SQM		0.00119			
20	AVEGAS	CUM/SEC		0.147			
21	AREA	SQM		1.81			
22	AVAREA	SQM		1.84			

Table G-46. Run 4.27.2 Data-Fit Results

Vary No.	Initial Value	Est Value	Stnd Dev	95% Conf Int Low Limit	95% Conf Int Up Limit
1	1.34	1.34	0.51	1.00	2.34
2	9787	9802	14616	5000	38450

	Var Name	Units	Meas Val	Est Val	Meas σ	Est σ	Norm Residue
1	GN2IN	MOL/HR	16707				
2	GH2OIN	MOL/HR	1424				
3	GCO2IN	MOL/HR	3276	3285	328	266	0.026
4	GCO2OT	MOL/HR	864	872	130	127	0.061
5	LK2CO3	MOL/HR	9916				
6	LPZ	MOL/HR	5446				
7	LH2O	MOL/HR	183469				
8	LCO2IN	MOL/HR	4142	4175	1242.6	1055	0.026
9	TGIN	C	40.04				
10	TLIN	C	39.3	39.27	0.79	0.72	-0.039
11	T4077	C	39.9	40.20	2.00	1.19	0.149
12	T4076	C	41.58	41.91	2.08	1.08	0.157
13	T4075	C	43.37	43.28	2.17	1.07	-0.041
14	T4073	C	44.76	44.48	2.24	1.18	-0.127
15	TLOUT	C	45.57	45.86	2.28	1.87	0.126
16	RHLDG			0.538			
17	LCO2RH	MOL/HR		16520			
18	LNLDG			0.459			
19	AVELIQ	SQM		0.00118			
20	AVEGAS	CUM/SEC		0.146			
21	AREA	SQM		1.42			
22	AVAREA	SQM		1.44			

Table G-47. Run 4.28.1 Data-Fit Results

Vary No.	Initial Value	Est Value	Stnd Dev	95% Conf Int Low Limit	95% Conf Int Up Limit
1	1.61	1.58	2.03	1.00	5.00
2	9923	10062	30970	5000	40000

	Var Name	Units	Meas Val	Est Val	Meas σ	Est σ	Norm Residue
1	GN2IN	MOL/HR	16753				
2	GH2OIN	MOL/HR	1445				
3	GCO2IN	MOL/HR	3390	3386	339	337	-0.013
4	GCO2OT	MOL/HR	1141	1142	228	228	0.004
5	LK2CO3	MOL/HR	7795				
6	LPZ	MOL/HR	4326				
7	LH2O	MOL/HR	155865				
8	LCO2IN	MOL/HR	3571	3443	1785.5	1520	-0.072
9	TGIN	C	40.07				
10	TLIN	C	38.88	38.54	5.83	5.08	-0.058
11	T4077	C	39.95	40.22	7.99	3.73	0.034
12	T4076	C	41.9	42.51	8.38	3.84	0.073
13	T4075	C	43.8	44.07	8.76	4.38	0.031
14	T4073	C	45.25	45.20	9.05	4.81	-0.005
15	TLOUT	C	45.8	45.30	6.87	5.19	-0.072
16	RHLDG			0.556			
17	LCO2RH	MOL/HR		13482			
18	LNLDG			0.464			
19	AVELIQ	SQM		0.00099			
20	AVEGAS	CUM/SEC		0.150			
21	AREA	SQM		1.55			
22	AVAREA	SQM		1.58			

Table G-48. Run 4.28.2 Data-Fit Results

Vary No.	Initial Value	Est Value	Stnd Dev	95% Conf Int Low Limit	95% Conf Int Up Limit
1	1.72	1.77	2.24	1.00	5.00
2	9855	11217	34506	5000	40000

	Var Name	Units	Meas Val	Est Val	Meas σ	Est σ	Norm Residue
1	GN2IN	MOL/HR	17247				
2	GH2OIN	MOL/HR	1477				
3	GCO2IN	MOL/HR	3055	3045	458	426	-0.022
4	GCO2OT	MOL/HR	939	940	282	275	0.004
5	LK2CO3	MOL/HR	7769				
6	LPZ	MOL/HR	4278				
7	LH2O	MOL/HR	156134				
8	LCO2IN	MOL/HR	3677	3496	1838.5	1366	-0.098
9	TGIN	C	40.04				
10	TLIN	C	38.39	38.16	3.84	3.32	-0.059
11	T4077	C	39.01	39.46	7.80	4.09	0.057
12	T4076	C	40.53	41.39	8.11	4.41	0.106
13	T4075	C	42.47	42.77	8.49	4.34	0.035
14	T4073	C	43.84	43.81	8.77	4.36	-0.003
15	TLOUT	C	45	44.30	6.75	6.05	-0.103
16	RHLDG			0.555			
17	LCO2RH	MOL/HR		13370			
18	LNLDG			0.468			
19	AVELIQ	SQM		0.00099			
20	AVEGAS	CUM/SEC		0.150			
21	AREA	SQM		1.74			
22	AVAREA	SQM		1.77			

Table G-49. Run 4.29.1 Data-Fit Results

Vary No.	Initial Value	Est Value	Stnd Dev	95% Conf Int Low Limit	95% Conf Int Up Limit
1	1.82	1.82	1.45	1.00	4.67
2	10342	10687	25087	5000	40000

	Var Name	Units	Meas Val	Est Val	Meas σ	Est σ	Norm Residue
1	GN2IN	MOL/HR	16966				
2	GH2OIN	MOL/HR	1406				
3	GCO2IN	MOL/HR	3116	3115	156	154	-0.007
4	GCO2OT	MOL/HR	777	777	155	154	-0.003
5	LK2CO3	MOL/HR	7947				
6	LPZ	MOL/HR	4394				
7	LH2O	MOL/HR	155707				
8	LCO2IN	MOL/HR	3478	3411	1043.4	850	-0.064
9	TGIN	C	39.97				
10	TLIN	C	39.42	39.17	3.94	2.99	-0.064
11	T4077	C	40.25	40.53	6.04	3.04	0.046
12	T4076	C	42.18	42.80	6.33	3.00	0.099
13	T4075	C	44.38	44.54	6.66	3.13	0.024
14	T4073	C	45.97	45.90	6.90	3.39	-0.010
15	TLOUT	C	46.36	46.00	4.64	4.28	-0.077
16	RHLDG			0.555			
17	LCO2RH	MOL/HR		13697			
18	LNLDG			0.460			
19	AVELIQ	SQM		0.00099			
20	AVEGAS	CUM/SEC		0.149			
21	AREA	SQM		1.79			
22	AVAREA	SQM		1.82			

Table G-50. Run 4.29.2 Data-Fit Results

Vary No.	Initial Value	Est Value	Stnd Dev	95% Conf Int Low Limit	95% Conf Int Up Limit
1	1.57	1.56	1.01	1.00	3.54
2	11111	11107	12872	5000	36336

	Var Name	Units	Meas Val	Est Val	Meas σ	Est σ	Norm Residue
1	GN2IN	MOL/HR	16703				
2	GH2OIN	MOL/HR	1415				
3	GCO2IN	MOL/HR	3316	3315	332	327	-0.004
4	GCO2OT	MOL/HR	894	894	134	134	-0.003
5	LK2CO3	MOL/HR	8125				
6	LPZ	MOL/HR	4456				
7	LH2O	MOL/HR	154674				
8	LCO2IN	MOL/HR	3394	3334	1357.6	982	-0.044
9	TGIN	C	39.87				
10	TLIN	C	39.49	39.40	1.97	1.84	-0.047
11	T4077	C	40.57	40.84	4.06	1.52	0.067
12	T4076	C	42.75	43.21	4.28	1.91	0.107
13	T4075	C	45	44.99	4.50	2.25	-0.002
14	T4073	C	46.77	46.39	4.68	2.37	-0.082
15	TLOUT	C	46.6	46.59	2.33	2.07	-0.006
16	RHLDG			0.552			
17	LCO2RH	MOL/HR		13880			
18	LNLDG			0.455			
19	AVELIQ	SQM		0.00099			
20	AVEGAS	CUM/SEC		0.149			
21	AREA	SQM		1.54			
22	AVAREA	SQM		1.56			

Table G-51. Run 4.30.1 Data-Fit Results

Vary No.	Initial Value	Est Value	Stnd Dev	95% Conf Int Low Limit	95% Conf Int Up Limit
1	1.19	1.19	0.54	1.00	2.24
2	17036	17036	28654	5000	40000

	Var Name	Units	Meas Val	Est Val	Meas σ	Est σ	Norm Residue
1	GN2IN	MOL/HR	17001				
2	GH2OIN	MOL/HR	1451				
3	GCO2IN	MOL/HR	3203	3207	641	640	0.006
4	GCO2OT	MOL/HR	565	565	113	113	0.004
5	LK2CO3	MOL/HR	11024				
6	LPZ	MOL/HR	6110				
7	LH2O	MOL/HR	176727				
8	LCO2IN	MOL/HR	4000	4051	1600	1573	0.032
9	TGIN	C	39.98				
10	TLIN	C	41.02	41.16	4.10	3.40	0.034
11	T4077	C	41.17	41.32	6.18	2.72	0.024
12	T4076	C	42.37	42.63	6.36	2.46	0.040
13	T4075	C	44.7	43.93	6.71	2.73	-0.115
14	T4073	C	46.2	45.24	6.93	3.25	-0.139
15	TLOUT	C	46.75	47.32	4.68	3.69	0.123
16	RHLDG			0.517			
17	LCO2RH	MOL/HR		17718			
18	LNLDG			0.440			
19	AVELIQ	SQM		0.00118			
20	AVEGAS	CUM/SEC		0.146			
21	AREA	SQM		1.29			
22	AVAREA	SQM		1.29			

Table G-52. Run 4.30.2 Data-Fit Results

Vary No.	Initial Value	Est Value	Stnd Dev	95% Conf Int Low Limit	95% Conf Int Up Limit
1	1.86	1.86	1.36	1.00	4.53
2	13908	13908	37502	5000	40000

	Var Name	Units	Meas Val	Est Val	Meas σ	Est σ	Norm Residue
1	GN2IN	MOL/HR	16636				
2	GH2OIN	MOL/HR	1411				
3	GCO2IN	MOL/HR	3476	3473	521	517	-0.005
4	GCO2OT	MOL/HR	714	710	107	107	-0.037
5	LK2CO3	MOL/HR	9361				
6	LPZ	MOL/HR	5168				
7	LH2O	MOL/HR	188825				
8	LCO2IN	MOL/HR	4031	4003	1209.3	1145	-0.023
9	TGIN	C	39.88				
10	TLIN	C	40.44	39.99	6.07	4.71	-0.075
11	T4077	C	40.62	41.17	6.09	3.34	0.091
12	T4076	C	42.46	43.10	6.37	2.86	0.101
13	T4075	C	44.46	44.68	6.67	3.34	0.032
14	T4073	C	45.91	45.98	6.89	3.95	0.010
15	TLOUT	C	46.5	46.40	6.98	4.61	-0.014
16	RHLDG			0.555			
17	LCO2RH	MOL/HR		16127			
18	LNLDG			0.460			
19	AVELIQ	SQM		0.00120			
20	AVEGAS	CUM/SEC		0.148			
21	AREA	SQM		1.97			
22	AVAREA	SQM		2.00			

Table G-53. Run 4.31.1 Data-Fit Results

Vary No.	Initial Value	Est Value	Stnd Dev	95% Conf Int Low Limit	95% Conf Int Up Limit
1	1.75	1.75	3.42	1.00	5.00
2	3417	3417	53990	100	40000

	Var Name	Units	Meas Val	Est Val	Meas σ	Est σ	Norm Residue
1	GN2IN	MOL/HR	27535				
2	GH2OIN	MOL/HR	2414				
3	GCO2IN	MOL/HR	5631	5627	845	834	-0.005
4	GCO2OT	MOL/HR	2725	2728	818	810	0.003
5	LK2CO3	MOL/HR	11535				
6	LPZ	MOL/HR	6332				
7	LH2O	MOL/HR	254388				
8	LCO2IN	MOL/HR	5700	5631	2850	2404	-0.024
9	TGIN	C	39.89				
10	TLIN	C	41.57	41.16	6.24	5.84	-0.067
11	T4077	C	42.48	43.47	8.50	3.76	0.117
12	T4076	C	45.38	45.88	9.08	4.48	0.055
13	T4075	C	47.51	47.34	9.50	4.84	-0.018
14	T4073	C	49.14	48.31	9.83	4.97	-0.084
15	TLOUT	C	47.06	46.99	7.06	4.99	-0.010
16	RHLDG			0.561			
17	LCO2RH	MOL/HR		20046			
18	LNLDG			0.480			
19	AVELIQ	SQM		0.00159			
20	AVEGAS	CUM/SEC		0.257			
21	AREA	SQM		2.02			
22	AVAREA	SQM		2.06			

Table G-54. Run 4.31.2 Data-Fit Results

Vary No.	Initial Value	Est Value	Stnd Dev	95% Conf Int Low Limit	95% Conf Int Up Limit
1	1.31	1.31	1.49	1.00	4.23
2	6010	6010	41139	100	40000

	Var Name	Units	Meas Val	Est Val	Meas σ	Est σ	Norm Residue
1	GN2IN	MOL/HR	27265				
2	GH2OIN	MOL/HR	2463	2422	1232	1180	-0.034
3	GCO2IN	MOL/HR	5525	5554	1381	1356	0.021
4	GCO2OT	MOL/HR	2639	2632	660	659	-0.011
5	LK2CO3	MOL/HR	11618				
6	LPZ	MOL/HR	6429				
7	LH2O	MOL/HR	253327				
8	LCO2IN	MOL/HR	5100	5157	2295	2195	0.025
9	TGIN	C	40.16				
10	TLIN	C	41.55	41.48	4.16	3.92	-0.016
11	T4077	C	42.37	43.32	10.59	3.11	0.090
12	T4076	C	45.11	45.53	11.28	3.19	0.038
13	T4075	C	47.21	47.00	7.08	3.70	-0.029
14	T4073	C	48.85	48.06	7.33	4.15	-0.108
15	TLOUT	C	47.02	47.40	4.70	3.51	0.080
16	RHLDG			0.546			
17	LCO2RH	MOL/HR		19701			
18	LNLDG			0.465			
19	AVELIQ	SQM		0.00158			
20	AVEGAS	CUM/SEC		0.253			
21	AREA	SQM		1.53			
22	AVAREA	SQM		1.55			

Table G-55. Run 4.32.1 Data-Fit Results

Vary No.	Initial Value	Est Value	Stnd Dev	95% Conf Int Low Limit	95% Conf Int Up Limit
1	1.60	1.60	2.18	1.00	5.00
2	5408	5408	739	5000	6856

	Var Name	Units	Meas Val	Est Val	Meas σ	Est σ	Norm Residue
1	GN2IN	MOL/HR	27482				
2	GH2OIN	MOL/HR	2421				
3	GCO2IN	MOL/HR	5902	5871	885	1029	-0.035
4	GCO2OT	MOL/HR	3075	3083	461	-	0.017
5	LK2CO3	MOL/HR	9502				
6	LPZ	MOL/HR	5196				
7	LH2O	MOL/HR	185596				
8	LCO2IN	MOL/HR	4383	4293	1314.9	6	-0.068
9	TGIN	C	39.95				
10	TLIN	C	43.53	42.51	6.53	-	-0.156
11	T4077	C	45.63	47.03	6.84	-	0.205
12	T4076	C	50.7	51.44	7.61	-	0.097
13	T4075	C	53.9	53.42	8.09	-	-0.059
14	T4073	C	55.84	54.11	8.38	-	-0.206
15	TLOUT	C	48.14	49.01	7.22	-	0.121
16	RHLDG			0.564			
17	LCO2RH	MOL/HR		16580			
18	LNLDG			0.469			
19	AVELIQ	SQM		0.00120			
20	AVEGAS	CUM/SEC		0.269			
21	AREA	SQM		1.68			
22	AVAREA	SQM		1.73			

Table G-56. Run 4.32.2 Data-Fit Results

Vary No.	Initial Value	Est Value	Stnd Dev	95% Conf Int Low Limit	95% Conf Int Up Limit
1	1.83	1.83	2.38	1.00	5.00
2	4932	4932	38566	100	40000

	Var Name	Units	Meas Val	Est Val	Meas σ	Est σ	Norm Residue
1	GN2IN	MOL/HR	27786				
2	GH2OIN	MOL/HR	2457				
3	GCO2IN	MOL/HR	5667	5601	1133	961	-0.058
4	GCO2OT	MOL/HR	2944	2946	589	564	0.003
5	LK2CO3	MOL/HR	9101				
6	LPZ	MOL/HR	5251				
7	LH2O	MOL/HR	187375				
8	LCO2IN	MOL/HR	4754	4453	1901.6	1198	-0.159
9	TGIN	C	39.87				
10	TLIN	C	43.72	43.14	4.37	4.26	-0.133
11	T4077	C	45.89	47.91	6.88	3.54	0.294
12	T4076	C	51.34	52.12	7.70	4.82	0.102
13	T4075	C	55.11	53.82	8.27	4.32	-0.156
14	T4073	C	56.56	54.27	8.48	4.18	-0.270
15	TLOUT	C	48.28	48.67	4.83	4.44	0.080
16	RHLDG			0.565			
17	LCO2RH	MOL/HR		16205			
18	LNLDG			0.471			
19	AVELIQ	SQM		0.00120			
20	AVEGAS	CUM/SEC		0.272			
21	AREA	SQM		1.94			
22	AVAREA	SQM		2.00			

Table G-57. Run 4.33.1 Data-Fit Results

Vary No.	Initial Value	Est Value	Stnd Dev	95% Conf Int Low Limit	95% Conf Int Up Limit
1	2.34	2.34	2.72	1.00	5.00
2	22168	22168	23542	5000	40000

	Var Name	Units	Meas Val	Est Val	Meas σ	Est σ	Norm Residue
1	GN2IN	MOL/HR	27716				
2	GH2OIN	MOL/HR	2382	2382	1191	1109	0.000
3	GCO2IN	MOL/HR	5917	5879	888	725	-0.043
4	GCO2OT	MOL/HR	3228	3240	484	457	0.026
5	LK2CO3	MOL/HR	7785				
6	LPZ	MOL/HR	4301				
7	LH2O	MOL/HR	155442				
8	LCO2IN	MOL/HR	3542	3468	1062.6	714	-0.069
9	TGIN	C	39.79				
10	TLIN	C	45.55	45.53	6.83	6.82	-0.003
11	T4077	C	54.28	54.59	8.14	7.50	0.039
12	T4076	C	57.75	57.15	8.66	4.54	-0.069
13	T4075	C	56.63	56.08	8.49	4.66	-0.065
14	T4073	C	53.7	54.46	8.06	4.84	0.094
15	TLOUT	C	46.16	46.09	6.92	4.04	-0.010
16	RHLDG			0.575			
17	LCO2RH	MOL/HR		13891			
18	LNLDG			0.466			
19	AVELIQ	SQM		0.00100			
20	AVEGAS	CUM/SEC		0.280			
21	AREA	SQM		2.28			
22	AVAREA	SQM		2.36			

Table G-58. Run 4.33.2 Data-Fit Results

Vary No.	Initial Value	Est Value	Stnd Dev	95% Conf Int Low Limit	95% Conf Int Up Limit
1	2.39	2.39	3.39	1.00	5.00
2	18555	18555	19876	5000	40000

	Var Name	Units	Meas Val	Est Val	Meas σ	Est σ	Norm Residue
1	GN2IN	MOL/HR	27927				
2	GH2OIN	MOL/HR	2516	2478	1258	1141	-0.030
3	GCO2IN	MOL/HR	5808	5687	871	733	-0.139
4	GCO2OT	MOL/HR	3203	3243	480	457	0.083
5	LK2CO3	MOL/HR	7451				
6	LPZ	MOL/HR	4320				
7	LH2O	MOL/HR	156637				
8	LCO2IN	MOL/HR	3822	3569	1146.6	740	-0.220
9	TGIN	C	40.1				
10	TLIN	C	45.08	45.00	6.76	6.74	-0.012
11	T4077	C	52.57	53.08	7.89	7.46	0.064
12	T4076	C	56.93	56.00	8.54	4.81	-0.109
13	T4075	C	55.98	55.39	8.40	4.78	-0.071
14	T4073	C	53.74	54.10	8.06	4.47	0.045
15	TLOUT	C	46.08	46.37	6.91	3.85	0.041
16	RHLDG			0.572			
17	LCO2RH	MOL/HR		13460			
18	LNLDG			0.468			
19	AVELIQ	SQM		0.00100			
20	AVEGAS	CUM/SEC		0.280			
21	AREA	SQM		2.30			
22	AVAREA	SQM		2.38			

Appendix H: Calibration Method for CO_2 Gas Analyzers

H.1 Absorber Inlet - Vaisala

1. Remove Vaisala probe from 8" PVC duct (1-1/8 inch nut)
2. Insert into CO_2 calibration chamber
3. Switch the calibration gas to flow to the INLET on the sample panel
4. Turn on desired calibration gas and check to see that the flow does not exceed the limits of the rotameter (the ball should be at approximately ½ to 2/3 of the way up
5. Run at least a zero and high range gas, a mid range gas is also preferable
6. See below for calibration gas operation

H.2 Absorber Outlet - Vaisala and Horiba

1. Remove Vaisala probe from 8" stainless line (1-1/8 inch nut)
2. Remove the ¼ inch tube for the Horiba from the 8" line (9/16 inch nut)
3. Unscrew the plugs from the CO_2 calibration chambers and insert the probe and ¼ line
4. Replace the holes in the column with the two plugs
5. Switch the calibration flow to the OUTLET on the sample panel
6. Be sure that the sample pump is turned on and that the cover is open (the sample pump will overheat if the cover is kept closed)
7. Turn on desired calibration gas and check to see that the flow does not exceed the limits of the rotameter (the ball should be at approximately ½ to 2/3 of the way up
8. Run at least a zero and high range gas, a mid range gas is also preferable
9. See below for calibration gas operation

H.3 Absorber Middle - Horiba

1. Disconnect the line going on the INLET of the 3-way valve for the calibration gases

2. Remove the cap from the ¼ inch line connect to the Horiba valve (bottom valve on the gas sampling side – left) and connect to the INLET of the 3-way valve
3. Turn on the Horiba sample valve
4. The calibration gases should flow directly to the Horiba analyzer
5. Make sure that the flow does not exceed the range of the rotameter

H.4 CALIBRATION GAS OPERATION

1. Open the main valve on the gas cylinder of the desired calibration gas
2. Be sure that the valve is backed off on the low pressure side of the regulator
3. Open the gate valve on the bottom of the sample panel for the desired calibration gas
4. The gases are arrange such that the largest concentration begins at the left
5. The zero gas is obtained by opening the valve for the nitrogen, located behind the operator in the 12 o'clock position
6. Gradually tighten the low pressure valve on the regulator until you see flow in the rotameter (1/2 – 2/3 of the way up the rotameter)
7. Additional adjustments can be made by adjusting the knob on the rotameter

H.5 CERTIFICATE OF ANALYSIS FOR CO_2 STANDARDS

PRAXAIR.

Praxair Distribution, Inc.
2801 Montopolis Drive
Austin, TX 78741
Tel: (512)389-2323
Fax: (512)389-2599

2/1/2005

Ut
10100 Burnet Road - Room 133
Austin, TX 78758-4445
USA

Attention: Balcones Resh CTR Seibert-Barz

Praxair Order No. **899848**
Customer Reference No. **18619**
Product Lot/Batch No. **530-5013-01**
Praxair Part No. **AI CD17P-K**

CERTIFICATE OF ANALYSIS
Primary Standard

Component	Requested Concentration	Certified Concentration	Analytical Principle	Analytical Accuracy
Carbon dioxide	**17.0 %**	**16.9 %**	**J**	**±0.1ppm**
Air	**balance**	**balance**	**O**	**±0.1ppm**

Analytical Instruments: **Varian~3400~GC - Gas Chromatograph~TCD - Thermal Conductivity Detector**
Servomex Co. Inc.~OA244~Percent Oxygen~Paramagnetic

Cylinder Style: **K**
Cylinder Pressure @70F: **2000 psig**
Cylinder Volume: **228 ft3**
Valve Outlet Connection: **590**
Cylinder No(s). **12622**

Filling Method: **Gravimetric**
Date of Fill: **1/13/2005**
Expiration Date: **12/31/2008**

Analyst: **Jason Heil**

The gas calibration cylinder standard prepared by Praxair Distribution is considered a certified standard. It is prepared by gravimetric, volumetric, or partial pressure techniques. The calibration standard provided is certified against Praxair Reference Materials which are either prepared by weights traceable to the National Institute of Standards and Technology (NIST) or by using NIST Standard Reference Materials where available.

Note: All expressions for concentration (e.g., % or ppm) are for gas phase, by volume (e.g., ppmv) unless otherwise noted.

Key to Analytical Techniques:

A	Flame Ionization with Methanizer	B	Gas Chromatography with Discharge Ionization Detector	C	Gas Chromatography with Electrolytic Conductivity Detector	D	Gas Chromatography with Flame Ionization Detector
E	Gas Chromatography with Flame Photometric Detector	F	Gas Chromatography with Helium Ionization Detector	G	Gas Chromatography with Methanizer Carbonizer	H	Gas Chromatography with Photoionization Detector
I	Gas Chromatography with Reduction Gas Analyzer	J	Gas Chromatography with Thermal Conductivity Detector	K	Gas Chromatography with Ultrasonic Detector	L	Infrared - FTIR or NDIR
M	Mass Spectrometry - MS or GC/MS	N	Proprietary	O	Paramagnetic	P	Specific Water Analyzer
Q	Total Hydrocarbon Analyzer	R	Wet Chemical	S	Detector Tube	T	Odor

IMPORTANT
The information contained herein has been prepared at your request by personnel within Praxair Distribution. While we believe the information is accurate within the limits of the analytical methods employed and is complete to the extent of the specific analyses performed, we make no warranty or representation as to the suitability of the use of the information for any particular purpose. The information is offered with the understanding that any use of the information is at the sole discretion and risk of the user. In no event shall liability of Praxair Distribution, Inc. arising out of the use of the information contained herein exceed the fee established for providing such information.

Pg.1 of 1

Figure H-1. Certificate of Analysis for 16.9% CO_2 Primary Gas Standard

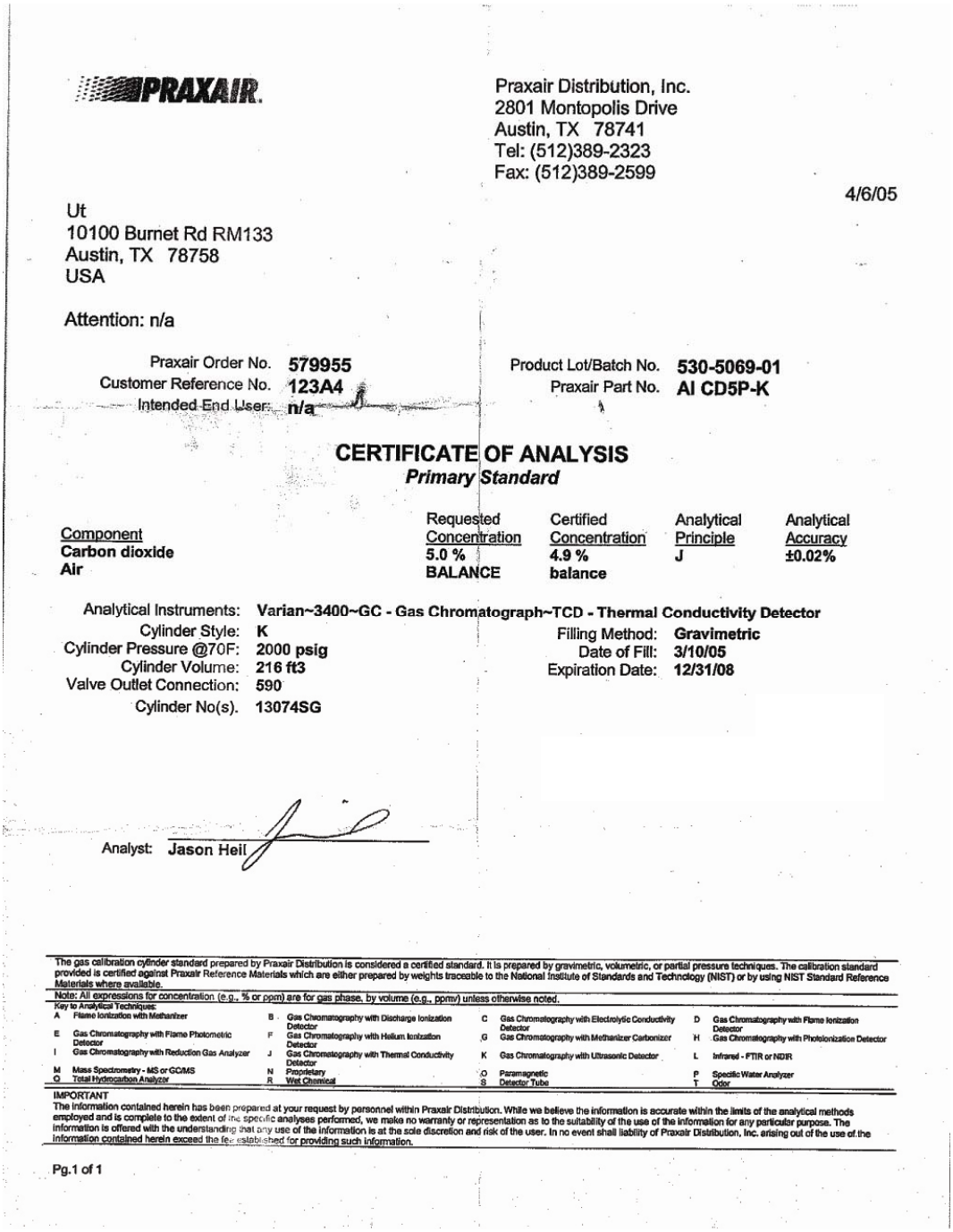

PRAXAIR.

Praxair Distribution, Inc.
2801 Montopolis Drive
Austin, TX 78741
Tel: (512)389-2323
Fax: (512)389-2599

4/6/05

Ut
10100 Burnet Rd RM133
Austin, TX 78758
USA

Attention: n/a

Praxair Order No. **579955**
Customer Reference No. **123A4**
Intended End User: **n/a**

Product Lot/Batch No. **530-5069-01**
Praxair Part No. **Al CD5P-K**

CERTIFICATE OF ANALYSIS
Primary Standard

Component	Requested Concentration	Certified Concentration	Analytical Principle	Analytical Accuracy
Carbon dioxide	**5.0 %**	**4.9 %**	**J**	**±0.02%**
Air	**BALANCE**	**balance**		

Analytical Instruments: **Varian~3400~GC - Gas Chromatograph~TCD - Thermal Conductivity Detector**
Cylinder Style: **K**
Cylinder Pressure @70F: **2000 psig**
Cylinder Volume: **216 ft3**
Valve Outlet Connection: **590**
Cylinder No(s). **13074SG**

Filling Method: **Gravimetric**
Date of Fill: **3/10/05**
Expiration Date: **12/31/08**

Analyst: **Jason Heil**

The gas calibration cylinder standard prepared by Praxair Distribution is considered a certified standard. It is prepared by gravimetric, volumetric, or partial pressure techniques. The calibration standard provided is certified against Praxair Reference Materials which are either prepared by weights traceable to the National Institute of Standards and Technology (NIST) or by using NIST Standard Reference Materials where available.

Note: All expressions for concentration (e.g., % or ppm) are for gas phase, by volume (e.g., ppmv) unless otherwise noted.

Key to Analytical Techniques:

A Flame Ionization with Methanizer	B Gas Chromatography with Discharge Ionization Detector	C Gas Chromatography with Electrolytic Conductivity Detector	D Gas Chromatography with Flame Ionization Detector
E Gas Chromatography with Flame Photometric Detector	F Gas Chromatography with Helium Ionization Detector	G Gas Chromatography with Methanizer Carbonizer	H Gas Chromatography with Photoionization Detector
I Gas Chromatography with Reduction Gas Analyzer	J Gas Chromatography with Thermal Conductivity Detector	K Gas Chromatography with Ultrasonic Detector	L Infrared - FTIR or NDIR
M Mass Spectrometry - MS or GC/MS	N Proprietary	O Paramagnetic	P Specific Water Analyzer
Q Total Hydrocarbon Analyzer	R Wet Chemical	S Detector Tube	T Odor

IMPORTANT
The information contained herein has been prepared at your request by personnel within Praxair Distribution. While we believe the information is accurate within the limits of the analytical methods employed and is complete to the extent of the specific analyses performed, we make no warranty or representation as to the suitability of the use of the information for any particular purpose. The information is offered with the understanding that any use of the information is at the sole discretion and risk of the user. In no event shall liability of Praxair Distribution, Inc. arising out of the use of the information contained herein exceed the fee established for providing such information.

Pg.1 of 1

Figure H-2. Certificate of Analysis for 4.9% CO_2 Primary Gas Standard

Appendix I: Liquid Sampling Procedure for Campaigns 2 and 4

I.1 Sample Vial Preparation

1. Label vials to be used. There are 5 sample points.
2. Tare scale with vial (without cap).
3. Add 30 mL of cold DI water to vials using the automatic pipette. DI water can be obtained from one of the 2 gallon jugs which are stored in the refrigerator in the back lab.
4. Record final weight of water in TOC logbook.
5. Tare scale with scale empty.
6. Record total weight of vial, cap, and water in TOC log book.
7. Repeat until all 5 vials are filled and weights recorded.
8. Put all 5 vials in the refrigerator until ready to be used.
9. Keep approximately 2 sets of 5 vials in the refrigerator at all times. This will make sure that one of the sets is chilled when needed.

I.2 Sample Collection

1. Connect sample bombs to sample bomb hoses and open valves to allow flow. All hoses and bombs are color coded. Color coded legend can be seen at the end of the SOP. Three connections are on the ground level (1st level) near the pumps (2 on the east side, 1 on the west). The other two bombs are connected to hoses coming directly off the columns. These connections are on the 3rd level of the plant, on the absorber and stripper scaffolds around the columns.
2. After a few seconds, verify that the flow is passing through the bombs. The bombs should heat up slightly from the warm sample.
3. Close the valves and remove the sample bombs.
4. Make sure to bring something to hold the sample bombs. Some of them will get very hot.
5. Make sure that the sample bombs are not leaking. Sometimes the valves will not close correctly and leak.
6. Now you can give the go ahead to change operating conditions.

7. Take the sample bombs to the back table of the back lab and also get the chilled water sample vials from the refrigerator.

I.3 SAMPLE INJECTION

1. Verify that the drain flask connected to the sample extraction device is empty. This is located under the back table of the back lab.
2. Connect the water/nitrogen connection to the sample extraction device.
3. Verify that the nitrogen and water valves on the water/nitrogen connector are closed. Make sure the water and nitrogen valves are open at their sources (under the counter for the nitrogen and at the sink for the water).
4. Open the drain valve.
5. Run water through the extraction device for approximately 10 seconds, then close the water valve on the water/nitrogen connection. Verify that water is draining into the large flask under the table.
6. Slowly and carefully open the nitrogen valve on the water/nitrogen connection. Once the initial burst of nitrogen passes, the flow will be more controlled.
7. Allow nitrogen to flow through the extraction device for approximately 10 seconds and then close the nitrogen valve.
8. **Close the drain valve.** If you forget to do this, the sample will drain out the bottom and be lost.
9. Connect one of the sample bombs to the sample extraction device.
10. Connect the quick connect valve to the top of the sample bomb.
11. Using a 10 mL syringe, extract ≈ 10 mL of sample through the "syringe extraction spot".
12. Loosen the cap of the vial which corresponds to the particular sample point. Do not take cap off though. Just loosen enough to allow air to escape.
13. Slowly inject the sample into the vial.
14. Tighten the cap of the vial.
15. Clean the 10 mL syringe by flushing DI water through it.
16. Tare the scale.
17. Record the weight of the vial (now containing vial, cap, sample, and water) into the TOC logbook next to the previous sample preparation entries for that particular vial. Be sure to record date and time of sample on vial and in TOC logbook.
18. Remove the quick connect valve from the sample bomb and remove the sample bomb from the extraction device.
19. Repeat this procedure for all 5 of the sample bombs and sample vials. Remember to clean using water and nitrogen between each sample.

20. Verify that the nitrogen and water valves on the water/nitrogen connector are closed. Make sure the water and nitrogen valves are closed at their sources (under the counter for the nitrogen and at the sink for the water).

I.4 SAMPLE COLOR CODES

Absorber Lean – Orange, Absorber Middle – Blue, Absorber Rich – Green, Stripper Lean – Red, Stripper Middle – White

Appendix J: Standard Operating Procedure for Shimadzu 5050A Total Organic Carbon Analyzer

J.1 Preparation of Standards

1. Sodium carbonate was heated in an oven at 225 °C for an hour and then let cool in a glass desiccator.
2. 3.50 g of reagent grade sodium hydrogen carbonate and 4.41 g of sodium carbonate were dissolved in zero water in a 1 liter measuring flask. Zero (carbon free) water was added to bring the total volume of the solution to the marked line.
3. The obtained standard solution contains 1000 mg C/liter, equivalent to 1000 ppm.
4. The 1000 ppm standard is to be stored in an air tight glass jar in the refrigerator.
5. Shelf life should not exceed one month.

J.2 Instrumentation Calibration

1. Prior to calibration, the zero baseline of the Shimadzu TOC-5050A Total Organic Carbon Analyzer was reset each day.
2. The water and phosphoric acid levels were checked to be adequate.
3. The IC solution was regenerated.
4. One hundred milliliters of 100, 200, 300 and 400 ppm standards were obtained from the 1000 ppm standard by using an auto pipette.
5. The four solutions were poured into the calibration vials and covered with parafilm to prevent and CO_2 transfer.
6. The concentrations of the calibration standards were input into the calibration subroutine.

7. Four water washes between samples, an injection volume of 8 μL, a minimum of two sample, a maximum of four samples, and a coefficient of variance of 2.0% were also input into the calibration program.
8. A calibration curve was generated by the TOC analyzer.

J.3 Analysis of Samples

1. Prior to use, the zero baseline of the Shimadzu TOC-5050A Total Organic Carbon Analyzer was reset each day.
2. The water and phosphoric acid levels were checked to be adequate.
3. The IC solution was regenerated.
4. Ten samples from the pilot plant were diluted and analyzed at a time. Since there are 5 sample points, two sample runs can be analyzed in the same TOC analyzer setup.
5. Sample solutions obtained from the pilot plant via the sample collection routine were used in creating more dilute solutions for the TOC analysis. Typical dilutions range from 1.2 to 2.0 g solution per 40 g of zero water to achieve carbon concentrations in the 200 ppm range. The range of the dilution depends on the CO_2 loading of the solution.
6. Once the diluted solutions were prepared, the capped vials were slowly inverted back and forth about 10 times to insure the solutions were uniform.
7. Approximately 10 mL of the solution were poured into the TOC vials and placed in the automatic sampler. Each vial was capped with parafilm to prevent any CO_2 loss to the surroundings.
8. Fifty mL of a 200 ppm standard were created from the 1000 ppm standard.
9. Three TOC vials were filled with the 200 ppm standard which was used as an internal standard. Again, these samples were covered with parafilm to prevent any CO_2 loss.
10. One standard was placed before the 10 pilot plant samples. One was placed after the 10 samples. One standard was placed between the 5th and 6th samples.
11. The auto sampling procedure was run after inputting the location of the 13 samples and the correct calibration curve to use.
12. The inorganic carbon concentrations were obtained from the printout of the TOC analyzer.
13. Before another set of runs can be tested, the water and phosphoric acid levels must be checked and the IC solution must be regenerated.

Appendix K: Sample Titration Method for Loading and Composition Determination for 5 m K^+/ 2.5 m PZ Solutions

1. Tare a 100 mL beaker on a scale.
2. Using a pipette, add 10 mL of sample to the beaker and record the mass.
3. Add approximately 5 drops of methyl orange indicator to the sample. If methyl orange is not fresh, you may need to use more.
4. Using a magnetic stir bar, stir the sample on a hot plate stirrer**.**
5. Fill one burette with certified 2N (±0.005) HCl.
6. Record the starting volume of HCl in the HCl burette.
7. Slowly add HCl to the solution until the sample turns from yellow to orange.
8. Record the final volume of HCl in the HCl burette.
9. On the hot plate stirrer, heat the sample to a boil to release CO_2 out of the solution.
10. Rapidly boil the solution for 2 minutes while still stirring it with the magnetic stir bar.
11. After 2 minutes, turn off the heat and allow the solution to return to ambient temperature.
12. Fill a second burette with certified 2N (± 0.02) NaOH.
13. Record the starting volume of NaOH in the NaOH burette.
14. Magnetically stir the solution while immersing a pH meter in the sample.
15. Add NaOH to the solution until the pH meter gives a reading of ≈ -265mV.
16. Record the final volume of NaOH in the NaOH burette.
17. Piperazine concentration is calculated by dividing the amount of HCl added by 2 because there are two nitrogen atoms in piperazine.
18. Potassium (K^+) concentration is calculated by taking the difference between the amount of HCl and NaOH added.

Appendix L: Ion Chromatography Method for Analysis of Piperazine and Potassium Concentration

L.1 Background Information

Configure the Ion Chromatograph (IC) for cation detection. Make sure the eluent bottles are filled. The 6 mM and 55 mM concentrations will be used for the Piperazine_5min procedure. To make new eluent, fill half of a 2 L volumetric flask with ultra-pure water and add 12 mL of 1 N monosulphonic acid (MSA) for the 6 mM concentration. QS the flask with ultra-pure water. For the 55 mM concentration, use 110 mL of 1 N MSA. Fill the eluent bottles by stopping the nitrogen flow (turn the knob on the casing to the right until it is no longer above the casing) and unscrew the lid. (Expect a hissing sound as the pressure is released from the bottles). Fill the bottles with the appropriate eluent concentration. Close the lid and open the valve on the casing to pressurize the eluent. Next, prime the pump. Note: Never allow the eluent bottles to become empty. Always make sure that there is more than sufficient eluent available to the IC.

When the eluent is refilled, the pump needs to be primed to allow any air bubbles that may be in the lines to be cleared before running the IC. To do this, set the concentration on the computer to 100% A. If the pump starts running when "Enter" is pressed, click the "Off" button. Click "Prime" and an error message will appear. Open the bottom compartment of the IC (under the

gradient mixer). On the upper left side of this compartment there is a black plastic peg. Turn it to the left and open it by loosening it. (If, after the pump is running, fluid can be seen dripping from the peg, simply tighten it a little. It just needs to be loose enough to release any back-pressure.) Then click "OK" on the error message and the pump will begin to run. On the bottom right of the compartment there is a loop of tubing. Hold it and watch for any air bubbles, which will be visible after a few seconds. Allow it to run for an additional ten seconds after the last air bubble is detected. Then click "Off". The eluent bottle A has just been primed. The process needs to be repeated for all of the other bottles that have been refilled. After priming the necessary eluent bottles, screw the peg back into place and close the compartment. (If there is a low pressure warning while trying to prime the pump, click the "Off' button, as the pump must still have been running. Click "Prime" and resume.)

Once the system is primed, one can begin to run the IC at the specifications that will be running with the program. To run the Piperzine_5min program, enter 30 for the %C, then press "Enter". The computer will automatically set the %A to 70. If not, enter it manually. If the pump is not already running, click "On" to enable it. Set the flow to 1.2 mL/s and the suppresser current to 73 mA. All of these settings are preset in the program Piperazine_5min. The machine is developing a constant baseline before measurements are taken. Allow the machine to run for approximately 10 minutes. Check to see if the base-line reading is steady. (It will still fluctuate within 0.001.) Look on the top monitor on the IC itself. If the screen is not lit, press one of the Arrow buttons. The Total μS reading should be no higher than 1.5; it should read below 1. If it is high, ask for assistance and begin troubleshooting. Once the reading is steady, the IC analysis can begin.

To set up a Sequence, change screens on the computer interface (Crtl+Tab). If the screen is not open, there is a button on the left side of the toolbar just below the menus that will open the window. Make a new sequence for each run that is done. The easiest way to do this is go to the last sequence that was done and click "Save As" with a new title containing the date and a letter 'A' afterwards, or the next consecutive letter. It is recommended to run the standards at the beginning of each day (0 ppm K^+/PZ, 10 ppm K^+/PZ, 20 ppm K^+/PZ, 30 ppm K^+/PZ, 40 ppm K^+/PZ, and 50 ppm K^+/PZ). The Type for these injections is Standards (the icon will be yellow). Then name the samples that will be injected. It is suggested to inject each sample twice (A and B). The Type for these injections is Unknown (the icon will be blue). One can Append Samples, Delete Samples and Insert Samples at this time, and even while the batch is running. (Make sure to save the screen after any changes are made.) On the tool bar or in the menu, select "Run Batch". A sub-screen will appear. Select the batch to run, and click "Ready Check". The program calculates the volume of eluent needed to run the sequence. Confirm that all is ready; then start the batch. An error message will appear, with a prompt to insert the sample. Rinse the 1 mL syringe with ultra-pure water a few times, flush with sample a few times, and insert about 1 mL. (The volume injected does not need to be precise. There is a sample coil that will be flushed and filled with the injection.)

L.2 INTERPRETATION OF CHROMATOGRAPHS

There is a water dip that will occur regularly around t=1.5 m. (The time events occur depends on the method.) There obviously should not be any detectible peaks in the 0 ppm K^+/PZ (ultra-pure water sample). There may be a small bump that is equivalent to about 200 ppb, but that is not cause for concern. If one were to change the program, increasing the flow moves the peaks left,

coming out at earlier times, and increasing the concentration of eluent primarily moves the peaks closer together. With the Piperazine_5min method, allow approximately 1 minute between the injection (t=30s) and the water dip. After another minute, the potassium peak appears. There is a minute to reestablish the baseline between peaks, then the piperazine peak, then another minute to reestablish the baseline before the method ends. Recently, the QNT or the calibration curve has been recalculated each time. It may be valuable to see how similar these are so that one only has to verify the standard.

L.3 FORMAL SOP FOR THE IC

1. Run the IC at method configurations to allow baseline to steady.
2. Run 0 ppm K^+/PZ and calibration standards.
3. Tare caged scale and measure clean sample vile.
4. Fill sample vile with 60 mL ultra-pure water. Record mass of water.
5. With a micro-auto pipette, add 60µL sample (x1000 dilution). Record total mass of solution. Cap vial.
6. Briefly agitate to ensure solution is mixed.
7. When the IC is ready for the next sample, rinse 1 mL syringe with ultra-pure water, flush once or twice with diluted sample, then fill with sample and inject into IC and press "Enter" on error message. Rinse the syringe with ultra-pure water.
8. Analyze each sample twice.
9. Enter actual concentrations of standards into QNT editor and set calibration curve.
10. Record the concentration of K^+ and PZ (ppm) along with actual dilution masses and calibration curve data.
11. To shut down, change flow to 0.4 mL/min and suppressor current to 25 mA. Leave the IC running to keep all parts wet. Make sure the eluent bottles have more than sufficient eluent remaining to last until the next run.

Note: A 4000x dilution should give a ppm reading around 30 for a 5 molal K^+ / 2.5 molal PZ solution. For Campaigns 2 and 4, the samples had already been diluted four times. The 1000 times dilution should be sufficient for these samples. In Campaign 1, the samples were not pre-diluted.

This method was developed with the help of Brian Daniels and Andrew Sexton.

Appendix M: Electrolyte-NRTL Physical and Transport Property Models and Equations

The following section lists the various models that are may be used depending upon the availability of certain parameters. These models are available as part of the default parameters for the electrolyte-NRTL model in Aspen Plus®.

M.1 RACKETT EQUATION FOR LIQUID MOLAR VOLUME

The Rackett equation is used to calculate the liquid molar volume of a pure component in the electrolyte-NRTL model. The Rackett equation is given by the following:

$$V_m^l = \frac{RT_c\left(Z_m^{RA}\right)^{\left[1+\left(1-T_r\right)^{2/7}\right]}}{P_c} \tag{M.1}$$

where,

$$T_c = \sum_i \sum_j x_i x_j V_{ci} V_{cj} \left(T_{ci} T_{cj}\right)^{1/2} \left(1 - k_{ij}\right) / V_{cm}^2 \tag{M.2}$$

$$\frac{T_c}{P_c} = \sum_i x_i \frac{T_{ci}}{P_{ci}} \tag{M.3}$$

$$Z_m^{RA} = \sum_i x_i Z_i^{*,RA} \tag{M.4}$$

$$V_{cm} = \sum_i x_i V_{ci} \tag{M.5}$$

$$T_r = \frac{T}{T_c} \tag{M.6}$$

where, P_c and T_c are the critical pressure and temperature, respectively. $Z_i^{*,RA}$ is the compressibility of the pure component given by the parameter RKTZRA. The default value for the RKTZRA parameter is the critical compressibility factor, ZC. The default value for V_{ci} is the critical volume, VC. T_r is the reduced temperature in absolute temperature units. k_{ij} is the interaction parameter for the Rackett equation and is given by the parameter RKTKIJ. The default value is calculated by the following equation:

$$k_{ij} = 1 - \frac{8\left(V_{ci}V_{cj}\right)^{1/2}}{\left(V_{ci}^{1/3} + V_{cj}^{1/3}\right)^3} \tag{M.7}$$

M.2 JONES–DOLE ELECTROLYTE CORRECTION FOR VISCOSITY

In the presence of electrolytes, the viscosity of the liquid mixture is corrected using the Jones–Dole model. This section lists the equations for the two other methods by which the parameter $\Delta\eta_{ca}^{l}$ can be calculated. As outlined in an earlier chapter, if the concentration of apparent electrolyte is greater than 0.1 M, the Breslau–Miller equation is used. However, when the concentration of apparent electrolyte is less than or equal to 0.1 M, the Jones–Dole equation is used. If the Jones–Dole parameters are not available, the Carbonell equation is used.

M.2.1 Jones–Dole Equation

The Jones–Dole equation is given by:

$$\Delta\eta_{ca}^{l} = A_{ca}\sqrt{c_{ca}^{a}} + B_{ca}c_{ca}^{a} \tag{M.8}$$

where is c_{ca}^{a} is the concentration of apparent electrolyte *ca*:

$$c_{ca}^{a} = \frac{x_{ca}^{a}}{V_{m}^{l}} \tag{M.9}$$

and x_{ca}^{a} is the mole fraction of apparent electrolyte *ca*. The other parameters are given by the following equations:

$$A_{ca} = \frac{1.45}{\eta_{solv}^{l}(2\varepsilon T)^{1/2}}\left[\frac{L_c + L_a}{4L_cL_a} - \frac{L_c - L_a}{\left(3+\sqrt{2}L_cL_a(L_c+L_a)\right)}\right] \tag{M.10}$$

$$L_a = l_{a,1} + l_{a,2}T \tag{M.11}$$

$$L_c = l_{c,1} + l_{c,2}T \tag{M.12}$$

$$B_{ca} = \left(b_{c,1} + b_{c,2}T\right) + \left(b_{a,1} + b_{a,2}T\right) \tag{M.13}$$

where l_1, l_2, b_1, and b_2 are the IONMOB/1, IONMOB/2, IONMUB/1, and IONMUB/2 parameters in Aspen Plus®.

M.2.2 Carbonell Equation

The Carbonell Equation is given by:

$$\Delta\eta_{ca}^{l} = \exp\left[0.48193\left(\sum_{k} M_k x_k^a\right)\frac{c_{ca}^{a}}{T}\right] - 1.0 \tag{M.14}$$

where M_k is the molecular weight of the apparent electrolyte component *k*. The other parameters are defined the same as in the preceding section.

Appendix N: RateSep™ Mass Transfer Correlation

N.1 Liquid and Vapor Mass Transfer Coefficients

The mass transfer coefficient for the liquid and gas were calculated using the Bravo et al. (1996) model available in RateSep™. In the Data-Fit analysis for Campaign 4, the model was also used to calculate the effective interfacial area in conjunction with the interfacial area factor. The binary liquid and vapor phase mass transfer coefficients are given by:

$$k_{i,k}^{L} = 2\sqrt{\frac{D_{i,k}^{L} u_{Le}}{\pi S C_E}} \tag{N.1}$$

and

$$k_{i,k}^{V} = 0.54 \frac{D_{i,k}^{V}}{S} \mathrm{Re}_{V}^{0.8} \, Sc_{V,i,k}^{0.333} \tag{N.2}$$

where $D_{i,k}^{L}$ and $D_{i,k}^{V}$ are the binary liquid and vapor diffusivity, respectively. C_E is correction factor for surface renewal and S is the slant height of a corrugation, The superficial liquid velocity, u_{Le}, is given by:

$$u_{Le} = \frac{u_s^L}{\varepsilon h_t \sin\theta} \tag{N.3}$$

where ε is the void fraction of the packing, u_s^L is the superficial vapor–liquid velocity, θ is the angle with the horizontal of the falling film or the corrugation channel. The fractional holdup, h_t, is given by the following equation:

$$h_t = \left(4\frac{F_t}{S}\right)^{2/3}\left(\frac{3\mu^L u_s^L}{\rho_t^L g_{eff}\varepsilon\sin\theta}\right)^{1/3} \tag{N.4}$$

where ρ_t^L is the liquid density and μ^L is the liquid viscosity. The effective gravity, g_{eff}, is given by:

$$g_{eff} = g\left(\frac{\rho_t^L - \rho_t^V}{\rho_t^L}\right)\left(1 - \frac{\Delta P/\Delta Z}{\Delta P/\Delta Z_{flood}}\right) \tag{N.5}$$

where g is the gravitational constant, ρ_t^L is the liquid density and ρ_t^V is the vapor density. $\Delta P/\Delta Z_{flood}$ is the pressure drop per unit height of packing at flooding. $\Delta P/\Delta Z$ is the pressure drop per unit of height of packing and is given by:

$$\frac{\Delta P}{\Delta Z} = \frac{\Delta P_d}{\Delta Z}\left(\frac{1}{1-(0.614+71.35S)h_t}\right)^5 \tag{N.6}$$

where $\Delta P_d/\Delta Z$ is the dry pressure drop per unit height of packing and is given by:

$$\frac{\Delta P_d}{\Delta Z} = \frac{0.177\rho_t^V}{S\varepsilon^2(\sin\theta)^2}\left(u_s^V\right)^2 + \frac{88.774\mu^V}{S^2\varepsilon\sin\theta}u_s^V \tag{N.7}$$

where ρ_t^V is the density of the vapor, μ^V is the viscosity of the vapor, and u_s^V is the superficial velocity of the vapor. The correction factor for total holdup due to the effective wetted area, F_t, is given by:

$$F_t = \frac{29.12(We_L Fr_L)^{0.15} S^{0.359}}{\mathrm{Re}_L^{0.2}\,\varepsilon^{0.6}(\sin\theta)^{0.3}(1-0.93\cos\gamma)} \tag{N.8}$$

where We_L is the Weber number of the liquid, Fr_L is the Froude number of the liquid, Re_L is the Reynolds number of the liquid and are given by the following equations:

$$We_L = \frac{\left(u_s^L\right)^2 \rho_t^L S}{\sigma} \tag{N.9}$$

$$Fr_L = \frac{\left(u_s^L\right)^2}{Sg} \tag{N.10}$$

$$\mathrm{Re}_L = \frac{u_s^L S \rho_t^L}{\mu^L} \tag{N.11}$$

The contact angle between the solid and liquid film, γ, is given by:

$$\cos\gamma = \begin{cases} 5.211x10^{-16.835\sigma} & for \sigma \geq 0.055 \\ 0.9 & for \sigma < 0.055 \end{cases} \tag{N.12}$$

The Reynolds number for the vapor, Re_V, is given by:

$$\mathrm{Re}_V = \frac{\left(u_{Ve} + u_{Le}\right) S \rho_t^V}{\mu^V} \tag{N.13}$$

where u_{Ve} is the effective velocity through the channel for the vapor and is given by:

$$u_{Ve} = \frac{u_s^V}{\varepsilon\left(1 - h_t\right)\sin\theta} \tag{N.14}$$

The Schmidt number for the vapor, $Sc_{V,i,k}$, is given by:

$$Sc_{V,i,k} = \frac{\mu^V}{\rho_t^V D_{i,k}^V} \tag{N.15}$$

N.2 Effective Interfacial Area

The total interfacial area for mass transfer is give by:

$$a^{I} = a_e A_t h_p \tag{N.16}$$

where A_t is the cross-sectional area of the column, h_p is the packed height of the column. a_e is the effective surface area per unit volume of the column and is given by:

$$a_e = F_t F_{se} a_p \tag{N.17}$$

where F_{se} is the factor for surface enhancement and a_p is the specific area of the packing.

Appendix O: RateSep™ Flux Equations for Mixed Flow

The following equations evaluate the flux for the Mixed flow model. In the Mixed flow model, the outlet conditions of the bulk property for the gas and liquid phases are used in the flux calculation. When other flow models are used, different conditions for the bulk properties of each phase are used as discussed in the absorber modeling chapter. The mass flux for the bulk liquid is given by the following equation:

$$\left[\mathbf{\Gamma}_j^L\right]\left(\mathbf{x}_j^I - \mathbf{x}_j\right) + \Delta\phi_j^E\left(\mathbf{x}_j \mathbf{z}_j\right) - \left[\mathbf{R}_j^L\right]\left(\mathbf{N}_j^L - N_t^L \mathbf{x}_j\right) = 0 \tag{O.1}$$

where:

$$\Gamma_{i,k,j}^L = \delta_{i,k} + x_{ij} \left.\frac{\partial \ln \varphi_{ij}^L}{\partial x_{kj}}\right|_{T_j^L, P_j, \Sigma} \tag{O.2}$$

where Σ represents fixing the mole fractions of all other components except the *n*th while evaluating the differentiation.

$$R_{i,i,j}^L = \frac{x_{ij}}{\overline{\rho}_j^L a_j^I k_{i,n,j}^L} + \sum_{\substack{m=1 \\ m \neq i}}^{n} \frac{x_{mj}}{\overline{\rho}_j^L a_j^I k_{i,m,j}^L} \quad for\ i = 1,\ldots,n-1 \tag{O.3}$$

$$R_{i,k,j}^L = -x_{ij}\left(\frac{1}{\overline{\rho}_j^L a_j^I k_{i,k,j}^L} - \frac{1}{\overline{\rho}_j^L a_j^I k_{i,n,j}^L}\right) \quad for\ i = 1,\ldots,n-1, i \neq k \tag{O.4}$$

When electrolytes are present, the driving force caused by the electric potential, $\Delta\phi_j^E\left(\mathbf{x}_j \mathbf{z}_j\right)$, in each film region is adjusted so that the electro-neutrality

conditions are satisfied at the right boundary of the film region. The mass flux for the bulk vapor is given by:

$$\left[\boldsymbol{\Gamma}_j^V\right]\left(\mathbf{y}_j^I - \mathbf{y}_j\right) + \left[\mathbf{R}_j^V\right]\left(\mathbf{N}_j^V - N_t^V \mathbf{y}_j\right) = 0 \tag{O.5}$$

where:

$$\Gamma_{i,k,j}^V = \delta_{i,k} + y_{ij} \left.\frac{\partial 1n\varphi_{ij}^V}{\partial y_{kj}}\right|_{T_j^V, P_j, \Sigma} \tag{O.6}$$

$$R_{i,i,j}^V = \frac{y_{ij}}{\overline{\rho}_j^V a_j^I k_{i,n,j}^V} + \sum_{\substack{m=1 \\ m \neq i}}^{n} \frac{y_{mj}}{\overline{\rho}_j^V a_j^I k_{i,m,j}^V} \quad for\ i = 1,\ldots,n-1 \tag{O.7}$$

$$R_{i,k,j}^V = -y_{ij}\left(\frac{1}{\overline{\rho}_j^V a_j^I k_{i,k,j}^V} - \frac{1}{\overline{\rho}_j^V a_j^I k_{i,n,j}^V}\right) \quad for\ i = 1,\ldots,n-1, i \neq k \tag{O.8}$$

The heat flux for the bulk liquid is given by the following equation:

$$a_j^I h_j^L \left(T_j^I - T_j^L\right) - q_j^L + \sum_{i=1}^{n} N_{ij}^L \overline{H}_{ij}^L = 0 \tag{O.9}$$

The heat flux for the bulk vapor is given by:

$$a_j^I h_j^V \left(T_j^V - T_j^I\right) - q_j^V + \sum_{i=1}^{n} N_{ij}^V \overline{H}_{ij}^V = 0 \tag{O.10}$$

Appendix P: RateSep™ Input File

```
Filename C:\Documents and Settings\chene\My Documents\UT Austin\CO2
Research\Aspen\2007\February\08.02.07 5k_2.5pz liq factor.inp
;



TITLE 'PZ, K2CO3, H2O and CO2 Absorber Model'

IN-UNITS SI MOLE-FLOW='mol/hr' PRESSURE=psi TEMPERATURE=C  &
      PDROP='N/sqm'

DEF-STREAMS CONVEN ALL

SIM-OPTIONS
   IN-UNITS MET VOLUME-FLOW='cum/hr' ENTHALPY-FLO='M m Kcal/hr'
&
      HEAT-TRANS-C='kcal/hr-sqm-K' PRESSURE=bar TEMPERATURE=C  &
      VOLUME=cum DELTA-T=C HEAD=meter MOLE-DENSITY='kmol/cum'
&
      MASS-DENSITY='kg/cum' MOLE-ENTHALP='kcal/mol'  &
      MASS-ENTHALP='kcal/kg' HEAT=M m Kcal MOLE-CONC='mol/l'  &
      PDROP=bar
   SIM-OPTIONS NPHASE=2

RUN-CONTROL MAX-TIME=1000.

DESCRIPTION "
   Electrolytes Simulation with Metric Units :
   C, bar, kg/hr, kmol/hr, M m Kcal/hr, cum/hr.

   Property Method: ELECNRTL

   Flow basis for input: Mole

   Stream report composition: Mole flow

   COPYRIGHT, THE UNIVERSITY OF TEXAS
   DEVELOPED BY ERIC CHEN (2007)
   "

DATABANKS ASPENPCD  / AQUEOUS  / SOLIDS  / INORGANIC  /  &
      PURE11

PROP-SOURCES ASPENPCD  / AQUEOUS  / SOLIDS  / INORGANIC  /  &
      PURE11

COMPONENTS
   H2O H2O /
   K2CO3 K2CO3 /
   KHCO3 KHCO3 /
   PZ C4H10N2 /
   K+ K+ /
   H3O+ H3O+ /
   CO2 CO2 /
   HCO3- HCO3- /
   OH- OH- /
   CO3--2 CO3-2 /
   PZH+ /
   PZCOO- /
   PZCOO-2 /
   HPZCOO /
   N2 N2

ADA-SETUP
   ADA-SETUP PROCEDURE=REL9

HENRY-COMPS GLOBAL CO2 N2

CHEMISTRY GLOBAL
   IN-UNITS MET VOLUME-FLOW='cum/hr' ENTHALPY-FLO='M m Kcal/hr'
&
      HEAT-TRANS-C='kcal/hr-sqm-K' PRESSURE=bar TEMPERATURE=C  &
```

```
      VOLUME=cum DELTA-T=C HEAD=meter MOLE-DENSITY='kmol/cum'
&
      MASS-DENSITY='kg/cum' MOLE-ENTHALP='kcal/mol'  &
      MASS-ENTHALP='kcal/kg' HEAT=M m Kcal MOLE-CONC='mol/l'  &
      PDROP=bar
   PARAM TAPP=0.
   DISS K2CO3 K+ 2 / CO3--2 1
   DISS KHCO3 K+ 1 / HCO3- 1
   STOIC 1 H2O -2 / H3O+ 1 / OH- 1
   STOIC 2 CO2 -1 / H2O -2 / H3O+ 1 / HCO3- 1
   STOIC 3 HCO3- -1 / H2O -1 / H3O+ 1 / CO3--2 1
   STOIC 4 PZH+ -1. / H2O -1. / PZ 1. / H3O+ 1.
   STOIC 5 PZ -1. / HCO3- -1. / PZCOO- 1. / H2O 1.
   STOIC 6 PZCOO- -1. / HCO3- -1. / PZCOO-2 1. / H2O 1.
   STOIC 7 HPZCOO -1. / PZ -1. / PZCOO- 1. / PZH+ 1.
   K-STOIC 1 A=132.89888 B=-13445.9 C=-22.4773 D=0
   K-STOIC 2 A=231.465439 B=-12092.1 C=-36.7816 D=0
   K-STOIC 3 A=216.05043 B=-12431.7 C=-35.4819 D=0
   K-STOIC 4 A=481.945 B=-33448.7 C=-69.7827 D=0.
   K-STOIC 5 A=-609.969 B=36511.7 C=87.075
   K-STOIC 6 A=-251.395 B=14080.2 C=36.7818
   K-STOIC 7 A=-488.753 B=27752.8 C=69.7831

FLOWSHEET
   BLOCK ABS-1 IN=GIN LIN OUT=GASOUT ABSRICH PSD1
   BLOCK LNFLASH IN=LNH2O OUT=LNFGAS LNFLIQ
   BLOCK ABS-FILM IN=GINFILM LINFILM OUT=GOUTFILM LOUTFILM  &
      PSD2
   BLOCK GASDUPL IN=GASIN OUT=GINFILM GIN
   BLOCK LIQDUP IN=LNFLIQ OUT=LIN LINFILM
   BLOCK STGFL1 IN=PSD1 OUT=SFVAP SFLIQ
   BLOCK STGFL2 IN=PSD2 OUT=SFVAP2 SFLIQ2

PROPERTIES ELECNRTL HENRY-COMPS=GLOBAL CHEMISTRY=GLOBAL
&
      TRUE-COMPS=YES
   PROPERTIES NRTL-RK

COMPARE K+ / H2O / K+ H2O

PROP-REPLACE ELECNRTL ELECNRTL
   PROP MULMX MULMX09

PROP-DATA DATA4
   IN-UNITS SI MOLE-FLOW='mol/hr' PRESSURE=psi TEMPERATURE=C  &
      MOLE-ENTHALP='kJ/kmol' MOLE-ENTROPY='cal/mol-K'  &
      PDROP='N/sqm'
   PROP-LIST CHARGE / IONTYP / MW / S025E / DHAQFM
   PVAL PZH+ 1.0 / 1.0 / 87.1469 / -104.8126015 /  &
      -129553.5032
   PVAL PZCOO- -1.0 / 3.0 / 129.1411 / -54.44301138 /  &
      -518314.8371
   PVAL PZCOO-2 -2.0 / 3.0 / 172.1432 / -4.07342124 /  &
      -950183.5167
   PROP-LIST CHARGE / IONTYP / MW / S025E / DHFORM
   PVAL HPZCOO 0 / 1.0 / 130.149 / -54.44301138 /  &
      -565493.0503

PROP-DATA DATA4
   IN-UNITS SI MOLE-FLOW='mol/hr' PRESSURE=bar TEMPERATURE=C  &
      MOLE-VOLUME='cc/mol' PDROP='N/sqm'
   PROP-LIST DGAQHG / DHAQHG / S25HG / OMEGHG / PC / TB /  &
      TC / ZC / VC / VB / RKTZRA / VLSTD / VCRKT
   PVAL PZH+ -90983047 / -100550000 / -470917.11 / 941008655 / &
      29.6882 / 68.75 / 234.25 / 0.26 / 369.445 / 140.903 / &
      0.25 / 0 / 250
   PVAL PZCOO- -490608390 / -542140000 / -400779.86 /  &
      1285873220 / 29.6882 / 68.75 / 234.25 / 0.26 /  &
      369.445 / 140.903 / 0.25 / 0 / 250
   PVAL PZCOO-2 -879555097 / -971930000 / -326881.53 /  &
      1852863480 / 29.6882 / 68.75 / 234.25 / 0.26 /  &
      369.445 / 140.903 / 0.25 / 0 / 250
   PVAL HPZCOO -533467731 / -589500000 / -415875.14 /  &
      772152519 / 29.6882 / 68.75 / 234.25 / 0.26 /  &
      369.445 / 140.9030000 / 0.25 / 0.0 / 250

PROP-DATA PZ
   IN-UNITS SI MOLE-FLOW='mol/hr' PRESSURE=psi TEMPERATURE=C  &
      PDROP='N/sqm'
   PROP-LIST VB
   PVAL PZ 0.129371

PROP-DATA REVIEW-1
```

```
  IN-UNITS MET VOLUME-FLOW='cum/hr' ENTHALPY-FLO='M m Kcal/hr'
&
     HEAT-TRANS-C='kcal/hr-sqm-K' PRESSURE=bar TEMPERATURE=C  &
     VOLUME=cum DELTA-T=C HEAD=meter MOLE-DENSITY='kmol/cum'
&
     MASS-DENSITY='kg/cum' MOLE-ENTHALP='kcal/mol'  &
     MASS-ENTHALP='kcal/kg' HEAT=M m Kcal MOLE-CONC='mol/l'  &
     PDROP=bar
  PROP-LIST DHFORM / DHVLB / RKTZRA
  PVAL PZ 3.917072705 / 9.999355116 / .2665202510

PROP-DATA REVIEW-1
  IN-UNITS MET VOLUME-FLOW='cum/hr' ENTHALPY-FLO='M m Kcal/hr'
&
     HEAT-TRANS-C='kcal/hr-sqm-K' PRESSURE=bar TEMPERATURE=C  &
     VOLUME=cum DELTA-T=C HEAD=meter MOLE-DENSITY='kmol/cum'
&
     MASS-DENSITY='kg/cum' MOLE-ENTHALP='kcal/mol'  &
     MASS-ENTHALP='kcal/kg' MOLE-VOLUME='cum/kmol' HEAT=M m
Kcal  &
     MOLE-CONC='mol/l' PDROP=bar
  PROP-LIST VB
  PVAL PZ 0.129371

PROP-DATA REVIEW-1
  IN-UNITS MET VOLUME-FLOW='cum/hr' ENTHALPY-FLO='M m Kcal/hr'
&
     HEAT-TRANS-C='kcal/hr-sqm-K' PRESSURE=bar TEMPERATURE=C  &
     VOLUME=cum DELTA-T=C HEAD=meter MOLE-DENSITY='kmol/cum'
&
     MASS-DENSITY='kg/cum' MOLE-ENTHALP='kcal/mol'  &
     MASS-ENTHALP='kcal/kg' HEAT=M m Kcal MOLE-CONC='mol/l'  &
     PDROP=bar
  PROP-LIST VLSTD
  PVAL H2O 18.04998800
  PVAL PZ 129.3710000
  PVAL CO2 53.55780000

PROP-DATA RKTZRA
  IN-UNITS SI MOLE-FLOW='mol/hr' PRESSURE=psi TEMPERATURE=C  &
     PDROP='N/sqm'
  PROP-LIST RKTZRA
  PVAL PZ 0.26652025

PROP-DATA CPAQ0-1
  IN-UNITS MET VOLUME-FLOW='cum/hr' ENTHALPY-FLO='M m Kcal/hr'
&
     HEAT-TRANS-C='kcal/hr-sqm-K' PRESSURE=bar TEMPERATURE=C  &
     VOLUME=cum DELTA-T=C HEAD=meter MOLE-DENSITY='kmol/cum'
&
     MASS-DENSITY='kg/cum' MOLE-ENTHALP='kcal/mol'  &
     MASS-ENTHALP='kcal/kg' HEAT=M m Kcal MOLE-CONC='mol/l'  &
     PDROP=bar
  PROP-LIST CPAQ0
  PVAL PZH+ 164.050109 0.071015035 0
  PVAL PZCOO- 172.9708577 0.521015035 0
  PVAL PZCOO-2 226.7359101 0.952615897 0

PROP-DATA CPDIEC-1
  IN-UNITS MET VOLUME-FLOW='cum/hr' ENTHALPY-FLO='M m Kcal/hr'
&
     HEAT-TRANS-C='kcal/hr-sqm-K' PRESSURE=bar TEMPERATURE=C  &
     VOLUME=cum DELTA-T=C HEAD=meter MOLE-DENSITY='kmol/cum'
&
     MASS-DENSITY='kg/cum' MOLE-ENTHALP='kcal/mol'  &
     MASS-ENTHALP='kcal/kg' HEAT=M m Kcal MOLE-CONC='mol/l'  &
     PDROP=bar
  PROP-LIST CPDIEC
  PVAL PZ 4.25304 1532.20 298.15

PROP-DATA CPIG-1
  IN-UNITS MET VOLUME-FLOW='cum/hr' ENTHALPY-FLO='M m Kcal/hr'
&
     HEAT-TRANS-C='kcal/hr-sqm-K' PRESSURE=bar TEMPERATURE=C  &
     VOLUME=cum DELTA-T=C HEAD=meter MOLE-DENSITY='kmol/cum'
&
     MASS-DENSITY='kg/cum' MOLE-ENTHALP='kcal/mol'  &
     MASS-ENTHALP='kcal/kg' HEAT=M m Kcal MOLE-CONC='mol/l'  &
     PDROP=bar
  PROP-LIST CPIG
  PVAL CO3--2 -1.054000669 0.0 0 0 0 0 0 -273.15 726.85  &
     7.943059138 5.08E-03 1.5
  PVAL PZH+ -1.054000669 0 0 0 0 0 -273.15 726.85  &
     7.943059138 5.08E-03 1.5
```

```
  PVAL PZCOO- -1.054000669 0 0 0 0 0 -273.15 726.85  &
    7.943059138 5.08E-03 1.5
  PVAL PZCOO-2 -1.054000669 0 0 0 0 0 -273.15 726.85  &
    7.943059138 5.08E-03 1.5
  PVAL HPZCOO 179.1101695 0.502615897 0 0 0 0 -273.15  &
    726.85 7.943059138 5.08E-03 1.5

PROP-DATA DHVLWT-1
  IN-UNITS MET VOLUME-FLOW='cum/hr' ENTHALPY-FLO='M m Kcal/hr'
&
    HEAT-TRANS-C='kcal/hr-sqm-K' PRESSURE=bar TEMPERATURE=C  &
    VOLUME=cum DELTA-T=C HEAD=meter MOLE-DENSITY='kmol/cum'
&
    MASS-DENSITY='kg/cum' MOLE-ENTHALP='kcal/mol'  &
    MASS-ENTHALP='kcal/kg' HEAT=M m Kcal MOLE-CONC='mol/l'  &
    PDROP=bar
  PROP-LIST DHVLWT
  PVAL HPZCOO 0 0 0

PROP-DATA IONMUB-1
  IN-UNITS MET VOLUME-FLOW='cum/hr' ENTHALPY-FLO='M m Kcal/hr'
&
    HEAT-TRANS-C='kcal/hr-sqm-K' PRESSURE=bar TEMPERATURE=C  &
    VOLUME=cum DELTA-T=C HEAD=meter MOLE-DENSITY='kmol/cum'
&
    MASS-DENSITY='kg/cum' MOLE-ENTHALP='kcal/mol'  &
    MASS-ENTHALP='kcal/kg' HEAT=M m Kcal MOLE-CONC='mol/l'  &
    PDROP=bar
  PROP-LIST IONMUB
  PVAL OH- 3056.175080 0.0
  PVAL PZCOO- 749.3994360 0.0
  PVAL PZCOO-2 2169.349130 0.0
  PVAL HCO3- 189.1691370 0.0
  PVAL CO3--2 619.9145130 0.0
  PVAL PZH+ -738.5092540 0.0

PROP-DATA PLXANT-1
  IN-UNITS SI
  PROP-LIST PLXANT
  PVAL H2O 72.550 -7206.70 .0 .0 -7.13850 .0000040460 2.0  &
    273.0 650.0
  PVAL PZH+ -1.00E+20 0 0 0 0 0 0 0 2000
  PVAL PZCOO- -1.00E+20 0 0 0 0 0 0 0 2000
  PVAL PZCOO-2 -1.00E+20 0 0 0 0 0 0 0 2000
  PVAL HPZCOO -1.00E+20 0 0 0 0 0 0 0 2000

PROP-DATA VLBROC-1
  IN-UNITS SI
  PROP-LIST VLBROC
  PVAL H2O .04640
  PVAL CO2 .09390

PROP-DATA HOCETA-1
  IN-UNITS ENG
  PROP-LIST HOCETA
  BPVAL H2O H2O 1.700000000
  BPVAL H2O CO2 .3000000000
  BPVAL CO2 H2O .3000000000
  BPVAL CO2 CO2 .1600000000

PROP-DATA ANDKIJ-1
  IN-UNITS ENG
  PROP-LIST ANDKIJ
  BPVAL PZ H2O -198.4399930 1.25683735E+5
  BPVAL H2O PZ -198.4399930 1.25683735E+5

PROP-DATA ANDMIJ-1
  IN-UNITS ENG
  PROP-LIST ANDMIJ
  BPVAL PZ H2O 4269.360160 -2.5189449E+6
  BPVAL H2O PZ 4269.360160 -2.5189449E+6

PROP-DATA HENRY-1
  IN-UNITS MET VOLUME-FLOW='cum/hr' ENTHALPY-FLO='M m Kcal/hr'
&
    HEAT-TRANS-C='kcal/hr-sqm-K' PRESSURE=bar TEMPERATURE=K  &
    VOLUME=cum DELTA-T=C HEAD=meter MOLE-DENSITY='kmol/cum'
&
    MASS-DENSITY='kg/cum' MOLE-ENTHALP='kcal/mol'  &
    MASS-ENTHALP='kcal/kg' HEAT=M m Kcal MOLE-CONC='mol/l'  &
    PDROP=bar
  PROP-LIST HENRY
  BPVAL CO2 H2O 159.1996745 -8477.711000 -21.95743000  &
    5.78074800E-3 273.0000000 500.0000000 0.0
```

```
   BPVAL N2 H2O -21.86242546 -2953.500000 10.39600000  &
     -.0540060000 273.1500000 345.6500000 0.0

PROP-DATA NRTL-1
   IN-UNITS MET VOLUME-FLOW='cum/hr' ENTHALPY-FLO='M m Kcal/hr'
&
      HEAT-TRANS-C='kcal/hr-sqm-K' PRESSURE=bar TEMPERATURE=K  &
      VOLUME=cum DELTA-T=C HEAD=meter MOLE-DENSITY='kmol/cum'
&
      MASS-DENSITY='kg/cum' MOLE-ENTHALP='kcal/mol'  &
      MASS-ENTHALP='kcal/kg' HEAT=M m Kcal MOLE-CONC='mol/l'  &
      PDROP=bar
   PROP-LIST NRTL
   BPVAL H2O CO2 10.06400000 -3268.135000 .2000000000 0.0 0.0  &
     0.0 273.1500000 473.1500000
   BPVAL CO2 H2O 10.06400000 -3268.135000 .2000000000 0.0 0.0  &
     0.0 273.1500000 473.1500000
   BPVAL H2O PZ 3.25045564 0.0 0.2 0 0 0 0 400
   BPVAL PZ H2O 6.64592945 -2789.4791 0.2 0 0 0 0 400
   BPVAL H2O HPZCOO -2.0805496 0.0 .2000000 0.0 0.0 0.0 0.0  &
     1000.000
   BPVAL HPZCOO H2O 7.14839988 0.0 .2000000 0.0 0.0 0.0 0.0  &
     1000.000
   BPVAL PZ CO2 0.0 0.0 .2000000 0.0 0.0 0.0 0.0 1000.000
   BPVAL CO2 PZ 0.0 0.0 .2000000 0.0 0.0 0.0 0.0 1000.000
   BPVAL PZ HPZCOO 0.0 0.0 .2000000 0.0 0.0 0.0 0.0  &
     1000.000
   BPVAL HPZCOO PZ 0.0 0.0 .2000000 0.0 0.0 0.0 0.0  &
     1000.000
   BPVAL CO2 HPZCOO 0.0 0.0 .2000000 0.0 0.0 0.0 0.0  &
     1000.000
   BPVAL HPZCOO CO2 0.0 0.0 .2000000 0.0 0.0 0.0 0.0  &
     1000.000

PROP-DATA VLCLK-1
   IN-UNITS MET VOLUME-FLOW='cum/hr' ENTHALPY-FLO='M m Kcal/hr'
&
      HEAT-TRANS-C='kcal/hr-sqm-K' PRESSURE=bar TEMPERATURE=C  &
      VOLUME=cum DELTA-T=C HEAD=meter MOLE-DENSITY='kmol/cum'
&
      MASS-DENSITY='kg/cum' MOLE-ENTHALP='kcal/mol'  &
      MASS-ENTHALP='kcal/kg' HEAT=M m Kcal MOLE-CONC='mol/l'  &
      PDROP=bar
   PROP-LIST VLCLK
   BPVAL K+ HCO3- 17.40077680 99.60622970
   BPVAL K+ CO3--2 10.39509860 124.6062640
   BPVAL K+ OH- 261.6117260 -1963.580210
   BPVAL K+ PZCOO-2 120.9666380 0.0
   BPVAL PZH+ PZCOO- 454.5238280 0.0
   BPVAL K+ PZCOO- 1.128907830 484.3426350
   BPVAL PZH+ OH- -428.9154410 0.0
   BPVAL PZH+ HCO3- -1325.643950 7476.869340
   BPVAL PZH+ CO3--2 196.3031750 0.0

PROP-DATA GMELCC-1
   IN-UNITS MET VOLUME-FLOW='cum/hr' ENTHALPY-FLO='M m Kcal/hr'
&
      HEAT-TRANS-C='kcal/hr-sqm-K' PRESSURE=bar TEMPERATURE=C  &
      VOLUME=cum DELTA-T=C HEAD=meter MOLE-DENSITY='kmol/cum'
&
      MASS-DENSITY='kg/cum' MOLE-ENTHALP='kcal/mol'  &
      MASS-ENTHALP='kcal/kg' HEAT=M m Kcal MOLE-CONC='mol/l'  &
      PDROP=bar
   PROP-LIST GMELCC
   PPVAL H2O ( H3O+ OH- ) 8.045000000
   PPVAL ( H3O+ OH- ) H2O -4.072000000
   PPVAL H2O ( H3O+ HCO3- ) 8.045000000
   PPVAL ( H3O+ HCO3- ) H2O -4.072000000
   PPVAL H2O ( H3O+ CO3--2 ) 8.045000000
   PPVAL ( H3O+ CO3--2 ) H2O -4.072000000
   PPVAL H2O ( H3O+ PZCOO- ) 8
   PPVAL ( H3O+ PZCOO- ) H2O -4
   PPVAL H2O ( H3O+ PZCOO-2 ) 8
   PPVAL ( H3O+ PZCOO-2 ) H2O -4
   PPVAL H2O ( K+ OH- ) 7.840673000
   PPVAL ( K+ OH- ) H2O -4.258696000
   PPVAL H2O ( K+ HCO3- ) 7.72747879
   PPVAL ( K+ HCO3- ) H2O -3.12841315
   PPVAL H2O ( K+ CO3--2 ) 9.21361281
   PPVAL ( K+ CO3--2 ) H2O -4.27485273
   PPVAL H2O ( K+ PZCOO- ) 8
   PPVAL ( K+ PZCOO- ) H2O -4
   PPVAL H2O ( K+ PZCOO-2 ) 7.01168545
   PPVAL ( K+ PZCOO-2 ) H2O -4
```

PPVAL H2O (PZH+ OH-) 8
PPVAL (PZH+ OH-) H2O -4
PPVAL H2O (PZH+ HCO3-) 9.08099491
PPVAL (PZH+ HCO3-) H2O -3.5427758
PPVAL H2O (PZH+ CO3--2) 8
PPVAL (PZH+ CO3--2) H2O -4
PPVAL H2O (PZH+ PZCOO-) 6.81507229
PPVAL (PZH+ PZCOO-) H2O -4
PPVAL H2O (PZH+ PZCOO-2) 8
PPVAL (PZH+ PZCOO-2) H2O -4
PPVAL CO2 (H3O+ OH-) 15.00000000
PPVAL (H3O+ OH-) CO2 -8.000000000
PPVAL CO2 (H3O+ HCO3-) 15.00000000
PPVAL (H3O+ HCO3-) CO2 -8.000000000
PPVAL CO2 (H3O+ CO3--2) 15.00000000
PPVAL (H3O+ CO3--2) CO2 -8.000000000
PPVAL CO2 (H3O+ PZCOO-) 10
PPVAL (H3O+ PZCOO-) CO2 -2
PPVAL CO2 (H3O+ PZCOO-2) 10
PPVAL (H3O+ PZCOO-2) CO2 -2
PPVAL CO2 (K+ OH-) 10
PPVAL (K+ OH-) CO2 -2
PPVAL CO2 (K+ HCO3-) 10
PPVAL (K+ HCO3-) CO2 -2
PPVAL CO2 (K+ CO3--2) 10
PPVAL (K+ CO3--2) CO2 -2
PPVAL CO2 (K+ PZCOO-) 10
PPVAL (K+ PZCOO-) CO2 -2
PPVAL CO2 (K+ PZCOO-2) 10
PPVAL (K+ PZCOO-2) CO2 -2
PPVAL CO2 (PZH+ OH-) 10
PPVAL (PZH+ OH-) CO2 -2
PPVAL CO2 (PZH+ HCO3-) 10
PPVAL (PZH+ HCO3-) CO2 -2
PPVAL CO2 (PZH+ CO3--2) 10
PPVAL (PZH+ CO3--2) CO2 -2
PPVAL CO2 (PZH+ PZCOO-) 10
PPVAL (PZH+ PZCOO-) CO2 -2
PPVAL CO2 (PZH+ PZCOO-2) 10
PPVAL (PZH+ PZCOO-2) CO2 -2
PPVAL PZ (H3O+ OH-) 10
PPVAL (H3O+ OH-) PZ -2
PPVAL PZ (H3O+ HCO3-) 10
PPVAL (H3O+ HCO3-) PZ -2
PPVAL PZ (H3O+ CO3--2) 10
PPVAL (H3O+ CO3--2) PZ -2
PPVAL PZ (H3O+ PZCOO-) 10
PPVAL (H3O+ PZCOO-) PZ -2
PPVAL PZ (H3O+ PZCOO-2) 10
PPVAL (H3O+ PZCOO-2) PZ -2
PPVAL PZ (K+ OH-) 10
PPVAL (K+ OH-) PZ -2
PPVAL PZ (K+ HCO3-) 10
PPVAL (K+ HCO3-) PZ -2
PPVAL PZ (K+ CO3--2) 4.79556769
PPVAL (K+ CO3--2) PZ -2
PPVAL PZ (K+ PZCOO-) 10
PPVAL (K+ PZCOO-) PZ -7.2514659
PPVAL PZ (K+ PZCOO-2) 10
PPVAL (K+ PZCOO-2) PZ -2
PPVAL PZ (PZH+ OH-) 10
PPVAL (PZH+ OH-) PZ -2
PPVAL PZ (PZH+ HCO3-) 10
PPVAL (PZH+ HCO3-) PZ -2
PPVAL PZ (PZH+ CO3--2) 10
PPVAL (PZH+ CO3--2) PZ -2
PPVAL PZ (PZH+ PZCOO-) 10
PPVAL (PZH+ PZCOO-) PZ -2
PPVAL PZ (PZH+ PZCOO-2) 10
PPVAL (PZH+ PZCOO-2) PZ -2
PPVAL HPZCOO (H3O+ OH-) 10
PPVAL (H3O+ OH-) HPZCOO -2
PPVAL HPZCOO (H3O+ HCO3-) 10
PPVAL (H3O+ HCO3-) HPZCOO -2
PPVAL HPZCOO (H3O+ CO3--2) 10
PPVAL (H3O+ CO3--2) HPZCOO -2
PPVAL HPZCOO (H3O+ PZCOO-) 10
PPVAL (H3O+ PZCOO-) HPZCOO -2
PPVAL HPZCOO (H3O+ PZCOO-2) 10
PPVAL (H3O+ PZCOO-2) HPZCOO -2
PPVAL HPZCOO (K+ OH-) 10
PPVAL (K+ OH-) HPZCOO -2
PPVAL HPZCOO (K+ HCO3-) 10
PPVAL (K+ HCO3-) HPZCOO -2

```
  PPVAL HPZCOO ( K+ CO3--2 ) 10
  PPVAL ( K+ CO3--2 ) HPZCOO -2
  PPVAL HPZCOO ( K+ PZCOO- ) 10
  PPVAL ( K+ PZCOO- ) HPZCOO -2
  PPVAL HPZCOO ( K+ PZCOO-2 ) 3.80551713
  PPVAL ( K+ PZCOO-2 ) HPZCOO -2
  PPVAL HPZCOO ( PZH+ OH- ) 10
  PPVAL ( PZH+ OH- ) HPZCOO -2
  PPVAL HPZCOO ( PZH+ HCO3- ) 10
  PPVAL ( PZH+ HCO3- ) HPZCOO -2
  PPVAL HPZCOO ( PZH+ CO3--2 ) 10
  PPVAL ( PZH+ CO3--2 ) HPZCOO -2
  PPVAL HPZCOO ( PZH+ PZCOO- ) 10
  PPVAL ( PZH+ PZCOO- ) HPZCOO -2
  PPVAL HPZCOO ( PZH+ PZCOO-2 ) 10
  PPVAL ( PZH+ PZCOO-2 ) HPZCOO -2

PROP-DATA GMELCD-1
  IN-UNITS MET VOLUME-FLOW='cum/hr' ENTHALPY-FLO='M m Kcal/hr'
&
     HEAT-TRANS-C='kcal/hr-sqm-K' PRESSURE=bar TEMPERATURE=C  &
     VOLUME=cum DELTA-T=C HEAD=meter MOLE-DENSITY='kmol/cum'
&
     MASS-DENSITY='kg/cum' MOLE-ENTHALP='kcal/mol'  &
     MASS-ENTHALP='kcal/kg' HEAT=M m Kcal MOLE-CONC='mol/l'  &
     PDROP=bar
  PROP-LIST GMELCD
  PPVAL H2O ( H3O+ OH- ) 0.0
  PPVAL ( H3O+ OH- ) H2O 0.0
  PPVAL H2O ( H3O+ HCO3- ) 0.0
  PPVAL ( H3O+ HCO3- ) H2O 0.0
  PPVAL H2O ( H3O+ CO3--2 ) 0.0
  PPVAL ( H3O+ CO3--2 ) H2O 0.0
  PPVAL H2O ( H3O+ PZCOO- ) 0.0
  PPVAL ( H3O+ PZCOO- ) H2O 0.0
  PPVAL H2O ( H3O+ PZCOO-2 ) 0.0
  PPVAL ( H3O+ PZCOO-2 ) H2O 0.0
  PPVAL H2O ( K+ OH- ) 773.3601000
  PPVAL ( K+ OH- ) H2O -305.6509000
  PPVAL H2O ( K+ HCO3- ) 0
  PPVAL ( K+ HCO3- ) H2O -129.141168
  PPVAL H2O ( K+ CO3--2 ) 0
  PPVAL ( K+ CO3--2 ) H2O -96.3329422
  PPVAL H2O ( K+ PZCOO- ) 0.0
  PPVAL ( K+ PZCOO- ) H2O 0.0
  PPVAL H2O ( K+ PZCOO-2 ) 0.0
  PPVAL ( K+ PZCOO-2 ) H2O 0.0
  PPVAL H2O ( PZH+ OH- ) 0.0
  PPVAL ( PZH+ OH- ) H2O 0.0
  PPVAL H2O ( PZH+ HCO3- ) 0.0
  PPVAL ( PZH+ HCO3- ) H2O 0.0
  PPVAL H2O ( PZH+ CO3--2 ) 0.0
  PPVAL ( PZH+ CO3--2 ) H2O 0.0
  PPVAL H2O ( PZH+ PZCOO- ) 0.0
  PPVAL ( PZH+ PZCOO- ) H2O 0.0
  PPVAL H2O ( PZH+ PZCOO-2 ) 0.0
  PPVAL ( PZH+ PZCOO-2 ) H2O 0.0
  PPVAL CO2 ( H3O+ OH- ) 0.0
  PPVAL ( H3O+ OH- ) CO2 0.0
  PPVAL CO2 ( H3O+ HCO3- ) 0.0
  PPVAL ( H3O+ HCO3- ) CO2 0.0
  PPVAL CO2 ( H3O+ CO3--2 ) 0.0
  PPVAL ( H3O+ CO3--2 ) CO2 0.0
  PPVAL CO2 ( H3O+ PZCOO- ) 0.0
  PPVAL ( H3O+ PZCOO- ) CO2 0.0
  PPVAL CO2 ( H3O+ PZCOO-2 ) 0.0
  PPVAL ( H3O+ PZCOO-2 ) CO2 0.0
  PPVAL CO2 ( K+ OH- ) 0.0
  PPVAL ( K+ OH- ) CO2 0.0
  PPVAL CO2 ( K+ HCO3- ) 0.0
  PPVAL ( K+ HCO3- ) CO2 0.0
  PPVAL CO2 ( K+ CO3--2 ) 0.0
  PPVAL ( K+ CO3--2 ) CO2 0.0
  PPVAL CO2 ( K+ PZCOO- ) 0.0
  PPVAL ( K+ PZCOO- ) CO2 0.0
  PPVAL CO2 ( K+ PZCOO-2 ) 0.0
  PPVAL ( K+ PZCOO-2 ) CO2 0.0
  PPVAL CO2 ( PZH+ OH- ) 0.0
  PPVAL ( PZH+ OH- ) CO2 0.0
  PPVAL CO2 ( PZH+ HCO3- ) 0.0
  PPVAL ( PZH+ HCO3- ) CO2 0.0
  PPVAL CO2 ( PZH+ CO3--2 ) 0.0
  PPVAL ( PZH+ CO3--2 ) CO2 0.0
  PPVAL CO2 ( PZH+ PZCOO- ) 0.0
```

```
PPVAL ( PZH+ PZCOO- ) CO2 0.0
PPVAL CO2 ( PZH+ PZCOO-2 ) 0.0
PPVAL ( PZH+ PZCOO-2 ) CO2 0.0
PPVAL PZ ( H3O+ OH- ) 0.0
PPVAL ( H3O+ OH- ) PZ 0.0
PPVAL PZ ( H3O+ HCO3- ) 0.0
PPVAL ( H3O+ HCO3- ) PZ 0.0
PPVAL PZ ( H3O+ CO3--2 ) 0.0
PPVAL ( H3O+ CO3--2 ) PZ 0.0
PPVAL PZ ( H3O+ PZCOO- ) 0.0
PPVAL ( H3O+ PZCOO- ) PZ 0.0
PPVAL PZ ( H3O+ PZCOO-2 ) 0.0
PPVAL ( H3O+ PZCOO-2 ) PZ 0.0
PPVAL PZ ( K+ OH- ) 0.0
PPVAL ( K+ OH- ) PZ 0.0
PPVAL PZ ( K+ HCO3- ) 0.0
PPVAL ( K+ HCO3- ) PZ 0.0
PPVAL PZ ( K+ CO3--2 ) 0.0
PPVAL ( K+ CO3--2 ) PZ 0.0
PPVAL PZ ( K+ PZCOO- ) 0.0
PPVAL ( K+ PZCOO- ) PZ 0.0
PPVAL PZ ( K+ PZCOO-2 ) 0.0
PPVAL ( K+ PZCOO-2 ) PZ 0.0
PPVAL PZ ( PZH+ OH- ) 0.0
PPVAL ( PZH+ OH- ) PZ 0.0
PPVAL PZ ( PZH+ HCO3- ) 0.0
PPVAL ( PZH+ HCO3- ) PZ 0.0
PPVAL PZ ( PZH+ CO3--2 ) 0.0
PPVAL ( PZH+ CO3--2 ) PZ 0.0
PPVAL PZ ( PZH+ PZCOO- ) 0.0
PPVAL ( PZH+ PZCOO- ) PZ 0.0
PPVAL PZ ( PZH+ PZCOO-2 ) 0.0
PPVAL ( PZH+ PZCOO-2 ) PZ 0.0
PPVAL HPZCOO ( H3O+ OH- ) 0.0
PPVAL ( H3O+ OH- ) HPZCOO 0.0
PPVAL HPZCOO ( H3O+ HCO3- ) 0.0
PPVAL ( H3O+ HCO3- ) HPZCOO 0.0
PPVAL HPZCOO ( H3O+ CO3--2 ) 0.0
PPVAL ( H3O+ CO3--2 ) HPZCOO 0.0
PPVAL HPZCOO ( H3O+ PZCOO- ) 0.0
PPVAL ( H3O+ PZCOO- ) HPZCOO 0.0
PPVAL HPZCOO ( H3O+ PZCOO-2 ) 0.0
PPVAL ( H3O+ PZCOO-2 ) HPZCOO 0.0
PPVAL HPZCOO ( K+ OH- ) 0.0
PPVAL ( K+ OH- ) HPZCOO 0.0
PPVAL HPZCOO ( K+ HCO3- ) 0.0
PPVAL ( K+ HCO3- ) HPZCOO 0.0
PPVAL HPZCOO ( K+ CO3--2 ) 0.0
PPVAL ( K+ CO3--2 ) HPZCOO 0.0
PPVAL HPZCOO ( K+ PZCOO- ) 0.0
PPVAL ( K+ PZCOO- ) HPZCOO 0.0
PPVAL HPZCOO ( K+ PZCOO-2 ) 0.0
PPVAL ( K+ PZCOO-2 ) HPZCOO 0.0
PPVAL HPZCOO ( PZH+ OH- ) 0.0
PPVAL ( PZH+ OH- ) HPZCOO 0.0
PPVAL HPZCOO ( PZH+ HCO3- ) 0.0
PPVAL ( PZH+ HCO3- ) HPZCOO 0.0
PPVAL HPZCOO ( PZH+ CO3--2 ) 0.0
PPVAL ( PZH+ CO3--2 ) HPZCOO 0.0
PPVAL HPZCOO ( PZH+ PZCOO- ) 0.0
PPVAL ( PZH+ PZCOO- ) HPZCOO 0.0
PPVAL HPZCOO ( PZH+ PZCOO-2 ) 0.0
PPVAL ( PZH+ PZCOO-2 ) HPZCOO 0.0

PROP-DATA GMELCE-1
  IN-UNITS MET VOLUME-FLOW='cum/hr' ENTHALPY-FLO='M m Kcal/hr'
&
     HEAT-TRANS-C='kcal/hr-sqm-K' PRESSURE=bar TEMPERATURE=C  &
     VOLUME=cum DELTA-T=C HEAD=meter MOLE-DENSITY='kmol/cum'
&
     MASS-DENSITY='kg/cum' MOLE-ENTHALP='kcal/mol'  &
     MASS-ENTHALP='kcal/kg' HEAT=M m Kcal MOLE-CONC='mol/l'  &
     PDROP=bar
  PROP-LIST GMELCE
  PPVAL H2O ( H3O+ OH- ) 0.0
  PPVAL ( H3O+ OH- ) H2O 0.0
  PPVAL H2O ( H3O+ HCO3- ) 0.0
  PPVAL ( H3O+ HCO3- ) H2O 0.0
  PPVAL H2O ( H3O+ CO3--2 ) 0.0
  PPVAL ( H3O+ CO3--2 ) H2O 0.0
  PPVAL H2O ( H3O+ PZCOO- ) 0.0
  PPVAL ( H3O+ PZCOO- ) H2O 0.0
  PPVAL H2O ( H3O+ PZCOO-2 ) 0.0
  PPVAL ( H3O+ PZCOO-2 ) H2O 0.0
```

PPVAL H2O (K+ OH-) -5.852382000
PPVAL (K+ OH-) H2O 4.754130000
PPVAL H2O (K+ HCO3-) 0
PPVAL (K+ HCO3-) H2O -2.78779375
PPVAL H2O (K+ CO3--2) 6.43696916
PPVAL (K+ CO3--2) H2O -0.142243146
PPVAL H2O (K+ PZCOO-) 0.0
PPVAL (K+ PZCOO-) H2O 0.0
PPVAL H2O (K+ PZCOO-2) 0.0
PPVAL (K+ PZCOO-2) H2O 0.0
PPVAL H2O (PZH+ OH-) 0.0
PPVAL (PZH+ OH-) H2O 0.0
PPVAL H2O (PZH+ HCO3-) 0.0
PPVAL (PZH+ HCO3-) H2O 0.0
PPVAL H2O (PZH+ CO3--2) 0.0
PPVAL (PZH+ CO3--2) H2O 0.0
PPVAL H2O (PZH+ PZCOO-) 0.0
PPVAL (PZH+ PZCOO-) H2O 0.0
PPVAL H2O (PZH+ PZCOO-2) 0.0
PPVAL (PZH+ PZCOO-2) H2O 0.0
PPVAL CO2 (H3O+ OH-) 0.0
PPVAL (H3O+ OH-) CO2 0.0
PPVAL CO2 (H3O+ HCO3-) 0.0
PPVAL (H3O+ HCO3-) CO2 0.0
PPVAL CO2 (H3O+ CO3--2) 0.0
PPVAL (H3O+ CO3--2) CO2 0.0
PPVAL CO2 (H3O+ PZCOO-) 0.0
PPVAL (H3O+ PZCOO-) CO2 0.0
PPVAL CO2 (H3O+ PZCOO-2) 0.0
PPVAL (H3O+ PZCOO-2) CO2 0.0
PPVAL CO2 (K+ OH-) 0.0
PPVAL (K+ OH-) CO2 0.0
PPVAL CO2 (K+ HCO3-) 0.0
PPVAL (K+ HCO3-) CO2 0.0
PPVAL CO2 (K+ CO3--2) 0.0
PPVAL (K+ CO3--2) CO2 0.0
PPVAL CO2 (K+ PZCOO-) 0.0
PPVAL (K+ PZCOO-) CO2 0.0
PPVAL CO2 (K+ PZCOO-2) 0.0
PPVAL (K+ PZCOO-2) CO2 0.0
PPVAL CO2 (PZH+ OH-) 0.0
PPVAL (PZH+ OH-) CO2 0.0
PPVAL CO2 (PZH+ HCO3-) 0.0
PPVAL (PZH+ HCO3-) CO2 0.0
PPVAL CO2 (PZH+ CO3--2) 0.0
PPVAL (PZH+ CO3--2) CO2 0.0
PPVAL CO2 (PZH+ PZCOO-) 0.0
PPVAL (PZH+ PZCOO-) CO2 0.0
PPVAL CO2 (PZH+ PZCOO-2) 0.0
PPVAL (PZH+ PZCOO-2) CO2 0.0
PPVAL PZ (H3O+ OH-) 0.0
PPVAL (H3O+ OH-) PZ 0.0
PPVAL PZ (H3O+ HCO3-) 0.0
PPVAL (H3O+ HCO3-) PZ 0.0
PPVAL PZ (H3O+ CO3--2) 0.0
PPVAL (H3O+ CO3--2) PZ 0.0
PPVAL PZ (H3O+ PZCOO-) 0.0
PPVAL (H3O+ PZCOO-) PZ 0.0
PPVAL PZ (H3O+ PZCOO-2) 0.0
PPVAL (H3O+ PZCOO-2) PZ 0.0
PPVAL PZ (K+ OH-) 0.0
PPVAL (K+ OH-) PZ 0.0
PPVAL PZ (K+ HCO3-) 0.0
PPVAL (K+ HCO3-) PZ 0.0
PPVAL PZ (K+ CO3--2) 0.0
PPVAL (K+ CO3--2) PZ 0.0
PPVAL PZ (K+ PZCOO-) 0.0
PPVAL (K+ PZCOO-) PZ 0.0
PPVAL PZ (K+ PZCOO-2) 0.0
PPVAL (K+ PZCOO-2) PZ 0.0
PPVAL PZ (PZH+ OH-) 0.0
PPVAL (PZH+ OH-) PZ 0.0
PPVAL PZ (PZH+ HCO3-) 0.0
PPVAL (PZH+ HCO3-) PZ 0.0
PPVAL PZ (PZH+ CO3--2) 0.0
PPVAL (PZH+ CO3--2) PZ 0.0
PPVAL PZ (PZH+ PZCOO-) 0.0
PPVAL (PZH+ PZCOO-) PZ 0.0
PPVAL PZ (PZH+ PZCOO-2) 0.0
PPVAL (PZH+ PZCOO-2) PZ 0.0
PPVAL HPZCOO (H3O+ OH-) 0.0
PPVAL (H3O+ OH-) HPZCOO 0.0
PPVAL HPZCOO (H3O+ HCO3-) 0.0
PPVAL (H3O+ HCO3-) HPZCOO 0.0

```
   PPVAL HPZCOO ( H3O+ CO3--2 ) 0.0
   PPVAL ( H3O+ CO3--2 ) HPZCOO 0.0
   PPVAL HPZCOO ( H3O+ PZCOO- ) 0.0
   PPVAL ( H3O+ PZCOO- ) HPZCOO 0.0
   PPVAL HPZCOO ( H3O+ PZCOO-2 ) 0.0
   PPVAL ( H3O+ PZCOO-2 ) HPZCOO 0.0
   PPVAL HPZCOO ( K+ OH- ) 0.0
   PPVAL ( K+ OH- ) HPZCOO 0.0
   PPVAL HPZCOO ( K+ HCO3- ) 0.0
   PPVAL ( K+ HCO3- ) HPZCOO 0.0
   PPVAL HPZCOO ( K+ CO3--2 ) 0.0
   PPVAL ( K+ CO3--2 ) HPZCOO 0.0
   PPVAL HPZCOO ( K+ PZCOO- ) 0.0
   PPVAL ( K+ PZCOO- ) HPZCOO 0.0
   PPVAL HPZCOO ( K+ PZCOO-2 ) 0.0
   PPVAL ( K+ PZCOO-2 ) HPZCOO 0.0
   PPVAL HPZCOO ( PZH+ OH- ) 0.0
   PPVAL ( PZH+ OH- ) HPZCOO 0.0
   PPVAL HPZCOO ( PZH+ HCO3- ) 0.0
   PPVAL ( PZH+ HCO3- ) HPZCOO 0.0
   PPVAL HPZCOO ( PZH+ CO3--2 ) 0.0
   PPVAL ( PZH+ CO3--2 ) HPZCOO 0.0
   PPVAL HPZCOO ( PZH+ PZCOO- ) 0.0
   PPVAL ( PZH+ PZCOO- ) HPZCOO 0.0
   PPVAL HPZCOO ( PZH+ PZCOO-2 ) 0.0
   PPVAL ( PZH+ PZCOO-2 ) HPZCOO 0.0

PROP-DATA GMELCN-1
   IN-UNITS MET VOLUME-FLOW='cum/hr' ENTHALPY-FLO='M m Kcal/hr'
&
      HEAT-TRANS-C='kcal/hr-sqm-K' PRESSURE=bar TEMPERATURE=C  &
      VOLUME=cum DELTA-T=C HEAD=meter MOLE-DENSITY='kmol/cum'
&
      MASS-DENSITY='kg/cum' MOLE-ENTHALP='kcal/mol'  &
      MASS-ENTHALP='kcal/kg' HEAT=M m Kcal MOLE-CONC='mol/l'  &
      PDROP=bar
   PROP-LIST GMELCN
   PPVAL H2O ( H3O+ OH- ) 0.2
   PPVAL H2O ( H3O+ HCO3- ) 0.2
   PPVAL H2O ( H3O+ CO3--2 ) 0.2
   PPVAL H2O ( H3O+ PZCOO- ) 0.2
   PPVAL H2O ( H3O+ PZCOO-2 ) 0.2
   PPVAL H2O ( K+ OH- ) 0.2
   PPVAL H2O ( K+ HCO3- ) 0.2
   PPVAL H2O ( K+ CO3--2 ) 0.2
   PPVAL H2O ( K+ PZCOO- ) 0.2
   PPVAL H2O ( K+ PZCOO-2 ) 0.2
   PPVAL H2O ( PZH+ OH- ) 0.2
   PPVAL H2O ( PZH+ HCO3- ) 0.2
   PPVAL H2O ( PZH+ CO3--2 ) 0.2
   PPVAL H2O ( PZH+ PZCOO- ) 0.2
   PPVAL H2O ( PZH+ PZCOO-2 ) 0.2
   PPVAL CO2 ( H3O+ OH- ) .1000000000
   PPVAL CO2 ( H3O+ HCO3- ) .1000000000
   PPVAL CO2 ( H3O+ CO3--2 ) .1000000000
   PPVAL CO2 ( H3O+ PZCOO- ) 0.2
   PPVAL CO2 ( H3O+ PZCOO-2 ) 0.2
   PPVAL CO2 ( K+ OH- ) 0.2
   PPVAL CO2 ( K+ HCO3- ) 0.2
   PPVAL CO2 ( K+ CO3--2 ) 0.2
   PPVAL CO2 ( K+ PZCOO- ) 0.2
   PPVAL CO2 ( K+ PZCOO-2 ) 0.2
   PPVAL CO2 ( PZH+ OH- ) 0.2
   PPVAL CO2 ( PZH+ HCO3- ) 0.2
   PPVAL CO2 ( PZH+ CO3--2 ) 0.2
   PPVAL CO2 ( PZH+ PZCOO- ) 0.2
   PPVAL CO2 ( PZH+ PZCOO-2 ) 0.2
   PPVAL PZ ( H3O+ OH- ) 0.2
   PPVAL PZ ( H3O+ HCO3- ) 0.2
   PPVAL PZ ( H3O+ CO3--2 ) 0.2
   PPVAL PZ ( H3O+ PZCOO- ) 0.2
   PPVAL PZ ( H3O+ PZCOO-2 ) 0.2
   PPVAL PZ ( K+ OH- ) 0.2
   PPVAL PZ ( K+ HCO3- ) 0.2
   PPVAL PZ ( K+ CO3--2 ) 0.2
   PPVAL PZ ( K+ PZCOO- ) 0.2
   PPVAL PZ ( K+ PZCOO-2 ) 0.2
   PPVAL PZ ( PZH+ OH- ) 0.2
   PPVAL PZ ( PZH+ HCO3- ) 0.2
   PPVAL PZ ( PZH+ CO3--2 ) 0.2
   PPVAL PZ ( PZH+ PZCOO- ) 0.2
   PPVAL PZ ( PZH+ PZCOO-2 ) 0.2
   PPVAL HPZCOO ( H3O+ OH- ) 0.2
   PPVAL HPZCOO ( H3O+ HCO3- ) 0.2
```

```
   PPVAL HPZCOO ( H3O+ CO3--2 ) 0.2
   PPVAL HPZCOO ( H3O+ PZCOO- ) 0.2
   PPVAL HPZCOO ( H3O+ PZCOO-2 ) 0.2
   PPVAL HPZCOO ( K+ OH- ) 0.2
   PPVAL HPZCOO ( K+ HCO3- ) 0.2
   PPVAL HPZCOO ( K+ CO3--2 ) 0.2
   PPVAL HPZCOO ( K+ PZCOO- ) 0.2
   PPVAL HPZCOO ( K+ PZCOO-2 ) 0.2
   PPVAL HPZCOO ( PZH+ OH- ) 0.2
   PPVAL HPZCOO ( PZH+ HCO3- ) 0.2
   PPVAL HPZCOO ( PZH+ CO3--2 ) 0.2
   PPVAL HPZCOO ( PZH+ PZCOO- ) 0.2
   PPVAL HPZCOO ( PZH+ PZCOO-2 ) 0.2

PROP-SET CPGMX CPMX UNITS='cal/mol-K' SUBSTREAM=MIXED
PHASE=V

PROP-SET CPLMX CPMX UNITS='cal/mol-K' SUBSTREAM=MIXED PHASE=L

PROP-SET D-HPZCOO DMX SUBSTREAM=MIXED COMPS=HPZCOO
PHASE=L

PROP-SET G-CO2 GAMUS SUBSTREAM=MIXED COMPS=CO2 PHASE=L

PROP-SET G-CO3 GAMMA SUBSTREAM=MIXED COMPS=CO3--2 PHASE=L

PROP-SET G-H2O
   IN-UNITS MET VOLUME-FLOW='cum/hr' ENTHALPY-FLO='M m Kcal/hr'
&
      HEAT-TRANS-C='kcal/hr-sqm-K' PRESSURE=bar TEMPERATURE=C  &
      VOLUME=cum DELTA-T=C HEAD=meter MOLE-DENSITY='kmol/cum'
&
      MASS-DENSITY='kg/cum' MOLE-ENTHALP='kcal/mol'  &
      MASS-ENTHALP='kcal/kg' HEAT=M m Kcal MOLE-CONC='mol/l'  &
      PDROP=bar
   PROPNAME-LIS GAMMA SUBSTREAM=MIXED COMPS=H2O PHASE=L

PROP-SET G-HCO3 GAMMA SUBSTREAM=MIXED COMPS=HCO3-
PHASE=L

PROP-SET G-HPZCOO GAMMA SUBSTREAM=MIXED COMPS=HPZCOO
PHASE=L

PROP-SET G-K+ GAMMA SUBSTREAM=MIXED COMPS=K+ PHASE=L

PROP-SET G-OH GAMMA SUBSTREAM=MIXED COMPS=OH- PHASE=L

PROP-SET G-PZ GAMMA SUBSTREAM=MIXED COMPS=PZ PHASE=L

PROP-SET G-PZCOO GAMMA SUBSTREAM=MIXED COMPS=PZCOO-
PHASE=L

PROP-SET G-PZCOO2 GAMMA SUBSTREAM=MIXED COMPS=PZCOO-2
PHASE=L

PROP-SET G-PZH+ GAMMA SUBSTREAM=MIXED COMPS=PZH+ PHASE=L

PROP-SET IONSTR IONSM SUBSTREAM=MIXED PHASE=L

PROP-SET MASSCONC
   IN-UNITS MET VOLUME-FLOW='cum/hr' ENTHALPY-FLO='M m Kcal/hr'
&
      HEAT-TRANS-C='kcal/hr-sqm-K' PRESSURE=bar TEMPERATURE=C  &
      VOLUME=cum DELTA-T=C HEAD=meter MOLE-DENSITY='kmol/cum'
&
      MASS-DENSITY='kg/cum' MOLE-ENTHALP='kcal/mol'  &
      MASS-ENTHALP='kcal/kg' HEAT=M m Kcal MOLE-CONC='mol/l'  &
      PDROP=bar
   PROPNAME-LIS MASSCONC SUBSTREAM=MIXED PHASE=L
;  "Mass concentration (component mass/liquid volume)"


PROP-SET MOLECONC
   IN-UNITS MET VOLUME-FLOW='cum/hr' ENTHALPY-FLO='M m Kcal/hr'
&
      HEAT-TRANS-C='kcal/hr-sqm-K' PRESSURE=bar TEMPERATURE=C  &
      VOLUME=cum DELTA-T=C HEAD=meter MOLE-DENSITY='kmol/cum'
&
      MASS-DENSITY='kg/cum' MOLE-ENTHALP='kcal/mol'  &
      MASS-ENTHALP='kcal/kg' HEAT=M m Kcal MOLE-CONC='mol/l'  &
      PDROP=bar
   PROPNAME-LIS MOLECONC UNITS='mol/l' SUBSTREAM=MIXED
PHASE=L
;  "Mole concentration (component mole/liquid volume)"
```

```
PROP-SET MUMX MUMX SUBSTREAM=MIXED PHASE=L

PROP-SET PPCO2 PPMX UNITS='Pa' SUBSTREAM=MIXED COMPS=CO2  &
     PHASE=V

PROP-SET PPH2O PPMX UNITS='Pa' SUBSTREAM=MIXED COMPS=H2O  &
     PHASE=V

PROP-SET PPPZ PPMX UNITS='Pa' SUBSTREAM=MIXED COMPS=PZ
PHASE=V

PROP-SET RHOMX RHOMX UNITS='kg/cum' SUBSTREAM=MIXED
PHASE=L

STREAM GASIN
   SUBSTREAM MIXED TEMP=40. PRES=0.01681693615 <psig>  &
      FREE-WATER=NO NPHASE=1 PHASE=V
   MOLE-FLOW H2O 2685.0358118 / CO2 5770.9797698 / N2  &
      27775.646121

STREAM LNH2O
   SUBSTREAM MIXED TEMP=40. PRES=-6.6 <in-water-g>  &
      FLASH-OPTION=NOFLASH
   MOLE-FLOW H2O 142200.83777 / K2CO3 6390.8612541 / PZ  &
      6391. / CO2 3405.9106826

BLOCK LNFLASH FLASH2
   PARAM TEMP=40. PRES=-6.1960359653 <in-water-g>

BLOCK STGFL1 FLASH2
   PARAM TEMP=40. VFRAC=1E-007 P-EST=14.

BLOCK STGFL2 FLASH2
   PARAM TEMP=45. VFRAC=1E-007 P-EST=14.

;=====================================================
;    RateFrac To RateSep (RadFrac) Conversion
;              (Version 2004.1)
;
; Conversion time: Mon Sep 11 11:03:30 2006
;
;=====================================================

BLOCK ABS-1 RADFRAC
   PARAM NSTAGE=50 EFF=MURPHREE ABSORBER=YES HYDRAULIC=YES
&
      MAXOL=50 TOLOL=0.001
   COL-CONFIG CONDENSER=NONE REBOILER=NONE
   RATESEP-ENAB CALC-MODE=RIG-RATE
   RATESEP-PARA RBTRFC=0.5 RBRXN=0.5 RBPACKEND=0.5  &
      RS-TOL=0.0001 RS-STABLE-IT=40 RS-MAXIT=50  &
      RS-STABLE-ME=DOGLEG CC-AVG-PARAM=1E-005 CONTIN-ITER=3  &
      DIAG-ITER=6 DISC-RATIO=6.
   DIAGNOSTICS MAIN=6
   FEEDS GIN 50 ON-STAGE / LIN 1 ON-STAGE
   PRODUCTS GASOUT 1 V / ABSRICH 50 L
   PSEUDO-STREA PSD1 2 MOLE-FLOW=10.
   P-SPEC 1 -5.9 <in-water-g>
   COL-SPECS DP-COL=5.52 <in-water>
   REAC-STAGES 1 50 KAX-H2O3
   T-EST 1 38. / 50 54.
   TRAY-REPORT TRAY-OPTION=ALL-TRAYS PROPERTIES=G-CO2 G-CO3
&
      G-H2O G-HCO3 G-HPZCOO G-K+ G-OH G-PZ G-PZCOO G-PZCOO2  &
      G-PZH+ PPCO2 PPH2O PPPZ D-HPZCOO MOLECONC CPGMX CPLMX
   PACK-RATE 1 1 50 FLEXIPAC VENDOR=KOCH PACK-MAT=STEEL  &
      PACK-SIZE="2Y" SPAREA=225.0000 VOIDFR=0.93 STICH1=5.  &
      STICH2=3. STICH3=0.45 PACK-HT=6.096 DIAM=16.8 <in>  &
      THETA=45. P-UPDATE=NO
   PACK-RATE2 1 RATE-BASED=YES LIQ-FILM=DISCRXN LIQ-CORRF=YES
&
      MTRFC-CORR=BRF-92 INTFA-CORR=BRF-92  &
      HOLDUP-CORR=PERCENT-DATA FLOW-MODEL=VPLUG-PAVG  &
      AREA-FACTOR=1.15 PERCENT-LHLD=1. LHLDP-FACTOR=1.  &
      NLPOINTS=3 STRUCT-SIDE=.0180340 S-RENEWAL-F=0.9  &
      HT-FACTOR=1.
   REPORT STDVPROF INT-PROFILE INT-AREA BULKRXN DIFF-COEFF  &
      MT-RATE MT-COEFF HT-RATE HT-COEFF FILMRXN S-DIMLESS  &
      V-DIMLESS
   HTLOSS-SEC SECNO=1 1 1 HTLOSS-SEC=0. / SECNO=2 2 2  &
      HTLOSS-SEC=0.
```

```
;=====================================================
;    RateFrac To RateSep (RadFrac) Conversion
;               (Version 2004.1)
;
; Conversion time: Mon Sep 11 11:03:30 2006
;
;=====================================================

BLOCK ABS-FILM RADFRAC
  PARAM NSTAGE=50 EFF=MURPHREE ABSORBER=YES HYDRAULIC=YES
&
     MAXOL=50 TOLOL=0.001
  COL-CONFIG CONDENSER=NONE REBOILER=NONE
  RATESEP-ENAB CALC-MODE=RIG-RATE
  RATESEP-PARA RS-TOL=0.0001 RS-STABLE-IT=40 RS-MAXIT=50  &
    RS-STABLE-ME=DOGLEG CC-AVG-PARAM=1E-005 CONTIN-ITER=3  &
    DIAG-ITER=6 DISC-RATIO=6.
  DIAGNOSTICS MAIN=6
  FEEDS GINFILM 50 ON-STAGE / LINFILM 1 ON-STAGE
  PRODUCTS GOUTFILM 1 V / LOUTFILM 50 L
  PSEUDO-STREA PSD2 4 MOLE-FLOW=10.
  P-SPEC 1 -5.9 <in-water-g>
  COL-SPECS DP-COL=5.52 <in-water>
  COMP-EFF 1 CO2 0.10336943 / 2 CO2 0.10181558 / 3 CO2  &
    0.09990972 / 4 CO2 0.09755632 / 5 CO2 0.09473571 /  &
    6 CO2 0.09145929 / 7 CO2 0.08774596 / 8 CO2  &
    0.083628 / 9 CO2 0.07916923 / 10 CO2 0.07447016 /  &
    11 CO2 0.06967231 / 12 CO2 0.06494452 / 13 CO2  &
    0.06046145 / 14 CO2 0.05637672 / 15 CO2 0.05280264 /  &
    16 CO2 0.04980273 / 17 CO2 0.04739682 / 18 CO2  &
    0.0455732 / 19 CO2 0.04430102 / 20 CO2 0.04354277 /  &
    21 CO2 0.04326015 / 22 CO2 0.04341941 / 23 CO2  &
    0.04399476 / 24 CO2 0.04497073 / 25 CO2 0.04634451 /  &
    26 CO2 0.04812791 / 27 CO2 0.05035017 / 28 CO2  &
    0.05306109 / 29 CO2 0.05633648
  REAC-STAGES 1 50 KAX-H2O3
  T-EST 1 38. / 50 52.
  TRAY-REPORT TRAY-OPTION=ALL-TRAYS PROPERTIES=G-CO2 G-CO3
&
     G-H2O G-HCO3 G-HPZCOO G-K+ G-OH G-PZ G-PZCOO G-PZCOO2  &
     G-PZH+ PPCO2 PPH2O PPPZ D-HPZCOO MOLECONC CPGMX CPLMX
  PACK-RATE 1 1 50 FLEXIPAC VENDOR=KOCH PACK-MAT=STEEL  &
     PACK-SIZE="2Y" SPAREA=225.0000 VOIDFR=0.93 STICH1=5.  &
     STICH2=3. STICH3=0.45 PACK-HT=6.096 DIAM=16.8 <in>  &
     THETA=45. P-UPDATE=NO
  PACK-RATE2 1 RATE-BASED=YES LIQ-FILM=DISCRXN LIQ-CORRF=YES
&
     MTRFC-CORR=BRF-92 INTFA-CORR=BRF-92  &
     HOLDUP-CORR=PERCENT-DATA FLOW-MODEL=VPLUG-PAVG  &
     AREA-FACTOR=1.5 PERCENT-LHLD=1. LHLDP-FACTOR=1.  &
     NLPOINTS=3 STRUCT-SIDE=.0180340 HT-FACTOR=1.
  REPORT STDVPROF INT-PROFILE INT-AREA BULKRXN DIFF-COEFF  &
     MT-RATE MT-COEFF HT-RATE HT-COEFF FILMRXN S-DIMLESS  &
     V-DIMLESS

BLOCK GASDUPL DUPL
  PROPERTIES ELECNRTL HENRY-COMPS=GLOBAL CHEMISTRY=GLOBAL

BLOCK LIQDUP DUPL

DESIGN-SPEC DS-1
  DEFINE GCO2OU MOLE-FLOW STREAM=GASOUT SUBSTREAM=MIXED
&
     COMPONENT=CO2
  SPEC "GCO2OU" TO "2623"
  TOL-SPEC "1"
  VARY BLOCK-VAR BLOCK=ABS-1 VARIABLE=AREA-FACTOR  &
    SENTENCE=PACK-RATE2 ID1=1
  LIMITS "1" "2"

EO-CONV-OPTI

CALCULATOR FLSHLDG
  DEFINE RCO2 MOLE-FLOW STREAM=SFLIQ SUBSTREAM=MIXED  &
    COMPONENT=CO2
  DEFINE RPZ MOLE-FLOW STREAM=SFLIQ SUBSTREAM=MIXED  &
    COMPONENT=PZ
  DEFINE SFLDG PARAMETER 13
  DEFINE RHPZCO MOLE-FLOW STREAM=SFLIQ SUBSTREAM=MIXED  &
    COMPONENT=HPZCOO
  DEFINE RPZCO2 MOLE-FLOW STREAM=SFLIQ SUBSTREAM=MIXED  &
    COMPONENT=PZCOO-2
  DEFINE RPZCOO MOLE-FLOW STREAM=SFLIQ SUBSTREAM=MIXED  &
    COMPONENT=PZCOO-
```

```
    DEFINE RCO3 MOLE-FLOW STREAM=SFLIQ SUBSTREAM=MIXED  &
      COMPONENT=CO3--2
    DEFINE RHCO3 MOLE-FLOW STREAM=SFLIQ SUBSTREAM=MIXED  &
      COMPONENT=HCO3-
    DEFINE RK MOLE-FLOW STREAM=SFLIQ SUBSTREAM=MIXED  &
      COMPONENT=K+
    DEFINE RPZH MOLE-FLOW STREAM=SFLIQ SUBSTREAM=MIXED  &
      COMPONENT=PZH+
F   SFLDG=(RCO2+RHPZCO+2*RPZCO2+RPZCOO+RCO3+RHCO3)/
F   (2*(RPZ+RPZH+RPZCOO+RPZCO2+RHPZCO)+RK)
F   WRITE(NTERM,*)SFLDG
    READ-VARS RCO2 RPZ RHPZCO RPZCO2 RPZCOO RCO3 RHCO3 RK  &
      RPZH
    WRITE-VARS SFLDG

CALCULATOR HTLOSS
    VECTOR-DEF TCOL PROFILE BLOCK=ABS-1 VARIABLE=TEMP  &
      SENTENCE=PROFILE
    DEFINE TAMB PARAMETER 20 PHYS-QTY=TEMPERATURE UOM="C"  &
      INIT-VAL=14.158333333
    DEFINE UA PARAMETER 21 INIT-VAL=0.
    DEFINE H1 BLOCK-VAR BLOCK=ABS-1 VARIABLE=HTLOSS-SEC  &
      SENTENCE=HTLOSS-SEC ID1=1
    DEFINE H2 BLOCK-VAR BLOCK=ABS-1 VARIABLE=HTLOSS-SEC  &
      SENTENCE=HTLOSS-SEC ID1=2
F   H1=UA*(TCOL(1)-TAMB)
F   H2=UA*(TCOL(2)-TAMB)
C   H3=UA*(TCOL(3)-TAMB)
C   H4=UA*(TCOL(4)-TAMB)
C   H5=UA*(TCOL(5)-TAMB)
C   H6=UA*(TCOL(6)-TAMB)
C   H7=UA*(TCOL(7)-TAMB)
C   H8=UA*(TCOL(8)-TAMB)
C   H9=UA*(TCOL(9)-TAMB)
C   H10=UA*(TCOL(10)-TAMB)
C   H11=UA*(TCOL(11)-TAMB)
C   H12=UA*(TCOL(12)-TAMB)
C   H13=UA*(TCOL(13)-TAMB)
C   H14=UA*(TCOL(14)-TAMB)
C   H15=UA*(TCOL(15)-TAMB)
C   H16=UA*(TCOL(16)-TAMB)
C   H17=UA*(TCOL(17)-TAMB)
C   H18=UA*(TCOL(18)-TAMB)
C   H19=UA*(TCOL(19)-TAMB)
C   H20=UA*(TCOL(20)-TAMB)
C   H21=UA*(TCOL(21)-TAMB)
C   H22=UA*(TCOL(22)-TAMB)
C   H23=UA*(TCOL(23)-TAMB)
C   H24=UA*(TCOL(24)-TAMB)
C   H25=UA*(TCOL(25)-TAMB)
C   H26=UA*(TCOL(26)-TAMB)
C   H27=UA*(TCOL(27)-TAMB)
C   H28=UA*(TCOL(28)-TAMB)
C   H29=UA*(TCOL(29)-TAMB)
C   H30=UA*(TCOL(30)-TAMB)
    READ-VARS UA TCOL TAMB
    WRITE-VARS H1 H2
    EXECUTE LAST

CALCULATOR KINFACTR
    DEFINE PZF PARAMETER 1 INIT-VAL=0.2
    DEFINE PZCOOF PARAMETER 2 INIT-VAL=0.2
    DEFINE KPZF REACT-VAR REACTION=KAX-H2O3 VARIABLE=PRE-EXP
&
      SENTENCE=RATE-CON ID1=3
    DEFINE KPZR REACT-VAR REACTION=KAX-H2O3 VARIABLE=PRE-EXP
&
      SENTENCE=RATE-CON ID1=4
    DEFINE KPZCF REACT-VAR REACTION=KAX-H2O3 VARIABLE=PRE-EXP
&
      SENTENCE=RATE-CON ID1=5
    DEFINE KPZCR REACT-VAR REACTION=KAX-H2O3 VARIABLE=PRE-EXP
&
      SENTENCE=RATE-CON ID1=6
    DEFINE PZF2 PARAMETER 3 INIT-VAL=0.2
    DEFINE PZCF2 PARAMETER 4 INIT-VAL=0.2
    DEFINE KPZHF REACT-VAR REACTION=KAX-H2O3 VARIABLE=PRE-EXP
&
      SENTENCE=RATE-CON ID1=7
    DEFINE KPZHR REACT-VAR REACTION=KAX-H2O3 VARIABLE=PRE-EXP
&
      SENTENCE=RATE-CON ID1=8
    DEFINE KPZCHF REACT-VAR REACTION=KAX-H2O3 VARIABLE=PRE-
EXP  &
```

```
     SENTENCE=RATE-CON ID1=17
   DEFINE KPZCHR REACT-VAR REACTION=KAX-H2O3 VARIABLE=PRE-
EXP  &
     SENTENCE=RATE-CON ID1=18
   DEFINE RF910 PARAMETER 5 INIT-VAL=0.2
   DEFINE RF1112 PARAMETER 6 INIT-VAL=0.2
   DEFINE RF1314 PARAMETER 7 INIT-VAL=0.2
   DEFINE RF1516 PARAMETER 8 INIT-VAL=0.2
   DEFINE RF1920 PARAMETER 9 INIT-VAL=0.2
   DEFINE RF2122 PARAMETER 10 INIT-VAL=0.2
   DEFINE RF2324 PARAMETER 11 INIT-VAL=0.2
   DEFINE RF12 PARAMETER 14 INIT-VAL=0.2
   DEFINE RXN9 REACT-VAR REACTION=KAX-H2O3 VARIABLE=PRE-EXP
&
     SENTENCE=RATE-CON ID1=9
   DEFINE RXN10 REACT-VAR REACTION=KAX-H2O3 VARIABLE=PRE-EXP
&
     SENTENCE=RATE-CON ID1=10
   DEFINE RXN11 REACT-VAR REACTION=KAX-H2O3 VARIABLE=PRE-EXP
&
     SENTENCE=RATE-CON ID1=11
   DEFINE RXN12 REACT-VAR REACTION=KAX-H2O3 VARIABLE=PRE-EXP
&
     SENTENCE=RATE-CON ID1=12
   DEFINE RXN13 REACT-VAR REACTION=KAX-H2O3 VARIABLE=PRE-EXP
&
     SENTENCE=RATE-CON ID1=13
   DEFINE RXN14 REACT-VAR REACTION=KAX-H2O3 VARIABLE=PRE-EXP
&
     SENTENCE=RATE-CON ID1=14
   DEFINE RXN15 REACT-VAR REACTION=KAX-H2O3 VARIABLE=PRE-EXP
&
     SENTENCE=RATE-CON ID1=15
   DEFINE RXN16 REACT-VAR REACTION=KAX-H2O3 VARIABLE=PRE-EXP
&
     SENTENCE=RATE-CON ID1=16
   DEFINE RXN19 REACT-VAR REACTION=KAX-H2O3 VARIABLE=PRE-EXP
&
     SENTENCE=RATE-CON ID1=19
   DEFINE RXN20 REACT-VAR REACTION=KAX-H2O3 VARIABLE=PRE-EXP
&
     SENTENCE=RATE-CON ID1=20
   DEFINE RXN21 REACT-VAR REACTION=KAX-H2O3 VARIABLE=PRE-EXP
&
     SENTENCE=RATE-CON ID1=21
   DEFINE RXN22 REACT-VAR REACTION=KAX-H2O3 VARIABLE=PRE-EXP
&
     SENTENCE=RATE-CON ID1=22
   DEFINE RXN23 REACT-VAR REACTION=KAX-H2O3 VARIABLE=PRE-EXP
&
     SENTENCE=RATE-CON ID1=23
   DEFINE RXN24 REACT-VAR REACTION=KAX-H2O3 VARIABLE=PRE-EXP
&
     SENTENCE=RATE-CON ID1=24
   DEFINE RXN1 REACT-VAR REACTION=KAX-H2O3 VARIABLE=PRE-EXP
&
     SENTENCE=RATE-CON ID1=1
   DEFINE RXN2 REACT-VAR REACTION=KAX-H2O3 VARIABLE=PRE-EXP
&
     SENTENCE=RATE-CON ID1=2
F    kpzf = pzf * 26801
F    kpzr = pzf * 2.7688
F
F    kpzcf = pzcoof * 19798
F    kpzcr = pzcoof * 14.0395
F
F    kpzhf = pzf2*1.5072E+08
F    kpzhr = pzf2*3.4841E+12
F
F    kpzchf = pzcf2*7.4224E+07
F    kpzchr = pzcf2*4.2601E+13
F
F    rxn9 = rf910*1.865E+10
F    rxn10 = rf910*2.411E+03
F
F    rxn11 = rf1112*3.6201E+10
F    rxn12 = rf1112*6.8163E+02
F
F    rxn13 = rf1314*3.9334E+11
F    rxn14 = rf1314*7.6235E+03
F
F    rxn15 = rf1516*4.6750E+11
F    rxn16 = rf1516*3.5207E-02
F
```

```
F    rxn19 = rf1920*3.6279e+10
F    rxn20 = rf1920*1.6960E+04
F
F    rxn21 = rf2122*1.9364E+11
F    rxn22 = rf2122*9.3182E+04
F
F    rxn23 = rf2324*1.8683e+10
F    rxn24 = rf2324*59954
F
F    rxn1 = rf12*9.2981e+6
F    rxn2 = rf12*0.0038419
  WRITE-VARS PZF PZCOOF KPZF KPZR KPZCF KPZCR PZF2 PZCF2  &
    KPZHF KPZHR KPZCHF KPZCHR RF910 RF1314 RF1112 RF1516  &
    RF1920 RF2122 RF2324 RF12 RXN10 RXN9 RXN11 RXN12  &
    RXN13 RXN14 RXN15 RXN16 RXN19 RXN20 RXN21 RXN22 RXN23  &
    RXN24 RXN1 RXN2
  EXECUTE FIRST

CALCULATOR RHLDG
  DEFINE RCO2 MOLE-FLOW STREAM=ABSRICH SUBSTREAM=MIXED  &
    COMPONENT=CO2
  DEFINE RPZ MOLE-FLOW STREAM=ABSRICH SUBSTREAM=MIXED  &
    COMPONENT=PZ
  DEFINE RHLDG PARAMETER 12
  DEFINE RHPZCO MOLE-FLOW STREAM=ABSRICH SUBSTREAM=MIXED
&
    COMPONENT=HPZCOO
  DEFINE RPZCO2 MOLE-FLOW STREAM=ABSRICH SUBSTREAM=MIXED
&
    COMPONENT=PZCOO-2
  DEFINE RPZCOO MOLE-FLOW STREAM=ABSRICH SUBSTREAM=MIXED
&
    COMPONENT=PZCOO-
  DEFINE RCO3 MOLE-FLOW STREAM=ABSRICH SUBSTREAM=MIXED  &
    COMPONENT=CO3--2
  DEFINE RHCO3 MOLE-FLOW STREAM=ABSRICH SUBSTREAM=MIXED  &
    COMPONENT=HCO3-
  DEFINE RK MOLE-FLOW STREAM=ABSRICH SUBSTREAM=MIXED  &
    COMPONENT=K+
  DEFINE RPZH MOLE-FLOW STREAM=ABSRICH SUBSTREAM=MIXED  &
    COMPONENT=PZH+
F   RHLDG=(RCO2+RHPZCO+2*RPZCO2+RPZCOO+RCO3+RHCO3)
F    WRITE(NTERM,*)RHLDG
  READ-VARS RCO2 RPZ RHPZCO RPZCO2 RPZCOO RCO3 RHCO3 RK  &
    RPZH
  WRITE-VARS RHLDG

CONV-OPTIONS
  PARAM CHECKSEQ=YES

STREAM-REPOR MOLEFLOW MOLEFRAC PROPERTIES=G-H2O PPPZ G-PZ
G-CO2  &
    G-CO3 G-HCO3 G-HPZCOO G-K+ G-PZCOO G-PZCOO2 G-PZH+  &
    IONSTR MOLECONC MASSCONC PPCO2 PPH2O

PROPERTY-REP PCES PROP-DATA DFMS

REACTIONS CONK-EQG REAC-DIST
  REAC-DATA 7 KINETIC CBASIS=MOLAR
  REAC-DATA 8 KINETIC CBASIS=MOLAR
  REAC-DATA 9 KINETIC CBASIS=MOLAR
  REAC-DATA 10 KINETIC CBASIS=MOLAR
  REAC-DATA 11 KINETIC CBASIS=MOLAR
  REAC-DATA 12 KINETIC CBASIS=MOLAR
  REAC-DATA 13 KINETIC CBASIS=MOLAR
  REAC-DATA 14 KINETIC CBASIS=MOLAR
  REAC-DATA 15 KINETIC CBASIS=MOLAR
  REAC-DATA 16 KINETIC CBASIS=MOLAR
  REAC-DATA 17 KINETIC CBASIS=MOLAR
  REAC-DATA 18 KINETIC CBASIS=MOLAR
  REAC-DATA 19 KINETIC CBASIS=MOLAR
  REAC-DATA 20 KINETIC CBASIS=MOLAR
  REAC-DATA 21 KINETIC CBASIS=MOLAR
  REAC-DATA 22 KINETIC CBASIS=MOLAR
  REAC-DATA 23 KINETIC CBASIS=MOLAR
  REAC-DATA 24 KINETIC CBASIS=MOLAR
  REAC-DATA 1 KINETIC CBASIS=MOLAR
  REAC-DATA 2 KINETIC CBASIS=MOLAR
  REAC-DATA 4 KINETIC CBASIS=MOLAR
  REAC-DATA 5 KINETIC CBASIS=MOLAR
  REAC-DATA 3 KINETIC CBASIS=MOLAR
  REAC-DATA 6 KINETIC CBASIS=MOLAR
  REAC-DATA 25
  REAC-DATA 27
```

```
REAC-DATA 28
REAC-DATA 29
K-STOIC 25 A=132.89888 B=-13445.9 C=-22.4773
K-STOIC 27 A=481.945 B=-33448.7 C=-69.7827
K-STOIC 28 A=-488.753 B=27752.8 C=69.7831
K-STOIC 29 A=216.05043 B=-12431.7 C=-35.4819
RATE-CON 7 PRE-EXP=2810.4 ACT-ENERGY=35020. <kJ/kmol> &
   T-REF=298.15 <K>
RATE-CON 8 PRE-EXP=23177000. ACT-ENERGY=88985.90085 <kJ/kmol> &
   T-REF=298.15 <K>
RATE-CON 9 PRE-EXP=143610. ACT-ENERGY=35020. <kJ/kmol> &
   T-REF=298.15 <K>
RATE-CON 10 PRE-EXP=0.0059841 ACT-ENERGY=147158.3638 <kJ/kmol> &
   T-REF=298.15 <K>
RATE-CON 11 PRE-EXP=328340. ACT-ENERGY=35020. <kJ/kmol> &
   T-REF=298.15 <K>
RATE-CON 12 PRE-EXP=0.0026999 ACT-ENERGY=154530.3585 <kJ/kmol> &
   T-REF=298.15 <K>
RATE-CON 13 PRE-EXP=679640. ACT-ENERGY=35020. <kJ/kmol> &
   T-REF=298.15 <K>
RATE-CON 14 PRE-EXP=1.2023 ACT-ENERGY=109394.981 <kJ/kmol> &
   T-REF=298.15 <K>
RATE-CON 15 PRE-EXP=8698100. ACT-ENERGY=35020. <kJ/kmol> &
   T-REF=298.15 <K>
RATE-CON 16 PRE-EXP=0.00058232 &
   ACT-ENERGY=145697.5341 <kJ/kmol> T-REF=298.15 <K>
RATE-CON 17 PRE-EXP=1873.6 ACT-ENERGY=35020. <kJ/kmol> &
   T-REF=298.15 <K>
RATE-CON 18 PRE-EXP=71086000. ACT-ENERGY=68331.06251 <kJ/kmol> &
   T-REF=298.15 <K>
RATE-CON 19 PRE-EXP=445440. ACT-ENERGY=35020. <kJ/kmol> &
   T-REF=298.15 <K>
RATE-CON 20 PRE-EXP=0.016851 ACT-ENERGY=133875.5201 <kJ/kmol> &
   T-REF=298.15 <K>
RATE-CON 21 PRE-EXP=452940. ACT-ENERGY=35020. <kJ/kmol> &
   T-REF=298.15 <K>
RATE-CON 22 PRE-EXP=3.6862 ACT-ENERGY=88740.14267 <kJ/kmol> &
   T-REF=298.15 <K>
RATE-CON 23 PRE-EXP=310540. ACT-ENERGY=35020. <kJ/kmol> &
   T-REF=298.15 <K>
RATE-CON 24 PRE-EXP=0.059532 ACT-ENERGY=126503.5254 <kJ/kmol> &
   T-REF=298.15 <K>
RATE-CON 1 PRE-EXP=17529. ACT-ENERGY=45600.27545 <kJ/kmol> &
   T-REF=298.15 <K>
RATE-CON 2 PRE-EXP=2.8933E-005 &
   ACT-ENERGY=113844.2621 <kJ/kmol> T-REF=298.15 <K>
RATE-CON 4 PRE-EXP=4.9935E-006 ACT-ENERGY=125056.905 <kJ/kmol> &
   T-REF=298.15 <K>
RATE-CON 5 PRE-EXP=24.632 ACT-ENERGY=47980.094 <kJ/kmol> &
   T-REF=298.15 <K>
RATE-CON 3 PRE-EXP=24.632 ACT-ENERGY=47980.094 <kJ/kmol> &
   T-REF=298.15 <K>
RATE-CON 6 PRE-EXP=2.5305E-005 &
   ACT-ENERGY=117684.9103 <kJ/kmol> T-REF=298.15 <K>
STOIC 7 PZ -1. / CO2 -1. / H2O -1. / PZCOO- 1. / &
   H3O+ 1.
STOIC 8 PZCOO- -1. / H3O+ -1. / PZ 1. / CO2 1. / &
   H2O 1.
STOIC 9 PZ -1. / CO2 -1. / PZCOO- 0. / HPZCOO 1.
STOIC 10 HPZCOO -1. / PZCOO- 0. / PZ 1. / CO2 1.
STOIC 11 PZ -2. / CO2 -1. / PZCOO- 1. / PZH+ 1.
STOIC 12 PZCOO- -1. / PZH+ -1. / PZ 2. / CO2 1.
STOIC 13 PZ -1. / CO2 -1. / CO3--2 -1. / PZCOO- 1. / &
   HCO3- 1.
STOIC 14 PZCOO- -1. / HCO3- -1. / PZ 1. / CO2 1. / &
   CO3--2 1.
STOIC 15 PZ -1. / CO2 -1. / OH- -1. / PZCOO- 1. / &
   H2O 1.
STOIC 16 PZCOO- -1. / H2O -1. / PZ 1. / CO2 1. / &
   OH- 1.
STOIC 17 PZCOO- -1. / CO2 -1. / H2O -1. / PZCOO-2 1. / &
   H3O+ 1.
STOIC 18 PZCOO-2 -1. / H3O+ -1. / PZCOO- 1. / CO2 1. / &
   H2O 1.
STOIC 19 PZCOO- -1. / CO2 -1. / PZ -1. / PZCOO-2 1. / &
   PZH+ 1.
STOIC 20 PZCOO-2 -1. / PZH+ -1. / PZCOO- 1. / CO2 1. / &
   PZ 1.
STOIC 21 PZCOO- -1. / CO2 -1. / CO3--2 -1. / PZCOO-2 &
   1. / HCO3- 1.
STOIC 22 PZCOO-2 -1. / HCO3- -1. / PZCOO- 1. / CO2 1. / &
   CO3--2 1.
STOIC 23 PZCOO- -2. / CO2 -1. / PZCOO-2 1. / HPZCOO &
   1.
```

```
  STOIC 24 PZCOO-2 -1. / HPZCOO -1. / PZCOO- 2. / CO2  &
    1.
  STOIC 1 CO2 -1. / OH- -1. / HCO3- 1.
  STOIC 2 HCO3- -1. / CO2 1. / OH- 1.
  STOIC 4 PZH+ -1. / HCO3- -1. / PZ 1. / CO2 1. / H2O  &
    1.
  STOIC 5 PZCOO- -1. / CO2 -1. / H2O -1. / HPZCOO 1. /  &
    HCO3- 1.
  STOIC 3 PZ -1. / CO2 -1. / H2O -1. / PZH+ 1. /  &
    HCO3- 1.
  STOIC 6 HPZCOO -1. / HCO3- -1. / PZCOO- 1. / CO2 1. /  &
    H2O 1.
  STOIC 25 H2O -2. / H3O+ 1. / OH- 1.
  STOIC 27 PZH+ -1. / H2O -1. / PZ 1. / H3O+ 1.
  STOIC 28 HPZCOO -1. / PZ -1. / PZCOO- 1. / PZH+ 1.
  STOIC 29 HCO3- -1. / H2O -1. / H3O+ 1. / CO3--2 1.
  POWLAW-EXP 7 PZ 1. / CO2 1. / H2O 0.
  POWLAW-EXP 8 PZCOO- 1. / H3O+ 1.
  POWLAW-EXP 9 PZ 1. / CO2 1. / PZCOO- 1.
  POWLAW-EXP 10 HPZCOO 1. / PZCOO- 1.
  POWLAW-EXP 11 PZ 2. / CO2 1.
  POWLAW-EXP 12 PZCOO- 1. / PZH+ 1.
  POWLAW-EXP 13 PZ 1. / CO2 1. / CO3--2 1.
  POWLAW-EXP 14 PZCOO- 1. / HCO3- 1.
  POWLAW-EXP 15 PZ 1. / CO2 1. / OH- 1.
  POWLAW-EXP 16 PZCOO- 1. / H2O 1.
  POWLAW-EXP 17 PZCOO- 1. / CO2 1. / H2O 1.
  POWLAW-EXP 18 PZCOO-2 1. / H3O+ 1.
  POWLAW-EXP 19 PZCOO- 1. / CO2 1. / PZ 1.
  POWLAW-EXP 20 PZCOO-2 1. / PZH+ 1.
  POWLAW-EXP 21 PZCOO- 1. / CO2 1. / CO3--2 1.
  POWLAW-EXP 22 PZCOO-2 1. / HCO3- 1.
  POWLAW-EXP 23 PZCOO- 2. / CO2 1.
  POWLAW-EXP 24 PZCOO-2 1. / HPZCOO 1.
  POWLAW-EXP 1 CO2 1. / OH- 1.
  POWLAW-EXP 2 HCO3- 1.
  POWLAW-EXP 4 PZH+ 1. / HCO3- 1.
  POWLAW-EXP 5 PZCOO- 1. / CO2 1. / H2O 0.
  POWLAW-EXP 3 PZ 1. / CO2 1. / H2O 0.
  POWLAW-EXP 6 HPZCOO 1. / HCO3- 1.

REACTIONS CONV-EQ REAC-DIST
  REAC-DATA 1
  REAC-DATA 3
  REAC-DATA 4
  REAC-DATA 7
  REAC-DATA 2
  REAC-DATA 5
  REAC-DATA 6
  K-STOIC 1 A=132.89888 B=-13445.9 C=-22.4773
  K-STOIC 3 A=216.05043 B=-12431.7 C=-35.4819
  K-STOIC 4 A=481.945 B=-33448.7 C=-69.7827
  K-STOIC 7 A=-488.753 B=27752.8 C=69.7831
  K-STOIC 2 A=98.566559 B=1353.8 C=-14.3043
  K-STOIC 5 A=-378.503561 B=24419.6 C=50.2934
  K-STOIC 6 A=-19.929561 B=1988.1
  STOIC 1 H2O -2. / H3O+ 1. / OH- 1.
  STOIC 3 HCO3- -1. / H2O -1. / H3O+ 1. / CO3--2 1.
  STOIC 4 PZH+ -1. / H2O -1. / PZ 1. / H3O+ 1.
  STOIC 7 HPZCOO -1. / PZ -1. / PZCOO- 1. / PZH+ 1.
  STOIC 2 CO2 -1. / OH- -1. / HCO3- 1.
  STOIC 5 PZ -1. / CO2 -1. / H2O -1. / PZCOO- 1. /  &
    H3O+ 1.
  STOIC 6 PZCOO- -1. / CO2 -1. / H2O -1. / PZCOO-2 1. /  &
    H3O+ 1.

REACTIONS EQUIL REAC-DIST
  REAC-DATA 1
  REAC-DATA 2
  REAC-DATA 3
  REAC-DATA 4
  REAC-DATA 5
  REAC-DATA 6
  REAC-DATA 7
  K-STOIC 1 A=132.89888 B=-13445.9 C=-22.4773
  K-STOIC 2 A=231.465439 B=-12092.1 C=-36.7816
  K-STOIC 3 A=216.05043 B=-12431.7 C=-35.4819
  K-STOIC 4 A=481.945 B=-33448.7 C=-69.7827
  K-STOIC 5 A=-609.969 B=36511.7 C=87.075
  K-STOIC 6 A=-251.395 B=14080.2 C=36.7818
  K-STOIC 7 A=-488.753 B=27752.8 C=69.7831
  STOIC 1 H2O -2. / H3O+ 1. / OH- 1.
  STOIC 2 CO2 -1. / H2O -2. / H3O+ 1. / HCO3- 1.
  STOIC 3 HCO3- -1. / H2O -1. / H3O+ 1. / CO3--2 1.
```

```
  STOIC 4 PZH+ -1. / H2O -1. / PZ 1. / H3O+ 1.
  STOIC 5 PZ -1. / HCO3- -1. / PZCOO- 1. / H2O 1.
  STOIC 6 PZCOO- -1. / HCO3- -1. / PZCOO-2 1. / H2O 1.
  STOIC 7 HPZCOO -1. / PZ -1. / PZCOO- 1. / PZH+ 1.

REACTIONS KAX-H2O3 REAC-DIST
  REAC-DATA 7 KINETIC CBASIS=MOLE-GAMMA
  REAC-DATA 8 KINETIC CBASIS=MOLE-GAMMA
  REAC-DATA 9 KINETIC CBASIS=MOLE-GAMMA
  REAC-DATA 10 KINETIC CBASIS=MOLE-GAMMA
  REAC-DATA 11 KINETIC CBASIS=MOLE-GAMMA
  REAC-DATA 12 KINETIC CBASIS=MOLE-GAMMA
  REAC-DATA 13 KINETIC CBASIS=MOLE-GAMMA
  REAC-DATA 14 KINETIC CBASIS=MOLE-GAMMA
  REAC-DATA 15 KINETIC CBASIS=MOLE-GAMMA
  REAC-DATA 16 KINETIC CBASIS=MOLE-GAMMA
  REAC-DATA 17 KINETIC CBASIS=MOLE-GAMMA
  REAC-DATA 18 KINETIC CBASIS=MOLE-GAMMA
  REAC-DATA 19 KINETIC CBASIS=MOLE-GAMMA
  REAC-DATA 20 KINETIC CBASIS=MOLE-GAMMA
  REAC-DATA 21 KINETIC CBASIS=MOLE-GAMMA
  REAC-DATA 22 KINETIC CBASIS=MOLE-GAMMA
  REAC-DATA 23 KINETIC CBASIS=MOLE-GAMMA
  REAC-DATA 24 KINETIC CBASIS=MOLE-GAMMA
  REAC-DATA 1 KINETIC CBASIS=MOLE-GAMMA
  REAC-DATA 2 KINETIC CBASIS=MOLE-GAMMA
  REAC-DATA 4 KINETIC CBASIS=MOLE-GAMMA
  REAC-DATA 5 KINETIC CBASIS=MOLE-GAMMA
  REAC-DATA 3 KINETIC CBASIS=MOLE-GAMMA
  REAC-DATA 6 KINETIC CBASIS=MOLE-GAMMA
  REAC-DATA 25 KBASIS=MOLE-GAMMA
  REAC-DATA 27 KBASIS=MOLE-GAMMA
  REAC-DATA 28
  REAC-DATA 29 KBASIS=MOLE-GAMMA
  K-STOIC 25 A=132.89888 B=-13445.9 C=-22.4773
  K-STOIC 27 A=481.945 B=-33448.7 C=-69.7827
  K-STOIC 28 A=-488.753 B=27752.8 C=69.7831
  K-STOIC 29 A=216.05043 B=-12431.7 C=-35.4819
  RATE-CON 7 PRE-EXP=8372000000. ACT-ENERGY=-17619. <kJ/kmol> &
    TEMP-EXPONEN=17.25 T-REF=298.15 <K>
  RATE-CON 8 PRE-EXP=3484000000000. ACT-ENERGY=185406. <kJ/kmol> &
    TEMP-EXPONEN=-33.04 T-REF=298.15 <K>
  RATE-CON 9 PRE-EXP=18650000000. ACT-ENERGY=-35394. <kJ/kmol> &
    TEMP-EXPONEN=25.7 T-REF=298.15 <K>
  RATE-CON 10 PRE-EXP=2411. ACT-ENERGY=214987. <kJ/kmol> &
    TEMP-EXPONEN=-24.59 T-REF=298.15 <K>
  RATE-CON 11 PRE-EXP=36200000000. ACT-ENERGY=-116263. <kJ/kmol> &
    TEMP-EXPONEN=44.43 T-REF=298.15 <K>
  RATE-CON 12 PRE-EXP=681.6 ACT-ENERGY=364854. <kJ/kmol> &
    TEMP-EXPONEN=-75.65 T-REF=298.15 <K>
  RATE-CON 13 PRE-EXP=393300000000. ACT-ENERGY=-54002. <kJ/kmol> &
    TEMP-EXPONEN=36.07 T-REF=298.15 <K>
  RATE-CON 14 PRE-EXP=7623. ACT-ENERGY=252380. <kJ/kmol> &
    TEMP-EXPONEN=-49.7 T-REF=298.15 <K>
  RATE-CON 15 PRE-EXP=467500000000. ACT-ENERGY=-31303. <kJ/kmol> &
    TEMP-EXPONEN=23.83 T-REF=298.15 <K>
  RATE-CON 16 PRE-EXP=0.03521 ACT-ENERGY=283511. <kJ/kmol> &
    TEMP-EXPONEN=-48.94 T-REF=298.15 <K>
  RATE-CON 17 PRE-EXP=4123000000. ACT-ENERGY=63251. <kJ/kmol> &
    TEMP-EXPONEN=-1.47 T-REF=298.15 <K>
  RATE-CON 18 PRE-EXP=4.26E+013 ACT-ENERGY=79780. <kJ/kmol> &
    TEMP-EXPONEN=-1.47 T-REF=298.15 <K>
  RATE-CON 19 PRE-EXP=36280000000. ACT-ENERGY=-35394. <kJ/kmol> &
    TEMP-EXPONEN=25.7 T-REF=298.15 <K>
  RATE-CON 20 PRE-EXP=16960. ACT-ENERGY=259228. <kJ/kmol> &
    TEMP-EXPONEN=-44.08 T-REF=298.15 <K>
  RATE-CON 21 PRE-EXP=193600000000. ACT-ENERGY=26868. <kJ/kmol> &
    TEMP-EXPONEN=17.35 T-REF=298.15 <K>
  RATE-CON 22 PRE-EXP=93180. ACT-ENERGY=146755. <kJ/kmol> &
    TEMP-EXPONEN=-18.14 T-REF=298.15 <K>
  RATE-CON 23 PRE-EXP=18680000000. ACT-ENERGY=45476. <kJ/kmol> &
    TEMP-EXPONEN=6.98 T-REF=298.15 <K>
  RATE-CON 24 PRE-EXP=59950. ACT-ENERGY=109361. <kJ/kmol> &
    TEMP-EXPONEN=6.98 T-REF=298.15 <K>
  RATE-CON 1 PRE-EXP=9298000. ACT-ENERGY=77495. <kJ/kmol> &
    TEMP-EXPONEN=-3.05 T-REF=298.15 <K>
  RATE-CON 2 PRE-EXP=0.003842 ACT-ENERGY=88750. <kJ/kmol> &
    TEMP-EXPONEN=11.25 T-REF=298.15 <K>
  RATE-CON 4 PRE-EXP=2.769 ACT-ENERGY=172473. <kJ/kmol> &
    TEMP-EXPONEN=-15.45 T-REF=298.15 <K>
  RATE-CON 5 PRE-EXP=19800. ACT-ENERGY=75784. <kJ/kmol> &
    TEMP-EXPONEN=-1.18 T-REF=298.15 <K>
  RATE-CON 3 PRE-EXP=26800. ACT-ENERGY=-5086. <kJ/kmol> &
    TEMP-EXPONEN=17.55 T-REF=298.15 <K>
```

```
RATE-CON 6 PRE-EXP=14.04 ACT-ENERGY=22606. <kJ/kmol> &
   TEMP-EXPONEN=35.61 T-REF=298.15 <K>
STOIC 7 PZ -1. / CO2 -1. / H2O -1. / PZCOO- 1. /  &
   H3O+ 1.
STOIC 8 PZCOO- -1. / H3O+ -1. / PZ 1. / CO2 1. /  &
   H2O 1.
STOIC 9 PZ -1. / CO2 -1. / PZCOO- 0. / HPZCOO 1.
STOIC 10 HPZCOO -1. / PZCOO- 0. / PZ 1. / CO2 1.
STOIC 11 PZ -2. / CO2 -1. / PZCOO- 1. / PZH+ 1.
STOIC 12 PZCOO- -1. / PZH+ -1. / PZ 2. / CO2 1.
STOIC 13 PZ -1. / CO2 -1. / CO3--2 -1. / PZCOO- 1. /  &
   HCO3- 1.
STOIC 14 PZCOO- -1. / HCO3- -1. / PZ 1. / CO2 1. /  &
   CO3--2 1.
STOIC 15 PZ -1. / CO2 -1. / OH- -1. / PZCOO- 1. /  &
   H2O 1.
STOIC 16 PZCOO- -1. / H2O -1. / PZ 1. / CO2 1. /  &
   OH- 1.
STOIC 17 PZCOO- -1. / CO2 -1. / H2O -1. / PZCOO-2 1. / &
   H3O+ 1.
STOIC 18 PZCOO-2 -1. / H3O+ -1. / PZCOO- 1. / CO2 1. / &
   H2O 1.
STOIC 19 PZCOO- -1. / CO2 -1. / PZ -1. / PZCOO-2 1. /  &
   PZH+ 1.
STOIC 20 PZCOO-2 -1. / PZH+ -1. / PZCOO- 1. / CO2 1. / &
   PZ 1.
STOIC 21 PZCOO- -1. / CO2 -1. / CO3--2 -1. / PZCOO-2  &
   1. / HCO3- 1.
STOIC 22 PZCOO-2 -1. / HCO3- -1. / PZCOO- 1. / CO2 1. / &
   CO3--2 1.
STOIC 23 PZCOO- -2. / CO2 -1. / PZCOO-2 1. / HPZCOO  &
   1.
STOIC 24 PZCOO-2 -1. / HPZCOO -1. / PZCOO- 2. / CO2  &
   1.
STOIC 1 CO2 -1. / OH- -1. / HCO3- 1.
STOIC 2 HCO3- -1. / CO2 1. / OH- 1.
STOIC 4 PZH+ -1. / HCO3- -1. / PZ 1. / CO2 1. / H2O  &
   1.
STOIC 5 PZCOO- -1. / CO2 -1. / H2O -1. / HPZCOO 1. /  &
   HCO3- 1.
STOIC 3 PZ -1. / CO2 -1. / H2O -1. / PZH+ 1. /  &
   HCO3- 1.
STOIC 6 HPZCOO -1. / HCO3- -1. / PZCOO- 1. / CO2 1. /  &
   H2O 1.
STOIC 25 H2O -2. / H3O+ 1. / OH- 1.
STOIC 27 PZH+ -1. / H2O -1. / PZ 1. / H3O+ 1.
STOIC 28 HPZCOO -1. / PZ -1. / PZCOO- 1. / PZH+ 1.
STOIC 29 HCO3- -1. / H2O -1. / H3O+ 1. / CO3--2 1.
POWLAW-EXP 7 PZ 1. / CO2 1. / H2O 0.
POWLAW-EXP 8 PZCOO- 1. / H3O+ 1.
POWLAW-EXP 9 PZ 1. / CO2 1. / PZCOO- 1.
POWLAW-EXP 10 HPZCOO 1. / PZCOO- 1.
POWLAW-EXP 11 PZ 2. / CO2 1.
POWLAW-EXP 12 PZCOO- 1. / PZH+ 1.
POWLAW-EXP 13 PZ 1. / CO2 1. / CO3--2 1.
POWLAW-EXP 14 PZCOO- 1. / HCO3- 1.
POWLAW-EXP 15 PZ 1. / CO2 1. / OH- 1.
POWLAW-EXP 16 PZCOO- 1. / H2O 1.
POWLAW-EXP 17 PZCOO- 1. / CO2 1. / H2O 0.
POWLAW-EXP 18 PZCOO-2 1. / H3O+ 1.
POWLAW-EXP 19 PZCOO- 1. / CO2 1. / PZ 1.
POWLAW-EXP 20 PZCOO-2 1. / PZH+ 1.
POWLAW-EXP 21 PZCOO- 1. / CO2 1. / CO3--2 1.
POWLAW-EXP 22 PZCOO-2 1. / HCO3- 1.
POWLAW-EXP 23 PZCOO- 2. / CO2 1.
POWLAW-EXP 24 PZCOO-2 1. / HPZCOO 1.
POWLAW-EXP 1 CO2 1. / OH- 1.
POWLAW-EXP 2 HCO3- 1.
POWLAW-EXP 4 PZH+ 1. / HCO3- 1.
POWLAW-EXP 5 PZCOO- 1. / CO2 1. / H2O 0.
POWLAW-EXP 3 PZ 1. / CO2 1. / H2O 0.
POWLAW-EXP 6 HPZCOO 1. / HCO3- 1.

PROP-TABLE 525 FLASHCURVE
   MOLE-FLOW H2O 55.5 / K2CO3 2.5 / PZ 2.5 / CO2 2.5
   STATE PRES=14.696
   VARY TEMP
   RANGE LOWER=20. UPPER=70. INCR=5.
   TABULATE PROPERTIES=RHOMX MUMX

PROP-TABLE 6416 FLASHCURVE
   MOLE-FLOW H2O 55.5 / K2CO3 3.2 / PZ 1.6 / CO2 2.58
   STATE PRES=14.696
   VARY TEMP
```

```
   RANGE LOWER=25. UPPER=70. INCR=5.
   TABULATE PROPERTIES=RHOMX MUMX

DISABLE
   BLOCK ABS-FILM STGFL2
;
;
;
;
;
```

Appendix Q: FORTRAN Interfacial Area Subroutine

```
      SUBROUTINE AREA(KSTG,   NCOMPS, IDX,    NBOPST, KPDIAG,
     1                XCOMPB, FRATEL, YCOMPB, FRATEV, PRESS,
     2                TLIQ,   TVAP,   AVMWLI, AVMWVA, VISCML,
     3                DENMXL, SIGMAL, VISCMV, DENMXV, AREAIF,
     4                COLTYP, USRCOR, TWRARA, COLDIA, HTPACK,
     5                PACSIZ, SPAREA, CSIGMA, PFACT,  PKPRMS,
     6                VOIDFR, IPAKAR, IPTYPE, IVENDR, IPMAT,
     7                IPSIZE, WEIRHT, DCAREA, ARAACT, FLOPTH,
     8                NPASS,  WEIRL,  IFMETH, SYSFAC, HOLEAR,
     9                ITTYPE, TRASPC, PITCH,  NINT,   INT,
     A                NREAL,  REAL)
      IMPLICIT NONE
      INTEGER KSTG, NCOMPS, IDX(NCOMPS), NBOPST(6), KPDIAG,
     +       COLTYP, USRCOR, IPAKAR, IPTYPE, IVENDR, IPMAT,  IPSIZE,
     +       NPASS, IFMETH, ITTYPE, NINT, INT(NINT), NREAL
      REAL*8  XCOMPB(NCOMPS), FRATEL, YCOMPB(NCOMPS), FRATEV,
     +       PRESS, TLIQ, TVAP, AVMWLI, AVMWVA, VISCML, DENMXL,
     +       SIGMAL, VISCMV, DENMXV, AREAIF, TWRARA, COLDIA,
     +       HTPACK, PACSIZ, SPAREA, CSIGMA, PFACT, PKPRMS(20),
     +       VOIDFR, WEIRHT, DCAREA, ARAACT, FLOPTH, WEIRL,
     +       SYSFAC, HOLEAR, TRASPC, PITCH, REAL(NREAL)
C***********************************************************************
C  LICENSED MATERIAL.  PROPERTY OF ASPEN TECHNOLOGY, INC.  TO
BE      *
C  TREATED AS ASPEN TECH PROPRIETARY INFORMATION UNDER THE
TERMS      *
C  OF THE ASPEN PLUS SUBSCRIPTION AGREEMENT.                    *
C***********************************************************************
C-----------------------------------------------------------------------
C        COPYRIGHT (C) 2004
C         ASPEN TECHNOLOGY, INC.
C         CAMBRIDGE, MA
C-----------------------------------------------------------------------
C
C    DESCRIPTION: User provided RateSep routine to calculate the
C                 specific interface area AREAIF (see NOTE-1).
C
C    VARIABLES IN ARGUMENT LIST
C
C    VARIABLE I/O TYPE   DIMENSION   DESCRIPTION AND RANGE
C    -------- --- ----  ---------  --------------------------------
C    KSTG     I  I       -      SEGMENT NUMBER
C    NCOMPS   I  I       -      NUMBER OF COMPONENTS
C    IDX      I  I     NCOMPS   COMPONENT INDEX VECTOR
C    NBOPST   I  I       6      PHYSICAL PROPERTY OPTION
C                               SET BEAD POINTER
C    KPDIAG   I  I       -      PHYSICAL PROPERTY
C                               DIAGOSTIC CODE
C    XCOMPB   I  R      NCOMPS   BULK LIQUID MOLE FRACTION
C    FRATEL   I  R       -      FLOW OF LIQUID (KMOL/SEC)
C    YCOMPB   I  R      NCOMPS   BULK VAPOR MOLE FRACTION
C    FRATEV   I  R       -      FLOW OF VAPOR (KMOL/SEC)
C    PRESS    I  R       -      PRESSURE (N/SQ.M)
C    TLIQ     I  R       -      LIQUID TEMPERATURE (K)
C    TVAP     I  R       -      VAPOR TEMPERATURE (K)
C    AVMWLI   I  R       -      AVERAGE MOLECULAR WEIGHT
C                               OF LIQUID MIXTURE
C                               (KG/KMOL)
C    AVMWVA   I  R       -      AVERAGE MOLECULAR WEIGHT
C                               OF VAPOR MIXTURE (KG/KMOL)
C    VISCML   I  R       -      VISCOSITY OF LIQUID
C                               (N-SEC/SQ.M)
C    DENMXL   I  R       -      DENSITY OF LIQUID MIXTURE
C                               (KMOL/CU.M)
C    SIGMAL   I  R       -      SURFACE TENSION OF LIQUID
C                               (N/M)
C    VISCMV   I  R       -      VISCOSITY OF VAPOR MIXTURE
C                               (N-SEC/SQ.M)
C    DENMXV   I  R       -      DENSITY OF VAPOR MIXTURE
C                               (KMOL/CU.M)
C    AREAIF   O  R       -      INTERFACIAL AREA
C                               (SEE NOTE-1 BELOW)
```

```
C   COLTYP  I  I     -     TYPE OF COLUMN
C                     1 = PACKED
C                     2 = TRAY
C   USRCOR  I  I     -     CALCULATION METHOD (I.E.
C                     CHOICE OF USER CORRELATION)
C                      1 = USER1
C                      2 = USER2
C                      3 = USER3
C                      4 = USER4
C   TWRARA  I  R     -     CROSS-SECTIONAL AREA OF
C                     TOWER (SQ.M)
C   COLDIA  I  R     -     COLUMN DIAMETER (M)
C   HTPACK  I  R     -     HEIGHT OF PACKING IN THE
C                     SEGMENT (M)
C   PACSIZ  I  R     -     SIZE OF PACKING (M)
C   SPAREA  I  R     -     SPECIFIC SURFACE AREA OF
C                     PACKING (SQ.M/CU.M)
C   CSIGMA  I  R     -     CRITICAL SURFACE TENSION
C                     OF PACKING MATERIAL (N/M)
C   PFACT   I  R     -     PACKING FACTOR (1/M)
C   PKPRMS  I  R     20    PACKING PARAMETERS
C                     PKPRMS(1) = STICHLMAIR CONSTANT C1
C                     PKPRMS(2) = STICHLMAIR CONSTANT C2
C                     PKPRMS(3) = STICHLMAIR CONSTANT C3
C                     PKPRMS(4) = CL IN BILLET 93
C                     PKPRMS(5) = CV IN BILLET 93
C                     PKPRMS(6) = B IN BRF 85
C                     PKPRMS(7) = S IN BRF 85
C                     PKPRMS(8) = H IN BRF 85
C                     PKPRMS(9) = Fse IN BRF 92
C                     PKPRMS(10) = CE IN BRF 92
C                     PKPRMS(11) = THETA IN BRF 92
C   VOIDFR  I  R     -     VOID FRACTION OF PACKING
C   IPAKAR  I  I     -     PACKING ARRANGEMENT
C                      1 = RANDOM
C                      2 = STRUCTURED
C   IPTYPE  I  I     -     PACKING TYPE
C                     See IPTYPE in packsr.f
C   IVENDR  I  I     -     PACKING VENDOR CODE
C   IPMAT   I  I     -     PACKING MATERIAL CODE
C   IPSIZE  I  I     -     PACKING SIZE CODE
C   WEIRHT  I  R     -     AVERAGE WEIR HEIGHT (M)
C   DCAREA  I  R     -     TOTAL AREA OF DOWNCOMER
C                     ON TRAY (SQ.M)
C   ARAACT  I  R     -     TOTAL ACTIVE AREA AVAILABLE
C                     ON TRAY (SQ.M)
C   FLOPTH  I  R     -     AVERAGE FLOWPATH LENGTH (M)
C   NPASS   I  I     -     NUMBER OF TRAY PASSES
C   WEIRL   I  R     -     AVERAGE WEIRH LENGTH (M)
C   IFMETH  I  I     -     FLOODING CALCULATION
C                     METHOD; REQUIRED FOR SIEVE
C                     TRAY
C   SYSFAC  I  R     -     SYSTEM FACTOR; REQUIRED FOR
C                     SIEVE TRAY
C   HOLEAR  I  R     -     HOLE AREA/ACTIVE AREA; REQUIRED
C                     FOR SIEVE TRAY
C   ITTYPE  I  I     -     TRAY TYPE
C                      1 - BUBBLE CAPS
C                      2 - SIEVE
C                      3 - GLITSCH BALLAST
C                      4 - KOCH FLEXITRAY
C                      5 - NUTTER FLOAT VALVE
C   TRASPC  I  R     -     TRAY SPACING (M)
C   PITCH   I  R     -     SIEVE TRAY HOLE PITCH (M)
C   NINT    I  I     -     Size of INT
C   INT     I/O I    NINT  User correlation INT array
C   NREAL   I  I     -     Size of REAL
C   REAL    I/O I    NREAL User correlation REAL array
C
C   NOTE-1:
C       SPECIFIC INTERFACIAL AREA "AREAIF" HAS THE FOLLOWING
UNITS.
C        FOR PACKED COLUMNS, THE UNITS IS "SQ.M/CU.M OF PACKING"
C        FOR TRAY COLUMNS, THE UNITS IS "SQ.M/SQ.M ACTIVE TRAY
AREA"
C
C***********************************************************************
C   Declare local variables used in the user correlations
C
      REAL*8 WeL,  dTemp,  uV,   rhoVms,
     +       uL,   rhoLms, ReL,  FrL,   uL2,
     +       ReV,  d,      Wprime,
     +       AREAE, At, hp, Ft, Fse, ap,
     +       S, cosg, pi, theta, ULIQ
```

```
C
C   Compute specific interface area as described above
C   Check COLTYP/USRCOR if providing multiple area correlations
C
    IF (COLTYP .EQ. 1) THEN
C
C**** PACKED COLUMN
C
      IF (USRCOR .EQ. 1) THEN
C       user subroutine example for packed column: Onda 68
C
C       Onda, K., Takeuchi, H. and Okumoto, Y., "Mass Transfer
C         Coefficients between Gas and Liquid Phases in Packed
C         Columns", J. Chem. Eng. Jap., 1, (1968) p. 56
C
        rhoLms = DENMXL * AVMWLI
        uL = FRATEL / TWRARA / DENMXL
        uL2 = uL * uL
        ReL = rhoLms * uL / VISCML / SPAREA
        FrL = SPAREA * uL2 / 9.81D0
C         WHERE 9.81D0 IS GRAVITY CONSTANT IN M/S**2
        WeL    = rhoLms * uL2 / SIGMAL / SPAREA
        dTemp = -1.45D0*((CSIGMA/SIGMAL)**0.75D0)
   +                *(ReL**0.1D0)*(FrL**(-0.05D0))
   +                *(WeL**0.2D0)
        dTemp = 1.D0 - DEXP(dTemp)

        AREAIF = SPAREA*dTemp

C       Uses specific area of the packing for both random and structured

      ELSEIF (USRCOR .EQ. 2) THEN

        AREAIF = SPAREA  !(sq.m/cu.m)

C       Uses the Rocha-Bravo-Fair (1992) Model as defined in Aspen Plus

      ELSEIF (USRCOR .EQ. 3) THEN

        IF (SIGMAL .GE. 0.055) THEN
          cosg = 5.211*(10**(-16.835 * SIGMAL))
        ELSE
          cosg = 0.9
        END IF

        pi     = 3.141592654
        theta   = PKPRMS(11)*pi/180

        rhoLms  = DENMXL * AVMWLI
        uL     = FRATEL / TWRARA / DENMXL
        uL2    = uL * uL
        S      = PKPRMS(7)

        WeL    = uL2 * rhoLms * S / SIGMAL
        FrL    = uL2 / (S * 9.81D0)
        ReL    = uL * S * rhoLms / VISCML
        Ft     = (29.12*((WeL*FrL)**0.15)*(S**0.359))/(ReL**0.2)
   +                /(VOIDFR**0.6)/(dsin(theta)**0.3)
   +                /(1-(0.93*cosg))


        Fse    = PKPRMS(9) !Surface enhancement factor
        ap     = SPAREA  !Specific area of packing
C         At     = TWRARA  (cross sectional area of column)
C         hp     = HTPACK  (height of packing)

        AREAIF  = Ft*Fse*ap

        IF (IPSIZE .eq. 606 .AND. IPTYPE .eq. 701) THEN
          AREAIF = AREAIF*1.147643+172.01
        ELSE
          AREAIF = AREAIF
        END IF

C         AREAIF = dsin(PKPRMS(11)*Pi)
C         WRITE (*,*) denmxl, avmwli, fratel, twrara, S

      ELSEIF (USRCOR .EQ. 4) THEN

      ULIQ = (FRATEL*3600) / TWRARA / DENMXL

      AREAIF = (0.5694 * ULIQ) + 204.57

      END IF
```

```
C       END OF IF (USRCOR)
C
      ELSE IF (COLTYP .EQ. 2) THEN
C
C**** TRAY COLUMN
C
        IF (USRCOR .EQ. 1) THEN
C         user subroutine example for tray column: Scheffe-Weiland 87
C
C         Scheffe, R.D. and Weiland, R.H., "Mass Transfer
C         Characteristics of Valve Trays." Ind. Eng. Chem. Res.
C         26, (1987) p. 228
C
C         The original paper only mentioned valve tray.
C         It is also used for bubble-cap tray and sieve tray.
C
C         CHARACTERISTIC LENGTH IS ALWAYS 1 METER.
          d = 1.0D0
          rhoLms = DENMXL * AVMWLI
          rhoVms = DENMXV * AVMWVA
          uL = FRATEL / TWRARA / DENMXL
          uV = FRATEV / TWRARA / DENMXV
          ReL = rhoLms * uL * d / VISCML
          ReV = rhoVms * uV * d / VISCMV
          Wprime = WEIRHT / d
          AREAIF = 0.27D0 * ReV**0.375D0 * ReL**0.247D0
          AREAIF = AREAIF * Wprime**0.515
        END IF
C       END OF IF (USRCOR)
C
       END IF
C     END OF IF (COLTYP)
C
      RETURN
      END
```

References

Aseyev, G. G., *Electrolytes. Transport Phenomena. Methods for Calculation of Multicomponent Solutions and Experimental Data on Viscosities and Diffusion Coefficients*. Begell House Inc. : New York, 1998; p 549.

Aseyev, G. G.; Zaytsev, I. D., *Volumetric Properties of Electrolyte Solutions - Estimation Methods and Experimental Data*. Begell House Inc.: New York, 1996; p 1572.

Aspen Technology Inc. *Aspen Plus Help File*, Cambridge, Massachusetts, 2006.

Aspiron, N., Surface Tension Models for Aqueous Blends. *Ind. Eng. Chem. Res.* **2005,** 44, 7270-7278.

Aspiron, N., Nonequilibrium Rate-Based Simulation of Reaction Systems: Simulation Model, Heat Transfer, and Influence of Film Discretization. *Ind. Eng. Chem. Res.* **2006,** 45, 2054-2069.

Billet, R.; Schultes, M., Predicting Mass Transfer in Packed Columns. *Chem. Eng. Technol.* **1993,** 16, (1), 1-9.

Bishnoi, S.; Rochelle, G. T., Absorption of Carbon Dioxide in Aqueous Piperazine/Methyldiethanolamine. *AIChE J.* **2002,** 48, 2788-2799.

Bosch, H.; Versteeg, G. F.; Van Swaaij, W. P. M., Gas-Liquid Mass Transfer with Parallel Reversible Reactions-II. Absorption of CO_2 into Amine-Promoted Carbonate Solutions. *Chem. Eng. Sci.* **1989,** 44, (11), 2735-2743.

Bravo, J. L.; Fair, J. R., Generalized Correlation for Mass Transfer in Packed Distillation Columns. *Ind. Eng. Chem. Proc. Des. Dev.* **1982,** 21, (1), 162-170.

Bravo, J. L.; Rocha, J. A.; Fair, J. R., Mass Transfer in Gauze Packings. *Hyd. Proc.* **1985,** 64, (1), 91-95.

Caplow, M., Kinetics of Carbamates Formation and Breakdown. *J. Am. Chem. Soc.* **1968,** 90, 6795-6803.

Chen, C.-C., Email from Aspen Tech Regarding HPZCOO IONMOB Adjustments. In 2006.

Chen, C. C.; Britt, H. I.; Boston, J. F.; Clarke, W. M., Thermodynamic Property Evaluation in Computer-Based Flowsheet Simulation for Aqueous Electrolyte Systems. *AIChE Symposium Series, Tutorial Lectures in Electrochemical Eng. and Tech. II, no. 229* **1983,** 79, 126.

Chilton, T. H.; Colburn, A. P., Mass Transfer (Absorption) Coefficients Prediction from Data on Heat Transfer and Fluid Friction. *Ind. Eng. Chem.* **1934,** 26, (11), 1183-1187.

CO2Net Capturing and Storing Carbon Dioxide: Technical Lessons Learned September 2004. www.co2net.com/infocentre/reports/technical_lessons_learned_final_report.pdf

Criss, C. M.; Cobble, J. W., The Thermodynamic Properties of High-Temperature Aqueous Solutions. V. The Calculation of Ionic Heat Capacities up to 200 Deg. Entropies and Heat Capacities Above 200 Deg. *J. Am. Chem. Soc.* **1964,** 86, (24), 5390-3.

Cullinane, J. T. Carbon Dioxide Absorption in Aqueous Mixtures of Potassium Carbonate and Piperazine. M.S. Thesis, The University of Texas as Austin, Austin, 2002.

Cullinane, J. T. Thermodynamics and Kinetics of Aqueous Piperazine with Potassium Carbonate for Carbon Dioxide Absorption. Ph.D. Dissertation, The University of Texas at Austin, Austin, 2005.

Danckwerts, P. V., The Reaction of Carbon Dioxide with Ethanolamines. *Chem. Eng. Sci.* **1979,** 34, 443-446.

deMontigny, D.; Aboudheir, A.; Tontiwachwuthikul, P.; Chakma, A., Modelling the Performance of a CO_2 Absorber Containing Structured Packing. *Ind. Eng. Chem. Res.* **2006,** 45, (8), 2594-2600.

Design Institute for Physical Properties (DIPPR), *Project 801 - Database of Physical and Thermodynamic Properties of Pure Chemicals*. American Institute of Chemical Engineers: New York, 2006.

Ducroux, R.; Jean-Bapiste, P. *Technologies, Methods, and Modelling for CO_2 Capture*, 7th International Greenhouse Gas Control Technologies, Vancouver, Canada, 2004.

Dugas, R. Pilot Plant Study of Carbon Dioxide Capture by Aqueous Monoethanolamine. M.S. Thesis, The University of Texas at Austin, Austin, 2006.

Escobillana, G. P.; Saez, J. A.; Perez-Correa, J. R.; Neuburg, H. J.; Kershenbaum, L. S., Behavior of Absorption/Stripping Columns for the CO_2-MEA System; Modeling and Experiments. *Can. J. Chem. Eng.* **1991,** 69, 969-977.

Freguia, S. Modeling of CO_2 Removal from Flue Gases with Monoethanolamine. M.S. Thesis, The University of Texas at Austin, Austin, 2002.

Furukawa, S. K.; Bartoo, R. K. Improved Benfield Process for Ammonia Plants. http://www.uop.com/gasprocessing/TechPapers/ImprovedBenfield.pdf (1/28),

Gabrielsen, J.; Michelsen, M. L.; Stenby, E. H.; Kontogeorgis, G. M., Modeling of CO_2 Absorber using an AMP Solution. *AIChE J.* **2006,** 52, (10), 3443-3451.

Hee-Moon, E.; Jun-Han, K.; Kyoung-Ryong, J.; Young-Mo, A. *CO_2 Recovery Pilot Plant*, 7th International Conference on Greenhouse Gas Control Technologies, Vancouver, Canada, 2004.

Hilliard, M. *CO_2 Capture by Absorption with Potassium Carbonate - First Quarterly Report*; U.S. Dept. of Energy: 2003.

Hilliard, M. Thermodynamics of Aqueous Piperazine, Potassium Carbonate, Carbon Dioxide Characterized by Electrolyte NRTL Model within Aspen Plus. M.S. Thesis, The University of Texas at Austin, Austin, 2005.

Hilliard, M.; Kim, I.; Rochelle, G. T.; Svendsen, H. F.; Hoff, K. A. *Thermodynamics of Carbon Dioxide in Aqueous Piperazine/Potassium Carbonate Systems at Stripper Conditions*, 8th International Conference on Greenhouse Gas Control Technologies, Trondheim, Norway, 2006.

Horvath, A. L., *Handbook of Aqueous Electrolyte Solutions*. Ellis Horwood, Ltd: Chichester, 1985.

Idem, R.; Wilson, M.; Tontiwachwuthikul, P.; Chakma, A.; Veawab, A.; Aroonwilas, A.; Gelowitz, D., Pilot Plant Studies of the CO_2 Capture Performance of Aqueous MEA and Mixed MEA/MDEA Solvents at the University of Regina CO_2 Capture Technology Development Plant and the Boundary Dam CO_2 Capture Demonstration Plant. *Ind. Eng. Chem. Res.* **2006,** 45, (8), 2414-2420.

Iijama, M.; Ishida, K.; Takashina, T.; Tanaka, H.; Hirata, T.; Yonekawa, T. *Carbon Dioxide Capture Technology for Coal Fired Boiler*, 7th International Conference on Greenhouse Gas Control Technologies Vancouver, Canada, 2004.

IPCC, *Special Report on Carbon Dioxide Capture and Storage. Prepared by Working Group III of the Intergovernmental Panel on Climate Change*. Cambridge University Press: Cambridge, 2005; p 442.

Kenig, E. Y.; Schneider, R.; Gorak, A., Reactive Absorption: Optimal Process Design Via Optimal Modeling. *Chem. Eng. Sci.* **2001,** 56, 343-350.

King, C. J., *Separation Processes*. 2nd ed.; McGraw-Hill Book Company: New York, 1980.

Knudsen, J. N.; Vilhelmsen, P.-J.; Biede, O.; Jensen, J. N. *CASTOR 1 t/h CO_2 Absorption Pilot Plant at the Elsam Kraft A/S Esberg Power Plant - First Year Operation Experience*, 8th International Conference on Greenhouse Gas Control Technologies, Trondheim, Norway, 2006.

Kohl, A. L.; Neilsen, R. B., *Gas Purification*. 5th ed.; Gulf Publishing Co.: Houston, 1997.

Krishna, R.; Standart, G. L., A Multicomponent Film Model Incorporating an Exact Matrix Method of Solution to the Maxwell-Stefan Equations. *AIChE J.* **1976,** 22, 383-389.

Kucka, L.; Muller, I.; Kenig, E. Y.; Gorak, A., On the Modeling and Simulation of Sour Gas Absorption by Aqueous Amine Solutions. *Chem. Eng. Sci.* **2003,** 58, 3571-3578.

Lewis, J. C.; Seibert, A. F.; Fair, J. R., Effective Mass Transfer Areas in Packed Absorbers. In *AIChE 2006 Annual Meeting*, San Francisco, CA, 2006.

Littel, R. J. Selective Carbonyl Sulfide Removal in Acid Gas Treating Processes. Ph.D. Dissertation, Twente University, 1991.

Littel, R. J.; Van Swaaij, W. P. M.; Versteeg, G. F., Kinetics of Carbon Dioxide with Tertiary Amines in Aqueous Solution. *AIChE J.* **1990,** 36, (11), 1633-1640.

Littel, R. J.; Versteeg, G. F.; Van Swaaij, W. P. M., Kinetics of CO_2 with Primary and Secondary Amines in Aqueous Solutions. I. Zwitterion Deprotonation Kinetics of DEA and DIPA in Aqueous Blends of Alkanolamines. *Chem. Eng. Sci.* **1992a,** 47, 2027-2035.

Littel, R. J.; Versteeg, G. F.; Van Swaaij, W. P. M., Kinetics of CO_2 with Primary and Secondary Amines in Aqueous Solutions. II. Influence of Temperature on Zwitterion Formation and Deprotonation Rates. *Chem. Eng. Sci.* **1992b,** 47, 2037-2045.

Marland, G.; Boden, T. A.; Andres, R. J. *Global, Regional, and National CO_2 Emissions. In Trends: A Compendium of Data on Global Change*; Carbon Dioxide Information Analysis Center, Oak Ridge National Laboratory, U.S. Department of Energy: Oak Ridge, Tenn., U.S.A., May 30, 2006.

McLees, J. Vapor-Liquid Equilibrium of Monoethanolamine, Piperazine, Water at 35-70 ^{o}C. M.S. Thesis, The University of Texas at Austin, Austin, 2006.

Ohishi, T.; Iwasaki, S.; Tanaka, H.; Hirata, T.; Iijama, M.; Ishida, K.; Yonekawa, T. *Long Term Testing of the Capture of CO_2 from a Coal-fired Boiler*, 8th International Conference on Greenhouse Gas Control Technologies, Trondheim, Norway, 2006.

Onda, K.; Takeuchi, H.; Okumoto, Y., Mass Transfer Coefficients between Gas and Liquid Phases in Packed Columns. *J. Chem. Eng. Japan* **1968,** 1, 56-62.

Oyenekan, B. Modeling of Strippers for CO_2 Capture by Aqueous Amines. Ph.D. Dissertation, The University of Texas at Austin, Austin, 2007.

Pacheco, M. A. Mass Transfer, Kinetics, and Rate-based Modeling of Reactive Absorption. Ph.D. Dissertation, The University of Texas at Austin, Austin, 1998.

Pacheco, M. A.; Rochelle, G. T., Rate-Based Modeling of Reactive Absorption of CO_2 and H_2S into Aqueous Methyldiethanolamine. *Ind. Eng. Chem. Fundam.* **1998,** 37, 4107-4117.

Pandya, J. D., Adiabatic Gas Absorption and Stripping with Chemical Reaction in Packed Towers. *Chem. Eng. Commun.* **1983,** 19, 343-361.

Peng, J. J., Email from Aspen Tech Regarding Liquid Holdup Specification in RateSep. In 2007.

Pintola, T.; Tontiwachwuthikul, P.; Meisen, A., A Simulation of Pilot Plant and Industrial CO_2-MEA Absorbers. *Gas Sep. Purif.* **1993,** 7, 47-52.

Pohorecki, R. M., Wladyslaw. , Kinetics of Reaction Between Carbon Dioxide and Hydroxyl Ions in Aqueous Electrolyte Solutions. . *Chem. Eng. Sci.* **1988,** 43, (7), 1677-1684.

Reid, R. C.; Prausnitz, J. M.; Poling, B. E., *The Properties of Gases and Liquids*. 4th ed.; McGraw-Hill: New York, 1987.

Rizzuti, L.; Augugliaro, V.; Cascio, G. L., The Influence of the Liquid Viscosity on the Effective Interfacial Area in Packed Columns. *Chem. Eng. Sci.* **1981,** 36, (6), 973-978.

Rocha, J. A.; Bravo, J. L.; Fair, J. R., Distillation Columns Containing Structured Packings: A Comprehensive Model for Their Performance. 1. Hydraulic Models. *Ind. Eng. Chem. Res.* **1993,** 32, 641-651.

Rocha, J. A.; Bravo, J. L.; Fair, J. R., Distillation Columns Containing Structured Packings: A Comprehensive Model for Their Performance. 2. Mass Transfer Model. *Ind. Eng. Chem. Res.* **1996,** 35, 1660-1667.

Sartori, G.; Savage, D. W., Sterically Hindered Amines for CO_2 Removal from Gases. *Ind. Eng. Chem. Fundam.* **1983,** 22, 239-249.

Saxena, M. N.; Flintoff, W., Engineering and Economics of CO_2 Removal and Sequestration. *Hyd. Proc.* **2006**, (December), 57-64.

Say, G. R.; Heinzelmann, F. J.; Iyengar, J. N.; Savage, D. W.; Bisio, A.; Sartori, G., A New, Hindered Amine Concept for Simultaneous Removal of CO_2 and H_2S from Gases. *Chem. Eng. Prog.* **1984,** 80, (10), 72-77.

Stichlmair, J.; Bravo, J. L.; Fair, J. R., General Model for Prediction of Pressure Drop and Capacity of Countercurrent Gas/Liquid Packed Columns. *Gas Sep. Purif.* **1989,** 3, 19-28.

Tontiwachwuthikul, P.; Meisen, A.; Lim, C. J., CO_2 Absorption by NaOH, Monoethanolamine and 2-Amino-2-Methyl-1-Propanol Solutions in a Packed Column. *Chem. Eng. Sci.* **1992,** 47, (2), 381-390.

Treybal, R. E., Adiabatic Gas Absorption and Stripping in Packed Towers. *Ind. Eng. Chem.* **1969,** 61, (7), 36-41.

Tseng, P. C.; Ho, W. S.; Savage, D. W., Carbon Dioxide Absorption into Promoted Carbonate Solutions. *AIChE J.* **1988,** 34, (6), 922-931.

Tseng, P. C.; Ho, W. S.; Savage, D. W., Carbon Dioxide Absorption into Promoted Carbonate Solutions. *AIChE. J.* **1998,** 34, (6), 922-931.

U.S. EPA *Inventory of U.S. Greenhouse Gas Emissions and Sinks: 1990-2004*; EPA 430R06002; Washington D.C., April 15, 2006, 2006.

Wang, G. Q.; Yuan, X. G.; Yu, K. T., Review of Mass-Transfer Correlations for Packed Columns. *Ind. Eng. Chem. Res.* **2005,** 44, (23), 8715-8729.

Wilke, C. R.; Chang, P., Correlation of Diffusion Coefficients in Dilute Solutions. *AIChE J.* **1955,** 2, 264-270.

Wilson, I. Gas-Liquid Contact Area of Random and Structured Packing. M.S. Thesis, The University of Texas at Austin, Austin, 2004.

Wilson, M.; Tontiwachwuthikul, P.; Chakma, A.; Idem, R.; Veawab, A.; Aroonwilas, A.; Gelowitz, D.; Henni, A.; Mahinpey, N. *The International Test Centre for Carbon Dioxide Capture (ITC)*, 7th International Conference on Greenhouse Gas Control Technologies, Vancouver, Canada, 2004a.

Wilson, M.; Tontiwachwuthikul, P.; Chakma, A.; Idem, R.; Veawab, A.; Aroonwilas, A.; Gelowitz, D.; Stobbs, R. *Evaluation of the CO_2 Capture Performance of the University of Regina CO_2 Technology Development Plant and the Boundary Dam CO_2 Demonstration Plant*, 7th International Conference on Greenhouse Gas Control Technologies, Vancouver, Canada, 2004b.

Xiao, J.; Li, C.-W.; Li, M.-H., Kinetics of Absorption of Carbon Dioxide into Aqueous Solutions of 2-Amino-2-Methyl-1-Propanol + Monoethanolamine. *Chem. Eng. Sci.* **2000,** 55, 161-175.

Yagi, Y.; Mimura, T.; Ishida, K.; Yoshiyama, R.; Kamijo, T.; Yonekawa, T. *Improvements of Carbon Dioxide Capture Technology from Flue Gas*, 7th International Conference on Greenhouse Gas Control Technologies, Vancouver, Canada, 2005.

This document does not include the vita page from the original.